Advances in Biochemical Engineering/Biotechnology 140
Series Editor: T. Scheper

Man Bock Gu
Hak-Sung Kim *Editors*

Biosensors Based on Aptamers and Enzymes

Springer

140
Advances in Biochemical Engineering/Biotechnology

For further volumes:
http://www.springer.com/series/10

Aims and Scope

This book series reviews current trends in modern biotechnology and biochemical engineering. Its aim is to cover all aspects of these interdisciplinary disciplines, where knowledge, methods and expertise are required from chemistry, biochemistry, microbiology, molecular biology, chemical engineering and computer science.

Volumes are organized topically and provide a comprehensive discussion of developments in the field over the past 3–5 years. The series also discusses new discoveries and applications. Special volumes are dedicated to selected topics which focus on new biotechnological products and new processes for their synthesis and purification.

In general, volumes are edited by well-known guest editors. The series editor and publisher will, however, always be pleased to receive suggestions and supplementary information. Manuscripts are accepted in English.

In references, Advances in Biochemical Engineering/Biotechnology is abbreviated as *Adv. Biochem. Engin./Biotechnol.* and cited as a journal.

Man Bock Gu · Hak-Sung Kim
Editors

Biosensors Based on Aptamers and Enzymes

With contributions by

Frieder W. Scheller · Aysu Yarman · Till Bachmann
Thomas Hirsch · Stefan Kubick · Reinhard Renneberg
Soeren Schumacher · Ulla Wollenberger · Carsten Teller
Frank F. Bier · Yeon Seok Kim · Man Bock Gu
Pui Sai Lau · Yingfu Li · Yu Xiang · Peiwen Wu
Li Huey Tan · Yi Lu · Maren Lönne · Guohong Zhu
Frank Stahl · Johanna-Gabriela Walter · Mahmoud Labib
Maxim V. Berezovski · Koichi Abe · Wataru Yoshida
Kazunori Ikebukuro · Butaek Lim · Young-Pil Kim
Yong Duk Han · Yo Han Jang · Hyun C. Yoon
Sven C. Feifel · Andreas Kapp · Fred Lisdat
Fabiana Arduini · Aziz Amine

Springer

Editors
Man Bock Gu
Korea University College of Life Sciences and Biotechnology
Seoul
Korea, Republic of South Korea

Hak-Sung Kim
Department of Biological Sciences
KAIST
Daejeon
Korea, Republic of South Korea

ISSN 0724-6145 ISSN 1616-8542 (electronic)
ISBN 978-3-642-54142-1 ISBN 978-3-642-54143-8 (eBook)
DOI 10.1007/978-3-642-54143-8
Springer Heidelberg New York Dordrecht London

Library of Congress Control Number: 2013958223

Printed on acid-free paper

Springer is part of Springer Science+Business Media (www.springer.com)

Preface

It is interesting to note that the first biosensor which emerged involved the use of an enzyme, while the most recent bioreceptor molecule is the aptamer. Therefore, the title and subject of this volume reminds us not only to look back to the history of biosensor development, but also to foresee the future of biosensors. We are really delighted to present this volume, even if it is true that a single volume cannot show all the progress in the biosensor development since it started. In this volume, therefore, after a brief introduction to the latest technology in biosensors, topical reviews are followed for the most recent advances in aptamer and enzyme biosensors. These contributions are by world renowned biosensor scientists and engineers who share their broad and deep experience and knowledge.

"Future of Biosensors: A Personal View" (Frieder W. Scheller, Aysu Yarman, Till Bachmann, Thomas Hirsch, Stefan Kubick, Reinhard Renneberg, Soeren Schumacher, Ulla Wollenberger, Carsten Teller and Frank F. Bier) gives a general overview of biosensors, which is a personal view on the future of biosensors. The chapter highlights that biosensors will be a very useful tool for decentralized and personalized online patient control or health check-ups in the future healthcare technology. They can also be widely used as a simple and rapid *on-site* measurement system, as a complement to the instrumental analysis methods, and for several applications including safety checks of drinking water and foods.

Since their first discovery in 1990, aptamers have received tremendous attention not only in academia but also from industrial sectors. During the last two decades, thousands of publications on aptamers or SELEX have been reported, numerous patents have been filed and granted, and several companies in pharmaceutical and diagnostic fields are now dealing with aptamers. Since the first FDA approved aptamer-drug (Macugen) entered onto the market, aptamers have become increasingly important as molecular probes for diagnostics and therapeutics. Especially, several advantages of aptamers, compared to natural receptors such as antibodies or enzymes, have attracted researchers to develop aptamer-based biosensors. Recently, various novel aptasensors have been developed from their intrinsic properties as nucleic acids, these show remarkable flexibility and convenience in the design of their structures. Moreover, a considerable understanding of aptamers' conformation and their ligand-binding properties combined with functional nanomaterials, such as gold nanoparticles or quantum dots, has led

to the emergence of a range of different styles of bioassay platforms. These issues are included in a different chapter of this book.

"Advances in Aptamer Screening and Small Molecule Aptasensors" (Gu and Kim) introduces the recent advances in aptamer screening methods, including a modified SELEX processes using graphene oxide (GO) from their own study, which enables aptamer isolation with higher affinity and selectivity through a less labor-efficient and time-efficient manner. This chapter also reviews aptasensors, especially for low-weight molecular targets, which have not been studied sufficiently, despite the increasing need in the fields of environmental monitoring, food safety, and defense and security.

In "Exploration of Structure-Switching in the Design of Aptamer Biosensors", Lau and Li review the recent progress on engineered structure-switching aptamer sensors. In this chapter, the authors introduce the origin and design of structure-switching aptamers and summarize their key applications for aptasensor development with the integration of fluorescent, electrochemical and colorimetric detection methods.

In "DNAzyme-Functionalized Gold Nanoparticles for Biosensing", Xiang, Wu, Tan, and Lu review the recent progress on analytical methods using DNAzyme and gold nanoparticles (AuNPs). In this chapter, various sensing methods using DNAzyme functionalized AuNPs are summarized. In addition, the intracellular applications of DNAzyme functionalized AuNPs are discussed.

In "Aptamer-Modified Nanoparticles as Biosensors" (Lonne, Zhu, Stahl, and Walter), the authors review both the utilization of aptamers in combination with various nanoparticles and discuss the analytical applications of aptamer-modified nanoparticles. Also, the authors address the medical applications of these aptamers in the detection of biomarkers and pathogens, cell targeting and imaging, and targeted drug delivery.

"Electrochemical Aptasensors for Microbial and Viral Pathogens" (Labib and Berezovski) summarizes the recent developments in electrochemical aptasensors for the detection of microbial and viral pathogens. In addition, the authors give a viability assessment of microorganisms, bacterial typing, identification of epitope-specific aptamers, and affinity measurement between aptamers and their respective targets.

Abe, Yoshida, and Ikebukuro also present electrochemical aptasensors in "Electrochemical Biosensors Using Aptamers for Theranostics", but this time focused on the theragnostics application, in which specific patients are selected for appropriate drug administration with diagnostics. The authors summarize the electrochemical aptamer-based sensing systems and discuss their advantages for theragnostics.

In spite of extensive advances in aptasensors, the market in biosensors is dominated by antibodies which are fully matured and standardized in the industry. One bottleneck in the commercialization of aptasensors is the isolation process of aptamers by in vitro selection which prevents widespread usages of aptamers. Only a limited number of aptamers are currently available. To overcome this issue, SELEX has been continuously advanced to make it simpler and quicker.

In addition, the understanding of whether any overarching rules govern aptamer functions is also important for optimal aptamer performance in assays and detection systems. Aptasensors are now starting to show their worth as a rival of traditional immunoassays in analytical fields.

In an effort to overcome the current limitations and expand the use of enzyme biosensors, many attempts have been made. This book describes some typical examples.

First, Lim and Kim in "Enzymatic Glucose Biosensors Based on Nanomaterials" describe the innovations in glucose biosensors that account for about 85 % of the entire biosensor market. Over the last few decades, glucose biosensors based on glucose oxidase (GOx) have played a pivotal role in simple glucose detection kits in blood as well as in vivo glucose monitoring, due to its mass production and easy availability. The major issues to be addressed in enzyme biosensors include the enhancement of biosensor performance such as sensitivity, selectivity, and detection range of analytes.

In "Cascadic Multienzyme Reaction-Based Electrochemical Biosensors", Yoon et al. describe a concept of cascadic multi-enzyme reaction employing more than two enzymes in the construction of biosensors to enhance their sensitivity and accuracy. They present fundamental principles for the development of electrochemical biosensors based on cascadic multienzyme reactions and their applications in clinical and environmental fields. Essential knowledge for the development of such biosensors includes a cascadic multi-enzyme reaction-based assay method and their multi-enzyme reaction mechanisms, electrochemical signaling principles, and multi-enzyme immobilization strategies. Obviously, a key step in the construction of biosensors is the immobilization process of enzymes that specifically recognizes the analyte. This crucial process is often limited by reduction in the catalytic activity of enzymes at the solid–liquid interface, which is related to the need for the biomaterial to be well-arranged on the surface, or within, an assembly. Furthermore, the number of biomolecules immobilized is connected to the sensitivity of the whole sensing device. This gives rise to the development of immobilization procedures which move away from simple mixing of the biocomponent with a matrix to methods allowing a layered and controlled deposition of the recognition element, resulting in multilayered architectures on the transducer surface.

In "Protein Multilayer Architectures on Electrodes for Analyte Detection", Feifel et al. present an overview of the methods available for arranging biomolecules in a layer-by-layer (LBL) design. Furthermore, applications in sensor construction are illustrated with the focus on electrochemical transduction. In particular, this chapter provides an overview of different assembly methodologies used for the construction of multilayer architectures with bio-molecules for application in sensors. The use of different building blocks is introduced for the formation of multilayers with a clear preference for polymers and nanoparticles.

Finally, as a new concept of enzyme biosensors, Arduini and Aminec in "Biosensors Based on Enzyme Inhibition" introduce a biosensor based on enzyme inhibition. The measurement of analytes can be performed by means of two

different approaches. If the enzyme metabolizes the analyte, the analyte can be determined measuring the enzymatic product. If the analyte inhibits the enzyme, the decrease in the enzymatic product formation can be measured and correlated to the analyte concentration. In this context, the authors describe the detection principle and the potential application of biosensors based on enzyme inhibition.

With a growing demand for sensitive and robust biosensors in the fields of healthcare, the environment, and bioprocesses, many advances in aptamer or enzyme biosensors are in high demand. In particular, the integration of new materials and nanotechnology with current biosensor technology will accelerate the development of new biosensors with greater potential. We hope that this volume provides some insight into the possible future developments of aptamer and enzyme biosensors.

Man Bock Gu
Hak-Sung Kim

Contents

Adv Biochem Eng Biotechnol (2014) 140: 1–28
DOI: 10.1007/10_2013_251

Published Online: 6 November 2013

Future of Biosensors: A Personal View

Frieder W. Scheller, Aysu Yarman, Till Bachmann, Thomas Hirsch, Stefan Kubick, Reinhard Renneberg, Soeren Schumacher, Ulla Wollenberger, Carsten Teller and Frank F. Bier

Abstract Biosensors representing the technological counterpart of living senses have found routine application in amperometric enzyme electrodes for decentralized blood glucose measurement, interaction analysis by surface plasmon resonance in drug development, and to some extent DNA chips for expression analysis and enzyme polymorphisms. These technologies have already reached a highly advanced level and need minor improvement at most. The dream of the "100-dollar" personal genome may come true in the next few years provided that the technological hurdles of nanopore technology or of polymerase-based single molecule sequencing can be overcome. Tailor-made recognition elements for biosensors including membrane-bound enzymes and receptors will be prepared by cell-free protein synthesis. As alternatives for biological recognition elements, molecularly imprinted polymers (MIPs) have been created. They have the potential to substitute antibodies in biosensors and biochips for the measurement of low-molecular-weight substances, proteins, viruses, and living cells. They are more stable than proteins and can be produced in large amounts by chemical synthesis. Integration of nanomaterials, especially of graphene, could lead to new miniaturized biosensors with high sensitivity and ultrafast response. In the future individual therapy will include genetic profiling of isoenzymes and polymorphic forms of drug-metabolizing enzymes especially of the cytochrome P450 family.

F. W. Scheller (✉) · A. Yarman · S. Kubick · S. Schumacher · C. Teller · F. F. Bier
Fraunhofer Institute for Biomedical Engineering IBMT, 14476 Potsdam, Germany
e-mail: fschell@uni-potsdam.de

F. W. Scheller · A. Yarman · U. Wollenberger · F. F. Bier
Institute of Biochemistry and Biology, University of Potsdam, Karl-Liebknecht-Str. 24–25, 14476 Potsdam, Germany

T. Bachmann
Division of Pathway Medicine, University of Edinburgh Chancellor's Building, 49 Little France Crescent, Edinburgh EH16 4SB, Scotland

T. Hirsch
Institute of Analytical Chemistry, Chemo- and Biosensors, University of Regensburg, 93053 Regensburg, Germany

R. Renneberg
Department of Chemistry, The Hong Kong University of Science and Technology, Clear Water Bay, Kowloon SAR Hong Kong, China

For defining the pharmacokinetics including the clearance of a given genotype enzyme electrodes will be a useful tool. For decentralized online patient control or the integration into everyday "consumables" such as drinking water, foods, hygienic articles, clothing, or for control of air conditioners in buildings and cars and swimming pools, a new generation of "autonomous" biosensors will emerge.

Keywords Biosensors · Molecularly imprinted polymers · Personalized medicine

Abbreviations

2D	Two-Dimensional
BCC	Business Communications Company, Inc
DNA	Deoxyribonucleic Acid
ELISA	Enzyme-Linked Immunosorbent Assay
ESBL	Extended-Spectrum Beta-Lactamase
FDA	Food and Drug Administration
FETs	Field Effect Transistors
GO	Graphene Oxide
HER-2	Human Epidermal Growth Factor Receptor 2
HVA	Homovanillic Acid
IUPAC	International Union of Pure and Applied Chemistry
IVD	In Vitro Diagnostics
KRAS	V-Ki-ras2 Kirsten Rat Sarcoma Viral Oncogene Homologue
LOD	Limit of Detection
MIP	Molecularly Imprinted Polymer
MRE	Molecular Recognition Element
NGS	Next-Generation Sequencing
pAP	p-Aminophenol
POC	Point of Care
PCR	Polymerase Chain Reaction
rGO	Reduced Graphene Oxide
RNA	Ribonucleic Acid
RT-PCR	Real-Time Polymerase Chain Reaction
SELEX	Systematic Evolution of Ligands by Exponential Enrichment
TSA	Transition State Analogue
TCP	2, 4, 6-Trichlorophenol
UV	Ultraviolet

Contents

1 Introduction

Enzymes and antibodies are well-established tools in clinical analysis, food control, and environmental analysis. Almost 50 years ago, a new category of analytical devices—biosensors—was created. According to the IUPAC definition, a biosensor is an integrated receptor-transducer device capable of providing selective quantitative or semi-quantitative analytical information using a biological recognition element [1]. The biosensor definition may also be extended to biomimetic recognition elements, for example, "mini-enzymes," synzymes, aptamers, and molecularly imprinted polymers (MIPs), which are derived from biology.The spatial integration of the recognition element with the transducer leads to a compact functional unit that allows reuse of the biological component and miniaturization of the sensor body (Fig. 1). These features allow for online measurements and are the basis of the combination of different recognition elements on one transducer array: the biochips. Integration of the biochemical and signal processing has been realized in "intelligent biosensors" and bio-FETs, respectively. The combination of biosensors with microfluidics and actuators on a chip has led to total microanalytical systems (μTAS).

In contrast to "traditional" bioanalytical assays such as Fehling's solution or measuring the optical rotation of sugar solution, biosensors combine highly specific, molecular recognition elements (MREs) with ultrasensitive signal transduction devices. Modern biosensorics has been established as a standalone branch of biotechnology at the interface between molecular and cell biology, and analytical chemistry and engineering, respectively.

The development of biosensors started with the enzyme electrode for blood glucose described by L. C. Clark in 1962 [2]. It combined the enzyme glucose oxidase with an amperometric oxygen electrode.

In spite of the large potential and the great expectations in the early 1980s, biosensors have found only limited application. The commercial sector is clearly dominated by the decentralized blood glucose measurement and the large forecasts in the field of DNA-based biochips have failed up to now [3].

After presenting the state of the art in this chapter we discuss the following key aspects of further development:

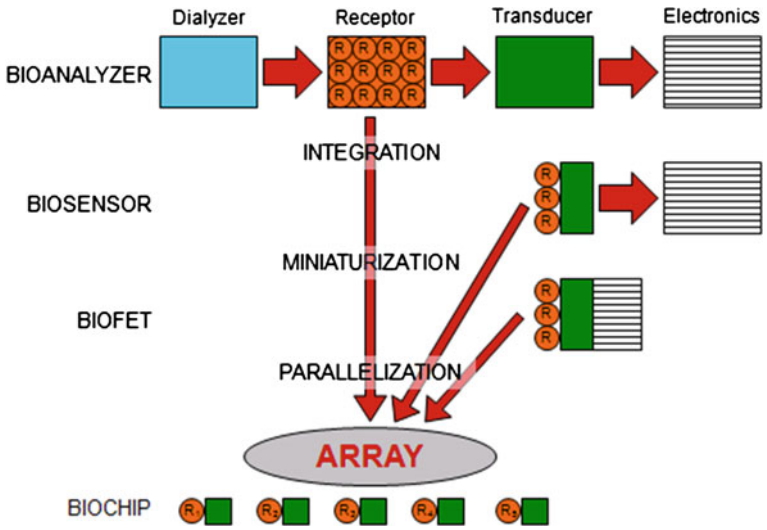

Fig. 1 The route from biosensor to biochip

- Physical, chemical, and biological enabling technologies for biosensors.
  - The "magic" of graphene.
  - The potential of bimimetic recognition elements.
  - Generation of proteins by cell-free synthesis.
- Biosensors for personalized medicine.

2 State of the Art

2.1 Blood Glucose Measurement

The blood glucose monitoring by biosensors is an integral part of diabetes management nowadays. Due to the permanently increasing incidence of diabetes both in industrialized countries and the "threshold" states such as China and India, blood glucose measurement is a rapidly growing market. The annual world market in 2012 was almost US $13 billion with a growth rate of almost 10 %. This value represents 87 % of the total market for all types of biosensors including DNA chips. The exceptional position of blood glucose sensors is also expected to last for the next decade [3].

There have been tremendous developments in the technologies behind commercial blood glucose devices resulting in cost-effectiveness and convenience for patients. Therefore these analyzers are simple and easy to use, have low sample requirements, and rapid response. The technology has already reached a highly advanced level and there are mostly possibilities for minor incremental

improvements of discontinuous extracorporeal blood glucose measurement [4, 5]. Nevertheless the following aspects still need further improvement and are the subjects of intensive research and development:

(i) The US Food and Drug Administration (FDA) recommends that glucose sensors must have an error of less than 20 % in the clinically relevant region between 1.65 and 22 mmol/L. Obviously, changes in the performance within one lot of single-use sensors are the reason for the insufficient accuracy of decentralized blood glucose analysis. Integrated recalibration could prevent scattering in many sensors. The present concepts of single-use sensors do not allow a calibration before the measurement, therefore they have to rely on the uniformity within each lot.

(ii) Elimination of interference, that is, "absolute" specificity for glucose both on the level of biological recognition and the transducer. In this line the traditional glucose-recognizing enzymes glucose oxidase and glucose dehydrogenase have engineered for improved substrate specificity [6]. Third-generation enzyme electrodes based on direct electron transfer between the active site of the biocatalyst e.g., cellobiose dehydrogenases [7] work at low electrode potential thus suppressing the interference of reducing sample constituents such as ascorbic acid or paracetamol (acetaminophen). As an alternative to enzymes, sugar-binding proteins in combination with an optical readout could be applied in glucose measurement.

(iii) Integration of all analysis steps from taking the sample to the measuring process including advanced lancing mechanisms and autonomous transfer of the sample to the sensor. Both micromechanical systems and manchetes with integrated lancets have been applied, however, the handling is not yet ripe.

Considerable efforts have been and will be devoted to continuous blood glucose [8, 9] measurement because it can provide valuable information on how to improve therapy. However, the difficulties in handling and the high costs are still limiting factors for the commercial success of the devices from Abbot, Medtronic, and DexCom.

Noninvasive blood glucose measurement is another prospective area. It would make all sample-dependent measurements obsolete. In spite of considerable efforts there has been no major success so far due to the absence of specificity.

2.2 Immunoassays

Immunoassays are a widely used analytical technology in biodiagnostics, including the determination of antigens, hormones, drugs, and antibodies. Immunoassays have been used in hospitals, laboratory medicine, and research since the mid-1960s. Their expansion is nowadays boosted by globalization of infectious diseases and the surge in cardiovascular and other chronic diseases. POC testing is one of the most rapidly growing segments as tests that were done in the central lab are now

available as near-patient tests. This has led to an explosion of new tests and technologies [10].

Lateral-flow assays have moved closer to the patient. A novel "digital-style" lateral-flow assay provides semi-quantitative results by simply counting the number of lines in the test without any expensive reading instrument. In addition, more and more lateral-flow tests using saliva, urine, and sweat for analysis can make them more patient-friendly.

Although it is impossible to duplicate analytes chemically yet, the analyte can be tagged with oligonucleotide markers that can be subsequently amplified with PCR and then identified by DNA detection [11, 12]. This approach is often referred to as immuno-PCR that allows the detection of proteins with DNA markers. A bio-barcode assay utilizes antibody-coated magnetic beads to capture and concentrate the analytes, which are subsequently labeled with gold nanoparticle probes conjugated with specific antibodies and DNA barcodes [13, 14]. The DNA barcodes are then released from the complex and detected via hybridization. This system allows signal amplification as the nanoparticle probe carries a large number of oligonucleotides per protein.

For the determination of haptens it would be desirable to provide a method that produces a response which increases with the concentration of the analyte. An immuno-threshold-based assay can give a signal directly proportional to the concentration of the hapten [15]. Also, a one-step, homogeneous noncompetitive immunoassay for haptens using a highly specific antibody against the immune complex (IC) formed between an antibody and an analyte has been demonstrated [16].

High-throughput multiplex immunoassays that measure hundreds of proteins in complex biological matrices in parallel have become significant tools for quantitative proteomics studies, diagnostic discovery, and biomarker-assisted drug development.

2.3 Lab-on-a-Chip Technologies in Bioanalysis

"Lab-on-chip technologies are believed to be one of the mainstream technologies within the next centuries." This sentence is familiar to any researcher in the field of lab-on-a-chip and biochip technology even if it is hard to find a citation for it. Nevertheless, according to BCC market researches about the Global Biochip Market published in 2011, the global market was believed to be as high as US $3.9 billion with an annual growth rate of 19.5 % which is a highly attractive market segment [17].

One of the key drivers in lab-on-a-chip systems are the huge research activities in biomedicine. Starting from the human genome project which was completed in 2003, researchers have gained more insights into the genome, proteome, or metabolome [18, 19, 20]. These activities boosted the technology because huge amounts of data per sample in an adequate time had to be delivered. Small sample

and reagent consumption, shorter reaction times, lower detection limits, and especially the possibility for multiparameter analysis made these systems superior to classical biochemical analysis. These advantages boosted research in areas such as empiric biomarker research, drug development, or high-throughput screening. In these areas, lab-on-a-chip systems are mostly used as research tools. For example, companies such as Affymetrix, Protagen, or Pepperprint offer high-density microarrays for biomarker identification.

These high-density arrays are used to evaluate differences between diseased and healthy patients. Starting with a broad spectrum of parameters, the number of biomarkers will be narrowed down to those analytes showing significant differences between healthy and diseased states. This lower number will be further evaluated as candidates in order to find a limited but sufficient number of markers for focused diagnostic decision making. This way of looking at molecular medicine offers great potential and benefits for patients. Whereas classical biochemistry looks at just one parameter in order to diagnose a certain disease, multiparameter analysis will allow us to verify the stage of the disease, to screen risks for predisposition, or to enable therapeutic control (Fig. 2).

This scientifically driven change in the diagnostic value chain will culminate in personalized medicine approaches. The frequent determination of a multiple of different parameter requests for new technologies that allow near-patient testing for direct therapeutic action. Many different analytical devices were developed for these applications including lab-on-a-disc systems or chip systems such as the Fraunhofer ivD-platform.

For example, in the Fraunhofer ivD-platform [21] a drop of blood is applied onto the credit card cartridge which is inserted into the base-unit for a fully automated processing of the assay. Within 10–15 min the results of immunological, serological, and DNA-based assays are obtained.

Multiplexed protein measurement for biomarker-based diagnostic and prognostic testing will become the largest growth segment of the immunodiagnostics industry [22]. It has the capacity to identify surrogates that will be integrated into clinical indices, treatment algorithms, and, ultimately, into dynamic disease models that permit real-time, data-driven patient management.

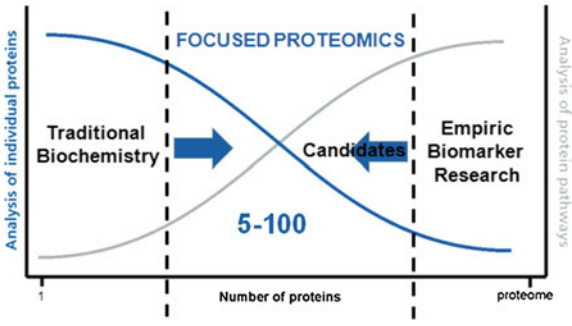

Fig. 2 Correlation of number of proteins with specific application areas such as traditional biochemistry, focused proteomics, and empiric biomarker research (adapted from [24])

Another very promising approach is next-generation sequencing (NGS). Elaborated systems such as the platform from Pacific Biosciences allow the sequencing of the whole genome. Within the platform, a single polymerase is attached to a waveguide. While synthesizing the complementary DNA strand each nucleotide is detected and the whole genome can be analyzed [23]. The ability to sequence the whole genome and to derive specific diagnostic statements such as genetic disposition gives rise to new molecular diagnostics. Since as the technology of sequencing is continually improving, the prices for whole genome sequencing will drop to an amount affordable for every patient. This trend is already here: for example, an app from Illumina is available called "My Genome" for exploring your own genome.

3 Enabling Technologies: Physical, Chemical, and Biological Approaches

3.1 Graphene in Biosensor Applications

In the family of carbon nanomaterials graphene has recently become the rising star. This was strengthened by the European Commission's choosing graphene as a future emerging technique. Research in Europe involving graphene will be funded in one of the first so-called flagship initiatives by €1,000 million for the next 10 years [25]. The scientific and technological roadmap of the graphene flagship lists graphene as a platform with many beneficial properties as a one-atom thick material with ultimate strength, but also high flexibility, as well as unique electrical and optical properties. The first components that can be transferred from academic research to industrial applications are proposed for 2015. Transistors are predicted to start the commercial success of the graphene story, followed by spin valves, flexible displays, RF tags, ultralight batteries, solar cells, ultrafast lasers, composite materials, and prostheses. Sensors and biosensors based on graphene are expected to be available on the market for 2017. To start, a ramp-up phase of 30 months with a total budget of €75 million is planned, where about 3–5 % will be spent in development of sensor technologies. Not only in Europe, but also in Asia, mainly Singapore, as well as in the United States, graphene is proclaimed as an important part of future key technologies. Therefore the question arises as to whether graphene could be smart enough to replace some of the currently used materials in biosensor technology.

The reasons why graphene has become so attractive to researchers are to be found in the extraordinary physical properties of this material. Simply, one can imagine graphene as a single layer of graphite with exactly one layer of a polycyclic aromatic hydrocarbon network, with all carbon atoms hexagonally arranged in a planar condensed ring system of quasi-infinite size [26]. It has a metallic character and consists solely of carbon and hydrogen. It was found for such a

material that the planar surface of 2,630 m^2 weighs only 1 g [27]. A Young's modulus of approximately 1,100 GPa indicates superior mechanical strength [28]. A high thermal conductivity of 5,000 Wm^{-1} K^{-1} and a high electrical conductivity of 1,738 S m^{-1} are further outstanding properties of graphene. Many more exciting properties have been discovered since Andre Geim and Konstantin Novoselov described in 2004 a simple way for producing and characterizing individual graphene flakes [29]. The idea to have all these supreme properties unified in one material is highly attractive. A combination of transparency, elasticity, and conductivity will immediately bring flexible sensor arrays with electrical addressing and/or optical read-out to one's mind.

This simple synthesis of graphene as described by Andre Geim and Konstantin Novoselov was performed by the so-called scotch-tape method: an adhesive tape is thereby placed onto a piece of highly ordered pyrolytic graphite and is then removed. The graphite layers that stick to the tape will be cleaved by repeating this procedure again and again. Graphite flakes are transferred from one tape to another and in each step there is a chance that this layered material will get disrupted. In a last step, to transfer the graphene, the adhesive tape will be placed onto and removed from a silicon wafer with a suitable oxide layer on top. The remaining graphene can be identified due to its high transparency simply by interference contrast with an optical microscope. This method allows distinguishing between single-, two-layer, and multilayer graphene and thus gives access to this carbon nanomaterial for the study of its physical properties. For any practical application this method is too laborious and inconvenient, therefore nearly a dozen methods have been developed thus far, to prepare graphene of various dimensions, shapes, and quality [30]. The methods used mostly are chemical vapor deposition [31], epitaxial growth on silicon carbide [32], or chemical exfoliation [33]. All of these methods are advantageous in some ways, and they are able to deliver large quantities of graphene, but the resulting products are not of the quality of defined molecules. Even within the same production technique an ill-defined material, which only somehow represents the ideal graphene at all, will be received, often with slightly different properties from batch to batch. The perfect graphene is characterized by quasi-infinite size. This cannot be achieved by any preparation method. Graphene comprises only surface; there is no bulk phase, but there is always a border. Therefore, as for every nanomaterial, the properties depend strongly on the size of the material. The smaller a perfect single flake, the higher the ratio of the surface to the border and the less the material can be claimed as perfect graphene. Furthermore, the structure itself can contain chemical functionalities or impurities, introduced by the synthesis or transfer of this material. For chemically derived graphene (rGO), for example, elemental analysis showed that about 5 % oxygen remains in this material. This has tremendous influence on the behavior and the properties of rGO, which are no longer the same as found for graphene prepared by the scotch-tape method. Additionally, many of the materials synthesized have not been adequately classified and so the term "graphene" is often used for materials that differ in chemical structure, shape, size, number of layers, and, therefore, in their properties. This problem was previously addressed

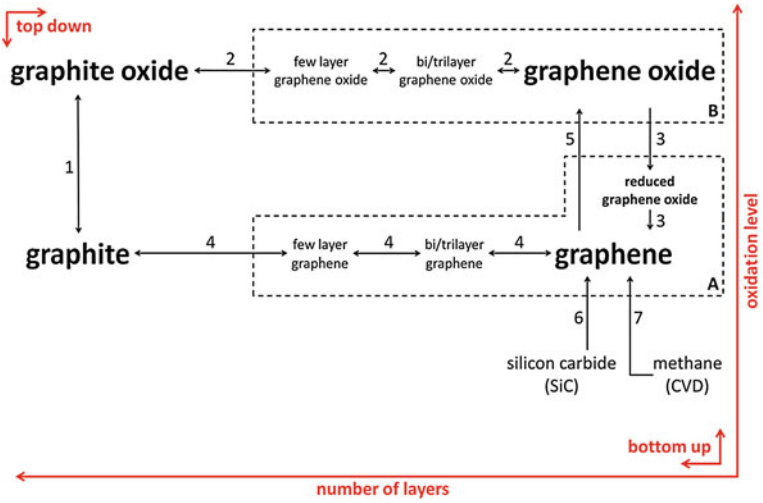

Fig. 3 Classification of graphene-related materials. Routes: (1) Oxidation of graphite to graphite oxide. (2) Stepwise exfoliation of graphite oxide to give graphene oxide in aqueous colloidal suspensions by sonication and stirring. (3) Reduction of graphene oxide by chemical reactions, thermal annealing, flash reduction, enzymatic reduction, or electrodeposition. (4) Mechanical exfoliation of graphite to give graphene (scotch-tape method). (5) Oxidation of graphene sheets to graphene oxide. (6) Thermal decomposition of a SiC wafer. (7) Growth of graphene films by chemical-vapor deposition. Group A includes graphene materials primarily used for their electronic properties, group B for their optical properties. (Adapted from [34] by permission from Elsevier.)

[26], but remains unresolved. It is therefore critical first to classify graphene materials before associating the materials with (biosensor) applications. Often this is neglected, and the term graphene is used without giving an exact characterization of the material. An urgent need, for all carbon nanomaterials in between *graphene* and *graphite* (Fig. 3), is to find a clear language in describing these manifold materials. Furthermore, a standard method is required that immediately depicts to any researcher the quality of the material, in terms of the number of layers, chemical doping, crystallite size, or presence of impurities. All this information can be obtained from Raman studies; therefore it should be mandatory for all works on and with graphene to present a Raman spectrum instead of defining the material by countless numbers of indiviual acronyms such as: CRGO, GO, RGO, GR, G, GNS, EG, GNP, CCG, GE, GP, ERGO, GF, EGO, GS, GN, TRGO, CMG, FG, ERGNO, CRGNO, and many more. This allows for a high risk of confusion (e.g., GO may stand for graphite oxide or graphene oxide).

For biosensor applications, it turned out that the chemically exfoliated graphene should be the most promising candidate. This material differs a lot from the perfect graphene, due to many defects in the chemical structure, and small flake sizes with high polydispersity, but it still has some interesting properties. First of all, graphene oxide (GO) can be dispersed in aqueous solutions and second, it can easily be modified by biomolecules via standard immobilization techniques. If the

flakes are small, such material shows a weak fluorescence that can be excited nearly over the whole visual range. After a reduction step, the previous highly distorted aromatic system will be recovered and such material turns out to have good electrical conductance as well as promising quenching abilities. The reduced GO, the chemically derived graphene (rGO), is also dispersible in water, but does not form stable solutions. It highly tends to aggregate due to excellent π-stacking properties. Nevertheless, chemically derived graphene as well as graphene oxide can be solution processed and therefore transferred to any sensor surface by dip coating, drop casting, or spin coating. As the starting material is very inhomogeneous this is also the case for such a sensor layer. Furthermore, there will not be the desired one-atom-thick layer, but more likely a few layers of graphene. The difference within the materials can be seen by investigating a literature survey on amperometric glucose sensors based on an electrode modified with graphene. More than 25 publications on this topic can be found for the last three years. The LODs in these studies, of more or less the same material—all talk about graphene—range from pM to mM, and the working potentials cover nearly the whole range possible in aqueous solutions from -0.8 to 1 V versus Ag/AgCl. This inconsistency is almost the same for any of the electrochemical biosensors used in amperometric or voltammetric transduction, with enzymes attached to graphene materials. Nevertheless, by this proof of principle two points turn out to be useful in the development of enzyme-based biosensors on graphene: the electrode potential can be significally lowered by introduction of graphene as a coupling material between electrode and enzyme, and therefore the selectivity of the sensor can be enhanced. Another benefit is that the electron transfer from the biomolecule to the electrode can be enhanced, which can result in higher sensitivity and faster response. Both could be interesting by thinking of electrodes completely fabricated out of graphene deposited on flexible substrates that can be further structured by laser beam writing to design mircroarrays. By this it would be possible to design cheap, miniaturized, disposable, multianalyte biosensors. Up to now, in biosensor technology, graphene and graphene-like materials have been used only as an additional layer on top of an already existing electrode, for example, on a carbon paste electrode. The improvements here may be of academic interest but there will be no impact on already commercially available biosensor applications. Furthermore, many of these studies do not demonstrate that they can be used in complex matrices such as whole blood or even serum.

Biosensors for the detection of proteins, mainly immunosensors, are also found in the literature in growing numbers. The common way is to immobilize antibodies onto individual graphene flakes. Sensor read-out is performed by differential pulse voltammetry, fluorescence, field effect transistors, impedance or electrochemiluminescence. Detection limits are in the range of nanogram per milliliter. The sensitive layer often comprises hybrid or composite materials in combination with gold or silver nanoparticles, ionic liquids, or membranes of nafion or chitosan. Explanations of why certain combinations of materials result in better sensitivity are poor. The function of the graphene is often allocated to increase the sensitive surface area. Sensors with fluorescence read-out seem to be more sensitive on the

order of one magnitude in contrast to the electrochemical ones. Interesting approaches report on electrochemiluminescent immunosensors for alpha fetoprotein (AFP) [35] or prostate protein antigen (PSA) [36] with detection limits of 0.2 fg/mL and 8 pg/mL. The electrochemiluminescence was induced by CdS nanoparticles in the case of AFP detection, for the PSA immunosensor luminol was used. It has been shown that the detection for PSA with this sensor could be performed in human blood serum. Biosensors for thrombin or IgE have been constructed by using aptamers immobilized on graphene as the bioreceptor. With differential pulse, voltammetry thrombin in concentrations as low as 0.45 fM has been detected [37]. The benefit of the graphene in this sensor platform is explained by the greatly enhanced charge transfer of this carbon nanomaterial.

In addition to enzymes and proteins, single-strand DNA has also been immobilized on electrochemical sensors based on graphene. It has been demonstrated that the hybridization of complementary strands can be monitored. The detection of single-base mismatch has been reported, but again, up to now there are no tremendous impacts that let one believe that graphene will soon become competitive with existing technologies. Fluorescence quenching can also be used as a detection principle for DNA sensors with graphene. A single strand of nucleic acids tends to bind to the aromatic system of the graphene via π-stacking of its nucleobases. After hybridization to a complementary strand the double strand is released from the graphene surface. By this, turn-on sensors can be constructed, where the probe DNA is labeled by a fluorescent dye, directly attached to the graphene before adding analyte DNA.

Many publications prove that graphene can be principally used in biosensors. Nevertheless, the advantages of using this material are not always apparent. The lack of a preparation method resulting in large-scale synthesis of well-defined graphene complicates the situation a lot. As long as there are no standards in material characterization a comparison of the results to existing concepts in sensor technology is difficult and success in using this material is hindered. A great perspective could be in chemical bottom-up synthesis of graphene. Surface-assisted coupling of molecular monomer precursors on metallic substrates has been successfully demonstrated by the group of Klaus Müllen [38]. To exploit all extraordinary properties of graphene at once it would be necessary to produce such high-quality material on insulating flexible materials. Graphene itself turned out to obtain high sensitivity but without any selectivity at all. One possibility to introduce selectivity can be by chemical modification. First results have already been described. Another possibility is to design composite materials together with other nanomaterials. The functionality of graphene should also be increased by expanding the one-atom-thick concept to other 2D atomic crystals, such as BN, $NbSe_2$, TaS_2, MoS_2, and many others. Many investigations in this field have very recently begun, and it is expected that the first biosensors with some of these materials or even with a combination of a stack of different 2D crystals will be reported soon.

For all these optimistic and promising perspectives of graphene, there will be three essential questions for the near future that are challenging for technology transfer. (1) Is there anything else beyond a good paper? (2) Will it be possible to

produce more than one device? (3) Does the market care? Up to now there are no convincing answers to any of these questions. Therefore one should not expect any biosensor based on graphene in the near future. Up to now graphene cannot compete with existing biosensors, and maybe it will never be able to do so. The most promising fields will not be in imitating and improving well-established sensor technologies. The focus needs to be driven to truly unique properties of carbon nanomaterials and how they can be exploited in new needs and markets. One of these properties may be the highest possible surface-to-volume ratio together with the ability to have transparent, conductive, as well as a flexible material at once, which could lead to new miniaturized biosensors and sensor arrays, with high sensitivity, high stability, multidetection capabilities, and ultrafast response.

3.2 Aptamers and Molecularly Imprinted Polymers as Recognition Elements in Biomimetic Sensors

Evolution has created biopolymers on the basis of amino acids and nucleotides showing high chemical selectivity and catalytic power. Molecular recognition and catalytic conversion of the target molecules by antibodies and enzymes take place in so-called epitopes or catalytic centers of the macromolecule that typically comprise 10–15 amino acids. Nucleic acids bind complementary single-stranded nucleic acids by base pairing (hybridization) but also interact highly specifically with proteins, for example, transcription factors, and low-molecular-weight molecules and even with ions.

As alternatives for biological binders and catalysts molecularly imprinted polymers and aptamers are generated using total chemical synthesis and "evolution in the test tube", respectively.

3.2.1 Aptamers

Aptamers are single-stranded DNA or RNA molecules prepared by in vitro selection from libraries of synthetic oligonucleotides. This combinatorial approach is known as SELEX (systematic evolution of ligands by exponential enrichment). The selection cycle is repeated 6–10 times leading by increasing the stringency of the binding conditions to aptamers with affinities comparable to those of antibodies.

Once the sequence of an aptamer is identified, it can be reproducibly synthesized with high purity. Aptamers can be easily modified by various tags or markers including electrochemical indicators and fluorescence probes. In contrast to antibodies, aptamers can be easily regenerated without loss of affinity and selectivity. On the other hand, immobilization of the aptamer to the transducer surface or

changes of the environment can influence the structure and therefore the interaction with the ligand. Furthermore, problems arise from degradation by the ubiquitous DNAses.

Today, aptamers for almost 250 different analytes including metal ions, organic dyes, drugs, amino acids, co-factors, antibiotics, and nucleic acids have been synthesized. Aptamers may even distinguish the chirality of molecules or the secondary structure of proteins.

The effective combination of aptamers with a transducer is still a challenge for the development of a sensor. The analyte recognition by the aptamer must be in close proximity to the surface of the signal-generating transducer. Therefore, the aptamer has to be immobilized directly at the surface [39, 40, 41].

In analogy with immunosensors and DNA chips aptamer sensors uses the following principles:

I. Competitive, displacement, or sandwich assays with fluorophores, enzyme, or redox labels.
II. Changes of permeability for an electrochemical probe (e.g., $[Fe(CN)_6]^3$).
III. Changes of accessibility of labels or markers, (e.g., intercalators, nanoparticles).
IV. Label-free evaluation of changes of the recognition layer upon binding of the analyte by potentiometry, FETs, conductometry, and impedance spectroscopy.

Aptamer-based sensors show several specific features:

- Analyte binding to aptamers—called molecular beacons—can induce drastic conformational changes that result in an enormous fluorescence or electrochemical signal.
- The exchange rate of the analyte–binder complex can be considerably higher than for antibodies. This behavior allows for sensor regeneration and even for "online measurements".

3.2.2 Antibody Mimics: Molecularly Imprinted Polymers

Molecular imprinting is a methodology used to create recognition sites in synthetic polymers by co-polymerizing a functional and a cross-linking monomer in the presence of the analyte. In the prepolymerization mixture, the dissolved target interacts by covalent (preorganized approach) or noncovalent (self-assembly approach) binding with the functional monomer responsible for localizing the chemically active moieties of the target molecules during co-polymerization. After polymerization the template molecules are removed, providing binding sites resembling size, shape, and functionality of the template, thus the template preferentially rebinds to the cavity (Fig. 4).

The most common functional monomers applied in thermal or photopolymerization are methacrylic acid, vinylimidazole, vinylpyridine, and their derivatives.

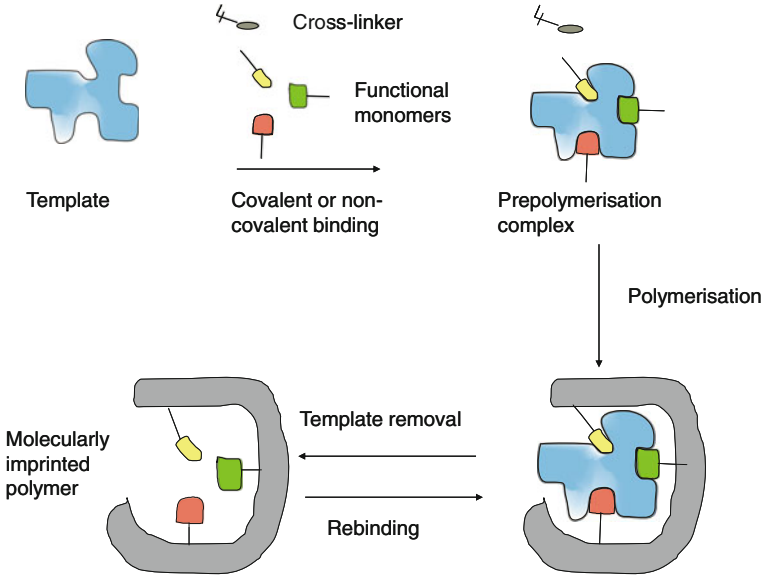

Fig. 4 Work flow of MIP preparation ([42] permission by Springer)

Surface imprinting of self-assembled monolayers of thiols on metal surfaces and electropolymerization of pyrrole, phenylenediamine, thiophene, p-aminophenylboronic acid, and their derivates in the presence of the target molecule allow the one-step preparation of MIPs for a broad spectrum of analytes [43, 44].

Molecularly imprinted polymers have the potential to substitute biological recognition elements, especially in affinity chromatography but also biosensors and biochips for the measurement of low-molecular-weight substances, proteins, viruses, and living cells. So far, however, the affinity and catalytic activity of MIPs have, in general, been well below the affinity and catalytic activity of their biological counterparts. The proteins are built up by 20 amino acids, however, MIPs are synthesized from only up to 5 different functional monomers. Combinatorial synthesis and molecular modeling should lead to further improvements.

3.2.3 Catalytically Active Molecularly Imprinted Polymers

In addition to binding MIPs, catalytically active MIPs have been developed for the application in sensors and syntheses for which no enzyme exists such as Diels–Alder reaction and Kemp elimination [45]. At the beginning the concept of catalytically active antibodies (Abzymes) was applied. In analogy to the generation of Abzymes stable analoga of the postulated transition state (TSA) of the catalyzed reaction are used as the template to mimic the active center of the enzyme. This concept is appropriate for the preparation of hydrolase-like MIPs, whenever the specific activity is several orders of magnitude lower as compared with that of

esterase enzymes [46, 47]. Obviously, the phosphonic acid esters that are generally applied as template insufficiently mimic the tetraetric TSA of the enzyme catalysis.

The first example of a MIP catalyst that had a higher catalytic activity than the respective catalytic antibodies applied a phosphonate, in the presence of an amidium-containing monomer and Zn^{2+} as TSA template [47] for the catalysis of carbonate hydrolysis.

Metal ions or metal complexes have been integrated into the polymer matrix of MIP in order to mimic redox enzymes. This concept takes advantage of the success in catalysis achieved by coordination chemistry [48]. Lakshmi et al. developed an electrochemical sensor for catechol and dopamine using hybrid materials that was capable of oxidizing the template [49]. In their approach they formed a conducting layer with a new monomer, N-phenylethylene diamine methacrylamide, on the gold electrode and grafted the MIP by UV light on this layer. The Cu^{2+}-containing MIP could mimic the catalysis of tyrosinase which can oxidize catechol in the presence of atmospheric oxygen. In addition the biomimetic approach applies redox-active groups of oxidoreductases, for example, heme, selenocystein, or flavine derivatives as the catalytic center.

For example, Cheng et al. used hemin as a co-monomer and homovanillic acid (HVA) as a template/substrate [50]. This HVA–MIP not only showed specificity towards HVA binding but it could also catalyze its oxidation in the presence of peroxide. It showed higher catalytic activity towards HVA as compared to structurally related substances such as (p-hydroxyphenyl) acetic acid and (p-hydroxyphenyl) propionic acid.

Kubato et al. prepared MIPs by bulk polymerization for pAP [51], serotonin [52], or epinephrine [53] by using hemin as the catalytic site and methacrylic acid. The MIPs were packed in a column that was inserted into a flow injection analysis system with an amperometric detector. Later, hemin-based catalytically active MIP was grafted on a glassy carbon electrode for the amperometric detecttion of pAP [54].

Recently Díaz-Díaz et al. described a MIP with chloroperoxidase-like activity towards the oxidation of 2, 4, 6-trichlorophenol (TCP) [55]. In this work hemin was used as the catalytical center and TCP as the template. It was seen that the presence of structurally similar substances did not change the kinetics of TCP, when 4-vinylpyridine was used as a functional monomer.

In the redox-active MIPs the creation of an appropriate binding pocket for the substrate is still a challenge. Up to now only one paper applied molecular modeling for the selection of functional monomers for optimal interaction in the prepolymerization complex. However, the reported catalytic efficiency for the oxidative dehalogenation as expressed by k_{cat}/K_M revealed no improvement as compared with the nonimprinted polymer [55].

In general the catalytic activities of MIPs are in aqueous media well below those of enzymes and comparable to Abzymes. Hybrids composed of a biocatalyst and MIP may combine the advantages of both components. But up to now the harsh conditions of MIP synthesis restricted this combination to enzyme labels in MIP-based binding assays and the integration of catalytically active prosthetic groups into the polymer backbone of catalytic MIPs.

Separation of MIP formation by electropolymerization and immobilization of the catalyst on top allowed the integration of the minizyme microperoxidase but also the enzyme-horseradish peroxidase (HRP) with a MIP layer in a sensor configuration. The peroxide-dependent substrate conversion takes place in the layer on top of a product-imprinted electropolymer on the indicator electrode. This architecture allowed the interference-free measurement of the drug aminopyrine [56]. This combination has the potential to be transferred to other enzymes, for example, P450 s, opening the way to clinically important analytes.

3.3 Cell-Free Synthesis of Biological Recognition Elements

Cell-free protein synthesis, also termed in vitro translation, has emerged as a powerful technology platform to produce correctly folded and functional proteins in reasonable amounts for further downstream applications. The development of translationally active cell lysates into highly productive systems, the generation and optimization of particular DNA and RNA templates for different cell-free systems and the optimization of reaction conditions in newly developed reaction systems are part of intense ongoing research activities. Recent advances have inspired new applications in the synthesis of protein libraries for functional genomics, the production of personalized medicines, and the expression of tailor-made biological recognition elements including membrane-bound enzymes and receptors.

Starting as a research tool to investigate the fundamentals of translation processes in vitro [57], cell-free protein synthesis has evolved to serve as a reliable and versatile protein production platform [58, 59]. In particular, cell-free protein synthesis has facilitated the successful production of pharmaceutical target proteins [60, 61, 62, 63] such as membrane proteins [64, 65, 66, 67, 68, 69, 70] and the high-throughput production of protein libraries [71, 72, 73]. The strategy of cell-free protein expression shows crucial advantages over conventional in vivo production methods [58, 57]. Protein production in living cells is always a compromise between the conditions required for efficient cell growth and viability and the conditions necessary for the synthesis of a functional target protein. Because cell-free systems represent open systems, reaction conditions can be adjusted according to the needs of the individual protein without consideration of the conditions necessary for cell cultivation. Moreover, cell-free protein synthesis can be performed using linear DNA templates, thereby omitting the need for time- and labor-consuming cloning steps. The basis of cell-free expression systems are crude cell extracts that can be obtained from different types of living cells. In particular, lysates gained from *Escherichia coli* (*E. coli*), wheat germ, rabbit reticulocytes, and insect cells [71] are very common and widely used. Every cell lysate has well-defined characteristics, therefore one has to consider carefully which type of lysate shall be used to express a desired protein. The expression of functional eukaryotic proteins not only requires the coordinated interplay of the translational machinery but also the integrity of components modulating co- and posttranslational

modifications. For reasons of economy and simplicity, lysates supplemented with mRNA or a mRNA-synthesizing subsystem and a NTP-regeneration subsystem are used most often. Prokaryotic cell lysates have the advantage of a long-lasting expertise, low costs, and high production yields but only very few posttranslational modifications can be carried out on target proteins [58, 74]. In contrast, eukaryotic lysates are well suited for the synthesis of complex proteins and proteins with posttranslational modifications not found in bacteria [75, 76, 68]. Such post-translational modifications, for example, glycosylation, signal peptide cleavage, phosphorylation, farnesylation, acetylation, palmitoylation, and disulfide bond formation have a great impact on protein folding, localization, and activity [77]. Because the majority of posttranslational modifications are processed inside the endoplasmic reticulum (ER) in living cells, novel in vitro translation systems have been developed that implement ER-derived microsomal vesicles in a translation-ally active eukaryotic cell lysate. These microsomal fractions are either derived from different types of cells [78, 79], or can be maintained in the lysate due to a sophisticated extract preparation procedure [67, 80, 70]. Using the latter type of lysate, posttranslational modifications on proteins such as glycosylation, lipidation, phosphorylation, signal peptide cleavage, and disulfide bond formation can be performed [81, 67, 82, 68, 83, 84].

The synthesis of functional membrane proteins in particular, depends on an efficient folding and modification machinery present in the cell-free expression system. Membrane proteins play a vital role in many biological functions and they have a tremendous potential in microsystem array platforms utilizing bioelectro-chemical methods for continuous use and label-free detection. Three quarters of all potential drug targets account for membrane proteins and recent advances in the self-assembly of biomimetic interfaces permit the development of biosensor arrays that harness the unique sensitivity and selectivity of membrane proteins [85]. In contrast, membrane proteins constitute a difficult-to-express class of proteins as their overexpression in vivo often leads to cytotoxic effects or results in protein aggregation, misfolding, and low yields [58]. However, in vitro translation can circumvent these obstacles. As cell-free systems provide open reaction conditions they can be supplemented with any kind of reagent that allows a solubilization of membrane proteins and supports their correct folding and assembly [86, 87]. The supplementation of lysates with natural or synthetic lipids or detergents [88], purified *E. coli* phospholipid bilayer vesicles [89], nanolipoprotein particles [90], or unilamellar liposomes [91] have shown to be promising strategies. Continuous cell-free translation systems combining eukaryotic cell lysates with the perpetual supply of consumable substrates and the removal of reaction by-products make the process of in vitro synthesis of membrane proteins and secreted proteins sustain-able and productive (Fig. 5). The development of this novel eukaryotic in vitro translation system now expands the possibilities of cell-free protein synthesis, inasmuch as membrane insertion and posttranslational modification significantly alter the physical and chemical properties of membrane proteins, including their folding and conformational distribution and these modifications are frequently a fundamental prerequisite for functional activity.

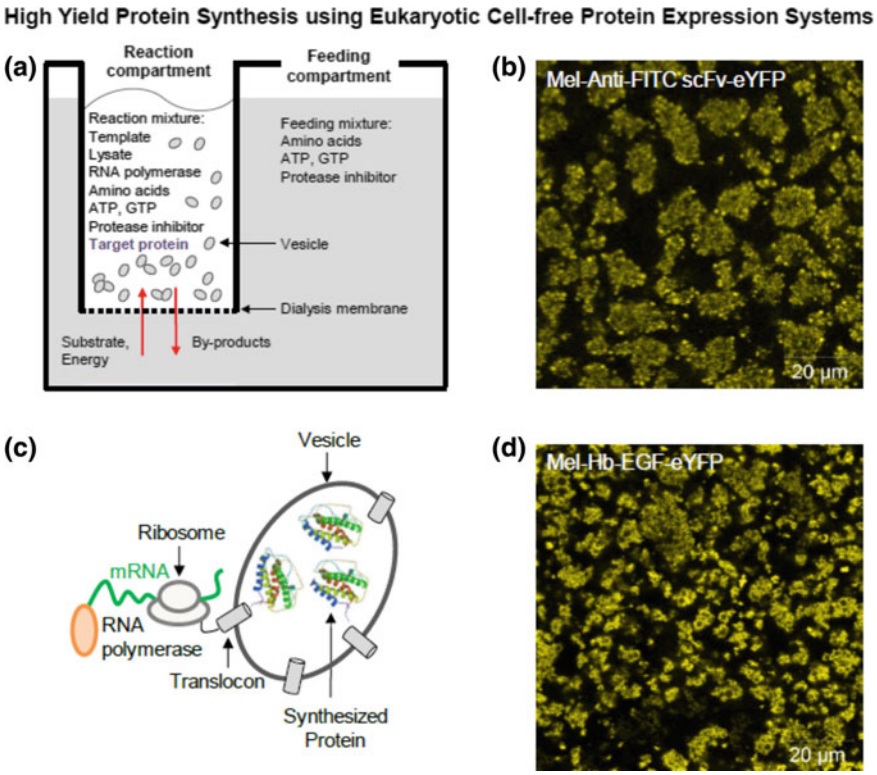

Fig. 5 High-yield protein synthesis using eukaryotic cell-free protein expression systems. **a** Schematic illustration of a cell-free reaction running in a continuous-exchange reactor device. The reaction compartment is separated from the feeding compartment by a semi-permeable dialysis membrane (molecular weight cut-off = 10 kDa). **b** Schematic presentation of the co-translational translocation of a secreted target protein into ER-derived vesicles that are present in the eukaryotic cell lysate. **c** CLSM image of the cell-free synthesized single-chain antibody fragment (scFv) Mel-Anti-FITC fused to eYFP (Mel-Anti-FITC scFv-eYFP). Strong emission intensity arising from the vesicles indicates translocation of the target protein into the lumen of the vesicles. **d** CLSM image of the cell-free synthesized transmembrane protein Mel-Hb-EGF fused to eYFP (Mel-Hb-EGF-eYFP). Strong emission intensity arising from the vesicular membrane indicates integration of the target membrane protein into the lipid bilayer. Samples for CLSM analysis were excited at 488 nm using an argon laser and fluorescence emission was recorded with a long-pass filter in the wavelength range above 505 nm

4 Biosensors for Personalized Medicine

Healthcare is seeing a dramatic change towards integration of stratified or even personalized approaches to drug therapy. This transformation is driven on the one hand by an increased understanding of disease etiologies but also by an increasing difficulty in the pharma industry to develop new drugs despite ever-increasing budgets and enormous efforts by introducing high-throughput screening, genomics, or molecular design in the drug development process. These developments are

underpinned by generally less than optimal efficacy rates for drugs in human therapy ranging from 80 % at the better end for analgesics to seriously concerning 20 % in oncology [92]. In summary, it is estimated that of 90 % of the drugs currently on the market only 40 % have the desired efficacy, resulting in US $350 billion ineffective prescriptions [93, 94]. The traditional blockbuster model is coming to its end and new models on niche busters and stratified treatments are gaining momentum [95]. One way to tailor a therapy to the specific needs of a patient and to ensure that a drug will reach its claimed efficacy and safety performance is to couple its application with the use of a diagnostic. The diagnostic then becomes the "companion diagnostic" for the drug in a constellation that is increasingly recognized by regulatory authorities. Other terminologies use "theranostics" to describe the combination of therapy and diagnostics. However, this term is easily misunderstood with multifunctional nanotechnological devices. As of 2012, there were 14 companion diagnostics approved by the US Food and Drug Administration. In addition, the pipelines of the pharma industry are packed with respective projects. In 2011 the Personalised Medicine Coalition already listed 74 drug–diagnostic partnerships [96]. Personalized medicine initially progressed with Herceptin and Gleevec for breast cancer and chronic myeloid leukemia therapy. For both drugs companion diagnostic tests were developed as predictive bioanalytical tests that determine the likelihood of response of a patient [97]. Meanwhile the personalized medicine portfolio grew beyond cancer, for example, into infectious diseases. For HIV therapy with Selzentry, the FDA requires testing of CCR5 tropism using a companion diagnostic test. For further drugs testing is either required, recommended, or informative tests are available.

The main metabolism route of xenobiotics is initiated by oxidative reactions called phase I metabolism, which are catalyzed by enzymes of the cytochrome P450 superfamily. Human cytochrome P450 enzymes act on more than 90 % of all drugs currently on the market [98].

The P450 catalysis leads to either activation of chemicals for bioavailability or detoxification with following excretion of drugs or reactive products and may also activate procancerogens. The amino acid sequence of the peptide chain can be quite diverse. P450 enzymes of the same family can differ by up to 60 % in their sequence; on the other hand, changes of only a single amino acid can alter the reactivity of the enzyme. Adverse effects in multidrug treatments have been seen in many patients originating from overlapping substrate specificities or inhibitory effects. Therefore for drug screening, assessment of toxicity and prediction of drug clearance the measurement of the substrate specificity and distribution of P450 isoenzymes and polymorphic enzymes would be of high clinical relevance.

P450-based enzyme electrodes utilizing a variety of isoenzymes in different surface architectures have been developed to detect various chemicals, such as chlorophenols, pesticides such as paraoxon, or drugs such as bupropion, bufuralol, warfarin, and cyclophosphamide [99, 100, 101, 102]. Also, microsomes combined with cytochrome P450 reductase were employed as in vitro sensor mimicking [103, 104, 105] for detection of drug conversion (i.e., Ketocanazole transformation). Kinetics of drug conversion of P450 isoenzymes and its polymorphic

variants have been addressed by forming fusion proteins bearing P450 and flavodoxin, which were then bound to gold electrodes modified with a self-assembled monolayer. The ability to engineer, express, and purify various P450 isoenzymes and polymorphic variants enabled development of P450-arrays for in vitro drug testing [101].

The current companion diagnostic tests predominantly use established and, to some degree traditional, laboratory-based technologies such as ELISA, RT-PCR, fluorescence/colorimetric in situ hybridization or DNA microarrays in some cases [106]. The dominating discipline in the field of companion diagnostics is molecular in vitro diagnostics. Here, biosensors traditionally have a strong domain and huge emerging potential. Not surprisingly, "personalized medicine" is a term that is increasingly found in biosensor-related publications to describe potential applications of the described new developments. Examples range from graphene-encapsulated nanoparticles to detect cancer biomarkers [107], piezoelectric microcantilevers for HER-2 biomarkers in serum of breast cancer patients [108], to electrical biosensors for the detection of circulating tumor cells associated with breast cancer [109]. Other biosensors detect the drug using carbon nanotube-based biosensors [110]. Next to HER-2 as an important cancer biomarker, KRAS mutations are strongly associated with poor responses to drugs targeting the epidermal growth factor receptor pathway. Consequently, a number of assays exist targeting this biomarker, mostly based on variations of PCR assays combined with nucleic acid probe technologies [111]. An interesting study dealt with the development of RNA aptamers to detect the mutated KRAS protein providing further potential for biosensor developments using aptamers [112, 113]. Although PCR and blood are the dominating sample matrix and technology, developments have been undertaken to improve PCR by moving to digital PCR formats and to target other sample matrices such as urine [114]. Great expectations are held in the use of exosomes as a source of useful biomarkers for therapy guidance in oncology and beyond [115].

Another major health problem of global scale where diagnostics and biosensors can make a difference is in infectious diseases. Infectious diseases are among the leading reasons for morbidity and death worldwide, especially in developing countries, for children and the elderly. In addition, antibiotic resistance is a worldwide threat to patients and healthcare systems. As an example, in the European Union 25,000 patients die annually from infection by four main pathogens [*Staphylococcus aureus*, *Enterococcus spp*., *Enterobacteriaceae* (e.g., *Escherichia coli*, *Klebsiella pneumoniae*, *Pseudomonas aeruginosa*) due to their antibiotic resistance [116]. The alarming rise of antibiotic resistance increasingly causes massive extra costs and problems to society. The problem is increasingly being recognized and reaches the global political arena as international [117] and national catastrophic threats together with climate change and terrorism [118]. Of particular concern is the increasing prevalence of multidrug-resistant Gram-negative pathogens in combination with the lack of antimicrobials against these pathogens in development may become one of the biggest and most pressing concerns in human healthcare if we run out of treatment options [119]. Beta-lactam antibiotics, conventionally used to target such infections

at present, make up more than half of antibiotics used in the world and these multiresistant Gram-negative strains pose a severe public health threat [120]. Rapid molecular diagnostics could help improve antibiotic stewardship and secure the precious resource of this important class of medications. Antibiotic prescriptions are often unnecessary (estimated 50 % in the United States) ([121, 122]), a situation that further drives the development of antibiotic resistance. To make things worse, the pipeline for new antibiotics is almost dry. Diagnostics could help in reducing this threat but current standard methods are too slow and lack information depth to enable tailored therapy decisions. To overcome this limitation molecular tools have been developed for rapid in vitro diagnostics of infectious diseases. In an ideal scenario such devices would be available at point of care to make therapy decisions possible at the site of the patient.

Conventional infectious disease diagnostic testing relies heavily on molecular amplification techniques such as quantitative real-time PCR, immunoassays, or cultivation-based tests. These tests may either be too slow or do not offer sufficient information in all cases to make a prospective therapy decision possible. Alternative methods described, among others, used DNA microarrays [123] and homogeneous multiplexing assays [124] for rapid genotyping of antibiotic resistances of bacterial pathogens (e.g., ESBL and carbapenemases). Although very sensitive, many of the molecular tests use optical read-out systems based on fluorescence which, in view of point-of-care testing, add unfavorably to the technical demands of a portable test device. Electrochemical biosensors instead offer the possibility to integrate the detection of molecular markers, such as PCR amplification products, in very simple systems paving the way for molecular diagnostics truly at the point of care [125]. The combination of such diagnostic tests with their linked antibiotic drug will enable a more stratified approach to antibiotic therapy.

The ultimate molecular diagnostic would be achieving target amplification-free determination of the entire genome sequence of interest, either in a host or tumor sample or in a pathogen. Although whole genome sequencing is well underway to become a key factor in clinical diagnostics, for example, in oncology [126] or infection outbreak tracking [127], it still has a considerable way to go until practicality issues including sample preparation, time to result, user interference, low complexity, and cost are overcome that have been solved for the traditional bioanalytical assays such as ELISA and PCR. Apparently, this has yet been impossible to achieve without target amplification in molecular tests. Interestingly, the recent advances in decoding genomic information delivered by next-generation sequencing techniques have not been associated with biosensor technologies in the perception of the public and scientific community, very much as in the case of DNA or protein arrays. Nevertheless, many of the technologies used for NGS are biosensor technologies [23, 128, 129] by definition, or have their roots in classic biosensor technologies and publications [130, 131]. Both fields, DNA arrays and NGS, aim for a massively parallel approach to holistically analyzing biological systems. It can be seen that biosensor research and development is steadily moving into this field and, with a view to personalized medicine, is gaining increasing momentum. It will be interesting to see how this development continues and impact is generated.

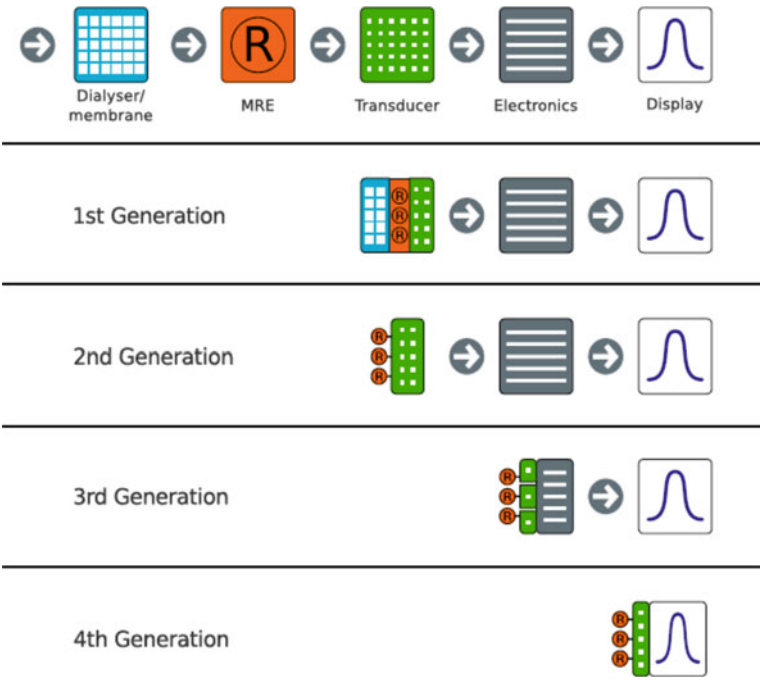

Fig. 6 The route to autonomous biosensors: from membrane-covered biosensor via direct immobilization of the MRE on the transducer surface and sensor arrays to complete integration of recognition and reporting within an autonomous biosensor unit

If a general prediction for biosensors for the future should be made, then their further development into simple-to-use tools that analyze the target system in an integrative manner at the site of demand with high connectivity into networks is most promising. This will enable their integration with the big data revolution and continued contribution to the improvement of healthcare and society.

5 Outlook

Current development is focused on a new generation: autonomous biosensor units for direct on-the-spot measurements. For decentralized online patient control or the integration into everyday "consumables" such as drinking water, foods, hygienic articles, or clothing [132] or for control of air conditioning in buildings and cars and swimming pools this new generation of "autonomous" biosensors will emerge. These fourth-generation biosensors can be autonomous data collectors that possess an internal energy supply and a wireless transmitter or sensor-actor-molecules—tailor-made MREs—that couple the recognition event to a direct read-out (Fig. 6). This kind of autonomy sets aside the need for complex equipment and training, and

enables usage in point-of-care diagnostic and fitness monitoring. Although the former is especially of great interest for medical care in sparsely populated areas, the latter application is receiving growing attention in the so-called "quantified self" movement. This term was coined to describe the measurement of bodily parameters, including heart rate and temperature as well as blood sugar level, lactate concentration, and ion balance. These data are collected and analyzed in order to achieve better knowledge about one's body and to take actions towards a higher quality of living.

References

1. Thévenot DR, Toth K, Durst RA, Wilson GS (1999) Pure Appl Chem 71:2333–2348
2. Clark LC Jr, Lyons C (1962) Ann N Y Acad Sci 102:29–45
3. Turner APF (2013) Biosensors: sense and sensibility. Chem Soc Rev 42:3184–3396
4. Vashist SK, Zheng D, Al-Rubeaan K, Luong JHT, Sheu F-S (2011) Anal Chim Acta 703:124–136
5. Wang J (2008) Chem Rev 108:814–825
6. Chen LQ, Zhang XE, Xie WH, Zhou YF, Zhang ZP, Cass AEG (2002) Biosens Biolectron 17:851–857
7. Ludwig R, Oritz R, Schulz C, Harreither W, Sygmund C, Gorton L (2013) Anal Bioanal Chem 405:3637–3658
8. Heller A, Feldman B (2008) Chem Rev 108:2482–2505
9. Wilson GS, Hu Y (2000) Chem Rev 100:2693–2704
10. Chan CP, Cheung Y, Renneberg R, Seydack M (2008) Adv Biochem Eng/Biotechnol 109:123–154
11. Sano T, Smith CL, Cantor CR (1992) Science 258:120–122
12. Zhou H, Fisher RJ, Papas TS (1993) Nucl Acids Res 21:6038–6039
13. Nam JM, Thaxton CS, Mirkin CA (2003) Science 301:1884–1886
14. Taton TA, Mirkin CA, Letsinger RL (2000) Science 289:1757–1760
15. Leung W, Chan P, Bosgoed F, Lehmann K, Renneberg I, Lehmann M, Renneberg R (2003) J Immunol Methods 281:109–118
16. Pulli T, Höyhtyä M, Söderlund H, Takkinen K (2005) Anal Chem 77:2637–2642
17. BCC Research (2011) http://www.bccresearch.com/report/global-biochip-markets-bio049d.html
18. Collins FS, Green ED, Guttmacher AE, Guyer MS (2003) Nature 24:835–847
19. Kaddurah-Daouk R, Kristal BS, Weinshilboum RM (2008) Annu Rev Pharmacol Toxicol 48:653–683
20. States DJ, Omenn GS, Blackwell TW, Fermin D, Eng J, Speicher DW, Hanash SM (2006) Nat Biotechnol 24:333–338
21. Schumacher S, Nestler J, Otto T, Wegener M, Ehrentreich-Förster E, Michel D, Wunderlich K, Palzer S, Sohn K, Weber A, Burgard M, Grzesiak A, Teichert A, Brandenburg A, Koger B, Albers J, Nebling E, Bier FF (2012) Lab Chip 12:464–473
22. Kingsmore SF (2006) Nat Rev Drug Discov 5:310–320
23. Eid J, Fehr A, Gray J, Luong K, Lyle J, Otto G, Peluso P, Rank D, Baybayan P, Bettman B, Bibillo A, Bjornson K, Chaudhuri B, Christians F, Cicero R, Clark S, Dalal R, Dewinter A, Dixon J, Foquet M, Gaertner A, Hardenbol P, Heiner C, Hester K, Holden D, Kearns G, Kong X, Kuse R, Lacroix Y, Lin S, Lundquist P, Ma C, Marks P, Maxham M, Murphy D, Park I, Pham T, Phillips M, Roy J, Sebra R, Shen G, Sorenson J, Tomaney A, Travers K, Trulson M, Vieceli J, Wegener J, Wu D, Yang A, Zaccarin D, Zhao P, Zhong F, Korlach J, Turner S (2009) Science 323:133–138

24. MacBeath G (2002) Nat Genet 32:526–532
25. Editorial, Nature Nanotechnology (2013) 8(221) http://www.nature.com/nnano/journal/v8/n4/pdf/nnano.2013.64.pdf
26. Dreyer DR, Ruoff RS, Bielawski CW (2010) Angew Chem Int Ed 49:9336–9344
27. Stoller MD, Park S, Zhu Y, An J, Ruoff RS (2008) Nano Lett 10:3498–3502
28. Lee C, Wei X, Kysar JW, Hone J (2008) Science 321:385–388
29. Novoselov KS, Geim AK, Morozov SV, Jiang D, Zhang Y, Dubonos SV, Grigorieva IV, Firsov AA (2004) Science 306:666–669
30. Novoselov KS, Fal′ko VI, Colombo L, Gellert PR, Schwab MG, Kim K (2012) Nature 490:192–200
31. Kim KS, Zhao Y, Jang H, Lee SY, Kim JM, Kim KS, Ahn J-H, Kim P, Choi J-Y, Hong BH (2009) Nature 457:706–710
32. Emtsev KV, Bostwick A, Horn K, Jobst J, Kellogg GL, Ley L, McChesney JL, Ohta T, Reshanov SA, Rohrl J, Rotenberg E, Schmid AK, Waldmann D, Weber HB, Seyller T (2009) Nat Mater 8:203–207
33. Park S, Ruoff RS (2009) Nat Nano 4:217–224
34. Kochmann S, Hirsch T, Wolfbeis OS (2012) TrAC-Trend. Anal Chem 39:87–113
35. Guo Z, Hao T, Duan J, Wang S, Wie D (2012) Talanta 89:27–32
36. Xu S, Liu Y, Wang T, Li J (2011) Anal Chem 83:3817–3823
37. Wang Y, Xiao Y, Ma X, Li N, Yang X (2012) Chem Commun 48:738–740
38. Cai JM, Ruffieux P, Jaafar R, Bieri M, Braun T, Blankenburg S, Muoth M, Seitsonen AP, Saleh M, Feng XL, Müllen K, Fasel R (2010) Nature 466:470–473
39. Hianik T, Wang J (2009) Electroanalysis 21:1223–1235
40. Song K-M, Lee S, Ban C (2012) Sensors 12:612–631
41. Zhou J, Battig MR, Wang Y (2010) Anal Bioanal Chem 398:2471–2480
42. Scheller FW, Yarman A (2012) Biomimetic Sensors. In: Bard AJ, Scholz F (eds) Electrochemical Dictionary 2nd edn. Springer, Heidelberg, pp 69–70
43. Malitesta C, Mazzotta E, Picca RA, Poma A, Chianella I, Piletsky SA (2012) Anal Bioanal Chem 402:1827–1846
44. Sharma PS, Pietrzyk-Le A, D'Souza F, Kutner W (2012) Anal Bioanal Chem 402:3177–3204
45. Servant A, Haupt K, Resmini M (2011) Chem Eur J 17:11052–11059
46. Lettau K, Warsinke A, Katterle M, Danielsson B, Scheller FW (2006) Angew Chem Int Ed Engl 45:6986–6990
47. Liu JQ, Wulff G (2004) Angew Chem Int Ed Engl 43:1287–1290
48. Lohmann W, Karst U (2008) Anal Bioanal Chem 391:79–96
49. Lakshmi D, Bossi A, Whitcombe MJ, Chianella I, Fowler SA, Subrahmanyam S, Piletska EV, Piletsky SA (2009) Anal Chem 81:3576–3584
50. Cheng Z, Zhang L, Li Y (2004) Chemistry 10:3555–3561
51. de Jesus Rodrigues Santos W, Lima PR, Tarley CR, Kubota LT (2007) Anal Bioanal Chem 389:1919–1929
52. de Jesus Rodrigues Santos W, Lima PR, Tarley CR, Höerh NF, Kubota LT (2009) Anal Chim Acta 31:170–176
53. Sartori LR, de Jesus Rodrigues Santos W, Lima PR, Kubota LT, Segatelli MG, Tarley CRT (2011) Mat Sci Eng C 31:114–119
54. Neto JRM, de Jesus Rodrigues Santos W, Lima PR, Tanaka SMCN, Tanaka AA, Kubota LT (2011) Sensor Actuat B Chem 152:220–225
55. Díaz-Díaz G, Diñeiro Y, Menéndez MI, Blanco-López MC, Lobo-Castañón MJ, Miranda-Ordieres AJ, Tuñón-Blanco P (2011) Polymer 52:2468–2473
56. Yarman A, Scheller FW (2013) Angew Chem Int Ed. doi:10.1002/anie.201305368
57. Nirenberg M, Matthaei J (1961) Proc Natl Acad Sci USA 47:1588–1602
58. Katzen F, Chang G, Kudlicki W (2005) Trends Biotechnol 23:150–156
59. Swartz J (2006) J Ind Microbiol Biotechnol 33:476–485
60. Goerke AR, Swartz JR (2008) Biotechnol Bioeng 99:351–367

61. Kanter G, Yang J, Voloshin A, Levy S, Swartz J, Levy R (2007) Blood 109:3393–3399
62. Yang J, Kanter G, Voloshin A, Michel-Reydellet N, Velkeen H, Levy R, Swartz JR (2005) Biotechnol Bioeng 89:503–511
63. Zawada JF, Yin G, Steiner AR, Yang J, Naresh A, Roy SM, Gold DS, Heinsohn HG, Murray CJ (2011) Biotechnol Bioeng 108:1570–1578
64. Gourdon P, Alfredsson A, Pedersen A, Malmerberg E, Nyblom M, Widell M, Berntsson R, Pinhassi J, Braiman M, Hansson Ö, Bonander N, Karlsson G, Neutze R (2008) Protein Expr Purif 58:103–113
65. Kalmbach R, Chizhov I, Schumacher MC, Friedrich T, Bamberg E, Engelhard M (2007) J Mol Biol 371:639–648
66. Klammt C, Löhr F, Schäfer B, Haase W, Dötsch V, Rüterjans H, Glaubitz C, Bernhard F (2004) Eur J Biochem 271:568–580
67. Kubick S, Gerrits M, Merk H, Stiege W, Erdmann VA (2009) In vitro synthesis of posttranslationally modified membrane proteins. "Membrane Protein Crystallization" Current Topics in Membranes Vol 63, Chapter 2, Academic Press Elsevier, 25–49
68. Sachse R, Wüstenhagen D, Šamalíková M, Gerrits M, Bier FF, Kubick S (2013) Eng Life Sci 13:39–48
69. Savage DF, Anderson CL, Robles-Colmenares Y, Newby ZE, Stroud RM (2012) Protein Sci 16:966–976
70. von Groll U, Kubick S, Merk H, Stiege W, Schäfer F (2007) Advances in insect-based cell-free protein expression. In: Kudlicki W, Katzen F, Bennett P (eds) Cell-free protein expression landes bioscience
71. Carlson ED, Gan R, Hodgman CE, Jewett MC (2012) Biotechnol Adv 30:1185–1194
72. Goshima N, Kawamura Y, Fukumoto A, Miura A, Honma R, Satoh R, Wakamatsu A, Yamamoto J, Kimura K, Nishikawa T, Andoh T, Iida Y, Ishikawa K, Ito E, Kagawa N, Kaminaga C, Kanehori K, Kawakami B, Kenmochi K, Kimura R, Kobayashi M, Kuroita T, Kuwayama H, Maruyama Y, Matsuo K, Minami K, Mitsubori M, Mori M, Morishita R, Murase A, Nishikawa A, Nishikawa S, Okamoto T, Sakagami N, Sakamoto Y, Sasaki Y, Seki T, Sono S, Sugiyama A, Sumiya T, Takayama T, Takayama Y, Takeda H, Togashi T, Yahata K, Yamada H, Yanagisawa Y, Endo Y, Imamoto F, Kisu Y, Tanaka S, Isogai T, Imai J, Watanabe S, Nomura N (2008) Nat Methods 5:1011–1017
73. Griffiths AD, Tawfik DS (2003) EMBO J 22:24–35
74. Schwarz D, Klammt C, Koglin A, Löhr F, Schneider B, Dötsch V, Bernhard F (2007) Methods 41:355–369
75. Chang H-C, Kaiser CM, Hartl FU, Barral JM (2005) J Mol Biol 353:397–409
76. Hillebrecht JR, Chong SA (2008) BMC Biotechnol 8:1790–1793
77. Mann M, Jensen ON (2003) Nat Biotech 21:255–261
78. Blobel G, Dobberstein B (1975) J Cell Biol 67:835–851
79. Walter P, Blobel G (1983) Preparation of microsomal membranes for cotranslational protein translocation. Methods Enzymol 96:84–93
80. Kubick S, Schacherl J, Fleischer-Notter H, Royall E, Roberts LO, Stiege W (2003) In vitro translation in an insect-based cell-free system. In: Swartz JR (ed) Cell-Free Protein Expression. Springer, New York, pp 209–217
81. Brödel AK, Raymond JA, Duman JG, Bier FF, Kubick S (2013) J Biotechnol 163:301–310
82. Merk H, Gless C, Maertens B, Gerrits M, Stiege W (2012) Biotechniques 53:153–160
83. Shaklee PM, Semrau S, Malkus M, Kubick S, Dogterom M, Schmidt T (2010) Chem Biochem 11:175–179
84. Stech M, Merk H, Schenk J, Stöcklein W, Wüstenhagen D, Micheel B, Duschl C, Bier F, Kubick S (2012) J Biotechnol 164:220–231
85. Khnouf R, Olivero D, Jin S, Coleman MA, Fan ZH (2010) Cell-Free expression of soluble and membrane proteins in an array device for drug screening. Anal Chem 82:7021–7026
86. Casteleijn MG, Urtti A, Sarkhel S (2013) Int J Pharm 440:39–47

87. Zanders ED, Kai L, Roos C, Haberstock S, Proverbio D, Ma Y, Junge F, Karbyshev M, Dötsch V, Bernhard F (2012) Systems for the cell-free synthesis of proteins, chemical genomics and proteomics, Humana Press, New York, pp 201–225
88. Klammt C, Schwarz D, Fendler K, Haase W, Dötsch V, Bernhard F (2005) FEBS J 272:6024–6038
89. Wuu JJ, Swartz JR (2008) Biochim Biophys Acta (BBA)—Biomembranes 1778:1237–1250
90. Doyle S, Cappuccio J, Hinz A, Kuhn E, Fletcher J, Arroyo E, Henderson P, Blanchette C, Walsworth V, Corzett M, Law R, Pesavento J, Segelke B, Sulchek T, Chromy B, Katzen F, Peterson T, Bench G, Kudlicki W, Hoeprich P Jr, Coleman M (2009) Cell-Free expression for nanolipoprotein particles: building a high-throughput membrane protein solubility platform, high throughput protein expression and purification. Humana Press, New Jersey, pp 273–295
91. Goren MA, Nozawa A, Makino S, Wrobel RL, Fox BG (2009) Methods Enzymol 463:647–673
92. Spear BB, Heath-Chiozzi M, Huff J (2001) Trends. Mol Med 5:201–204
93. Editorial, Nature Biotechnology (2012) 30(1) http://www.nature.com/nbt/journal/v30/n1/pdf/nbt.2096.pdf
94. Roche Business Overview (2011) www.roche.com/diagnosticsbrochure.pdf
95. Blair ED (2009) Predictive tests and personalised medicine. Drug Discov World 22:27–31
96. The Case for Personalized Medicine http://www.personalizedmedicinecoalition.org/sites/default/files/files/Case_for_PM_3rd_edition.pdf
97. Arteaga CL, Sliwkowski MX, Osborne CK, Perez EA, Puglisi F, Gianni L (2011) Nat Rev Clin Oncol 2011(9):16–32
98. Yarman A, Wollenberger U, Scheller FW (2013) Electrochim. Acta doi: org/10.1016/j.electacta.2013.03.154
99. Carrara S, Cavallini A, Erokhin V, De Micheli G (2011) Biosens Bioelectron 26:3914–3919
100. Liu SQ, Peng L, Yang XD, Wu YF, He L (2008) Anal Biochem 375:209–216
101. Panicco P, Dodhia VR, Fantuzzi A, Gilardi G (2011) Anal Chem 83:2179–2186
102. Yang ML, Kabulski JL, Wollenberg L, Chen XQ, Subramanian M, Tracy TS, Lederman D, Gannett PM, Wu N (2009) Drug Metab Dispos 37:892–899
103. Huang M, Xu X, Yang H, Liu S (2012) RSC Adv 2:12844–12850
104. Krishnan S, Wasalathanthri D, Zhao LL, Schenkman JB, Rusling JF (2011) J Am Chem Soc 133:1459–1465
105. Mie Y, Suzuki M, Komatsu Y (2009) J Am Chem Soc 131:6646–6647
106. Allison M (2008) Nat Biotechnol 26:509–517
107. Myung S, Solanki A, Kim C, Park J, Kim KS, Lee KB (2011) Adv Mater 23:2221–2225
108. Loo L, Capobianco JA, Wu W, Gao X, Shih WY, Shih WH, Pourrezaei K, Robinson MK, Adams GP (2011) Anal Chem 83:3392–3399
109. Munzone E, Nolé F, Goldhirsch A, Botteri E, Esposito A, Zorzino L, Curigliano G, Minchella I, Adamoli L, Cassatella MC, Casadio C, Sandri MT (2010) Clin Breast Cancer 10:392–397
110. Baj-Rossi C, De Micheli C, Carrara S (2012) Sensors 12:6520–6537
111. Hirani R, Connolly AR, Putral L, Dobrovic A, Trau M (2011) Anal Chem 83:8215–8221
112. Jeong S, Han SR, Lee YJ, Kim JH, Lee SW (2010) Oligonucleotides 20:155–161
113. Nonaka Y, Yoshida W, Abe K, Ferri S, Schulze H, Bachmann TT, Ikebukuro K (2013) Anal Chem 85:1132–1137
114. Shen F, Du W, Kreutz JE, Fok A, Ismagilov RF (2010) Lab Chip 10:2666–2672
115. Théry C, Ostrowski M, Segura E (2009) Nat Rev Immunol 9:581–593
116. ECDC/EMEA Joint Technical Report (2009) http://www.ecdc.europa.eu/en/publications/Publications/0909_TER_The_Bacterial_Challenge_Time_to_React.pdf
117. World More at Risk from Markets and Mother Nature—Global Risks (2013) Report. http://www.weforum.org/globalrisks2013

118. Annual Report of the Chief Medical Officer (2011) Volume Two, UK Department of Health https://www.gov.uk/government/uploads/system/uploads/attachment_data/file/138331/CMO_Annual_Report_Volume_2_2011.pdf
119. Kumarasamy KK, Toleman MA, Walsh TR, Bagaria J, Butt F, Balakrishnan R, Chaudhary U, Doumith M, Giske CG, Irfan S, Krishnan P, Kumar AV, Maharjan S, Mushtaq S, Noorie T, Pater-son DL, Pearson A, Perry C, Pike R, Rao B, Ray U, Sarma JB, Sharma M, Sheridan E, Thirunara-yan MA, Turton J, Upadhyay S, Warner M, Welfare W, Livermore DM, Woodford N (2010) Lancet Infect Dis 10:597–602
120. Elander RP (2003) Appl Microbiol Biotechnol 61:385–392
121. Pichichero ME (2002) JAMA 287:3133–3135
122. Centers for Disease Control and Prevention (CDC) (2011) MMWR Morb Mortal Wkly Rep 60:1153–1156
123. Leinberger DM, Grimm V, Rubtsova M, Weile J, Schröppel K, Wichelhaus TA, Knabbe C, Schmid RD, Bachmann TT (2010) J Clin Microbiol 48:460–471
124. Pierce KE, Peter H, Bachmann TT, Volpe C, Mistry R, Rice JE, Wangh LJ (2013) J Mol Diagn 15:291–298
125. Corrigan DK, Schulze H, Henihan G, Ciani I, Giraud G, Terry JG, Walton AJ, Pethig R, Ghazal P, Crain J, Campbell CJ, Mount AR, Bachmann TT (2012) Biosens Bioelectron 34:178–184
126. Gerlinger M, Rowan AJ, Horswell S, Larkin J, Endesfelder D, Gronroos E, Martinez P, Matthews N, Stewart A, Tarpey P, Varela I, Phillimore B, Begum S, McDonald NQ, Butler A, Jones D, Raine K, Latimer C, Santos CR, Nohadani M, Eklund HNCAC, Spencer-Dene B, Clark G, Pickering L, Stamp G, Gore M, Szallasi Z, Downward J, Futreal A, Swanton C (2012) N Engl J Med 366:883–892
127. Harris SR, Cartwright EJ, Török ME, Holden MT, Brown NM, Ogilvy-Stuart AL, Ellington MJ, Quail MA, Bentley SD, Parkhill J, Peacock SJ (2013) Lancet Infect Dis 13:130–136
128. Purushothaman S, Toumazou C, Georgiou J (2002) Towards fast solid state DNA sequencing, IEEE international symposium on circuits and systems, Phoenix, Arizona, 26–29 May 2002, New York, IEEE 2002, pp 169–172
129. Schneider GF, Dekker C (2012) Nat Biotechnol 30:326–328
130. Bergveld P (2003) Sensor Actuat B Chem 88:1–20
131. Wise KD, Angell JB, Starr A (1970) IEEE Trans Biomed Eng BME 17:238–247
132. Windmiller J, Wang J (2013) Electroanalysis 25:29–46

Adv Biochem Eng Biotechnol (2014) 140: 29–67
DOI: 10.1007/10_2013_225

Published Online: 13 July 2013

Advances in Aptamer Screening and Small Molecule Aptasensors

Yeon Seok Kim and Man Bock Gu

Abstract It has been 20 years since *aptamer* and *SELEX* (systematic evolution of ligands by exponential enrichment) were described independently by Andrew Ellington and Larry Gold. Based on the great advantages of aptamers, there have been numerous isolated aptamers for various targets that have actively been applied as therapeutic and analytical tools. Over 2,000 papers related to aptamers or SELEX have been published, attesting to their wide usefulness and the applicability of aptamers. SELEX methods have been modified or re-created over the years to enable aptamer isolation with higher affinity and selectivity in more labor- and time-efficient manners, including automation. Initially, most of the studies about aptamers have focused on the protein targets, which have physiological functions in the body, and their applications as therapeutic agents or receptors for diagnostics. However, aptamers for small molecules such as organic or inorganic compounds, drugs, antibiotics, or metabolites have not been studied sufficiently, despite the ever-increasing need for rapid and simple analytical methods for various chemical targets in the fields of medical diagnostics, environmental monitoring, food safety, and national defense against targets including chemical warfare. This review focuses on not only recent advances in aptamer screening methods but also its analytical application for small molecules.

Keywords Aptamers · SELEX · Small molecule aptasensors

Y. S. Kim
Future Technology R and D Center, SK Telecom, 9-1 Sunae-dong, Bundang-gu, Seongnam 463-838, Republic of Korea

M. B. Gu (✉)
School of Life Sciences and Biotechnology, Korea University, Anam-dong, Seongbuk-Gu, Seoul 136-791, Republic of Korea
e-mail: mbgu@korea.ac.kr

Contents

1 Introduction

As one of the most popular biomaterials for molecular recognition, antibodies have been widely used for more than three decades in various fields, especially in medical diagnostics and therapeutics. The new class of oligonucleotide-based molecular recognition elements has more recently emerged as a rival of antibody-based methods. These oligonucleotide sequences are called "aptamers," derived from a linguistic chimera composed of the Latin word *aptus* (meaning "to fit") and the Greek suffix "*-mer*" [1, 2]. Aptamers can bind to a wide range of target molecules that include proteins, peptides, nucleotides, amino acids, antibiotics, low-molecular organic or inorganic compounds, and even whole cells with high affinity and specificity [3]. Aptamers can be developed in vitro by systematic evolution of ligands by exponential enrichment (SELEX), which makes it possible to isolate functional oligonucleotides against a specific target from a random single strand (ss)DNA or RNA library (usually 10^{15} different sequences). The higher-order structure of oligonucleotides is accomplished by changing intramolecular base pairing. This means that a random library is actually a library of three-dimensional (3D) structural DNA or RNA. Some sequences among the nucleic acid library are folded into unique 3D structures having a combination of stems, loops, quadruplexes, pseudoknots, bulges, or hairpins [4]. The molecular recognition of aptamers results from intermolecular interactions such as the stacking of aromatic rings, electrostatic and van der Waals interactions, or hydrogen bonding with a target compound. In addition, the specific interaction between an aptamer and its target is complemented through an induced fit mechanism, which requires the aptamer to adopt a unique folded structure to its target [4–6].

Over the last 20 years, a large and diverse collection of aptamers for hundreds of targets has been developed from combinatorial ssDNA or RNA pools by basic or advanced SELEX processes. The dissociation constant (K_d) of aptamers to their targets is typically from the micromolar to picomolar range, which is comparable

to or sometimes even better than the affinity of antibodies to their antigens. Aptamers have high specificity, which makes it possible to discriminate specific target molecules from their derivatives, as demonstrated in previous reports for a theophyllin binding aptamer, which showed a 10,000-fold higher binding capacity against caffeine (difference of only a methyl group) [7], by an $_{L}$-arginine binding aptamer with 12,000-fold affinity against $_{D}$-arginine [8], and by an oxytetracycline binding aptamer against tetracycline (difference of only an OH-group) [9].

In addition to high affinity and specificity, aptamers have a number of advantages as molecular recognition elements in comparison to antibodies. First, aptamers are easy to handle due to their thermostability. Aptamers can be also regenerated easily within a few minutes after denaturation because aptamers undergo reversible denaturation. This excellent flexibility of the aptamer structure is useful in developing new types of sensing methods. Second, aptamers are easily modified, linked with labeling molecules such as dyes, or immobilized on the surface of beads or substrates for different applications. This is a tremendous advantage for diagnostic and biosensor applications, because the uniform alignment and immobilization of receptors are very important in analytical systems. Labeling with signal-generating molecules is a common method for signal production or amplification in biosensors. Third, there is no or rare immunogenicity when aptamers are applied to an in vivo system. Aptamers also enable easy control of bioavailability and delivery durability due to their small size (generally less than 20 kDa). This facilitates their penetration into cells and their delivery or immobilization in any medium, similar to liposomes. Fourth, nucleic acid aptamers can be easily amplified by polymerase chain reaction (PCR), unlike other synthetic receptors such as antibodies, oligopeptides, or molecular imprinted polymers (MIP), and also can be expressed inside cells containing a plasmid that includes the aptamer sequence [10]. Finally, the most important advantage of using aptamers is that these receptors do not require animals for selection and production. There is no need for an in vivo immunization to obtain an aptamer, which can be isolated and chemically synthesized in vitro. This is the main advantage of aptamers because it is not easy to produce antibodies against some targets, such as proteins, that are structurally similar to endogenous proteins and toxic compounds. In contrast, aptamers are not limited to their targets. In vitro synthesis makes it possible for the production of purified aptamers with low cost and without batch-to-batch variation. In vitro selection is also proper to develop a high-throughput or automated system for aptamer isolation. Based on these properties of aptamers, the screening method, the SELEX process, has been modified or evolutionarily changed over the years to develop aptamers with higher affinity and selectivity in more efficient, less time-consuming, or automatic ways.

In addition, one of the most successful applications of aptamers is as a recognition probe for medical diagnostics and biosensor development. Various benefits of aptamers as sensing elements (i.e., high affinity and specificity, small size, easy modification and labeling, high stability, no limitation against any kinds of targets, and reversible denaturation) have been verified [11]. Concerning the aptamer-based biosensors, several novel strategies have been devised with

different signal transducers [12]. Most studies on aptamer-based biosensing have focused on protein targets for medical diagnostics. However, the aptamers for small molecules such as organic or inorganic compounds, drugs, antibiotics, or metabolites have not been studied sufficiently, despite the ever-increasing demand for rapid and simple analytical methods for chemical targets in the fields of medical diagnostics, environmental monitoring, food safety, and national defense against targets including chemical warfare agents.

Therefore, this review focuses on recent advances in aptamer screening techniques and aptamer-based biosensors for small molecule detection.

2 Recent Advances in Aptamer Screening Methods

2.1 General Process of Aptamer Screening

In 1990, three laboratories independently described a technique for isolation of functional oligonucleotides, showing the affinity to their target molecule or enzymatic activity, from a randomly synthesized nucleic acid library composed of more than 10^{15} different sequences [1, 2, 13]. This was accomplished by repetition of selection and amplification. This method of in vitro selection is commonly known as SELEX. Since this early introduction of aptamers and the SELEX process, numerous papers about aptamer isolation, their applications in various fields, and the modifications of the SELEX process have been reported. SELEX has become a general and powerful method for isolating nucleic acid aptamers. Figure 1 is a schematic diagram depicting the basic SELEX process including repeated cycles of selection and amplification. This aptamer screening process is affected by many parameters such as target features, design of the random DNA library, selection conditions, and the efficiency of the partitioning methods.

As with any other combinatorial method, the SELEX process starts with the chemical synthesis of a single-stranded (ss)DNA library comprised of random sequences at the center flanked by defined primer binding sites at each 5' and 3' terminus. Individual ssDNA has a different sequence. Compared to other libraries, the randomized ssDNA pool can be easily prepared by a standard DNA synthesizer, because the coupling efficiency of the A, T, G, and C phosphoramidites is very similar. The random ssDNA library can be produced with the mixture of phosphoramidites in a ratio of 1.5: 1.25: 1.15: 1.0 (A: C: G: T) [14]. The diversity of the library depends on the length of the random region. Although one generates 4^n different sequences for n nucleotides long, about 10^{15} diversity is a practical limitation, which corresponds to a length of about 25 nucleotides. Because 30–60 nucleotides at random regions are a commonly used DNA pool, unfortunately, the full theoretical diversity is not covered for a randomly synthesized DNA library in real experiments [14]. Normally, an initial ssDNA pool comprised of around 10^{15} different sequences allowing a generation of a high possibility of sequences

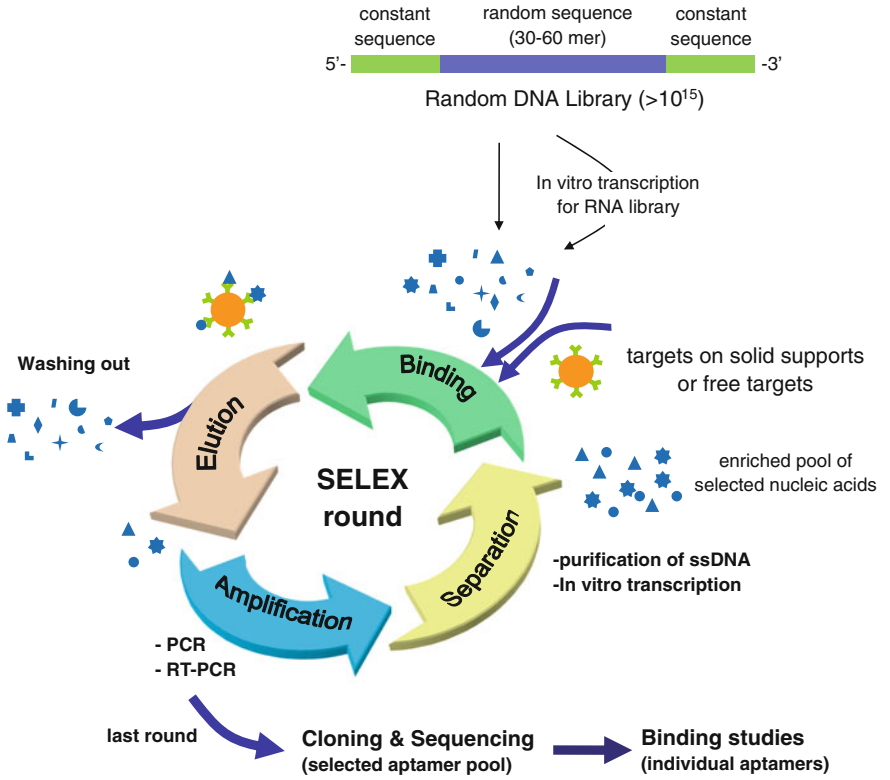

Fig. 1 SELEX technology aptamer screening process

specific for a target is used. Only the short part of full aptamer sequences is sufficient for binding to a target [15]. This suggests that a short library, which is cost-effective and easier to manage, can be used for successful aptamer screening as well. However, long random sequences in a library are more appropriate for providing higher structural complexity, which is important in isolating aptamers with high affinity. Therefore, a longer library may increase the possibility for successful aptamer selection [16]. The constant region as a primer binding site should be well designed to avoid primer–dimer pairs and self-priming during PCR amplification, and to reduce the probability of base pairing between the two constant regions. The design of a constant region is important, because the DNA pool should undergo many rounds of amplification. Therefore, any unwanted nucleotides could be amplified in the final aptamer population by hundreds of PCR cycles [17]. An initial random ssDNA library then is incubated with a target molecule. In this step, however, the ssDNA library must be transformed to a RNA library before the incubation with the target is conducted for the selection of RNA aptamers. In an early stage of aptamer research, RNA libraries were frequently used for aptamer selection because RNA is better at folding into complex 3D

structures that provide stronger molecular interactions with the target. RNA also has an additional hydroxyl group that might facilitate the formation of additional hydrogen bonds between the aptamer and the target. For these reasons, the ability of RNA aptamers is generally reported to be superior to DNA aptamers in terms of their affinity and specificity. For in vivo applications such as therapeutics, molecular imaging, or drug delivery, both RNA and DNA aptamers have to be modified to achieve resistance in degradation against nucleases, which is very expensive work. For in vitro applications such as biosensor development, the modification of DNA aptamers for enhancing stability is not necessary, whereas RNA aptamers should still be modified due to their low stability. Nowadays, therefore, ssDNA pools and DNA aptamers are widely used for the isolation of aptamers and for the development of aptamer-based biosensors or separation systems. In fact, DNA aptamers are much cheaper than RNA aptamers, and DNA is easier to manipulate during the SELEX process [16]. Furthermore, ssDNA folds into a 3D configuration containing stems and loops, even though the folded ssDNAs are less stable than the folded structure of the corresponding RNA sequences [18, 19]. It should also be noted that the conformations of DNA aptamers differ from the corresponding RNA aptamer sequences.

The essential steps of the normal SELEX process are binding, selection, amplification, and partitioning. The most critical step of this process is the selection step. In the first step of SELEX, the random DNA or RNA library is incubated with the target. The nucleic acid–target complex is subsequently partitioned from unbound and weakly bound nucleotides. This is one of the most critical steps to isolate high affinity and specificity aptamers among the extremely diverse oligonucleotide library. During this incubation step, target molecules are either interacted with the nucleic acid pool as a free form or a form that is immobilized on a certain substrate. Fixation of the target on a solid support facilitates easy separation of bound nucleic acids to target from unbound and weakly bound nucleotides. Consequently, this method is very efficient for low-molecular targets. But, the immobilization of the target may result in its conformational change and cause interference on the binding of the library with the conjugation side of the target molecules [20]. The abundant nonspecific interaction of nucleic acid with the solid supports or linker molecules is also notable. Furthermore, it must be remarked that the elution of the strongly bound nucleic acids from the target is difficult, especially in an affinity chromatography type operation, which can restrict the isolation of the extremely high affinity of aptamers. This technique also requires a large amount of targets for elution. In previous studies, therefore, most of the highest affinity aptamers with subnanomolar or picomolar K_d values were obtained by SELEX with free-form target molecules [21, 22]. In addition, a free-form target can avoid all of these issues. However, the separation of a free target–nucleotide complex from unbound nucleotides is difficult or impossible in some cases, especially for low-molecular targets. Therefore, this method is proper only for macromolecular targets. This method normally produces low separation efficiency, which significantly affects the efficiency of the SELEX

process. An efficient partitioning method can reduce the required number of SELEX rounds.

Filtrations using a nitrocellulose membrane or affinity chromatography column containing the target immobilized beads are traditional and conventional methods for partitioning in the SELEX process [1, 2, 22, 23]. In the filtration method, unbound oligonucleotides to targets are removed from aptamer–target complexes based on the molecular weight difference between nucleic acids and the oligonucleotide–target complex. Affinity chromatography separates oligonucleotides interacted with the target molecules from the pool of nucleic acids by using a column packed with the target-immobilized beads. These separation methods, however, often show low resolution and efficiency in separation. Therefore, many cycles of SELEX rounds are required. In addition, it is not easy to elute nucleic acids that are strongly bound to targets using an affinity chromatography type operation. Recently, many advanced separation methods have been developed to improve separation efficiency, which are detailed later in this review. The affinity of nucleotides to their targets might be affected by the selection conditions. In some cases, the binding and washing conditions (i.e., concentration of target, buffer composition, time, and volume) are changed stringently in later SELEX rounds to obtain the aptamers with high affinity and specificity [16]. The nucleotides that bind to the target can be eluted through the heating, the change of ionic strength or pH, the competitive elution by the excessive addition of target, or the addition of denaturing substances including urea, sodium dodecyl sulfate (SDS), or ethylenediamine tetraacetic acid (EDTA) after the harsh washing step [8, 24–28].

In principle, it is expected that only a few oligonucleotide sequences among the initial oligonucleotide library having an extreme diversity might bind to the target molecules. However, it is very difficult or impossible to separate these from a library readily at a time, due to the low partitioning coefficient of normal separation techniques. Therefore, the repetition of the selection step is required in practical protocols of aptamer screening. To perform this repeated selection, the bound oligonucleotides to the targets should be amplified by reverse transcription (RT)-PCR for a RNA library or PCR for a DNA library, which generates a new population of oligonucleotides for the next round of SELEX. PCR is one of the major steps in the aptamer screening process and, therefore, is important to achieve successive PCR amplification with high efficiency. PCR efficiency in the SELEX process is normally not high, mainly due to the central random sequence regions of the nucleotide pool. Therefore, the PCR conditions including the number of cycles should be optimized depending on the design of the primers and library.

Too many PCR cycles might cause unexpected DNA banding (normally a longer DNA band), whereas the excessive amplification of the selected DNA is not required. Normally, 10–20 amplifications are sufficient within 10–20 cycles [29] for the next round of selection. Improvements of the SELEX process have been accomplished in this amplification step, the preparation of the random nucleotides' pool, or the modification of the SELEX procedure. Normally, for practical reasons, the library of random nucleic acids cannot contain all possible sequences. Mutagenic PCR and nonhomologous random recombination (NRR) have been applied

to increase the diversity of the DNA pool during PCR amplification. In error-prone PCR techniques, point mutations occur with a frequency of 1–10 % per base per PCR reaction. This evolution by mutagenic PCR increases the diversity of the oligonucleotide pool. Consequently, the probability to select the more efficient aptamers can be increased [30]. However, the degree of evolution by point mutation is still not sufficient. Liu and co-workers applied NRR to already defined DNA aptamers for a streptavidin target. NRR enabled random recombination of the nucleic acid fragments in a length-controlled manner. As a result, the affinity of aptamers was improved by 15- to 20-fold compared to aptamers enhanced by mutagenic PCR and 27- to 46-fold higher than the original aptamers [31].

After PCR amplification, the enriched oligonucleotide pool exists as double-stranded DNAs. This dsDNA pool is separated to individual ssDNAs and then a forward strand DNA pool is incubated with targets as the next round of SELEX. For the selection of RNA aptamers, the ssDNA pool has to be converted to a RNA pool by reverse transcription. The streptavidin/biotin interaction is widely used for this. In this method, a biotin molecule is incorporated into the unwanted strands during PCR amplification with biotinylated reverse primer. Then, biotin-labeled dsDNAs (only reverse-strand biotinylated) are incubated or passed through a column of streptavidin-coated beads. Forward strands originating from nucleic acids bound to the target are separated by alkaline denaturation or affinity purification, whereas the biotinylated reverse strands are captured on the streptavidin-coated supports [29, 32–34]. Asymmetric PCR is one possible approach to generate enriched ssDNAs from the eluted ssDNA pool. In this technique, only one or a significant portion of one primer is used for PCR [35]. The forward strand can dominate in a mixture of the ss- or ds-DNA pool by asymmetric PCR amplification. Another method was also developed, based on the size difference between strands. Williams and Bartel used a primer linked with a hexaethyleneglycol (HEGL) spacer and an additional 20 adenine nucleotides to provide a size difference between strands [36]. The different-sized strands were easily discriminated and visible in denaturing polyacrylamide gel electrophoresis (PAGE) by ultraviolet (UV) shadowing or by fluorescence using dye-modified primer in PCR [24, 37–39].

During repeated cycles of selection and amplification, the diversity in an oligonucleotide pool is decreased and a high affinity of oligonucleotides to target can result, because low or no affinity of oligonucleotides have no chance to interact with the target. In general, only a few sequences that can bind to targets with high affinity dominate in an oligonucleotide pool after around 8–15 cycles of selection and amplification. The progress of the SELEX process (enrichment of target-bound oligonucleotides) can be monitored by the quantification of target-bound oligonucleotides among the pools of incubated oligonucleotides at each round of SELEX. Radioactive markers are widely used for the quantification of target-bound oligonucleotides during SELEX due to their high sensitivity, even though they have many drawbacks such as the need for an isotope laboratory, high cost, and health risk for experimenters [1, 40, 41]. Fluorescence dyes are also attractive labeling materials for the quantification of target-bound oligonucleotides, because

they are sufficiently sensitive, relatively economical, and easy to handle and measure [24, 38, 39, 42].

Typically during the SELEX process, a counter-selection (negative selection) is normally involved and is necessary to exclude oligonucleotides that are nonspecifically bound to the membrane or bead surface in the absence of the target [7, 43, 44]. The oligonucleotides that bind to structurally similar compounds or abundant molecules in a real sample such as serum albumin proteins can also be removed by counter-selection. During the counter-selection, these undesirable molecules are incubated with the pool of oligonucleotides instead of the target molecule itself, and the oligonucleotides bound to undesirable molecules are eliminated from the oligonucleotide pool. Counter-selection can enhance the specificity of aptamers, but too much counter-selection might decrease the efficiency of the entire SELEX procedure. Subtractive selection is also similar to counter-selection, but it purposefully improves aptamer selectivity against complex targets such as whole cells. Subtractive selection excludes the oligonucleotides bound to the uninteresting regions of the complex target. One study isolated aptamers that can discriminate target cells (leukemia cells) and other cells using the normal human lymphoma cell line as subtractive cells [45]. This technique has become widely used and is powerful for the isolation of highly selective aptamers against cancer cells or bacterial cells [29, 46].

The selection is stopped when oligonucleotides bound to the target are fully dominant in the pool of oligonucleotides or when no significant enhancement of target-bound oligonucleotides is observed during two or three successive SELEX rounds. At this time, most selected oligonucleotides can be regarded as potential aptamer sequences. These selected oligonucleotides are amplified with unmodified primers. Subsequently, the sequences of individually selected oligonucleotides are identified by cloning and sequencing of the selected clones. The number of different aptamer sequences screened by the SELEX process might depend on the stringency of the selection conditions and target characteristics [47]. In general, about 50 or more colonies among many colonies are sequenced. Sequence analysis can give some useful information about selected oligonucleotides. Regions of homologous sequences differing only by a few points can be identified by sequence analysis. These highly conserved regions or some unique sequence patterns are often an essential part of an aptamer for target binding (see Sect. 2.2.1 for details). DIALIGN and CLUSTAL are frequently used sequence alignment programs (http://bibiserv.techfak.uni-bielefeld.de/dialign/ and http://www.ebi.ac.uk/clustalw/) [48–51]. Secondary structure analysis of aptamers can also provide binding site information that can be predicted easily by a computer program. A representative program “m-fold” for the secondary structure prediction of ssDNA or RNA at various conditions is available at http://frontend.bioinfo.rpi.edu/applications/mfold/cgi-bin/dna-form1.cgi [52]. This program is based on a free energy minimization algorithm. Consensus motifs in predicted secondary structures of different aptamers are mainly located in stem-loop structures and are rarely in G-rich structures such as G-quadruplexes or pseudoknot structures [53–55]. These structurally conserved motifs normally correspond

closely with consensus regions of aptamer sequences and are often regarded as binding sites of aptamer to target. After the selection and identification of aptamers, the affinity and specificity of individual aptamers is evaluated by various methods. In some cases, however, the oligonucleotide pool obtained from the last SELEX round can be characterized according to binding ability and used as a mixture, such as polyclonal antibodies [56]. Exact assessment of the aptamer's affinity (dissociation constant, K_d) and specificity is very important for further applications of aptamers. These characteristics of aptamers can be influenced by the conditions of the binding assay.

The normal SELEX process for aptamer screening is universally performed by the repetition of three main steps: selection, amplification, and partitioning. However, there is no standard aptamer screening protocol for any target groups. The SELEX process has been continuously modified to improve screening efficiency and make possible aptamer screening against inaccessible targets by using new efficient separation techniques, automation of the process, or new design of oligonucleotide libraries. The following section describes these advances in the SELEX process in detail.

2.2 Advanced Methods for Aptamer Screening

2.2.1 Oligonucleotide Libraries

Several modifications of the random nucleic acid library in the SELEX process have been developed. Basically, modification is done with the aim of improving aptamer potency by increasing the affinity of aptamers to targets, by offering nuclease resistance, or by providing higher stability. Among the approximately 10^{15} different oligonucleotides, a very small portion of sequences are folded to the 3D structure that allows them to bind to the specific target. Based on this knowledge, Liu and co-workers examined the relationship between the degree of secondary structure in a nucleic acid library and its ability to yield aptamers [57]. They designed a patterned nucleic acid library with a remarkably high degree of secondary structure and ability to accommodate loops and bulges normally observed in the aptamer structures, and demonstrated that the use of a patterned oligonucleotide library had a higher potential to isolate the higher affinity of aptamers than the same size of an unpatterned random library to the same targets.

For in vivo applications, aptamers should be modified to endow nuclease-resistant ability because DNA, and especially RNA, is very sensitive to nucleases [58]. Thus, some methods to transform aptamers into nuclease-resistant moieties by modifying the ribose ring at the 2′-position or by modifying the pyrimidine nucleotide specifically have been reported [59, 60]. Because most nucleases in biological fluids are pyrimidine-specific nucleases, the specific modification with 2′-amino and 2′-fluoro functional groups at the 2′-position of the pyrimidine nucleotide is the commonly used method to increase resistance from nucleases,

increasing half-life up to 15 h [61]. Macugen® marketed by Pfizer and several aptamers currently in clinical development were generated with a library containing 2′-fluoro-pyrimidines. A large number of modifications including substitution at the 2′ position (2′-*O*-methyl, 2′fluoro) and phosphate modifications (phosphorothioate, phosphoraminate, morpholino) have been developed [62–64]. In some cases, these kinds of modifications are limited in their application to the SELEX process because the polymerase cannot effectively amplify DNA with these modified nucleotides. Therefore, some researchers have tried to develop modification schemes that protect DNA or RNA from nuclease-mediated degradation while maintaining the availability of modified nucleotides for PCR amplification by using a special DNA polymerase such as KOD Dash DNA polymerase [65, 66]. These SELEX processes with a modified nucleic acid library can endow not only the nuclease-resistant ability to aptamers, but also accessibility to difficult or impossible targets [67].

A photo-SELEX method performed by incorporating modified nucleic acids activated by absorption of light instead of normal nucleotides has been introduced [68]. In this technique, fluorophore-modified nucleotides, such as 5′ bromodeoxyuridineITP or 5′ iodouracil, were used. The modified ssDNA aptamers can bind to photocross-linking the target molecule and were identified by photo-SELEX [68]. These modified aptamers can make a photo-induced covalent bond with the target molecules, which is very useful in developing sensitive assays. This method screens the high affinity and specificity of aptamers via strong covalent cross-linking between nucleic acid and the target, but the false-positive rate is also high. So the cross-linking conditions should be optimized well.

Genomic SELEX used ssDNA or RNA libraries derived from the whole genome of a certain organism. *Escherichia coli, Saccharomyces cerevisiae*, and the human genomic DNA library were used for genomic SELEX in previous studies [23, 69, 70]. All other steps in the genomic SELEX are similar to the normal SELEX. This method provides great potential for the study of regulation networks between proteins and nucleic acids, and interaction between bioactive molecules and nucleic acids.

The full aptamer sequence is generally not essential for binding to the target [71, 72]. Therefore, several different truncation series of aptamer sequences were arrayed on a chip with high density and DNA microarray experiments with these chips were conducted with dye-labeled target molecules to ascertain which sequence among the full aptamer sequence was essential for the target binding. Fluorescence intensity at each spot well represented the binding ability of truncated aptamer sequences to the target. These massively parallel sequence-function analyses with an aptamer microarray demonstrated that the consensus sequence and common stem-loop structures of aptamers were important for target binding.

In addition, the exclusion of primer sequences was generally not necessary for target binding. However, truncation of primer sequences did not affect the binding ability in all cases. Wen and Gray developed a primer-free SELEX with a bacteriophage-derived genomic library to avoid the influence of primers [73]. Recently, Pan and co-workers reported a minimal primer and primer-free SELEX

protocol with a random DNA library [74]. In these techniques, primer sequences were excluded from the DNA pool before incubation with the target and were incorporated again at the amplification step. Tailored SELEX as a similar approach was successively demonstrated with a random library flanked by short oligonucleotide sequences (only 10 nucleotides) that formed complementary base pairing [75]. In this manner, primers were added to both ends by bridge sequences during amplification; then these primers were eliminated by an alkali treatment. This newly prepared short oligonucleotide pool can then be used in the next round of SELEX. As a result, short aptamer sequences originated from all randomized DNA libraries not incorporated with primer sequences could be screened directly, with no need for a truncation study as a post-SELEX process to use screened aptamers in practical applications.

Burke and Willis varied the SELEX protocol in the generation of a starting nucleic acid pool to develop bifunctional aptamers [76]. At first, they prepared a chimera RNA by simple junction of aptamers previously identified for different targets. These chimera RNAs showed some binding ability to both targets, but their binding activity was not satisfactory probably due to misfolding. To solve this problem, a recombined RNA population was generated by an overlap extension method in PCR with different two aptamers and was used in the SELEX process to both target molecules, instead of a random nucleic acid library (chimeric SELEX). By this technique, dual-functional aptamers having high-binding ability to both targets were screened. Similar to the chimeric SELEX, multistage SELEX was introduced [35]. In this method, each SELEX process was first performed individually with different targets. Then, after five to six rounds of SELEX, two nucleic acid pools were fused to form longer oligonucleotides that were used in the next round of SELEX for both targets.

2.2.2 Selection Methods

In the normal SELEX process, counter-selection is strongly suggested to improve the specificity of aptamers to their target, which is essential for aptamer use, especially in medical diagnostic or therapeutic applications. However, in some applications such as bioseparation and environmental monitoring, the universal binding (low specificity to single target molecules) of aptamer to a group of structurally similar molecules can be more useful [38, 77]. In order to screen the aptamers having high universality, the sequential screening of the nucleic acid pool should be performed with a group of target analogues [22, 25, 38]. Based on this strategy, White and co-workers suggested a toggle-SELEX process, in which two different target molecules are switched during alternating rounds of selection [22]. This method allowed the identification of aptamers that can recognize both human and porcine thrombin with K_d values of 1–4 nM and less than 1 nM, respectively. This technique suggests a useful approach for new therapies when aptamers isolated against human targets may not progress to clinical trials due to their therapeutic efficacy in animal models. Gu's group also developed DNA

aptamers that can bind to two structurally similar antibiotics, oxytetracycline and tetracycline [38]. These aptamers might be more useful in aptasensors to estimate the total concentration of three different tetracycline antibiotics, meaningful information in environmental monitoring, than a combination of aptamers to individual tetracyclines. Toggle-SELEX is available for structurally similar targets whereas chimeric SELEX and multistage-SELEX are less limited to structural similarity between targets.

SELEX is a time-consuming and laborious process because it requires many repetitions of selection and amplification. Therefore, time, cost, or labor can be effectively reduced if the round of SELEX is decreased by enhancement of separation efficiency. If the separation efficiency of the selection method is low, more cycles are needed to screen the aptamers having high affinity and specificity. To this end, many separation tools were applied in the SELEX process. Stoltenburg and co-workers introduced a FluMag-SELEX process based on magnetic beads and fluorescence-labeled forward primers [24], which is a more advanced method than the technique using magnetic beads [78]. In this method, target molecules are immobilized on the surface of the magnetic beads. Unbound oligonucleotides can be efficiently removed from oligonucleotides bound to targets immobilized on magnetic beads by magnetic separation, which is very simple and also does not require a large amount of target, expensive instruments, or skilled people. The evolution of an oligonucleotide pool amplified by using fluorescence-labeled forward primer is also monitored by measuring fluorescence during SELEX rounds [9, 24, 38, 39]. Many kinds of magnetic beads, functionalized to immobilize any target molecules having a functional group, are commercially provided. Tok and Fischer suggested a similar method based on a single microbead to which target proteins were immobilized [79]. They used only a single bead to reduce the amount of targets incubated with the nucleic acid library. It was asserted that small amounts of targets were better to isolate most strongest and specific aptamers. After two cycles, eight aptamers were identified.

Improvement of the partitioning coefficient of the selection methods can also decrease the rounds of SELEX. In this regard, capillary electrophoresis is an attractive method for aptamer researchers. The first application of capillary electrophoresis in the SELEX process (CE-SELEX) was demonstrated by Mendonsa and Bowser [80]. In this separation system, unbound oligonucleotides can be easily partitioned from oligonucleotide–target complexes with high resolution based on the difference of migration velocity between unbound oligonucleotides and oligonucleotide–target complexes [81–83]. The high efficiency of CE-SELEX aptamer selection was verified by the isolation of IgE specific aptamers identified after only four cycles, whereas normal SELEX required 18 cycles to obtain a similar affinity of aptamers. In addition, CE-SELEX does not need to consider the nonspecific adsorption of oligonucleotides on the matrix because the target interacts with oligonucleotides as a free form. However, CE-SELEX is limited in terms of its properties and target size. Especially, low-molecular weight targets such as small organic compounds are not suitable in CE-SELEX because the migration velocity of oligonucleotide–target complexes is not effectively

discriminated with one of the unbound oligonucleotides. In addition, because a very small volume of sample (nL level) can be injected without overloading the capillary, only a small amount of the library having low diversity (typically 10^{13}) has a chance to interact with the target.

Non-SELEX is also a highly efficient and fast method for aptamer screening. This process is performed by repetitive selection without an intervening PCR amplification step. The selected target-bound oligonucleotide pool selected from the previous round is directly used in the next round of selection. In this method, nonequilibrium capillary electrophoresis of equilibrium mixtures (NECEEM) is used for separation. This method enables the selection of aptamers with predefined kinetic/thermodynamic parameters (such as K_d), because the migration time of the aptamer–target complexes in the capillary depends on the K_d. Berezovski and co-workers first showed that the high affinity of aptamer (K_d: 0.3 nM) for hRas was screened in only three selection cycles [21]. However, the mechanism of this method is still unclear and reports of aptamers screened by this method are very few. Therefore, additional investigations of non-SELEX for various targets are required to establish an efficient method for aptamer screening.

Faster and greater high-throughput methods for aptamer screening are strongly demanded. To this goal, automatic, high-throughput, and simultaneous aptamer selection methods have and continue to be devised. The first automated SELEX process was developed based on the Biomek 2000 pipetting robot (Beckman Coulter) by Cox and Ellington in 1998 [84]. The authors reported that this robotic workstation could carry out aptamer screening for eight targets simultaneously with the process completed in about 12 rounds of selection in two days. The authors immobilized biotinylated lysozyme on strepavidin-coated beads and then conducted an automated repetition of cycles of separation and amplification [85]. Even if lysozyme aptamers were isolated by automatic SELEX, just pipetting, not the whole SELEX process, was automatically operated in this system. This automated SELEX process using a robotic workstation was also demonstrated for some other protein targets such as CYT-18, MEK-1, and Rho [86]. The robotic workstation for automatic SELEX was improved by the addition of a generation part of protein targets that are directly produced from the respective gene in vitro on station [87]. This can accelerate the SELEX process for protein targets.

Eulberg and co-workers developed a modified automatic SELEX system whose design was based on the optimum aptamer screening conditions including buffer components, pH, and PCR conditions, which could be varied according to the target's features [88]. In this system, the Amp 4200E robotic workstation (MWG Biotech Ebersberg) was incorporated with an ultrafiltration system, fluorescence detector, and semi-quantitative PCR under some flexibility [89]. Recently, an upgraded version of the automatic SELEX process was developed using a microfluidic system [90]. This automatic SELEX system, as a microfluidic, microline-based assembly, enables a start-to-finish SELEX including transcription, selection, RT-PCR, and partitioning. The prototype of this automated system is smaller, simpler, and relatively less expensive than previous robotic workstations. In spite of the rapid improvement of the SELEX process, it has still not been

standardized for any type of target. The automated SELEX system can be a favorable approach to establish a standard SELEX protocol. In addition, the automated SELEX system enables fast and high-throughput aptamer screening, and improves the accessibility of SELEX to many nonspecialized researchers.

Most recently, a sol-gel microfluidic chip was also adapted for the SELEX process, in the form of a "SELEX-on-a-chip" [91]. In this system, the binding and elution are performed on a microelectromechanical systems (MEMS) chip for the simultaneous examination of multiple targets. The microfluidic chip was designed to incorporate five sol-gel droplets in which different molecules were embedded as targets or control. The droplets are located on top of individually addressable electrical microheaters used to elute target-bound nucleic acids in the sol-gel droplets. They have demonstrated the specific binding of aptamers to their respective protein targets, and the selective elution by microheating. This SELEX-on-a-chip system demonstrated high selection efficiency and consequent decrease of selection cycles to isolate high-affinity aptamers. This method needs only a very small reagent volume for selection and induces the competitive binding of oligonucleotides to multiple targets embedded in each droplet, which is useful to increase the specificity of aptamers. In addition, the process can be easily extended for larger arrays of sol-gel–embedded proteins. Another microfluidic chip-based aptamer selection method, termed microfluidic SELEX (M-SELEX), was developed [92, 93]. In this system, the magnetic bead-based SELEX process (using target immobilized micromagnetic beads for selection) is integrated with microfluidics technology, which enables the precise manipulation of a small number of beads and selection of target-bound oligonucleotides from the library with a high partitioning coefficient. M-SELEX successively isolated high-affinity DNA aptamers (nM level K_d values) that strongly bound to the light chain of recombinant *Botulinum* neurotoxin type A after only a single round of selection.

2.2.3 Target Features

The SELEX process has no limitation on various classes of targets. Large molecules such as proteins are the best-suited targets in the SELEX process because they provide a large surface for interaction with aptamers. However, low-molecular–weight targets such as inorganic components (Zn^{2+}, Ni^{2+}, As) [94–96] and small organic molecules including cholic acid, cocaine, theophylline, tyrosinimide, ethanolamine, malachite green, and oxytetracycline [1, 7, 9, 97–101] are also proper in the SELEX process. The affinity of these aptamers for small molecules is normally low in a range of submicro- to micromolar K_d values. The major difficulty in aptamer screening for low-molecular–weight targets is that the target should be immobilized on a solid substrate to separate the target unbound oligonucleotides from the oligonucleotide–target complex. If a target interacts with oligonucleotides as a free form, it is very difficult to separate them due to the lack of a significant difference between their molecular weights. Unfortunately, the fixation of targets (especially small molecular targets) has the potential to decrease

the specificity of aptamers, especially towards the immobilization part of the target [20]. In addition, many small molecular targets such as pesticides are not easy to immobilize on any solid substrates.

To overcome this problem in SELEX for small molecular targets, Gu and co-workers recently developed an immobilization-free aptamer screening method using graphene oxide (GO-SELEX) [102]. It had already been proven that ssDNA can avidly adsorb on graphene or a graphene oxide sheet via π–π stacking interactions [103]. Based on this knowledge, the ssDNA library was adsorbed on graphene oxide and the DNA species were interacted with target molecules. ssDNA binding to target was target-induced detached from the graphene oxide sheet and separated from the unbound ssDNA pool still adsorbed on the graphene oxide sheet by centrifugation. By this GO-SELEX method, ssDNA aptamers having submicromolar K_d values were successively isolated for Nampt, an adipokine protein. Even in the absence of reports about aptamers for small molecules screened by GO-SELEX, the approach can be easily extended to low-molecular–weight targets because GO-SELEX is based on the competitive interaction among oligonucleotides, graphene sheet, and target molecules, and not on the size difference between unbound oligonucleotide and an oligonucleotide target complex. Another useful approach for immobilization-free SELEX was introduced by Nutiu and Li in 2005 [104]. This method was based on the structural-switching property of aptamers. In this reported SELEX method, an oligonucleotide library was designed as a 15 nt specific sequence flanked by two random sequences of 10 and 20 nt. The central specific sequence was complementary to a biotinylated capture oligonucleotide. Thus, the library could be immobilized on avidin-coated beads by hybridization. Oligonucleotides binding to targets were released from the beads via structure-switching for the formation of a complex that was subsequently separated from the library.

Sometimes the preparation of pure protein is not easy, or the aptamers for a pure protein are not useful (e.g., membrane proteins and ion channel proteins). As well, some researchers are more interested in complex targets such as whole cells. Fortunately, the SELEX process is also suitable for these complex targets or mixtures when detailed information about their individual target is not available, which is very attractive in studies of diseases such as cancer. The structural or molecular change on the surface of cells is normally associated with their state, but information is lacking in many cases. In recent years, an interest in aptamers for complex targets such as mammalian cells, tissues, bacteria, and viruses has spurred the development of a new SELEX process dubbed cell-SELEX or whole cell-SELEX [46, 105–107]. This method is very similar to the normal SELEX process, except for the use of whole cells or tissues, instead of purified targets. But, serious hurdles remain. Because receptors or proteins expressed on the cell surface are so complex and multifarious, it is not easy to isolate the aptamers specific to target proteins. Cerchia and co-workers solved this problem using a new strategy in which target proteins were overexpressed on the cell surface [106]. Another study reported improvements by excessive negative selection using counter-cells having almost same composition of membrane proteins on the cell surface, except for a

specific target receptor [107]. These kinds of cell-SELEX processes are very useful approaches for diagnostics, imaging, drug delivery, and therapy for cancer or any other disease.

3 Recent Advances in Aptasensors for Small Molecule Detection

The need for the development of chemical biosensors is continuously increasing because the rapid and on-site detection of low-weight compounds, such as residual antibiotics or medicines, illegal drugs, environmental toxicants, chemical warfare agents, and heavy metals, is increasingly important in aspects that include public health, environmental monitoring, food safety, and antiterrorism. In addition, the need for the accurate detection of small molecules, such as disease-related metabolites or medically relevant bioactive compounds, is also increasing in disease diagnosis through the multiparameter analysis of disease-related proteins and newly discovered metabolite biomarkers. However, biosensors for these low-weight compounds have not been extensively studied as much as protein targets have. In addition to the fact that proteins are very significant compared to other molecules, another critical reason is that the recognition elements for these targets are often very difficult to develop. Antibody- or enzyme-based assays are still regarded as standard and well-established assays for the detection of proteins and small chemicals, but they are restricted to some targets, such as toxicants or nonimmunogenic compounds and also often show low specificity due to structurally diverse similar analogues that can exist in the sample. One more important concern for chemical sensing is related to the transducer platform for signal production. For the detection of small molecules, mass-dependent detection methods, including surface plasmon resonance (SPR), quartz crystal microbalance (QCM), and cantilevers, are not efficient because it is very difficult for small molecular targets to generate a signal effectively upon the molecular interaction, due to their low molecular weight in mass-dependent affinity-based assays [108]. A sandwich assay format, one of most powerful methods in immunoassay, is also unsuitable for the detection of low-weight compounds because these targets are normally pocketed inside the cleft of the capturing probes, leaving little space for interaction with secondary probes [109]. The single-site binding, which is the normal assay configuration for small molecules, is not suitable for signal amplification. Subsequently, the highly sensitive detection of small molecules is very restricted. However, environmentally hazardous components can cause a significant problem as they are present in very low concentration in many cases.

Nucleic acid aptamers are very attractive bioreceptors for low-weight compounds due to their many advantages in biosensor development. Aptamer screening for toxic target molecules or for molecules with no or low immunogenicity is possible. Denatured aptamers can be regenerated easily within minutes, which is a useful property in a bioassay. Aptamers are also promising because of their high specificity to low molecular targets from structurally similar analogues.

Concerning signal production, the structural flexibility of aptamers enables the development of novel and unique aptamer-based sensing platforms [110]. Nucleic acid aptamers fold into a flexible but well-defined three-dimensional structure upon binding to their target molecules. Another approach is the use of the inherent property of aptamers as nucleic acids. Nucleic acid aptamers can form a double-helix structure by hybridization with their complementary sequences. This double-helix structure can be easily destroyed by the binding of aptamers to targets by competitive interaction. There are few reports about aptasensors for low-weight compounds, but some compelling aptasensor developments for small molecules have been introduced based on the conformational change of aptamers, hybridized aptamers, or other strategies with optical or electrochemical platforms.

3.1 Fluorescence-Based Analysis

Fluorescence analysis is the most popular technique in bioanalytical chemistry. Several conventional fluorescent or quencher molecules are available and their detection is very sensitive. These various dye molecules can be easily conjugated with nucleic acid aptamers and are also inherently suitable for real-time detection. In addition, the high flexibility of the aptamer structure is very useful to establish various types of fluorescent aptasensors, such as a fluorescence resonance energy transfer (FRET) assay, which is based on the energy transfer between two fluorescent molecules (donor and acceptor). A frequently adopted method is an aptamer-based molecular beacon (aptabeacon). If aptamers have a hairpin structure, the aptamer can be used as a molecular beacon by labeling with a fluorescent compound and quenching dye at the 5′ and 3′ end of the aptamer, respectively. In the presence of targets, the aptamer undergoes a conformational change from the hairpin structure to the unfolded form, and fluorescence of the dye molecules is recovered because the distance between the fluorescence dyes and quencher molecules is beyond that for efficient quenching [111]. Similarly, for aptabeacons, a theophylline-specific aptamer double-labeled with a fluorophore and a quencher dye was examined for the detection of theophylline with a target-dependent allosteric ribozyme [112]. In the presence of theophylline, the ribozyme domain was altered to an active conformation by the action of a theophylline-specific aptamer domain. Thus, the quencher was positioned away from the fluorophore by substrate cleavage, resulting in an increase of the fluorescence signal.

Nutiu and Li developed a more generalized aptamer-based FRET assay by DNA displacement [113]. They hybridized aptamers with two partial complementary sequences labeled with fluorescence dye and quencher, respectively. In the absence of the target, the fluorescence was quenched by the nearby quencher molecule hybridization, whereas the aptamer preferred to form an aptamer–target complex when the target was added. As a result, a strong fluorescence signal could be generated by dissociation of short quenching DNA. This approach can be adopted in sandwich fluorescence assay in which fluorescent nanoparticles and

quenching (or capturing particles) are networked by sandwich hybridization between aptamers and their complementary DNAs. This network is broken by the formation of the target–aptamer complex, resulting in the enhancement or quenching of the fluorescence signal. This target-induced displacement strategy might be useful to improve the universality of the methods and to develop aptasensors when an aptamer has no beacon structure or prior information about its secondary or tertiary structure [114, 115]. Most recently, another general excimer signaling approach for aptasensors was reported by Wu and co-workers [116]. In this method, the aptamer was split into two fragments conjugated with pryene molecules, abrogating the aptamer's binding ability. Target molecules (cocaine) induced the self-assembly of the split pieces, allowing the pyrene molecules to approach close enough to establish a pryene excimer. This resulted in a wavelength shift of fluorescence.

Gold nanoparticles (AuNPs) have been widely used in an aptamer-based FRET assay as a fluorescence acceptor, based on the knowledge that AuNPs can superquench fluorescence through an energy/charge transfer process [117]. In general, the quenching effect of AuNPs is several orders of magnitude higher than that of an organic quencher [118]. AuNPs have a broad quenching ability for almost all organic dyes, which enables a multiplex detection of several analytes in homogeneous solution by the anchoring of multiple aptamers on AuNPs without rational design and optimization of fluorophore–quencher pairs [119–121]. Besides AuNPs, carbon nanotube (CNT), graphene, and graphene oxide have been recently applied in aptamer-based FRET assays as effective fluorescence acceptors. Yang and co-workers demonstrated the potency of a CNT–aptamer complex-based fluorescent biosensor. In this method, dye-labeled aptamer was adsorbed on CNT via π–π stacking interaction between bases of aptamer and CNT sidewalls. Fluorescence was quenched by the electron or energy transfer from the fluorophore to the CNT. The fluorescence signal was recovered by the addition of the target due to the competitive interaction between aptamer and target [122]. The FRET assay using graphene and graphene oxide has been applied in aptasensors using almost the same mechanism as the CNT-based assay [123, 124]. In some cases, target-induced conformational change of aptamers brings the donor and acceptor in close proximity, which causes fluorescence quenching (signal-off mode). One example is a cocaine-binding aptamer having a three-way junction [125]. This aptamer, which is double labeled with the donor and acceptor at each end, exists as a free form in the absence of cocaine. But the addition of cocaine induces a conformational change of the aptamer, leading to the close apposition of the acceptor and donor, and consequent quenching of the fluorescence.

A double-labeled thrombin-binding aptamer was also used as a signal-off mode to detect Pb^{2+} and Hg^{2+} [126]. The conformation of this random coil structure aptamer was changed to a G-quadruplex by the interaction with Pb^{2+} or to a hairpin structure by interaction with Hg^{2+}, respectively. As a result, the fluorescence was decreased by FRET between the fluorophore and quencher. Similarly, $_L$-argininamide-binding aptamer was used for detection of $_L$-argininamide [127]. Although some of the aptamer-based FRET assays have been conducted only for a

protein target (mostly thrombin), these principles have no restriction on being expanded for small molecular detection.

All of the aforementioned methods used fluorescence and quencher-labeled nucleic acids. But, label-free aptamers involving fluorescence aptasensors for low-weight components using intercalating agents have been studied [128–130]. In these techniques, fluorescence dyes such as N,Ndimethyl-2,7-diazapyrenium dication (DMDAP) and 2-amino-5,6,7-trimethyl-1,8-naphthyridine (ATMND) are intercalated in single or duplex form of aptamers and quenched by acceptors. These intercalating agents are displaced upon target binding, resulting in increased fluorescence. Another approach of the label-free aptamer-based fluorescence assay was developed based on target-binding induced quencher deactivation or removal. In these methods, quenchers were located close to donors, such as fluorescence dye and quantum dots, by conjugation on beads or hybridization with aptamer [131, 132]. In some cases, label-free fluorescent aptasensors were developed using fluorescent dyes including 4′,6-diamidino-2-phenylindol (DAPI), Hoechst, malachite green (MG), acridine orange (AO), and OliGreen (OG) without quencher molecules [133–137]. These fluorescent dyes emit very weak fluorescence when they are free in solution, but their fluorescence is significantly enhanced by interaction with specific regions of aptamers such as stem structure or capturing with dye-binding aptamers. As one example, the aptamer has no stable stem structure for dye binding in the absence of targets ($_{L}$-argininamide), whereas target binding to an aptamer leads to stable stem formation, resulting in enhancement of fluorescence by the binding of dye (DAPI or Hoechst). The interaction between aptamer and fluorescent dye does not affect the binding ability of the aptamer because the stem structure of aptamers is not normally a binding domain. Conversely, AO and OG dyes interact well with the free form of aptmers in the absence of target, but are displaced by the formation of an aptamer–target complex (signal-off mode) [138, 139].

Recently, an interesting fluorescence assay was reported, which is based on selective fluorescent CuNP formation by accumulation in the major groove of the DNA duplex [140]. Based on this phenomenon, small molecular targets including ATP and cocaine were sensitively detected using dsDNA formed by hybridization between aptamers and their complementary ssDNA. In the absence of targets, the formation of CuNPs associated with the dsDNA template induces the fluorescence emission from CuNPs. But the fluorescence signal cannot be observed in the presence of the target because the dsDNA is broken by the formation of the aptamer–target complex, in which CuNPs cannot be grown due to the absence of dsDNA.

3.2 Colorimetric Assay

The colorimetric assay is a very attractive method because detection can be accomplished simply using the naked eye, which eliminates the need for expensive analytical instruments. Based on these features, colorimetric biosensors are a

compelling point-of-care (POC) analysis, which is frequently requested for the real-life application of biosensors. Based on these advantages, colorimetric aptasensors have been recently studied for the detection of low-molecular–weight components, such as small chemicals and heavy metal ions. An initial colorimetric aptasensor for a small molecule (cocaine) was developed based on the intermolecular displacement of the dye from an aptamer–dye complex in the presence of the cocaine target [99]. In this method, cocaine displaced the dye by forming a cocaine–aptamer complex, causing an immediate attenuation of absorbance and eventual precipitation of the dye. In a similar approach, heavy metal ions (Pb^{2+} and Cu^{2+}) were also detected using DNAzymes [141, 142].

Nowadays, AuNPs are more widely used materials in colorimetric assays due to their unique optical properties, the size-dependent SPR. AuNPs have high extinction coefficients and show size-dependent colors [143]. The dispersed AuNPs that are approximately 13 nm in diameter appear red in color due to their intense SPR absorbance at 520 nm, but the red color changes to purple when they aggregate. This red-to-purple color change can be easily observed by the naked eye. Based on this optical property of AuNPs, as a more recent technology, aptamer-based colorimetric analyses using AuNPs have been extensively described. In this technique, AuNPs are connected to each other by hybridization between aptamers and two different sequenced DNA probes, which are individually immobilized on AuNPs. Due to the aggregation, the solution of AuNPs appears purple. In the presence of target, the networking between AuNPs is broken and they disperse, changing the color to red [144]. This principle was adopted in a "dipstick" type of aptasensor for the detection of small molecules (adenosine and cocaine) [145]. In this system, target-specific, aptamer-linked NP aggregates were loaded onto a lateral flow device, resulting in a simpler and, more excitingly, more sensitive dipstick test than the colorimetric assay in solution. In the absence of target, aggregated nanostructures did not move along the membrane and show a purple line in the conjugation pad. This dipstick type of aptasensor is very attractive in a practical application format, similar to the pregnancy test strip.

Similarly, aptamer was partially hybridized with a probe immobilized on AuNPs. In this state, the AuNPs are not aggregated by the addition of salt. Upon binding of the target, aptamers that are partially hybridized with probes are released from the AuNPs. Then, the AuNPs will aggregate in the salt addition, which screens the electrostatic repulsion between AuNPs. Consequently, the color of the AuNP solution is changed from red to purple [146]. In a converse format for networking between AuNPs, some macromolecular targets having multibinding moieties for aptamers including thrombin and platelet-derived growth factor can induce interparticle cross-linking aggregation of AuNPs by sandwich binding, resulting in the colorimetric change from red to purple in the presence of the target [147]. Unfortunately, this method cannot be adopted for small molecular detection because small molecules do not possess sufficient binding moieties to enable sandwich binding. However, some metal ions, such as Hg^{2+} and Ag^{+}, can be detected by this target-induced cross-linked aggregation of AuNPs. Thymine–thymine (T–T) and cytosine–cytosine (C–C) base pairs selectively capture

mercury and silver ions, respectively, and the metallo-base pairs, T–Hg^{2+}–T and C–Ag^{+}–C, are formed in DNA duplexes with high stability [148]. This phenomenon was successfully adopted in colorimetric metal ion detection [149–151]. In this method, Hg^{2+} and Ag^{+} led to the aggregation of AuNPs by the formation of T–Hg^{2+}–T and C–Ag^{+}–C, respectively, resulting in the red-to-purple color change.

In most cases, AuNP-based colorimetric aptasensors used the modified AuNPs with aptamers or their specific probes for the cross-linking of AuNPs. However, the use of unmodified AuNPs should be more convenient, cost-effective, and time-saving because the synthesis of thiolated aptamers is very expensive and the immobilization of aptamers on AuNPs is time-consuming. Li and Rothberg have described a new strategy of colorimetric assay using unmodified AuNPs for DNA detection, which is based on the different electrostatic interactions between ssDNA and dsDNA on AuNPs. The selective adsorption of ssDNA on AuNPs prevents the aggregation of AuNPs at a salt concentration that screens the repulsive interactions of citrate ions [152]. Inspired by this phenomenon, many unmodified AuNP-based colorimetric aptasensors have been recently developed. Dong's group has developed a simple unmodified AuNP-based colorimetric assay for Pb^{2+} detection using 17E DNAzyme, which cleaves its substrate, 17DS, in the presence of Pb^{2+} [153]. The ssDNA released from the 17E − 17DS duplex is adsorbed on the AuNPs, preventing the aggregation of the AuNPs. In another approach, the target-induced conformational change of aptamers was applied in an unmodified AuNP-based colorimetric aptasensor for the detection of small molecules or ions.

The detection for several low-weight components (K^{+}, Hg^{2+}, oxytetracycline) was accomplished using unmodified AuNPs and aptamers with a simple experimental design [154–157]. In the assay, unfolded aptamers were strongly adsorbed on AuNPs and stabilized the AuNPs in a high salt buffer. In the presence of targets the conformation of aptamers transits to a folded state that is not easily adsorbed on AuNPs. Subsequently, the red color of the dispersed AuNPs is changed to a purple color due to the aggregation of AuNPs.

However, not all of the aptamers undergo a sufficient conformational change. To overcome this limitation, Fan and co-workers have developed a displacement-based assay [158]. In this strategy, aptamers were hybridized with their complementary DNA. By the addition of targets, the aptamers detached from the duplex form to interact with target molecules. A released complementary ssDNA from complex stabilizes AuNPs against aggregation and the color of the AuNPs appears as red. This strategy can be generally applied to any kind of aptamer structure. Most recently, Fan's group have reported a more advanced design of an unmodified AuNP-based colorimetric assay. In this assay, aptamers are partitioned to two pieces of ssDNA, which reassemble into the original tertiary structure of aptamers in the presence of target molecules [143]. By this strategy, small molecules (cocaine, adenosine, and K^{+}) were detected in the micromolar range within minutes, which is based on the knowledge that the short-sized DNA fragments are more rapidly adsorbed on AuNPs. Surprisingly, almost all of colorimetric aptasensors used only a few aptamers as cocaine, adenosine, and K^{+} binding aptamers, because these aptamers have been extensively studied concerning their structure

and binding. Unfortunately, however, it is true that the information on the structure of many aptamers is not available or elucidated. As an answer to this issue, Gu's group demonstrated that long-sized aptamers (76 mer) can also be used in an unmodified AuNP-based colorimetric assay directly after SELEX without studies on the truncation and structure, although the sensitivity for some targets was not satisfactory for use in real samples. They also showed signal enhancement by modulating the interaction between aptamers and AuNPs through the exchange of AuNP capping agents. [156–158]

In addition to AuNP-based assays, other colorimetric aptasensors have been reported using polydiacetylene (PDA) liposomes and colored polymers. Kim and co-workers introduced colorimetric aptasensors incorporated with PDA liposome, which is very sensitive and changes its color by external stimuli including ligand interaction, temperature, solvent, and pH. In this technique, aptamers are conjugated on the surface of PDA liposomes. Binding of target to aptamers induces the color change of the liposomes. The detection of K^+ was successfully performed by this method [159, 160]. In another way, a colorimetric detection of mercury ion was accomplished using conjugated polymer, poly(3-(3′-*N*,*N*,*N*-triethylamino-1′-propyloxy)-4-methyl-2,5-thiophene hydrochloride) (PMNT) and Hg^{2+} specific T-rich ssDNA. The optical properties of polythiophene are highly sensitive to conformational change of its conjugated backbone. In the absence of Hg^{2+}, T-rich ssDNA has a stretched structure that readily forms an electrostatic complex with cationic PMNT in aqueous solution. This leads to a planar conformation of PMNT with a characteristic red color. In the presence of Hg^{2+}, T-rich ssDNA forms a stem-loop structure by binding with Hg^{2+} and is surrounded by PMNT. This conformational change of PMNT induces a color change from red to yellow [161].

Colorimetric aptasensors are very useful for the on-site detection of low-weight components with high simplicity, but the relatively low sensitivity compared with other methods remains a significant hurdle for real applications.

3.3 Electrochemical Analysis

Electrochemical analysis is one of the most attractive sensing platforms due to its great simplicity, rapidity in detection, cost-effectiveness, and the ease of miniaturization, which are necessary for POC applications of biosensors. An electrochemical biosensor is also suitable for multitarget detection through the design of arrayed electrode chips. Recently, many papers have described the incorporation of aptamer-based biosensors in electrochemical detection systems based on distinct properties of aptamers. In electrochemistry, the state change of an electrode surface that occurs by the interaction between targets and immobilized receptors modifies the resistance and capacitance of the electrode–solution interface. Therefore, voltammetry and impedance analyses are very effective and widely used techniques in electrochemical biosensors. The first electrochemical aptasensors developed were mainly based on the analysis of current or faradic

impedance change occurring by simple binding events. In these systems, the electron transfer resistance between redox mediators such as $[Fe(CN)_6]^{-3/-4}$ in solution and electrode is changed by the capturing of target by aptamers immobilized on the electrode. The direction of current or resistance change is greatly affected by electrical properties of the targets [162, 163]. These single-binding methods result in very sensitive and simple detection at the fM level for some protein targets such as thrombin [164]. However, this electrochemical detection based on simple binding is still limited for the development of sensitive aptasensors for small molecules, because the electron transfer resistance or current that can be changed by the simple binding of small molecular targets is generally insignificant, compared to macromolecules [165, 166]. To overcome this problem of low sensitivity, various strategies for the design and signal amplification methods of electrochemical signal production have been incorporated in novel and sensitive electrochemical aptasensors, based on the signals produced by the direct conformational change of aptamers and target-induced displacement.

Hegger and Plaxco have developed new types of electrochemical aptasensors based on the conformational change that occurs when aptamers are bound to target molecules [167–169]. In this technique, the current is changed depending on the distance between electroactive compounds (methylene blue or ferrocene) labeled with aptamers and the electrode surface, which is well distinguished in the absence or presence of any type of target. One example is a thrombin detection using redox-active methylene blue- (MB) labeled thrombin-binding aptamer immobilized on an electrode. The flexible conformation of the aptamer labeled with MB enables the electrical contact of the MB with the electrode, and a voltammetric response of the MB. This sensing principle was successfully expanded to low-weight components such as cocaine and K^+. But, this signal-off sensing format has the disadvantage of a negative readout signal.

To solve this defect, several signal-on aptasensors have been developed. One approach is to use a bifunctionalized aptamer labeled with a terminal electroactive ferrocene as a redox group and a thiol group at the second terminus of the aptamer [168, 170]. The long, flexible aptamer strand prevents electrical contact of the ferrocene with the electrode. The formation of an aptamer–target complex makes a rigid configuration and results in the orientation of the ferrocene towards the electrode. This leads to the generation of a positive signal in the presence of targets such as cocaine. In another approach, a DNA duplex structure consisting of a ferrocene-labeled aptamer and its complementary DNA was used [171–173]. In the absence of target molecules (cocaine, ATP, Pb^{2+}), the hybridized aptamer adopts a partially unfolded state, whereas in the presence of targets, the aptamer folds to bind to the targets. Consequently, an electroactive ferrocene is closed to the electrode, and the signal is increased. As another approach, a target-induced displacement format is a very effective method. This strategy is based on the separation of the two strands of duplex nucleic acids, composed of an aptamer strand and partially complementary sequence, induced by the presence of target molecules. In the presence of a target, duplex DNA separates and the aptamer folds and binds to the target. The displacement of a complementary sequence decreases

the electron-flow resistance. The separation of duplex DNA is dependent on target concentration. Thus, this method enables the sensitive detection of small molecules [173–176].

The other method for an electrochemical aptasensor uses a redox-active reporter that intercalates into double-stranded DNA rather than being covalently tethered to the aptamer. In this method, intercalating redox-active molecules such as MB are used for signal enhancement. The hairpin structure of aptamers is immobilized on a gold electrode, and MB intercalated in the duplex stem structure of the probe hairpin. The binding of target with the aptamer opens the hairpin structure, thus releasing the intercalated redox-active MB. As a result, the electrochemical signal decreases proportionally to the target (theophylline) concentration [177]. Shao and co-workers suggested a sensitive chronocoulometric aptasensor for adenosine monophosphate (AMP) detection using $[Ru(NH_3)_6]^{3+}$ (RuHex) [178]. In this report, the aptamers hybridized with short complementary ssDNA were immobilized on a gold surface and many RuHex molecules were associated with the duplex form of the aptamer complex to produce a coulometric signal. Short complementary ssDNA was displaced from the aptamer with RuHex by addition of the target (AMP). Thus, the charge was reduced in proportion to the AMP concentration. Similarly, the sensitivity of adenosine detection was improved as low as 1 nM by MB intercalation into the DNA duplex formed by hybridization between an adenosine-binding aptamer and probe DNA immobilized on the electrode [179]. The addition of adenine induced the displacement of adenine-binding aptamers from the duplex form, followed by the releasing of MB. As a result, the current was decreased.

Other effective signal amplification methods in electrochemical detection have been accomplished by the incorporation of NPs. AuNPs are the most popular NPs used for signal amplification in electrochemical aptasensors due to their large surface area, favorable electronic properties, and electrocatalytic activity. The strategies of AuNP-based signal amplification in electrochemical aptasensors are classified into two different approaches. The first method is an attachment of AuNPs on an electrode for enlargement of the electrode surface. The second method is the use of AuNPs as the carrier of signaling materials for amplification of the electrochemical signal. Zhang and co-workers reported a sensitive electrochemical aptasensor for cocaine detection based on the signal enhancement supported by the self-assembly of AuNPs on a gold electrode [180]. In this report, cocaine-binding aptamers conjugated with a redox-active ferrocene and thiol group, respectively, were immobilized on the AuNP-modified electrode. The target-induced conformational change of aptamers may increase the current due to the close proximity between ferrocene and the electrode in the presence of cocaine. As a result, the sensitivity of aptasensors using an AuNP-modified electrode was enhanced tenfold compared to aptasensors using a naked gold electrode. As a converse method, a signal-off electrochemiluminescence (ECL) aptasensor was developed for the detection of small molecules using a gold electrode modified by the complex of AuNPs and ECL substrate $(Ru(bpy)_3^{2+})$ [181]. An adenine-binding aptamer conjugated with ferrocene was immobilized on a modified gold electrode

and stretched by the hybridization with complementary DNA. In the presence of adenine, complementary DNA was dehybridized by the formation of an adenine–aptamer complex. The ferrocene probe was closed to the electrode by the folding of the aptamers. Consequently, the ECL intensity was decreased by the quenching effect of ferrocene to the $Ru(bpy)_3^{2+}$.

AuNP-based electrochemical signal amplification in aptasensors has been developed mainly in the sandwich configuration. Use of AuNPs conjugated with secondary aptamers is a very simple and powerful method for signal amplification in electrochemical aptasensors, but they are not available for small molecular detection due to the sparse binding space of small molecule-binding aptamers. Therefore, almost all sandwich structures in aptasensors consist of duplex DNA formed by hybridization between aptamers and their complementary sequences (as capture and reporter probes conjugated with AuNPs). Zhu and co-workers proposed a method for the detection of Hg^{2+} using AuNPs [182]. In this method, mercury-ion–specific ssDNAs were heavily loaded on AuNPs which were linked on the electrode. This led to the extensive capture of a large amount of Hg^{2+}, resulting in a decrease of the electrochemical signal. The sensitivity of this method for Hg^{2+} was improved by three orders of magnitude compared with one of simple binding of Hg^{2+} by Hg^{2+}-specific ssDNA on an electrode. Similarly, the sensitive electrochemical aptasensor for ATP detection was also reported [183]. In this method, many ATP-binding aptamers were grafted on AuNPs by the hybridization with partially complemented ssDNA. Then the aptamer-grafted AuNPs were held on the gold electrode by the hybridization between the single-sequenced region of aptamer and another partially complemented capture DNA immobilized on the electrode. The MB bound to the dsDNA and also bound to guanine bases for the generation of strong electrochemical signal. The duplex structure was destroyed by the addition of ATP, which decreased the amount of MB on the electrode. As a result, a peak current was significantly decreased. This aptasensor could detect ATP as low as 0.1 nM, which is a markedly amplified sensitivity compared with use of a single ATP-binding aptamer.

4 Future Perspectives

Many researchers have demonstrated that aptamers are very useful bioreceptors in various fields such as therapeutics, medical diagnostics, biosensors for environmental monitoring and food safety, bioseparation, and bioimaging. In addition, the success of Macugen® (Pfizer), the first FDA-approved aptamer drug, in the pharmaceutical industry has accelerated researchers' interest in the isolation and applications of aptamers. However, aptamers for other targets remain few compared with antibodies, and only a few aptamers have been isolated and used in reports describing aptamer applications. Therefore, aptamers for more varied targets are required because it is expected that the spectrum of analytes will be greatly expanded in various applications. To meet the extensive requirement of

Table 1 Examples of modified SELEX process

Designation	Description	References
Negative-SELEX	- Include selection without targets to exclude nonspecifically bound nucleic acids to solid matrix	[76]
Counter-SELEX or	- Exclude the nucleic acids bound to structurally similar or abundant molecules in real samples	[29, 43–47]
Subtractive SELEX	- To improve the specificity of aptamers	
Photo-SELEX	- Using photoreactive molecule-modified nucleic acids library to induce cross-linking between targets and nucleic acids	[69]
Genomic SELEX	- Using nucleic acids library derived from organism's genome	[23, 70, 71]
	- Useful for studies on regulation or interaction between biological target molecules and nucleic acids	
Primer-free SELEX	- Primer sequences are excluded from library before incubation with target and are incorporated at PCR step	[74, 75]
	- Useful for screening of short aptamers	
Tailored SELEX	- Using random library flanked by short bridge sequences for primers that are linked and removed during SELEX process	[76]
	- Useful for screening of short aptamers	
Chimeric SELEX	- Using recombined nucleic acids library that originate from two or more different aptamer sequences	[35]
	- Generate bifunctional aptamers	
Multistage SELEX	- After five to six rounds of SELEX, two nucleic acid pools are fused to form a new longer nucleic acid library used in the next round for both targets	[77]
	- Generate bifunctional aptamers	
Toggle-SELEX	- Switching between different targets during alternating rounds of selection	[22, 38]
	- Generate aptamers having high universality	
FluMag-SELEX	- Targets are immobilized on magnetic beads	[9, 24, 38, 39]
	- Unbound nucleic acids are removed by magnetic separation	
	- Using fluorescein-modified nucleic acids pool	

(continued)

Table 1 (continued)

Designation	Description	References
CE-SELEX	- Using capillary electrophoresis to separate target-bound nucleic acids from unbound or weakly bound nucleic acids pool - Not suitable for low-weight molecular targets	[81–84]
Non-SELEX	- Performing repetitive selections without PCR amplification - Nonequilibrium capillary electrophoresis of equilibrium mixtures (NECEEM) is used for separation	[21]
Automatic SELEX	- Using robotic workstation for repetitive separation and amplification - To improve SELEX efficiency	[85–91]
SELEX-on-a chip	- Performing competitive binding for multiple targets and individual elution on MEMS chip - Targets are embedded in sol-gel droplets	[92]
Microfluidic SELEX	- Integration of microfluidics chip with magnetic separation - Manipulating small amount of beads with high partitioning coefficient	[93, 94]
GO-SELEX	- Graphene oxide (GO) used as an absorbent of nucleic acid pool - Target induces the displacement of nucleic acids from GO	[103]
Cell-SELEX or Tissue SELEX	- For aptamer screening to complex targets such as whole cells or tissues - Various molecules on cells or tissues are targets of selected aptamers	[47, 106–108]

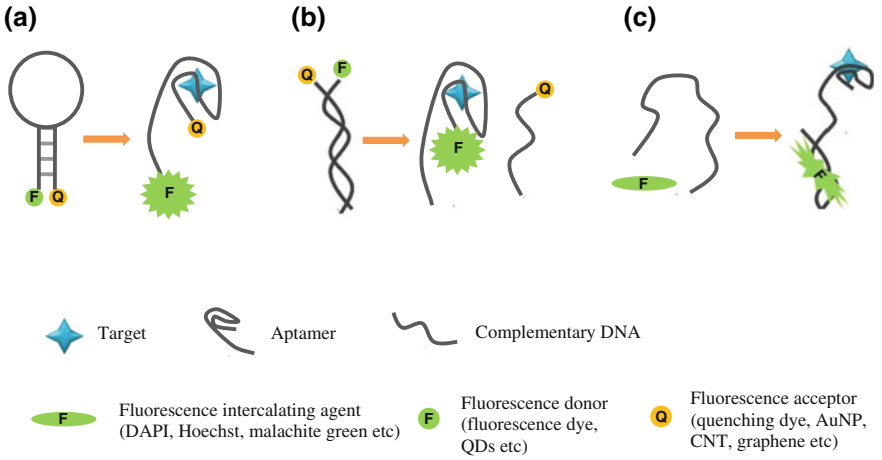

Fig. 2 Various types of fluorescent aptasensors. (**a**) FRET assay using aptabeacon conjugated with fluorescence donor and acceptor; (**b**) fluorescent assay based on target-induced displacement of complementary DNA (CD) from aptamer–CD duplex; (**c**) label-free fluorescence aptasensor using intercalating fluorescence dye

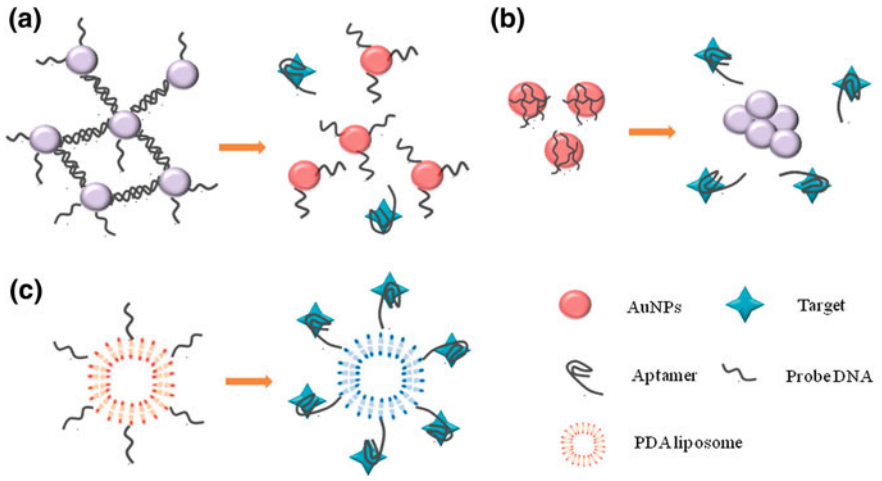

Fig. 3 Various types of colorimetric aptasensors. (**a**) Colorimetric assay using AuNP aggregates cross-linked via aptamers and probe DNA; (**b**) unmodified AuNP-based colorimetric aptasensing; (**c**) PDA liposome-based colorimetric aptasensing

aptamers for various targets, researchers will be continuously trying to advance the SELEX process by improving the automation degree and efficiency, development of more high-throughput processes and new screening techniques, and reducing the limitation to targets. Towards these goals, a clearer understanding of the binding mechanism of aptamers to targets and their binding structure in various conditions is needed.

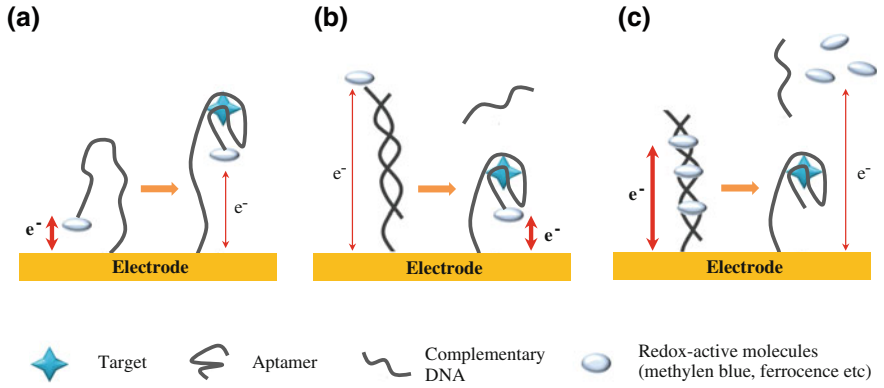

Fig. 4 Various types of electrochemical aptasensors. (**a**) Target-induced conformation change-based electrochemical aptasensing using redox active molecules modified aptamer (signal-off mode); (**b**) electrochemical aptasensing based on target-induced displacement format (signal-on mode); (**c**) electrochemical signal amplification in aptasensors using intercalating electroactive component

There is no doubt that studies on aptasensors will be continuously and actively increasing based on various merits of aptamers as bioreceptors. In spite of these bright perspectives, aptamer-based biosensors also have some hurdles to overcome. Aptasensor technology is immature compared to immunoassays, and the biosensing and diagnostic market is still largely dominated by antibodies. Only a few aptamer-based biosensors are commercially available.

However, aptasensors have one promising area for detection of small molecules in biological systems, the environment, and food safety because it is very difficult to produce highly specific antibodies for small molecules. For successful commercial applications of aptasensors for low-molecular–weight components, some technical issues should be overcome. First, a stronger affinity of aptamers for small molecules is needed because the affinity of aptamers significantly affects sensitivity. In many cases, especially in the environment, small molecules exist in very low concentrations. Related to this, the post-SELEX including truncation and study of the binding site will become a more conventional step to downsize the aptamers and improve the aptamers' affinity. Truncations of isolated aptamers can not only reduce the synthetic cost meaningfully, but also raise the affinity of original aptamers to targets in some cases. More powerful signal amplification methods are expected to be developed by implementation of various NPs as powerful probe materials, and new sensing mechanisms. Secondly, most aptasensors were tested in defined buffer solution. They should be examined on complex real samples for practical applications. The sensitivity of aptasensors often declines remarkably in real biological or environmental samples. To overcome this problem, aptamer screening has been attempted in real samples, not defined buffer solution. Finally, simpler, more cost-effective, and high-throughput aptasensors are needed. To meet these requirements, the development of

aptasensors should be label-free, real-time, multiplex, and miniaturized systems. All of these efforts on aptasensors will facilitate their commercialization (Table 1, Figs. 2, 3, 4).

References

1. Ellington AD, Szostak JW (1990) In vitro selection of RNA molecules that bind specific ligands. Nature 346:818–822
2. Tuerk C, Gold L (1990) Systematic evolution of ligands by exponential enrichment: RNA ligands to bacteriophage T4 DNA-polymerase. Science 249:505–510
3. Jayasena SD (1999) Aptamers: an emerging class of molecules that rival antibodies in diagnostics. Clinic Chem 45:1628–1650
4. Patel DJ, Suri AK, Jiang F, Jiang LC, Fan F, Kumar RA, Nonin S (1997) Structure, recognition and adaptive binding in RNA aptamer complex. J Mol Biol 272:645–664
5. Hermann T, Patel DJ (2000) Adaptive recognition by nucleic acid aptamers. Science 87:820–825
6. Osborne SE, Ellington AE (1997) Nucleic acid selection and the challenge of combinatorial chemistry. Chem Rev 97:349–370
7. Jenison RD, Gill SC, Pardi A, Polisky B (1994) High-resolution molecular discrimination by RNA. Science 263:1425–1429
8. Geiger A, Burgstaller P, Von der Eltz H, Roeder A, Famulok M (1996) RNA aptamers that bind L-arginine with sub-micromolar dissociation constants and high enantioselectivity. Nucleic Acids Res 24:1029–1036
9. Niazi JH, Lee SJ, Kim YS, Gu MB (2008) ssDNA aptamers that selectively bind oxytetracycline. Bioorg Med Chem 16:1254–1261
10. You KM, Lee SH, Im A, Lee SB (2003) Aptamers as functional nucleic acids: in vitro selection and biotechnological applications. Biotech Bioprocess Eng 8:64–75
11. Tombelli S, Minunni M, Mascini M (2005) Analytical application of aptamers. Biosens Bioelectron 20:2424–2434
12. Baldrich E, Acero JL, Reekmans G, Laureyn W, O'Sullivan CK (2005) Displacement enzyme linked aptamer assay. Anal Chem 77:4774–4784
13. Robertson DL, Joyce GF (1990) Selection in vitro of an RNA enzyme that specifically cleaves single-stranded DNA. Nature 344:467–468
14. Ho SP, Britton DH, Stone BA, Behrens DL, Leffet LM, Hobbs FW, Miller JA, Trainor GL (1996) Potent antisense oligonucleotides to human multidrug resistance-1 mRNA are rationally selected by mapping RNA-accessible sites with oligonucleotide libraries. Nucleic Acids Res 24:1901–1907
15. Bock LC, Griffin LC, Latham JA, Vermaas EH, Toole JJ (1992) Selection of single-stranded DNA molecules that bind and inhibit human thrombin. Nature 355:564–566
16. Marshall KA, Ellington AD (2000) In vitro selection of RNA aptamers. Meth Enzymol 318:19–214
17. Sampson T (2003) Aptamers and SELEX: the technology. World Patent Inf 25:123–129
18. Harada K, Frankel AD (1995) Identification of two novel arginine binding DNAs. EMBO J 23:5798–5811
19. Hamula C, Guthrie J, Zhang H, Li XF, Le XC (2006) Selection and analytical applications of aptamers. Tr Anal Chem 25:681–691
20. Reinemann C, Stoltenburg R, Strehlitz B (2009) Investigations on the specificity of DNA aptamers binding to ethanolamine. Anal Chem 81:3973–3978

21. Berezovski M, Drabovich A, Krylova SM, Musheev M, Okhonin V, Petrov A, Krylov SN (2005) Nonequilibrium capillary electrophoresis of equilibrium mixtures: a universal tool for development of aptamers. J Am Chem Soc 127:3165–3171
22. White R, Rusconi C, Scardino E, Wolberg A, Lawson J, Hoffman M, Sullenger B (2001) Generation of species cross-reactive aptamers using "toggle" SELEX. Mol Ther 4:567–573
23. Shimada T, Fujita N, Maeda M, Ishihama A (2005) Systematic search for the Cra-binding promoters using genomic SELEX system. Genes Cells 10:907–917
24. Stoltenburg R, Reinemann C, Strehlitz B (2005) FluMag-SELEX as an advantageous method for DNA aptamer selection Anal. Bioanal Chem 383:83–91
25. Bianchini M, Radrizzani M, Brocardo MG, Reyes GB, Gonzalez SC, Santa-Coloma TA (2001) Specific oligobodies against ERK-2 that recognize both the native and the denatured state of the protein. J Immunol Methods 252:191–197
26. Theis MG, Knorre A, Kellersch B, Moelleken J, Wieland F, Kolanus W, Famulok M (2004) Discriminatory aptamer reveals serum response element transcription regulated by cytohesin-2. Proc Natl Acad Sci 101:11221–11226
27. Weiss S, Proske D, Neumann M, Groschup MH, Kretzschmar HA, Famulok M, Winnacker EL (1997) RNA aptamers specifically interact with the prion protein PrP. J Virol 71:8790–8797
28. Bridonneau P, Chang YF, Buvoli VB, O'Connell D, Parma D (1999) Site directed selection of oligonucleotide antagonists by competitive elution. Antisens. Nucleic A 9:1–11
29. Sefah K, Shangguan D, Xiong X, O'Donoghue MB, Tan W (2010) Development of DNA aptamers using cell-SELEX. Nat Protocol 5:1169–1185
30. Cadwell RC, Joyce GF (1994) Mutagenic PCR. PCR methods Appl 3:S136–S140
31. Bittker JA, Le BV, Liu DR (2002) Nucleic acids evolution and minimization by nonhomologous random recombination. Nat Biotechnol 20:1204–1209
32. Paul A, Avci-Adali M, Ziemer G, Wendel HP (2009) Streptavidin-coated magnetic beads for DNA strand separation implicate a multitude of problems udirng cell-SELEX. Oligonucleotides 19:243–254
33. Fitzwater T, Polisky B (1996) A SELEX primer Methods Enzymol 267:275–301
34. Naimuddin M, Kitamura K, Kinoshita Y, Honda-Takahashi Y, Murakami M, Ito M, Yamamoto K, Hanada K, Husimi Y, Nishigaki K (2007) Selection-by-function: efficient enrichment of cathepsin E inhibitors from a DNA library. J Mol Recognit 20:58–68
35. Wu LH, Curran JF (1999) An allosteric synthetic DNA. Nucleic Acids Res 27:1512–1516
36. Williams KP, Bartel DP (1995) PCR product with strands of unequal length. Nucleic Acids Res 23:4220–4221
37. Hendry P, Hannan G (1996) Detection and quantitation of unlabeled nucleic acids in polyacrylamide gels. Biotechniques 20:258–264
38. Niazi JH, Lee SJ, Gu MB (2008) Single stranded DNA aptamers specific for antibiotics tetracyclines. Bioorg Med Chem 16:7245–7253
39. Kim YS, Hyun CJ, Kim IA, Gu MB (2010) Isolation and characterization of enantioselective DNA aptamers for ibuprofen. Bioorg Med Chem 18:3467–3473
40. Shi H, Fan XC, Ni ZY, Lis JT (2002) Evolutionary dynamics and population control during in vitro selection and amplification with multiple targets. RNA 8:1461–1470
41. Beinoraviciute-Kellner R, Lipps G, Krauss G (2005) In vitro selection of DNA binding sites for ABF1 protein from Saccharomyces cerevisiae. FEBS Lett 579:4535–4540
42. Rhie A, Kirby L, Sayer N, Wellesley R, Disterer P, Sylvester I, Gill A, Hope J, James W, Tahiri-Alaoui A (2003) Characterization of 2'-fluoro-RNA aptamers that bind preferentially to disease-associated conformations of prion protein and inhibit conversion. J Biol Chem 278:39697–39705
43. Ellington AD, Szostak JW (1992) Selection in vitro of single-stranded DNA molecules that fold into specific ligand-binding structures. Nature 355:850–852
44. Wang W, Jia L (2009) Progress in aptamer screening methods. Chin J Anal Chem 37:454–460

45. Wang CL, Zhang M, Yang G, Zhang DJ, Ding HM, Wang HX, Fan M, Shen BF, Shao NS (2003) Single-stranded DNA aptamers that bind differentiated but not parental cells: subtractive systematic evolution of ligands by exponential enrichment. J Biotechnol 102:15–22
46. Shangguan D, Li Y, Tang Z, Cao ZC, Chen HW, Mallikaratchy P, Sefah K, Yang CZ, Tan W (2006) Aptamers evolved from live cells as effective molecular probes for cancer study. Proc Natl Acad Sci 103:11838–11843
47. Conrad RC, Baskerville S, Ellington AD (1995) In vitro selection methodologies to probe RNA function and structure. Mol Div 1:69–78
48. Thompson JD, Higgins DG, Gibson TJ (1994) CLUSTAL W: improving the sensitivity of progressive multiple sequence alignment through sequence weighting, position-specific gap penalties and weight matrix choice. Nucleic Acids Res 22:4673–4680
49. Chenna R, Sugawara H, Koike T, Lopez R, Gibson TJ, Higgins DG, Thompson JD (2003) Multiple sequence alignment with the clustal series of programs. Nucleic Acids Res 31:3497–3500
50. Morgenstern B (2004) DIALIGN: multiple DNA and Protein Sequence Alignment at BiBiServ. Nucleic Acids Res 32:W33–W36
51. Morgenstern B, Prohaska SJ, Pöhler D, Stadler PF (2006) Multiple sequence alignment with user-defined anchor points. Algorithms Mol Boil 1:6
52. Zuker M (2003) Mfold web server for nucleic acid folding and hybridization prediction. Nucleic Acids Res 31:3406–3415
53. Horn WT, Convery MA, Stonehouse NJ, Adams CJ, Liljas L, Phillips SEV, Stockley PG (2004) The crystal structure of a high affinity RNA stem-loop complexed with the bacteriophage MS2 capsid: further challenges in the modeling of ligand-RNA interactions. RNA 10:1776–1782
54. Macaya RF, Schultze P, Smith FW, Roe JA, Feigon J (1993) Thrombin binding DNA aptamer forms a unimolecular quadruplex structure in solution. Proc Natl Acad Sci 90:3745–3749
55. Chaloin L, Lehmann MJ, Sczakiel G, Restle T (2002) Endogenous expression of a high-affinity pseudoknot RNA aptamer suppresses replication of HIV-1. Nucleic Acids Res 30:4001–4008
56. Bruno JG, Kiel JL (1999) In vitro selection of DNA aptamers to anthrax spores with electrochemiluminescence detection. Biosens Bioelectron 14:457–464
57. Ruff KM, Snyder TM, Liu DR (2010) Enhanced functional potential of nucleic acid aptamer library patterned to increase secondary structure. J Am Chem Soc 132:9453–9464
58. Wilson C, Keefe AD (2006) Building oligonucleotide therapeutics using non-natural chemistries. Curr Opin Chem Biol 10:607–614
59. Kusser W (2000) Chemically modified nucleic acid aptamers for in vitro selections: evolving evolution. J Biotechnol 74:27–38
60. Pieken W, Olsen DB, Benseler F, Aurup H, Eckstein HF (1991) Kinetic characterization of ribonuclease-resistant 2′-modified hammerhead ribozymes. Science 253:314–317
61. Heidenreich O, Eckstein F (1992) Hammerhead ribozyme-mediated cleavage of the long terminal repeat RNA of human immunodeficiency virus type 1. J Biol Chem 267:1904–1909
62. Kubik MF, Bell C, Fitzwater T, Watson SR, Tasset DM (1997) Isolation and characterization of 2'-fluoro-, 2'-amino-, and 2'-fluoro-/amino- modified RNA ligands to human INF-gamma that inhibit receptor binding. J Immunol 159: 259–267
63. Prakash TP, Bhat B (2007) 2'-modified oligonucleitides for antisense therapeutics. Curr Top Med Chem 7:641–649
64. Koizumi M (2007) True antisense oligonucleotides with modified nucleotides restricted in the N-conformation. Curr Top Med Chem 7:661–665
65. Sawai H, Ozaki A, Satoh F, Ohbayashi T, Masud M, Ozaki H (2001) Expansion of structural and functional diversities of DNA using new 5-substituted deoxyuridine

derivatives by PCR with superthermophilic KOD Dash DNA polymerase, Chem Commun 24:2604–2605
66. Kuwahara M, Hanawa K, Ohsawa K, Kitagata R, Ozaki H, Sawai H (2006) Direct PCR amplification of various modified DNAs having amino acids: convenient preparation of DNA libraries with high-potential activities for in vitro selection. Bioorg Med Chem 14:2518–2526
67. Keefe AD, Cload ST (2008) SELEX with modified nucleotides. Curr Opion Chem Biol 12:448–456
68. Golden MC, Collins BD, Willis MC, Koch TH (2000) Diagnostic potential of photoSELEX-evolved ssDNA aptamers. J Biotechnol 81:167–178
69. Singer BS, Shtatland T, Brown D, Gold L (1997) Libraries for genomic SELEX. Nucleic Acids Res 25:781–786
70. Shtatland T, Gill SC, Javornik BE, Johansson HE, Singer BS, Uhlenbeck OC, Zichi DA, Gold L (2000) Interactions of Escherichia coli RNA with bacteriophage MS2 coat protein: genomic SELEX. Nucleic Acids Res 28:E93
71. Fischer NO, Tok J, Tarasow TM (2008) Massively parallel interrogation of aptamer sequence, structure and function. PLoS ONE 3:e2720
72. Katilius E, Flores C, Woodbury NW (2007) Exploring the sequence space of a DNA aptamer using microarrays. Nucleic Acids Res 35:7626–7635
73. Wen JD, Gray DM (2004) Selection of genomic sequences that bind tightly to Ff gene 5 protein: primer-free genomic SELEX. Nucleic Acids Res 32:e182
74. Pan WH, Xin P, Clawson GA (2008) Minimal primer and primer-free SELEX protocols for selection of aptamers from random DNA libraries. Biotechniques 44:351–360
75. Vater A, Jarosch F, Buchner K, Klussmann S (2003) Short bioactive Spiegelmers to migraine-associated calcitonin gene-related peptide rapidly identified by a novel approach: tailored-SELEX. Nucleic Acids Res 31:e130
76. Burke DH, Willis JH (1998) Recombination, RNA evolution, and bifunctional RNA molecules isolated through Chimeric SELEX. RNA 4:1165–1175
77. Deng Q, German I, Buchanan D, Kennedy RT (2001) Retention and separation of adenosine and analogues by affinity chromatography with an aptamer stationary phase. Anal Chem 73:5415–5421
78. Bruno JG, Kiel JL (2002) Use of magnetic beads in selection and detection of biotoxin aptamers by electrochemiluminescence and enzymatic methods. Biotechniques 32(178–180): 182–173
79. Tok JB, Fischer NO (2008) Single microbead SELEX for efficient ssDNA aptamer generation against botulinum neurotoxin. Chem Comm 16:1883–1885
80. Mendonsa SD, Bowser MT (2004) In vitro selection of high-affinity DNA ligands for human IgE using capillary electrophoresis. Anal Chem 76:5387–5392
81. Tang JJ, Xie JW, Shao NS, Yan Y (2006) The DNA aptamers that specifically recognize ricin toxin are selected by two in vitro selection methods. Electrophoresis 27:1303–1311
82. Drabovich AP, Berezovski M, Okhonin V, Krylov SN (2006) Selection of smart aptamers by methods of kinetic capillary electrophoresis. Anal Chem 78:3171–3178
83. Mosing RK, Mendonsa SD, Bowser MT (2005) Capillary electrophoresis-SELEX selection of aptamers with affinity for HIV-1 reverse transcriptase. Anal Chem 77:6107–6112
84. Cox JC, Rudolph P, Ellington AD (1998) Automated RNA selection. Biotechnol Prog 14:845–850
85. Cox JC, Ellington AD (2001) Automated selection of anti-protein aptamers. Bioorg Med Chem 9:2525–2531
86. Cox JC, Rajendran M, Riedel T, Davidson EA, Sooter LJ, Bayer TS, Schmitz BM, Ellington AD (2002) Automated acquisition of aptamer sequences. Comb Chem High Throughput Screening 5:289–299
87. Cox JC, Hayhurst A, Hesselberth J, Bayer TS, Georgiou G, Ellington AD (2002) Automated selection of aptamers against protein targets translated in vitro: from gene to aptamer. Nucleic Acids Res 30:e108

88. Hianik T, Ostatna V, Sonlajtnerova M, Grman I (2007) Influence of ionic strength, pH, and aptamer configuration for binding affinity to thrombin. Biochem 70:127–133
89. Eulberg D, Buchner K, Maasch C, Klussmann S (2005) Development of an automated in vitro selection protocol to obtain RNA-based aptamers: identification of a biostable substance P antagonist. Nucleic Acids Res 33:e45
90. Hybarger G, Bynum J, Williams RF, Valdes JJ, Chambers JP (2006) A microfluidic SELEX prototype. Anal Bioanal Chem 384:191–198
91. Park SM, Ahn JY, Jo MJ, Lee D, Lis JT, Craighead HG, Kim S (2009) Selection and elution of aptamers using nanoporous sol-gel arrays with integrated microheaters. Lab Chip 9:1206–1212
92. Lou X, Qian J, Xiao Y, Viel L, Gerdon AE, Lagally ET, Atzberger P, Tarasow TM, Heeger AJ, Soh HT (2009) Micromagnetic selection of aptamers in microfluidic channels. Proc Natl Acad Sci 106:2989–2994
93. Gian J, Lou X, Zhang Y, Xiao Y, Soh HT (2009) Generation of high specific aptamers via micromagnetic selection. Anal Chem 81:5490–5495
94. Ciesiolka J, Gorski J, Yarus M (1995) Selection of an RNA domain that binds Zn2+. RNA 1:538–550
95. Hofmann HP, Limmer S, Hornung V, Sprinzl M (1997) Ni2 + -binding RNA motifs with an asymmetric purine-rich internal loop and a G-A base pair. RNA 3:1289–1300
96. Kim M, Um HJ, Bang S, Lee SH, Oh SJ, Han JH, Kim KW, Min J, Kim YH (2009) Arsenic removal from Vietnamese groundwater using the Arsenic-binding DNA aptamer. Environ Sci Technol 43:9335–9340
97. Mann D, Reinemann C, Stoltenburg R, Strehlitz B (2005) In vitro selection of DNA aptamers binding ethanolamine. Biochem Biophys Res Commun 338:1928–1934
98. Grate D, Wilson C (2001) Inducible regulation of the S-cerevisiae cell cycle mediated by an RNA aptamer-ligand complex. Bioorg Med Chem 9:2565–2570
99. Stojanovic MN, Landry DW (2002) Aptamer-based colorimetric probe for cocaine. J Am Chem Soc 124:9678–9679
100. Kato T, Takemura T, Yano K, Ikebukuro K, Karube I (2000) In vitro selection of DNA aptamers which bind to cholic acid. Biochim Biophys Acta 1493:12–18
101. Vianini E, Palumbo M, Gatto B (2001) In vitro selection of DNA aptamers that bind L-tyrosinamide. Bioorg Med Chem 9:2543–2548
102. Park JW, Tatavarty R, Kim DW, Jung HE, Gu MB (2012) Immobilization-free screening of aptamers assisted by graphene oxide. Chem Com 48:2071–2073
103. Wu M, Kempaiah R, Huang PJJ, Maheshwari V, Liu J (2011) Adsorption and desorption of DNA on graphene oxide studies by fluorescently labeled oligonucleotides. Langmuir 27:2731–2738
104. Nutiu R, Li YF (2005) In vitro selection of structure-switching signaling aptamers. Angew Chem Int Edit 44:1061–1065
105. Daniels DA, Chen H, Hicke BJ, Swiderek KM, Gold L (2003) A tenascin-C aptamer identified by tumor cell SELEX: systematic evolution of ligands by exponential enrichment. Proc Natl Acad Sci 100:15416–15421
106. Cerchia L, Duconge F, Pestourie C, Boulay J, Aissouni Y, Gombert K, Tavitian B, de Franciscis V, Libri D (2005) Neutralizing aptamers from whole-cell SELEX inhibit the RET receptor tyrosine kinase. PLoS Biol 3:697–704
107. Tang Z, Shangguan D, Wang K, Shi H, Sefah K, Mallikratchy P, Chen HW, Li Y, Tan W (2007) Selection of aptamers for molecular recognition and characterization of cancer cells. Anal Chem 79:4900–4907
108. Kim YS, Jung HS, Matsuura T, Lee HY, Kawai T, Gu MB (2007) Electrochemical detection of 17β-estradiol using DNA aptamer immobilized gold electrode chip. Biosens Bioelectron 22:2525–2531
109. Song S, Wang L, Li J, Zhao J, Fan C (2008) Aptamer-based biosensors. Trends Anal Chem 27:108–117

110. Li D, Song S, Fan C (2010) Target-responsive structural switching for nucleic acid-based sensors. Acc Chem Res 43:631–614
111. Yamamoto R, Baba T, Kumar PK (2000) Molecular beacon aptamer fluorescence in the presence of Tat protein of HIV-1. Genes Cells 5:389–396
112. Frauendorf CA, Jaschke A (2001) Detection of small organic analytes by fluorescing molecular switches. Bioorg Med Chem 9:2521–2524
113. Song Y, Zhao C, Ren J, Qu X (2009) Rapid and ultra-sensitive detection of AMP using a fluorescent and magnetic nano-silica sandwich complex. Chem Commun 15:1975–1977
114. Nutiu R, Li Y (2003) Structure-switching signaling aptamers. J Am Chem Soc 125:4771–4778
115. Cruz-Aguado JA, Penner G (2008) Fluorescence polarization based displacement assay for the determination of small molecules with aptamers. Anal Chem 80:8853–8855
116. Wu C, Yan L, Wang C, Lin H, Wang C, Chen X, Yang CJ (2010) A general excimer signaling approach for aptamer sensors. Biosens Bioelectron 25:2232–2237
117. Liu JW, Lee JH, Lu Y (2007) Quantum dot encoding of aptamer-linked nanostructures for one-pot simultaneous detection of multiple analytes. Anal Chem 79:4120–4125
118. Fan C, Wang S, Hong JW, Bazan GC, Plaxco KW, Heeger AJ (2003) Beyond superquenching: hyper-efficient energy transfer from conjugated polymers to gold nanoparticles. Proc Natl Acad Sci 100:6297–6301
119. Song S, Liang Z, Zhang J, Wang L, Li G, Fan C (2009) Gold-nanoparticle-based multicolor nanobeacons for sequence-specific DNA analysis. Angew Chem Int Ed 48:8670–8674
120. Zhang J, Wang L, Zhang H, Boey F, Song S, Fan C (2010) Aptamer-based multicolor fluorescent gold nanoparticles for multiplex detection in homogenous solution. Small 6:201–204
121. Kim YS, Jurng J (2011) Gold nanoparticle-based homogeneous fluorescent aptasensor for multiplex detection. Analyst 136:3720–3724
122. Yang R, Tang Z, Yan J, Kang H, Kim Y, Zhu Z, Tan W (2008) Noncovalent assembly of carbon nanotubes and single-stranded DNA: an effective sensing platform for probing biomolecular interactions. Anal Chem 80:7408–7413
123. Chang H, Tang L, Wang Y, Jiang J, Li J (2010) Graphene fluorescence resonance energy transfer aptasensor for the thrombin detection. Anal Chem 82:2341–2346
124. Sheng L, Ren J, Miao Y, Wang J, Wang E (2011) PVP-coated graphene oxide for selective determination of ochratoxin A via quenching fluorescence of free aptamer. Biosens Bioelectron 26:3494–3499
125. Stojanovic MN, de Prada P, Landry DW (2001) Aptamer-based folding fluorescent sensor for cocaine. J Am Chem Soc 123:4928–4931
126. Liu CW, Huang CC, Chang HT (2009) Highly selective DNA-based sensor for lead(II) and mercury(II) ions. Anal Chem 81:2383–2387
127. Ozaki H, Nishihira A, Wakabayashi M, Kuwahara M, Sawai H (2006) Biomolecular sensor based on fluorescence-labeled aptamer. Bioorg Med Chem Lett 16:4381–4384
128. Xiang Y, Tong A, Lu Y (2009) Abasic site-containing DNAzyme and aptamer for label-free fluorescent detection of Pb2 + and adenosine with high sensitivity, selectivity, and tunable dynamic range. J Am Chem Soc 131:15352–15357
129. Xiang Y, Wang Z, Xing H, Wong NY, Lu Y (2010) Label-free fluorescent functional DNA sensors using unmodified DNA: a vacant site approach. Anal Chem 82:4122–4129
130. Xu Z, Morita K, Sato Y, Dai Q, Nishizawa S, Teramae N (2009) Label-free aptamer-based sensor using abasic site-containing DNA and a nucleobase-specific fluorescent ligand. Chem Commun 42:6445–6447
131. Li B, Qin C, Li T, Wang L, Dong S (2009) Fluorescent switch constructed based on hemin-sensitive anionic conjugated polymer and its applications in DNA-related sensors. Anal Chem 81:3544–3550
132. Zhang CY, Johnson LW (2009) Single quantum-dot-based aptameric nanosensor for cocaine. Anal Chem 81:3051–3055

133. Zhu Z, Yang C, Zhou X, Qin J (2011) Label-free aptamer-based sensors for L-argininamide by using nucleic acid minor groove binding dyes. Chem Commun 47:3192–3194
134. Xu W, Lu Y (2010) Label-free fluorescent aptamer sensor based on regulation of malachite green fluorescence. Anal Chem 82:574–578
135. Babendure JR, Adams SR, Tsien RY (2003) Aptamers switch on fluorescence of triphenylmethane dyes. J Am Chem Soc 125:14716–14717
136. Sando S, Narita A, Hayami M, Aoyama Y (2008) Transcription monitoring using fused RNA with a dyebinding light-up aptamer as a tag: a blue fluorescent RNA. Chem Commun 33:3858–3860
137. Furutani C, Shinomiya K, Aoyama Y, Yamada K, Sando S (2010) Modular blue fluorescent RNA sensors for label-free detection of target molecules. Mol BioSyst 6:1569–1571
138. Shi Y, Huang WT, Luo HQ, Li NB (2011) A label-free DNA reduced graphene oxide-based fluorescent sensor for highly sensitive and selective detection of hemin. Chem Commun 47:4676–4678
139. Huang CC, Chang HT (2008) Aptamer-based fluorescence sensor for rapid detection of potassium ions in urine. Chem Commun 12:1461–1463
140. Rotaru A, Dutta S, Jentzsch E, Gothelf K, Mokhir A (2010) Selective dsDNA-templated formation of copper nanoparticles in solution. Angew Chem Int Ed 49:5665–5667
141. Liu J, Lu Y (2003) A colorimetric lead biosensor using DNAzyme-directed assembly of gold nanoparticles. J Am Chem Soc 125:6642–6643
142. Liu J, Lu Y (2007) A DNAzyme catalytic beacon sensor for paramagnetic Cu2 + ions in aqueous solution with high sensitivity and selectivity. J Am Chem Soc 129:9838–9839
143. Zhang J, Wang L, Pan D, Song S, Boey F, Zhang H, Fan C (2008) Visual cocaine detection with gold nanoparticles and rationally engineered aptamer structures. Small 4:1196–1200
144. Liu J, Lu Y (2006) Fast colorimetric sensing of adenosine and cocaine based on a general sensor design involving aptamers and nanoparticles. Angew Chem Int Ed 45:90–94
145. Liu J, Mazumdar D, Lu Y (2006) A simple and sensitive "dipstick" test in serum based on lateral flow separation of aptamer-linked nanostructures. Angew Chem Int Ed 45: 7955–7959
146. Zhao WA, Chiuman W, Brook MA, Li YF (2007) Simple and rapid colorimetric biosensors based on DNA aptamer and noncrosslinking gold nanoparticle aggregation. ChemBioChem 8:727–731
147. Huang CC, Huang YF, Cao Z, Tan W, Chang HT (2005) Aptamer-modified gold nanoparticles for colorimetric determination of platelet-derived growth factors and their receptors. Anal Chem 77:5735–5741
148. Ono A, Torigou H, Tanaka Y, Okamoto I (2011) Binding of metal ions by pyrimidine base pairs in DNA duplexes. Chem Soc Rev 40:5855–5866
149. Lee JS, Han MS, Mirkin CA (2007) Colorimetric detection of mercuric ion (Hg2+) in aqueous media using DNA-functionalized gold nanoparticles. Angew Chem Int Ed 46:4093–4096
150. Xu H, Wang Y, Huang X, Li Y, Zhang H, Zhong X (2012) Hg2+ -mediated aggregation of gold nanoparticles for colorimetric screening of biothiols. Analyst 137:924–931
151. Li B, Du Y, Dong S (2009) DNA based gold nanoparticles colorimetric sensors for sensitive and selective detection of Ag(I) ions. Anal Chimi Acta 644:78–82
152. Li H, Rothberg L (2004) Colorimetric detection of DNA sequences based on electrostatic interactions with unmodified gold nanoparticles. Proc Natl Acad Sci 101:14036–14039
153. Wei H, Li B, Li J, Dong S, Wang E (2008) DNAzyme-based colorimetric sensing of lead (Pb2 +) using unmodified gold nanoparticle probes. Nanotechnology 19:1–5
154. Wang L, Liu X, Hu X, Song S, Fan C (2006) Unmodified gold nanoparticles as a colorimetric probe for potassium DNA aptamers. Chem Commun 28:3780–3782
155. Liu CW, Hsieh YT, Huang CC, Lin ZH, Chang HT (2008) Detection of mercury(II) based on Hg2 + –DNA complexes inducing the aggregation of gold nanoparticles. Chem Commun ***2242–2244

156. Kim YS, Kim JH, Kim IA, Lee SJ, Jurng J, Gu MB (2010) A novel colorimetric aptasensor using gold nanoparticle for a highly sensitive and specific detection of oxytetracycline. Biosens Bioelectron 26:1644–1649
157. Kim YS, Kim JH, Kim IA, Lee SJ, Gu MB (2011) The affinity ratio—Its pivotal role in gold nanoparticle-based competitive colorimetric aptasensor. Biosens Bioelectron 26:4058–4063
158. Wang J, Wang L, Liu X, Liang Z, Song S, Li W, Li G, Fan W (2007) A gold nanoparticle-based aptamer target binding readout for ATP assay. Adv Mater 19:3943–3946
159. Lee J, Kim HJ, Kim J (2008) Polydiacetylene liposome arrays for selective potassium detection. J Am Chem Soc 130:5010–5011
160. Lee J, Seo S, Kim J (2012) Colorimetric detection of warfare gases by polydiacetylenes toward equipment-free detection. Adv Func Mater 22:1632–1638
161. Liu X, Tang Y, Wang L, Zhang J, Song S, Fan C, Wang S (2007) Optical detection of mercury(II) in aqueous solutions by using conjugated polymers and label-free oligonucleotides. Adv Mater 19:1471–1474
162. Rodriguez MC, Kawde AN, Wang J (2005) Aptamer biosensor for label-free impedance spectroscopy detection of proteins based on recognition-induced switching of the surface charge. Chem Commun 2005:4267–4269
163. Radi AE, Sanchez JLA, Baldrich E, O'Sullivan CK (2005) Reusable impedimetric aptasensor. Anal Chem 77:6320–6323
164. Xu Y, Yang L, Ye XY, He PA, Fang YZ (2006) An aptamer-based protein biosensor by detecting the amplified impedance signal. Electroanal 18:1449–1456
165. Kim YS, Niazi JH, Gu MB (2009) Sepecific detection of oxytetracycline using DNA aptamer-immobilized interdigitated array electrode chip. Anal Chim Acta 634:250–254
166. Kim YJ, Kim YS, Niazi JH, Gu MB (2010) Electrochemical aptasensor for tetracycline detection. Bioprocess Biosyst Eng 33:31–37
167. Xiao Y, Lubin AA, Heeger AJ, Plaxco KW (2005) Label-free electronic detection of thrombin in blood serum by using an aptamer-based sensor. Angew Chem Int Ed 44:5456–5459
168. Baker BR, Lai RY, Wood MS, Doctor EH, Heeger AJ, Plaxco KW (2006) An electronic, aptamer-based small-molecule sensor for the rapid, label-free detection of cocaine in adulterated samples and biological fluids. J Am Chem Soc 128:3138–3139
169. Zuo X, Song S, Zhang J, Pan D, Wang L, Fan C (2007) A target-responsive electrochemical aptamer switch (TREAS) for reagentless detection of nanomolar ATP. J Am Chem Soc 129:1042–1043
170. Li X, Qi H, Shen L, Gao Q, Zhang C (2008) Electrochemical aptasensor for the determination of cocaine incorporating gold nanoparticles modification. Electroanalysis 13:1475–1482
171. Xiao Y, Piorek BD, Plaxco KW, Heeger AJ (2005) A reagentless signal-on architecture for electronic, aptamer-based sensors via target-induced strand displacement. J Am Chem Soc 127:17990–17991
172. Xiao Y, Rowe AA, Plaxco KW (2007) Electrochemical detection of parts-per-billion lead via an electrode-bound DNAzyme assembly. J Am Chem Soc 129:262–263
173. Lu Y, Li X, Zhang L, Yu P, Su L, Mao L (2008) Aptamer-based electrochemical sensors with aptamer-complementary DNA oligonucleotides as probe. Anal Chem 80:1883–1890
174. Wu Z, Guo M, Zhang S, Chen C, Jiang J, Shen G, Yu R (2007) Reusable electrochemical sensing platform for highly sensitive detection of small molecules based on structure-switching signaling aptamers. Anal Chem 79:2933–2939
175. Du Y, Li B, Wei H, Wang Y, Wang E (2008) Multifunctional label-free electrochemical biosensor based on an integrated aptamer. Anal Chem 80:5110–5117
176. Feng K, Sun C, Kang Y, Chen J, Jiang J, Shen G, Yu R (2008) Label-free electrochemical detection of nanomolar adenosine based on target-induced aptamer displacement. Electrochem Comm 10:531–535

177. Zhu Z, Su Y, Li J, Li D, Zhang J, Song S, Zhao Y, Li G, Fan C (2009) Highly sensitive electrochemical sensor for mercury(II) ions by using a mercury-specific oligonucleotide probe and gold nanoparticle-based amplification. Anal Chem 81:7660–7666
178. Ferapontova EE, Olsen EM, Gothelf KV (2008) An RNA aptamer-based electrochemical biosensor for detection of theophylline in resum. J Am Chem Soc 130:4256–4258
179. Feng K, Sun C, Kang Y, Chen J, Jiang JH, Shen GL, Yu RQ (2008) Electrochem Commun 10:531–535
180. Li X, Qi HL, Shen LH, Gao Q, Zhang CX (2008) Electrochemical aptasensor for the determination of cocaine incorporating gold nanoparticles modification. Electroanalysis 20:1475–1482
181. Wang X, Dong P, He PG, Fang YZ (2010) A solid-state electrochemiluminescence sensing platform for detection of adenosine based on ferrocene-labeled structure-switching signaling aptamer. Anal Chim Acta 658:128–132
182. Shen L, Chen Z, Li Y, Jing P, Xie S, He S, He P, Shao Y (2007) A chronocoulometric aptamer sensor for adenosine monophosphate. Chem Commun 21:2169–2171.
183. Du Y, Li B, Wang F, Dong S (2009) Au nanoparticles grafted sandwich platform used amplified small molecules electrochemical aptasensor. Biosens Bioelectron 24:1979–1983

Adv Biochem Eng Biotechnol (2014) 140: 69–92
DOI: 10.1007/10_2013_223

Published Online: 13 July 2013

Exploration of Structure-Switching in the Design of Aptamer Biosensors

Pui Sai Lau and Yingfu Li

Abstract The process of "structure-switching" enables biomolecular switches to function as effective biosensing tools. Biomolecular switches can be activated or inactivated by binding to a specific target that triggers a precise conformational change in the biomolecules involved. Although many examples of aptamer-based biomolecular switches can be found in nature, substantial effort has been made in the last decade to engineer structure-switching aptamer sensors by coupling aptamers to a signal transduction method to generate a readout signal upon target binding to the aptamer domain. This chapter focuses on the progress of research on engineered structure-switching aptamer sensors. We begin by discussing the origin of the structure-switching aptamer design, highlight the key developments of structure-switching DNA aptamers for fluorescence-, electrochemistry-, and colorimetry-based detection, and introduce our recent efforts in exploring RNA aptamers to create structure-switching molecular sensors.

Keywords Aptamer · DNA · RNA · Sensor · Structure-switching

Contents

P. S. Lau · Y. Li (✉)
Department of Biochemistry and Biomedical Sciences,
Department of Chemistry and Chemical Biology,
and Michael D. DeGroote Infectious Disease Research Institute,
McMaster University, 1280 Main Street West,
Hamilton ON, L8S 4K1, Canada
e-mail: liying@mcmaster.ca

1 Introduction

Nature has evolved biomolecular switches in all domains of life as biosensing tools to monitor its complex environmental surroundings. Made of nucleic acids or proteins, biomolecular switches effectively detect specific chemical signals (targets) to carry out precise biochemical functions within a cell. Through "structure-switching," nature's biosensors can become active/inactive, by target binding that induces specific conformational change of the biomolecules involved [1].

To date, the only known group of natural nucleic-acid-based biomolecular switches are riboswitches. Discovered by Ronald Breaker's group in 2002, riboswitches are RNA-based regulatory systems found in diverse organisms that respond to specific small molecules to regulate gene expression [2]. Typically composed of a molecular recognition element (aptamer domain) that binds to a specific target and a downstream expression domain, riboswitches operate through structure-switching events whereby target binding to the aptamer domain results in an overall change in the structure of the designated RNA to switch the expression domain to the "on" or "off" state.

Although the number of novel classes of riboswitches that respond to different metabolites continues to grow [3–5], many research groups have successfully engineered artificial riboswitches to broaden the versatility of controlling gene expression by RNA switches [6–14]. Interestingly, even before the discovery of riboswitches, the laboratories of Jack Szostak and Larry Gold independently developed a method to derive artificial aptamers in 1990 [15, 16]. Termed systematic evolution of ligands by exponential enrichment, or SELEX, this test-tube–based selection technique has been extensively used to isolate aptamers specific to a target of choice from random-sequence DNA or RNA libraries [17, 18]. Through the mechanism of structure-switching, many of these aptamers have been coupled to a signal transduction method to relay a readout signal produced by target binding to the aptamer domain [19, 20]. This is the subject of the current chapter.

Exploration of structure-switching for the design of aptamer-based biosensors is attractive for two particular reasons. First, structure-switching processes can ensure high detection specificity; that is because structure-switching can only be induced through specific target–aptamer interactions (which are difficult to imitate by noncognate targets). Second, structure-switching is highly compatible with a variety of signal transduction mechanisms for signal generation; the aptamer–ligand binding also brings about pronounced structural/physical rearrangement of the aptamer, which can be effortlessly coupled to many prevailing signal production mechanisms for the generation of an easily detectable signal, such as a change in fluorescence intensity, color appearance, and electrochemical readout.

The exploration of aptamers for engineering biosensors also comes with a number of advantages that reflect the innate properties of nucleic acids. These include the chemical stability of DNA, intricate folding capability of DNA and RNA, tendency of both DNA and RNA to form predictable duplex structural elements, ease of immobilization of DNA and RNA onto solid supports, and their

amenability to various chemical modifications [21]. This chapter focuses on research progress in structure-switching aptamer sensors made over the past decade. We discuss the origin of structure-switching aptamer design; highlight the key developments in investigating structure-switching DNA aptamers for biosensing in connection with fluorescent, electrochemical, and colorimetric platforms; and introduce our recent efforts in exploring RNA aptamers for the design of structure-switching molecular sensors.

2 The Origin of Structure-Switching DNA Aptamers

Early accounts of engineered structure-switching aptamer sensors began using DNA aptamers. Inspired by natural biomolecular switches and motivated to improve upon previous aptamer sensor designs that lacked wide applicability towards diverse aptamers, our group developed structure-switching DNA aptamers [22]. This approach takes advantage of the ability of aptamers to form both an aptamer–target complex and a DNA–DNA duplex with complementary sequences. By creating a DNA duplex composed of an extended DNA aptamer strand partly hybridized to complementary strands of fluorophore-labeled DNA (FDNA) and quencher-labeled DNA (QDNA), a low fluorescent signal is obtained due to the close proximity of the fluorophore and quencher moieties (the "off" mode). The addition of a target, however, facilitates formation of the target–aptamer complex and subsequent displacement of QDNA, generating a high fluorescent signal (the "on" mode; Fig. 1a). In this way, signaling reporters were successfully created for both anti-ATP [23] and anti-thrombin [24] aptamers.

The ATP reporter exhibited target specificity comparable to the original aptamer (which primarily recognizes the common adenosine group), and generated 10- to 14-fold fluorescence increase in the presence of adenosine and related analogues such as ATP, ADP, AMP, and dATP. Expectedly, no fluorescence increase was generated in the presence of CTP, UTP, or GTP. Similarly, the thrombin reporter only recognized the thrombin target, produced $\sim$12-fold fluorescence increase, but exhibited no signal for BSA and human factors Xa and IXa. The structure-switching design served well despite differences in binding affinity and size of the aptamers tested, thus demonstrating generality of the strategy [22].

To further extend the generality, our group developed three other structure-switching designs [22]. These alternative designs include the attachment of the fluorophore to the end of an aptamer (Fig. 1b) or at an internal nucleotide (Fig. 1c), and the hybridization of FDNA and QDNA with an aptamer without the addition of extra nucleotides (Fig. 1d). Notably, there are also examples of sensing strategies that make use of target-induced structure-switching, but do not involve the dissociation of a complementary oligonucleotide [25, 26].

Aptamers are artificially created through the SELEX process [15, 16]. In this technique, a randomized library of $\sim 10^{15}$ single-stranded DNA or RNA sequences is subjected to a selective pressure to separate molecules that pass a functional test

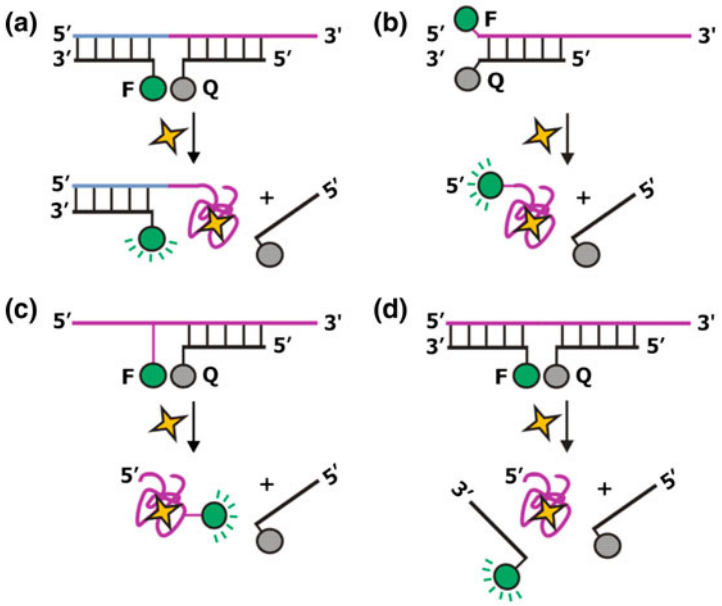

Fig. 1 Variations of the structure-switching design strategy. All examples make use of the ability of a DNA aptamer (*purple*) to form a duplex with a complementary DNA sequence, or a complex with a designated target (*star*). F and Q signify fluorophore and quencher, respectively. See main text for details

(i.e., target binding) from those that do not. Successful sequences are copied, and used to carry out the same procedure for another round. Through iterative rounds of selection and amplification, functional molecules "evolve," so that only the most effective sequences survive in the end (Fig. 2a).

Our group has developed a strategy to create structure-switching reporters directly through SELEX [27]. The potential advantage of this approach is that post-SELEX modification and optimization steps do not need to be taken to convert the selected aptamer into a signaling probe. In this study, the DNA library was specially designed to contain a central fixed-sequence domain flanked by two random-sequence domains, each of which was further flanked by a primer-binding sequence. The central fixed-sequence domain was purposely designed to be complementary to an antisense oligonucleotide biotinylated at its 5′-end (BDNA), which permitted immobilization of the DNA library onto streptavidin-coated beads. The immobilized DNA duplex was then exposed to a solution containing the target of interest. Oligonucleotides that were able to form the DNA/target complex were separated from the beads and were released into solution. These molecules were then collected, amplified by PCR, and processed for the next round of enrichment (Fig. 2b). Interestingly, all classes of ATP-binding aptamers obtained contained the previously isolated ATP-binding aptamer, which reinforces that SELEX often finds the same solution to a given problem. Other groups have

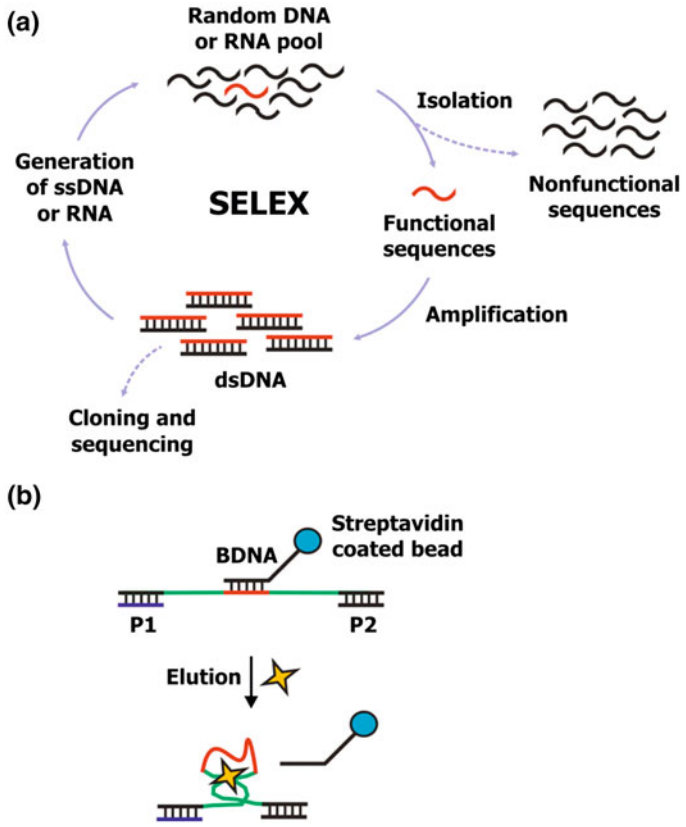

Fig. 2 **a** General SELEX scheme. **b** Application of SELEX to develop structure-switching reporters. Isolation step is depicted: DNA sequences are designed with two randomized sites (*green*) and fixed regions that hybridize with primers (*P1, P2*), and biotinylated DNA (*BDNA*). Only sequences capable of target (*star*) binding, and thus structure-switching, are eluted from the streptavidin beads and carried on for further SELEX rounds

also independently reported selection of the same ATP-binding motif [23, 28], despite differences in library designs and SELEX strategies used. Additionally, conserved nucleotides were also found outside the target-binding sites, suggesting that these regions are important for the structure-switching process. All selected reporters readily responded to ATP, however, the fluorescence increase was only ~4.5-fold. A possible explanation for this may lie in the finding that all selected aptamers acquired one or two nucleotide mutations in the site that binds to BDNA. Although a weaker aptamer–BDNA duplex enabled easier structure-switching throughout the course of SELEX, it also contributed to a higher background signal of the aptamer-based sensor. Therefore, improved structure-switching reporters may be developed in the future by using a more stringent SELEX design (i.e.,

elevated temperature during the functional selection step to eliminate weaker duplex structures) [27].

Since conception, structure-switching DNA aptamers have been expanded to detect various targets including GTP [27], mercury [29, 30], quinine [31], cocaine [32], arginine [33], IgE [34], L-tyrosinamide [35], cathepsin D [36], lysozyme [37], and PDGF [38], although most studies to date have predominantly focused on the anti-ATP and anti-thrombin DNA aptamers, which have become model systems for biosensor development. Moreover, the versatility of the structure-switching design has been adapted to function with other signal transduction methods including electrochemical and colorimetric platforms. In the following sections, we discuss some of the key advancements of structure-switching sensors using fluorescent, colorimetric, and electrochemical signal transduction mechanisms. To facilitate comparative analysis, we examine examples primarily based on the well-characterized anti-ATP and anti-thrombin DNA aptamers.

3 Structure-Switching DNA Aptamers in Fluorescent Sensors

Fluorescence is a commonly used method of signal transduction for aptamer sensors due to the ease of conjugation of various fluorophores and quenchers to DNA, and the convenience of detection conferred by widely available commercial instruments. Using the classic structure-switching design [22], our lab discovered that the ATP reporter produced a K_d of $\sim$600 μM [22], which is 60-fold lower in affinity than the original aptamer ($K_d = \sim 10$ μM) [23]. The thrombin reporter produced a K_d of $\sim$400 nM [22], which is a twofold reduction in affinity compared to the original aptamer ($K_d = 200$ nM) [24]. These findings suggest that the QDNA displacement step affects the target-binding affinity of aptamers with inherently low affinity more so than those with high affinity. Possible explanations for the reduced affinities of the structure-switching reporters include: (i) QDNA hybridization partially blocks the aptamer site, so the target must compete with QDNA for binding, and (ii) the low level of fluorescence generated from the signaling duplex (extended aptamer–FDNA–QDNA) itself may make it difficult to detect small increases in fluorescence from low target concentrations, which may be obscured within the background fluorescence associated with a large excess of unswitched duplex.

To enhance detection sensitivity, signal amplification methods can provide solutions. A commonly used assay format based on structure-switching involves a capture probe to bind a desired ligand at one site for immobilization, and a signaling probe to bind the ligand at another site for detection (Fig. 3a). In this way, Xiaogang Qu and colleagues have created an assay that makes use of fluorescent silica nanoparticles (FNPs), which can entrap many fluorophores in a single particle [39]. Compared with traditional fluorophores, FNPs are advantageous as they provide fluorescent signal amplification and higher photostability. The design by the Qu group involved use of magnetic silica microspheres functionalized with

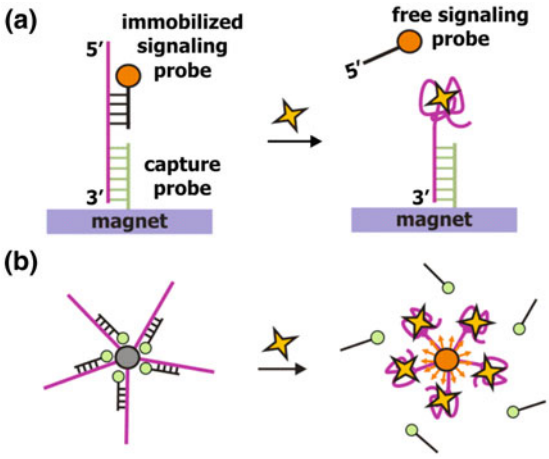

Fig. 3 **a** A structure-switching assay for fluorescence-based detection. The capture probe immobilizes the aptamer, and the signaling probe anneals to provide a readout signal upon target-induced structure-switching. Only the signal in solution from displaced signaling probes is measured after the magnetic separation step. **b** Quantum dots for multiplex detection; use of multiple aptamers, for many target-induced structure-switching events and high increase in fluorescent signal

DNA that hybridizes to a part of the anti-ATP aptamer (capture probe), and FNPs functionalized with DNA that hybridizes to another part of the aptamer (signaling probe). In the absence of the target, the capture probe-aptamer-signaling probe complex was separated from the solution magnetically, which resulted in low fluorescence in solution. However, when the target was introduced, the binding of the target to the aptamer resulted in a structure-switching event that separated FNPs from the complex and produced a high level of fluorescence in solution. This method exhibited a much improved detection limit of 0.1 μM.

Quantum dots (QDs) have also been explored for the purpose of signal amplification. From a molecular recognition perspective, the surface of QDs can be easily functionalized with multiple oligonucleotides to facilitate multiple binding interactions (Fig. 3b). From a signaling perspective, QDs provide higher photostability, sharper emission bands, and versatility for multiplex detection (QDs respond to the same excitation wavelength, but can be tuned to emit at different wavelengths). The Ellington group has designed a strategy whereby QDs were functionalized with multiple copies of an extended thrombin aptamer [40]. Hybridization of a complementary, quencher-modified DNA to the QD-aptamer resulted in low fluorescence due to the close proximity of the QD and quencher. The addition of thrombin, however, led to multiple target–aptamer binding interactions, and displacement of many quencher-modified DNA strands. The result of multiple structure-switching events generated signal amplification and a 19-fold fluorescence enhancement.

Yi Lu's group has taken QDs one step further for simultaneous detection of multiple targets within one pot [41]. Their design takes advantage of a number of properties of gold nanoparticles (AuNPs): the ability of AuNPs to quench fluorescence when in close proximity to QDs, the tunability of fluorescence quenching by controlling the aggregation or dispersal state of AuNPs, and the color changes associated with aggregation or dispersal of AuNPs due to surface plasmon resonance. In brief, when no target was added, AuNPs and QDs functionalized with complementary DNA sequences hybridized to an extended aptamer sequence. In this state, the AuNP–QD–aptamer complex aggregated to generate low fluorescence (due to close proximity of QD and AuNP), as well as a blue color from the AuNPs. In the presence of the target, however, target–aptamer binding occurred, which caused the functionalized QDs and AuNPs to dehybridize and disperse the aggregate. This subsequently led to high fluorescence signaling (separation of QD from AuNP), and a color change to red. Using this design, two different aptamer-based reporters were created to detect ATP and cocaine, respectively. The associated QDs for each reporter emitted at characteristic wavelengths of 525 and 585 nm, although the same excitation wavelength was used for both systems. ATP and cocaine were accurately detected simultaneously in the same solution using fluorescent and colorimetric means.

Over the last few years, structure-switching fluorescent reporters have started to move into the realm of more "real-life" detection involving the use of automation and complex samples. For drug discovery, our group implemented a structure-switching assay to search for enzyme inhibitors in a high-throughput screen (HTS) [42]. The therapeutic target used in this case was adenosine deaminase (ADA), a problematic metabolic enzyme in severe combined immunodeficiency diseases that irreversibly converts adenosine into inosine [43]. The well-established anti-ATP structure-switching aptamer reporter provided a suitable solution as a screening assay because the aptamer has a high affinity for adenosine, but does not bind inosine [23]. In the presence of adenosine, the target–aptamer complex formed and structure-switching occurred to generate high fluorescent signaling. However, in the presence of inosine (after ADA conversion of adenosine), the fluorescein-labeled aptamer bound to the complementary QDNA sequence, and fluorescence was quenched. The use of this screening assay resulted in the identification of small-molecule inhibitors of ADA out of a collection of 44,400 compounds [42].

Another automated approach that was demonstrated to be highly amenable with structure-switching sensors is fluorescence-activated cell sorting (FACS), a method that can sort fluorescent cells faster than 10^4 cells a second [44]. Juewen Liu and colleagues immobilized the anti-ATP structure-switching aptamer onto magnetic microparticles, and implemented FACS to sort out microparticles that underwent target-induced structure-switching (high fluorescence) from those that retained the duplex of fluorescein-labeled aptamer and QDNA (low fluorescence) [45]. Furthermore, sorting was also demonstrated in serum without significant change in the performance of the reporter. In another FACS-based study, Chad Mirkin's group functionalized AuNPs with duplexes made of the ATP aptamer

hybridized to a fluorophore-modified complementary DNA sequence, forming the aptamer "nanoflare" [46]. In this state, the close proximity of fluorophore to the AuNP resulted in fluorescence quenching. However, the addition of ATP resulted in target–aptamer complex formation and the release of fluorophore-modified complementary DNA (high fluorescence from reporter "flares"). This reporter was readily taken up by living cells, and FACS was implemented to measure fluorescence intensity and quantify intracellular levels of ATP.

Other efforts have also resulted in the successful immobilization of structure-switching reporters in sol–gel- [47, 48], hydrogel- [49], and cellulose- [50] based materials, which have shown comparable sensing capabilities as solution-based studies. These findings will help extend the utility of structure-switching sensors towards real-world applications in medical diagnostics, environmental monitoring, and food safety.

4 Structure-Switching DNA Aptamers in Electrochemical Sensors

Electrochemistry has become another well-established signal transduction method for structure-switching designs (Fig. 4a). Some of the major advantages include high sensitivity and selectivity, fast and accurate detection, requirement of only simple instrumentation, and possible miniaturization for portability [51]. Signals generated by aptamer-based electrochemical sensors involve the transfer of electrons between redox-active moieties in an electrically conductive medium (electrolyte) and a conductive support (electrode) to which the aptamer is typically immobilized. The electrical changes produced by target binding to the aptamer can be measured based on changes in voltage (potentiometric), current (amperometric), or the ability to transport charge (conductometric) [52].

Electrochemical sensors can be classified as "signal-off" or "signal-on" sensor types depending on whether target binding decreases or increases the measured electrochemical signal (Fig. 4b). One of the earlier signal-off sensor designs involved hybridization of an immobilized anti-ATP aptamer with a complementary DNA sequence labeled with a redox-tag [53]. In this state, the close proximity of the redox-tag to the electrode surface facilitated electron transfer and an intense electrochemical signal. However, in the presence of ATP, the aptamer sequence binds to its target, and displaces the redox-tag–labeled DNA strand. The separation of the redox-tag from the electrode resulted in substantial signal reduction. Alternatively, in a reported signal-on design, the anti-ATP aptamer was labeled with the redox-tag [54]. When the aptamer sequence formed a duplex structure with the complementary DNA strand, a low electrochemical signal was produced due to the rather large distance of the redox-tag from the electrode surface. The presence of target, however, resulted in target–aptamer complex formation, and displacement of the complementary DNA. In this state, the redox tag was brought

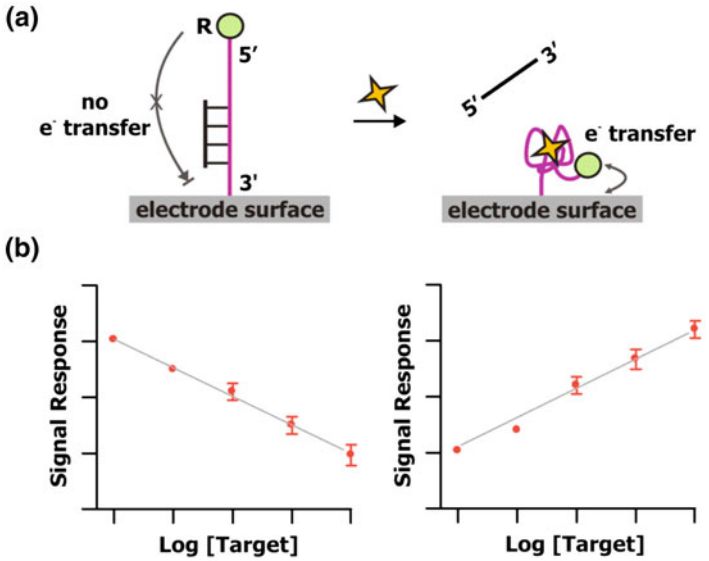

Fig. 4 **a** Structure-switching design for electrochemical detection. **b** Sensor "off" switch involves a decrease in signal upon target detection (*left*). Sensor "on" switch involves signal increase upon target addition (*right*)

in close proximity to the electrode surface for electron transfer to occur. The aforementioned designs are considered to be "labeled" methods as they involve direct labeling of the aptamer or aptamer-related sequence with a redox tag (Fig. 5a).

"Label-free" structure-switching designs, on the other hand, have also been demonstrated and involve a free redox mediator in solution; the aptamer and aptamer-related sequences are free of any direct labeling (Fig. 5b). One notable label-free example involved hybridization of an extended anti-ATP aptamer sequence to a complementary DNA segment that was immobilized to an electrode support [55]. Methylene blue was used as the free redox indicator, as it has the ability to interact with guanine to form a complex. This way, methylene blue molecules effectively tag the aptamer sequence. As a signal-off design, the high electrochemical signal generated in this state was significantly reduced upon addition of ATP, as structure-switching resulted in displacement of the target–aptamer complex, as well as methylene blue molecules away from the electrode surface.

Whether classified as signal-off or signal-on, labeled or label-free, electrochemical structure-switching designs based on the anti-ATP aptamer produce detection limits in the μM to nM range [53–55], which is an improvement on fluorescence-based designs. Nevertheless, signal amplification methods have also been successfully applied to lower the limit of detection further. Shaojun Dong and colleagues have designed an assay using AuNPs functionalized with multiple copies of a complementary DNA sequence in duplex with the anti-ATP aptamer

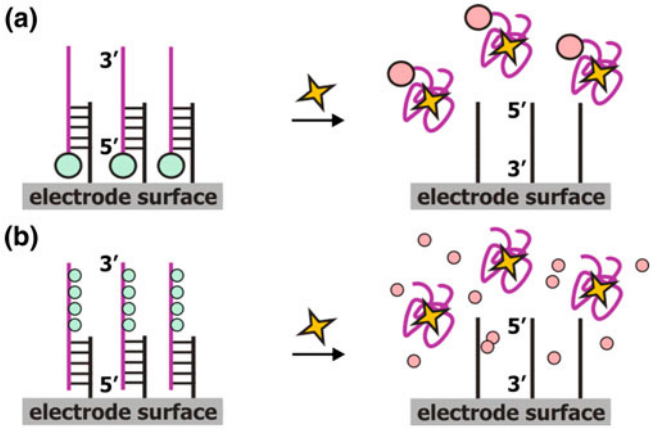

Fig. 5 **a** Electrochemical detection with "labeled" design involves direct coupling of the aptamer or aptamer-related sequence with a signaling molecule. **b** A "label-free" design involves the use of a free signaling molecule in solution

[56]. Methylene blue molecules intercalate along the DNA sequences immobilized to the electrode surface for redox tagging. The intense electrochemical signal produced in this state was significantly reduced when ATP was added to induce multiple structure-switching events, and subsequent displacement of multiple target–aptamer complexes, as well as methylene blue indicators. The detection limit was determined to be 100 pM, which is well below the reported K_d value of the original aptamer. Another notable signal amplification method involved a three-step procedure and made use of silver microspheres (SMSs) as a separation element, and graphene–mesoporous silica AuNP hybrids (GSGHs) to enhance the performance of the electrode surface [57]. In the first step, SMSs were functionalized with the anti-ATP aptamer, which formed a duplex with a complementary DNA sequence (blocker strand). In the presence of ATP, the blocker strand was displaced through structure-switching. SMSs linked with the aptamer–target complexes were then removed, leaving only the blocker strands in solution. In step two, hairpin probes that were complementary in sequence to the blocker strand were incorporated. The blocker strands opened the hairpin probes by the well-established toehold-based strand displacement strategy to generate an accumulation of duplex donor probes. In the last step, the duplex donor probes were captured to form Ag^+-stabilized DNA triplex structures with ssDNA acceptor probes that were immobilized onto the GSGH-electrode platform. Given the numerous DNA triplex structures formed and the enhanced nature of the electrode surface implemented, this design provided substantial signal amplification and yielded an incredible detection limit of $\sim$23 pM.

In addition to continual advancements in sensing capabilities for electrochemistry-based detection, many sensing designs have been applied in complex sample matrixes including serum [58], urine [59], and cell extracts [60]. Furthermore, the structure-switching design has also been used for multiplex

detection. Through implementation of a bifunctional aptamer, whereby the anti-ATP aptamer was linked to the anti-thrombin aptamer, parallel detection of both targets was effectively demonstrated [61]. Arguably, the most successful commercially available electrochemical sensor to date is the glucose sensor, which is widely used by diabetic patients around the world [62, 63]. Taking advantage of the convenience, portability, and low cost of personal glucose meters (PGMs), Yi Lu's group strategically adapted commercially available PGMs and the structure-switching design to quantify adenosine among other nonglucose-related targets [64]. In this approach, magnetic beads were functionalized with the designated aptamer in duplex with a complementary DNA sequence labeled with invertase enzyme. The addition of the target resulted in structure-switching: the aptamer–target–bead complexes were separated magnetically, and the invertase-labeled DNA strands were left in solution. Invertase was then able to catalyze the conversion of sucrose into glucose for detection by the PGM. Because the concentration of released invertase-labeled DNA is directly proportional to the concentration of the target, the readings produced by the PGM can be used for target quantification. Although this integrated method of detection is not as simple as current usage of PGMs, further progress towards automation can perhaps take this prototype system into mainstream usage for convenient medical and environmental monitoring in the near future.

5 Structure-Switching DNA Aptamers in Colorimetric Sensors

Colorimetric detection is an attractive option for biosensor development as a simple color change in the presence of the target is readily observable by the naked eye without the use of complex instruments (Fig. 6). This advantage is particularly useful for on-site qualitative analysis in resource-limited regions. As nucleic acids do not absorb light in the visible spectrum, colorimetry-based detection requires coupling aptamers to a color-producing molecule to generate a color change upon target binding. For structure-switching designs, AuNPs (10–50 nm in diameter) have been a popular choice. Due to the optical phenomenon of surface plasmon resonance, the color of AuNPs in aqueous solution can be reversibly changed from a red (dispersed state) to a blue color (aggregated state). The surface of AuNPs can be easily functionalized to immobilize desired DNA sequences, which allows the tunability of color changes by target–aptamer interactions. A "cross-linking" design was created by Yi Lu's group, whereby AuNPs were functionalized with one of two DNA sequences that were complementary to different sites of an extended anti-ATP aptamer [65].

Once all components were hybridized to each other, the extended aptamer cross-linked both types of functionalized AuNPs to form an aggregate and produce a blue color. Upon the addition of adenosine, target–aptamer binding occurred to induce structure-switching and subsequent displacement of functionalized AuNPs. Dispersal of AuNPs produced a red color. Although this method is a clear

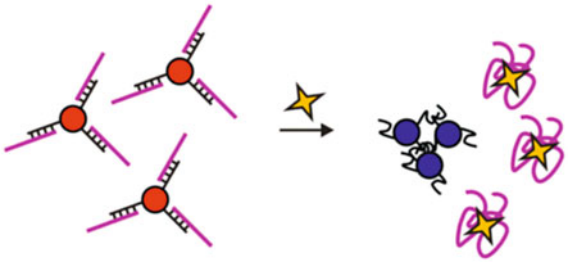

Fig. 6 Structure-switching reporter for colorimetric detection. A gold nanoparticle (AuNP)-based system is illustrated. See main text for details

demonstration of technology transfer of the original structure-switching design into a novel signal transduction platform, the obtained sensitivity was not as high as for typical fluorescent-based designs, and generated a detection limit of 300 μM. Our group has improved the sensitivity of the ATP structure-switching reporter by applying a "non-cross–linking" strategy [66]. This design makes use of AuNPs functionalized with a segment of DNA to hybridize to the ATP aptamer. Under specific salt conditions, the aptamer–AuNPs remained well dispersed and produced a red color. The addition of the target, however, resulted in a structure-switching event, which led to aggregation of the AuNPs and a color change to blue. The detection limit was determined to be $\sim$10 μM, which is identical to the reported K_d of the original aptamer [23]. Alternatively, a "label-free" method of structure-switching was also demonstrated to provide improved detection sensitivity. Developed by Chunhai Fan and colleagues, this design makes use of the anti-ATP aptamer in duplex with its complementary sequence [67]. In a mixture of DNA duplex and AuNPs, the addition of salt resulted in aggregation of the AuNPs (blue color). However, when ATP was initially added to the duplex DNA and AuNP mixture, the target–aptamer complex formation resulted in structure-switching and displacement of the complementary DNA strand. The free DNA strand was then able to adsorb onto the surface of AuNPs, which provided protection and stability against the effect of salt. As a result, the AuNPs remained dispersed and appeared red in color. The reported detection limit was $\sim$0.6 μM.

Although less extensively studied than fluorescence and electrochemistry-based structure-switching aptamer reporters, AuNPs have also started to move into the realm of real-world applications. AuNPs using the cross-linking strategy have been successfully applied for multiplex detection, which enables the detection of multiple targets within the same environmental conditions and the investigation of co-operative binding. Based on the original cross-linking system, Yi Lu's group created design variations whereby AuNPs were functionalized with multiple complementary DNA sequences to hybridize to designated sites on the anti-ATP and anti-cocaine aptamers [68]. The aggregated state of the AuNPs resulted in a blue color. Depending on the system, the AuNP aggregates were dispersed to produce a red color change, by the addition of both ATP and cocaine targets (high co-operativity), or simply by either one of the targets alone (no co-operativity).

To take one step further towards practical application, the cross-linking design has also been applied to a "dip-stick" assay format using lateral flow to separate

dispersed aptamer-linked AuNPs from those aggregated [69]. This adaptation enhances the user-friendliness of detection, and the use of effective separation was also shown to provide better sensitivity than solution-based tests due to lower background interference. Furthermore, the assay retained function even in complex sample matrices, such as blood serum.

6 Structure-Switching RNA Aptamers

Metabolite-binding RNA aptamers exist in cells as parts of riboswitches to regulate gene expression [2]. These RNA regulatory systems are composed of a well-conserved aptamer domain that recognizes a specific metabolite, and a downstream expression domain, which converts the aptamer–metabolite binding interaction to a change in the level of gene expression. Based on variations of the structure-switching mechanism, riboswitches control gene expression through regulation of transcription, translation, or alternative RNA splicing [3–5]. To date, riboswitches have been discovered to respond to nucleobases [70–72] and their derivatives [73–82], amino acids [83–86] and their derivatives [87–93], vitamins [2, 94, 95], sugar derivatives [96], and even metal ions [97, 98]. Metabolite binding alters expression of genes typically associated with biosynthesis, transport, or utilization of the metabolite involved. Remarkably, without assistance from protein effectors, riboswitches can detect a specific metabolite in the complex cellular environment with an affinity typically in the picomolar to micromolar range. More details on this topic can be found in comprehensive reviews published in recent years [99–103].

In addition to the growing number of riboswitches that have been discovered, numerous artificial RNA aptamers have also been isolated through SELEX to recognize wide-ranging molecular targets [15–18]. Similar to natural RNA aptamers, many artificial RNA aptamers also exhibit superior binding affinity and specificity [93, 104–106]. These excellent RNA aptamers constitute an attractive reservoir of molecular recognition elements for biosensor development. However, reports on exploring RNA aptamers for biosensing applications are relatively limited, largely due to the poor chemical stability of RNA and its susceptibility to nuclease degradation. The primary cause of chemical instability stems from the characteristic 2′-hydroxyl group on the ribose ring of RNA [107]. Absent in DNA, the 2′-hydroxyl group enables more intricate folding of RNA to facilitate target recognition [108]; however, this functional group can also readily act as a nucleophile to attack the adjacent phosphodiester linkage in RNA, causing cleavage of the RNA backbone [107]. Additionally, the prevalence of nucleases is another cause of degradation, which predominantly targets RNA rather than DNA [107].

To explore RNA aptamers as sensing elements, we have developed a generalizable rational strategy to create structure-switching reporters from existing RNA aptamers. Conceptually based on the previously reported DNA structure-switching reporters, the newly adapted design makes use of the ability of RNA aptamers to

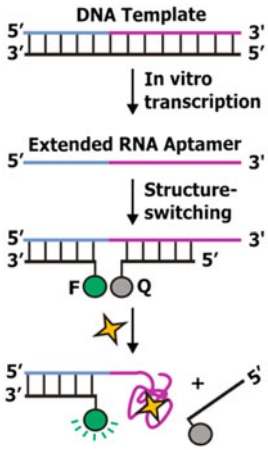

Fig. 7 Overview of a general procedure for designing structure-switching reporters based on RNA aptamers

form both an aptamer–target complex and an RNA–DNA duplex with a complementary sequence [109]. As part of a three-component system, the hybridization of an in vitro transcribed aptamer-containing RNA sequence to chemically synthesized sequences of fluorophore-modified DNA (FDNA) and quencher-modified DNA (QDNA) resulted in low fluorescence through quenching. The addition of target released the QDNA from the aptamer, which subsequently led to high fluorescence enhancement (Fig. 7). Using this strategy, we successfully created two reporters based on first, an RNA aptamer developed through SELEX to bind theophylline [106], and second, a riboswitch-derived RNA aptamer that recognizes thiamine pyrophosphate (TPP) metabolite [105]. Both reporters retained the binding specificity of the original aptamer, and presented comparable detection limits (10 × higher than the K_d of the original aptamers). Despite differences in origin, size, and affinity of the aptamers tested, our strategy functioned well and was shown to be generalizable.

In contrast to the previous DNA aptamer reporters [22], a number of modifications were critical to the design for RNA aptamers. First, a greater number of base pairs in duplex between the FDNA and the extended aptamer sequence were required in order to reduce background fluorescence and obtain a higher level of target-induced signal enhancement. Second, a longer QDNA length was determined to be optimal for the RNA aptamer-based systems to produce the most desirable balance of background fluorescence and signaling rate. Third, the use of a longer QNDA also necessitated the use of a longer extension domain (nucleotides immediately upstream of the aptamer domain that participate in the binding of QDNA, but not in the binding of target) for better signal enhancement [109].

The use of in vitro transcription to generate RNA aptamers was shown to be an effective approach as it bypasses the need for chemical synthesis of RNA, which is inefficient relative to that of DNA [110, 111]. Furthermore, this method facilitates the long-term storage of the sensing components. The aptamer-encoding DNA template is more stable than its RNA counterpart and can be readily transcribed

when needed. In addition, hybridization of RNA with fluorescently labeled DNA circumvents the need for modified RNA, which is prone to degradation and can contribute to higher background fluorescence [109].

To help address the issue of RNA degradation as the next step, both theophylline and TPP structure-switching reporters were successfully immobilized in sol–gel derived material for solid-phase sensor development. Both RNA reporters demonstrated sensitivity and specificity comparable to free aptamers in solution, when entrapped in a composite material derived from 40 % (v/v) methyltrimethoxysilane/tetramethoxysilane [112]. Furthermore, this material conferred protection of the RNA reporters from nuclease degradation, and afforded long-term chemical stability, which enabled storage for up to one month without significant loss of sensing ability for both reporters.

Immobilization within sol–gel–derived materials [112], as well as other RNA protection methods such as chemical modification of nucleotides [113–117], Spiegelmer technology [118, 119], and locked nucleic acids (LNAs) [120, 121] have made considerable advancements to improve the stability of RNA aptamers. Nevertheless, combating the technical challenges of RNA also requires implementation of appropriate experimental controls to ensure the validity of results produced by RNA aptamer-based detection. External experiments commonly used to assess RNA integrity include agarose gel electrophoresis of stained RNA [122–124], calculation of absorbance ratio at 260 and 280 nm by spectrophotometer [125, 126], and microfluidic capillary electrophoresis by a bioanalyzer [127, 128]. Alternatively, a simple biosensing strategy that incorporates an internal control to monitor RNA integrity continuously would be highly beneficial to ensure the quality of detection throughout the duration of the bioanalysis. Structure-switching designs typically require the formation of DNA–DNA or RNA–DNA duplexes as critical structural elements [22, 109]. Unintentional structural denaturation, however, can occur at times caused by a variety of factors (high temperature, unfavorable pH, suboptimal metal ion concentration, presence of organic species such as alcohol, formamide, urea, detergents, etc.) [129]. Having a detection strategy with an internal control in place would help pin-point defective samples in real-time, which could otherwise contribute to a higher background signal (hence lower sensitivity) in some situations, or be mistaken as an authentic target-induced signal in others. For similar reasons, an RNA aptamer detection strategy that can internally monitor quality control would also be useful in different cases of RNA degradation. We previously found that longer RNA sequences undergo more spontaneous degradation than shorter sequences in solution by comparing the activity of structure-switching reporters using RNA aptamers of different lengths over long-term storage [112]. Under physiological conditions, the rate of degradation for RNA is $\sim$100,000-fold higher than that of DNA [130]. If experimental conditions are not optimal, additional factors can further increase the rate of degradation (i.e., pH, metal ion concentration, temperature, etc.). In addition, quality control monitoring would serve well to report the effects of nucleases, which are highly prevalent. Previously, we illustrated the potent function of nucleases on RNA structure-switching reporters, inasmuch as the addition of

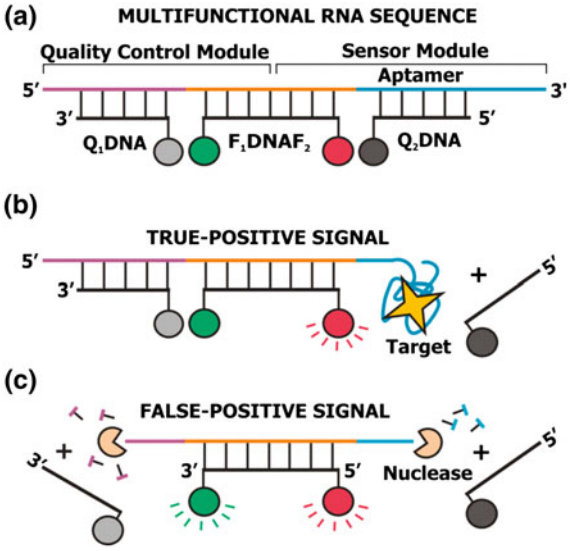

Fig. 8 Structure-switching RNA aptamers with a quality control element. **a** Hybridization of a multifunctional RNA with Q_1DNA, F_1DNAF_2, and Q_2DNA. **b** True-positive signal: addition of target (*star*) results in target–aptamer complex formation and separation of Q_2DNA, which leads to an F_2 signal. **c** False-positive signal: system destruction (e.g., from a nuclease) would lead to both F_1 and F_2 signals

RNase A or RNase H resulted in complete RNA digestion [112]. Hence, continuous system monitoring is critical; depending on the level of the denaturation or degradation source, defects can occur sporadically or may only become apparent over time. Having a simple strategy that can detect system malfunction would ensure the reliability and reproducibility of RNA aptamer-based sensing.

We have recently developed a fluorescent aptamer biosensor design strategy that exploits an internal control (or quality control) element to distinguish target binding from false-positive signals in real-time (Fig. 8) [131]. The DNA sequence encoding both the quality control (QC) and aptamer elements was chemically synthesized and amplified via PCR with the necessary primers to produce a double-stranded DNA template. The template was then used for in vitro transcription to generate the required multifunctional RNA (mfRNA) for a given aptamer. Each mfRNA is designed to form three consecutive short duplexes with Q_1DNA, F_1DNAF_2, and Q_2DNA (Fig. 8a). Target addition is expected to release Q_2DNA from the duplex assembly through structure-switching and produce the expected true-positive signal from F_2 (Fig. 8b). Incorporation of the Q_1F_1 pair is intended to facilitate the distinction of a true-positive signal from a false-positive signal that may arise from unexpected system malfunctions such as the destruction of the DNA/RNA assembly by nucleases (Fig. 8c). Using this design, structure-switching reporters were created to detect theophylline, and thrombin, respectively. Both reporters exhibited sensitivity and specificity comparable to the original aptamer [106, 132], confirming the generality of the design. The QC element was able to report a true-positive signal for both reporters (production of F_2 signal and lack of F_1 signal), and also reliably report a system malfunction when treated with known chemical denaturants and nucleases, as well as unspecified nucleases in human serum (production of both F_1 and F_2 signals).

These results demonstrate the intended utility of the QC element, and showcase the generality of the design strategy. In testing the human serum samples doped with theophylline, we discovered that simple filtration of the drug–serum mixture prior to addition to the theophylline reporter removed all contaminating nucleases, but was able to retain the drug target for detection. However, for the thrombin reporter, simple filtration was not a feasible correction method because protein targets and common nucleases are similar in size. In this case, we found that treatment of the protein–serum mixture with nuclease inhibitors substantially reduced nuclease degradation, and allowed accurate detection of thrombin. These analyses indicate that the incorporation of a QC element can help identify remedy methods to eliminate false-positive signals.

Given the success of the structure-switching reporters based on DNA aptamers, RNA aptamer reporters with a QC element are expected to find a variety of applications where high quality of detection is necessary.

7 Concluding Thoughts

Looking back over the past decade, structure-switching aptamers have garnered considerable success. Structure-switching DNA aptamer sensors have been utilized for a variety of bioanalytical tasks using different signal transduction methods, and novel strategies have been developed to lower the boundaries of detection limits. Reporting systems based on structure-switching RNA aptamers have begun to emerge. Given the continual advancements in RNA protection technology and the incorporation of quality control elements in the design, structure-switching RNA aptamers are expected to find increasing application in bioanalysis.

Further expansion of exploiting structure-switching aptamer reporters for bioanalytical applications requires use of aptamers beyond the model anti-ATP and anti-thrombin systems. This is feasible because diverse aptamers have been, and will continue to be, discovered by the SELEX approach or in biological systems. With the availability of many different aptamers, the structure-switching design will certainly be explored for more challenging analytical tasks or innovations, such as multiplex detection in a single assay and automated testing for multiple analytes in parallel using real-life biological samples. Several aptamers are currently at various stages of clinical trials [133] and structure-switching may offer unique solutions to accelerating the progress of diagnostics and therapeutics using these aptamers. Many challenges remain to be addressed for real-life applications, which include simplification of assay procedures for greater efficiency and lower cost, integration of streamlined assays into automated multifunctional systems for high-throughput analysis, assurance of accurate detection directly in complex samples, and protection against the possibility of false-positive signals. Nevertheless, ongoing research with structure-switching aptamers is expected to reveal more answers in the next decade and beyond.

References

1. Gerstein M, Krebs W (1998) A database of macromolecular motions. Nucleic Acids Res 26:4280–4290
2. Nahvi A, Sudarsan N, Ebert MS et al (2002) Genetic control by a metabolite binding mRNA. Chem Biol 9:1043–1049
3. Roth A, Breaker RR (2009) The structural and functional diversity of metabolite-binding riboswitches. Annu Rev Biochem 78:305–334
4. Tucker BJ, Breaker RR (2005) Riboswitches as versatile gene control elements. Curr Opin Struct Biol 15:342–348
5. Mandal M, Breaker RR (2004) Gene regulation by riboswitches. Nat Rev Mol Cell Biol 5:451–463
6. Topp S, Gallivan JP (2010) Emerging applications of riboswitches in chemical biology. ACS Chem Biol 5:139–148
7. Werstuck G, Green MR (1998) Controlling gene expression in living cells through small molecule-RNA interactions. Science 282:296–298
8. Thompson KM, Syrett HA, Knudsen SM, Ellington AD (2002) Group I aptazymes as genetic regulatory switches. BMC Biotechnol 2:21
9. Suess B, Hanson S, Berens C et al (2003) Conditional gene expression by controlling translation with tetracycline-binding aptamers. Nucleic Acids Res 31:1853–1858
10. Suess B, Fink B, Berens C et al (2004) A theophylline responsive riboswitch based on helix slipping controls gene expression in vivo. Nucleic Acids Res 32:1610–1614
11. Desai SK, Gallivan JP (2004) Genetic screens and selections for small molecules based on a synthetic riboswitch that activates protein translation. J Am Chem Soc 126:13247–13254
12. Weigand JE, Sanchez M, Gunnesch EB et al (2008) Screening for engineered neomycin riboswitches that control translation initiation. RNA 14:89–97
13. Topp S, Gallivan JP (2007) Guiding bacteria with small molecules and RNA. J Am Chem Soc 129:6807–6811
14. Topp S, Gallivan JP (2008) Random walks to synthetic riboswitches-a high-throughput selection based on cell motility. ChemBioChem 9:210–213
15. Ellington AD, Szostak JW (1990) In vitro selection of RNA molecules that bind specific ligands. Nature 346:818–822
16. Tuerk C, Gold L (1990) Systematic evolution of ligands by exponential enrichment: RNA ligands to bacteriophage T4 DNA polymerase. Science 249:505–510
17. Bunka DH, Stockley PG (2006) Aptamers come of age—at last. Nat Rev Microbiol 4:588–596
18. Lee JF, Hesselberth JR, Meyers LA, Ellington AD (2004) Aptamer database. Nucleic Acids Res 32:D95–100
19. Lau PS, Li Y (2011) Functional nucleic acids as molecular recognition elements for small organic and biological molecules. Curr Org Chem 15:557–575
20. Vallee-Belisle A, Plaxco KW (2010) Structure-switching biosensors: inspired by Nature. Curr Opin Struct Biol 20:518–526
21. Klussmann S (2006) The Aptamer handbook. Wiley, Weinheim
22. Nutiu R, Li Y (2003) Structure-switching signaling aptamers. J Am Chem Soc 125:4771–4778
23. Huizenga DE, Szostak JW (1995) A DNA aptamer that binds adenosine and ATP. Biochemistry 34:656–665
24. Bock LC, Griffin LC, Latham JA et al (1992) Selection of single-stranded DNA molecules that bind and inhibit human thrombin. Nature 355:564–566
25. Han K, Liang Z, Zhou N (2010) Design strategies for aptamer-based biosensors. Sensors 10:4541–4557
26. White RJ, Rowe AA, Plaxco KW (2010) Re-engineering aptamers to support reagentless, self-reporting electrochemical sensors. Analyst 135:589–594

27. Nutiu R, Li Y (2005) In vitro selection of structure-switching signaling aptamers. Angew Chem Int Ed 44:1061–1065
28. Lin CH, Patel DJ (1997) Structural basis of DNA folding and recognition in an AMP-DNA aptamer complex: distinct architectures but common recognition motifs for DNA and RNA aptamers complexed to AMP. Chem Biol 4:817–832
29. Wang ZD, Lee JH, Lu Y (2008) Highly sensitive "turn-on" fluorescent sensor for Hg2 + in aqueous solution based on structure-switching DNA. Chem Commun (Camb) 6005–6007
30. Wu DH, Zhang Q, Chu X et al (2010) Ultrasensitive electrochemical sensor for mercury (II) based on target-induced structure-switching DNA. Biosens Bioelectron 25:1025–1031
31. Taylor SK, Pei RJ, Moon BC et al (2009) Triggered release of an active peptide conjugate from a DNA device by an orally administrable small molecule. Angew Chem Int Ed 48:4394–4397
32. Liu J, Lu Y (2005) Fast colorimetric sensing of adenosine and cocaine based on a general sensor design involving aptamers and nanoparticles. Angew Chem Int Ed 45:90–94
33. Null EL, Lu Y (2010) Rapid determination of enantiomeric ratio using fluorescent DNA or RNA aptamers. Analyst 135:419–422
34. Feng KJ, Sun CH, Jiang JH, Yu RQ (2011) An aptamer-based competitive fluorescence quenching assay for IgE. Anal Lett 44:1301–1309
35. Zhu ZY, Schmidt T, Mahrous M et al (2011) Optimization of the structure-switching aptamer-based fluorescence polarization assay for the sensitive tyrosinamide sensing. Anal Chim Acta 707:191–196
36. Niu WZ, Jiang N, Hu YH (2007) Detection of proteins based on amino acid sequences by multiple aptamers against tripeptides. Anal Biochem 362:126–135
37. Liu DY, Zhao Y, He XW, Yin XB (2011) Electrochemical aptasensor using the tripropylamine oxidation to probe intramolecular displacement between target and complementary nucleotide for protein array. Biosens Bioelectron 26:2905–2910
38. Yang L, Fung CW, Cho EJ, Ellington AD (2007) Real-time rolling circle amplification for protein detection. Anal Chem 79:3320–3329
39. Song YJ, Zhao C, Ren JS, Qu XG (2009) Rapid and ultra-sensitive detection of AMP using a fluorescent and magnetic nano-silica sandwich complex. Chem Commun (Camb) 15:1975–1977
40. Levy M, Cater SF, Ellington AD (2005) Quantum-dot aptamer beacons for the detection of proteins. ChemBioChem 6:2163–2166
41. Liu JW, Lee JH, Lu Y (2007) Quantum dot encoding of aptamer-linked nanostructures for one-pot simultaneous detection of multiple analytes. Anal Chem 79:4120–4125
42. Elowe NH, Nutiu R, Allah-Hassani A et al (2006) Small-molecule screening made simple for a difficult target with a signaling nucleic acid aptamer that reports on deaminase activity. Angew Chem Int Ed 45:5648–5652
43. Aldrich MB, Blackburn MR, Kellems RE (2000) The importance of adenosine deaminase for lymphocyte development and function. Biochem Biophys Res Commun 272:311–315
44. Fowler CC, Brown ED, Li Y (2008) A FACS-based approach to engineering artificial riboswitches. ChemBioChem 9:1906–1911
45. Huang PJJ, Liu JW (2010) Flow cytometry-assisted detection of adenosine in serum with an immobilized aptamer sensor. Anal Chem 82:4020–4026
46. Zheng D, Seferos DS, Giljohann DA et al (2009) Aptamer nano-flares for molecular detection in living cells. Nano Lett 9:3258–3261
47. Rupcich N, Nutiu R, Li Y, Brennan JD (2005) Entrapment of fluorescent signaling DNA aptamers in sol-gel-derived silica. Anal Chem 77:4300–4307
48. Carrasquilla C, Li Y, Brennan JD (2011) Surface immobilization of structure-switching DNA aptamers on macroporous Sol-Gel-derived films for solid-phase biosensing applications. Anal Chem 83:957–965
49. El-Hamed F, Dave N, Liu J (2011) Stimuli-responsive releasing of gold nanoparticles and liposomes from aptamer-functionalized hydrogels. Nanotechnology 22:494011–494017

50. Su SX, Nutiu R, Filipe CDM et al (2007) Adsorption and covalent coupling of ATP-binding DNA aptamers onto cellulose. Langmuir 23:1300–1302
51. Radi AE, Acero Sanchez JL, Baldrich E, O'Sullivan CK (2006) Reagentless, reusable, ultrasensitive electrochemical molecular beacon aptasensor. J Am Chem Soc 128:117–124
52. Luong JH, Male KB, Glennon JD (2008) Biosensor technology: technology push versus market pull. Biotechnol Adv 26:492–500
53. Yoshizumi J, Kumamoto S, Nakamura M, Yamana K (2008) Target-induced strand release (TISR) from aptamer-DNA duplex: A general strategy for electronic detection of biomolecules ranging from a small molecule to a large protein. Analyst 133:323–325
54. Zuo XL, Song SP, Zhang J et al (2007) A target-responsive electrochemical aptamer switch (TREAS) for reagentless detection of nanomolar ATP. J Am Chem Soc 129:1042–1043
55. Wang JL, Wang F, Dong SJ (2009) Methylene blue as an indicator for sensitive electrochemical detection of adenosine based on aptamer switch. J Electroanal Chem 626:1–5
56. Du Y, Li BL, Wang F, Dong SJ (2009) Au nanoparticles grafted sandwich platform used amplified small molecule electrochemical aptasensor. Biosens Bioelectron 24:1979–1983
57. Guo SJ, Du Y, Yang X et al (2011) Solid-state label-free integrated aptasensor based on graphene-mesoporous silica-gold nanoparticle hybrids and silver microspheres. Anal Chem 83:8035–8040
58. Zhang SS, Xia JP, Li XM (2008) Electrochemical biosensor for detection of adenosine based on structure-switching aptamer and amplification with reporter probe DNA modified Au nanoparticles. Anal Chem 80:8382–8388
59. Li W, Nie Z, Xu XH et al (2009) A sensitive, label free electrochemical aptasensor for ATP detection. Talanta 78:954–958
60. Zhang XR, Zhao YQ, Li SG, Zhang SS (2010) Photoelectrochemical biosensor for detection of adenosine triphosphate in the extracts of cancer cells. Chem Commun (Camb) 46:9173–9175
61. Du Y, Li BL, Wei H et al (2008) Multifunctional label-free electrochemical biosensor based on an integrated aptamer. Anal Chem 80:5110–5117
62. Clark LC Jr, Lyons C (1962) Electrode systems for continuous monitoring in cardiovascular surgery. Ann NY Acad Sci 102:29–45
63. Montagnana M, Caputo M, Giavarina D, Lippi G (2009) Overview on self-monitoring of blood glucose. Clin Chim Acta Int J Clin Chem 402:7–13
64. Xiang Y, Lu Y (2011) Using personal glucose meters and functional DNA sensors to quantify a variety of analytical targets. Nature Chem 3:697–703
65. Liu JW, Lu Y (2006) Fast colorimetric sensing of adenosine and cocaine based on a general sensor design involving aptamers and nanoparticles. Angew Chem Int Ed 45:90–94
66. Zhao WA, Chiuman W, Brook MA, Li Y (2007) Simple and rapid colorimetric biosensors based on DNA aptamer and noncrosslinking gold nanoparticle aggregation. ChemBioChem 8:727–731
67. Wang J, Wang LH, Liu XF et al (2007) A gold nanoparticle-based aptamer target binding readout for ATP assay. Adv Mater 19:3943–3946
68. Liu JW, Lu Y (2006) Smart nanomaterials responsive to multiple chemical stimuli with controllable cooperativity. Adv Mater 18:1667–1671
69. Liu JW, Mazumdar D, Lu Y (2006) A simple and sensitive "dipstick" test in serum based on lateral flow separation of aptamer-linked nanostructures. Angew Chem Int Ed 45:7955–7959
70. Johansen LE, Nygaard P, Lassen C et al (2003) Definition of a second Bacillus subtilis pur regulon comprising the pur and xpt-pbuX operons plus pbuG, nupG (yxjA), and pbuE (ydhL). J Bacteriol 185:5200–5209
71. Mandal M, Breaker RR (2004) Adenine riboswitches and gene activation by disruption of a transcription terminator. Nat Struct Mol Biol 11:29–35
72. Mandal M, Boese B, Barrick JE et al (2003) Riboswitches control fundamental biochemical pathways in Bacillus subtilis and other bacteria. Cell 113:577–586

73. Roth A, Winkler WC, Regulski EE et al (2007) A riboswitch selective for the queuosine precursor preQ1 contains an unusually small aptamer domain. Nat Struct Mol Biol 14:308–317
74. Meyer MM, Roth A, Chervin SM et al (2008) Confirmation of a second natural preQ1 aptamer class in Streptococcaceae bacteria. RNA 14:685–695
75. Mironov AS, Gusarov I, Rafikov R et al (2002) Sensing small molecules by nascent RNA: a mechanism to control transcription in bacteria. Cell 111:747–756
76. Rodionov DA, Vitreschak AG, Mironov AA, Gelfand MS (2002) Comparative genomics of thiamin biosynthesis in procaryotes. New genes and regulatory mechanisms. J Biol Chem 277:48949–48959
77. Cheah MT, Wachter A, Sudarsan N, Breaker RR (2007) Control of alternative RNA splicing and gene expression by eukaryotic riboswitches. Nature 447:497–500
78. Wachter A, Tunc-Ozdemir M, Grove BC et al (2007) Riboswitch control of gene expression in plants by splicing and alternative 3′ end processing of mRNAs. Plant Cell 19:3437–3450
79. Croft MT, Moulin M, Webb ME, Smith AG (2007) Thiamine biosynthesis in algae is regulated by riboswitches. Proc Natl Acad Sci USA 104:20770–20775
80. Bocobza S, Adato A, Mandel T et al (2007) Riboswitch-dependent gene regulation and its evolution in the plant kingdom. Genes Dev 21:2874–2879
81. Winkler WC, Cohen-Chalamish S, Breaker RR (2002) An mRNA structure that controls gene expression by binding FMN. Proc Natl Acad Sci USA 99:15908–15913
82. Sudarsan N, Lee ER, Weinberg Z et al (2008) Riboswitches in eubacteria sense the second messenger cyclic di-GMP. Science 321:411–413
83. Mandal M, Lee M, Barrick JE et al (2004) A glycine-dependent riboswitch that uses cooperative binding to control gene expression. Science 306:275–279
84. Grundy FJ, Lehman SC, Henkin TM (2003) The L box regulon: lysine sensing by leader RNAs of bacterial lysine biosynthesis genes. Proc Natl Acad Sci USA 100:12057–12062
85. Rodionov DA, Vitreschak AG, Mironov AA, Gelfand MS (2003) Regulation of lysine biosynthesis and transport genes in bacteria: yet another RNA riboswitch? Nucleic Acids Res 31:6748–6757
86. Sudarsan N, Wickiser JK, Nakamura S et al (2003) An mRNA structure in bacteria that controls gene expression by binding lysine. Genes Dev 17:2688–2697
87. Gilbert SD, Rambo RP, Van Tyne D, Batey RT (2008) Structure of the SAM-II riboswitch bound to S-adenosylmethionine. Nat Struct Mol Biol 15:177–182
88. Corbino KA, Barrick JE, Lim J et al (2005) Evidence for a second class of S-adenosylmethionine riboswitches and other regulatory RNA motifs in alpha-proteobacteria. Genome Biol 6:R70
89. Epshtein V, Mironov AS, Nudler E (2003) The riboswitch-mediated control of sulfur metabolism in bacteria. Proc Natl Acad Sci USA 100:5052–5056
90. Fuchs RT, Grundy FJ, Henkin TM (2006) The S(MK) box is a new SAM-binding RNA for translational regulation of SAM synthetase. Nat Struct Mol Biol 13:226–233
91. McDaniel BA, Grundy FJ, Artsimovitch I, Henkin TM (2003) Transcription termination control of the S box system: direct measurement of S-adenosylmethionine by the leader RNA. Proc Natl Acad Sci USA 100:3083–3088
92. Winkler WC, Nahvi A, Sudarsan N et al (2003) An mRNA structure that controls gene expression by binding S-adenosylmethionine. Nat Struct Biol 10:701–707
93. Wang JX, Lee ER, Morales DR et al (2008) Riboswitches that sense S-adenosylhomocysteine and activate genes involved in coenzyme recycling. Mol Cell 29:691–702
94. Borovok I, Gorovitz B, Schreiber R et al (2006) Coenzyme B12 controls transcription of the Streptomyces class Ia ribonucleotide reductase nrdABS operon via a riboswitch mechanism. J Bacteriol 188:2512–2520
95. Warner DF, Savvi S, Mizrahi V, Dawes SS (2007) A riboswitch regulates expression of the coenzyme B12-independent methionine synthase in Mycobacterium tuberculosis: implications for differential methionine synthase function in strains H37Rv and CDC1551. J Bacteriol 189:3655–3659

96. Winkler WC, Nahvi A, Roth A et al (2004) Control of gene expression by a natural metabolite-responsive ribozyme. Nature 428:281–286
97. Cromie MJ, Shi Y, Latifi T, Groisman EA (2006) An RNA sensor for intracellular Mg(2+). Cell 125:71–84
98. Baker JL, Sudarsan N, Weinberg Z et al (2012) Widespread genetic switches and toxicity resistance proteins for fluoride. Science 335:233–235
99. Breaker RR (2011) Prospects for riboswitch discovery and analysis. Mol Cell 43:867–879
100. Ferre-D'Amare AR, Winkler WC (2011) The roles of metal ions in regulation by riboswitches. Met Ions Life Sci 9:141–173
101. Serganov A, Patel DJ (2012) Molecular recognition and function of riboswitches. Curr Opin Struct Biol 22:279–286
102. Wittmann A, Suess B (2012) Engineered riboswitches: Expanding researchers' toolbox with synthetic RNA regulators. FEBS Lett 586:2076–2083
103. Batey RT (2012) Structure and mechanism of purine-binding riboswitches. Q Rev Biophys 45:345–381
104. Huang L, Serganov A, Patel DJ (2010) Structural insights into ligand recognition by a sensing domain of the cooperative glycine riboswitch. Mol Cell 40:774–786
105. Welz R, Breaker RR (2007) Ligand binding and gene control characteristics of tandem riboswitches in Bacillus anthracis. RNA 13:573–582
106. Jenison RD, Gill SC, Pardi A, Polisky B (1994) High-resolution molecular discrimination by RNA. Science 263:1425–1429
107. Fowler CC, Navani NK, Brown ED, Li Y (2008) Aptamers and their potential as recognition elements for the detection of bacteria. In: Zourob M, Elwary S, Turner A (eds) Principles of bacterial detection: biosensors, recognition receptors and microsystems, Springer, Chapter 25, pp 689–714
108. Cate JH, Gooding AR, Podell E et al (1996) Crystal structure of a group I ribozyme domain: principles of RNA packing. Science 273:1678–1685
109. Lau PS, Coombes BK, Li Y (2010) A general approach to the construction of structure-switching reporters from RNA aptamers. Angew Chem Int Ed 49:7938–7942
110. Scaringe SA, Wincott FE, Caruthers MH (1998) Novel RNA synthesis method using 5′-*O*-silyl-2′-*O*-orthoester protecting groups. J Am Chem Soc 120:11820–11821
111. Khakshoor O, Kool ET (2011) Chemistry of nucleic acids: impacts in multiple fields. Chem Commun (Camb) 47:7018–7024
112. Carrasquilla C, Lau PS, Li Y, Brennan JD (2012) Stabilizing structure-switching signaling RNA aptamers by entrapment in sol-gel derived materials for solid-phase assays. J Am Chem Soc 134:10998–11005
113. Jellinek D, Green LS, Bell C et al (1995) Potent 2′-amino-2′-deoxypyrimidine RNA inhibitors of basic fibroblast growth factor. Biochemistry 34:11363–11372
114. Lin Y, Qiu Q, Gill SC, Jayasena SD (1994) Modified RNA sequence pools for in vitro selection. Nucleic Acids Res 22:5229–5234
115. Biesecker G, Dihel L, Enney K, Bendele RA (1999) Derivation of RNA aptamer inhibitors of human complement C5. Immunopharmacology 42:219–230
116. Ruckman J, Green LS, Beeson J et al (1998) 2′-Fluoropyrimidine RNA-based aptamers to the 165-amino acid form of vascular endothelial growth factor (VEGF165). Inhibition of receptor binding and VEGF-induced vascular permeability through interactions requiring the exon 7-encoded domain. J Biol Chem 273:20556–20567
117. Green LS, Jellinek D, Bell C et al (1995) Nuclease-resistant nucleic acid ligands to vascular permeability factor/vascular endothelial growth factor. Chem Biol 2:683–695
118. Klussmann S, Nolte A, Bald R et al (1996) Mirror-image RNA that binds D-adenosine. Nat Biotechnol 14:1112–1115
119. Nolte A, Klussmann S, Bald R et al (1996) Mirror-design of L-oligonucleotide ligands binding to L-arginine. Nat Biotechnol 14:1116–1119
120. Kumar R, Singh SK, Koshkin AA et al (1998) The first analogues of LNA (locked nucleic acids): phosphorothioate-LNA and 2′-thio-LNA. Bioorg Med Chem Lett 8:2219–2222

121. Petersen M, Wengel J (2003) LNA: a versatile tool for therapeutics and genomics. Trends Biotechnol 21:74–81
122. Le Pecq JB, Paoletti C (1966) A new fluorometric method for RNA and DNA determination. Anal Biochem 17:100–107
123. Vendrely R, Alexandrov K, De Sousa Lechner MC, Coirault Y (1968) Fractionation of ribonucleic acids by 'Sephadex' agarose gel electrophoresis. Nature 218:293–294
124. Lehrach H, Diamond D, Wozney JM, Boedtker H (1977) RNA molecular weight determinations by gel electrophoresis under denaturing conditions, a critical reexamination. Biochemistry 16:4743–4751
125. Manchester KL (1995) Value of A260/A280 ratios for measurement of purity of nucleic acids. BioTechniques 19:208–210
126. Glasel JA (1995) Validity of nucleic acid purities monitored by 260 nm/280 nm absorbance ratios. BioTechniques 18:62–63
127. Mueller O, Hahnenberger K, Dittmann M et al (2000) A microfluidic system for high-speed reproducible DNA sizing and quantitation. Electrophoresis 21:128–134
128. Bustin SA (2002) Quantification of mRNA using real-time reverse transcription PCR (RT-PCR): trends and problems. J Mol Endocrinol 29:23–39
129. Doktycz MJ (1997) Nucleic acids: thermal stability and denaturation. Encyclopedia of Life Sciences
130. Li Y, Breaker RR (1999) Kinetics of RNA degradation by specific base catalysis of transesterification involving the 2′-hydroxyl group. J Am Chem Soc 121:5364–5372
131. Lau PS, Lai CK, Li Y (2013) Quality control certification of RNA aptamer-based detection. ChemBioChem. doi:10.1002/cbic.201300134
132. Kubik MF, Stephens AW, Schneider D, Marlar RA, Tasset D (1994) High-affinity RNA ligands to human alpha-thrombin. Nucleic Acids Res 22:2619–2626
133. Ni X, Castanares M, Mukherjee A, Lupold SE (2011) Nucleic acid aptamers: clinical applications and promising new horizons. Curr Med Chem 18:4206–4214

Adv Biochem Eng Biotechnol (2014) 140: 93–120
DOI: 10.1007/10_2013_242

Published Online: 12 September 2013

DNAzyme-Functionalized Gold Nanoparticles for Biosensing

Yu Xiang, Peiwen Wu, Li Huey Tan and Yi Lu

Abstract Recent progress in using DNAzyme-functionalized gold nanoparticles (AuNPs) for biosensing is summarized in this chapter. A variety of methods, including those for attaching DNA on AuNPs, detecting metal ions and small molecules by DNAzyme-functionalized AuNPs, and intracellular applications of DNAzyme-functionalized AuNPs are discussed. DNAzyme-functionalized AuNPs will increasingly play more important roles in biosensing and many other multi-disciplinary applications.

Keywords Biosensing · DNAzyme · Gold nanoparticle · Intracellular imaging

Abbreviations

AuNP	Gold Nanoparticle
DNA	Deoxyribonucleic Acid
dsDNA	Double-stranded DNA
PEG	Poly-(Ethylene Glycol)
SERS	Surface Enhanced Raman Spectroscopy
SPR	Surface Plasmon Resonance
ssDNA	Single-stranded DNA

Contents

Y. Xiang · P. Wu · L. H. Tan · Y. Lu (✉)
Department of Chemistry and Beckman Institute,
University of Illinois at Urbana-Champaign, Urbana IL, 61801, USA
e-mail: yi-lu@illinois.edu

1 Introduction: DNAzymes and Gold Nanoparticles

Deoxyribonucleic acid (DNA) is a biopolymer made of four types of deoxynucleotides: adenosine (A), thymidine (T), guanosine (G), and cytidine (C). Complementary DNA strands assemble into a double helix (DNA duplex) via the formation of A–T and G–C base pairs [1, 2]. Such DNA was long considered solely a genetic material to encode the inheritable information of many organisms through its sequence. However, this understanding was challenged in the 1990s when DNAs with catalytic activities [3–5] and ligand-binding abilities [6–9] were discovered from libraries containing random DNA sequences through combinatorial techniques such as in vitro selection (Fig. 1) or systematic evolution of ligands by exponential enrichment (SELEX) [3–9]. The DNAs with catalytic activities are DNAzymes (also called deoxyribozymes or catalytic DNAs). Since their discovery, many different DNAzymes have been isolated by different research groups to catalyze the cleavage [3, 10–18], ligation [4, 19, 20], phosphorylation [21], adenylation [22], depurination [23], and thymine dimer repair [24, 25] of nucleic acids, as well as formation of nucleopeptide linkage [26, 27], porphyrin metallation [28], and other chemical reactions [29–31]. DNAzymes are generally more stable than protein and ribozymes due to the prominent stability of DNA against hydrolysis and denaturation, and many artificial modifications can be further introduced into DNAzymes to enhance their resistance to nuclease degradation [32, 33]. As a result of these properties, DNAzymes have been widely applied in many research fields, including biosensing [34–45], logical DNA computing and machines [39, 46–48], gene therapy [49–54], and others [55–60].

Among many nanomaterials, gold nanoparticle (AuNP) is one of the most studied [61]. The growing research interest on AuNPs is mainly because of their excellent properties such as high stability, strong plasmonic effects, good catalytic activities, and low cytotoxicity [62]. Many techniques have been developed for the synthesis of AuNPs of different sizes and shapes [63–68], including Au spheres [69–72], rods [73–80], prisms [81–84], cages [85–87], and wires [88, 89]. AuNPs are widely applied in nanoassembly [90–99], chemical catalysis [90, 100–106], sensing [96, 107–122], and biological applications [90, 123–131].

In this chapter, we focus on DNAzyme-functionalized AuNPs in biosensing and dynamic assembly [43, 96, 98, 121, 132–138]. The related works that have been conducted in our group are also introduced. Readers are directed to other outstanding reviews about more general perspectives of DNAzymes [34–60, 139–172], AuNPs [61, 62, 90], and biomolecule-functionalized nanomaterials [92, 95, 97–99, 122, 173–178].

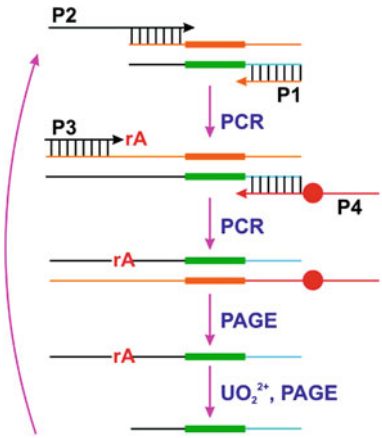

Fig. 1 A scheme of in vitro selection technique for selecting DNAzymes specifically using uranyl ions (UO_2^{2+}) as a cofactor to catalyze nucleic acid cleavage. The random DNA library is amplified by PCR using primers P1 and P2, and repeated using P3 and P4 containing rA as a cleavage site and an overhang/spacer as a tag, respectively. After PCR and PAGE purification, the DNA library is incubated with UO_2^{2+}. DNA sequences (containing both DNAzyme (*bold* and *green*) and substrate (*black* and *rA*) motifs) that undergo cleavage in the presence of UO_2^{2+} are isolated and used for the next round of selection. After a few rounds of selection, UO_2^{2+}-specific DNAzymes are identified by cloning and sequencing (Adapted from Ref. [16])

2 DNAzyme-Functionalized Gold Nanoparticles for Biosensing

2.1 Fabrication of DNA-Functionalized AuNPs

Before AuNPs can be used with DNAzymes, they have to be functionalized with DNA through strong ligand–Au bindings or in some other cases by weaker DNA–Au interactions. AuNPs synthesized by various methods are generally coated by ligands to stabilize the colloid aqueous solutions [62, 63, 71]. These ligands on the surface of AuNPs can be efficiently replaced by thiol-containing molecules because of the thiophilic nature of Au [179–181]. Based on this principle, thiol-modified DNAs (thiol-DNAs) were successfully functionalized onto the surface of AuNPs to direct the assembly of AuNPs via DNA hybridization (Fig. 2a) [182, 183]. After DNA functionalization, the AuNPs were stabilized by the strong electrostatic repulsion between negatively charged DNA strands. A fluorescence-based method could be utilized to quantify the surface coverage and hybridization efficiency of thiol-DNAs on AuNPs, using mercaptoethanol to displace the surface-bound fluorophore-labeled thiol-DNAs [184]. DNA loading on AuNPs of different sizes can be significantly enhanced by aging in concentrated salt solution or introducing a PEG spacer to the DNA [185]. Gel electrophoresis was used to study the conformation of thiol-DNA attached on AuNPs [186] and separate DNA-functionalized AuNPs containing different DNA coverage or in different

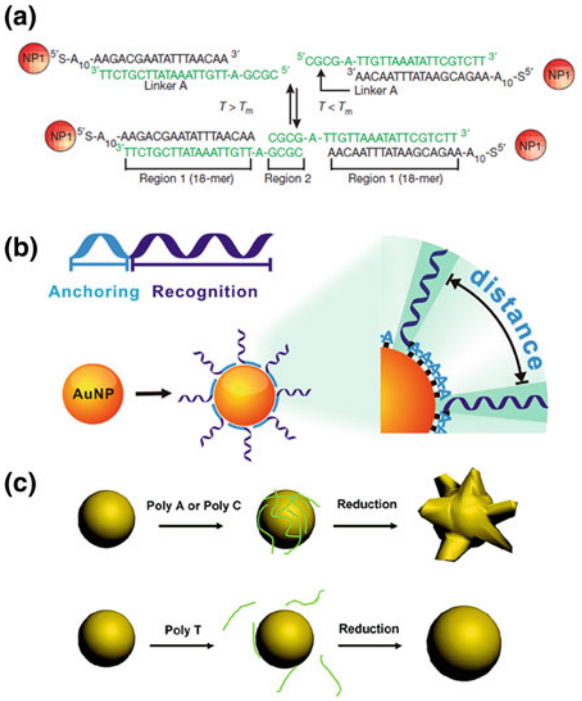

Fig. 2 Functionalization of DNA on AuNPs through **a** thiol–Au interaction, **b** poly A tags, and **c** in situ embedding during AuNP growth (Adapted from Ref. [182, 193, 196])

assemblies [183, 187–190]. In addition to the DNA-functionalized AuNPs with multiple DNA strands on each AuNP, mono-DNA-functionalized AuNPs (one DNA strand per AuNP) could also be prepared and purified [183, 187, 191, 192]. In addition to thiol-DNA, DNA with a poly A block was found to bind AuNPs with sufficient affinity to form DNA-functionalized AuNPs, and the lateral spacing and surface density of DNA strands on AuNPs was controlled by adjusting the length of the poly A block (Fig. 2b) [193].

In our lab, DNAzymes and their nucleic acid substrates were used as cross-linkers to form assemblies of DNA-functionalized AuNPs via DNA hybridizations on both binding arms, and the assemblies underwent disassembly upon cleavage of the substrates by the DNAzymes in the presence of metal ion cofactors [194, 195]. In addition to the postsynthetic methods that attach DNA on the surface of pre-formed AuNPs, our lab developed a new in situ method to prepare DNA-functionalized AuNPs simultaneously during the growth of AuNPs in the presence of DNA (Fig. 2c) [196, 197]. In this approach, DNA noncovalently bound to the surface of spherical Au nanoseeds through its poly A or poly C blocks, and then Au salts and reductants were added to initiate the growth of the nanoseeds into larger flower-shaped AuNPs. DNA was partially embedded in the newly formed Au layers during the growth of these Au "nanoflowers", and the DNA fragment on the surface of the AuNPs was still active to hybridize with AuNPs functionalized with a complementary DNA strand to form nanoassemblies [196]. One advantage

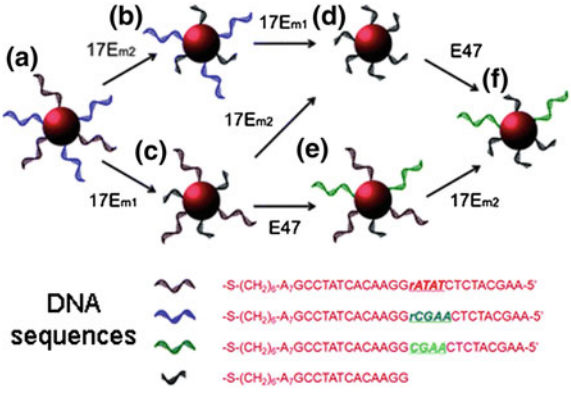

Fig. 3 Selective and stepwise modification of DNA sequences immobilized on AuNPs using DNAzymes (Adapted from Ref. [204])

of this in situ DNA-functionalization method over postsynthetic methods is that the attachment of DNA on the AuNPs by embedding is so stable that the treatment of high concentrations of coadsorbed diluent molecules such as mercaptoethanol could not displace the DNA from the AuNPs [196], whereas under this condition thiol-DNA on the surface of AuNPs was efficiently removed from the AuNPs [184]. The mechanism on how DNA is embedded and which sequence is preferred for the embedding during the growth of Au nanoseeds is currently not clear. Further studies are under way in our lab to answer these questions to enable more efficient DNA functionalization on AuNPs and better preservation of DNA activities.

On the other hand, despite the above progress made to attach DNA on AuNPs, few methods are capable of modifying the DNA sequences already attached [189, 198–203]. The "post-attachment" modification can enable more flexible transformations of DNA sequences to control AuNP nanoassemblies and tune their functions [189, 198–203]. We have recently developed a DNAzyme-based method to modify the sequences of DNA on AuNPs (Fig. 3). The DNA is processed by DNAzymes to cut off (cleave) unwanted fragments and then add (ligate) desired new fragments, enabling DNA sequence modifications to provide new DNA functions to the DNA-functionalized AuNPs [204]. More importantly, the DNA sequence modifications catalyzed by the DNAzymes are sequence-specific [3, 4], so that multiple DNA sequences on one AuNP can be modified selectively and in a stepwise manner [204]. Another advantage of this method is that the size of DNAzymes is comparable to that of DNA attached on AuNPs, thus little steric effect is present [203, 204]; whereas protein enzymes that catalyze sequence-specific DNA cleavage and ligation are much larger and may encounter low efficiency or incomplete cleavage of DNA on AuNPs [198–201]. In our current method, a ribonucleotide (rA) serves as the designed cleavage site in the DNA when DNAzymes are present. This rA is not necessary if a recently discovered new DNAzyme that can catalyze the cleavage of unmodified DNA is utilized [18].

2.2 DNAzyme-Functionalized AuNPs for Biosensing

The major application of DNAzyme-functionalized AuNPs is biosensing [43, 98, 121, 132, 135, 137]. DNA-functionalized AuNPs were first found to assemble via DNA hybridization between complementary DNA strands in 1996 [182, 183], where a color change from red to blue was observed. A red shift in absorption spectra was observed when discrete AuNPs assembled into macroscopic aggregates [182]. Due to the extremely large extinction coefficient of AuNPs compared to organic dyes and their other prominent properties such as light scattering, surface enhanced Raman spectroscopy (SERS), and surface plasmon resonance (SPR), AuNPs have been widely applied for highly sensitive enzyme-free detection of nucleic acids [205–240].

By introducing DNAzymes into such DNA–AuNP systems and taking advantage of AuNPs, a new series of DNAzyme-based biosensors has been developed for a broad range of targets [194, 221, 241–278]. In most of these studies, DNAzymes have played two distinct roles in target recognition and in signal enhancement. In the former case, nucleic acid cleaving or ligating DNAzymes [3, 4, 165] are used to recognize specific cofactors such as metal ions and small organic molecules; then the DNAzyme-catalyzed cleavage or ligation of the nucleic acid substrates alters AuNP assemblies, producing physically detectable signal changes for sensing the cofactors as targets [194, 241–252, 255–261, 263, 265–267, 269, 271–275, 277, 278]. In the latter case, peroxidase-mimicking DNAzymes [28, 29, 40, 169], usually containing G-quadruplex motifs, serve as signal generators or enhancers on AuNPs to transform target recognition by other molecules into physically detectable signals [221, 253, 254, 262, 264, 268, 270, 275, 276].

In addition to the above examples of in vitro detection, cellular or in vivo biosensing is also an active field of research and can provide useful information of the analytes in live cells and organisms. Although DNA-functionalized AuNPs have been successfully applied to biosensing of nucleic acids and small molecules in cells based on nucleic acid hybridization and aptamers [230, 279–282], such application based on DNAzymes and AuNPs for metal ion detection in live cells is still very challenging and has been reported only recently [283].

2.2.1 Nucleic Acid Cleaving/Ligating DNAzymes and AuNPs for Biosensing

In 2003, a colorimetric biosensor for lead ion (Pb^{2+}) was developed based on the DNA-directed assembly of 13 nm AuNPs in our lab (Fig. 4a) [194]. DNA-functionalized AuNPs were mixed with 8–17 DNAzymes and nucleic acid substrates. The nucleic acid substrates cross-linked the AuNPs into aggregates via DNA hybridization after mild heating at 50 °C and annealing, resulting in a blue solution and an absorption band around 700 nm. However, in the presence of the target (Pb^{2+}, the cofactor of the DNAzyme), the nucleic acid substrates that crosslinked

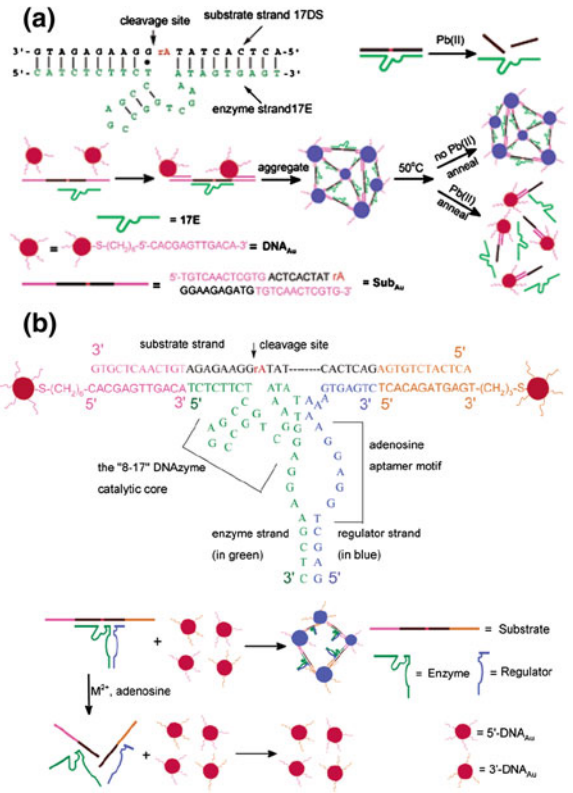

Fig. 4 Colorimetric detection of (**a**) Pb^{2+} and (**b**) adenosine using DNAzyme-functionalized AuNPs by an 8–17 DNAzyme and an adenosine-specific aptazyme, respectively (Adapted from Ref. [194, 244])

the AuNP together were cleaved by the DNAzymes so that no AuNPs aggregates could form. A red color and an absorption band at 522 nm were observed in this case. When an inactive DNAzyme was used, the DNA-directed assembly of AuNPs still occurred, but no color change was observed regardless of whether the samples contained Pb^{2+}. Interestingly, by changing the ratio of active and inactive DNAzymes, the dynamic range of the biosensor could be tuned from 0.1 $\sim$ 4 to 10 $\sim$ 200 μM [194]. This method was further optimized by testing the biosensor using different DNAzyme lengths, AuNP alignments, stoichiometries of DNAzyme to its substrate, buffer pH, and temperatures [242].

To enable fast Pb^{2+} detection at ambient temperature, the "tail-to-tail" alignment of 42-nm AuNPs was used for the biosensor design. The alignment and size of AuNPs were the major determining factors to achieve fast color changes and assembly of AuNP aggregates [241]. In another work, DNA functionalized AuNPs first assembled into aggregates cross-linked by 8–17 DNAzymes and substrates. Then, the aggregates were used as a biosensor system to detect Pb^{2+} by disassembling them in the presence of Pb^{2+} with the assistance of invasive DNA, resulting in color changes from blue to red and a blue shift in absorption spectra [245]. Compared with the previous methods [194, 241, 242], this new design

exhibited a "light-up" response to Pb^{2+} rather than a "light-down," and thus was less vulnerable to interference from other species that could inhibit the DNAzyme activity [245]. To eliminate the requirement of invasive DNA usage, an improved design using asymmetric DNAzymes to form the AuNP aggregates as the biosensor system was also developed [246].

In addition to Pb^{2+}, the biosensor system was further modified to detect adenosine by replacing the 8–17 DNAzyme with a DNA aptazyme (Fig. 4b). The aptazyme was a combination of an 8–17 DNAzyme and an adenosine aptamer, with the latter sequence inserted to one binding arm of the 8–17 DNAzyme. In this case, only in the presence of both adenosine and Pb^{2+} could the DNAzyme motif be activated to cleave its substrate and disassemble the AuNP aggregates [244].

In addition to the 8–17 DNAzyme that is specific to Pb^{2+}, other DNAzymes such as a nucleic acid ligating E47 DNAzyme for cupric ion (Cu^{2+}) and a nucleic acid cleaving 39E DNAzyme for uranyl ion (UO_2^{2+}) were also functionalized with AuNPs for the detection of Cu^{2+} and UO_2^{2+} through the color change of AuNP assemblies [247, 248]. In the former case, the E47 DNAzyme catalyzed the ligation of two short DNA strands into a long strand in the presence of Cu^{2+}. The long DNA strand could then bind two types of DNA-functionalized AuNPs by linking two short DNA fragments via DNA hybridization, respectively, to form blue colored aggregates as a response to Cu^{2+} in the solution [247]. In the latter case, the 39E DNAzyme induced the cleavage of a nucleic acid substrate with UO_2^{2+} as the cofactor. Upon the addition of UO_2^{2+} to AuNP aggregates cross-linked by 39E DNAzymes and their substrates, the cross-linker substrates were cleaved and caused the disassembly of the AuNP aggregates, resulting in color changes from blue to red [248].

In contrast to the above examples of AuNP aggregate formation by DNA cross-linkers [182], non-crosslinking DNA hybridization could also induce rapid aggregation of AuNPs [284]. For example, Li and coworkers utilized the 8–17 DNAzymes and substrates to functionalize discrete AuNPs without cross-linking, where Pb^{2+}-induced cleavage of the substrates reduced the stability of the AuNP colloid solution and caused aggregation. The detection of Pb^{2+} in this simple method was successfully achieved by monitoring the color change from red to purple or the red shift in absorption spectra due to the Pb^{2+}-induced aggregation of AuNPs [285].

To make the metal ion detection more user-friendly, lateral-flow devices were also developed based on DNAzymes and AuNPs for dipstick tests. In one design, the 8–17 DNAzymes and substrates were modified with biotin and functionalized on AuNPs. In the absence of Pb^{2+}, the AuNPs in the lateral-flow device were captured by the streptavidins immobilized on the device in the control zone, thus showing a colored band in this zone as a sign of Pb^{2+} free samples (Fig. 5a). However, when Pb^{2+} was present, the cleavage of the substrates removed the biotin labels from AuNPs and allowed them to go through the control zone on the device to reach the test zone containing immobilized complementary DNA, where biotin-free AuNPs were captured and displayed a colored band, indicating the presence of Pb^{2+} in the samples [256]. In another design by Zeng and coworkers, a

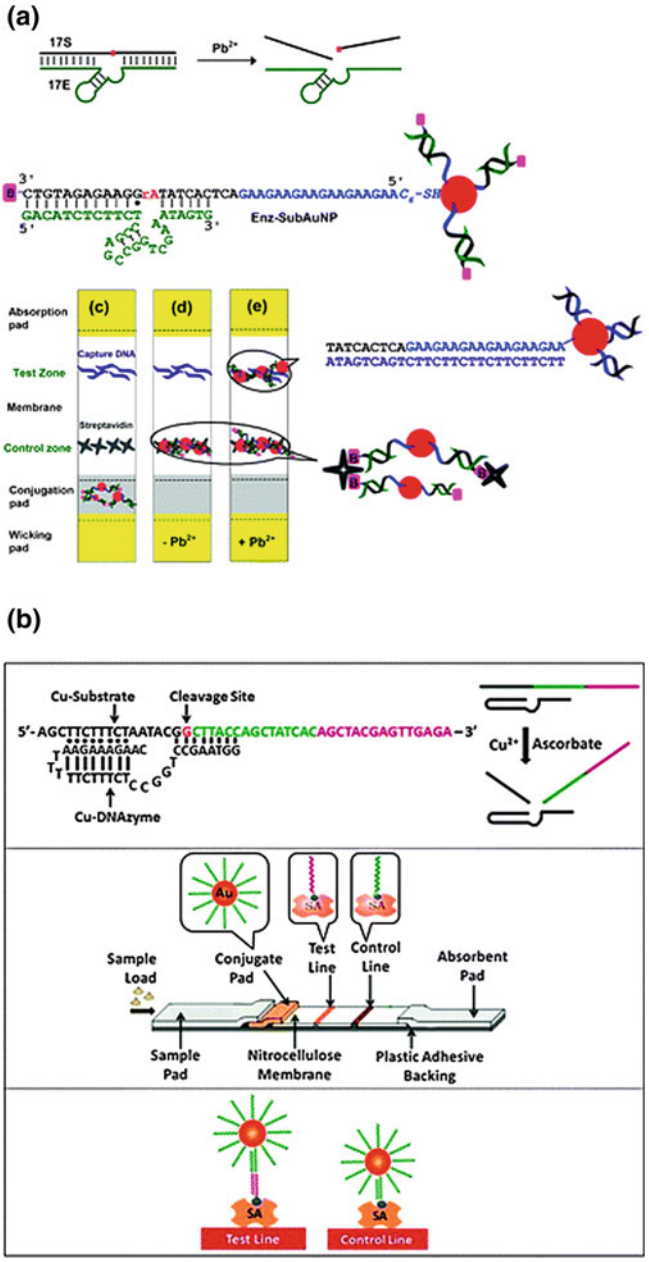

Fig. 5 Lateral-flow devices using DNAzyme-functionalized AuNPs for the detection of (**a**) Pb^{2+} and (**b**) Cu^{2+} (Adapted from Ref. [255, 256])

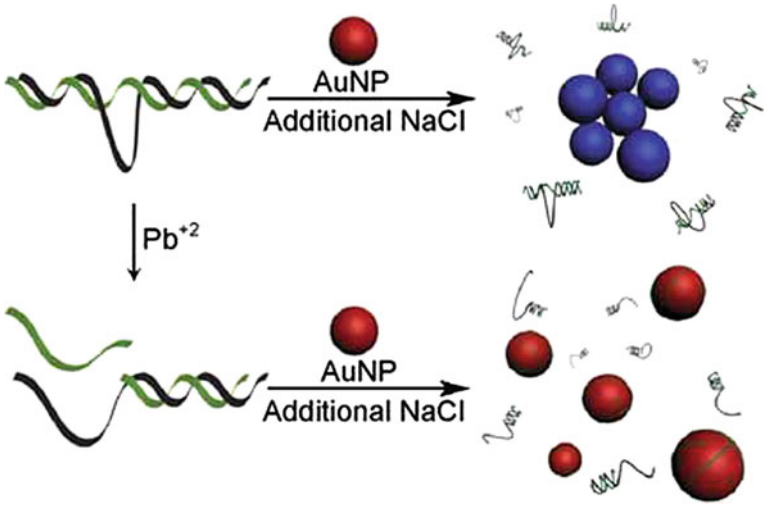

Fig. 6 Label-free detection of Pb^{2+} using DNAzymes and unmodified AuNPs (Adapted from Ref. [250])

nucleic acid cleaving DNAzyme specific for Cu^{2+} and its substrate were used without being prefunctionalized on AuNPs. The target Cu^{2+} interacted with the DNAzyme and substrate first, releasing a single-stranded DNA (ssDNA) piece that could link DNA-functionalized AuNPs to the test line by DNA hybridization (Fig. 5b). In the absence of Cu^{2+}, however, no release of the ssDNA occurred, thus the AuNPs moved across the test line and were captured on the control line where complementary DNA was immobilized. Therefore, a red line appeared on the test line only when Cu^{2+} was present in the samples [255]. Later, the same research group further incorporated a catalytic DNA circuit that could amplify the release of a ssDNA by the 8–17 DNAzyme and its substrate, achieving the detection of Pb^{2+} on a lateral-flow device with high sensitivity [277].

In addition to the lateral-flow device, an interesting study by Yu and coworkers utilized a conventional compact disc as the platform for Pb^{2+} detection based on DNAzymes and AuNPs. In their method, Pb^{2+}-induced cleavage of the substrate strand prevented the attachment of DNA-functionalized AuNPs onto the disc coated with complementary DNA. When Pb^{2+} was present in samples, fewer AuNPs were decorated on the disc to induce error in disc reading. Any optical drive from a computer could be used as a reader for this Pb^{2+} detection with the disc [265]. We also developed a method to use a low-cost commercial device, a glucose meter, to detect Pb^{2+} using DNAzymes, although no AuNPs were involved in the method [286].

In 2008, unmodified AuNPs were found to have the ability to couple with label-free DNAzymes and substrates for Pb^{2+} detection (Fig. 6) [250, 251]. The approach was based on a previous finding by Rothberg and coworkers that ssDNA

and double-stranded DNA (dsDNA) had distinct binding affinities and stabilization effects on unmodified AuNPs [218–220, 287]. Upon cleavage of the nucleic acid substrate by the 8–17 DNAzyme in the presence of Pb^{2+}, a ssDNA fragment was released from the DNA duplex to bind unmodified AuNPs. Because this ssDNA fragment had a stronger binding affinity to AuNPs to stabilize the colloid solution, the red color of the solution was only preserved when Pb^{2+} was present. By measuring the absorbance ratio at two wavelengths, the Pb^{2+} concentration was quantified [250, 251]. Through a very similar design but using another nucleic acid cleaving DNAzyme for Cu^{2+} with unmodified AuNPs, Yang and coworkers also developed a label-free method for detection of Cu^{2+} [257].

In addition to the above colorimetric methods based on DNAzyme-functionalized AuNPs, other analytical techniques have also been utilized to detect the target-induced change of DNAzyme-substrate duplexes and AuNPs. For example, AuNP-induced light scattering was used to develop biosensor systems for the detection of Pb^{2+} (Fig. 7a) and Cu^{2+} [263, 271, 273, 274]. The approach was based on the cleavage of substrates in the presence of metal ions by DNAzymes to either disassemble the DNA cross-linked AuNP aggregates [263] or prevent the aggregation of unmodified AuNPs [271, 273, 274]. In all these studies, the quantification of metal ions was achieved by measuring the difference in light-scattering properties between discrete AuNPs and aggregates [263, 271, 273, 274]. SERS [267] and SPR [275] (Fig. 7b) were also used to detect Pb^{2+} by measuring the release of AuNPs [267] and the activation of catalytic motifs [275] by the DNAzyme-catalyzed cleavage of substrates on surfaces, respectively.

Instead of generating signals directly, AuNPs can also serve as efficient fluorescence quenchers for the design of fluorescent biosensors [224, 288]. Following this principle, a Pb^{2+} sensor was developed by attaching fluorophore-labeled 8–17 DNAzymes and substrates to AuNPs, which underwent fluorescence enhancement in the presence of Pb^{2+} as a result of the increase in fluorophore-AuNP distance upon DNAzyme-catalyzed cleavage of the substrate [260]. Another study used a similar design for a Cu^{2+}-specific DNAzyme but was applied for ascorbic acid detection rather than Cu^{2+}, taking advantage of the requirement of ascorbic acid to reduce Cu^{2+} for the DNAzyme's activity [272]. Similarly, rod-shaped AuNPs coated with positively charged surfactants acted as binders and quenchers for flurophore-labeled 8–17 DNAzymes and substrates, allowing the detection of Pb^{2+} by fluorescence enhancement [266]. In addition to fluorescence quenching, AuNPs could serve as fluorescence anisotropy generators for the coated fluorophores due to the large size compared to free fluorophores and DNA. Based on this principle, a fluorescence anisotropy sensor was constructed using DNAzyme-functionalized AuNPs for the detection of Cu^{2+} and Pb^{2+} [259]. Finally, DNAzyme-functionalized AuNPs were also incorporated with electrochemically active substances for biosensor applications. Electrochemical sensors for Pb^{2+} were reported using Pb^{2+}-induced cleavage of nucleic acid substrates on AuNPs by 8–17 DNAzymes to enable the detachment (Fig. 7c) [249] or attachment [258] of AuNPs onto a DNA-coated electrode. The DNA on AuNPs permits attachment of large amounts of

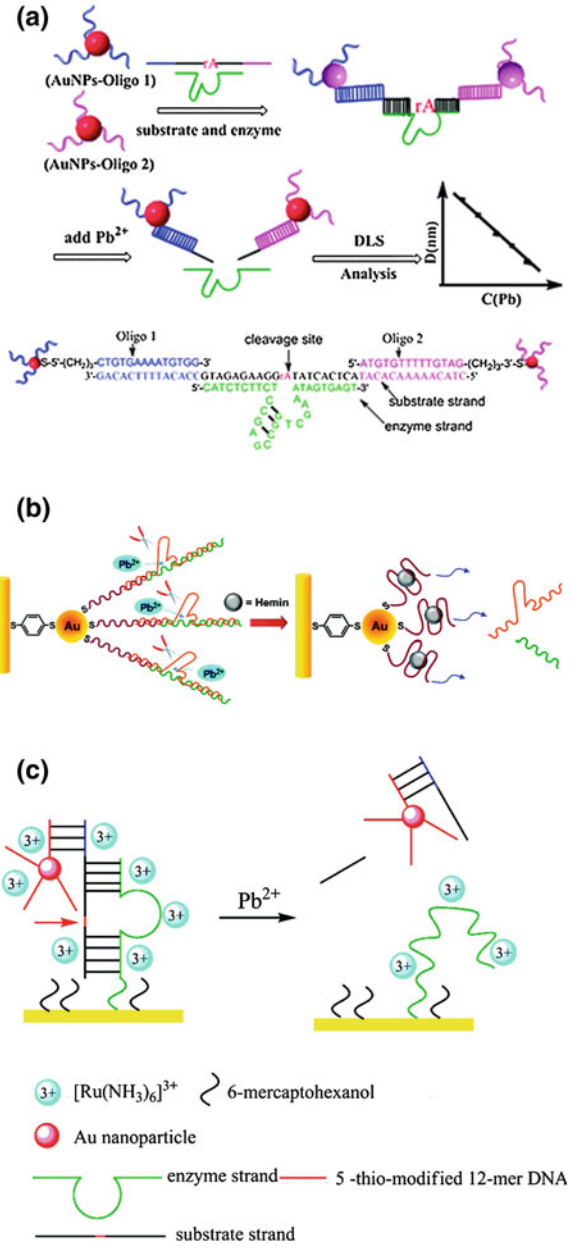

Fig. 7 DNAzyme-functionalized AuNPs for the detection of Pb^{2+} using (**a**) dynamic light scattering, (**b**) SPR, and (**c**) electrochemistry (Adapted from Ref. [249, 263, 275])

electrochemically active metal complexes, thus providing a large signal enhancement on the electrode in the presence of Pb^{2+} [249, 258]. Graphene sheets decorated by DNAzyme-functionalized AuNPs were also used to detect L-histidine and Pb^{2+} as the cofactors of two DNAzymes, respectively [261, 278].

2.2.2 Peroxidase-mimicking DNAzymes and AuNPs for Biosensing

Unlike the nucleic acid cleaving or ligating DNAzymes mentioned above that could recognize the target molecules and transform the recognition event into changes of AuNPs, peroxidase-mimicking DNAzymes [28, 29, 40, 169] usually serve as signal generators or enhancers by catalyzing the production of optically active substances, with AuNPs as carriers of many such DNAzymes for signal amplification. Willner and coworkers developed a telomerase activity assay using DNAzyme-functionalized AuNPs (Fig. 8a). In their method, the DNA immobilized on a surface was extended with telomere repeat units to capture the AuNPs via DNA hybridization. Then, the DNAzymes on the surface-bound AuNPs catalyzed the production of chemiluminescence. The more telomerase activity was present in samples, the more DNAzymes and AuNPs were immobilized, generating more intense chemiluminescence [221].

A similar design using magnetic particles as the surface was reported for the colorimetric detection of nucleic acids, where the target-induced immobilization of DNAzyme-functionalized AuNPs catalyzed the production of colored $ABTS^+$ from H_2O_2 and ABTS (Fig. 8b) [253]. By functionalizing AuNPs with both DNAzymes and antibodies, sandwich immunoassays were successfully achieved using the DNAzymes on AuNPs to generate color [254], electrochemiluminescence (Fig. 8c) [262], and chemiluminescence [264] signals for the detection of α-fetoprotein and carcinoembryonic antigen. Pb^{2+} detection using Pb^{2+}-specific DNAzymes [275] or Pb^{2+}-binding G-quarduplex [270] and AuNPs as carriers for peroxidase-mimicking DNAzymes were also achieved by electrochemistry [275] and fluorescence [270] measurements. Another study used AuNPs as carriers of two halves of a peroxidase-mimicking DNAzyme. The two halves were released when target nucleic acids or small molecules interacted with the DNA or aptamers on the surface of the AuNPs, respectively. Then the released halves formed active DNAzymes in solution and generated chemiluminescence for sensitive detection [276].

2.2.3 DNAzyme-Functionalized AuNPs for Intracellular Biosensing

AuNPs were first found by Mirkin and coworkers as an efficient material for the delivery of DNA into cells for intracellular gene regulation and the detection of mRNA and ATP [230, 279, 280]. By functionalizing AuNPs with DNAzymes, delivery of DNAzymes into cells to sequence-specifically cleave mRNA [281] and perform RNAi-independent gene regulation [282] were achieved. Despite these achievements, there are still very few studies using DNAzyme-functionalized AuNPs for intracellular biosensing.

Recently, our group has developed a new method to attach fluorophore-labeled UO_2^{2+}-specific DNAzymes and substrates onto AuNPs for intracellular UO_2^{2+} detection (Fig. 9). The UO_2^{2+}-specific 39E DNAzyme was conjugated to the AuNP through a thiol tag, and the substrate strand was modified with a Cy3

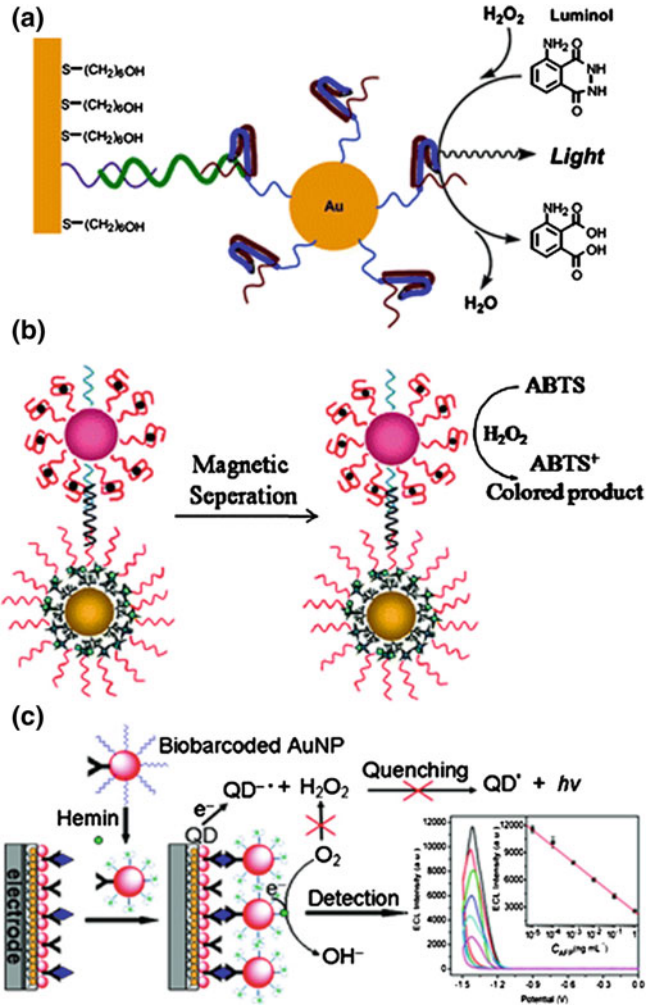

Fig. 8 Detection of (**a**) telomerase activity, (**b**) nucleic acid, and (**c**) protein biomarker using AuNPs as support for peroxidase-mimicking DNAzymes (Adapted from Ref. [211, 253, 262])

fluorophore and a molecular quencher to reduce background. In the absence of UO_2^{2+}, the fluorescence of the Cy3 was quenched by both the AuNP and the molecular quencher. In the presence of UO_2^{2+}, the DNAzyme cleaved the fluorophore-labeled substrate strand, resulting in the release of the shorter ssDNA containing the Cy3, and accompanied by fluorescence enhancement. We demonstrated that this DNAzyme–AuNP biosensor could readily enter cells and serve as a UO_2^{2+} sensor within a cellular environment, making it the first demonstration of DNAzymes as intracellular metal ion sensors [283].

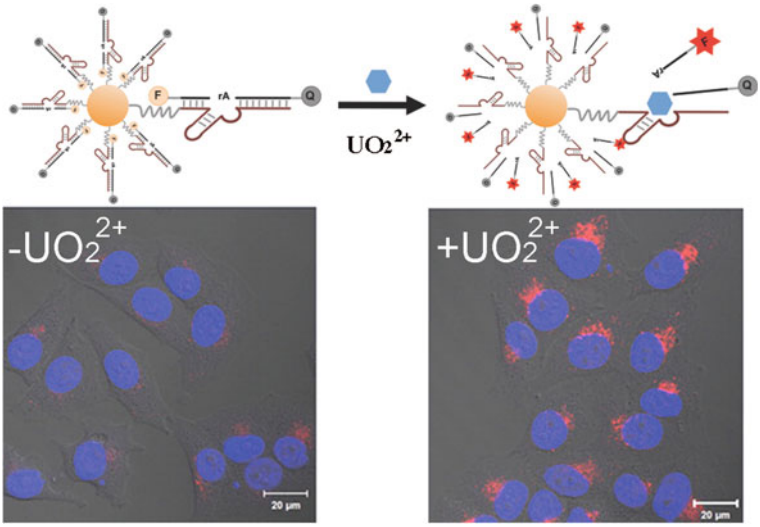

Fig. 9 Fluorescent UO_2^{2+}-specific DNAzyme immobilized onto AuNP as selective turn-on UO_2^{2+} sensors inside live cells. The scale bar is 20 μm (Adapted from Ref. [283])

3 Summary and Outlook

Since the discovery of the first DNAzyme that catalyzed the cleavage of RNA in 1994, more and more DNAzymes with diverse functions have been obtained by the in vitro selection technique and are being actively pursued for many applications including biosensing, especially for metal ion detection in both the environment and biology. AuNPs, on the other hand, are ideal materials for biosensing due to their prominent properties as efficient signal reporters, DNA carriers, and cellular delivery materials. Therefore, intensive research has been carried out in recent years to utilize DNAzyme-functionalized AuNPs for biosensing and other applications, and there is no doubt that the future work and impact of this field will continue to grow.

One challenge in this field is the discovery of new DNAzymes to cover more metal ions and other target molecules. DNAzymes specific for Mg^{2+}, Zn^{2+}, Pb^{2+}, Cu^{2+}, Co^{2+}, Hg^{2+}, and UO_2^{2+} have been selected from random DNA libraries and biochemically characterized [3, 4, 10–20]. However, many other important molecules and especially metal ions, such as iron (Fe^{2+} and Fe^{3+}), Cr^{3+}, Ni^{2+}, and Mn^{2+} in biology, still do not have a DNAzyme to selectively recognize each of them. Introducing modified DNA bases or backbone into random DNA libraries is one promising method to extend the possibility of obtaining these candidates. However, the available techniques for amplifying DNA with artificial modifications for in vitro selection are still limited and require active collaboration from many disciplines such as chemistry, chemical biology, and biochemistry.

On the other hand, although AuNPs provide many unique properties for signal amplification, one hurdle for wide adoption in commercial products is batch-to-batch variations and quality controls. Overcoming this hurdle is critical to translate the technology from bench to the field, clinics, and home.

Another challenge is the application of DNAzyme-functionalized AuNPs in intracellular biosensing. Although AuNPs can efficiently deliver DNAzymes and substrates into cells and serve as part of the sensor systems, such as signal reporters for light scattering and SERS or quenchers for fluorescence, the intracellular localization and activation of such sensors are still difficult and demand more general methods to be developed because many intracellular targets are not evenly distributed in cells. In addition, most DNAzymes currently available are not selected under cellular conditions, so they may need optimization and reselection to ensure their activities are still viable inside cells and on the surface of AuNPs to recognize specific targets. Stability of DNAzymes in a cellular environment has not been well understood and DNA modifications are required to make DNAzymes more resistant to enzymatic degradation while still retaining their activities.

Finally, the cytotoxicity and biological effects of nanomaterials such as AuNPs on different cells are not well understood currently, and how DNAzyme functionalization will affect these properties of AuNPs is still an open question to be answered. These are critical for the future applications of DNAzyme-functionalized AuNPs in cellular and in vivo biosensing. Given the progress made in this area in the past 10 years, more efficient DNAzyme–AuNP-based sensors will be developed in the near future.

Acknowledgments We thank the Lu group members who contributed to the work described in this chapter and the U.S. National Institutes of Health (ES16865), Department of Energy (DE-FG02-08ER64568), and National Science Foundation (CTS-0120978) for financial support.

References

1. Watson JD, Crick FHC (1953) Molecular structure of nucleic acids: a structure for deoxyribose nucleic acid. Nature 171:737–738
2. Saenger W (1984) Principles of nucleic acid structure. Springer, New York
3. Breaker RR, Joyce GF (1994) A DNA enzyme that cleaves RNA. Chem Biol 1:223–229
4. Cuenoud B, Szostak JW (1995) A DNA metalloenzyme with DNA ligase activity. Nature 375:611–614
5. Robertson DL, Joyce GF (1990) Selection in vitro of an RNA enzyme that specifically cleaves single-stranded-DNA. Nature 344:467–468
6. Bock LC, Griffin LC, Latham JA, Vermaas EH, Toole JJ (1992) Selection of single-stranded-DNA molecules that bind and inhibit human thrombin. Nature 355:564–566
7. Ellington AD, Szostak JW (1992) Selection invitro of single-stranded-DNA molecules that fold into specific ligand-binding structures. Nature 355:850–852
8. Tuerk C, Gold L (1990) Systematic evolution of ligands by exponential enrichment: RNA ligands to bacteriophage T4 DNA polymerase. Science 249:505–510
9. Ellington AD, Szostak JW (1990) In vitro selection of RNA molecules that bind specific ligands. Nature 346:818–822

10. Breaker RR, Joyce GF (1995) A DNA enzyme with Mg2 + -dependent RNA phosphoesterase activity. Chem Biol 2:655–660
11. Carmi N, Shultz LA, Breaker RR (1996) In vitro selection of self-cleaving DNAs. Chem Biol 3:1039–1046
12. Santoro SW, Joyce GF (1997) A general purpose RNA-cleaving DNA enzyme. Proc Natl Acad Sci USA 94:4262–4266
13. Carmi N, Balkhi SR, Breaker RR (1998) Cleaving DNA with DNA. Proc Natl Acad Sci USA 95:2233–2237
14. Feldman AR, Sen D (2001) A new and efficient DNA enzyme for the sequence-specific cleavage of RNA. J Mol Biol 313:283–294
15. Liu J, Lu Y (2007) Rational design of "Turn-On" allosteric DNAzyme catalytic beacons for aqueous mercury ions with ultrahigh sensitivity and selectivity. Angew Chem Int Ed 46:7587–7590
16. Liu JW, Brown AK, Meng XL, Cropek DM, Istok JD, Watson DB, Lu Y (2007) A catalytic beacon sensor for uranium with parts-per-trillion sensitivity and millionfold selectivity. Proc Natl Acad Sci USA 104:2056–2061
17. Hollenstein M, Hipolito C, Lam C, Dietrich D, Perrin DM (2008) A highly selective DNAzyme sensor for mercuric ions. Angew Chem Int Ed 47:4346–4350
18. Chandra M, Sachdeva A, Silverman SK (2009) DNA-catalyzed sequence-specific hydrolysis of DNA. Nat Chem Biol 5:718–720
19. Sreedhara A, Li YF, Breaker RR (2004) Ligating DNA with DNA. J Am Chem Soc 126:3454–3460
20. Purtha WE, Coppins RL, Smalley MK, Silverman SK (2005) General deoxyribozyme-catalyzed synthesis of native 3′-5′ RNA linkages. J Am Chem Soc 127:13124–13125
21. Li YF, Breaker RR (1999) Phosphorylating DNA with DNA. Proc Natl Acad Sci USA 96:2746–2751
22. Li YF, Liu Y, Breaker RR (2000) Capping DNA with DNA. Biochemistry 39:3106–3114
23. Sheppard TL, Ordoukhanian P, Joyce GF (2000) A DNA enzyme with N-glycosylase activity. Proc Natl Acad Sci USA 97:7802–7807
24. Chinnapen DJF, Sen D (2004) A deoxyribozyme that harnesses light to repair thymine dimers in DNA. Proc Natl Acad Sci USA 101:65–69
25. Thorne RE, Chinnapen DJF, Sekhon GS, Sen D (2009) A deoxyribozyme, Sero1C, uses light and serotonin to repair diverse pyrimidine dimers in DNA. J Mol Biol 388:21–29
26. Pradeepkumar PI, Hobartner C, Baum DA, Silverman SK (2008) DNA-catalyzed formation of nucleopeptide linkages. Angew Chem Int Ed 47:1753–1757
27. Sachdeva A, Silverman SK (2010) DNA-catalyzed serine side chain reactivity and selectivity. Chem Commun 46:2215–2217
28. Li YF, Sen D (1996) A catalytic DNA for porphyrin metallation. Nat Struct Biol 3:743–747
29. Travascio P, Li YF, Sen D (1998) DNA-enhanced peroxidase activity of a DNA aptamer-hemin complex. Chem Biol 5:505–517
30. Poon LCH, Methot SP, Morabi-Pazooki W, Pio F, Bennet AJ, Sen D (2011) Guanine-rich RNAs and DNAs that bind heme robustly catalyze oxygen transfer reactions. J Am Chem Soc 133:1877–1884
31. Chandra M, Silverman SK (2008) DNA and RNA can be equally efficient catalysts for carbon–carbon bond formation. J Am Chem Soc 130:2936–2937
32. Kurreck J (2003) Antisense technologies—improvement through novel chemical modifications. Eur J Biochem 270:1628–1644
33. Schubert S, Gul DC, Grunert HP, Zeichhardt H, Erdmann VA, Kurreck J (2003) RNA cleaving '10-23' DNAzymes with enhanced stability and activity. Nucleic Acids Res 31:5982–5992
34. Kuwabara T, Warashina M, Taira K (2000) Allosterically controllable ribozymes with biosensor functions. Curr Opin Chem Biol 4:669–677
35. Navani NK, Li YF (2006) Nucleic acid aptamers and enzymes as sensors. Curr Opin Chem Biol 10:272–281

36. Vannela R, Adriaens P (2006) DNAzymes in environmental sensing. Crit Rev Environ Sci Technol 36:375–403
37. Mok W, Li YF (2008) Recent progress in nucleic acid aptamer-based biosensors and bioassays. Sensors 8:7050–7084
38. Palchetti I, Mascini M (2008) Nucleic acid biosensors for environmental pollution monitoring. Analyst 133:846–854
39. Willner I, Shlyahovsky B, Zayats M, Willner B (2008) DNAzymes for sensing, nanobiotechnology and logic gate applications. Chem Soc Rev 37:1153–1165
40. Kosman J, Juskowiak B (2011) Peroxidase-mimicking DNAzymes for biosensing applications: a review. Anal Chim Acta 707:7–17
41. Ma DL, Chan DSH, Man BYW, Leung CH (2011) Oligonucleotide-based luminescent detection of metal Ions. Chem Asian J. 6:986–1003
42. Lu Y, Liu JW, Li J, Bruesehoff PJ, Pavot CMB, Brown AK (2003) New highly sensitive and selective catalytic DNA biosensors for metal ions. Biosens Bioelectron 18:529–540
43. Liu JW, Cao ZH, Lu Y (2009) Functional nucleic acid sensors. Chem Rev 109:1948–1998
44. Nagraj N, Lu Y (2011) Catalytic nucleic acid biosensors for environmental monitoring. In: Mascini M, Palchetti I (eds) Nucleic acid biosensors for environmental pollution monitoring. Royal Society of Chemistry, Cambridge
45. Zhang XB, Kong RM, Lu Y (2011) Metal ion sensors based on DNAzymes and related DNA molecules. Annu Rev Anal Chem 4:105–128
46. Stojanovic MN (2008) Molecular computing with deoxyribozymes. Prog Nucleic Acid Res Mol Biol 82:199–217
47. Chen X, Ellington AD (2010) Shaping up nucleic acid computation. Curr Opin Biotechnol 21:392–400
48. Teller C, Willner I (2010) Functional nucleic acid nanostructures and DNA machines. Curr Opin Biotechnol 21:376–391
49. Pyle AM, Chu VT, Jankowsky E, Boudvillain H (2000) Using DNAzymes to cut, process, and map RNA molecules for structural studies or modification. Methods Enzymol 317:140–146
50. Scherer LJ, Rossi JJ (2003) Approaches for the sequence-specific knockdown of mRNA. Nat Biotechnol 21:1457–1465
51. Sioud M, Iversen PO (2005) Ribozymes, DNAzymes and small interfering RNAs as therapeutics. Curr Drug Targets 6:647–653
52. Bhindi R, Fahmy RG, Lowe HC, Chesterman CN, Dass CR, Cairns MJ, Saravolac EG, Sun LQ, Khachigian LM (2007) Brothers in arms—DNA enzymes, short interfering RNA, and the emerging wave of small-molecule nucleic acid-based gene-silencing strategies. Am J Pathol 171:1079–1088
53. Isaka Y (2007) DNAzymes as potential therapeutic molecules. Curr Opin Mol Ther 9:132–136
54. Tan ML, Choong PFM, Dass CR (2009) DNAzyme delivery systems: Getting past first base. Expert Opin Drug Deliv 6:127–138
55. Sun LQ, Cairns MJ, Saravolac EG, Baker A, Gerlach WL (2000) Catalytic nucleic acids: From lab to applications. Pharmacol Rev 52:325–347
56. Emilsson GM, Breaker RR (2002) Deoxyribozymes: new activities and new applications. Cell Mol Life Sci 59:596–607
57. Breaker RR (2004) Natural and engineered nucleic acids as tools to explore biology. Nature 432:838–845
58. Peracchi A (2005) DNA catalysis: potential, limitations, open questions. ChemBioChem 6:1316–1322
59. Silverman SK (2005) In vitro selection, characterization, and application of deoxyribozymes that cleave RNA. Nucleic Acids Res 33:6151–6163
60. Baum DA, Silverman SK (2008) Deoxyribozymes: useful DNA catalysts in vitro and in vivo. Cell Mol Life Sci 65:2156–2174

61. Sardar R, Funston AM, Mulvaney P, Murray RW (2009) Gold nanoparticles: Past, present, and future. Langmuir 25:13840–13851
62. Schmid G, Corain B (2003) Nanoparticulated gold: syntheses, structures, electronics, and reactivities. Eur J, Inorg Chem, pp 3081–3098
63. Zhao P, Li N, Astruc D (2013) State of the art in gold nanoparticle synthesis. Coord Chem Rev 257:638–665
64. Pileni MP (2003) The role of soft colloidal templates in controlling the size and shape of inorganic nanocrystals. Nat Mater 2:145–150
65. Grzelczak M, Perez-Juste J, Mulvaney P, Liz-Marzan LM (2008) Shape control in gold nanoparticle synthesis. Chem Soc Rev 37:1783–1791
66. Tao AR, Habas S, Yang P (2008) Shape control of colloidal metal nanocrystals. Small 4:310–325
67. Xia Y, Xiong Y, Lim B, Skrabalak SE (2009) Shape-controlled synthesis of metal nanocrystals: simple chemistry meets complex physics? Angew Chem Int Ed 48:60–103
68. Sau TK, Murphy CJ (2004) Room temperature, high-yield synthesis of multiple shapes of gold nanoparticles in aqueous solution. J Am Chem Soc 126:8648–8649
69. Brust M, Walker M, Bethell D, Schiffrin DJ, Whyman R (1994) Synthesis of thiol-derivatized gold nanoparticles in a 2-phase liquid–liquid system. J Chem Soc, Chem Commun 7:801–802
70. Brust M, Fink J, Bethell D, Schiffrin DJ, Kiely C (1995) Synthesis and reactions of functionalized gold nanoparticles. J Chem Soc, Chem Commun 16:1655–1656
71. Park J, Joo J, Kwon SG, Jang Y, Hyeon T (2007) Synthesis of monodisperse spherical nanocrystals. Angew Chem Int Ed 46:4630–4660
72. Link S, El-Sayed MA (1999) Size and temperature dependence of the plasmon absorption of colloidal gold nanoparticles. J Phys Chem B 103:4212–4217
73. Yu YY, Chang SS, Lee CL, Wang CRC (1997) Gold nanorods: electrochemical synthesis and optical properties. J Phys Chem B 101:6661–6664
74. Jana NR, Gearheart L, Murphy CJ (2001) Wet chemical synthesis of high aspect ratio cylindrical gold nanorods. J Phys Chem B 105:4065–4067
75. Kim F, Song JH, Yang PD (2002) Photochemical synthesis of gold nanorods. J Am Chem Soc 124:14316–14317
76. Murphy CJ, Jana NR (2002) Controlling the aspect ratio of inorganic nanorods and nanowires. Adv Mater 14:80–82
77. Nikoobakht B, El-Sayed MA (2003) Preparation and growth mechanism of gold nanorods (NRs) using seed-mediated growth method. Chem Mater 15:1957–1962
78. Perez-Juste J, Pastoriza-Santos I, Liz-Marzan LM, Mulvaney P (2005) Gold nanorods: synthesis, characterization and applications. Coord Chem Rev 249:1870–1901
79. Busbee BD, Obare SO, Murphy CJ (2003) An improved synthesis of high-aspect-ratio gold nanorods. Adv Mater 15:414–416
80. Huang X, Neretina S, El-Sayed MA (2009) Gold nanorods: from synthesis and properties to biological and biomedical applications. Adv Mater 21:4880–4910
81. Shankar SS, Rai A, Ankamwar B, Singh A, Ahmad A, Sastry M (2004) Biological synthesis of triangular gold nanoprisms. Nat Mater 3:482–488
82. Metraux GS, Mirkin CA (2005) Rapid thermal synthesis of silver nanoprisms with chemically tailorable thickness. Adv Mater 17:412–415
83. Millstone JE, Park S, Shuford KL, Qin LD, Schatz GC, Mirkin CA (2005) Observation of a quadrupole plasmon mode for a colloidal solution of gold nanoprisms. J Am Chem Soc 127:5312–5313
84. Millstone JE, Metraux GS, Mirkin CA (2006) Controlling the edge length of gold nanoprisms via a seed-mediated approach. Adv Funct Mater 16:1209–1214
85. Chen J, Saeki F, Wiley BJ, Cang H, Cobb MJ, Li ZY, Au L, Zhang H, Kimmey MB, Li XD, Xia YN (2005) Gold nanocages: bioconjugation and their potential use as optical imaging contrast agents. Nano Lett 5:473–477

86. Skrabalak SE, Chen J, Sun Y, Lu X, Au L, Cobley CM, Xia Y (2008) Gold nanocages: synthesis, properties, and applications. Acc Chem Res 41:1587–1595
87. Xia Y, Li W, Cobley CM, Chen J, Xia X, Zhang Q, Yang M, Cho EC, Brown PK (2011) Gold nanocages: from synthesis to theranostic applications. Acc Chem Res 44:914–924
88. Kondo Y, Takayanagi K (2000) Synthesis and characterization of helical multi-shell gold nanowires. Science 289:606–608
89. Wu B, Heidelberg A, Boland JJ (2005) Mechanical properties of ultrahigh-strength gold nanowires. Nat Mater 4:525–529
90. Daniel MC, Astruc D (2004) Gold nanoparticles: assembly, supramolecular chemistry, quantum-size-related properties, and applications toward biology, catalysis, and nanotechnology. Chem Rev 104:293–346
91. Vigderman L, Khanal BP, Zubarev ER (2012) Functional gold nanorods: synthesis, self-assembly, and sensing applications. Adv Mater 24:4811–4841
92. Storhoff JJ, Mirkin CA (1999) Programmed materials synthesis with DNA. Chem Rev 99:1849–1862
93. Ofir Y, Samanta B, Rotello VM (2008) Polymer and biopolymer mediated self-assembly of gold nanoparticles. Chem Soc Rev 37:1814–1823
94. Prasad BLV, Sorensen CM, Klabunde KJ (2008) Gold nanoparticle superlattices. Chem Soc Rev 37:1871–1883
95. Niemeyer CM, Simon U (2005) DNA-based assembly of metal nanoparticles. Eur J Inorg Chem 18:3641–3655
96. Lu Y, Liu JW (2007) Smart nanomaterials inspired by biology: Dynamic assembly of error-free nanomaterials in response to multiple chemical and biological stimuli. Acc Chem Res 40:315–323
97. Crookes-Goodson WJ, Slocik JM, Naik RR (2008) Bio-directed synthesis and assembly of nanomaterials. Chem Soc Rev 37:2403–2412
98. Wang ZD, Lu Y (2009) Functional DNA directed assembly of nanomaterials for biosensing. J Mater Chem 19:1788–1798
99. Kumar A, Hwang JH, Kumar S, Nam JM (2012) Tuning and assembling metal nanostructures with DNA. Chem Commun 49:2597–2609
100. Chen MS, Goodman DW (2006) Catalytically active gold: from nanoparticles to ultrathin films. Acc Chem Res 39:739–746
101. Hvolbaek B, Janssens TVW, Clausen BS, Falsig H, Christensen CH, Norskov JK (2007) Catalytic activity of Au nanoparticles. Nano Today 2:14–18
102. Min BK, Friend CM (2007) Heterogeneous gold-based catalysis for green chemistry: Low-temperature CO oxidation and propene oxidation. Chem Rev 107:2709–2724
103. Corma A, Garcia H (2008) Supported gold nanoparticles as catalysts for organic reactions. Chem Soc Rev 37:2096–2126
104. Xu WL, Shen H, Liu GK, Chen P (2009) Single-molecule kinetics of nanoparticle catalysis. Nano Res 2:911–922
105. Ma Z, Dai S (2011) Development of novel supported gold catalysts: a materials perspective. Nano Res 4:3–32
106. Stratakis M, Garcia H (2012) Catalysis by supported gold nanoparticles: beyond aerobic oxidative processes. Chem Rev 112:4469–4506
107. Ghosh SK, Pal T (2007) Interparticle coupling effect on the surface plasmon resonance of gold nanoparticles: from theory to applications. Chem Rev 107:4797–4862
108. Guo S, Wang E (2007) Synthesis and electrochemical applications of gold nanoparticles. Anal Chim Acta 598:181–192
109. Murphy CJ, Gole AM, Hunyadi SE, Stone JW, Sisco PN, Alkilany A, Kinard BE, Hankins P (2008) Chemical sensing and imaging with metallic nanorods. Chem Commun 5:544–557
110. Porter MD, Lipert RJ, Siperko LM, Wang G, Narayanana R (2008) SERS as a bioassay platform: fundamentals, design, and applications. Chem Soc Rev 37:1001–1011
111. Wilson R (2008) The use of gold nanoparticles in diagnostics and detection. Chem Soc Rev 37:2028–2045

112. Guo S, Dong S (2009) Biomolecule-nanoparticle hybrids for electrochemical biosensors. TRAC-Trend Anal Chem 28:96–109
113. Wang Z, Ma L (2009) Gold nanoparticle probes. Coord Chem Rev 253:1607–1618
114. Cao X, Ye Y, Liu S (2011) Gold nanoparticle-based signal amplification for biosensing. Anal Biochem 417:1–16
115. Lin Y-W, Huang C-C, Chang H-T (2011) Gold nanoparticle probes for the detection of mercury, lead and copper ions. Analyst 136:863–871
116. Liu D, Wang Z, Jiang X (2011) Gold nanoparticles for the colorimetric and fluorescent detection of ions and small organic molecules. Nanoscale 3:1421–1433
117. Jans H, Huo Q (2012) Gold nanoparticle-enabled biological and chemical detection and analysis. Chem Soc Rev 41:2849–2866
118. Lei JP, Ju HX (2012) Signal amplification using functional nanomaterials for biosensing. Chem Soc Rev 41:2122–2134
119. Saha K, Agasti SS, Kim C, Li X, Rotello VM (2012) Gold nanoparticles in chemical and biological sensing. Chem Rev 112:2739–2779
120. Zhao W, Brook MA, Li YF (2008) Design of gold nanoparticle-based colorimetricbiosensing assays. ChemBioChem 9:2363–2371
121. Lin Y-W, Liu C-W, Chang H-T (2009) DNA functionalized gold nanoparticles for bioanalysis. Anal Methods 1:14–24
122. Zanoli LM, D'Agata R, Spoto G (2012) Functionalized gold nanoparticles for ultrasensitive DNA detection. Anal Bioanal Chem 402:1759–1771
123. Hu M, Chen J, Li Z-Y, Au L, Hartland GV, Li X, Marquez M, Xia Y (2006) Gold nanostructures: engineering their plasmonic properties for biomedical applications. Chem Soc Rev 35:1084–1094
124. Huang XH, El-Sayed IH, Qian W, El-Sayed MA (2006) Cancer cell imaging and photothermal therapy in the near-infrared region by using gold nanorods. J Am Chem Soc 128:2115–2120
125. Huang X, Jain PK, El-Sayed IH, El-Sayed MA (2007) Gold nanoparticles: interesting optical properties and recent applications in cancer diagnostic and therapy. Nanomedicine 2:681–693
126. Murphy CJ, Gole AM, Stone JW, Sisco PN, Alkilany AM, Goldsmith EC, Baxter SC (2008) Gold nanoparticles in biology: beyond toxicity to cellular imaging. Acc Chem Res 41:1721–1730
127. Qian X, Peng X-H, Ansari DO, Yin-Goen Q, Chen GZ, Shin DM, Yang L, Young AN, Wang MD, Nie S (2008) In vivo tumor targeting and spectroscopic detection with surface-enhanced Raman nanoparticle tags. Nat Biotechnol 26:83–90
128. Sperling RA, Rivera gil P, Zhang F, Zanella M, Parak WJ (2008) Biological applications of gold nanoparticles. Chem Soc Rev 37:1896–1908
129. Boisselier E, Astruc D (2009) Gold nanoparticles in nanomedicine: Preparations, imaging, diagnostics, therapies and toxicity. Chem Soc Rev 38:1759–1782
130. Giljohann DA, Seferos DS, Daniel WL, Massich MD, Patel PC, Mirkin CA (2010) Gold nanoparticles for biology and medicine. Angew Chem Int Ed 49:3280–3294
131. Dreaden EC, Alkilany AM, Huang X, Murphy CJ, El-Sayed MA (2012) The golden age: gold nanoparticles for biomedicine. Chem Soc Rev 41:2740–2779
132. Lu Y, Liu JW (2006) Functional DNA nanotechnology: emerging applications of DNAzymes and aptamers. Curr Opin Biotechnol 17:580–588
133. Lu Y, Liu JW (2009) Catalyst-functionalized nanomaterials. WIREs Nanomed Nanobi. 1:35–46
134. Lee JH, Yigit MV, Mazumdar D, Lu Y (2010) Molecular diagnostic and drug delivery agents based on aptamer-nanomaterial conjugates. Adv Drug Delivery Rev 62:592–605
135. Sato K, Hosokawa K, Maeda M (2007) Colorimetric biosensors based on DNA-nanoparticle conjugates. Anal Sci 23:17–20
136. Knecht MR, Sethi M (2009) Bio-inspired colorimetric detection of Hg2 + and Pb2 + heavy metal ions using Au nanoparticles. Anal Bioanal Chem 394:33–46

137. Wang H, Yang RH, Yang L, Tan WH (2009) Nucleic acid conjugated nanomaterials for enhanced molecular recognition. ACS Nano 3:2451–2460
138. de la Escosura-Muniz A, Medina M, Merkoci A (2011) New trends in DNA sensors for environmental applications: nanomaterials, miniaturization, and lab-on-a-chip technology. In: Mascini M, Palchetti I (eds) Nucleic acid biosensors for environmental pollution monitoring. Royal Society of Chemistry, Cambridge
139. Sen D, Geyer CR (1998) DNA enzymes. Curr Opin Chem Biol 2:680–687
140. Famulok M, Jenne A (1999) Catalysis based on nucleic acid structures. In: Schmidtchen FP (ed) Implementation and redesign of catalytic function in biopolymers. Springer, Berlin
141. Kurz M, Breaker RR (1999) In vitro selection of nucleic acid enzymes. In: Famulok M, Winnacker E-L, Wong C-H (eds) Combinatorial Chemistry in Biology. Springer, Berlin
142. Joyce GF (2001) RNA cleavage by the 10–23 DNA enzyme. Methods Enzymol 341:503–517
143. Bittker JA, Phillips KJ, Liu DR (2002) Recent advances in the in vitro evolution of nucleic acids. Curr Opin Chem Biol 6:367–374
144. Cairns MJ, Saravolac EG, Sun LQ (2002) Catalytic DNA: a novel tool for gene suppression. Curr Drug Targets 3:269–279
145. Achenbach JC, Chiuman W, Cruz RPG, Li Y (2004) DNAzymes: from creation in vitro to application in vivo. Curr Pharm Biotechnol 5:321–336
146. Joyce GF (2004) Directed evolution of nucleic acid enzymes. Annu Rev Biochem 73:791–836
147. Peracchi A (2004) Prospects for antiviral ribozymes and deoxyribozymes. Rev Med Virol 14:47–64
148. Schubert S, Kurreck J (2004) Ribozyme- and deoxyribozyme-strategies for medical applications. Curr Drug Targets 5:667–681
149. Fiammengo R, Jaschke A (2005) Nucleic acid enzymes. Curr Opin Biotechnol 16:614–621
150. Lu Y (2006) Metalloprotein and metallo-DNA/RNAzyme design: current approaches, success measures, and future challenges. Inorg Chem 45:9930–9940
151. Hobartner C, Silverman SK (2007) Recent advances in DNA catalysis. Biopolymers 87:279–292
152. Benson VL, Khachigian LM, Lowe HC (2008) DNAzymes and cardiovascular disease. Br J Pharmacol 154:741–748
153. Dass CR, Choong PFM, Khachigian LM (2008) DNAzyme technology and cancer therapy: cleave and let die. Mol Cancer Ther 7:243–251
154. Pan WH, Clawson GA (2008) Catalytic DNAzymes: derivations and functions. Expert Opin Biol Ther 8:1071–1085
155. Silverman SK (2008) Catalytic DNA (deoxyribozymes) for synthetic applications—current abilities and future prospects. Chem Commun 14:3467–3485
156. Burton AS, Lehman N (2009) DNA before proteins? Recent discoveries in nucleic acid catalysis strengthen the case. Astrobiology 9:125–130
157. Silverman SK (2009) Deoxyribozymes: selection design and serendipity in the development of DNA catalysts. Acc Chem Res 42:1521–1531
158. Silverman SK, Baum DA (2009) Use of deoxyribozymes in RNA research. Methods Enzymol 469:95–117
159. Tan ML, Choon PFM, Dass CR (2009) Cancer, chitosan nanoparticles and catalytic nucleic acids. J Pharm Pharmacol 61:3–12
160. Franzen S (2010) Expanding the catalytic repertoire of ribozymes and deoxyribozymes beyond RNA substrates. Curr Opin Mol Ther 12:223–232
161. Heinisch T, Ward TR (2010) Design strategies for the creation of artificial metalloenzymes. Curr Opin Chem Biol 14:184–199
162. Kuwahara M, Sugimoto N (2010) Molecular evolution of functional nucleic acids with chemical modifications. Molecules 15:5423–5444
163. Mastroyiannopoulos NP, Uney JB, Phylactou LA (2010) The application of ribozymes and DNAzymes in muscle and brain. Molecules 15:5460–5472

164. McManus SA, Li YF (2010) The structural diversity of deoxyribozymes. Molecules 15:6269–6284
165. Schlosser K, Li YF (2010) A versatile endoribonuclease mimic made of DNA: characteristics and applications of the 8–17 RNA-cleaving DNAzyme. ChemBioChem 11:866–879
166. Sigel RKO, Sigel H (2010) A stability concept for metal Ion coordination to single-stranded nucleic acids and affinities of individual sites. Acc Chem Res 43:974–984
167. Deuss PJ, den Heeten R, Laan W, Kamer PCJ (2011) Bioinspired catalyst design and artificial metalloenzymes. Chem Eur J 17:4680–4698
168. Lau PS, Li YF (2011) Functional nucleic acids as molecular recognition elements for small organic and biological molecules. Curr Org Chem 15:557–575
169. Sen D, Poon LCH (2011) RNA and DNA complexes with hemin Fe(III) heme are efficient peroxidases and peroxygenases: how do they do it and what does it mean? Crit Rev Biochem Mol Biol 46:478–492
170. Takezawa Y, Shionoya M (2012) Metal-mediated DNA base pairing: alternatives to hydrogen-bonded watson-crick base pairs. Acc Chem Res 45:2066–2076
171. Lu Y (2002) New transition-metal-dependent DNA-zymes as efficient endonucleases and as selective metal biosensors. Chem Eur J 8:4589–4596
172. Lu Y (2009) DNAzyme and aptamer sensors for on-site and real-time detection of a broad range of environmental toxins. Environ Mol Mutagen 50:534
173. Wang G, Wang Y, Chen L, Choo J (2010) Nanomaterial-assisted aptamers for optical sensing. Biosens Bioelectron 25:1859–1868
174. Roh YH, Ruiz RCH, Peng S, Lee JB, Luo D (2011) Engineering DNA-based functional materials. Chem Soc Rev 40:5730–5744
175. Tan SJ, Campolongo MJ, Luo D, Cheng WL (2011) Building plasmonic nanostructures with DNA. Nat Nanotechnol 6:268–276
176. Xing H, Ngo Yin W, Xiang Y, Lu Y (2012) DNA aptamer functionalized nanomaterials for intracellular analysis, cancer cell imaging and drug delivery. Curr Opin Chem Biol 16:429–435
177. Willner I, Willner B, Katz E (2007) Biomolecule-nanoparticle hybrid systems for bioelectronic applications. Bioelectrochemistry 70:2–11
178. Sau TK, Rogach AL, Jaeckel F, Klar TA, Feldmann J (2010) Properties and applications of colloidal nonspherical noble metal nanoparticles. Adv Mater 22:1805–1825
179. Jadzinsky PD, Calero G, Ackerson CJ, Bushnell DA, Kornberg RD (2007) Structure of a thiol monolayer-protected gold nanoparticle at 1.1 angstrom resolution. Science 318:430–433
180. Heaven MW, Dass A, White PS, Holt KM, Murray RW (2008) Crystal structure of the gold nanoparticle N(C8H17)(4) Au-25(SCH2CH2Ph)(18). J Am Chem Soc. 130:3754–3755
181. Hakkinen H (2012) The gold-sulfur interface at the nanoscale. Nature Chem 4:443–455
182. Mirkin CA, Letsinger RL, Mucic RC, Storhoff JJ (1996) A DNA-based method for rationally assembling nanoparticles into macroscopic materials. Nature 382:607–609
183. Alivisatos AP, Johnsson KP, Peng XG, Wilson TE, Loweth CJ, Bruchez MP, Schultz PG (1996) Organization of 'nanocrystal molecules' using DNA. Nature 382:609–611
184. Demers LM, Mirkin CA, Mucic RC, Reynolds RA, Letsinger RL, Elghanian R, Viswanadham G (2000) A fluorescence-based method for determining the surface coverage and hybridization efficiency of thiol-capped oligonucleotides bound to gold thin films and nanoparticles. Anal Chem 72:5535–5541
185. Hurst SJ, Lytton-Jean AKR, Mirkin CA (2006) Maximizing DNA loading on a range of gold nanoparticle sizes. Anal Chem 78:8313–8318
186. Parak WJ, Pellegrino T, Micheel CM, Gerion D, Williams SC, Alivisatos AP (2003) Conformation of oligonucleotides attached to gold nanocrystals probed by gel electrophoresis. Nano Lett 3:33–36
187. Zanchet D, Micheel CM, Parak WJ, Gerion D, Alivisatos AP (2001) Electrophoretic isolation of discrete Au nanocrystal/DNA conjugates. Nano Lett 1:32–35

188. Ackerson CJ, Sykes MT, Kornberg RD (2005) Defined DNA/nanoparticle conjugates. Proc Natl Acad Sci USA 102:13383–13385
189. Claridge SA, Mastroianni AJ, Au YB, Liang HW, Micheel CM, Frechet JMJ, Alivisatos AP (2008) Enzymatic ligation creates discrete multinanoparticle building blocks for self-assembly. J Am Chem Soc 130:9598–9605
190. Mastroianni AJ, Claridge SA, Alivisatos AP (2009) Pyramidal and chiral groupings of gold nanocrystals assembled using DNA scaffolds. J Am Chem Soc 131:8455–8459
191. Claridge SA, Liang HW, Basu SR, Frechet JMJ, Alivisatos AP (2008) Isolation of discrete nanoparticle—DNA conjugates for plasmonic applications. Nano Lett 8:1202–1206
192. Li ZT, Cheng EJ, Huang WX, Zhang T, Yang ZQ, Liu DS, Tang ZY (2011) Improving the Yield of Mono-DNA-Functionalized Gold Nanoparticles through Dual Steric Hindrance. J Am Chem Soc 133:15284–15287
193. Pei H, Li F, Wan Y, Wei M, Liu HJ, Su Y, Chen N, Huang Q, Fan CH (2012) Designed diblock oligonucleotide for the synthesis of spatially isolated and highly hybridizable functionalization of DNA-gold nanoparticle nanoconjugates. J Am Chem Soc 134:11876–11879
194. Liu JW, Lu Y (2003) A colorimetric lead biosensor using DNAzyme-directed assembly of gold nanoparticles. J Am Chem Soc 125:6642–6643
195. Liu J, Lu Y (2006) Preparation of aptamer-linked gold nanoparticle purple aggregates for colorimetric sensing of analytes. Nat Protoc 1:246–252
196. Wang ZD, Zhang JQ, Ekman JM, Kenis PJA, Lu Y (2010) DNA-mediated control of metal nanoparticle shape: one-pot synthesis and cellular uptake of highly stable and functional gold nanoflowers. Nano Lett 10:1886–1891
197. Wang ZD, Tang LH, Tan LH, Li JH, Lu Y (2012) Discovery of the DNA "genetic code" for abiological gold nanoparticle morphologies. Angew Chem Int Ed 51:9078–9082
198. Pena SRN, Raina S, Goodrich GP, Fedoroff NV, Keating CD (2002) Hybridization and enzymatic extension of Au nanoparticle-bound oligonucleotides. J Am Chem Soc 124:7314–7323
199. Kanaras AG, Wang ZX, Bates AD, Cosstick R, Brust M (2003) Towards multistep nanostructure synthesis: Programmed enzymatic self-assembly of DNA/gold systems. Angew Chem Int Ed 42:191–194
200. Xu X, Rosi NL, Wang Y, Huo F, Mirkin CA (2006) Asymmetric functionalization of gold nanoparticles with oligonucleotides. J Am Chem Soc 128:9286–9287
201. Huo F, Lytton-Jean AKR, Mirkin CA (2006) Asymmetric functionalization of nanoparticles based on thermally addressable DNA interconnects. Adv Mater 18:2304–2306
202. Zhao WA, Gao Y, Kandadai SA, Brook MA, Li YF (2006) DNA polymerization on gold nanoparticles through rolling circle amplification: towards novel scaffolds for three-dimensional periodic nanoassemblies. Angew Chem Int Ed 45:2409–2413
203. Zhao W, Lam JCF, Chiuman W, Brook MA, Li Y (2008) Enzymatic cleavage of nucleic acids on gold nanoparticles: a generic platform for facile colorimetric biosensors. Small. 4:810–816
204. Xiang Y, Wang ZD, Xing H, Lu Y (2013) Expanding DNAzyme functionality through enzyme cascades with applications in single nucleotide repair and tunable DNA-directed assembly of nanomaterials. Chem Sci 4:398–404
205. Thaxton CS, Georganopoulou DG, Mirkin CA (2006) Gold nanoparticle probes for the detection of nucleic acid targets. Clin Chim Acta 363:120–126
206. He L, Musick MD, Nicewarner SR, Salinas FG, Benkovic SJ, Natan MJ, Keating CD (2000) Colloidal Au-enhanced surface plasmon resonance for ultrasensitive detection of DNA hybridization. J Am Chem Soc 122:9071–9077
207. Patolsky F, Ranjit KT, Lichtenstein A, Willner I (2000) Dendritic amplification of DNA analysis by oligonucleotide-functionalized Au-nanoparticles. Chem Commun 12:1025–1026
208. Taton TA, Mirkin CA, Letsinger RL (2000) Scanometric DNA array detection with nanoparticle probes. Science 289:1757–1760

209. Zhou XC, O'Shea SJ, Li SFY (2000) Amplified microgravimetric gene sensor using Au nanoparticle modified oligonucleotides. Chem Commun 11:953–954
210. Authier L, Grossiord C, Brossier P, Limoges B (2001) Gold nanoparticle-based quantitative electrochemical detection of amplified human cytomegalovirus DNA using disposable microband electrodes. Anal Chem 73:4450–4456
211. Cai H, Xu C, He PG, Fang YZ (2001) Colloid Au-enhanced DNA immobilization for the electrochemical detection of sequence-specific DNA. J Electroanal Chem 510:78–85
212. Dubertret B, Calame M, Libchaber AJ (2001) Single-mismatch detection using gold-quenched fluorescent oligonucleotides. Nat Biotechnol 19:365–370
213. Wang J, Xu DK, Kawde AN, Polsky R (2001) Metal nanoparticle-based electrochemical stripping potentiometric detection of DNA hybridization. Anal Chem 73:5576–5581
214. Cao YWC, Jin RC, Mirkin CA (2002) Nanoparticles with Raman spectroscopic fingerprints for DNA and RNA detection. Science 297:1536–1540
215. Maxwell DJ, Taylor JR, Nie SM (2002) Self-assembled nanoparticle probes for recognition and detection of biomolecules. J Am Chem Soc 124:9606–9612
216. Park SJ, Taton TA, Mirkin CA (2002) Array-based electrical detection of DNA with nanoparticle probes. Science 295:1503–1506
217. Ozsoz M, Erdem A, Kerman K, Ozkan D, Tugrul B, Topcuoglu N, Ekren H, Taylan M (2003) Electrochemical genosensor based on colloidal gold nanoparticles for the detection of Factor V Leiden mutation using disposable pencil graphite electrodes. Anal Chem 75:2181–2187
218. Li HX, Rothberg L (2004) Colorimetric detection of DNA sequences based on electrostatic interactions with unmodified gold nanoparticles. Proc Natl Acad Sci USA 101:14036–14039
219. Li HX, Rothberg LJ (2004) DNA sequence detection using selective fluorescence quenching of tagged oligonucleotide probes by gold nanoparticles. Anal Chem 76:5414–5417
220. Li HX, Rothberg LJ (2004) Label-free colorimetric detection of specific sequences in genomic DNA amplified by the polymerase chain reaction. J Am Chem Soc 126:10958–10961
221. Niazov T, Pavlov V, Xiao Y, Gill R, Willner I (2004) DNAzyme-functionalized Au nanoparticles for the amplified detection of DNA or telomerase activity. Nano Lett 4:1683–1687
222. Storhoff JJ, Lucas AD, Garimella V, Bao YP, Muller UR (2004) Homogeneous detection of unamplified genomic DNA sequences based on colorimetric scatter of gold nanoparticle probes. Nat Biotechnol 22:883–887
223. Bao YP, Huber M, Wei TF, Marla SS, Storhoff JJ, Muller UR (2005) SNP identification in unamplified human genomic DNA with gold nanoparticle probes. Nucleic Acids Res 33:e15
224. Dyadyusha L, Yin H, Jaiswal S, Brown T, Baumberg JJ, Booy FP, Melvin T (2005) Quenching of CdSe quantum dot emission, a new approach for biosensing. Chem Commun 25:3201–3203
225. Endo T, Kerman K, Nagatani N, Takamura Y, Tamiya E (2005) Label-free detection of peptide nucleic acid-DNA hybridization using localized surface plasmon resonance based optical biosensor. Anal Chem 77:6976–6984
226. Stoeva SI, Huo FW, Lee JS, Mirkin CA (2005) Three-layer composite magnetic nanoparticle probes for DNA. J Am Chem Soc 127:15362–15363
227. Li YA, Wark AW, Lee HJ, Corn RM (2006) Single-nucleotide polymorphism genotyping by nanoparticle-enhanced surface plasmon resonance imaging measurements of surface ligation reactions. Anal Chem 78:3158–3164
228. Ray PC (2006) Diagnostics of single base-mismatch DNA hybridization on gold nanoparticles by using the hyper-Rayleigh scattering technique. Angew Chem Int Ed 45:1151–1154
229. Zhang J, Song SP, Zhang LY, Wang LH, Wu HP, Pan D, Fan CH (2006) Sequence-specific detection of femtomolar DNA via a chronocoulometric DNA sensor (CDS): effects of nanoparticle-mediated amplification and nanoscale control of DNA assembly at electrodes. J Am Chem Soc 128:8575–8580

230. Seferos DS, Giljohann DA, Hill HD, Prigodich AE, Mirkin CA (2007) Nano-flares: probes for transfection and mRNA detection in living cells. J Am Chem Soc 129:15477–15479
231. Zhang J, Song SP, Wang LH, Pan D, Fan CH (2007) A gold nanoparticle-based chronocoulometric DNA sensor for amplified detection of DNA. Nat Protoc 2:2888–2895
232. Song SP, Liang ZQ, Zhang J, Wang LH, Li GX, Fan CH (2009) Gold-Nanoparticle-Based Multicolor Nanobeacons for Sequence-Specific DNA Analysis. Angew Chem Int Ed 48:8670–8674
233. Xue X, Xu W, Wang F, Liu X (2009) Multiplex single-nucleotide polymorphism typing by nanoparticle-coupled DNA-templated reactions. J Am Chem Soc 131:11668–11669
234. Bai X, Shao C, Han X, Li Y, Guan Y, Deng Z (2010) Visual detection of sub-femtomole DNA by a gold nanoparticle seeded homogeneous reduction assay: toward a generalized sensitivity-enhancing strategy. Biosens Bioelectron 25:1984–1988
235. Chen JIL, Chen Y, Ginger DS (2010) plasmonic nanoparticle dimers for optical sensing of DNA in complex media. J Am Chem Soc 132:9600–9601
236. Jung YL, Jung C, Parab H, Cho D-Y, Park HG (2011) Colorimetric SNP genotyping based on allele-specific PCR by using a thiol-labeled primer. ChemBioChem 12:1387–1390
237. Oh JH, Lee JS (2011) Designed hybridization properties of DNA-gold nanoparticle conjugates for the ultraselective detection of a single-base mutation in the breast cancer gene BRCA1. Anal Chem 83:7364–7370
238. Acuna GP, Moller FM, Holzmeister P, Beater S, Lalkens B, Tinnefeld P (2012) Fluorescence enhancement at docking sites of DNA-directed self-assembled nanoantennas. Science 338:506–510
239. Deng H, Xu Y, Liu YH, Che ZJ, Guo HL, Shan SX, Sun Y, Liu XF, Huang KY, Ma XW, Wu Y, Liang XJ (2012) Gold nanoparticles with asymmetric polymerase chain reaction for colorimetric detection of DNA sequence. Anal Chem 84:1253–1258
240. Gao F, Zhu Z, Lei J, Geng Y, Ju H (2013) Sub-femtomolar electrochemical detection of DNA using surface circular strand-replacement polymerization and gold nanoparticle catalyzed silver deposition for signal amplification. Biosens Bioelectron 39:199–203
241. Liu JW, Lu Y (2004) Accelerated color change of gold nanoparticles assembled by DNAzymes for simple and fast colorimetric Pb2 + detection. J Am Chem Soc 126:12298–12305
242. Liu JW, Lu Y (2004) Optimization of a Pb2 + -directed gold nanoparticle/DNAzyme assembly and its application as a colorimetric biosensor for Pb2+. Chem Mater 16:3231–3238
243. Liu JW, Lu Y (2004) Colorimetric biosensors based on DNAzyme-assembled gold nanoparticles. J Fluoresc 14:343–354
244. Liu JW, Lu Y (2004) Adenosine-dependent assembly of aptazyme-functionalized gold nanoparticles and its application as a colorimetric biosensor. Anal Chem 76:1627–1632
245. Liu J, Lu Y (2005) Stimuli-responsive disassembly of nanoparticle aggregates for light-up colorimetric sensing. J Am Chem Soc 127:12677–12683
246. Liu JW, Lu Y (2006) Design of asymmetric DNAzymes for dynamic control of nanoparticle aggregation states in response to chemical stimuli. Org Biomol Chem 4:3435–3441
247. Liu J, Lu Y (2007) Colorimetric Cu2 + detection with a ligation DNAzyme and nanopairticles. Chem Commun 46:4872–4874
248. Lee JH, Wang ZD, Liu JW, Lu Y (2008) Highly sensitive and selective colorimetric sensors for Uranyl (UO22 +): development and comparison of labeled and label-free DNAzyme-gold nanoparticle systems. J Am Chem Soc 130:14217–14226
249. Shen L, Chen Z, Li YH, He SL, Xie SB, Xu XD, Liang ZW, Meng X, Li Q, Zhu ZW, Li MX, Le XC, Shao YH (2008) Electrochemical DNAzyme sensor for lead based on amplification of DNA-Au bio-bar codes. Anal Chem 80:6323–6328
250. Wang ZD, Lee JH, Lu Y (2008) Label-free colorimetric detection of lead ions with a nanomolar detection limit and tunable dynamic range by using gold nanoparticles and DNAzyme. Adv Mater 20:3263–3267

251. Wei H, Li BL, Li J, Dong SJ, Wang EK (2008) DNAzyme-based colorimetric sensing of lead (Pb(2 +)) using unmodified gold nanoparticle probes. Nanotechnology 19:095501
252. Zhao WA, Lam JCF, Chiuman W, Brook MA, Li YF (2008) Enzymatic cleavage of nucleic acids on gold nanoparticles: a generic platform for facile colorimetric biosensors. Small 4:810–816
253. Fu R, Li T, Park HG (2009) An ultrasensitive DNAzyme-based colorimetric strategy for nucleic acid detection. Chem Commun 39:5838–5840
254. Zhou WH, Zhu CL, Lu CH, Guo XC, Chen FR, Yang HH, Wang XR (2009) Amplified detection of protein cancer biomarkers using DNAzyme functionalized nanoprobes. Chem Commun 28:6845–6847
255. Fang ZY, Huang J, Lie PC, Xiao Z, Ouyang CY, Wu Q, Wu YX, Liu GD, Zeng LW (2010) Lateral flow nucleic acid biosensor for Cu2 + detection in aqueous solution with high sensitivity and selectivity. Chem Commun 46:9043–9045
256. Mazumdar D, Liu JW, Lu G, Zhou JZ, Lu Y (2010) Easy-to-use dipstick tests for detection of lead in paints using non-cross-linked gold nanoparticle-DNAzyme conjugates. Chem Commun 46:1416–1418
257. Wang Y, Yang F, Yang XR (2010) Label-free colorimetric biosensing of copper(II) ions with unimolecular self-cleaving deoxyribozymes and unmodified gold nanoparticle probes. Nanotechnology 21:205502
258. Yang XR, Xu J, Tang XM, Liu HX, Tian DB (2010) A novel electrochemical DNAzyme sensor for the amplified detection of Pb2 + ions. Chem Commun 46:3107–3109
259. Yin BC, Zuo P, Huo H, Zhong XH, Ye BC (2010) DNAzyme self-assembled gold nanoparticles for determination of metal ions using fluorescence anisotropy assay. Anal Biochem 401:47–52
260. Kim JH, Han SH, Chung BH (2011) Improving Pb(2 +) detection using DNAzyme-based fluorescence sensors by pairing fluorescence donors with gold nanoparticles. Biosens Bioelectron 26:2125–2129
261. Liang JF, Chen ZB, Guo L, Li LD (2011) Electrochemical sensing of L-histidine based on structure-switching DNAzymes and gold nanoparticle-graphene nanosheet composites. Chem Commun 47:5476–5478
262. Lin DJ, Wu J, Yan F, Deng SY, Ju HX (2011) Ultrasensitive immunoassay of protein biomarker based on electrochemiluminescent quenching of quantum dots by hemin bio-bar-coded nanoparticle tags. Anal Chem 83:5214–5221
263. Miao XM, Ling LS, Shuai XT (2011) Ultrasensitive detection of lead(II) with DNAzyme and gold nanoparticles probes by using a dynamic light scattering technique. Chem Commun 47:4192–4194
264. Wang C, Wu J, Zong C, Ju HX, Yan F (2011) Highly sensitive rapid chemiluminescent immunoassay using the DNAzyme label for signal amplification. Analyst 136:4295–4300
265. Wang HL, Ou LML, Suo YR, Yu HZ (2011) Computer-readable DNAzyme assay on disc for ppb-level lead detection. Anal Chem 83:1557–1563
266. Wang L, Jin Y, Deng J, Chen GZ (2011) Gold nanorods-based FRET assay for sensitive detection of Pb2 + using 8-17DNAzyme. Analyst 136:5169–5174
267. Wang YL, Irudayaraj J (2011) A SERS DNAzyme biosensor for lead ion detection. Chem Commun 47:4394–4396
268. Yuan YL, Gou XX, Yuan R, Chai YQ, Zhuo Y, Mao L, Gan XX (2011) Electrochemical aptasensor based on the dual-amplification of G-quadruplex horseradish peroxidase-mimicking DNAzyme and blocking reagent-horseradish peroxidase. Biosens Bioelectron 26:4236–4240
269. Jo H, Lee S, Min K, Ban C (2012) Detection of the strand exchange reaction using DNAzyme and Thermotoga maritima recombinase A. Anal Biochem 421:313–320
270. Li CL, Huang CC, Chen WH, Chiang CK, Chang HT (2012) Peroxidase mimicking DNA-gold nanoparticles for fluorescence detection of the lead ions in blood. Analyst 137:5222–5228

271. Liu QY, Wei L, Wang LS, Liang AH, Jiang ZL (2012) A label-free deoxyribozymes resonance rayleigh scattering assay for trace lead(II) based on nanogold catalysis of chloroauric acid-vitamin C particle reaction. Anal Lett 45:2737–2748
272. Malashikhina N, Pavlov V (2012) DNA-decorated nanoparticles as nanosensors for rapid detection of ascorbic acid. Biosens Bioelectron 33:241–246
273. Miao XM, Ling LS, Cheng D, Shuai XT (2012) A highly sensitive sensor for Cu2 + with unmodified gold nanoparticles and DNAzyme by using the dynamic light scattering technique. Analyst 137:3064–3069
274. Miao XM, Ling LS, Shuai XT (2012) Detection of Pb2 + at attomole levels by using dynamic light scattering and unmodified gold nanoparticles. Anal Biochem 421:582–586
275. Pelossof G, Tel-Vered R, Willner I (2012) Amplified surface plasmon resonance and electrochemical detection of Pb2 + ions using the Pb2 + -dependent DNAzyme and Hemin/G-Quadruplex as a label. Anal Chem 84:3703–3709
276. Zhou MY, Liu Y, Tu YF, Tao GH, Yan JL (2012) DNAzyme-based turn-on chemiluminescence assays in homogenous media. Biosens Bioelectron 35:489–492
277. Chen JH, Zhou XM, Zeng LW (2013) Enzyme-free strip biosensor for amplified detection of Pb2 + based on a catalytic DNA circuit. Chem Commun 49:984–986
278. Wen YQ, Li FBY, Dong XC, Zhang J, Xiong QH, Chen P (2013) The electrical detection of Lead ions using Gold-nanoparticle- and DNAzyme-functionalized graphene device. Adv Healthc Mater 2:271–274
279. Rosi NL, Giljohann DA, Thaxton CS, Lytton-Jean AKR, Han MS, Mirkin CA (2006) Oligonucleotide-modified gold nanoparticles for intracellular gene regulation. Science 312:1027–1030
280. Zheng D, Seferos DS, Giljohann DA, Patel PC, Mirkin CA (2009) Aptamer nano-flares for molecular detection in living cells. Nano Lett 9:3258–3261
281. Tack F, Noppe M, Van Dijck A, Dekeyzer N, Van Der Leede BJ, Bakker A, Wouters W, Janicot M, Brewster ME (2008) Delivery of a DNAzyme targeting c-myc to HT29 colon carcinoma cells using a gold nanoparticulate approach. Pharmazie 63:221–225
282. Yehl K, Joshi JR, Greene BL, Dyer RB, Nahta R, Salaita K (2012) Catalytic deoxyribozyme-modified nanoparticles for RNAi-independent gene regulation. ACS Nano 6:9150–9157
283. Wu PW, Hwang K, Lan T, Lu Y (2013) A DNAzyme-gold nanoparticle probe for uranyl ion in living cells. J Am Chem Soc 135:5254–5257. doi:10.1021/ja400150v
284. Sato K, Hosokawa K, Maeda M (2003) Rapid aggregation of gold nanoparticles induced by non-cross-linking DNA hybridization. J Am Chem Soc 125:8102–8103
285. Zhao W, Chiuman W, Lam JCF, Brook MA, Li Y (2007) Simple and rapid colorimetric enzyme sensing assays using non-crosslinking gold nanoparticle aggregation. Chem Commun 36:3729–3731
286. Xiang Y, Lu Y (2013) An invasive DNA approach toward a general method for portable quantification of metal ions using a personal glucose meter. Chem Commun 49:585–587
287. Li HX, Rothberg L (2005) Detection of specific sequences in RNA using differential adsorption of single-stranded oligonucleotides on gold nanoparticles. Anal Chem 77:6229–6233
288. Dulkeith E, Morteani AC, Niedereichholz T, Klar TA, Feldmann J, Levi SA, van Veggel F, Reinhoudt DN, Moller M, Gittins DI (2002) Fluorescence quenching of dye molecules near gold nanoparticles: radiative and nonradiative effects. Phys Rev Lett 89:203002

Adv Biochem Eng Biotechnol (2014) 140: 121–154
DOI: 10.1007/10_2013_231

Published Online: 4 July 2013

Aptamer-Modified Nanoparticles as Biosensors

Maren Lönne, Guohong Zhu, Frank Stahl and Johanna-Gabriela Walter

Abstract Aptamers are short oligonucleotides that are capable of selectively binding to their corresponding target. Therefore, they can be thought of as a nucleic acid-based alternative to antibodies and can substitute for their amino acid-based counterparts in analytical applications, including as receptors in biosensors. Here they offer several advantages because their nucleic acid nature and their binding via an induced fit mechanism enable novel sensing strategies. In this article, the utilization of aptamers as novel bio-receptors in combination with nanoparticles as transducer elements is reviewed. In addition to these analytical applications, the medical relevance of aptamer-modified nanoparticles is described.

Keywords Aptamer · Aptasensor · Biosensor · Nanoparticle

Abbreviations

AgNP	Silver nanoparticle
ATP	Adenosine triphosphate
AuNP	Gold nanoparticle
BOBO-3	(1,1′-(4,4,7,7-tetramethyl-4,7-diazaundecamethylene)-bis-4-[3-methyl-2,3-dihydro-(benzo-1,3-thiazole)-2-methylidene]-pyridinium tetraiodide)
CdSNP	CdS nanoparticles
CRET	Chemiluminescence resonance energy transfer
Cy3	Carbocyanine 3
Cy5	Carbocyanine 5
DABCYL	4-([4-(Dimethylamino)phenyl]azo)benzoic acid
DMDAP	*N,N*-dimethyl-2,7-diazapyrenium dication
DNA	Deoxyribonucleic acid
dsDNA	Double-stranded DNA

M. Lönne · G. Zhu · F. Stahl · J.-G. Walter (✉)
Institut für Technische Chemie, Gottfried Wilhelm Leibniz Universität Hannover, Callinstr. 5, 30167 Hannover, Germany
e-mail: walter@iftc.uni-hannover.de

FACS	Fluorescence activated cell sorting
FRET	Förster resonance energy transfer
G-quadruplex	Guanosine-quadruplex
IgM	Immunoglobulin M
LOD	Limit of detection
LSPR	Localized surface plasmon resonance
MB	Methylene blue
MNP	Magnetic nanoparticle
MRI	Magnetic resonance imaging
nd	Not determined
NIR	Near-infrared
NIR-NP	Near-infrared fluorescent nanoparticles
NMR	Nuclear magnetic resonance
PDGF	Platelet-derived growth factor
PEG	Polyethylene glycol
PEG-PCL	Poly(ethyleneglycol)-poly(ε-caprolactone)
PLGA	Poly(D, L lactic-co-glycolic acid)
PLGA-b-PEG	Poly(D,L-lactic-*co*-glycolic acid)-*block*-poly(ethylene glycol)
PLA-PEG	Poly(lactic acid)-block-polyethylene glycol
PEI	Polyethylenimine
PrP^C	Cellular prion protein
RNA	Ribonucleic acid
RNase	Ribonuclease
PTK 7	Protein tyrosine kinase-7
PSMA	Prostate-specific membrane antigen
QCM	Quartz crystal microbalance
QD	Quantum dot
SELEX	Systematic evolution of ligands by exponential enrichment
SERS	Surface-enhanced Raman scattering
SERRS	Surface-enhanced resonance Raman scattering
SiNP	Silica nanoparticle
siRNA	Small interfering RNA
SPR	Surface plasmon resonance
ssDNA	Single-stranded DNA
TAMRA	Carboxytetramethylrhodamine
TEM	Transmission electron microscopy
TID	Target-induced dissociation
TIR	Target-induced reassembling of aptamer fragments
TISS	Target-induced structure switching
UCNP	Upconversion nanoparticle

Contents

1 Introduction

Nanotechnology is playing an increasingly important role in the development of biosensor systems [1]. In biosensors, nanoparticles (NPs) have enabled new techniques for signal transduction based on their unique characteristics. Because of these properties, aptamer-modified NPs have been investigated intensively in the last decade, which can be tracked by the exponential increase of publications in this area (Fig. 1a). In addition to bioanalytical applications, aptamer-modified nanoparticles have also attracted attention in medical applications, including as vehicles for drug delivery (Fig. 1b).

Although not exhaustive, this review aims to highlight the broad diversity of aptamer-modified nanoparticles for sensor applications and the underlying detection modes. In the first part, aptamers are described, with a focus on their binding properties and possible chemical modifications. In the next section, the role of aptamers in nanosensors is summarized and categorized according to the mechanism underlying the sensing. The use of aptamer-modified nanoparticles for the detection of different analytes is reviewed. Different aptamer-modified nanoparticles are classified according to the material of the nanoparticle, the type of sensor enabled by this nanoparticle (e.g. optical, electrochemical sensor), and the underlying mode of detection. Finally, potential medical applications are outlined.

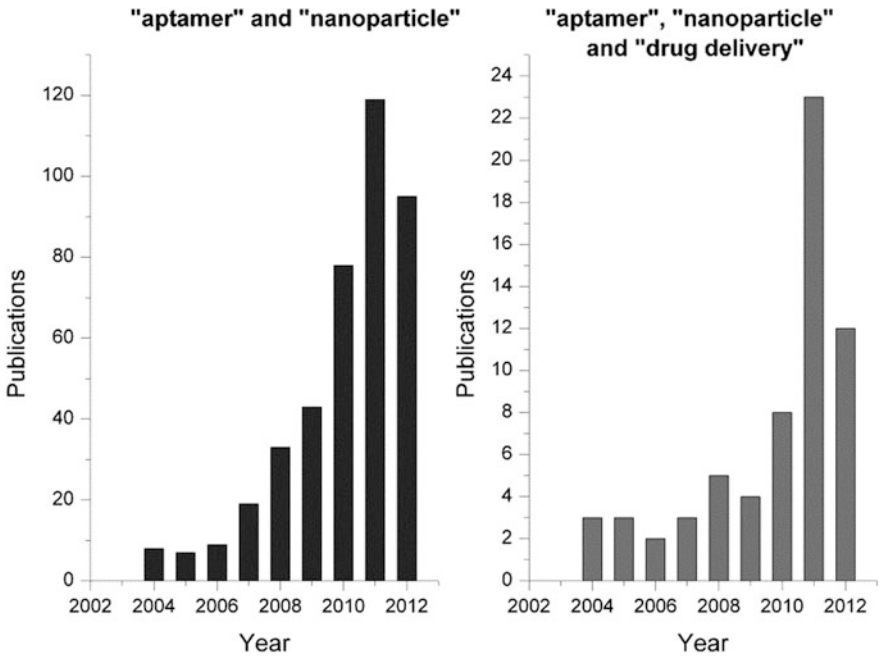

Fig. 1 Publications dealing with aptamer-modified nanoparticles. *Left* publications containing the terms "aptamer" and "nanoparticle." *Right* Publications additionally containing the term "drug delivery." Data was created using MEDSUM: an online MEDLINE summary tool by Galsworthy, MJ. Hosted by the Institute of Biomedical Informatics (IBMI), Faculty of Medicine, University of Ljubljana, Slovenia. URL: www.medsum.info

2 Aptamers

Aptamers are single-stranded DNA or RNA molecules consisting of 15–80 mononucleotides. Because an elongated primary molecular structure is energetically unfavorable, some unpaired nucleobases interact with each other, generating typical secondary structural motifs such as different loop structures. Additional interactions between these motifs result in more complex tertiary structures, which generate a sequence-dependent three-dimensional conformation allowing specific target recognition and binding. However, in some cases the ligand-binding domain of the unbound aptamer remains completely unstructured until ligand binding [2].

Aptamers bind their ligands by folding around and encapsulating them via an "induced fit mechanism." Only during the binding process is the final bioactive aptamer conformation achieved because the interaction between the target and aptamer induces the formation of new secondary and tertiary structure elements.

2.1 Aptamer Folding and Target Recognition

Typical nucleic acid secondary structure elements are k-turn, stem-loop or pseudoknot motifs, but higher-ranking tertiary motifs such as coaxial stacking or G-quadruplexes are also formed (Fig. 2).

The k-turn motif comprises a three-nucleotide bulge flanked by regular paired bases and introduces a tight kink into the helical aptamer. K-turn motifs are conserved to a high degree and they are renowned as important protein recognition elements [3]. Loops, especially tetraloops, are the most common motifs in aptamer folding, which may be stabilized by mismatch base pairing and base stacking during target binding [4]. Pseudoknot structures are more complex because they contain two nested stem-loop elements. As the half of one stem intercalates between the two halves of the other stem, a distinct tertiary structure is built up. Further, guanine-rich aptamer sequences are capable of forming higher ordered structures named G-quadruplexes. Here, four Hoogsteen-paired guanine bases arrange in a planar guanine tetrad, which can stack on top of another tetrad. In the center of the quadruplex motif, monovalent or divalent cations can be incorporated, which stabilize the three-dimensional (3D)-structure via electrostatic interactions. Due to different steric demands, the effective quadruplex geometry depends on the ion identity [5, 6].

All associations and aptamer structures are based on intra- and intermolecular hydrogen bonds, hydrophobic effects, or electrostatic interactions. Intramolecular hydrogen bonds can induce both match and mismatch base pairing. In addition to typical Watson–Crick-match base pairs, resulting in regular helical structures, aptamer folding is also affected by extraordinary base pairing geometrics, base triples, and "mismatches" [4, 7]. In particular, all mismatch-paired or unpaired bases are highly involved in target recognition because they can build up additional hydrogen bonds towards the target molecules, which in turn stabilize the aptamer conformation. Moreover, the hydroxyl groups of the ribose backbone can contribute to target binding as well.

For aptamer folding, stacking effects are even more important than hydrogen bonds. Here, the planar carbon ring systems of the nucleobases orient in parallel to each other, allowing dipole–dipole interactions between the aromatic bases [8]. Those interactions may also be important for target binding because planar molecules can be sandwiched by two stacking nucleobase pairs in aptamer complexes [9].

Although hydrogen bonds and stacking effects take place between nucleobases and sugar molecules, the negatively charged phosphate group can induce electrostatic interactions towards other charged molecules or functional groups. In particular, the presence of metal cations ("diffused" or "chelated" ions) can strongly affect the aptamer folding, explaining the strong buffer dependency of aptamer-based assays. while diffused ions interact with the aptamer without any physical contact, chelated ions get in direct contact with an electronegative chelating site. Thereby, water molecules, hydrating the ion, are partially or entirely displaced [10].

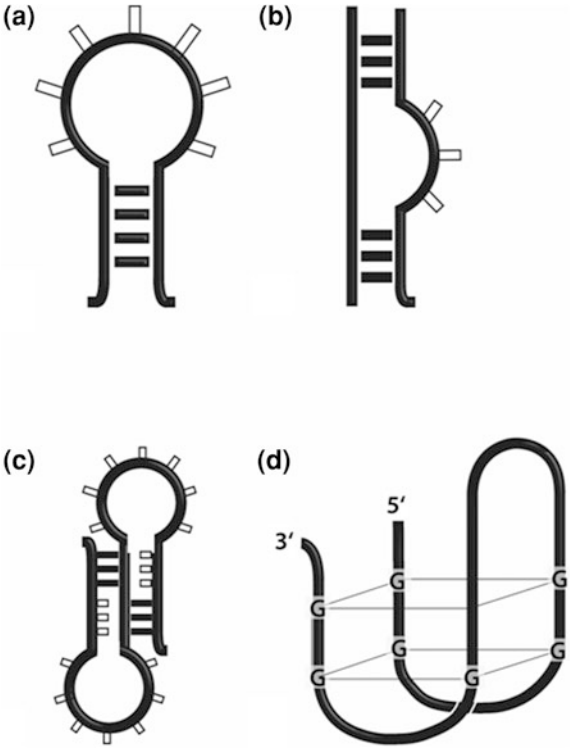

Fig. 2 Secondary structures of aptamers. (**a**) Stem-loop (**b**) K-turn (**c**) Pseudoknot (**d**) G-quadruplex

Specific target binding of aptamers is achieved by interplay of various discriminatory contacts based on the three referred interactions and additional steric effects [9]. Which of these effects contributes to the recognition of a particular target depends on its molecular structure. Binding of small targets is often achieved by intercalation between two nucleobases, especially when the target contains either nucleobase-similar structure elements or planar aromatic ring systems.

Because proteins are much larger, they provide a huge number of secondary structure elements and thus potential binding sites. Aptamers can accommodate minimal elements of this secondary structure by forming sterically restricted pockets that are only accessed by elected amino acids. Typical recognition elements are the guanidinium groups of arginine side chains, which form an "electrostatic zippering" with the phosphate backbone, and aromatic side chains, which intercalate into the oligonucleotide [4].

2.2 Modification of Aptamers

Because aptamers are generated during an in vitro selection process (SELEX) based on polymerase chain reaction, the initially selected aptamers were

chemically identical with naturally occurring oligonucleotides. Because both RNA- and DNA- degrading nucleases are omnipresent in nearly all biological fluids, any biological or pharmaceutical application of aptamers may be limited due to degradation. To overcome those stability problems, a multiplicity of pre- and post-SELEX modifications were developed over the years.

During the amplification step of the SELEX process, diverse nucleoside triphosphates analogues can be incorporated into the oligonucleotide, provided that they are suitable polymerase substrates. Typical modifications include masking the 2′-OH-group of the ribose by replacing it with amino, O-methyl [11], or fluoro [12] groups. Moreover, 4′-thioribonucleotides possess a sulfur atom instead of the furanose ring oxygen atom. All ribose-modified nucleotides show enhanced RNase resistance [13]. Further, the phosphate backbone of nucleotides can be replaced with phosphorothioate [11] or boranophosphate [14], which are isoelectronic and isosteric with the natural phosphodiester but show reduced nuclease affinity.

Another common strategy to improve aptamer stability and in some cases also the affinity towards the molecular target is the derivatization of nucleobases [11]. The 5′ position of pyrimidine bases and the 7′ or 8′ position of purine bases are the most permissive sites for modifications because these modifications are accepted by polymerases, enabling an efficient SELEX process [14, 15]. Moreover, aptamers consisting of unnatural L-sugar backbones named “spiegelmers” are not degraded by nucleases, as these enzymes show stereospecific substrate recognition [16]. For biological applications, there are some further exercises beside aptamer stability that can be solved with post-SELEX modifications. Those are generally initialized by introducing a functional group (usually amine or thiol) at C-terminus or N-terminus of the aptamer linking it to another molecule. Typical binding partners for pharmaceutical applications are polyethylene glycol (PEG), which enhances the plasma half-life and distribution of aptamers [17], enzymes restoring the activity in enzyme-deficient cells [18], and siRNA molecules inhibiting specific gene expression [19].

Due to their high specificity, aptamers have found many applications in medicine [20–22], biotechnology [23–25] and bioanalysis [26–31]. For using aptamers as recognition molecules, they can be linked to organic chromophores such as Cy3 or Cy5, or nanoparticles, which are the topic of this review.

3 Detection Modes of Aptamer-Based Biosensors

Based on specific binding to their corresponding targets, aptamers can be used as recognition elements in biosensors. Here, they can be used to substitute for antibodies, thereby enabling the application of detection modes known from conventional antibody-based biosensors:

- *Sandwich mode*: In the sandwich mode, two aptamers directed against different "epitopes" of the target are used. Usually, one aptamer is immobilized on the sensor surface. This aptamer captures the target, which is consequently bound by a second aptamer that is labeled for detection.
- *Competitive replacement*: In a competitive assay, one component (either the aptamer or the analyte) is immobilized on the sensor's surface. In the case of immobilized aptamers, a labeled target is bound to the aptamer. Competitive replacement of the labeled target by an unlabeled target originating from the sample results in a decrease of the signal.
- *Simple binding mode*: Using labeled aptamers, surface-bound targets can be detected.

In addition, due to their oligonucleotide nature and their adaptive mechanism of binding, aptamers enable novel detection strategies [29, 32]:

- *Target-induced structure switching (TISS):* TISS is based on the induced fit binding mechanism [9]. Here, conformational changes during the binding of the target are used to generate a signal.
- *Target-induced dissociation (TID)*: Because aptamers are oligonucleotides, complementary oligonucleotides can be designed, which hybridize with the aptamer in the absence of the target. In the presence of the target, the complementary sequence dissociates from the aptamer and is replaced by the target.
- *Target-induced reassembling of aptamer fragments (TIR)*: The aptamer can be cut into two pieces that do not interact with each other in the absence of the target. In the presence of the target, the aptamer fragments reassemble to form a three-molecular complex with the target.

These modes of detection enabled by the specific properties of nucleic acid-based aptamers are summarized in Fig. 4, using the example of aptamer-modified gold nanoparticles.

4 Aptamer-Modified Nanoparticles in Analytical Applications

4.1 Gold Nanoparticles

Noble-metal nanoparticles with a size less than 100 nm exhibit unique properties for biosensing, including structural, electronic, optical, and catalytic properties. Features such as localized surface plasmon resonance (LSPR) and strong light scattering, in combination with the lack of photobleaching, qualify them as a platform for robust and sensitive detection.

Most aptamer-modified noble metal nanoparticles described in the literature are gold nanoparticles (AuNPs). The immobilization of DNA to AuNPs has been well established by the groups of Alivisatos and Mirkin [33, 34]. This two-step process

involving the chemical synthesis of AuNPs and subsequent modification of AuNPs with DNA via ligand exchange with thiolated DNA has already been successfully transferred to aptamers [35, 36]. More recently, it was shown that AuNPs can also be produced by laser ablation of gold in a liquid environment [37, 38], and that AuNPs can be modified with aptamers during laser ablation based AuNP generation in a one-step procedure [39].

Due to strong localized LSPR and high extinction coefficients in the visible region, AuNPs are especially suitable for colorimetric sensing. The state-of-the-art of aptamer-modified AuNP-based biosensors has been reviewed by Du et al. [40]. Due to their high biocompatibility, aptamer-modified AuNPs have also been used extensively in medical applications (as discussed in Sect. 5 of this review). Within the text of this section, only a few examples for analytical applications of aptamer-modified AuNPs are outlined; a more comprehensive review of the current literature is given in Table 1.

4.1.1 Colorimetric Sensing with Aptamer-Modified AuNPs

Typically, colloidal spherical AuNPs exhibit a red color arising from their LSPR maximum ($LSPR_{Max}$) at approximately 520 nm. LSPR strongly depends on the size and shape of AuNPs, as well as on the surrounding media and interparticle distance of AuNPs. If the distance of AuNPs decreases, a red-to-purple or even blue color change can be observed as a result of plasmon coupling between vicinal AuNPs. The distance-dependent optical properties can be exploited to design colorimetric aptasensors. In these sensors, the binding of the target to aptamer-modified AuNPs results in a color shift from red (non-agglomerated AuNPs) to purple or blue (agglomerated AuNPs), or vice versa. Because the LSPR absorption of AuNPs is in the visible region, these changes can be observed by the naked eye or, more precisely, by monitoring the absorption spectra. According to the classification of sensing modes described in Sect. 3, the application of aptamer-modified AuNPs in colorimetric sensors is summarized in the following paragraphs.

Sandwich-Based Colorimetric Sensing

In the sandwich assay, two (or more) aptamer-modified AuNPs bind to one target molecule. Thereby, AuNP interparticle distance decreases, resulting in a blue-shift of AuNP's $LSPR_{Max}$. For the construction of a sandwich assay, either two aptamers directed against different "epitopes" of one target or targets comprising two or more equivalent "epitopes" are necessary. The latter variant was applied by Huang et al. for the detection of platelet-derived growth factor (PDGF) [36]. They have modified AuNPs with a DNA aptamer directed against PDGF. Because PDGF is a homodimeric protein, it is able to bind two aptamer-modified AuNPs, resulting in decreased distances of AuNPs and thus in a blue-shift of $LSPR_{Max}$ (Fig. 3).

Exploiting the visible absorption of AuNPs, Xu et al. have developed a lateral flow device platform with aptamer-modified AuNP readout in the sandwich mode [41]. Two DNA aptamers directed against thrombin were applied; one of them was

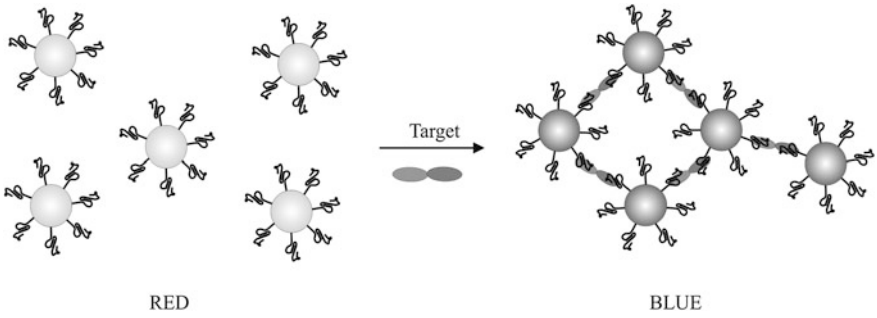

Fig. 3 Detection of a homodimeric target using Aptamer-modified gold nanoparticles in the sandwich mode. Adapted from Huang et al. [36]

immobilized on a membrane via biotin-streptavidin interaction to form the test zone. The other aptamer was immobilized on AuNPs. In the presence of thrombin, the aptamer-modified AuNPs concentrate in the test zone to form a red line. Thrombin detection could also be performed in human plasma samples, indicating the suitability of the device for diagnostic applications.

Using two different DNA aptamers selected against Ramos cells via cell SELEX, Liu et al. have developed a similar dipstick assay for the detection of circulating cancer cells [42]. Again, one of the aptamers was immobilized on the membrane via biotin-streptavidin interaction, whereas the other aptamer was immobilized on AuNPs. The cells were captured by the membrane-bound aptamer and consequently stained with aptamer-modified AuNPs.

Direct Capture-Based Colorimetric Sensing

Because of their characteristic adsorption in the visible region, aptamer-modified AuNPs can be used for colorimetric detection of the target by direct capture. For instance, Wang et al. have developed a dot-blot assay for detection of thrombin [43]. Thrombin was immobilized on a nitrocellulose membrane and anti-thrombin aptamer-modified AuNPs were used for detection. Spots were visible with a limit of detection (LOD) of 0.115 pmol thrombin. The sensitivity was further increased by silver enhancement, resulting in a LOD of 14 fmol and detection of thrombin in complex samples was demonstrated by spiking thrombin to 1 % human plasma. We have used a similar approach to verify the functionality of aptamer-modified AuNPs produced by laser ablation-based in situ conjugation using aptamers directed against streptavidin [39]. Many approaches for the detection of cells, such as the detection of prostate cancer cells via aptamer-modified AuNPs [39], belong to direct capture-based assays.

TISS-Based Colorimetric Sensing

The stability of AuNPs against salt-induced aggregation depends on the interplay of interparticle attraction and repulsion forces. Major possibilities to stabilize AuNPs are to maximize electrostatic and steric repulsion forces. Because aptamers

are polyelectrolytes bearing a negatively charged phosphate backbone, they enable the effective stabilization of AuNPs at elevated ionic strength. Moreover, different states of aptamers—in particular, folded and unfolded conformations—have a different stabilizing effect.

Zhao et al. have exploited this effect to design an aptamer-based sensor for adenosine and potassium ions [44]. They have immobilized an aptamer directed against adenosine on the surface of AuNPs. Target-induced structure switching of this aptamer results in an increased stability of AuNPs (Fig. 4c). In the absence of adenosine, the AuNPs agglomerated at 30 mM $MgCl_2$. In contrast, in the presence of adenosine, the AuNPs remained stable. The authors assumed that the adoption of a rigid, compact conformation induced by target binding in contrast to random conformation in the absence of the target results in better electrostatic and steric stabilization.

In a similar approach, Chen et al. used aptamer-modified AuNPs to sense ATP in an aggregation-based assay. Aptamer-modified AuNPs were aggregated in the absence of ATP under high salt conditions, resulting in a red-to-purple color change. In contrast, in the presence of ATP, no agglomeration occurred because the target induces the folding of the aptamer into a G-quadruplex containing conformation [45].

Another type of sensor using TISS mode is based on unmodified AuNPs (Fig. 4d). It is known that short ssDNA can be adsorbed to AuNPs and stabilizes them against salt-induced aggregation. Wang et al. have developed this sensor type by using an aptamer directed against potassium ions [46]. In the absence of the target, the aptamer is adsorbed on AuNPs via nitrogen of nucleobases, thereby electrostatically stabilizing the AuNPs against salt-induced aggregation. After the addition of K^+, the aptamer folds into a G-quadruplex that does not significantly adsorb on AuNPs. Due to agglomeration of AuNPs, a blue-shift of $LSPR_{Max}$ was observed. A similar assay was developed using aptamers directed against thrombin and adenosine, which also contain G-quadruplex structures [47, 48].

TID-Based Colorimetric Sensing

To translate the binding of the target into a signal, oligonucleotides complementary to the aptamer can be designed. The binding between this oligonucleotide and the aptamer has to be strong enough to be stable in the off-state of the sensor. Otherwise, the binding must not be too strong in order to guarantee sufficient replacement of the oligonucleotide by the target. Here, the binding strength can be tuned by variation of the length of the complementary oligonucleotide.

A TID-based sensor for the detection of adenosine has been developed by Liu and Lu [49, 50]. They have extended the anti-adenosine aptamer sequence and have used AuNPs that were modified with two oligonucleotides complementary to the extension and a portion of the original aptamer. In the absence of adenosine, the extended aptamer hybridizes with the complementary oligonucleotides, thereby agglomerating the AuNPs. The presence of the target induces aptamer folding and dissociation from the complementary oligonucleotides and thus an AuNP disassembly-based red shift (Fig. 4a). To show the general applicability of

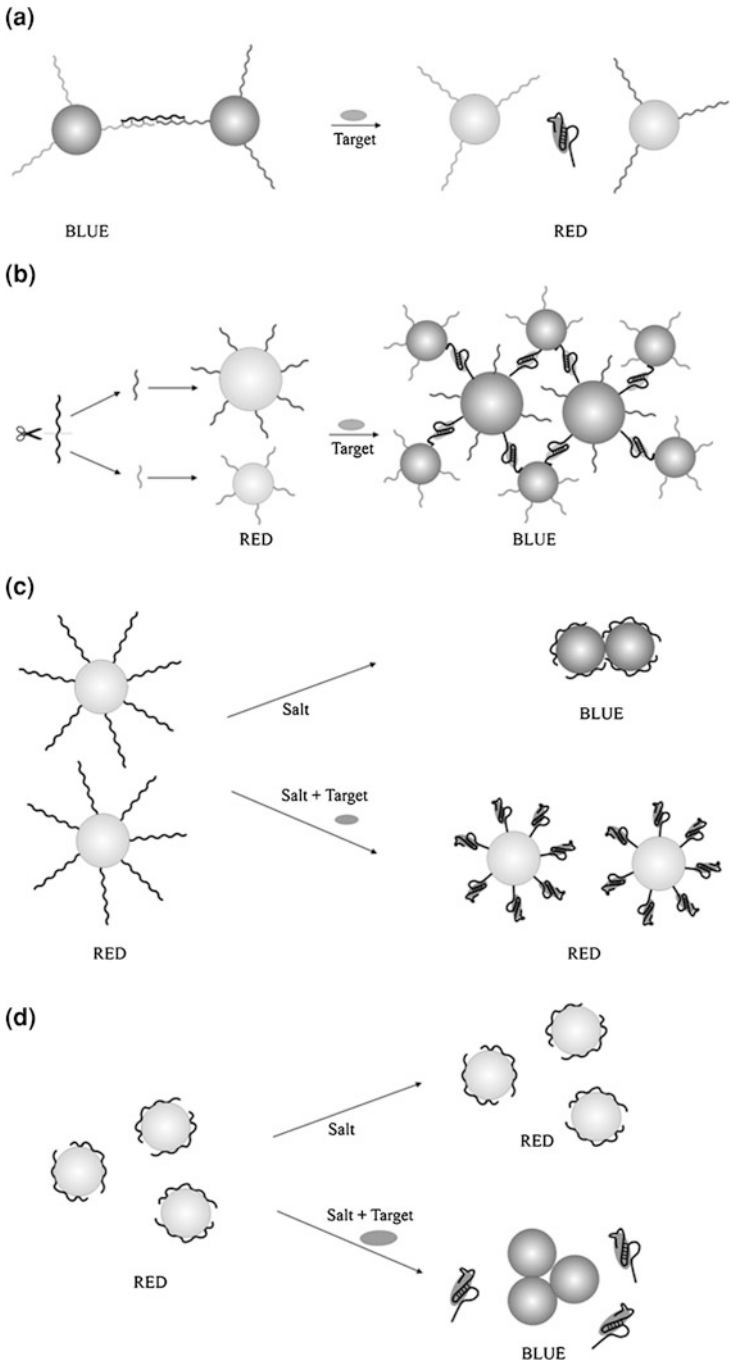
(a)
Target
BLUE
RED
(b)
Target
RED
BLUE
(c)
Salt
BLUE
Salt + Target
RED
RED
(d)
Salt
RED
Salt + Target
RED
BLUE

◄**Fig. 4** Detection modes enabled by the specific properties of aptamers. **a** Target-induced dissoziation (TID), **b** Target-induced reassembling of aptamer fragments (TIR). **c** Target-induced structuring switching (TISS). **d** Target-induced structuring switching (TISS)

this concept, the sensor design has been transferred to an aptamer directed against cocaine. The same authors have combined their sensor systems for adenosine and cocaine detection to create a sensor that only responds in the presence of both targets [51].

Due to their visible color, aptamer-modified AuNPs can be used not only in homogeneous assays, but they can also be applied to dipstick assays. Based on the TID mode, Liu et al. have developed a dipstick assay for the detection of adenosine. Here, aptamers against adenosine were hybridized with complementary oligonucleotides that were immobilized on AuNPs. In addition, the AuNPs were modified with biotin. In the absence of adenosine, large agglomerates were formed that were not able to migrate through the membrane of the dipstick assay. The addition of adenosine induces disassembly of agglomerates and the single AuNPs were able to migrate into the membrane, where they were captured by streptavidin that was immobilized to the test zone; consequently, a red line could be detected. The assay was also successfully applied for the detection of cocaine in human serum [52].

Although in the former aptasensors crosslinking of AuNPs was achieved via hybridization of aptamers and complementary oligonucleotides, Zhao et al. have reported a noncrosslinking agglomeration assay [53]. Here the phenomenon of salt-induced aggregation of AuNPs was exploited. AuNPs were modified with short oligonucleotides, which were complementary to the terminus of an aptamer directed against adenosine. After hybridization with the aptamer, the AuNPs were stable to a given salt concentration. Upon addition of the target, the aptamer dissociated from the oligonucleotide-modified AuNP. Because the AuNPs were electrostatically stabilized by the aptamer, the dissociation of the aptamer resulted in agglomeration and thus a blue-shift of $LSPR_{Max}$-. Based on different susceptibilities to salt-induced agglomeration of AuNPs carrying the aptamer and those only carrying the short oligonucleotide, sensing of adenosine was performed.

TIR-Based Colorimetric Sensing

Because the sandwich assay requires at least two aptamers binding to one target molecule, this detection scheme is limited to large molecules such as proteins, whereas small molecules do not offer sufficient surface to simultaneously bind to two aptamers. Here, target-induced reassembling of aptamer fragments offers a "sandwich-like" alternative. Li et al. first developed this method by cutting a DNA aptamer against adenosine into two fragments and immobilizing these fragments on different AuNPs [54]. After mixing of the particles and addition of the target, the aptamer fragments reassemble into the intact aptamer and form a three-molecule complex with adenosine (Fig. 4b). The agglomeration of AuNPs was visible by the naked eye and, using ultraviolet (UV)-Vis spectroscopy, the sensor was

capable of detecting adenosine in the low micromolar range. Moreover, the general applicability of this detection mode was demonstrated by successful application of another aptamer directed against cocaine.

4.1.2 Fluorescence Sensing with Aptamer-Modified AuNPs

Although most AuNPs (except those smaller than 3 nm) exhibit no fluorescence, they can be used in fluorescence assays as a "superquencher" for almost all dyes. The Stern–Volmer quenching constants for dye-AuNP pairs are usually several orders of magnitude higher than for typical dye-small molecule quencher pairs [55]. Therefore, they allow increased sensitivity and efficiency in Förster resonance energy (FRET)-based biosensors [56]. AuNPs can also be used to quench the fluorescence of semiconductor nanocrystals. Within this review, these sensors are discussed in Sect. 4.2.

Competitive Binding-Based Fluorescence Sensing

Huang et al. have developed a competitive assay for PDGF by using two differently sized AuNPs [57]. AuNPs with a diameter of 2 nm were modified with PDGF. Due to their small size, these AuNPs exhibit photoluminescence and were used as a donor in the FRET system. Larger AuNPs (diameter 13 nm) were modified with an aptamer and used as an acceptor. In the absence of PDGF, PDGF-modified AuNPs were bound to aptamer-modified AuNPs and the photoluminescence of the 2 nm AuNPs was quenched by the larger AuNPs. Free PDGF in the sample displaced PDGF-modified AuNPs and the release of these AuNPs results in an increase of photoluminescence signal. The LOD was 80 pM for PDGF and the assay was also used for sensing of PDGF α-receptor with a LOD of 250 pM.

TISS-Based Fluorescence Sensing

Huang et al. have developed a fluorescence sensor for PDGF based on the quenching properties of AuNPs [58]. They exploited the DNA-intercalating fluorescence dye *N,N*-dimethyl-2,7-diazapyrenium dication (DMDAP), which was intercalated to a DNA aptamer immobilized on AuNP. In the off-state, the DMDAP was almost completely quenched by the AuNP. The fluorescence strongly increased after the addition of PDGF. The authors assume this to be a result of conformational changes of the aptamer during the binding of PDGF. The LOD was 8 pM and additionally the assay was transferred to the detection of thrombin (LOD: 250 pM). The sensor was also reported to be useful for the detection of PDGF in cell culture media (LOD: 1 nM), but in this case preconcentration of the sample was required.

TID-Based Fluorescence Sensing

A TID-based fluorescence assay to sense thrombin was reported by Wang et al. [59]. The anti-thrombin aptamer was immobilized on AuNPs and a complementary TAMRA-modified oligonucleotide was hybridized to the aptamer. In the absence

of thrombin, the TAMRA dye was effectively quenched by the AuNP. In the presence of thrombin, the oligonucleotide dissociates from the aptamer and is thus released from the AuNP, resulting in an increased TAMRA fluorescence signal. The LOD was 0.14 nM for this system. The authors also constructed a similar system in which the complementary oligonucleotide is immobilized on the AuNP while the aptamer is TAMRA labeled. This sensor showed a LOD of 3.5 nM.

The TID-approach has also been used to realize multiplexed detection of small molecules [60]. In this case, the AuNPs were simultaneously modified with three different oligonucleotides complementary to the terminal bases of aptamers directed against adenosine, potassium ion, and cocaine, respectively. The three aptamers were labeled with different dyes and were allowed to hybridize to the corresponding oligonucleotides immobilized on the AuNPs surface. As a result of the close proximity to the AuNPs surface, the fluorescence of the dyes is quenched in the "off" state of the resulting nanosensor. In response to the target-induced dissociation of the aptamer, the sensor switches to the "on" state, allowing the simultaneous detection of the three analytes.

4.1.3 Electrochemical Sensing with Aptamer-Modified AuNPs

In addition to their excellent optical properties, AuNPs exhibit redox properties qualifying them as electrochemical labels. Du et al. identified two general applications of aptamer-modified AuNPs in electrochemical sensors [40]:

(i) AuNPs can be immobilized on the sensor's surface in order to increase the surface area and thus the loading of capture probe, thereby enhancing signal intensity. This application of AuNPs as a substrate in electrochemical sensors has been widely used [61–66].
(ii) AuNPs can be used as labels for amplification of the detection signal.

Within this section, we focus on the latter class of electrochemical sensors.

Sandwich-Based Electrochemical Detection

He et al. have developed an aptamer-modified AuNP-based approach for the electrochemical detection of thrombin, in which an anti-thrombin antibody was immobilized in order to capture thrombin from the applied sample. [67]. The captured thrombin was sandwiched by aptamer-modified AuNPs. Alkaline solution was used to release aptamer-modified AuNPs and the aptamers were degraded by acid or nuclease treatment. The redoxactivity of adenine was directly measured on pyrolytic graphite electrodes. Because the AuNP carries large amounts of aptamers, AuNPs were used to amplify the signal. As a result, the sensor shows excellent sensitivity with an LOD of approximately 3 pM. Another sandwich-based sensor for thrombin was developed by Li et al. who used two aptamers—one for the capture of thrombin and one for the detection. Also, this assay was very sensitive (20 pM) [68].

Moreover, Ding et al. have used a similar approach to detect thrombin. Here, AuNPs were additionally modified with CdS nanoparticles, which were detected via differential pulse voltammetry. A detection limit of 0.55 fM emphasizes the extraordinary sensitivity of the developed electrochemical sensor, which was also successfully used to quantify thrombin in clinical serum samples [69]. More examples for the high sensitivity of electrochemical sensors can be found in Table 1.

TID-Based Electrochemical Detection

Although the sandwich assay shows extreme sensitivity, it is not necessarily applicable for all targets, such as small molecule targets. Using an aptamer directed against ATP and two oligonucleotides partially complementary to this aptamer, Du et al. developed an electrochemical aptasensor for ATP detection [70]. One of the complementary oligonucleotides was immobilized on the sensor's surface, whereas the other was immobilized to AuNPs. Both oligonucleotides bind the aptamer via hybridization in a "sandwich-like" manner. Methylene blue (MB) was intercalated in the resultant DNA duplexes. In the presence of ATP, the aptamer was released from the oligonucleotides; thus, the differential pulse voltammetry (DVP) signal decreases. The AuNP was used to amplify the signal by carrying many copies of MB-intercalating DNA duplexes. The detection limit was 100 nM.

A similar TID-based electrochemical sensor for adenosine was developed using $[Ru(NH_3)_6]^{3+}$ as a redox indicator. A LOD of 180 pM and successful detection of adenosine in human serum samples was reported [71].

TIR-Based Electrochemical Detection

Another method to detect small molecules in a sandwich-like assay is the TIR-mode. Sharon et al. realized an electrochemical sensor for detection of cocaine based on TIR [72]. The anti-cocaine aptamer was divided into two fragments. One of the fragments was immobilized on the sensor's surface; the other was immobilized on AuNPs. The addition of cocaine resulted in the formation of a complex containing the two fragments and the target; consequently, AuNPs were bound to the sensor's surface. Because the AuNPs exhibit a highly negative charge as a consequence of multiple oligonucleotide loading, the interfacial electron transfer resistance increased when a negatively charged redox-label was used.

4.1.4 Other Sensing Techniques Applied to Aptamer-Modified AuNPs

Noble metal nanoparticles can be used in a variety of biosensing applications [56]. In addition to the optical and electrochemical applications discussed above, they can be used in Raman spectroscopy and imaging to enhance signals. Wang et al. have used aptamer-modified AuNPs to develop a surface-enhanced Raman scattering (SERS) sensor for thrombin in a sandwich mode. A thrombin-binding aptamer was immobilized on a gold surface. After capturing thrombin, a sandwich was formed with aptamer-modified AuNPs, which also carry the Raman reporter R6G. Raman signal was enhanced utilizing AgNPs, resulting in a sensitivity of

Table 1 Analytical applications of aptamer-modified AuNPs, including the target of the aptamer, the mode of detection, the applied sensor type, and the limit of detection

Target	Principle	Sensor type	LOD	References
Thrombin	Sandwich	Colorimetric	20 nM	[35]
PDGF	Sandwich	Colorimetric	2.5–10 nM	[36]
Thrombin	Sandwich	Colorimetric (dipstick)	2.5 nM (buffer) 0.6 μM (human plasma)	[41]
Ramos cells	Sandwich	Colorimetric (dipstick)	4000 cells (naked eye) 800 cells (with readout system)	[42]
Thrombin	Simple binding	Colorimetric (dot blot)	0.115 pmol (naked eye) 14 fmol (silver enhancement)	[43]
Mercury ions	TISS	Colorimetric	1 nM	[80]
ATP	TISS	Colorimetric	10 nM	[45]
Adenosine K^+	TISS	Colorimetric	Approx. 20 μM	[44]
K^+	TISS	Colorimetric	1 mM	[46]
Thrombin	TISS	Colorimetric	0.83 nM	[47]
Adenosine	TISS	Colorimetric	51.5 nM	[48]
Adenosine cocaine	TID	Colorimetric	0.3 mM (adenosine) 50 μM (cocaine)	[49–51]
Adenosine	TID	Colorimetric	100 mM	[81]
Adenosine	TID	Colorimetric	10 μM	[53]
Adenosine cocaine	TID	Colorimetric (dipstick)	20 μM (adenosine) 10 μM (cocaine in buffer) 200 μM cocaine (in human blood serum)	[52]
Adenosine cocaine	TIR	Colorimetric	0.25 mM (adenosine) 0.1 mM (cocaine)	[54]
Adenosine		Colorimetric		[82]
PDGF	Competitive	Fluorescence	80 pM	[57]
PDGF Thrombin	TISS	Fluorescence	8 pM (PDGF) 1 nM (PDGF in complex sample) 250 pM (thrombin)	[58]
Adenosine	TISS	Fluorescence	5.5 nM	[83]
Thrombin	TID	Fluorescence	0.14 nM	[59]
Thrombin	Sandwich	Electrochemical	3 pM	[67]
Thrombin	Sandwich	Electrochemical	20 pM	[68]
Thrombin	Sandwich	Electrochemical	0.55 fM	[69]
Thrombin	Sandwich	Electrochemical	100 fM	[84]
PDGF	Sandwich	Electrochemical	10 fM (purified samples) 1 pM (blood serum)	[61]
Thrombin	Sandwich	Electrochemical	7.82 aM	[85]
Adenosine	TID	Electrochemical	180 pM	[71]
ATP	TID	Electrochemical	200 pM	[86]
Adenosine lysozyme	TID	Electrochemical	20 pM (adenosine) 670 pM (lysozyme)	[87]
Thrombin	TID	Electrochemical	662 fM	[88]

(continued)

Table 1 (continued)

Target	Principle	Sensor type	LOD	References
Adenosine thrombin	TID	Electrochemical	8.8 pM (adenosine) 0.78 pM (thrombin)	[89]
ATP	TID	Electrochemical	100 nM	[70]
Cocaine	TIR	Electrochemical	1 μM	[72]
Adenosine thrombin	TID Sandwich	Electrochemical	2.2 pM (adenosine) 12 fM	[90]
IgE	Sandwich	SPR	0.001 μg/ml	[78]
Thrombin	Sandwich	SERS	0.5 nM	[73]
Thrombin	TISS	SERRS	100 pM 1 nM in 10 % fetal calf serum	[75]
Thrombin	TISS	SERS	20 pM	[74]
Adenosine	TID	SPR	100 nM – 100 pM (linear range)	[77]
Adenosine	TID	SPR	1 nM – 1 μM (linear range)	[91]
Adenosine	TIR	SPR	1.5 pM	[76]
Thrombin	Sandwich	QCM	0.1 nM	[92]

ATP adenosine triphosphate; *IgE* immunogloblin E; *LOD* limit of detection; *PDGF* platelet-derived growth factor; *QCM* quartz crystal microbalance; *SERS* surface-enhanced Raman scattering; *SERRS* surface-enhanced resonance Raman scattering; *SPR* surface plasmon resonance; *TID* target-induced dissociation; *TIR* target-induced reassembling of aptamer fragments; *TISS* target-induced structure switching

0.5 nM [73]. Other SERS-based sensors for thrombin based on TISS-based detection mode have been described with LODs in the picomolar range [74, 75].

Aptamer-modified AuNPs can also be used to enhance signals in surface plasmon resonance (SPR) sensors. This is especially useful for the detection of small molecules, which do not result in sufficient changes in refractive index upon binding to SPR sensor surfaces. To overcome this limitation, Wang et al. developed a TIR-based SPR sensor for the detection of adenosine. The aptamer directed against adenosine was divided in two pieces—one immobilized on the sensor's gold surface, the other to AuNPs. In the presence of adenosine, both fragments reassemble to form a sandwich-like complex with the target. Electronic coupling of the localized plasmon of AuNP and Au surface plasmon wave thereby occurs and enhances the SPR signal. The detection limit for adenosine was 1.5 pM and detection in complex samples was successfully performed [76]. Aptamer-modified AuNPs have also been used for signal enhancement in other SPR sensors [77–79]. More details can be found in Table 1.

4.2 Quantum Dots

Quantum dots (QDs) are semiconductor nanocrystals. Upon excitation with UV light, QDs emit fluorescence; the emission maximum is directly dependent on the QD's diameter. Due to their unique optical properties such as broad adsorption

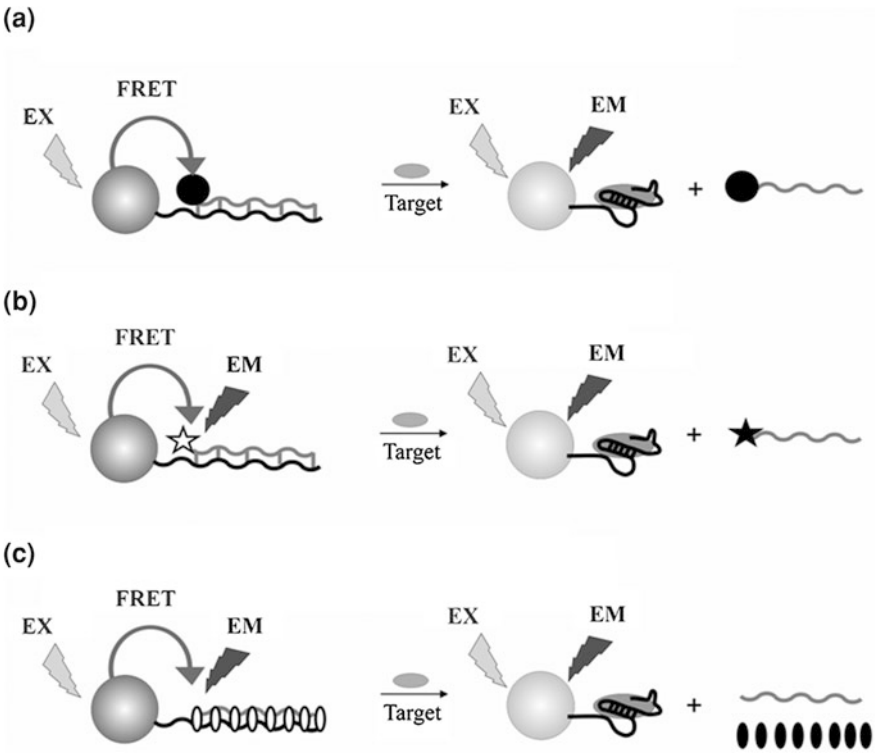

Fig. 5 Target-induced dissociation-based Förster resonance energy transfer (FRET) approaches using aptamer-modified quantum dots. **a** FRET utilizing quencher-modified oligonucleotides. **b** FRET utilizing dye-modified oligonucleotides. FRET utilizing dsDNA interlealated dyes. Adapted from Zhou [93]

spectrum, narrow and tunable emission spectrum, and low photobleaching, they are valuable platforms for analytical devices as well as for biological imaging.

Based on their broad absorption in combination with narrow emission, QDs are particularly attractive for Förster resonance energy transfer (FRET)-based sensors. Here, the excitation wavelength can be chosen from a broad range and narrow emission spectra qualify them especially for multiplexing approaches [93]. Based on the broad absorption, the use of QDs as FRET acceptors is limited, although they are excellent donors [93].

In general, FRET sensors rely on a target-induced change of the distance between donor (in this case a QD) and receptor (a dye that is excited by the emission of the QD or a quencher). Therefore, for FRET sensors, the TID and TISS modes of detection are especially useful. Different TID-based FRET approaches, which are displayed in Fig. 5, are described in the following paragraph and summarized in Table 2.

Table 2 Analytical applications of aptamer-modified quantum dots

Target	Principle	Sensor type	LOD	References
Thrombin	TISS	FRET	1 nM (in buffer) 50– 500 nM (linear range in 15 % serum)	[96]
Thrombin	TID	FRET	Nd	[94]
PDGF	TID	FRET	0.4 nM	[97]
Cocaine	TID	FRET	0. 5 μM	[95]
ATP	TID	FRET	24 μM	[98]
ATP	TID	Fluorescence	0.1 mM	[99]
ATP	TIR	CRET	185 nM	[100]
ATP	TIR	Electrochemical	30 nM	[101]
Cocaine			50 nM	

ATP adenosine triphosphate; *CRET* chemiluminescence resonance energy transfer; *FRET* Förster resonance energy transfer; *LOD* limit of detection; *PDGF* platelet-derived growth factor; *TID* target-induced dissociation; *TIR* target-induced reassembling of aptamer fragments; *TISS* target-induced structure switching

TID-Based FRET

Levy et al. have developed a FRET-based approach for detection of proteins [94]. They have modified QDs with an anti-thrombin aptamer. In the off-state of the sensor, the QD's fluorescence was quenched by a quencher-modified oligonucleotide that was hybridized to the aptamer. Binding of thrombin to the aptamer induces dissociation of the quencher-modified oligonucleotide and thus enhances QD fluorescence (Fig. 5a).

In addition to the utilization of quencher-modified complementary oligonucleotides, oligonucleotides modified with fluorescent dyes also have been successfully applied to FRET-based sensors (Fig. 5b). For instance, Zhang et al. have used this strategy to create a sensor for cocaine detection [95]. Here, the aptamer was immobilized on the QD and subsequently hybridized with a complementary oligonucleotide which was modified with Cy5. In the absence of cocaine, Cy5 was positioned in close proximity to the QD and could thus be excited by the QD. Cocaine addition results in dissociation of the Cy5-modified oligonucleotide from the aptamer and thus a decrease of Cy5 fluorescence was observed for increasing cocaine concentrations.

Although the aforementioned approaches necessitate the chemical modification of the complementary oligonucleotide, it is also possible to design FRET-based sensors with nonmodified oligonucleotides. Here, dsDNA-intercalating dyes can be incorporated in the duplex formed by the aptamer and the complementary oligonucleotide (Fig. 5c).

TISS-Based FRET

Using the conformational changes of an aptamer directed against thrombin, Chi et al. have developed an aptamer-modified QD-based sensor for thrombin. They have immobilized the aptamer on QDs. In the absence of the target, the aptamer adopts a stem-loop structure. The dsDNA region of this structure was intercalated

with the fluorescence dye (1,1′-(4,4,7,7-tetramethyl-4,7-diazaundecamethylene)-bis-4-[3-methyl-2,3-dihydro-(benzo-1,3-thiazole)-2-methylidene]-pyridinium tetraiodide) (BOBO-3), which was excited by the QD's fluorescence. The addition of thrombin results in a conformational rearrangement of the aptamer into a G-quadruplex, which is not capable of binding to BOBO-3. Consequently, BOBO-3 fluorescence decreases upon binding of thrombin.

Multiplexing with Quantum Dots

One of the main advantages of quantum dots is their high potential for multiplex analysis. Liu et al. have developed a quantum dot-based multiplex sensor for the simultaneous detection of adenosine and cocaine [102]. They have used two quantum dots emitting at different wavelengths and AuNPs as a quencher. In a TID mode, the nanoparticles were modified with short oligonucleotides complementary to parts of extended aptamers. In the sensor's off-state, AuNPs quench the QDs emission. Target molecules binding to the aptamer result in increased QD fluorescence. The authors have developed and tested these systems first for the detection adenosine and cocaine separately. Afterwards, they have mixed QDs and AuNPs for the simultaneous detection of both analytes. They were able to detect both analytes in a one-pot assay. Beside the fluorescence of the QD that increases with increasing analyte concentrations, also the change in $LSPR_{Max}$ of AuNPs could be exploited for sensing. Here, the disassembly of agglomerated AuNPs results in a red shift of $LSPR_{Max}$. The analytical applications of aptamer-modified QDs are summarized in Table 2.

4.3 Other Nanoparticles

4.3.1 Magnetic Nanoparticles

One problem associated with QDs and AuNPs is the background interference due to scattering, absorption, and autofluorescence of biological samples. In contrast to these nanoparticles, magnetic nanoparticles (MNPs) do not interfere with biological samples, which exhibit virtually no magnetic background [103].

MNPs are able to enhance the magnetic resonance from surrounding water molecules. Aggregation of MNPs induces the coupling of magnetic spin moments, resulting in a strong local magnetic field. Thus, aggregation and dissociation of MNPs result in a change in proton relaxation times, which can be read out via NMR, magnetic resonance imaging (MRI), or relaxometry.

Based on this effect, Bamrungsap et al. have described the use of aptamer-modified MNPs for the detection of lysozyme [104]. Here, iron oxide nanoparticles were modified with an anti-lysozyme aptamer. A linker oligonucleotide was designed, which is complementary to the terminal fraction of the aptamer. In absence of lysozyme, the linker leads to agglomeration of the MNPs; in presence of lysozyme, the linker is replaced, resulting in the dissociation of agglomerates

and thus an increase of proton relaxation time. Thus, this sensor is one example for the TISS mode of detection. The sensor was able to detect lysozyme concentrations as low as 0.5 nM and was also used to determine the level of lysozyme in cell lysates [104].

MNPs can also be used in combination with other nanoparticles. For example, Zheng et al. have developed a sandwich-based assay for the detection of thrombin that uses MNPs and AuNPs. The nanoparticles, MNPs and AuNPs, were modified with aptamers directed against the target. In presence of thrombin, a sandwich was formed. Signal amplification was performed by the addition of thiocyanuric acid, which results in the formation of a network-like thiocyanuric acid/AuNP structure. Due to this signal amplification, an excellent LOD of 7.82 aM was reported [85].

As described before for AuNPs, MNPs can also be used to enhance SPR signals. In this context, aptamer-modified MNPs have been used to enhance the sensitivity for the detection of adenosine by Wang et al. [105].

4.3.2 Silica Nanoparticles

Dye-doped silica nanoparticles (SiNPs) offer several advantages over organic dyes. A large number of dyes can be incorporated in the SiNP, resulting in high optical intensity. Moreover, photobleaching is minimized within the nanoparticle and the dye is protected from environmental influences.

Babu et al. have recently constructed a TISS-based sensor for thrombin based on aptamer-modified SiNPs [106]. The system consists of SiNPs doped with $[Ru(dpsphen)_3]^{4-}$ (dpsphen-4,7-diphenyl-phenanthroline disulfonate) ion. The nanoparticles were further modified with anti-thrombin aptamers, which were covalently attached to the SiNP via their 5′ terminus, whereas the 3′ terminus was modified with a DABCYL quencher. In the presence of thrombin, the aptamer adopts its specific G-quadruplex conformation in which the DABCYL quencher comes in close proximity to the SiNP surface. Thus, in this sensor, the luminescence signal decreases with increasing thrombin concentration.

In a TID-based approach, Cai et al. have used SiNPs to detect ATP [107]. The SiNP was modified with an oligonucleotide complementary to an ATP-binding aptamer. Thus, the addition of ATP causes the release of the aptamer from the SiNP and a reduction of dsDNA on the particle surface. This was read out using Hoechst33258, a dye which preferentially binds to AT-rich sequences of dsDNA. This approach necessitates the separation of SiNPs from the sample prior to the addition of the dye. Due to the high density of silica, this can be easily achieved by centrifugation. Therefore, despite the necessity of several steps, this ATP assay can be easily performed and does not necessitate the use of expensive labeled aptamers. The authors assumed their platform to be universally applicable to other aptamers [107].

A sandwich-based approach based on SiNPs has been realized by Wang et al. [108]. They have immobilized an aptamer directed against thrombin on SiNPs. After capture of thrombin by the aptamer, a fluorescently-labeled aptamer directed

against thrombin was bound. Signal amplification was performed with a cationic conjugated polymer, resulting in excellent LOD of 1.06 nM.

4.3.3 DNA and Protein Nanoparticles

DNA can be used to construct three-dimensional DNA polyhedrons. By using six DNA sequences with partial complementary sequences, Chang et al. have designed a six-point-star motif that further assembles to form a rigid DNA icosahedra due to hybridization of sticky ends of the oligonucleotides [114]. Because one of the DNA strands contains a DNA aptamer directed against the tumor surface marker MUC 1 and this aptamer erects at the outside of the DNA polyhedral during the self-assembly, the particle is able to bind to human breast cancer cell line MCF-7. Moreover, the DNA nanoparticles were internalized via endocytosis. The double-stranded DNA of the nanoparticle was used as a carrier for the DNA-intercalating drug doxorubicin. The targeted delivery of doxorubicin to MCF-7 cells was demonstrated and doxorubicin's fluorescence was used for the imaging of internalization.

Kim et al. have modified ferritin nanoparticles composed of ferritin heavy chain and green fluorescent protein with an anti-PDGF aptamer. These nanoparticles were used to detect the growth factor in a sandwich format [113].

5 Aptamer-Modified Nanoparticles in Medical Applications

Based on their potential in analytical applications and their specific binding, aptamer-modified nanoparticles attracted attention in diagnostics and therapeutical applications. Depending on the analyte of interest, three different diagnostic applications of aptamer-modified nanoparticles can be distinguished:

(i) detection of soluble biomarkers,
(ii) intracellular detection of biomarkers, and
(iii) detection of cell-surface-bound biomarkers.

These diagnostic applications are described in the following paragraphs and reviewed in Table 4. Potential therapeutic applications are outlined in Sect. 5.4.

5.1 Detection of Soluble Biomarkers

Several examples for the detection of soluble biomarkers have already been given in the previous section. For example, thrombin regulates the process of blood coagulation and its concentration is associated with thrombosis, hemostasis, and heart diseases. Therefore, it is a target for therapy as well as diagnostics. PDGF is

Table 3 Applications of other nanoparticles in aptamer-based sensors

Target	Nanoparticle	Principle	Sensor type	LOD	References
Thrombin	SiNP	TISS	Luminescence	4 nM	[106]
ATP	SiNP	TID	Fluorescence	20 μM	[107]
ATP	SiNP	TID		34 μM	[109]
Thrombin Lysozyme	SiNP	Sandwich	Fluorescence	1.06 nM (thrombin)	[108]
Thrombin Lysozyme	SiNP	Sandwich	Fluorescence	1.06 nM (thrombin)	[108]
Adenosine	MNP	TID	SPR	10– 10 μM (linear range)	[105]
Lysozyme	MNP	TID	Magnetic relaxation switch detection	1 nM (in serum)	[104]
Thrombin	MNP	Sandwich	Magnetic relaxation switch detection	1 nM	[110]
Thrombin	MNP	Sandwich	Magnetic resonance imaging	25 nM (in serum)	[111]
Ochratoxin A	MNP/UCNP	TID	Luminescence	0.1 pg/ml	[112]
PDGF	Ferritin	Sandwich	Fluorescence	100 fM	[113]

ATP adenosine triphosphate; *LOD* limit of detection; *MNP* magnetic nanoparticle; *PDGF* platelet-derived growth factor; *SiNP* silica nanoparticle; *SPR* surface plasmon resonance; *TID* target-induced dissociation; *TISS* target-induced structure switching; *UCNP* upconversion nanoparticle

known to be related with tumor growth. These and other examples for the detection of soluble biomarkers can be found in Tables 1, 2, and 3.

5.2 Intracellular Detection

Oligonucleotide-modified AuNPs are known to be internalized by cells [115]. This cellular uptake is dependent on the oligonucleotide loading, in which higher loadings result in better uptake. Giljohan et al. have investigated this effect systematically and have proposed that AuNPs carrying a dense oligonucleotide monolayer adsorb a large number of proteins on their surface, which facilitates cellular uptake [115]. On this basis, Mirkin and co-workers have developed an aptamer-modified AuNP that enables the detection of ATP within living cells [116]. The so-called aptamer nanoflares consist of AuNPs modified with a dense monolayer of anti-ATP aptamer. The detection was based on TID mode; therefore, the aptamer was hybridized with a Cy5-labelled complementary oligonucleotide. It was shown that nanoflares were effectively taken up by HeLa cells. Moreover, the conjugate resists nuclease degradation. Within the cell, ATP binds to the aptamer, resulting in dissociation of Cy5-labeled complementary strands from the quenching AuNP and thus in increased fluorescence signals. The sensor was

Table 4 Applications of aptamer-modified nanoparticles in cell detection

Target	Nanoparticle	Mode of Detection	Application (LOD)	References
CEM cells, Ramos cells, Toledo cells	SiNP	Simple binding	Multiplex cancer cell monitoring	[117]
PTK7 receptor IgM	MNP	TID	Detection of cancer cells (10 cells/250 μl in PBS, 100 cells in biological liquids)	[103]
PSMA	AuNP	Simple binding	Detection of prostate cancer cells in human tissue sections	[39]
PSMA	MNP	Simple binding	Prostate cancer imaging	[122]
Tenascin-C	QD	Simple binding	Targeting of glioma cells	[123]
Mucin 1	QD	FRET	Detection of tumor marker	[124]
CCRF-CEM	NIR-NP	Simple binding	Detection of cancer cells in whole blood	[125]
C. jejuni surface proteins	QD	Sandwich	Detection of food-borne pathogens (*C. jejuni*) (2.5 cfu in buffer; 10–250 cfu in food matrices)	[121]
Bacillus thuringiensis spores	QD	Simple binding	Detection of *Bacillus thuringiensis* spores (1000 cfu/ml)	[120]
Salmonella typhimurium Staphylococcus aureus	MNP/UCNP	Sandwich	Simultaneous detection of *S. Typhimurium* (5 cfu/ml) and *S. aureus* (8 cfu/ml)	[119]
Hemagglutinin	QD	Simple binding	Detection of influenza A virus particles	[126]
Prion protein	AgNP	Simple binding	Intracellular imaging of prion protein in human bone marrow blastoma cells	[118]

AgNP silver nanoparticle; *AuNP* gold nanoparticle; *FRET* Förster resonance energy transfer; *LOD* limit of detection; *MNP* magnetic nanoparticle; *NIR-NP* near-infrared fluorescent nanoparticles; *PBS* phosphate-buffered saline; *PSMA* prostate-specific membrane antigen; *QD* quantum dot; *SiNP* silica nanoparticle; *TID* target-induced dissociation; *UCNP* upconversion nanoparticle

capable of quantifying ATP concentration in a physiological range (0.1–3 mM). The authors expect this approach to be extendable to other intracellular analytes.

5.3 Detection of Cell Surface-Bound Biomarkers

The specific detection of subpopulations of cells is especially important in cancer diagnosis. Other diagnostic applications include the detection of pathogens. These

diagnostic applications of aptamer-modified nanoparticles are outlined in the next paragraphs; more examples can be found in Table 4.

5.3.1 Cell Targeting and Imaging

Bamrungsap et al. have used aptamer-modified magnetic nanoparticles to detect cancer cells [103]. As described in Sect. 4.4.1, the aggregation of MNPs results in changes of proton relaxation times. In this case, the aptamers were directed against cancer-specific cell surface proteins (IgM, PTK 7) and binding of the aptamer to the surface bound target lead to aggregation of MNPs on the cell surface. The sensor was able to detect the applied cell lines. By using an array of MNPs conjugated with seven aptamers directed against cancer-associated targets, it was possible to distinguish between different cancer cell lines based on differential expression of the respective cell surface markers. The sensors' sensitivity was as high as 10 cells in 150 μl [103].

Chen et al. developed a dye-doped SiNP-based system for the simultaneous detection of multiple cancer cells [117]. They used three different aptamers directed against different cancer cell lines (Ramos, CEM, Toledo). Aptamers were immobilized on dye-doped SiNPs via biotin-streptavidin interaction. The SiNPs were doped with three different dyes and mixtures thereof. The dyes exhibit overlapped excitation and emission wavelengths and thus enable fluorescence energy transfer (FRET). As a result, by using one single excitation wavelength, three dyes could be detected simultaneously, resulting in simplification of instrumentation requirements. In early experiments, aptamer-modified SiNPs were shown to selectively bind to the corresponding target cells, as monitored by FACS. Moreover, simultaneous detection of three cancer cell lines was performed and examined via confocal microscopy. To simulate complex samples, the measurements were also performed in cell culture media supplemented with 10 % fetal bovine serum. Although the experiments were only performed with cell lines so far, the authors believe that the method is applicable for the multiplexed detection of cancer cells.

Beside their potential in diagnostic applications, aptamer-modified nanoparticles can also be exploited in medical research. For instance, Chen et al. have modified AgNPs with an aptamer directed against cellular prion protein (PrP^C), which is a cell-surface-bound protein. They have used this aptamer-modified AgNP to investigate the internalization pathway of PrP^C. Here the excellent light scattering properties of silver nanoparticles (AgNPs) were exploited for dark-field light scattering microscopy and the AgNP was also used as a contrast imaging agent for TEM in order to localize aptamer-modified AgNPs after internalization. The results support a caveolae-dependent endocytosis pathway. Moreover, internalized aptamer-modified AgNPs were subjected to single nanoparticle spectral analysis. Because the surrounding of AgNPs influences spectral characteristics, the authors assume that these nanoparticles might be useful for intercellular microenvironment analysis [118].

5.3.2 Detection of Pathogens

Recently, Duan et al. have developed a highly sensitive aptamer-conjugated nanoparticle-based platform for the simultaneous detection of *Salmonella* Typhimurium and *Staphylococcus aureus* [119]. They have used two different nanoparticles, MNPs and lanthanide-doped near-infrared (NIR)-to-visible upconversion nanoparticles (UCNPs), in a sandwich-based assay. Both nanoparticles were modified with aptamers. The MNPs were used to capture and concentrate the target pathogen, whereas the UCNP was used for detection of MNP-bound targets. The sensor has a LOD of 5 cfu/ml and 8 cfu/ml for *S. Typhimurinum* and *S. aureus,* respectively. The sensor's applicability to real samples was investigated by analyzing authentic water samples. Comparative measurements with classical counting methods revealed good agreement of both methods.

Ikanovic et al. have described the use of aptamer-modified quantum dots for the detection of *Bacillus thuringiensis* spores [120]. In a more advanced approach, the same group has constructed a sandwich assay consisting of aptamer-modified magnetic beads and aptamer-modified QDs for the detection of *Campylobacter jejuni* [121]. Here, a sandwich of the aptamer-modified particles and the target was formed and the magnetic beads were used to concentrate the analyte, resulting in a LOD of 2.5 cfu in buffer and 10–250 cfu in complex food samples.

5.4 Targeted Drug Delivery

In medical applications, aptamer-modified nanoparticles can be used not only for cell targeting but also for drug delivery, as well as combinations of both [127, 128]. Here, the possibility to use nanoparticles as a platform to design multifunctional constructs is exploited. The nanoparticle itself serves a transducer and offers surface and/or volume for further modification. The surface can carry the aptamer and other functional molecules can be immobilized. These may include drugs or polymers controlling the internalization of nanoparticles into cells or the fate of nanoparticles within the cell. In case of polymer-based nanoparticles, the nanoparticle's volume can carry drugs and the nature of the polymer can facilitate controlled release of this drug and biodegadation. These manifold functionalities of aptamer-modified nanoparticles have accelerated their use as vehicles for targeted delivery. In this section, some of these approaches will be summarized. A more comprehensive review of the literature is given in Table 5.

In targeted delivery, the aptamer is exploited to enhance the specificity of a therapy. By binding of the aptamer-modified nanoparticle to the cell-surface-bound target, the drug is localized directly at the desired cells or tissues that shall be treated. Thereby, in contrast to systemic therapy, the local concentration of the drug can be enhanced while side effects to healthy tissue are minimized.

As a consequence of their high loading capacity, especially liposomes, polymeric nanoparticles and hybrid systems of both can be applied for targeted

Table 5 Applications of aptamer-modified nanoparticles in drug delivery

Target	Nanoparticle	Application/Cell type	References
PSMA	PLGA-*b*-PEG	Targeted drug delivery/LNCaP	[137]
PSMA	PLGA-*b*-PEG	Co-delivery of multiple drugs/LNCaP	[138]
PSMA	PLGA-*b*-PEG	Targeted drug delivery/LNCaP	[139]
Nucleolin	PLGA-lecithin-PEG	Tumor cell targeting drug delivery/MCF-7 and GI-1	[129]
U87 cells	PEG-PCL	Targeted delivery/U87 glioma cells	[140]
PSMA	PLA-PEG	Targeted drug delivery/LNCaP	[141]
IgM	Micelle	Potential application in drug delivery/Ramos	[142]
ATP	SiNP	Stimulus-responsive controlled release/Ramos	[135]
CCRF-CEM cells	SiNP	Targeted delivery and detection/CCRF-CEM	[134]
Thrombin	Lipid-coated SiNP	Inhibition of tumor cell proliferation, drug delivery/HeLa	[133]
PSMA	QD	Targeted delivery/C4-2B cells	[131]
PSMA	QD	Targeted delivery/LNCaP cells	[130]
PSMA	MNP	Targeted delivery and imaging/LNCaP	[122]
MUC 1	DNA	Drug delivery/MCF-7 breast cancer cell line	[114]
gp 120	RNA	Delivery of siRNA and HIV-1 inhibition/infected human PBMCs	[143]

ATP adenosine triphosphate; *HIV* human immunodeficiency virus; *IgM* immunoglobulin M; *PBMC* peripheral blood mononuclear cell; *PEG* polyethylene glycol; *PEG-PCL* poly(ethylene-glycol)-poly(***ε*-caprolactone); *PLGA* poly(D, L lactic-co-glycolic acid); *PLGA-b-PEG* poly(D,L-lactic-co-glycolic acid)-block-poly(ethylene glycol); *PLA-PEG* poly(lactic acid)-block-polyethylene glycol; *PSMA* prostate-specific membrane antigen; *QD* quantum dot; *SiNP* silica nanoparticle

delivery. Biocompatible polymeric nanoparticles enable the encapsulation of hydrophobic drugs and the drug release rate can be controlled by choice of the polymer; it is also possible to achieve triggered drug release that is initiated by pH changes, for example. Biodegradable liposomes offer advantageous features for drug delivery. They can be used for the encapsulation of hydrophilic drugs within their core. They can also carry hydrophobic drugs within the lipid bilayer, although in this case the loading capacity is rather low. Other disadvantages include the burst release of drugs. In order to overcome these limitations, lipid-polymer hybrids can be used [129].

In this context, Aravind et al. have designed a lipid-polymer hybrid nanoparticle consisting of a poly(D, L lactic-co-glycolic acid) (PLGA) core, a lipid layer of lecithin and pegylated phospholipids [129]. The pegylated lipids were functionalized with an anti-nucleolin aptamer to enable targeting of cancer cells overexpressing nucleolin receptors. The core was loaded with paclitaxel for cancer treatment and with Nile red to monitor cellular uptake. It was shown that the aptamer significantly increases uptake of conjugates to MCF-7 breast cancer cell line, whereas no toxicity was observed for normal cells (HMEC).

Further, anorganic nanoparticles can be used for targeted delivery. For example, Bagalkot et al. have designed aptamer-modified quantum dots for synchronous

cancer imaging and therapy [130]. Here, quantum dots were modified with an RNA aptamer directed against PSMA. In addition to its function to guide the conjugate to the desired cells, the aptamer was also used as a carrier for the nucleic acid-intercalating drug doxorubicin. Besides the potential use for doxorubicin delivery, the conjugates also allow the detection of conjugate binding and doxorubicin release. Doxorubicin exhibits fluorescence, which is quenched by intercalation in the double-stranded regions of the RNA aptamer. Thus, gradual release of doxurubicin can be monitored after cellular uptake. Moreover, doxorubicin quenches the quantum dot's fluorescence, resulting in a simultaneous increase of quantum dot fluorescence during doxorubicin release. Thus, this system not only delivers the drug into the cells, but it also senses the delivery.

Beside conventional small-molecule drugs, siRNA has been delivered to cells via aptamer-conjugated nanoparticles. Bagalkot and Gao have designed a siRNA-aptamer chimera, which was immobilized on polyethylenimine (PEI)-modified QDs [131]. Based on an RNA aptamer directed against PSMA, these conjugates bind to PSMA-positive cells and are internalized. Moreover, due to the proton sponge effect of PEI [132], endosomal escape of siRNA was improved and effective gene silencing was observed.

Gao et al. have investigated the use of mesoporous SiNPs for the inhibition of tumor cell proliferation [133]. The SiNPs were lipid-coated and additionally modified with an anti-thrombin aptamer. Moreover, the lipid layer was used to incorporate the anticancer drug docetaxel. These multifunctional hybrid SiNPs were shown to suppress HeLa cell growth by inhibiting thrombin and thus disturbing PAR-1 receptor signaling, which is activated by thrombin to accelerate tumor cell proliferation. Moreover, the SiNPs were internalized via endocytosis, resulting in delivery of docetaxel.

SiNPs have also been used by He et al. for targeted delivery of doxorubicin to leukemia CCRF-CEM cells [134]. To enable targeted delivery, the SiNPs were modified with an aptamer directed against the cells. The SiNP allows sustained release of doxorubicin and in vitro studies revealed an effective killing of tumor cells after endocytic uptake. The first animal experiments were performed with SiNPs not modified with an aptamer by injection in tumor-bearing mice. These nontargeting SiNPs were shown to accumulate in the lung, kidney, and the tumor-tissue. The authors assume that the SiNPs passively target the tumor due to enhanced permeability and retention effects, which has to be resolved before in vivo application.

Recently, He et al. have developed a stimulus-responsive controlled release system by using aptamer-modified mesoporous SiNPs [135]. As a model for incorporated drugs, the dye $Ru(biphy)_3^{2+}$ was incorporated in SiNPs and ATP binding aptamers were used to design a cap to block the release of the dye. Here, a TID approach was used in which two oligonucleotides were immobilized on the SiNPs surface, which are partially complementary to the anti-ATP aptamer and bind the aptamer in a sandwich-like manner. Binding of ATP to the aptamer dissociates the aptamer from the cap and flexible single-stranded oligonucleotides no longer block the pores of SiNP. The capping efficiency was high and after

addition of 20 mM ATP, 83.2 % of the dye was released within 7 h. The system was stable in serum at 37 °C. This proof-of-concept study may enable the development of other stimulus-responsive systems in the future.

Besides their application as vehicles for drug delivery, aptamer-modified nanoparticles may also be used for selective surgery. In this context, Nair et al. have used aptamer-modified MNPs to perform surgical actions. The so-called nanosurgeon can selectively target cancer cells and be moved by external magnetic fields. By applying a rotating magnetic field, cell death was induced. Thus, the authors assume that the nanosurgeon will be a useful tool in the removal of complex cancers [136].

Within this section, only a few examples of the application of aptamer-modified nanoparticles have been given. More examples are summarized in Table 5.

6 Summary, Conclusions, Outlook

The use of aptamer-modified nanoparticles in analytical and medical applications was intensively investigated in the last decade. Within the literature reviewed in this article, a broad diversity of applications was revealed. Many different analytes, including small molecules, proteins, and even cells, have already been detected successfully using aptamer-modified nanoparticles composed of manifold anorganic and inorganic materials. Today, most reports deal with aptamer-modified AuNPs, which enable different detection techniques, including colorimetric, fluorescent, and electrochemical detection. Among these techniques, electrochemical sensing has particularly enabled the ultrasensitive detection of analytes with LODs in the femto- or even atomolar range.

Despite this high sensitivity, most reports on aptamer-modified nanoparticles are proof-of-concept studies using pure targets. Only a few investigations have been performed for the applicability of these sensors for the analysis of real, complex samples. Nonetheless, these rare cases, such as the detection of PDGF in complex samples [58], point out the potential of aptamer-modified nanoparticles in complex analytical problems.

Especially for the detection of small molecules, the use of aptamers as bioreceptors has proven to be advantageous. Here the conformational changes of aptamers during binding of the target can be exploited for the detection of the target. Also, different "sandwich-like" sensor systems have been developed based on the oligonucleotide structure of the aptamer. Target-induced dissociation of complementary oligonucleotides (TID) and target-induced rearrangement of aptamer fragments (TIR) have been used for the detection of small molecules. Here, LODs in the nano- and picomolar range have been achieved.

In summary, the application of aptamer-modified nanoparticles in bioanalysis shows highly promising results. To tap the full potential, more applications to complex analytical problems have to be performed and optimized, if necessary. The same is true for medical applications of aptamer-modified nanoparticles. Most

of the studies have been performed using cell lines or mixtures of different cell lines. Within the body or biological samples, aptamer-modified nanoparticles will be confronted with a much more complex environment that challenges their specificity.

References

1. Jianrong C, Yuqing M, Nongyue H, Xiaohua W, Sijiao L (2004) Biotechnol Adv 22(7):505–518
2. Schwalbe H, Buck J, Fürtig B, Noeske J, Wöhnert J (2007) Angew Chem Int Ed 46(8):1212–1219
3. Heppell B, Lafontaine DA (2008) Biochemistry 47(6):1490–1499
4. Patel D (1997) Curr Opin Chem Biol 1(1):32–46
5. Keniry MA (2000) Biopolymers 56(3):123–146
6. Nagatoishi S, Tanaka Y, Tsumoto K (2007) Biochem Biophys Res Commun 352(3):812–817
7. Leontis NB, Westhof E (2001) RNA (New York, NY) 7 (4):499–512
8. Cai S, Lau C, Lu J (2011) Anal Chem 83(15):5844–5850
9. Hermann T, Patel DJ (2000) Science 287(5454):820–825
10. Lambert D, Leipply D, Shiman R, Draper DE (2009) J Mol Biol 390(4):791–804
11. Green LS, Jellinek D, Bell C, Beebe LA, Feistner BD, Gill SC, Jucker FM, Janjić N (1995) Chem Biol 2(10):683–695
12. Ruckman J, Green LS, Beeson J, Waugh S, Gillette WL, Henninger DD, Claesson-Welsh L, Janjic N (1998) J Biol Chem 273(32):20556–20567
13. Kato Y, Minakawa N, Komatsu Y, Kamiya H, Ogawa N, Harashima H, Matsuda A (2005) Nucleic Acids Res 33(9):2942–2951
14. Keefe AD, Cload ST (2008) Curr Opin Chem Biol 12(4):448–456
15. Kuwahara M, Sugimoto N (2010) Molecules 15(8):5423–5444
16. Eulberg D, Klussmann S (2003) ChemBioChem 4(10):979–983
17. Tucker CE, Chen LS, Judkins MB, Farmer JA, Gill SC, Drolet DW (1999) J Chromatogr B. Biomed. Sci Appl 732(1):203–212
18. Chen C-hB, Dellamaggiore KR, Ouellette CP, Sedano CD, Lizadjohry M, Chernis GA, Gonzales M, Baltasar FE, Fan AL, Myerowitz R, Neufeld EF (2008) Proc Natl Acad Sci 105(41):15908–15913
19. Kim E, Jung Y, Choi H, Yang J, Suh J-S, Huh Y-M, Kim K, Haam S (2010) Biomaterials 31(16):4592–4599
20. Strehlitz B, Reinemann C, Linkorn S, Stoltenburg R (2012) Bioanal Rev 4(1):1–30
21. Blank M, Blind M (2005) Curr Opin Chem Biol 9(4):336–342
22. Brody EN, Gold L (2000) J Biotechnol 74(1):5–13
23. Famulok M, Hartig JS, Mayer G (2007) Chem Rev 107(9):3715–3743
24. Kökpinar Ö, Walter J-G, Shoham Y, Stahl F, Scheper T (2011) Biotechnology and Bioengineering May 2. doi: 10.1002/bit.23191. [Epub ahead of print]
25. Walter J-G, Stahl F, Scheper T (2012) Eng Life Sci 12(5):496–506
26. Clark SL, Remcho VT (2002) Electrophoresis 23(9):1335–1340
27. Spiridonova VA, Kopylov AM (2002) Biochemistry (Mosc) 67(6):706–709
28. Walter J, Kokpinar O, Friehs K, Stahl F, Scheper T (2008) Anal Chem 80(19):7372–7378
29. Walter J-G, Heilkenbrinker A, Austerjost J, Stahl F, Scheper T (2012) Z Naturforsch 67b:976-986
30. Lübbecke M, Walter J-G, Stahl F, Scheper T (2012) Engineering in life sciences accepted article. doi:10.1002/elsc.201100100

31. Zhu G, Lübbecke M, Walter J, Stahl F, Scheper T (2011) Chem Eng Technol 34(12):2022–2028
32. Han K, Liang Z, Zhou N (2010) Sensors 10(5):4541–4557
33. Alivisatos AP, Johnsson KP, Peng XG, Wilson TE, Loweth CJ, Bruchez MP, Schultz PG (1996) Nature 382(6592):609–611
34. Mirkin CA, Letsinger RL, Mucic RC, Storhoff JJ (1996) Nature 382(6592):607–609
35. Pavlov V, Xiao Y, Shlyahovsky B, Willner I (2004) J Am Chem Soc 126(38):11768–11769
36. Huang CC, Huang YF, Cao Z, Tan W, Chang HT (2005) Anal Chem 77(17):5735–5741
37. Sylvestre JP, Kabashin AV, Sacher E, Meunier M (2005) Appl Phys A: Mater Sci & Process 80(4):753–758
38. Barcikowski S, Hahn A, Kabashin AV, Chichkov BN (2007) Appl Phys A: Mater Sci & Process 87(1):47–55
39. Walter J, Petersen S, Barcikowski S, Stahl F, Scheper T (2010) J Nanobiotechnol 8 (21):doi: 10.1186/1477-3155-1188-1121
40. Du Y, Li B, Wang E (2010) Bioanal Rev 1 (187-208)
41. Xu H, Mao X, Zeng Q, Wang S, Kawde AN, Liu G (2009) Anal Chem 81(2):669–675
42. Liu G, Mao X, Phillips JA, Xu H, Tan W, Zeng L (2009) Anal Chem 81(24):10013–10018
43. Wang Y, Li D, Ren W, Liu Z, Dong S, Wang E (2008) Chem Commun (Camb) (22):2520–2522
44. Zhao W, Chiuman W, Lam JC, McManus SA, Chen W, Cui Y, Pelton R, Brook MA, Li Y (2008) J Am Chem Soc 130(11):3610–3618
45. Chen SJ, Huang YF, Huang CC, Lee KH, Lin ZH, Chang HT (2008) Biosens Bioelectron 23(11):1749–1753
46. Wang LH, Liu XF, Hu XF, Song SP, Fan CH (2006) Chem Commun 36:3780–3782
47. Wei H, Li BL, Li J, Wang EK, Dong SJ (2007) Chem Commun 36:3735–3737
48. Liu XP, Zhou ZH, Zhang LL, Tan ZY, Shen GL, Yu RQ (2009) Chin J Chem 27(10):1855–1859
49. Liu J, Lu Y (2005) Angew Chem Int Ed Engl 45(1):90–94
50. Liu JW, Lu Y (2007) J Am Chem Soc 129(27):8634–8643
51. Liu JW, Lu Y (2006) Adv Mater 18 (13):1667-+
52. Liu JW, Mazumdar D, Lu Y (2006) Angew Chemie Int Ed 45(47):7955–7959
53. Zhao W, Chiuman W, Brook MA, Li Y (2007) ChemBioChem 8(7):727–731
54. Li F, Zhang J, Cao X, Wang L, Li D, Song S, Ye B, Fan C (2009) Analyst 134(7):1355–1360
55. Dulkeith E, Morteani AC, Niedereichholz T, Klar TA, Feldmann J, Levi SA, van Veggel FC, Reinhoudt DN, Moller M, Gittins DI (2002) Phys Rev Lett 89(20):203002
56. Doria G, Conde J, Veigas B, Giestas L, Almeida C, Assuncao M, Rosa J, Baptista PV (2012) Sensors (Basel) 12(2):1657–1687
57. Huang C–C, Chiang C-K, Lin Z-H, Lee K-H, Chang HT (2008) Anal Chem 80:1497–1504
58. Huang CC, Chiu SH, Huang YF, Chang HT (2007) Anal Chem 79(13):4798–4804
59. Wang W, Chen C, Qian M, Zhao XS (2008) Anal Biochem 373(2):213–219
60. Zhang J, Wang L, Zhang H, Boey F, Song S, Fan C (2010) Small 6(2):201–204
61. Wang J, Meng W, Zheng X, Liu S, Li G (2009) Biosens Bioelectron 24(6):1598–1602
62. Wu ZS, Guo MM, Zhang SB, Chen CR, Jiang JH, Shen GL, Yu RQ (2007) Anal Chem 79(7):2933–2939
63. Feng KJ, Sun CH, Kang Y, Chen JW, Jiang JH, Shen GL, Yu RQ (2008) Electrochem Commun 10(4):531–535
64. Li XX, Qi HL, Shen LH, Gao Q, Zhang CX (2008) Electroanalysis 20(13):1475–1482
65. Suprun E, Shurnyantseva V, Bulko T, Rachmetova S, Rad'ko S, Bodoev N, Archakov A (2008) Biosens Bioelectron 24(4):825–830
66. Fang LY, Lv ZZ, Wei H, Wang E (2008) Anal Chim Acta 628(1):80–86
67. He P, Shen L, Cao Y, Li D (2007) Anal Chem 79(21):8024–8029
68. Li B, Wang Y, Wei H, Dong S (2008) Biosens Bioelectron 23(7):965–970
69. Ding C, Ge Y, Lin JM (2010) Biosens Bioelectron 25(6):1290–1294

70. Du Y, Li B, Wang F, Dong S (2009) Biosens Bioelectron 24(7):1979–1983
71. Zhang S, Xia J, Li X (2008) Anal Chem 80(22):8382–8388
72. Sharon E, Freeman R, Tel-Vered R, Willner I (2009) Electroanalysis 21(11):1291–1296
73. Wang Y, Wei H, Li B, Ren W, Guo S, Dong S, Wang E (2007) Chem Commun (Camb) (48):5220-5222
74. Hu J, Zheng PC, Jiang JH, Shen GL, Yu RQ, Liu GK (2009) Anal Chem 81(1):87–93
75. Cho H, Baker BR, Wachsmann-Hogiu S, Pagba CV, Laurence TA, Lane SM, Lee LP, Tok JBH (2008) Nano Lett 8(12):4386–4390
76. Wang Q, Huang JH, Yang XH, Wang KM, He LL, Li XP, Xue CY (2011) Sens Actuators B Chem 156(2):893–898
77. Wang JL, Munir A, Zhou HS (2009) Talanta 79(1):72–76
78. Wang JL, Munir A, Li ZH, Zhou HS (2009) Biosens Bioelectron 25(1):124–129
79. Wang J, Zhou HS (2008) Anal Chem 80(18):7174–7178
80. Li L, Li B, Qi Y, Jin Y (2009) Anal Bioanal Chem 393(8):2051–2057
81. Zhang Z, Chen CL, Zhao XS (2009) Electroanalysis 21(11):1316–1320
82. Liu J, Lu Y (2004) Anal Chem 76(6):1627–1632
83. Chen SJ, Huang CC, Chang HT (2010) Talanta 81(1–2):493–498
84. Deng C, Chen J, Nie Z, Wang M, Chu X, Chen X, Xiao X, Lei C, Yao S (2009) Anal Chem 81(2):739–745
85. Zheng J, Feng W, Lin L, Zhang F, Cheng G, He P, Fang Y (2007) Biosens Bioelectron 23(3):341–347
86. Li W, Nie Z, Xu X, Shen Q, Deng C, Chen J, Yao S (2009) Talanta 78(3):954–958
87. Deng C, Chen J, Nie L, Nie Z, Yao S (2009) Anal Chem 81(24):9972–9978
88. Zheng J, Cheng GF, He PG, Fang YZ (2010) Talanta 80(5):1868–1872
89. Li X, Liu J, Zhang S (2010) Chem Commun (Camb) 46(4):595–597
90. Chai Y, Tian D, Cui H (2012) Anal Chim Acta 715:86–92
91. Wang JL, Zhou HS (2008) Anal Chem 80(18):7174–7178
92. Chen Q, Tang W, Wang D, Wu X, Li N, Liu F (2010) Biosens Bioelectron 26(2):575–579
93. Zhou D (2012) Biochem Soc Trans 40(4):635–639
94. Levy M, Cater SF, Ellington AD (2005) ChemBioChem 6(12):2163–2166
95. Zhang CY, Johnson LW (2009) Anal Chem 81(8):3051–3055
96. Chi CW, Lao YH, Li YS, Chen LC (2011) Biosens Bioelectron 26(7):3346–3352
97. Kim GI, Kim KW, Oh MK, Sung YM (2009) Nanotechnology 20(17):175503
98. Chen Z, Li G, Zhang L, Jiang J, Li Z, Peng Z, Deng L (2008) Anal Bioanal Chem 392(6):1185–1188
99. Bogomolova A, Aldissi M (2011) Biosens Bioelectron 26(10):4099–4103
100. Zhou ZM, Yu Y, Zhao YD (2012) Analyst 137(18):4262–4266
101. Zhang H, Jiang B, Xiang Y, Zhang Y, Chai Y, Yuan R (2011) Anal Chim Acta 688(2):99–103
102. Liu J, Lee JH, Lu Y (2007) Anal Chem 79(11):4120–4125
103. Bamrungsap S, Chen T, Shukoor MI, Chen Z, Sefah K, Chen Y, Tan W (2012) ACS Nano 6(5):3974–3981
104. Bamrungsap S, Shukoor MI, Chen T, Sefah K, Tan W (2011) Anal Chem 83(20):7795–7799
105. Wang JL, Munir A, Zhu ZZ, Zhou HS (2010) Anal Chem 82(16):6782–6789
106. Babu E, Mareeswaran PM, Rajagopal S (online first, doi:10.1007/s10895-012-1127-0) J Fluoresc
107. Cai L, Chen ZZ, Dong XM, Tang HW, Pang DW (2011) Biosens Bioelectron 29(1):46–52
108. Wang Y, Liu B (2009) Langmuir 25(21):12787–12793
109. Wang Y, Liu B (2008) Nanotechnology 19(41):415605
110. Liang G, Cai S, Zhang P, Peng Y, Chen H, Zhang S, Kong J (2011) Anal Chim Acta 689(2):243–249
111. Yigit MV, Mazumdar D, Lu Y (2008) Bioconjug Chem 19(2):412–417
112. Wu S, Duan N, Wang Z, Wang H (2011) Analyst 136(11):2306–2314

113. Kim SE, Ahn KY, Park JS, Kim KR, Lee KE, Han SS, Lee J (2011) Anal Chem 83(15):5834–5843
114. Chang M, Yang CS, Huang DM (2011) ACS Nano 5(8):6156–6163
115. Giljohann DA, Seferos DS, Patel PC, Millstone JE, Rosi NL, Mirkin CA (2007) Nano Lett 7(12):3818–3821
116. Zheng D, Seferos DS, Giljohann DA, Patel PC, Mirkin CA (2009) Nano Lett 9(9):3258–3261
117. Chen X, Estevez MC, Zhu Z, Huang YF, Chen Y, Wang L, Tan W (2009) Anal Chem 81(16):7009–7014
118. Chen LQ, Xiao SJ, Peng L, Wu T, Ling J, Li YF, Huang CZ (2010) J Phys Chem B 114(10):3655–3659
119. Duan N, Wu S, Zhu C, Ma X, Wang Z, Yu Y, Jiang Y (2012) Anal Chim Acta 723:1–6
120. Ikanovic M, Rudzinski WE, Bruno JG, Allman A, Carrillo MP, Dwarakanath S, Bhahdigadi S, Rao P, Kiel JL, Andrews CJ (2007) J Fluoresc 17(2):193–199
121. Bruno JG, Phillips T, Carrillo MP, Crowell R (2009) J Fluoresc 19(3):427–435
122. Wang AZ, Bagalkot V, Vasilliou CC, Gu F, Alexis F, Zhang L, Shaikh M, Yuet K, Cima MJ, Langer R, Kantoff PW, Bander NH, Jon S, Farokhzad OC (2008) ChemMedChem 3(9):1311–1315
123. Chen XC, Deng YL, Lin Y, Pang DW, Qing H, Qu F, Xie HY (2008) Nanotechnology 19(23):235105
124. Cheng AK, Su H, Wang YA, Yu HZ (2009) Anal Chem 81(15):6130–6139
125. Deng T, Li J, Zhang LL, Jiang JH, Chen JN, Shen GL, Yu RQ (2010) Biosens Bioelectron 25(7):1587–1591
126. Cui ZQ, Ren Q, Wei HP, Chen Z, Deng JY, Zhang ZP, Zhang XE (2011) Nanoscale 3(6):2454–2457
127. Xiao Z, Farokhzad OC (2012) ACS Nano 6(5):3670–3676
128. Farokhzad OC, Karp JM, Langer R (2006) Expert Opin Drug Deliv 3(3):311–324
129. Aravind A, Jeyamohan P, Nair R, Veeranarayanan S, Nagaoka Y, Yoshida Y, Maekawa T, Kumar DS (2012) Biotechnol Bioeng 109(11):2920–2931
130. Bagalkot V, Zhang L, Levy-Nissenbaum E, Jon S, Kantoff PW, Langer R, Farokhzad OC (2007) Nano Lett 7(10):3065–3070
131. Bagalkot V, Gao X (2011) ACS Nano 5(10):8131–8139
132. Yezhelyev MV, Qi L, O'Regan RM, Nie S, Gao X (2008) J Am Chem Soc 130(28):9006–9012
133. Gao L, Cui Y, He Q, Yang Y, Fei J, Li J (2011) Chemistry 17(47):13170–13174
134. He X, Hai L, Su J, Wang K, Wu X (2011) Nanoscale 3(7):2936–2942
135. He X, Zhao Y, He D, Wang K, Xu F, Tang J (2012) Langmuir 28(35):12909–12915
136. Nair BG, Nagaoka Y, Morimoto H, Yoshida Y, Maekawa T, Kumar DS (2010) Nanotechnology 21(45):455102
137. Farokhzad OC, Cheng J, Teply BA, Sherifi I, Jon S, Kantoff PW, Richie JP, Langer R (2006) Proc Natl Acad Sci U S A 103(16):6315–6320
138. Zhang L, Radovic-Moreno AF, Alexis F, Gu FX, Basto PA, Bagalkot V, Jon S, Langer RS, Farokhzad OC (2007) ChemMedChem 2(9):1268–1271
139. Dhar S, Gu FX, Langer R, Farokhzad OC, Lippard SJ (2008) Proc Natl Acad Sci U S A 105(45):17356–17361
140. Gao H, Qian J, Yang Z, Pang Z, Xi Z, Cao S, Wang Y, Pan S, Zhang S, Wang W, Jiang X, Zhang Q (2012) Biomaterials 33(26):6264–6272
141. Farokhzad OC, Jon S, Khademhosseini A, Tran TN, Lavan DA, Langer R (2004) Cancer Res 64(21):7668–7672
142. Wu YR, Sefah K, Liu HP, Wang RW, Tan WH (2010) Proc Natl Acad Sci USA 107(1):5–10
143. Zhou J, Shu Y, Guo P, Smith DD, Rossi JJ (2011) Methods 54(2):284–294

Adv Biochem Eng Biotechnol (2014) 140: 155–181
DOI: 10.1007/10_2013_229

Published Online: 6 August 2013

Electrochemical Aptasensors for Microbial and Viral Pathogens

Mahmoud Labib and Maxim V. Berezovski

Abstract Aptamers are DNA and RNA oligonucleotides that can bind to a variety of nonnucleic acid targets with high affinity and specificity. Pathogen detection is a promising area in aptamer research. One of its major advantages is the ability of the aptamers to target and specifically differentiate microbial and viral strains without previous knowledge of the membrane-associated antigenic determinants or molecular biomarkers present in that particular microorganism. Electrochemical sensors emerged as a promising field in the area of aptamer research and pathogen detection. An electrochemical sensor is a device that combines a recognition element and an electrochemical transduction unit, where aptamers represent the latest addition to the large catalog of recognition elements. This chapter summarizes and evaluates recent developments of electrochemical aptamer-based sensors for microbial and viral pathogen detection, viability assessment of microorganisms, bacterial typing, identification of epitope-specific aptamers, affinity measurement between aptamers and their respective targets, and estimation of the degree of aptamer protection of oncolytic viruses for therapeutic purposes.

Keywords Affinity · Aptamers · Aptasensor · Bacteria · Electrochemical · Epitope · Oncolytic viruses · Pathogen · Viability

Contents

M. Labib · M. V. Berezovski (✉)
Department of Chemistry, University of Ottawa, 10 Marie Curie,
Ottawa ON K1N 6N5, Canada
e-mail: Maxim.Berezovski@uottawa.ca

1 Introduction

Pathogen surveillance is critical to the diagnosis, control, and prevention of infectious diseases. Common diagnostic and surveillance methods include culture-based tests, biochemical assays, antibody-based methods including agglutination and enzyme-linked assays, and molecular methods [1]. These techniques are either time-consuming or require sophisticated equipment and highly trained personnel, hence increasing the analysis cost. Therefore, there is a continued need for point-of-care assays that are simple, reliable, user-friendly, rapid, sensitive, and economical [2]. According to Lazcka et al. biosensor technology is the fastest growing area in rapid pathogen detection [3]. The commonly used biological recognition elements in biosensor platforms are whole cells [4], receptors [5], antibodies [6, 7], proteins [8–10], peptides [11–15], histones [16], molecularly imprinted polymers [17], and nucleic acid probes [18, 19]. Aptamers are specific nucleic acid sequences that can bind to a wide range of targets with high affinity and specificity [20, 21]. This group of synthetic nucleic acid molecules can be generated in vitro against virtually any target analyte. The affinity of aptamers to their targets is comparable to, or even higher, than most monoclonal antibodies. Typical dissociation constants for aptamer-target complexes are found in the picomolar to low micromolar range [22]. Aptamers possess key advantages over antibodies, including lower cost and less batch-to-batch variation. Furthermore, toxins and molecules that are poisonous or do not elicit any good immune response can be used to generate high affinity aptamers [23]. Besides the advantages discussed above, aptamers can undergo conformational changes and become reusable, allowing some of the aptasensor platforms to become recyclable. Also, aptamers have long shelf-lives and thus can be used to coat devices for point-of-care applications for which these devices could potentially be reused after heating due to the thermal stability of aptamers. In addition, aptamers can be chemically modified and incorporated into a variety of simple assays for pathogen detection, including flow cytometry, cell imaging, and aptasensors. The global market for aptamers is expected to expand rapidly in the near future. BCC Research estimates that the market was $10 million in 2009 and it will grow to $1.9 billion in 2014 [24]. Aptamer therapeutic markets were valued at $10 million in 2009 and should increase at a 55 % compound annual growth rate to $1.2 billion in 2014. Aptamer

diagnostic markets were worth $26 million in 2010 and are expected to increase in value to $659 million in 2014, a compound annual growth rate of 124 %.

This chapter summarizes and evaluates recent developments in electrochemical aptasensors for microbial and viral pathogens detection, viability assessment of microorganisms, bacterial typing, identification of epitope-specific aptamers, affinity measurement between aptamers and their respective targets, and estimation of the degree of aptamer protection of oncolytic viruses for therapeutic purposes. One of the main advantages of electrochemical aptasensors is that the sensitivity can be enhanced by attaching biocatalytic labels to the aptamer-target complexes to amplify the signal. Furthermore, electrochemical aptasensors are more convenient for on-field applications because they do not require expensive optical instruments. Additionally, it is possible to use label-free and reusable detection systems [25].

2 Aptasensors for Microbial and Viral Pathogen Detection

In this section, we focus on electrochemical aptasensors developed for the detection of pathogens and comprising aptamers specific to whole bacterial cells, bacterial toxins, whole viral cells, and viral nucleic acids.

2.1 Detection of Whole Bacterial Cells

In 2008, Crespo and his coworkers showed that single-walled carbon nanotubes (SWCNTs) can act as efficient ion-to-electron transducers in potentiometric assays [26]. The notable charge-transfer capability between the heterogeneous phases of SWCNTs [27] together with their remarkable double-layer capacitance [28] might explain their transducing behavior. Moreover, aptamers can self-assemble on carbon nanotubes by π–π stacking interactions between the puric and pyrimidic bases and the carbon nanotube walls [29], thus forming a hybrid material that can be applied in the development of aptasensors [30]. In this context, So et al. reported on aptamer-functionalized single-walled carbon nanotube field-effect transistor (SWCNTs-FET) arrays as a screening tool for *Escherichia coli* [31]. Notably, *E. coli* is the bacterium inhabiting the lower intestine of warm-blooded animals, and the level of *E. coli* provides an indicator of food and water pollution. Also, *E. coli* can cause intestinal and extraintestinal infections; some strains of the bacteria, such as *E. coli* (O157:H7), can be fatal [32]. The developed sensor was based on *E. coli*-specific RNA aptamers. The binding of the bacterium to the immobilized aptamers resulted in a more than 50 % decrease in conductance in less than 20 min. Furthermore, the SWCNTs-FET did not show a noticeable change in conductance when exposed to a high-density *Salmonella typhimurium* solution, indicating the high selectivity of the developed sensor.

In 2009, Zelada-Guillén et al. employed an RNA aptamer specific to IVB pili of *Salmonella typhi*, previously developed by Pan and coworkers [33], to develop a

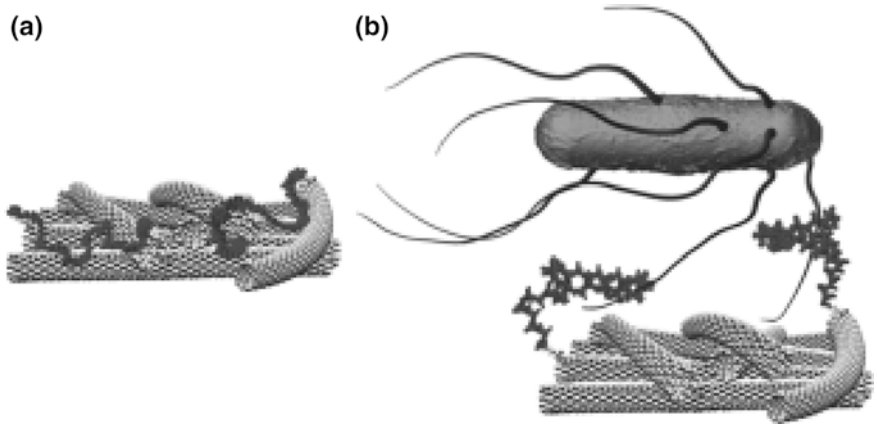

Fig. 1 **a** Possible conformations of the aptamers that are self-assembled on carbon nanotubes. **b** Schematic representation of the interaction between the target bacteria and the hybrid aptamer–SWCNT system. From Zelada-Guillen et al. [34], with permission

SWCNT-based potentiometric sensor for the detection of *S. typhi* [34], a major cause of many food poisoning cases worldwide [35]. The developed sensor was based on the well-known carbodiimide-mediated wet-chemistry approach to form amide bonds between the amine spacer of the synthetic aptamer and the carboxylic moieties on the sidewalls of the nanotubes [36], as shown in Fig. 1. The developed sensor allowed the detection of ultralow concentrations of the bacteria with a dynamic range of four logarithmic units (0.2–10^3 CFU mL^{-1}) in close to real time, thus making the detection of the pathogen as easy as measuring the pH value. Also, the sensor was easily regenerated by dissociating the bacteria from the immobilized aptamers in 2 M NaCl for 30 min. Furthermore, the most important strength of this aptasensor is that simple positive/negative tests can be carried out in real zero-tolerance conditions and without cross reaction with other bacteria.

Similarly, the same group reported on an SWCNT-based potentiometric aptasensor for detection of *E. coli* (CECT 675) [37] as a nonpathogenic surrogate for the pathogenic *E. coli* (O157:H7), the causative agent of a wide spectrum of human diseases ranging from some types for hemorrhagic and nonhemorrhagic diarrhea, kidney failure, hemolytic uremic syndrome, and death due to ingestion of contaminated food [38]. The developed sensor allowed the interrogation of the *E. coli* level in a couple of minutes and at concentrations as low as 6 CFU mL^{-1} in complex matrices as milk or 26 CFU mL^{-1} in apple juice and up to 10^4 CFU mL^{-1}. Also, the authors assessed the selectivity of the sensor against different microorganisms, including *Salmonella enterica*, *Lactobacillus casei*, and *E. coli* (CECT 4558), and they found that none of them gave a detectable potentiometric signal. Remarkably, the sensor can also be regenerated with 2 M NaCl for at least five regeneration cycles before the sensitivity and limit of detection are affected.

In 2012, the same group reported two SWCNT-based potentiometric sensors for the detection of *Staphylococcus aureus*, a Gram-positive pathogen that can cause a wide range of diseases, including several types of dermatitis, gastrointestinal tract infections, and endotoxin-related food poisoning worldwide [39]. Furthermore, the microorganism is also responsible for many other life-threatening infections such as pneumonia, septicemia, osteomyelitis, toxic shock syndrome, and about one third of endocarditis cases worldwide. The developed sensors were based on a tailored DNA aptamer that can recognize conserved epitopes on the surface of *S. aureus* [40]. These aptamers were attached to a homogenous layer of SWCNTs using two functionalization strategies, including a covalent and a noncovalent approach. The covalent approach consisted of attaching the aptamers to the nanotubes chemically by the amide bonds formed between the carboxylic groups of previously carboxylated SWCNTs and an amine moiety introduced at the 3′ end of the aptamer by the carbodiimide mediated chemistry [36]. The noncovalent approach was performed by direct adsorption onto the SWCNT side walls of pyrenil moieties previously introduced at the 3′ end of the aptamer. It is worth noting that the pyrenil groups strongly interact with the sidewalls of the nanotubes by π-stacking, and this property is commonly used to attach pyrenil-modified biomolecules to carbon nanotubes by drop casting [41]. Both of these approaches yielded functional biosensors but there were large differences in the minimum detectable bacteria concentration and sensitivity values. With covalent functionalization, the minimum concentration detected was 8×10^2 CFU mL^{-1} and the sensitivity was 0.36 mV/Decade. With the noncovalent approach, the sensitivity was higher (1.52 mV/Decade) but the minimum concentration detected was greatly affected (10^7 CFU mL^{-1}). In both cases, potential as a function of Decade of bacteria concentration was linear, as shown in Fig. 2.

Two reasons might explain the lower affinity of the biosensors prepared by noncovalent functionalization. First, an excess of Pyr-Aptamer molecules closely adsorbed during the drop casting procedure probably resulted in random molecular overlapping; therefore, the recognition of the target bacteria by the biosensor was compromised by self-entanglement of Pyr-Aptamer molecules, which could clearly reduce the availability of aptamers that are able to recognize their targets. A second possibility is the progressive leaching of the aptamer-bacteria complex, which was probably caused by an excessive accumulation of aptamers, which may have reduced the fixation strength of outer aptamer layers to the nanotube sidewalls by inner layers of more strongly adsorbed aptamers.

Electrochemical impedance spectroscopy (EIS) is one of the most powerful electrochemical techniques for directly probing the interfacial reaction mechanisms and monitoring the dynamics of biomolecular interactions. Also, EIS is widely used to characterize variations in the electronic properties of bulk materials, as well as for investigating surface and interfacial processes on electrodes. Compared to other electrochemical methods, EIS has a less destructive effect on the measured biological interactions because it is usually performed at a very narrow range of small potentials [42]. Recently, Labib and coworkers reported two impedimetric aptasensors for detection of *Salmonella enteritidis* [43] and

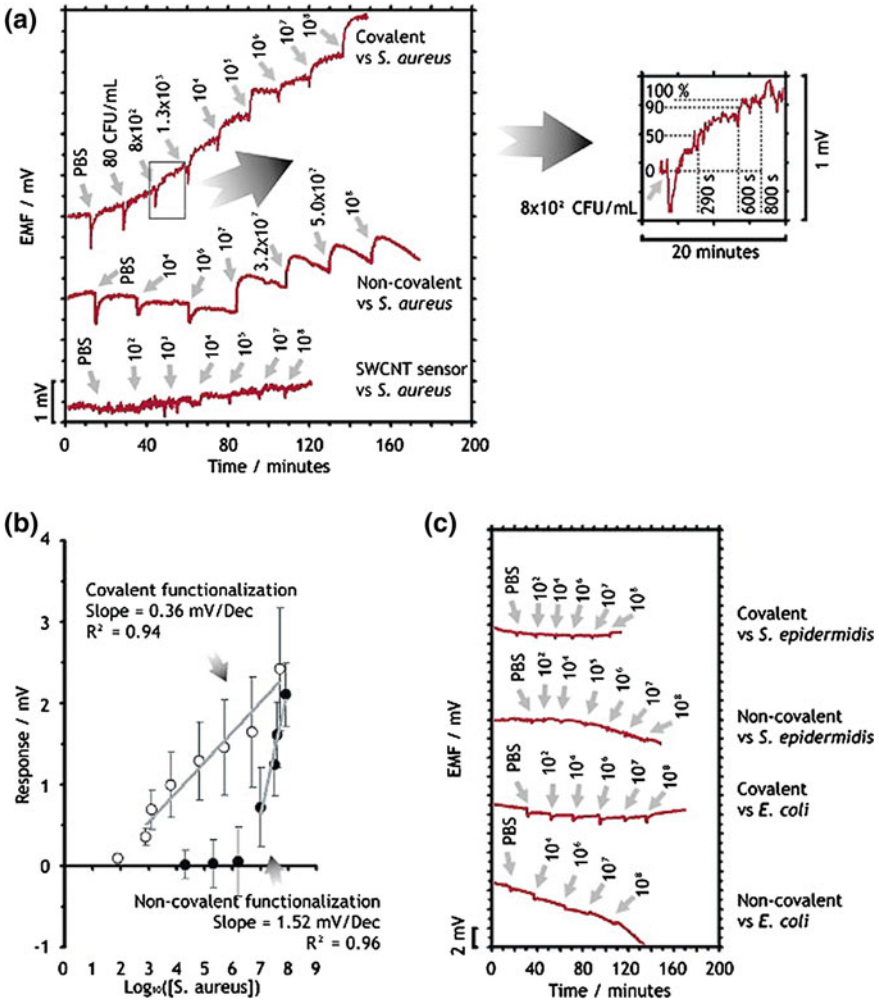

Fig. 2 Performance of biosensors prepared by covalent functionalization with NH_2-aptamer and noncovalent functionalization with Pyr-aptamer. **a** Change in Electromotive Force (EMF) recorded as a function of time for different biosensors when exposed to *S. aureus* (*right*, amplification of the curve after inoculation with 8×10^2 CFU mL^{-1}). **b** Potentiometric response as a function of concentration of bacteria in decade units (the *circles* represent the average responses of three different biosensors; *error bars* are standard deviations). **c** Change in EMF recorded as a function of time, when biosensors were exposed to stepwise increasing concentrations of different microorganisms (values are in CF mL^{-1}), *S. aureus*, *E. coli*, *S. epidermidis* and a SWCNTs-based sensor without aptamer to *S. aureus*. From Zelada-Guillen et al. [39], with permission

Salmonella typhimurium [44]. The developed sensors were based on the self-assembly of thiolated DNA aptamers onto gold nanoparticle-modified screen-printed carbon electrodes (GNPs-SPCEs). Remarkably, the developed sensors

exhibited high selectivity and allowed the detection of both bacterial species at levels down to 600 CFU mL^{-1} in 10 min.

2.2 Detection of Bacterial Toxins

Botulinum neurotoxin (*Bo*NT) is one of the most toxic substances known. Among the seven defined serotypes of *Bo*NT, A to G, type A represents the most frequent cause of human botulism [45]. In 2009, Wei and coworkers proposed an electrochemical aptasensor coupled with an enzymatic amplification step for detection of *Bo*NT type A toxoid [46]. A toxoid-specific DNA aptamer was dual-labeled with a reporting tag, fluorescein, and an anchoring tag, biotin. In the signal amplification step, an anti-fluorescein antibody conjugated with horseradish peroxidase (HRP) was introduced to bind to the fluorescein label on the aptamer. Subsequently, 3,3′,5,5′ tetramethylbenzidine (TMB/H_2O_2) was added for the signal readout under −200 mV. TMB acts as a mediator and is reduced at −200 mV; consequently, HRP reduces H_2O_2 to $2H_2O$. In the absence of the target, the aptamer remained in the closed conformation and prevented the anti-fluorescein-HRP from accessing the reporting tag and thus inhibited the signal amplification [47]. After binding of the toxoid, the aptamer conformation opened up and permitted access of the HRP reporter, generating an electrochemical current signal, as shown in Fig. 3. The developed sensor allowed the determination of as low as 40 pg mL^{-1} of the toxoid.

Ochratoxins are byproducts of several fungal species that can contaminate food and beverage and cause food poisoning. Ochratoxin A (OTA) is the most toxic serotype; it can cause hepatotoxicity, nephrotoxicity, and teratogenicity to a wide variety of mammalian species [48]. In 2010, Kuang and coworkers reported an electrochemical aptasensor for detection of OTA [49]. In the proposed technique, an OTA-specific DNA aptamer was immobilized on the surface of the electrode through base-pairing with an immobilized linker DNA (DNA 1), which is complementary to the lower part of the aptamer. Subsequently, a gold nanoparticle (GNP)-functionalized DNA sequence (DNA 2), complementary to the upper part of the aptamer, was hybridized with aptamer to amplify the sensing signal. Methylene blue was used as an electrochemical probe and its amount was proportional to the amount of DNA on the sensor surface. Upon binding between OTA and its specific aptamer, the aptamer was forced to dissociate from its complex with DNA 1 and DNA 2. Hence, the displacement of the aptamer from the surface of the electrode into the bulk solution brought about a significant reduction of methylene blue redox current, "signal-off," which was measured via cyclic voltammetry, as shown in Fig. 4. Importantly, using GNPs caused a nearly fivefold amplification of signal intensity, which greatly improved the sensitivity of the sensor, presumably due to enhancing the electron transfer between the redox mediator and the electrode. The developed sensor allowed a linear quantification of the level of OTA in the dynamic range of 0.1–20 ng mL^{-1} with an Limit of

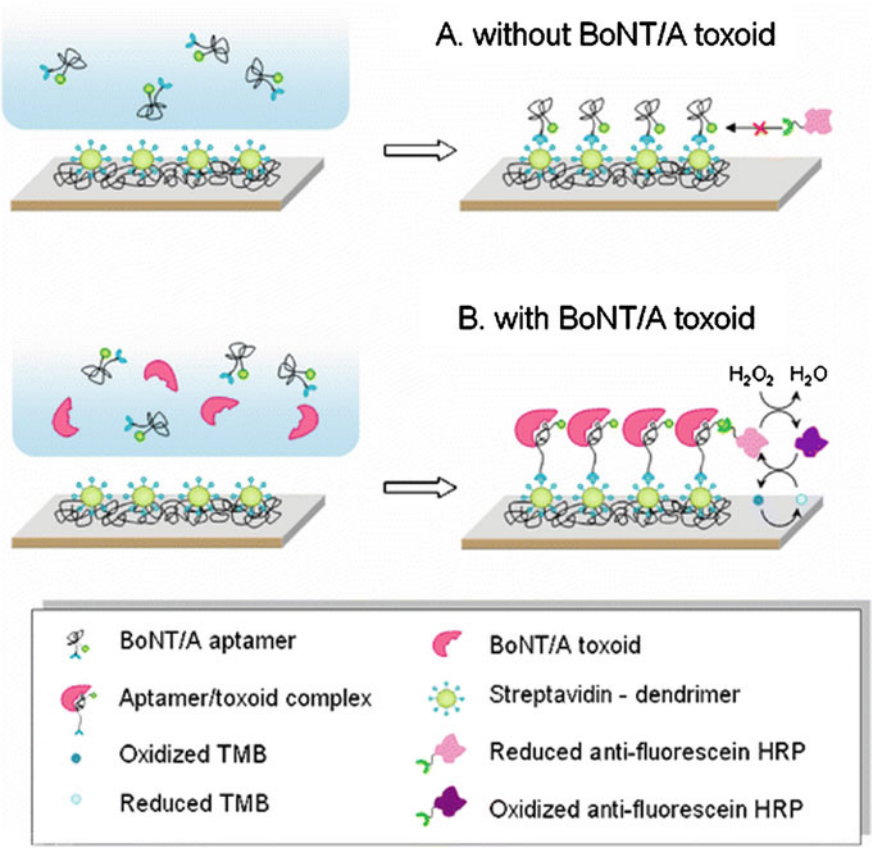

Fig. 3 Aptamer-based electrochemical detection of *Bo*NT/A toxoid. *BoNY* Botulinum neurotoxin, *HRP* horseradish peroxidase, *TMB* tetramethylbenzidine. From Wei and Ho [46], with permission

Detection (LOD) of 0.03 ng mL^{-1}, which is much lower than the acceptable safe OTA concentration of 10 ng mL^{-1}.

Microcystins are potent hepatotoxins produced by cyanobacteria. The health hazard of microcystin contamination prompted a World Health Organization (WHO) evaluation of the tolerable daily intake level of 0.01 μg/kg/day of microcystins [50]. This strict regulation called for rapid, sensitive, and reliable detection method for microcystins. In 2012, Ng and coworkers developed an electrochemical aptasensor for the detection of several microcystin congeners, including microcystin LR (MC-LR), MC-LA, and MC-YR [51]. In the proposed technique, microcystin-specific DNA aptamers were immobilized onto the electrode surface by self-assembly via thiol-chemistry and exposed to a solution containing the redox cations $[Ru(NH_3)_6]^{3+}$. In the absence of the target, the redox cations bound to the phosphate backbone of the immobilized aptamers gave a large

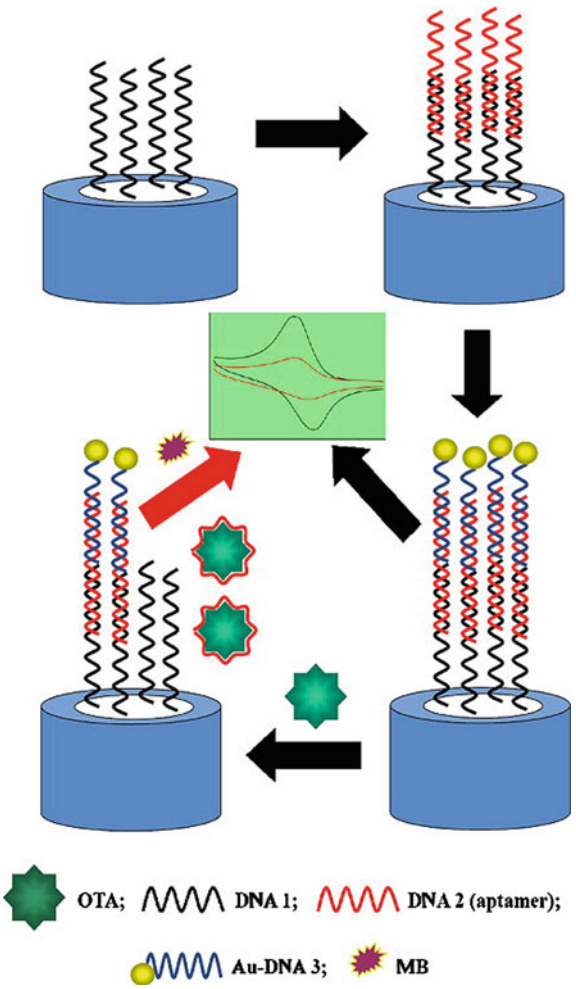

Fig. 4 The aptamer-based sensing mechanism of the ochratoxin A (OTA) using Methylene Blue (MB) as an electrochemical probe. From Kuang et al. [49], with permission

reduction peak measured via square wave voltammetry, as shown in Fig. 5. Introduction of microcystins caused a decrease in the voltammetric current within the dynamic range of 10 pM to 10 nM microcystin, with an LOD of 7.5–12.8 pM.

Endotoxin is the major component of the lipopolysaccharide outer membrane of gram-negative bacteria, which upon internalization into mammalian cells may trigger a fatal septic shock [52]. Recently, Kim and coworkers developed an electrochemical impedimetric aptasensor for detection of endotoxin [53]. The developed aptasensor was based on a thiol-modified endotoxin-specific DNA aptamer self-assembled onto a gold disc electrode. Binding of endotoxin to its respective aptamer brought about an increase in the resistance to charge transfer (R_{CT}) in the range of 0.01–1 ng mL^{-1}, as shown in Fig. 6. This range is comparable to the endotoxin detection range reported by the conventional Limulus amoebocyte lysate assay.

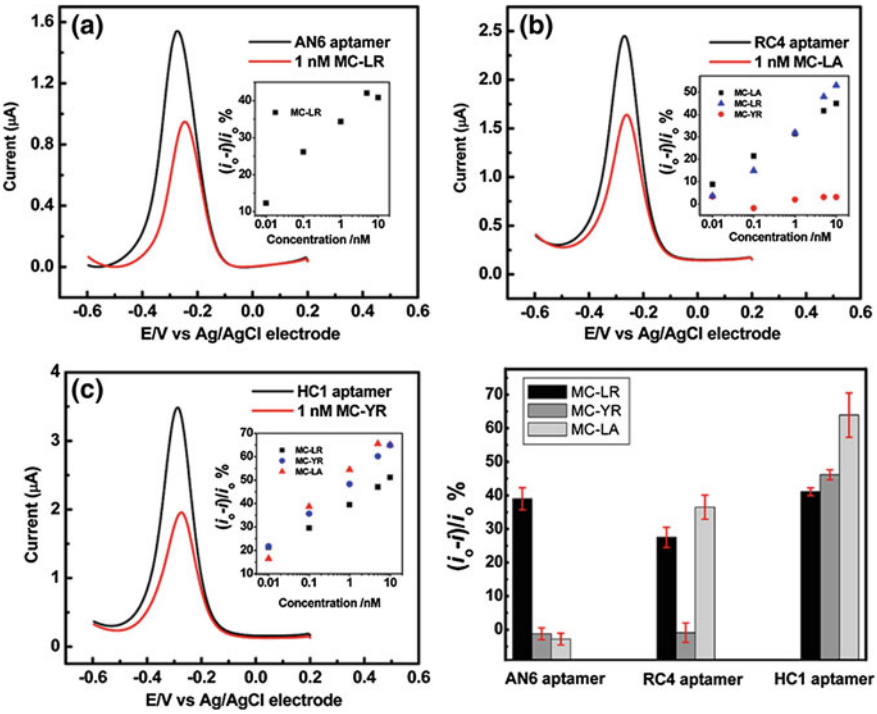

Fig. 5 Electrochemical detection of microcystin. Square Wave Voltammetry (SWV) of 5.0 μM $[Ru(NH_3)_6]^{3+}$ on AN6 aptamer (**a**), RC4 aptamer, (**b**), HC1 aptamer, (**c**), modified gold electrodes in 10 mM Tris buffer at pH 7.4 before (*black line*) and after (*red line*) incubation with 1 nM microcystin (MC)-LR, -LA, and -YR. **d** Percentage of electrochemical signal change showing congener selectivity of the aptasensor. The *inset* is the *calibration curves* based on the change of the % SWV peak current change versus the logarithm of the concentrations. From Ng et al. [51], with permission

2.3 Detection of Whole Viral Particles

Vaccinia virus (VACV), a member of the *Orthopoxvirus* genus of *Poxviridae* family, served as a live vaccine to eradicate smallpox, which is caused by another orthopoxvirus, variola virus, in a worldwide vaccination program organized by the WHO in the last century [54]. Recently, there has been a renewed interest in the use of VACV vaccine as a defense against the deliberate release of variola virus, as an act of bioterrorism [55]. This has led to the rebuilding of VACV vaccine stocks and created an urge for the development of rapid and sensitive methods for quantifying VACV. Recently, Labib and coworkers selected anti-VACV DNA aptamers and developed an electrochemical impedimetric aptasensor for VACV analysis. The developed sensor was based on the formation of a self-assembled monolayer of a hybrid of a thiolated DNA capture probe and the aptamers [19]. It was demonstrated that the interfacial resistance decreased linearly with increasing

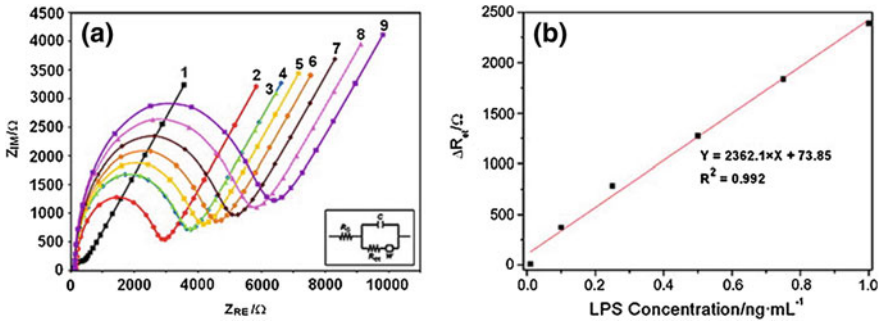

Fig. 6 **a** Nyquist plots for the gold electrode during modification (1–3: bare, aptamer deposition, 6-mercapto-1-hexanol (MCH) deposition and detection (4–9: 0.01, 0.1, 0.25, 0.5, 0.75, and 1 ng mL^{-1} of Lipopolysaccharide (LPS) processes and the equivalent circuit (*inner*) used to model electrochemical impedance spectroscopy data. **b** The linear relationship between ΔR_{et} and endotoxin concentration. From Kim et al. [53], with permission

the number of VACV particles, in the range from 500 to 3,000 plaque forming units (PFU) with an LOD of 330 PFU.

Vesicular stomatitis virus (VSV) is an arthropod-borne RNA virus that primarily affects rodents, cattle, swine, and horses but can also infect humans [56]. Based on the same sensing platform previously adopted for VACV analysis and using an anti-VSV DNA aptamer, the same group has developed an electrochemical impedimetric sensor for VSV analysis [57]. EIS was employed to quantitate VSV in the dynamic range of 800–2,200 PFU, with an LOD of 600 PFU.

2.4 Detection of Viral Nucleic Acid

Avian influenza virus (AIV) infections are the major cause of diseases ranging from asymptomatic infection to acute, fatal respiratory diseases in poultry. The virus is subtyped according to the antigenic type of the hemagglutinin (H) and neuraminidase (N). Unfortunately, AIV has crossed the species barrier recently and infected humans [58]. Through September 2009, 442 cases of AIV H5N1 infection of humans occurred and led to 262 deaths [59]. Driven by the severity of the disease, several electrochemical aptasensors were developed for the detection of AIV nucleic acid. The utilized aptamers can discriminate between target nucleic acids on the basis of subtle structural differences, such as the presence and absence of chemical groups [60] and the dimensional structure [61]. Therefore, they have two different modes of binding to target DNA sequences: (i) hybridization and (ii) preferred dimensional orientation. In 2008, Kukol and coworkers developed an electrochemical impedimetric aptasensor for detection of 30-nt DNA sequence obtained by reverse translation of an amino acid sequence that exists in highly pathogenic AIV [62]. The developed hybridization sensor was based on the self-

assembly of a thiolated complementary DNA probe onto a gold electrode surface. Incubation with the target DNA caused an increase in the interfacial resistance measured via EIS. Interestingly, the authors observed that the incubation of the sensor with shorter sequences (23-nt) brought about a higher detection signal than longer sequences (120-nt). This was ascribed to the space constraints on the sensor surface where non-hybridized stretches of the DNA sequence might have prevented the hybridization at neighboring probe molecules. Therefore, although longer nucleotides may confer greater specificity, shorter counterparts may give rise to greater sensitivity.

In 2009, Zhu and coworkers developed a novel electrochemical aptasensor based on the combination of multi-walled carbon nanotubes-cobalt phthalocyanine (MWCNTs-CoPc) nanocomposite and poly amidoamine (PAMAM) dendrimer on a glassy carbon electrode for detection of 21-nt DNA sequence characteristic to highly pathogenic AIV [63]. In the proposed technique, a complementary DNA probe was immobilized on the modified electrode by covalent coupling between the amino group of the PAMAM and the 5′-end phosphate group of the DNA probe. Differential pulse voltammetry (DPV) is a well-established electrochemical technique known for providing better peak resolution and current sensitivity. In addition, the charging current contribution to the background current, which is a limiting factor in analytical measurements, is negligible in the DPV mode [64]. In this work, DPV measurements revealed that increasing the target DNA concentration between 0.01 and 500 ng mL^{-1} caused a proportional decrease in the guanine oxidation signal.

In 2011, Liu and coworkers developed a sensitive electrochemical aptasensor for the detection of the AIV H5N1 gene sequence using a DNA aptamer immobilized onto a gold electrode modified with MWCNTs, polypyrrole nanowires (PPNWs), and gold nanoparticles (GNPs) [65]. The hybrid nanomaterials (MWCNTs/PPNWs/GNPs) provided a porous structure with a large effective surface area, highly electrocatalytic activities, and electronic conductivity. Recognition of the target DNA was performed using tris91,10-phenanthroline cobalt (III) percholrate as a redox indicator, which cannot bind to the single-stranded DNA aptamer before recognition. After recognition, the response signal was associated with the redox process involving the intercalation of the indicator into the formed double-stranded DNA hybrid. DPV measurements showed that the oxidation peak current of the indicator increased linearly with the target concentration within the dynamic range between 5×10^{-12} and 1×10^{-9} M, with an LOD of 4.3×10^{-13} M.

Lai and coworkers presented a miniaturized complementary metal oxide semiconductor (CMOS) sensor for nonfaradic impedimetric detection of AIV oligonucleotides [66]. The CMOS sensor impedimetric sensor is based on measuring the interface impedance changes using a potentiostatic step method where small potential steps were applied to the working electrode and the transient current responses, as determined by the time constant of the interface resistance and capacitance, were measured accordingly. In contrast to faradic EIS, nonfaradic impedance spectroscopy does not require the inclusion of any redox indicators.

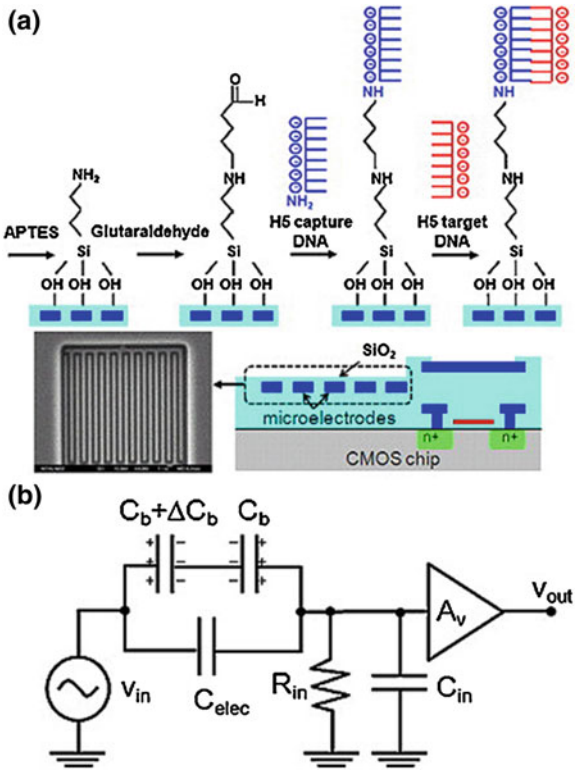

Fig. 7 **a** Surface modification and functionalization for impedimetric detection of avian influenza virus H5 DNA hybridization using complementary metal oxide semiconductor (CMOS) interdigitated microelectrodes. The scanning electron micrograph shows the top view of the electrodes. **b** The equivalent-circuit model for impedimetric detection. From Lai et al. [66], with permission

The associated impedance change is predominantly capacitive due to a dielectric thin film on the top of the interdigitated microelectrodes with the charge transfer resistance being omitted. Also, the small gap (<μm) between the interdigitated sensing electrodes was found to improve the sensing resolution by promoting signal coupling efficiency, as shown in Fig. 7. The developed CMOS sensor achieved a highly sensitive detection of AIV nucleotides, down to 6.1 fg mL^{-1}.

3 Aptasensors for Viability Assessment of Microorganisms

Conventional methods used to assess the viability of microorganisms (bacteria and viruses) involve the use of specific enrichment media to separate, identify, and count viable cells. For instance, the conventional bacteriological method used to assess the presence of pathogenic bacteria and to determine whether they are alive or dead is based on pre-enrichment in a nonselective media, followed by selective plating and subsequent biochemical and serological confirmation, which often takes 2–3 days for presumptive results and up to 7–10 days for confirmation [67]. This method is time-consuming, labor-intensive, and is not valid for detection of

viable but nonculturable (VBNC) bacteria. Similarly, the conventional cell-culture based method for viability assessment of viruses is the plaque-forming assay. A viral plaque is formed when a virus infects a cell within a fixed monolayer of cells. However, plaque formation may take 3–14 days, depending of the virus being analyzed. This section focuses on electrochemical aptasensors as a rapid and sensitive alternative to the previous conventional techniques for the viability assessment of bacteria and viruses.

3.1 Viability Assessment of Bacteria

In 2012, Labib et al. reported the first aptamer-based viability impedimetric sensor for bacteria (AptaVISens-B) that can distinguish between live and heat-killed *Salmonella typhimurium*, a major cause of many food poisoning cases worldwide [44]. The idea of the sensor is based on tailoring the selectivity of the aptamers by positive selection against live *S. typhimurium* cells, whereas the counter selection was performed against the heat-killed bacteria. Several rounds of selection were performed against the live target to increase the affinity and against the dead target to improve the selectivity. The developed sensor was based on the self-assembly of the thiol-modified live *S. typhimurium*-specific DNA aptamer onto a gold nanoparticle-modified screen-printed carbon electrode (GNPs-SPCE), as shown in Fig. 8. Interestingly, incubation of the heat-killed *S. typhimurium* with the developed sensor caused only a 13.8 % increase in the R_{CT} value, compared with 100 % obtained with live cells. In addition, incubation with proteinase K-digested cells caused only a 4.2 % increase in the R_{CT} value, which confirmed the high selectivity of the developed sensor.

3.2 Viability Assessment of Viruses

Recently, Labib and coworkers reported the first aptamer-based viability impedimetric sensor for viruses (AptaVISens-V) that can distinguish between live and heat-killed vaccinia virus [18]. Similar to the previously discussed AptaVISens-B, the idea of the sensor is based on tailoring the selectivity of the aptamers by performing several rounds of positive selection against viable intact vaccinia virus particles and counter-selection against the heat-killed virus particles. The selected DNA aptamer was thiolated and self-assembled onto a GNPs-SPCE. Subsequently, EIS measurement revealed that the incubation of the developed sensor with heat-killed vaccinia virus caused only a 13.8 % decrease in the R_{CT} value, in contrast with 100 % obtained with intact virus particles. In addition, incubation with proteinase-K digested virus brought about a negligible change in the interfacial resistance, which ensured the selectivity of the sensor, as shown in Fig. 9. Viability sensors are envisaged to open a new venue for the development of a variety

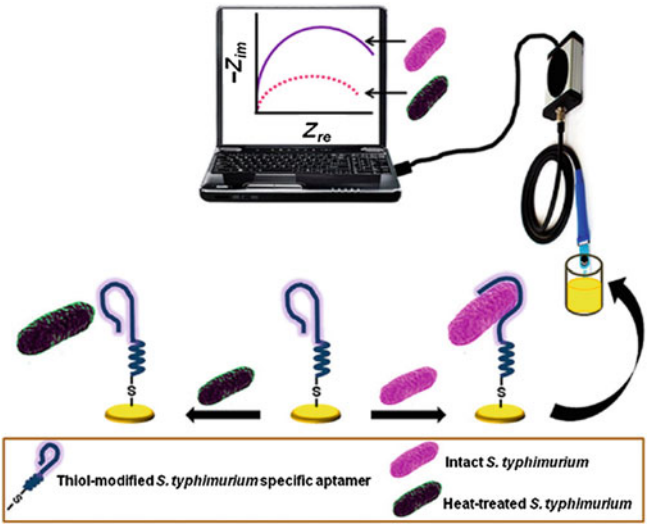

Fig. 8 Schematic diagram of the aptamer-mediated electrochemical detection of live *Salmonella typhimurium* bacteria. From Labib et al. [44], with permission

of sensors for viability assessment of many microorganisms and spores. This is particularly important in sterility tests and for validating the efficiency of sterilization.

4 Aptasensors for Bacterial Typing

Although serotyping using the Kauffman-White scheme represents the gold standard for serovar determination, it is not free from significant deficiencies including high cost, inability to serotype between 5 and 8 % of the isolates, and the long time (3 or more days) that is required for a highly trained technician to produce results [68]. In addition, genotyping methods require highly skilled personnel, sophisticated equipment, and centralized laboratories. Furthermore, both sero- and genotyping methods require a pre-enrichment step, which takes 2–3 days for presumptive results and 7–10 days for confirmation, thus adding to the time and complexity of these methods [69]. Recently, Labib and coworkers reported the first aptamer-based impedimetric sensor for typing of bacteria (AIST-B) [43]. The idea of the sensor is based on tailoring the selectivity of the aptamers by positive selection against live *Salmonella enteritidis* bacteria and counter selection against other related pathogens, including *Salmonella typhimurium*, *Escherichia coli*, *Staphylococcus aureus*, *Pseudomonas aeruginosa*, and *Citrobacter freundii*. The thiol-modified selected DNA aptamer was self-assembled onto GNPs-SPCE. EIS experiments showed that the incubation of the sensor with *S. typhimurium* caused

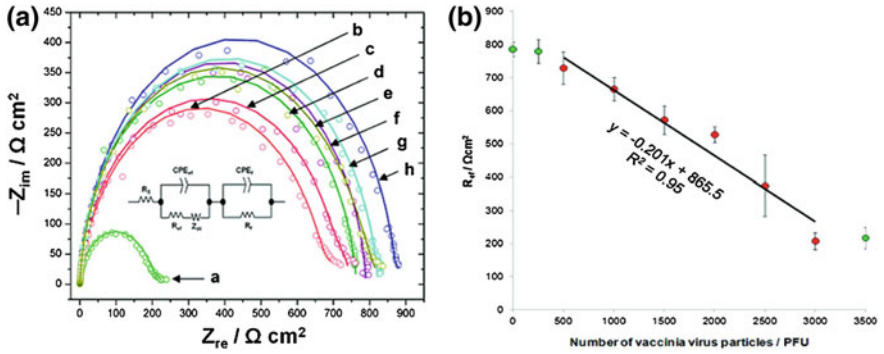

Fig. 9 **a** Nyquist plot (−Zim vs. Zre) of impedance spectra of the vaccinia virus (VACV) viability aptasensor obtained using (*a*) 60 PFU μL^{-1} (equivalent to 3,000 PFU) VACV, (*b*) heat-treated 60 PFU mL^{-1} VACV for 30 min at 90 °C, (*c*) 60 PFU μL^{-1} vesicular stomatitis virus (VSV), (*d*) buffer alone, (*e*) 20 mg mL^{-1}proteinase K alone, (*f*) 5.1 mg mL^{-1} Human Serum Albumin (HSA), (*g*) 60 PFU μL^{-1} VACV treated with 1.0 μL of 20 mg mL^{-1} proteinase K, and (*h*) 60 PFU μL^{-1} VACV using DNA library instead of the anti-VACV aptamer pool. The inset represents the circuit employed to fit to electrochemical impedance spectroscopy-measured data. The circuit consists of the ohmic resistance; R_S, of the electrolyte solution, electrolyte/film interface resistance R_{ef}, and capacity CPE_{ef}, film resistance R_f and capacity CPE_f, and the Warburg impedance, Z_w, resulting from diffusion of the redox probe. **b** Titration plot of R_{ef} *vs* number of VACV particles ranging from 0 to 3,500 PFU. From Labib et al. [18], with permission

26.2 % increase in the R_{CT} value, whereas incubation with *S. choleraesuis* caused an 18.1 % increase in the R_{CT} value, when compared with 100 % obtained with *S. enteritidis*. The developed sensor is envisaged to open a new venue for the development of a genus-specific array chip comprising highly specific aptamers for each species, to enable typing of a variety of pathogens. Although there is a long road ahead for establishing such a typing format, it is attainable considering the substantial efforts of many researchers to produce highly specific aptamers and the recent advances in selection technologies. Both trends are foreseen to produce species-specific aptamers with the same ease of analyzing the species genome.

5 Aptasensors for Identification of Epitope-Specific Aptamers

Although aptamers can be selected in vitro against purified target molecules, their applications to detect whole live cells can sometimes be limited because the binding sites of the cell-surface molecules differ from their isolated forms. Therefore, whole live cells have become common targets for aptamer selection. This is because aptamer selection using whole cells allows epitopes to be targeted in their native conformation on the cell surface. It also negates the need for target partitioning and complex purification steps.

In 2012, Labib et al. introduced a novel technology for electrochemical differentiation of epitope-specific aptamers (eDEA) using an electrochemical aptasensor without selecting aptamers against individual antigenic determinants [19]. In this work, the authors selected aptamers against VACV followed by cloning and sequencing of the selected aptamers. Next, electrochemical aptasensors were produced based on the formation of a self-assembled monolayer of a hybrid of a thiolated DNA capture probe and each of the selected anti-VACV aptamers onto gold microelectrodes. Subsequently, the interfacial resistance was recorded via EIS. Afterward, the developed sensors were incubated with VACV and the interfacial resistance at the biosensing interface were measured via EIS. It was observed that incubation with VACV caused a decrease in the interfacial resistance. It is noteworthy that the VACV membrane is associated with at least 19 different viral proteins [70]; among them, only six—L1R [71], A27L [72], D8L [73], H3L [74], A28 [75], and B5R [76]—are the targets of neutralizing antibodies.

All the developed aptasensors were then incubated with a high concentration of a monoclonal antibody specific to any of the VACV epitopes, such as the anti-L1R protein specific antibody, and EIS was measured again. Two situations were encountered, If the immobilized aptamer sequence was specific to L1R protein, then the added anti-L1R protein antibody at high concentration, relative to the small concentration of the aptamers immobilized onto the gold microelectrode surface, forced the virus to dissociate from its complex with the immobilized aptamer, causing a shift-back in the interfacial resistance. Hence, all the aptasensors that exhibited a shift-back in signal were sorted out and the involved aptamer sequences specific to L1R protein were registered. In the other situation, incubation with the antibody caused a further decrease in impedance, indicating that the immobilized aptamers were not specific to the target epitope, as shown in Fig. 10. Subsequently, these aptasensors were exposed to a monoclonal antibody specific to another VACV epitope. This technology is envisaged to open a new venue for the production of aptamers specific to target molecules in their native state and conformation. Hence, it surpasses the limitation of many conventional methods for the development of aptamers against recombinant proteins, which may not possess the native folding and post-translational modifications.

6 Aptasensors for Affinity Estimation Between Aptamers and Their Targets

Conventional methods for measuring the affinity of aptamers to proteins include dialysis [77], ultrafiltration [78], gel [79] and capillary electrophoresis [80], high-performance liquid chromatography [81], isothermal titration calorimetry [82], circular dichroism [83], surface Plasmon resonance [84], and flow cytometry [85]. However, there is an urge for simple, rapid, economic, and ultrasensitive techniques that are capable of distinguishing between the binding affinities of aptamers

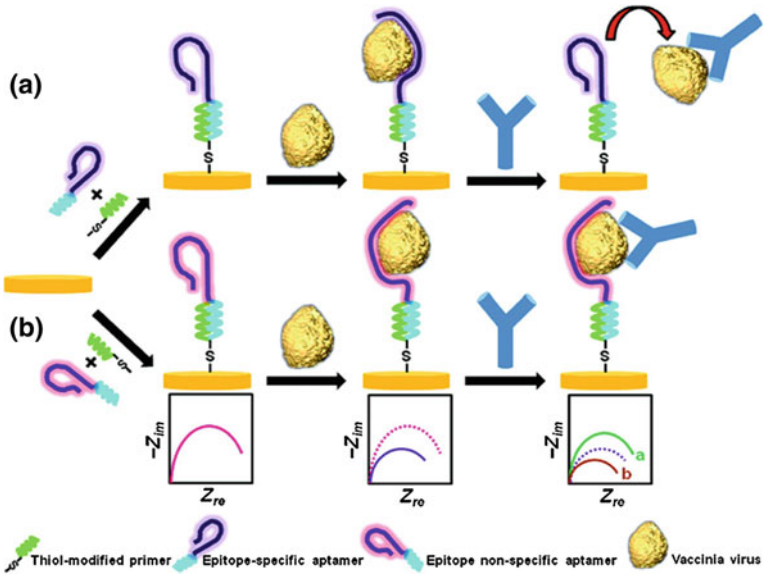

Fig. 10 Schematic diagram of the electrochemical differentiation of the epitope-specific aptamers (eDEA) technique. A thiolated DNA primer is hybridized with a complementary end of a vaccinia virus (VACV)-specific aptamer (either specific or nonspecific to a viral epitope). The hybrid is self-assembled onto a gold microelectrode surface. Binding of the virus to the immobilized aptamer causes a decrease in impedance, measured by electrochemical impedance spectroscopy. Introduction of epitope-specific anti-VACV neutralizing antibody could either **a** force the virus to dissociate from the virus–aptamer complex, causing a shift back in impedance in the case of an epitope-specific aptamer, or **b** bind to a vacant epitope on the surface of the virus, causing a further decrease in interfacial resistance if the aptamer is nonspecific to the epitope. According to the electrochemical data, all DNA aptamers can be categorized as either immunoshielding aptamers or analytical probes. From Labib et al. [19], with permission

to their targets, particularly between aptamers showing relatively close affinities to their target.

In 2012, Labib et al. reported two electrochemical aptasensors for measuring the affinity of the selected aptamers to vesicular stomatitis virus (VSV) [57] and VACV [19]. The idea is based on selecting aptamers from a native single-stranded DNA library that consists of a randomized region of nucleotides flanked by two constant hybridization sites. Afterward, a hybrid of thiolated DNA capture probe complementary to one hybridization site and the selected anti-virus aptamer itself was self-assembled onto a gold microelectrode. Subsequently, the developed sensor was titrated with several concentrations of the target virus and the dynamic range was determined using EIS. Next, a set of aptasensors were produced; each contained one of the selected aptamers hybridized with the universal capture probe and immobilized onto the electrode surface. Consequently, each aptasensor was incubated with a fixed concentration of virus particles that lies within the dynamic range to avoid saturation of the sensor surface. EIS was measured before and after

virus binding to guard against any possible variations in the baseline interfacial resistance values that might be caused by the different aptamers adopting different conformations on the electrode surface, thereby affecting the charge transfer through the formed film. Thus, the change in interfacial resistance after target binding can be used as an estimate for the affinity between the selected aptamer and its respective target. Interestingly, this method can be used for rapid screening of aptamers using an array chip and a rapid and sensitive electrochemical technique, such as SWV or DPV. In addition, this method is highly useful in the case of small targets for which conventional techniques such as flow cytometry may not be able to distinguish between aptamers exhibiting close affinities to their target.

7 Aptasensors for Estimation of the Degree of Aptamer Protection of Oncolytic Viruses

Oncolytic viruses (OVs) are promising therapeutics that selectively replicate in and kill tumor cells. However, repetitive administration of OVs provokes the generation of neutralizing antibodies (nAbs) that can diminish their anticancer effects. Although VSV has been extensively used as a laboratory tool for probing aspects of cellular physiology, it was only during the last decade that its potential as a cancer therapeutic has been appreciated. VSV replication in normal cells is usually thwarted by the innate immune response. Defects in antiviral innate immune responses in transformed cells, involving the interferon (IFN) system, play a prominent role in allowing VSV to robustly replicate and invoke cytolysis [86]. In this context, VSV proves to be superior to DNA viruses for oncolytic applications, for a variety of reasons. For example, VSV is a relatively innocuous virus that, even in its most virulent state, causes mild disease in ruminants and humans. Furthermore, VSV rapidly replicates to very high levels that it can effectively shut off host-mRNA export and take over the protein synthesis machinery of the transformed cell for its own specific use, within a few hours of infection.

Owing to its short generation time, VSV can be produced at very high titers in bioreactors or in well-characterized mammalian cell lines [87]. OVs administered intravenously can be particularly effective against metastatic cancers, which are difficult to treat using conventional therapy. However, OVs can be deactivated by nAbs and rapidly cleared from circulation. Thus, a prerequisite for a successful virotherapy is that the virus must gain access to the tumor cell; this requires an extended circulation time without depletion by nAbs. The current approaches to extend the circulation time exploit polymer-coating technologies with poly-[N-(2-hydroxypropyl) methacrylamide] (HPMA) [88] and polyethylene glycol (PEG) [89] or preinfected T cells as carriers for the delivery of OVs to tumor sites [90]. However, these methods suffer from many drawbacks, including the permanent polymer coating of the virus causing a loss of infectivity. The latter requires the

isolation of the patient's T cells and activation followed by back-infusion to the patient, which makes it impractical for clinical use. Development of aptamers specific for VSV seems promising in terms of changing the viral interaction with the immune system. In other words, protecting the VSV surface with specific nonimmunogenic aptamers could allow the virus to escape the host immune mechanism and neutralization by the circulating antibodies. This is only feasible if the aptamers can specifically bind to the vulnerable epitopes on the virus surface that are attacked by nAbs.

In 2012, Labib et al. developed a novel technology called aptamer-facilitated virus immunoshielding (AptaVISH) to protect oncolytic viruses from their respective nAbs [57]. In this work, several anti-VSV DNA aptamers were selected and an electrochemical impedimetric aptasensor was developed for measuring the degree of protection (DoP) imparted by each aptamer for the virus. The aptasensor is based on the formation of a self-assembled monolayer (SAM) of a thiolated DNA capture probe and an anti-VSV aptamer as a detection probe. An electrochemical displacement assay was performed to ensure that the selected aptamers can protect the virus and prevent its binding to nAbs, as shown in Fig. 11.

Each selected aptamer pool was immobilized onto an electrode and incubated with VSV. The electrode was then washed and incubated with a high concentration of an anti-VSV polyclonal antibody. It was observed that the addition of anti-VSV antibody caused a shift-back in impedance due to the reduction of the interfacial resistance. This could be ascribed to the binding of the antibody, at such a high concentration, to VSV with the subsequent dissociation of the virus from its complex with the immobilized aptamers. Thus, the ratio between the shift-back signal and the original signal observed after VSV coupling can thus be used to estimate the degree of protection (DoP) of VSV by the selected aptamers. This can be calculated from the formula DoP $= (R1_{ef} - R2_{ef})/R1_{ef}$ (%), where $R1_{ef}$ represents the change in in the electrolyte/film interfacial resistance $R1_{ef}$ after VSV coupling ($R1_{ef}$—baseline), whereas $R2_{ef}$ represents the change in $R2_{ef}$ after VSV dissociation from its complex with the immobilized aptamer by the added antibody ($R2_{ef}$—baseline). Importantly, the DoP value indicates the affinity of an aptamer to a virus, whereas its sign shows if the aptamer can protect the virus or not. Thus, a positive DoP indicates virus protection from nAb, whereas a negative DoP indicates noncompetitive binding of the aptamer to the virus.

Compared to VSV, VACV has a genome of approximately 190 kbp and can potentially express more than 200 proteins, allowing an exceptional degree of independence from the host [91]. VACV replication is associated with activation of the epidermal growth factor receptor (EGFR)-Ras signalling pathway, which is activated in most human cancers [92], indicating that the virus could be broadly applied in cancer therapy. Recently, Labib et al. developed a similar aptasensor for measuring the DoP imparted by DNA aptamers specific to VACV [19].

Development of aptamers specific to nAbs seems promising in terms of shielding nAbs with aptamers, allowing the virus to escape the host immune mechanism and following neutralization. This can be feasible if the aptamer is selected against the antigen-binding fragment (Fab) of nAbs [93]. Antibodies can

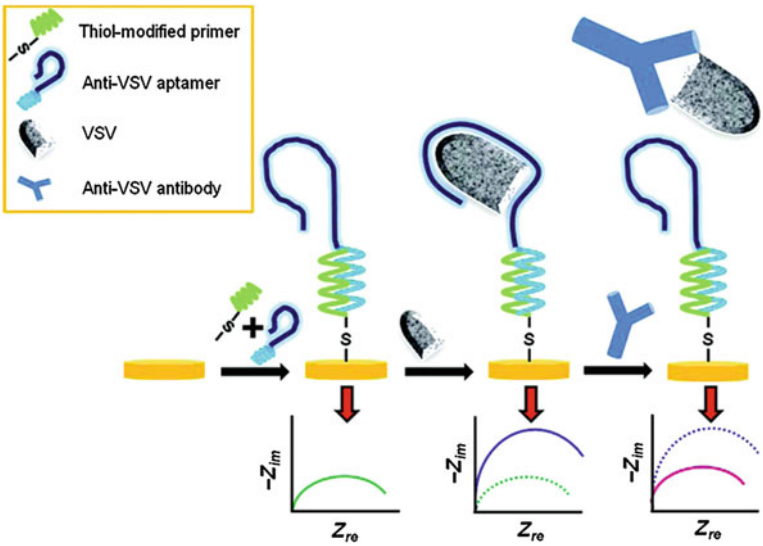

Fig. 11 Schematic diagram of an electrochemical sensor applied for the development of aptamer-facilitated virus immunoshielding (AptaVISH). A thiolated DNA primer is hybridized with the complementary end of vesicular stomatitis virus (VSV)-specific aptamer and the hybrid was self-assembled on a gold microelectrode surface. Binding of VSV to the immobilized aptamer causes an increase in impedance, whereas the introduction of the neutralizing anti-VSV antibody causes a shift-back in impedance. From Labib et al. [57], with permission

exist in two physical forms: a soluble form that is secreted from plasma B cells and a membrane-bound form that is attached to the surface of B cells, referred to as the B cell receptor [94]. Ideally, aptamers should bind to free antibodies, which mimic the soluble form of antibodies, and this binding can be tested using flow cytometry. On the other hand, aptamers should have a high affinity to immobilized antibodies or B-cell receptors. The latter can be tested using an immunosensor where nAbs are immobilized onto the gold electrode.

Recently, Muharemagic and coworkers developed an aptamer-mediated neutralizing antibodies shielding (AptaNAS) technology to enhance the survival of oncolytic viruses and efficiency of anticancer treatment [95]. An electrochemical immunosensor was developed to ensure that the selected aptamers can adequately shield the anti-VSV nAbs and thus can be further used to enhance VSV delivery into tumor cells. The developed biosensor was employed for screening of aptamers based on their degree of shielding (DoS) of the antibodies in order to find aptamer clones showing the highest shielding effect. The evaluation is based on measuring the impedimetric signal that resulted from the binding of VSV to aptamer-shielded immobilized nAbs when compared to the nonshielded counterpart, as shown in Fig. 12. Briefly, EIS was performed and the R_{CT} baseline value was determined after the immunosensor preparation (R_{CTb}), after aptamer binding (R_{CTa}), and after the virus capture (R_{CTv}). Correspondingly, the change of R_{CT} upon virus binding

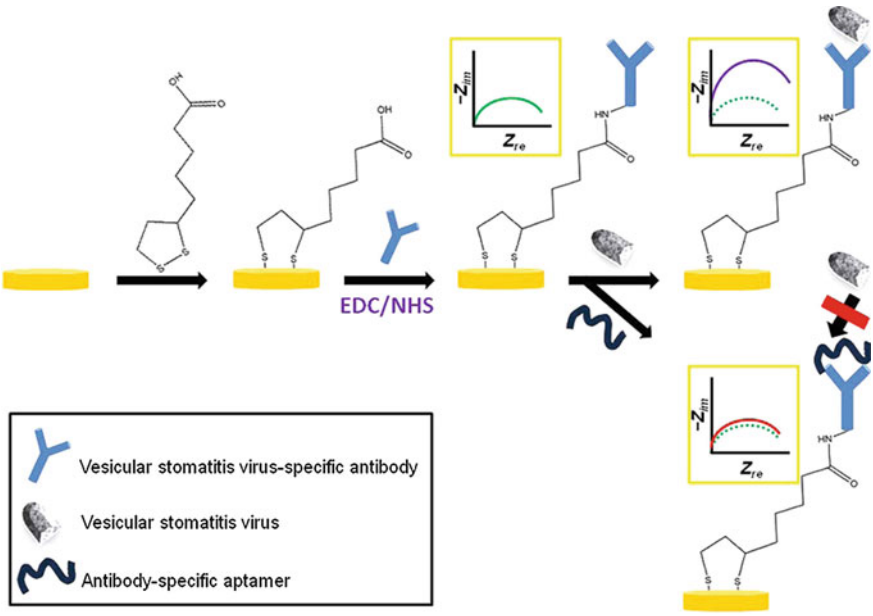

Fig. 12 Principle of aptamer-mediated neutralizing antibody shielding (AptaNAS). **a** Anti-vesicular stomatitis virus-neutralizing antibodies bind to the virus, which causes aggregation, blocks the attachment of the virus to the cell membrane, or prevents uncoating of the virus inside the cell. **b** With aptamers binding to the Fab fragment of antibodies, the virus is free to infect a cell. From Zhu et al. [95], with permission

(R_{CTv}) was calculated for each aptamer-shielded anti-VSV nAbs by subtracting R_{CTb} from R_{CTv}. The reference R_{CTv} value for the non-shielded anti-VSV nAbs was determined by incubating the immunosensor, without prior shielding, with VSV under the same incubation conditions. Hence, the DoS value can be calculated from the formula: DoS = (R_{CTv} for non-shielded nAbs − R_{CTv} for shielded nAbs)/R_{CTv} for non-shielded nAbs (%).

8 Forthcoming Challenges and Concluding Remarks

In this chapter, we described the current applications of electrochemical aptasensors specific for microbial and viral pathogens, starting from the classical detection application to the latest applications of viability assessment and estimation of the degree of aptamer protection of oncolytic viruses. Although aptamers are one of the most attractive recognition elements for integration into sensing devices, their potential application in complex matrices continues to be a major challenge for point-of-care systems. Therefore, complementary strategies involving nanomaterials have been the subject of intense study. We are presently

in the early days of the emerging technology of using aptamers and nanostructured materials to develop sensing devices. Nevertheless, it is foreseen that nanomaterial-based aptasensors will soon be used for the diagnosis and therapeutic follow-up of diseases.

References

1. Gerber MA, Shulman ST (2004) Rapid diagnosis of pharyngitis caused by group A streptococci. Clin Microbiol Rev 17(3):571–580 (table of contents)
2. Alocilja EC, Radke SM (2003) Market analysis of biosensors for food safety. Biosens Bioelectron 18(5–6):841–846
3. Lazcka O, Del Campo FJ, Munoz FX (2007) Pathogen detection: a perspective of traditional methods and biosensors. Biosens Bioelectron 22(7):1205–1217
4. Kostrzynska M, Leung KT, Lee H, Trevors JT (2002) Green fluorescent protein-based biosensor for detecting SOS-inducing activity of genotoxic compounds. J Microbiol Methods 48(1):43–51
5. Subrahmanyam S, Piletsky SA, Turner AP (2002) Application of natural receptors in sensors and assays. Anal Chem 74(16):3942–3951
6. Labib M, Hedström M, Amin M, Mattiasson B (2009a) A capacitive biosensor for detection of staphylococcal enterotoxin B. Anal Bioanal Chem 393(5):1539–1544
7. Labib M, Hedström M, Amin M, Mattiasson B (2009b) A capacitive immunosensor for detection of cholera toxin. Anal Chim Acta 634(2):255–261
8. Labib M, Hedström M, Amin M, Mattiasson B (2009c) A multipurpose capacitive biosensor for assay and quality control of human immunoglobulin G. Biotechnol Bioeng 104(2): 312–320
9. Labib M, Hedström M, Amin M, Mattiasson B (2010a) Competitive capacitive biosensing technique (CCBT): a novel technique for monitoring low molecular mass analytes using glucose assay as a model study. Anal Bioanal Chem 397(3):1217–1224
10. Labib M, Hedström M, Amin M, Mattiasson B (2010b) A novel competitive capacitive glucose biosensor based on concanavalin A-labeled nanogold colloids assembled on a polytyramine-modified gold electrode. Anal Chim Acta 659(1–2):194–200
11. Labib M, Martić S, Shipman PO, Kraatz HB (2011a) Electrochemical analysis of HIV-1 reverse transcriptase serum level: exploiting protein binding to a functionalized nanostructured surface. Talanta 85(1):770–778
12. Labib M, Shipman PO, Martić S, Kraatz H-B (2011b) A bioorganometallic approach for rapid electrochemical analysis of human immunodeficiency virus type-1 reverse transcriptase in serum. Electrochimica Acta 56(14):5122–5128
13. Labib M, Shipman PO, Martić S, Kraatz HB (2011c) Towards an early diagnosis of HIV infection: an electrochemical approach for detection of HIV-1 reverse transcriptase enzyme. Analyst 136(4):708–715
14. Martić S, Labib M, Kraatz HB (2011a) Electrochemical investigations of sarcoma-related protein kinase inhibition. Electrochimica Acta 56:10676–10682
15. Martić S, Labib M, Kraatz HB (2011b) On chip electrochemical detection of sarcoma protein kinase and HIV-1 reverse transcriptase. Talanta 85(5):2430–2436
16. Du X, Sasaki S, Nakamura H, Karube I (2001) The determination of DNA based on light-scattering of a complex formed with histone. Talanta 55(1):93–98
17. Uludag Y, Piletsky SA, Turner AP, Cooper MA (2007) Piezoelectric sensors based on molecular imprinted polymers for detection of low molecular mass analytes. FEBS J 274(21):5471–5480

18. Labib M, Zamay AS, Muharemagic D, Chechik AV, Bell JC, Berezovski MV (2012a) Aptamer-based viability impedimetric sensor for viruses. Anal Chem 84(4):1813–1816
19. Labib M, Zamay AS, Muharemagic D, Chechik AV, Bell JC, Berezovski MV (2012b) Electrochemical differentiation of epitope-specific aptamers. Anal Chem 84(5):2548–2556
20. Berezovski M, Musheev M, Drabovich A, Krylov SN (2006) Non-SELEX selection of aptamers. J Am Chem Soc 128(5):1410–1411
21. Berezovski MV, Lechmann M, Musheev MU, Mak TW, Krylov SN (2008) Aptamer-facilitated biomarker discovery (AptaBiD). J Am Chem Soc 130(28):9137–9143
22. White RR, Sullenger BA, Rusconi CP (2000) Developing aptamers into therapeutics. J Clin Invest 106(8):929–934
23. Proske D, Blank M, Buhmann R, Resch A (2005) Aptamers–basic research, drug development, and clinical applications. Appl Microbiol Biotechnol 69(4):367–374
24. BCC-Research (2010) Nucleic acid aptamers for diagnostics and therapeutics: global markets. BCC Research, Wellesley, MA
25. Lee JO, So HM, Jeon EK, Chang H, Won K, Kim YH (2008) Aptamers as molecular recognition elements for electrical nanobiosensors. Anal Bioanal Chem 390(4):1023–1032
26. Crespo GA, Macho S, Rius FX (2008) Ion-selective electrodes using carbon nanotubes as ion-to-electron transducers. Anal Chem 80(4):1316–1322
27. Dai H (2002) Carbon nanotubes: synthesis, integration, and properties. Acc Chem Res 35(12):1035–1044
28. Crespo GA, Macho S, Bobacka J, Rius FX (2009) Transduction mechanism of carbon nanotubes in solid-contact ion-selective electrodes. Anal Chem 81(2):676–681
29. Zheng M, Jagota A, Strano MS, Santos AP, Barone P, Chou SG, Diner BA, Dresselhaus MS, McLean RS, Onoa GB, Samsonidze GG, Semke ED, Usrey M, Walls DJ (2003) Structure-based carbon nanotube sorting by sequence-dependent DNA assembly. Science 302(5650):1545–1548
30. Star A, Tu E, Niemann J, Gabriel JC, Joiner CS, Valcke C (2006) Label-free detection of DNA hybridization using carbon nanotube network field-effect transistors. Proc Natl Acad Sci USA 103(4):921–926
31. So HM, Park DW, Jeon EK, Kim YH, Kim BS, Lee CK, Choi SY, Kim SC, Chang H, Lee JO (2008) Detection and titer estimation of Escherichia coli using aptamer-functionalized single-walled carbon-nanotube field-effect transistors. Small 4(2):197–201
32. Rahal EA, Kazzi N, Nassar FJ, Matar GM (2012) Escherichia coli O157: H7-Clinical aspects and novel treatment approaches. Front Cell Infect Microbiol 2:138
33. Pan Q, Zhang XL, Wu HY, He PW, Wang F, Zhang MS, Hu JM, Xia B, Wu J (2005) Aptamers that preferentially bind type IVB pili and inhibit human monocytic-cell invasion by *Salmonella enterica* serovar typhi. Antimicrob Agents Chemother 49(10):4052–4060
34. Zelada-Guillen GA, Riu J, Duzgun A, Rius FX (2009) Immediate detection of living bacteria at ultralow concentrations using a carbon nanotube based potentiometric aptasensor. Angew Chem Int Ed Engl 48(40):7334–7337
35. Chiu CH, Tang P, Chu C, Hu S, Bao Q, Yu J, Chou YY, Wang HS, Lee YS (2005) The genome sequence of *Salmonella enterica* serovar Choleraesuis, a highly invasive and resistant zoonotic pathogen. Nucleic Acids Res 33(5):1690–1698
36. Wong SS, Joselevich E, Woolley AT, Cheung CL, Lieber CM (1998) Covalently functionalized nanotubes as nanometre-sized probes in chemistry and biology. Nature 394(6688):52–55
37. Zelada-Guillen GA, Bhosale SV, Riu J, Rius FX (2010) Real-time potentiometric detection of bacteria in complex samples. Anal Chem 82(22):9254–9260
38. Decludt B, Bouvet P, Mariani-Kurkdjian P, Grimont F, Grimont PA, Hubert B, Loirat C (2000) Haemolytic uraemic syndrome and Shiga toxin-producing *Escherichia coli* infection in children in France. The Societe de Nephrologie Pediatrique. Epidemiol Infect 124(2):215–220

39. Zelada-Guillen GA, Sebastian-Avila JL, Blondeau P, Riu J, Rius FX (2012) Label-free detection of Staphylococcus aureus in skin using real-time potentiometric biosensors based on carbon nanotubes and aptamers. Biosens Bioelectron 31(1):226–232
40. Cao X, Li S, Chen L, Ding H, Xu H, Huang Y, Li J, Liu N, Cao W, Zhu Y, Shen B, Shao N (2009) Combining use of a panel of ssDNA aptamers in the detection of Staphylococcus aureus. Nucleic Acids Res 37(14):4621–4628
41. Chen RJ, Zhang Y, Wang D, Dai H (2001) Noncovalent sidewall functionalization of single-walled carbon nanotubes for protein immobilization. J Am Chem Soc 123(16):3838–3839
42. Bogomolova A, Komarova E, Reber K, Gerasimov T, Yavuz O, Bhatt S, Aldissi M (2009) Challenges of electrochemical impedance spectroscopy in protein biosensing. Anal Chem 81(10):3944–3949
43. Labib M, Zamay AS, Kolovskaya OS, Reshetneva IT, Zamay GS, Kibbee RJ, Sattar SA, Zamay TN, Berezovski MV (2012c) Aptamer-based impedimetric sensor for bacterial typing. Anal Chem 84(19):8114–8117
44. Labib M, Zamay AS, Kolovskaya OS, Reshetneva IT, Zamay GS, Kibbee RJ, Sattar SA, Zamay TN, Berezovski MV (2012d) Aptamer-based viability impedimetric sensor for bacteria. Anal Chem 84(21):8966–8969
45. Arnon SS, Schechter R, Inglesby TV, Henderson DA, Bartlett JG, Ascher MS, Eitzen E, Fine AD, Hauer J, Layton M, Lillibridge S, Osterholm MT, O'Toole T, Parker G, Perl TM, Russell PK, Swerdlow DL, Tonat K (2001) Botulinum toxin as a biological weapon: medical and public health management. JAMA 285(8):1059–1070
46. Wei F, Ho CM (2009) Aptamer-based electrochemical biosensor for Botulinum neurotoxin. Anal Bioanal Chem 393(8):1943–1948
47. Wei F, Wang J, Liao W, Zimmermann BG, Wong DT, Ho CM (2008) Electrochemical detection of low-copy number salivary RNA based on specific signal amplification with a hairpin probe. Nucleic Acids Res 36(11):e65
48. Breitholtz A, Olsen M, Dahlback A, Hult K (1991) Plasma ochratoxin A levels in three Swedish populations surveyed using an ion-pair HPLC technique. Food Addit Contam 8(2):183–192
49. Kuang H, Chen W, Xu D, Xu L, Zhu Y, Liu L, Chu H, Peng C, Xu C, Zhu S (2010) Fabricated aptamer-based electrochemical "signal-off" sensor of ochratoxin A. Biosens Bioelectron 26(2):710–716
50. Pearson L, Mihali T, Moffitt M, Kellmann R, Neilan B (2010) On the chemistry, toxicology and genetics of the cyanobacterial toxins, microcystin, nodularin, saxitoxin and cylindrospermopsin. Mar Drugs 8(5):1650–1680
51. Ng A, Chinnappan R, Eissa S, Liu H, Tlili C, Zourob M (2012) Selection, characterization, and biosensing application of high affinity congener-specific microcystin-targeting aptamers. Environ Sci Technol 46(19):10697–10703
52. Preston A, Mandrell RE, Gibson BW, Apicella MA (1996) The lipooligosaccharides of pathogenic gram-negative bacteria. Crit Rev Microbiol 22(3):139–180
53. Kim SE, Su W, Cho M, Lee Y, Choe WS (2012) Harnessing aptamers for electrochemical detection of endotoxin. Anal Biochem 424(1):12–20
54. Damon I (2007) Poxviridae and their replication. In: Fields BN, Knipe DM et al (eds) Fields virology. Raven Press Ltd., New York, pp 2079–2081
55. Whitley RJ (2003) Smallpox: a potential agent of bioterrorism. Antiviral Res 57(1–2):7–12
56. Mead D, Ramberg F, Besselsen D, Mare C (2000) Transmission of vesicular stomatitis virus from infected to non-infected black flies co-feeding on non viremic deer mice. Science 287:486–487
57. Labib M, Zamay AS, Muharemagic D, Chechik A, Bell JC, Berezovski MV (2012e) Electrochemical sensing of aptamer-facilitated virus immunoshielding. Anal Chem 84(3):1677–1686
58. Sakudo A, Ikuta K (2008) Efficient capture of infectious H5 avian influenza virus utilizing magnetic beads coated with anionic polymer. Biochem Biophys Res Commun 377(1):85–88

59. Qi C, Tian XS, Chen S, Yan JH, Cao Z, Tian KG, Gao GF, Jin G (2010) Detection of avian influenza virus subtype H5 using a biosensor based on imaging ellipsometry. Biosens Bioelectron 25(6):1530–1534
60. Jenison RD, Gill SC, Pardi A, Polisky B (1994) High-resolution molecular discrimination by RNA. Science 263(5152):1425–1429
61. Sassanfar M, Szostak JW (1993) An RNA motif that binds ATP. Nature 364(6437):550–553
62. Kukol A, Li P, Estrela P, Ko-Ferrigno P, Migliorato P (2008) Label-free electrical detection of DNA hybridization for the example of influenza virus gene sequences. Anal Biochem 374(1):143–153
63. Zhu X, Ai S, Chen Q, Yin H, Xu J (2009) Label-free electrochemical detection of Avian Influenza Virus genotype utilizing multi-walled carbon nanotubes-cobalt phthalocyanine-PAMAM nanocomposite modified glassy carbon electrode. Electrochem Commun 11:1543–1546
64. Shen L, Chen Z, Li Y, He S, Xie S, Xu X, Liang Z, Meng X, Li Q, Zhu Z, Li M, Le XC, Shao Y (2008) Electrochemical DNAzyme sensor for lead based on amplification of DNA-Au bio-bar codes. Anal Chem 80(16):6323–6328
65. Liu X, Cheng Z, Fan H, Ai S, Han R (2011) Electrochemical detection of avian influenza virus H5N1 gene sequence using a DNA aptamer immobilized onto a hybrid nanomaterial-modified electrode. Electrochimica Acta 56:6266–6270
66. Lai WA, Lin CH, Yang YS, Lu MS (2012) Ultrasensitive and label-free detection of pathogenic avian influenza DNA by using CMOS impedimetric sensors. Biosens Bioelectron 35(1):456–460
67. June GA, Sherrod PS, Hammack TS, Amaguana RM, Andrews WH (1996) Relative effectiveness of selenite cystine broth, tetrathionate broth, and rappaport-vassiliadis medium for recovery of *Salmonella* spp. from raw flesh, highly contaminated foods, and poultry feed: collaborative study. J AOAC Int 79(6):1307–1323
68. Edwards RA, Olsen GJ, Maloy SR (2002) Comparative genomics of closely related salmonellae. Trends Microbiol 10(2):94–99
69. Eyigor A, Carli KT, Unal CB (2002) Implementation of real-time PCR to tetrathionate broth enrichment step of Salmonella detection in poultry. Lett Appl Microbiol 34(1):37–41
70. Condit RC, Moussatche N, Traktman P (2006) In a nutshell: structure and assembly of the vaccinia virion. Adv Virus Res 66:31–124
71. Wolffe EJ, Vijaya S, Moss B (1995) A myristylated membrane protein encoded by the vaccinia virus L1R open reading frame is the target of potent neutralizing monoclonal antibodies. Virology 211(1):53–63
72. Rodriguez JF, Janeczko R, Esteban M (1985) Isolation and characterization of neutralizing monoclonal antibodies to vaccinia virus. J Virol 56(2):482–488
73. Hsiao JC, Chung CS, Chang W (1999) Vaccinia virus envelope D8L protein binds to cell surface chondroitin sulfate and mediates the adsorption of intracellular mature virions to cells. J Virol 73(10):8750–8761
74. Davies DH, McCausland MM, Valdez C, Huynh D, Hernandez JE, Mu Y, Hirst S, Villarreal L, Felgner PL, Crotty S (2005) Vaccinia virus H3L envelope protein is a major target of neutralizing antibodies in humans and elicits protection against lethal challenge in mice. J Virol 79(18):11724–11733
75. Nelson GE, Sisler JR, Chandran D, Moss B (2008) Vaccinia virus entry/fusion complex subunit A28 is a target of neutralizing and protective antibodies. Virology 380(2):394–401
76. Hooper JW, Custer DM, Schmaljohn CS, Schmaljohn AL (2000) DNA vaccination with vaccinia virus L1R and A33R genes protects mice against a lethal poxvirus challenge. Virology 266(2):329–339
77. Cruz-Aguado JA, Penner G (2008) Determination of ochratoxin a with a DNA aptamer. J Agric Food Chem 56(22):10456–10461
78. Czerwinski JD, Hovan SC, Mascotti DP (2005) Quantitative nonisotopic nitrocellulose filter binding assays: bacterial manganese superoxide dismutase-DNA interactions. Anal Biochem 336(2):300–304

79. Tahiri-Alaoui A, Frigotto L, Manville N, Ibrahim J, Romby P, James W (2002) High affinity nucleic acid aptamers for streptavidin incorporated into bi-specific capture ligands. Nucleic Acids Res 30(10):e45
80. Mendonsa SD, Bowser MT (2004) In vitro evolution of functional DNA using capillary electrophoresis. J Am Chem Soc 126(1):20–21
81. Michaud M, Jourdan E, Villet A, Ravel A, Grosset C, Peyrin E (2003) A DNA aptamer as a new target-specific chiral selector for HPLC. J Am Chem Soc 125(28):8672–8679
82. Muller M, Weigand JE, Weichenrieder O, Suess B (2006) Thermodynamic characterization of an engineered tetracycline-binding riboswitch. Nucleic Acids Res 34(9):2607–2617
83. del Toro M, Gargallo R, Eritja R, Jaumot J (2008) Study of the interaction between the G-quadruplex-forming thrombin-binding aptamer and the porphyrin 5,10,15,20-tetrakis-(N-methyl-4-pyridyl)-21,23H-porphyrin tetratosylate. Anal Biochem 379(1):8–15
84. Wang J, Lv R, Xu J, Xu D, Chen H (2008) Characterizing the interaction between aptamers and human IgE by use of surface plasmon resonance. Anal Bioanal Chem 390(4):1059–1065
85. Zhang WY, Zhang W, Liu Z, Li C, Zhu Z, Yang CJ (2012) Highly parallel single-molecule amplification approach based on agarose droplet polymerase chain reaction for efficient and cost-effective aptamer selection. Anal Chem 84(1):350–355
86. Stojdl DF, Lichty B, Knowles S, Marius R, Atkins H, Sonenberg N, Bell JC (2000) Exploiting tumor-specific defects in the interferon pathway with a previously unknown oncolytic virus. Nat Med 6(7):821–825
87. Rose NF, Marx PA, Luckay A, Nixon DF, Moretto WJ, Donahoe SM, Montefiori D, Roberts A, Buonocore L, Rose JK (2001) An effective AIDS vaccine based on live attenuated vesicular stomatitis virus recombinants. Cell 106(5):539–549
88. Fisher KD, Stallwood Y, Green NK, Ulbrich K, Mautner V, Seymour LW (2001) Polymer-coated adenovirus permits efficient retargeting and evades neutralising antibodies. Gene Ther 8(5):341–348
89. Doronin K, Shashkova EV, May SM, Hofherr SE, Barry MA (2009) Chemical modification with high molecular weight polyethylene glycol reduces transduction of hepatocytes and increases efficacy of intravenously delivered oncolytic adenovirus. Hum Gene Ther 20(9):975–988
90. Ong HT, Hasegawa K, Dietz AB, Russell SJ, Peng KW (2007) Evaluation of T cells as carriers for systemic measles virotherapy in the presence of antiviral antibodies. Gene Ther 14(4):324–333
91. Goebel SJ, Johnson GP, Perkus ME, Davis SW, Winslow JP, Paoletti E (1990) The complete DNA sequence of vaccinia virus. Virology 179(1):247–266
92. Yu YA, Shabahang S, Timiryasova TM, Zhang Q, Beltz R, Gentschev I, Goebel W, Szalay AA (2004) Visualization of tumors and metastases in live animals with bacteria and vaccinia virus encoding light-emitting proteins. Nat Biotechnol 22(3):313–320
93. Fabris L, Dante M, Braun G, Lee SJ, Reich NO, Moskovits M, Nguyen TQ, Bazan GC (2007) A heterogeneous PNA-based SERS method for DNA detection. J Am Chem Soc 129(19):6086–6087
94. Borghesi L, Milcarek C (2006) From B cell to plasma cell: regulation of V(D)J recombination and antibody secretion. Immunol Res 36(1–3):27–32
95. Muharemagic D, Labib M, Ghobadloo SM, Zamay AS, Bell JC, Berezovski MV (2012) Anti-fab aptamers for shielding virus from neutralizing antibodies. J Am Chem Soc 134(41): 17168–17177

Adv Biochem Eng Biotechnol (2014) 140: 183–202
DOI: 10.1007/10_2013_226

Published Online: 20 July 2013

Electrochemical Biosensors Using Aptamers for Theranostics

Koichi Abe, Wataru Yoshida and Kazunori Ikebukuro

Abstract Theranostics, a new term consisting of the words "therapy" and "diagnostics," represents the concept of selecting specific patients for appropriate drug administration using diagnostics. For the development of a molecular targeting drug, the theranostics approach is effective. Therefore, the market for molecular diagnostics is likely to grow at an extraordinary rate over the next 10 years. In this review, we focus on aptamer-based electrochemical biosensors for theranostics. Aptamers are molecular recognition elements that can bind to various target molecules from small compounds to proteins with affinities and specificities comparable to those of antibodies. Inasmuch as various molecules would be targeted for analysis using theranostics, aptamer-based biosensors would be an attractive format because they can be developed for various molecules using the same sensing format. Although a diverse sensing system can be constructed, we focus on electrochemical biosensors in this review because they can measure biomarkers rapidly in a miniaturized sensing system with low cost, such as blood glucose sensors. We summarize the sensing systems of aptamer-based electrochemical biosensors and discuss their advantages for theranostics.

Keywords Aptamer · Biosensor · Electrochemical detection · Theranostics

Contents

K. Abe · W. Yoshida · K. Ikebukuro (✉)
Tokyo University of Agriculture and Technology, Tokyo, Japan
e-mail: ikebu@cc.tuat.ac.jp

1 Introduction

Molecular target drugs have been developed for various diseases. Because molecular target drugs are efficacious for patients whose cells express the target molecules of the drug, evaluation of the amount of target molecules or other alternative biomarkers is essential prior to the administration of the drug, in order to select the patient. Theranostics, a coined term combining the words "therapy" and "diagnostics" (also called "companion diagnostics"), is defined as using diagnostics testing to identify the disease, select a treatment regimen, and monitor the response of the patient to therapy. The US Food and Drug Administration (FDA) recently recognized companion diagnostics as being increasingly important in decision making by introducing guidelines according to which targeted drugs will be reviewed for approval only in the presence of matching companion diagnostics (http://www.fda.gov/downloads/MedicalDevices/DeviceRegulationandGuidance/GuidanceDocuments/UCM262327.pdf).

Trastuzumab (Herceptin®), an antibody drug for breast cancer, is a representative example of theranostics. HER-2, the target protein of trastuzumab, is overexpressed in 25–30 % of breast cancers [1], and trastuzumab inhibits the growth of tumors overexpressing HER-2 but not that of tumors in which this molecule is not expressed. To administer trastuzumab to patients, the HER-2 expression level must be evaluated by immunohistochemistry (IHC) and/or in situ hybridization by fluorescence (FISH).

For infectious diseases, there is a need for rapid (<1 h) and accurate diagnostic tests to enable optimal patient management and treatment [2]. To administer neuraminidase inhibitors, which are therapeutics for influenza, the presence of the influenza virus in a specimen is evaluated by immunochromatography, which is a lateral flow assay using a gold nanoparticle-labeled antibody. It can detect the influenza virus within 15 min, although it is limited to qualitative detection.

For theranostics, the sensing system should measure biomarkers rapidly and easily with low cost. Because rapid measurement with low cost is required for point-of-care testing (POCT) to allow physicians to tailor the selection of either drugs or drug doses quickly, POCT technology would help in the development of theranostics. In addition, it is necessary to analyze various kinds of molecules such as DNA, RNA, proteins, and metabolites to decide on the appropriate therapeutic in terms of safety and efficiency. As we describe later, because aptamers can be selected against various molecules, we can construct a sensing system for various molecules from DNA/RNA to small compounds using the same sensing platform.

This is an attractive feature because it would repress the cost of development and it would allow us to construct multiple biomarker detection systems.

In this review, we summarize electrochemical aptamer sensors in the field of theranostics and describe their advantages.

2 Aptamers

Aptamers are nucleic acids that exhibit binding ability toward various molecules with unique three-dimensional structures [3, 4]. Some aptamers have comparable affinity and specificity to antibodies. Compared to antibodies, aptamers have some advantages originating from their nucleic acid properties. They can be easily synthesized and labeled with various molecules. Aptamers, especially DNA aptamers, are more stable than antibodies at room temperature and they are renaturable after denaturation by heating. These properties are advantageous in their use as molecular recognition tools in commercialized biosensors because the cost can potentially be repressed and the molecule would endure severe storage conditions. Furthermore, aptamers can be selected by an in vitro selection method named SELEX (systematic evolution of ligand exponential enrichment) [3]. SELEX consists of four simple steps: incubation of a combinatorial nucleic acid library of about 10^{15} sequences with the target, removal of unbound nucleic acids, extraction of bound nucleic acids from the target, and amplification of the collected nucleic acids. The aptamers are selected by repeating these steps. These steps enable us to automate and shorten the developmental period for molecular recognition elements for biosensors [5]. Using SELEX, we can select aptamers that bind to various targets such as small compounds, peptides, proteins, and even cells including toxins and antigens that do not induce immune responses in host animals for antibody production. Most aptamers recognize target molecules with unique three-dimensional structures and some aptamers can discriminate between slight differences in the target [6]. By combining this property with negative selection against other molecules or cells, we can select specific aptamers that can distinguish slight changes in the target. Williams et al. selected aptamers bound to histone H4 acetylated at lysine 16 (H4-K16Ac), and not histone H4 that is notacetylated at lysine 16. The selected aptamer showed higher specificity to H4-K16Ac than did the anti-H4-K16Ac antibody [7]. Furthermore, we can select aptamers that recognize the conformation and assembly state of the target. Sayer et al. reported aptamers that selectively bind disease-associated β-sheet rich forms of the prion protein but not its α form [8]. We have reported aptamers that bind to the amyloidogenic soluble oligomer of α-synuclein and amyloid β [9]. These aptamers recognize only the soluble amyloidogenic oligomer but not the monomeric state and amyloid fibril of α-synuclein and amyloid β. Soluble amyloidogenic oligomers are known as the most toxic species and cause neurodegenerative diseases such as Alzheimer's disease, Parkinson's disease, Huntington disease, and

prion disease. Aptamers would be useful diagnostic tools for these diseases and for the analysis of the molecular mechanisms of these diseases.

Additionally, aptamers against cells can be selected directly by Cell-SELEX [10]. Protein expression levels on the cell surface help us discriminate between cancer cells and normal cells. Most antibodies are used for cell typing based on protein expression on the cell surface. The target proteins for antibody therapy are expressed on the cell membrane, therefore evaluation of target protein expression is important for the selection of patients for antibody therapy. However, it is difficult to purify membrane proteins for immunization. Although peptide immunization sometimes helps in generating antibodies, the selected antipeptide antibody often shows low binding ability toward the target protein. In addition, aptamers selected against purified target membrane proteins often do not bind to the target protein on the cell surface, because the purified protein might have a conformation that is different from that seen on the cell surface [11]. On the other hand, Cell-SELEX, a SELEX method that directly uses the cells as the targets, can select aptamers against membrane proteins with native structure without protein purification. Aptamers selected by Cell-SELEX show strong binding to the target cells [10]. However, inasmuch as Cell-SELEX has the potential to obtain aptamers that bind to membrane proteins other than the target protein, we need to introduce adequate counter-selections in Cell-SELEX [12].

SELEX against unpurified proteins, including Cell-SELEX, can be utilized to identify biomarkers. Polyacrylamide gel electrophoresis (PAGE) can separate proteins from crude samples and aptamers can be selected against the protein transferred onto a nitrocellulose membrane [13]. The membrane-bound protein of interest is excised, and nucleic acids bound to the protein of interest are extracted from the membrane. Thereby, we can obtain aptamers against the unpurified protein. By comparing samples of normal and tumor cells resolved by PAGE, we can identify aptamers recognizing proteins that represent only tumor cells. Using these selected aptamers, the target protein can be easily purified and identified. For the validation of biomarkers, many samples from patients should be evaluated. Aptamers would allow us to analyze the protein amount in the sample and facilitate biomarker discovery.

Many aptamer sensors based on selected aptamers have been developed. As described later, conformational changes that occur in aptamers upon binding to target molecules are utilized in many biosensors. Fluorescence resonance energy transfer (FRET) can transduce binding signals generated by a conformational change in the aptamer. This feature represents an advantage of using aptamers over antibodies for the construction of biosensors. However, engineering aptamers for biosensors based on conformational change requires a detailed knowledge of the aptamer sequence and structure. Rajendran and Ellington have reported screening using aptamer beacons, an optical sensing format that detects conformational change, in a random library [14]. They used complementary strands immobilized on beads. The complementary strand was modified with a quencher and the DNA library was modified with the fluorescence molecule. When the DNA binds to the target molecule, the DNA is dissociated from the beads, resulting in increased

fluorescence intensity. The collected DNA was amplified by PCR and these steps were repeated. By iterative cycles, they succeeded in obtaining aptamer beacons.

3 Electrochemical Biosensors Using Aptamers

Since the first reports of aptamers became public two decades ago, many researchers have reported various aptamer sensors for biomarker detection based on optical or electrochemical detection. Among these, electrochemical methods have attracted particular attention in the development of aptamer sensors because of their high sensitivity, inherent simplicity, miniaturization, and low cost. We describe biosensors using aptamers as alternatives to antibodies, and using aptamers with unique features not present in antibodies.

3.1 Sandwich Assay

Because aptamers have comparable affinity and specificity to antibodies, they are often used as an alternative to antibodies in biosensors. The sandwich assay format is a widely used method to measure diagnostic markers in commercialized sensing systems (Fig. 1). We have reported a simple electrochemical sandwich assay of thrombin using two antithrombin aptamers that simultaneously bind to different parts of thrombin. A 15-mer thrombin aptamer was immobilized on a gold electrode and a biotinylated 29-mer thrombin aptamer was labeled with avidin-conjugated flavin adenine dinucleotide-dependent glucose dehydrogenase (FADGDH) [15] or pyrroloquinoline quinone-dependent glucose dehydrogenase (PQQGDH) [16, 17] via avidin–biotin interactions. An electrochemical current was observed with a dependence on thrombin concentration upon adding D-glucose. GDH has high catalytic activity and an electrochemical current can be obtained by the addition of D-glucose, which is a very cheap substrate. The sandwich assay format enables the removal of nonspecific binding and amplification of the binding signal using an enzyme [18] or other nanomaterials such as Pt nanoparticles [19], which catalyze the reduction of H_2O_2, and CdS [20], detectable by an ion-selective electrode following the dissolution of CdS with hydrogen peroxide, resulting in highly sensitive detection with high specificity. Many researchers have therefore reported various sensing systems based on the sandwich assay using aptamers. Centi et al. optimized the sandwich assay for thrombin using alkaline phosphatase-conjugated streptavidin [21]. They immobilized aptamers on magnetic beads, facilitating the effective mixing and washing of the beads. After the preparation of the sandwich complex on the beads, beads were applied on screen-printed carbon electrodes. This method resulted in the successful detection of thrombin with a lower detection limit of 0.45 nM.

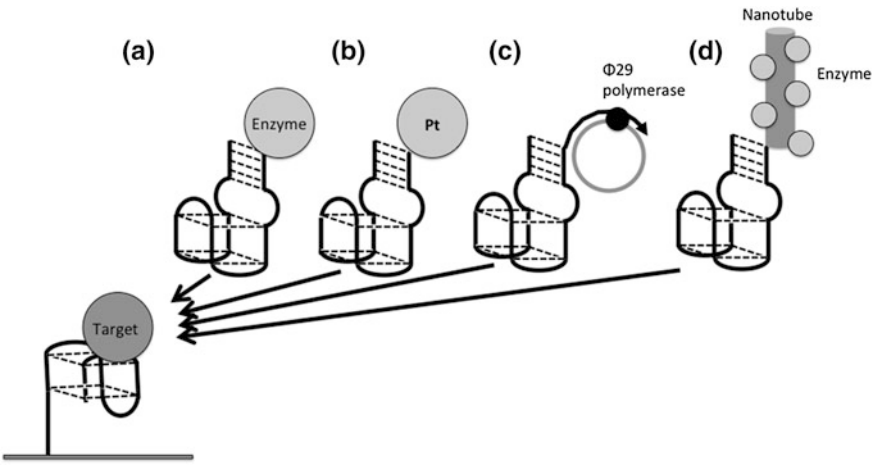

Fig. 1 Sandwich assay using aptamers combining various signal amplification methods: **a** enzyme, **b** nanoparticle, **c** rolling cycle amplification, **d** multiple enzyme-labeled carbon nanotube

3.2 Signal Amplification in Sandwich Assay Format

To construct a highly sensitive detection system, some researchers have attempted the conjugation of multiple enzymes on an aptamer. Xiang et al. used a single-walled carbon nanotube (SWCNT) to conjugate several alkaline phosphatases (ALP) for highly sensitive detection. Aptamer-labeled ALP conjugated to CNTs recognizes target molecules captured by an immobilized aptamer on the electrode. Combined with signal amplification by diahorase, this method allowed the successful detection of thrombin with a lower detection limit of 10 fM.

Zhou et al. used rolling cycle amplification (RCA) for signal amplification in the sandwich assay [22]. Inasmuch as aptamers themselves can be amplified by a polymerase, we can amplify signals without labeling the aptamers. RCA can amplify the aptamer by several thousands isothermally via ϕ29 polymerase, resulting in the amplification of a site to which an enzyme-labeled probe sequence can be hybridized. Zhou et al. used platelet-derived growth factor-BB (PDGF-BB) aptamer with an attached primer site that hybridized to a padlock probe. When sandwich complexes are formed on the electrode, ϕ29 polymerase amplifies the padlock probe sequence. Zhou et al. used ALP-conjugated avidin and biotinylated complementary DNA and measured ALP activity based on enzymatic silver deposition via ascorbic acid that is generated from ascorbic acid 2-phosphate by ALP. They succeeded in PDGF-BB detection with a low detection limit of 10 fM by linear sweep voltammetry.

Polymerase chain reaction (PCR) is an attractive methodology to amplify signals because PCR can amplify the signal exponentially. Many researchers have utilized PCR for aptamer sensors. PCR is often used in biosensors combined with

antibodies and this sensing system called immuno-PCR. Although immuno-PCR allows the construction of a highly sensitive detection system, antibodies should be modified with probe DNA. On the other hand, the aptamer does not need to be labeled with probe DNA and can be directly applied to PCR [23]. Many researchers have reported aptamer-based immuno-PCR. Most of these studies have used real-time PCR based on fluorescence detection. Xiang et al. reported the electrochemical detection of PCR products. They focused on the guanosine as the electric probe [24]. After PCR amplification, they treated purified PCR products with H_2SO_4 and heat, which enhance the depurination of DNA, and measured the released guanosine by chronopotentiometric measurements. The detection limit was 5.4 fM, significantly lower than the detection limit without PCR (8 nM).

The sandwich assay format requires two aptamers that bind to the target simultaneously. Therefore, it is difficult to apply it to sensing systems for small compounds, proteins that have only one superior aptamer, and monomeric proteins. We have constructed a bound/free separation (B/F separation) system for versatile biosensors using an aptamer (Fig. 2). We have reported two types of biosensors using an aptamer. These systems consist of two parts: an aptamer and its complementary DNA. One system utilizes the inhibition of hybridization of complementary DNA with an aptamer upon target binding. Target molecule binding to the aptamer stabilizes its structure, thereby inhibiting the hybridization of complementary DNA (Fig. 2a) [25, 26]. Furthermore, when we use DNA that is complementary to the target-binding region, the complementary DNA cannot hybridize with the aptamer because of steric hindrance. Another system utilizes the conformational change of an aptamer. We created a "capturable" aptamer by adding a sequence to it that gave it a new structure (Fig. 2b) [27, 28]. Upon target binding, the aptamer would form a structure suitable for target recognition, and the attached DNA would be free. The conformationally altered aptamer–target complex can be captured by an immobilized DNA that is complementary to the attached DNA sequence. These B/F separation systems can remove excess aptamer labeled with an enzyme. Therefore, we can utilize enzymes to amplify signals for target sensing. We have designed these sensing systems for thrombin, prion, IgE, and vascular endothelial growth factor (VEGF).

3.3 Label-Free Aptamer Sensor

Because aptamers can be immobilized on the electrode using thiol-labeled aptamers, aptamers are easily applicable to the development of electrochemical biosensors. Electrochemical impedance spectrometry (EIS) and field-effect transistor (FET) methodology can detect signals originating from the molecular recognition of immobilized ligands. EIS measures alternating current impedance, reflecting changes in a diffusion-limited electrochemical process, presumably due to steric hindrance created by the bound molecules to immobilized aptamer and repulsion between electron mediators and immobilized molecules. Xu et al. reported IgE

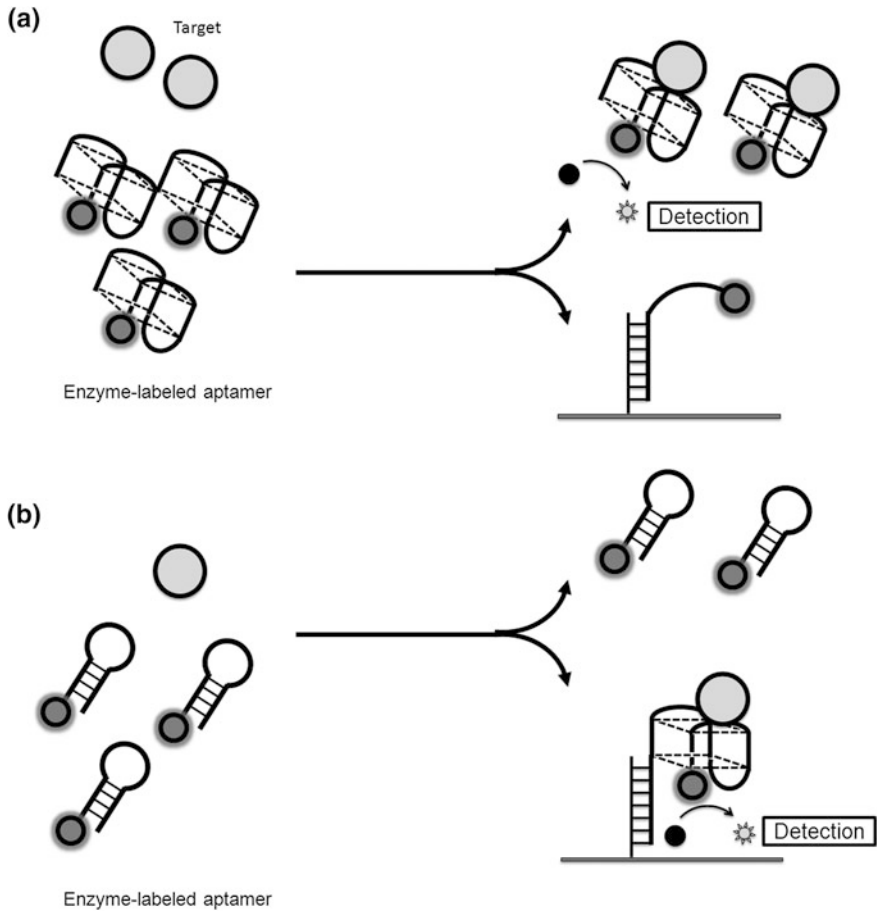

Fig. 2 Bound/free separation system using an aptamer. **a** In the absence of a target molecule, the aptamers are trapped by immobilized beads containing a DNA sequence complementary to that of the aptamer, whereas in the presence of the target protein, aptamers that bind to the target are not trapped. **b** The aptamer, which can be captured, undergoes a conformational change upon binding to the target molecule. This change induces the exposure of a partial single strand that hybridizes with the complementary DNA. Otherwise, any unbound capturable aptamer does not hybridize with the complementary DNA, and it is removed by the bound/free separation system

sensing using the IgE aptamer and compared this with detection using antibodies [29]. They observed lower background impedance using the IgE aptamer-immobilized electrode than with an anti-IgE antibody-immobilized electrode, presumably due to the small size and simple structure of aptamers. In addition, the ratio of the signal change upon IgE binding to the IgE aptamer to the background signal was higher than that of the anti-IgE antibody. Therefore, EIS would be an attractive detection approach for aptamer-based biosensors, and many researchers have reported aptamer sensors based on EIS for small molecules, protein, viruses,

and bacteria [30–32]. EIS can measure slight changes in the electric charge transfer resistance (Rct) on the electrode surface, therefore we can trace the fabrication process of the electrode. On the other hand, the background signal must be suppressed for highly sensitive detection, especially for serum samples, because EIS is sensitive to nonspecific interaction. Qi et al. investigated surface treatment for thrombin detection [33]. Thiol-containing compounds can mask the gold electrode to suppress nonspecific interaction. They found that treatment of the gold electrode by dithiothreitol suppresses nonspecific interaction and enhances the signal-to-noise ratio. They succeeded in detecting thrombin in undiluted serum with a lower detection limit of 0.3 ng/mL (8 pM) based on EIS.

Deng et al. introduced gold nanoparticle-labeled aptamers (Apt-AuNP) to enhance signal amplification in an EIS-based sensor [34]. Apt-AuNP formed a sandwich structure with thrombin and immobilized a 15-mer thrombin-binding aptamer. To enhance charge transfer resistance, they used enlarged sodium dodecyl sulfate (SDS)-stabilized Apt-AuNP. As expected, Apt-AuNP increased Rct because of steric hindrance by the enlarged gold nanoparticle and electrostatic repulsion between the SDS-stabilized Apt-AuNPs and the redox probe, $[Fe(CN)_6]^{3-/4-}$. Using Apt-AuNPs, thrombin was detected with a lower detection limit of 100 fM.

EIS is an easy sensing methodology, but its sensitivity is dependent on target charges and sizes. Wang et al. utilized graphene to control Rct based on the conformational change of an ATP-binding aptamer to amplify signals for the detection of small molecules [35]. Graphene has ultrahigh electron transfer ability and it interacts with single-stranded DNA nonspecifically due to strong π–π interactions. Adsorption of graphene onto the aptamer immobilized on the electrode decreases the Rct because of the high electron transferability of graphene. ATP binding to the aptamer induces a conformational change in the aptamer and decreases the adsorption of graphene to the aptamer, resulting in no decrease of Rct. The Rct depends on the ATP concentration, with a lower detection limit of 15 nM. They also fabricated a sensing system for Hg^{2+}, a highly toxic metal ion, using a thymine-rich mercury-binding oligonucleotide, with a lower detection limit of 0.5 nM. The change in impedance caused by the binding of small compounds would be lower than that caused by protein. The change ratio of Rct can be increased by the use of graphene.

FET methodology can also detect target molecules without labeling the molecular recognition element. FET biosensors measure binding events between aptamers and target proteins within the Debye length, defined as the typical distance required for screening the surplus charge carried by mobile carriers present in a material; therefore, FET biosensors that use antibodies require careful control of the Debye length [36]. Because most aptamers have sizes that are smaller than the Debye length, aptamers would be useful molecular recognition elements. Maehashi et al. reported the development of FET sensors for IgE using aptamers and compared the performance with FET biosensors using antibody [37]. Inasmuch as IgE has a large size ($\sim$10 nm), complex IgEs and anti-IgE antibodies

easily exceed the Debye length. They succeeded in detecting IgE using the anti-IgE aptamer but not the anti-IgE antibody under similar conditions.

3.4 Aptamer Sensors Based on Conformational Change

Because aptamers are a type of biopolymer consisting of nucleic acids that have many negative charges, their tertiary structures are destabilized by the repulsion between phosphate backbones. Furthermore, some aptamers have the ability to form different structures because there are many possible combinations for Watson–Crick base pairing with similar energy states. Target molecule binding stabilizes a particular structure, even though the structure would have little chance of forming without the target molecule. Aptamers therefore have the potential to change conformation, and in some cases, drastically so. Their conformational changes upon target binding are not limited to protein binding but also occur upon the binding of small molecules. Therefore, aptamer sensors based on conformational change have potential applications as biosensors for various molecules. Many aptamer sensors have been reported and they rely on the transduction of structural changes into detectable signals [38]. Aptamer beacons are optical sensors based on FRET accompanied by a conformational change in the aptamer upon target binding [39, 40]. To measure the conformational change in the aptamer based on electrochemistry, a redox tag such as methylene blue or ferrocene is used, and the distance between the redox tag and electrode surface is controlled to measure biomarkers based on the electrochemical current change. Bang et al. focused on a feature that methylene blue can intercalate with double-stranded DNA [41]. They added a complementary sequence at the 5′ terminal that hybridizes with 3′ region of the thrombin aptamer. The immobilized designed aptamer on the electrode folds into a stem-loop structure without thrombin. Methylene blue recognizes double-stranded DNA regions, resulting in increased electric current (Fig. 3a). Upon thrombin binding to the aptamer, the thrombin aptamer folds into a chair-type G-quadruplex structure that does not have a stem structure, resulting in a decrease in electric current because of the dissociation of methylene blue from immobilized DNA. However, this sensing system is limited to G-quadruplex-type aptamers.

Xiao et al. reported the development of a thrombin sensor using a methylene blue-labeled aptamer immobilized on a gold electrode [42]. Their group has previously constructed DNA sensors based on controlling the distance between methylene blue and the electrode. In the absence of the target, the immobilized 32-mer thrombin aptamer is thought to remain relatively unfolded, thereby allowing the attached methylene blue moiety to collide with (or weakly bind to) the electrode and transfer an electron (Fig. 3b). Upon thrombin binding, electron transfer is inhibited (signal-off sensor), presumably due to a binding-induced conformational change in the aptamer. Radi et al. reported a similar sensing system for thrombin using a ferrocene-labeled aptamer in the same period, but this sensing

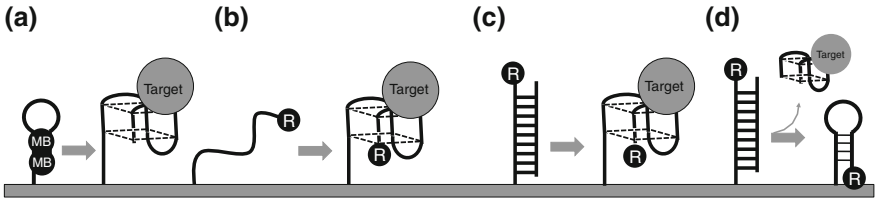

Fig. 3 Electrochemical aptamer sensor format based on conformational change. **a** In the absence of the target molecule, immobilized DNA forms a stem-loop structure and methylene blue associates with the stem-loop structure, resulting in an increase in electric current. Upon target molecule binding, immobilized DNA forms a G-quadruplex structure and methylene blue (MB) dissociates from immobilized DNA, resulting in a decrease in electric current. **b** Immobilized redox-probe–modified DNA does not form a stable structure and the redox probe can easily access the electrode. Upon target binding, the redox probe is fixed at a certain position, resulting in an increase or decrease of electric current dependent on the aptamer structure. **c** The duplex of the redox-probe–modified DNA aptamer and the complementary DNA is immobilized on the electrode. Upon target binding, the aptamer folds and the complementary DNA dissociates from the electrode, resulting in the fixation of the redox probe at the proximal side of electrode. **d** The duplex of the DNA aptamer and the redox-probe–modified complementary DNA are immobilized on the electrode. Upon target binding, the aptamer folds and dissociates from the electrode. The immobilized complementary DNA folds into a stem-loop, resulting in the fixation of the redox probe at the proximal side of the electrode

system shows the opposite signal change (signal-on sensor) [43]. They used a ferrocene-labeled short 15-mer thrombin aptamer. The distance between the electrode and the labeled ferrocene decreased significantly upon thrombin binding, resulting in enhancement of electron transfer. This strategy resulted in the successful detection of thrombin with a lower detection limit of 0.5 nM.

This strategy is useful for small molecule detection. Baker et al. reported cocaine sensors using methylene blue-labeled aptamers [44]. The cocaine aptamer formed a stable three-way junction. Stojanovic et al. engineered the cocaine aptamer to form a three-way junction in the presence of cocaine but not in the absence of cocaine by destabilizing the stem structure formed between the 5′ and 3′ ends [45]. Upon cocaine binding, the distance between the 5′ and 3′ ends is decreased, leading to the successful construction of an optical cocaine sensor based on FRET. Baker et al. applied cocaine aptamers to an electrochemical aptamer-based sensor (E-AB sensor) [44]. The immobilized methylene blue-labeled aptamer was partially folded and the methylene blue was attached at the 3′ terminal of the aptamer at varying distances relative to the electrode. Binding of the target molecule induces the folding of the aptamer resulting in the restriction of the aptamer structure at the position close to the electrode. Subsequently, electron transfer from methylene blue to the electrode is presumably facilitated. This resulted in the successful detection of cocaine with a lower detection limit of 10 μM. Lai et al. also reported platelet-derived growth factor (PDGF) sensing using methylene blue-labeled aptamers, and they succeeded in the detection of PDGF with a lower detection limit of 1 nM in undiluted serum and 50 pM in twofold diluted serum[46]. Because we do not need to wash to detect signals using the

conformational change of the aptamer, we can detect target molecules rapidly. Baker et al. detected cocaine in 4 min, and PDGF in 30 min. This method is very attractive for use in constructing biosensors for theranostics.

Although this sensing system is not limited to G-quadruplex-type aptamers, it is not easy to construct biosensors with any kind of aptamer because some aptamers have a rigid structure regardless of binding to the target. Xiao et al. hypothesized that if binding of the target to the aptamer restricts the movement of the immobilized aptamer, the electric current would change with a dependence on the target concentration [47]. They tried to measure thrombin and IgE using the corresponding aptamer. Although Xiao et al. succeeded in the detection of thrombin and IgE, they found that only about 3 % of the signaling current was changed when saturated IgE (200 nM) was applied. Inasmuch as IgE has a high molecular weight, it is expected that IgE binding to the aptamer would efficiently restrict the movement of the aptamer. However, methylene blue is presumably sufficiently close to the electrode in the absence of target molecules, because IgE aptamer has a restricted structure in the absence of target binding, resulting in a slight current change upon target addition. This indicates that the restricted movement of an aptamer upon target binding depends on the aptamer sequence but not the target size. Therefore, we need to engineer the structures of aptamers to apply them to E–AB sensors.

To apply E–AB methodology to any aptamer, complementary DNA has often been used to induce a conformational change in the aptamer before target binding. The complementary DNA induces a conformational change in the aptamer forming a double-stranded DNA structure. The complementary DNA dissociates from the aptamer upon target binding. Xiao et al. reported thrombin sensing by E–AB using complementary DNA [48]. The immobilized DNA consists of the aptamer and the hybridization region with the complementary DNA sequence. The complementary DNA partially hybridizes with the aptamer sequence, and the terminus of the sequence that hybridizes with the aptamer sequence is labeled with methylene blue. In the absence of the target, the complementary DNA hybridizes with the aptamer region and methylene blue is restricted at a considerable distance from the electrode. Upon target binding, the complementary DNA presumably dehybridizes from the aptamer, bringing the methylene blue closer to the electrode. In the absence of the complementary DNA, it is difficult to control the signal change. In the thrombin-sensing system, the electric current associated with the thrombin concentration decreases (signal-off sensor). On the other hand, in the cocaine and PDGF detection system, the electric current associated with the PDGF concentration increases (signal-on sensor). For highly sensitive detection, the signal-on sensor is more suitable than the signal-off sensor because it is easier to decrease noise in such a system than in the signal-off sensor in the absence of the target. Using complementary DNA, the authors succeeded in constructing a signal-on sensor for thrombin and DNA with lower detection limits of 3 nM and 400 fM, respectively.

Zuo et al. reported an aptamer sensor for adenosine based on a similar strategy [49]. The adenosine aptamer was immobilized on a gold electrode and the opposite terminal was labeled with ferrocene. Ferrocene does not have the ability to

intercalate with dsDNA, therefore it was considered a better choice than methylene blue. In the absence of adenosine, a complementary DNA was hybridized with the aptamer. Upon target binding, the complementary DNA presumably dissociated from the aptamer, bringing the ferrocene close to the electrode (Fig. 3c). On the other hand, Lu et al. immobilized the complementary DNA on the electrode [50]. They designed a complementary DNA to the aptamer that forms a stem-loop structure in the absence of aptamer hybridization. In the absence of the target molecule, the aptamer hybridizes with the complementary DNA. Upon target binding to the aptamer, the aptamers confined to the electrode surface dissociate from the complementary DNA, allowing the complementary DNA to form the stem-loop structure. The 3′ terminal of the aptamer was labeled with ferrocene and the formation of the stem-loop structure resulted in an increase in electric current via the reduction of the ferrocene (Fig. 3d).

Das et al. reported a versatile aptamer sensor platform by using a polycationic polymer-modified peptide nucleic acid (PNA), designated the neutralizer [51] (Fig. 4). Because aptamers possess many negative charges, some researchers have utilized these negative charges in the development of biosensors [52, 53]. Upon target binding, most of the negative charges would be neutralized, resulting in a decrease in the amount of $Ru(NH_3)_6^{3+}$ bound to the aptamer. However, the neutralization efficiency upon binding to the target molecule depends on the size of the target molecule. To apply this platform in a biosensor to measure any molecule using aptamers, the high background signal originating from the nonspecific interaction of $Ru(NH3)_6^{3+}$ with immobilized aptamers would pose a problem. Das et al. resolved this problem using a neutralizer. PNA is entirely a synthetic DNA mimic and can hybridize to complementary DNA or RNA strands. In PNA, the negatively charged phosphate backbone of the nucleic acid is replaced by an uncharged *N*-(2-aminoethyl)-glycine scaffold. Using this polycationic polymer-modified PNA, the negative charge of the immobilized aptamer is neutralized, resulting in a decrease in the background signal from $Ru(NH3)_6^{3+}$ binding. Upon target binding, the neutralizer is replaced by the target molecule, resulting in the binding of $Ru(NH3)_6^{3+}$ to the exposed phosphate backbone of the immobilized aptamer. The authors combined $Ru(NH3)_6^{3+}$ and $Fe(CN)_6^{3-}$, which would permit the turnover of $Ru(NH3)_6^{3+}$ by regenerating the oxidized form, resulting in signal amplification. The use of this technology resulted in the successful detection of ATP (1 μM), cocaine (1 μg/mL), DNA (100 aM), bacteria (0.15 cfu/mL), and thrombin (10 fM). Because PNA can hybridize with DNA more strongly than can DNA, strand displacement seems not to occur rapidly. The authors introduced mismatches in the PNA such that the target bound to the immobilized aptamer more rapidly and robustly, leading to the displacement of the neutralizer. Signal change in ATP detection occurred within 1 min, and the signal change in the absence of ATP is not significant even after 20 min.

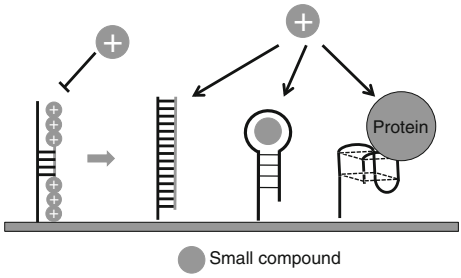

Fig. 4 Aptamer sensors using peptide nucleic acid-modified cationic polymer as the neutralizer. Upon target binding, the neutralizer dissociates from DNA immobilized on the electrode and the ruthenium complex associates with the immobilized DNA, resulting in an increase in electric current

3.5 Sensing System for POCT Using Aptamers

To measure biomarkers for POCT, the sensing system should be miniaturized and capable of rapid measurement at low cost. In general, immunochromatography formats are widely utilized for POCT. Immobilized antibodies trap targets such as virus, bacteria, and the like and gold nanoparticle-modified antibodies form a sandwich structure with the immobilized antibody–target complex. Inasmuch as gold nanoparticles undergo a color change when they form assemblies, we can estimate the presence of virus, bacteria, or other biomarkers in the sample by observing the presence of a line at the spot where the antibodies are immobilized. This methodology is useful in the estimation of infectious disease in order to administer a suitable medicine. However, it is limited to partial quantification because we evaluated it only by the presence of the line.

Most successful biosensors are glucose-sensing systems for self-monitoring blood glucose (SMBG). Most glucose sensors for SMBG are based on electrochemical detection using glucose oxidase or glucose dehydrogenase [54]. Glucose sensors can measure the blood glucose concentration in 0.15 μL blood within 1 s [55]. Whole systems are optimized well, and some glucose sensors contain an enzyme that removes the effect of redox active molecules such as ascorbic acid and uric acid included in blood. We focus on glucose dehydrogenase as the labeling enzyme. Glucose dehydrogenase has high catalytic activity (PQQGDH shows 5,000 U/mg protein) that is measurable by an optimized minimal glucose-sensing format. Therefore, we could potentially construct a highly sensitive detection system for various biomarkers for POCT, and we have reported aptamer sensors using glucose dehydrogenase as the labeling enzyme and an aptamer that binds to PQQGDH and FADGDH [15–17, 56–58].

Using the FADGDH-binding aptamer, we have reported a novel sensing system based on nanostructure control by target molecule binding [57]. The FADGDH binding aptamer selected by SELEX forms a G-quadruplex structure composed of two successive stretches of six guanines each, with a sandwiched sequence

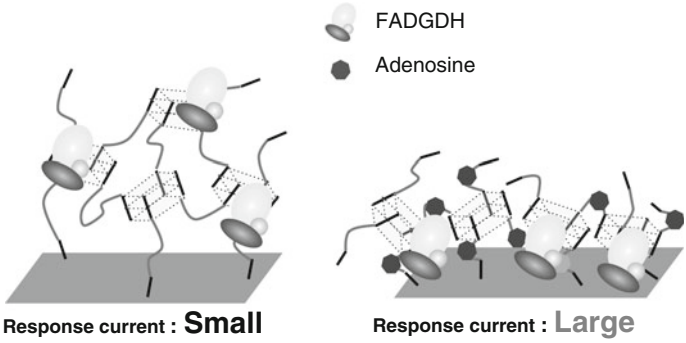

Fig. 5 G-quadruplex–based nanostructure biosensing format using FADGDH that has an electron transfer subunit. In the absence of the target molecule, the electron transfer subunit is distant from the electrode. Upon target molecule binding, the G-quadruplex structure changes, resulting in increased electron transfer from the enzyme subunit to the electrode

between these sequences. Through the analysis of truncated mutants, we found that this aptamer formed a polymerized G-quadruplex structure called a G-wire, and a mutant that broke the G-wire structure lost its ability to bind to FADGDH. Surprisingly, we found that the central sequence sandwiched by consecutive guanines was not related to FADGDH binding. FADGDH derived from *Burkholderia cepacia* has three subunits, one of which has electron transfer activity to the electrode from the catalytic subunit [59]. It has been utilized in a glucose sensing system based on direct electron transfer without an electron mediator [60]. We therefore hypothesized that replacing the central sequence with an aptamer in the structure of the G-wire would change the distance between the electrode and FADGDH upon target binding (Fig. 5). When we inserted the adenosine aptamer into the FADGDH aptamer, it retained its ability to bind adenosine and FADGDH. The aptamer was immobilized on a gold electrode and incubated with FADGDH. After washing the electrode to remove excess FADGDH, the electrode with the immobilized adenosine aptamer containing the insertion of the G-wire–FADGDH complex was further incubated with various concentrations of adenosine. As expected, we observed a concentration-dependent increase in electric current with adenosine in the absence of electron mediator. Although the sensitivity of this system is low because nanostructure control is a complicated process, this sensing system is very attractive because it can utilize signal amplification by the enzyme without B/F separation.

Xiang et al. reported the development of biosensors using commercialized glucose sensors for various target molecules based on strand displacement [61] (Fig. 6). To apply the glucose sensor to a sensing system for not only glucose but also various other biomarkers, they focused on an invertase, which catalyzes the hydrolysis of sucrose to glucose. The aptamer was immobilized on beads via partially complementary DNA to the 5′-region of the aptamer and invertase-modified complementary DNA was hybridized with the 3′-region of the aptamer.

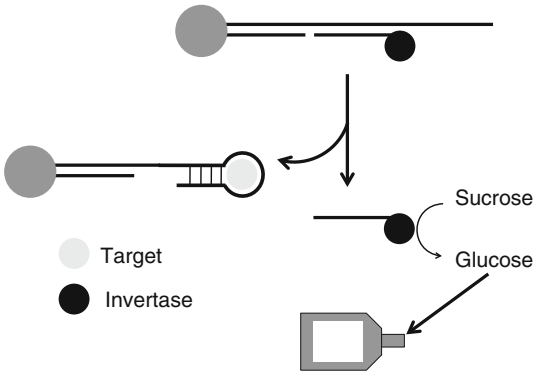

Fig. 6 Versatile aptamer sensor using a glucose meter. Aptamers are immobilized on the beads via complementary DNA. Invertase-modified DNA is hybridized with the aptamer. Upon target binding, invertase-modified DNA dissociates from the beads. Glucose that is converted from sucrose by invertase is measured using a glucose meter

Upon binding of the target molecule, the invertase-modified complementary DNA was released from the beads into solution. When sucrose was added to the supernatant after removing the beads by magnetic separation, sucrose was hydrolyzed to glucose and fructose with a dependence on the amount of invertase within a short time. More important, because of its highly efficient enzymatic turnover, even nanomolar levels of invertase are capable of converting millimolar concentrations of sucrose into millimolar amounts of glucose whose range can be measured by commercialized glucose sensors. The authors measured cocaine (3.4 μM detection limit), adenosine (18 μM detection limit), and interferon-gamma of tuberculosis (2.6 nM detection limit). They also used DNAzyme for the on-site detection of toxic metal ions such as uranium (UO_2^{2+}). Biotinylated DNA was immobilized on magnetic beads, and the invertase-conjugated DNA probe was connected to the UO_2^{2+}-dependent DNAzyme via 12-base–pair hybridization. Upon the binding of UO_2^{2+} to the DNAzyme, the DNAzyme cleaved the complementary probe immobilized on the beads, resulting in the release of the invertase-conjugated DNA probe. The group of Dr. Ya-Qin Chai has also reported the development of biosensors using invertase-modified nanoparticles [62, 63]. They utilized antibodies or DNA probes immobilized on the nanoparticle. After B/F separation, sucrose was converted to glucose in a target DNA concentration-dependent manner. They succeeded in sensing carcinoembryonic antigen or DNA with a lower detection limit comparable to that of conventional ELISA. Therefore, invertase would be an attractive enzyme for signal amplification because its activity can be measured in a miniaturized glucose sensing system.

3.6 Future Perspective

Diagnostics are increasingly important to achieve personalized medicine, therefore the development of molecular recognition elements and detection systems should be accelerated. Aptamers are expected to be useful as alternatives to antibodies because they can be selected by in vitro selection with comparable affinity and

specificity in a short time and possibly with low cost. To develop theranostics, we need to develop biosensing systems for various biomarkers with low cost and rapid sensing. An electrochemical sensing system can miniaturize the sensing system at low cost and it can be fabricated by lithography-based technology, allowing us to construct multiple biomarker detection systems by using a chip. Aptamers are the most suitable molecular recognition element for use with an electrochemical sensing system because they can be easily modified for immobilization on the electrode. For conventional diagnostics, antibody-based chemiluminescent detection systems are widely used clinically. However, their sensing systems are relatively big. Electrochemical sensors using aptamers would allow us to measure multiple biomarkers by a chip rapidly and with low cost to allow physicians to tailor the selection of either drugs or drug doses quickly. We expect that these biosensors will facilitate the development of theranostics and personalized medicine.

References

1. Slamon DJ, Godolphin W, Jones LA, Holt JA, Wong SG, Keith DE, Levin WJ, Stuart SG, Udove J, Ullrich A et al (1989) Studies of the HER-2/neu proto-oncogene in human breast and ovarian cancer. Science 244:707–712
2. Picard FJ, Bergeron MG (2002) Rapid molecular theranostics in infectious diseases. Drug Discov Today 7:1092–1101
3. Tuerk C, Gold L (1990) Systematic evolution of ligands by exponential enrichment: RNA ligands to bacteriophage T4 DNA polymerase. Science 249:505–510
4. Ellington AD, Szostak JW (1990) In vitro selection of RNA molecules that bind specific ligands. Nature 346:818–822
5. Cox JC, Ellington AD (2001) Automated selection of anti-protein aptamers. Bioorg Med Chem 9:2525–2531
6. Jenison RD, Gill SC, Pardi A, Polisky B (1994) High-resolution molecular discrimination by RNA. Science 263:1425–1429
7. Williams BA, Lin L, Lindsay SM, Chaput JC (2009) Evolution of a histone H4–K16 acetyl-specific DNA aptamer. J Am Chem Soc 131:6330–6331
8. Sayer NM, Cubin M, Rhie A, Bullock M, Tahiri-Alaoui A, James W (2004) Structural determinants of conformationally selective, prion-binding aptamers. J Biol Chem 279:13102–13109
9. Tsukakoshi K, Harada R, Sode K, Ikebukuro K (2012) Screening of DNA aptamer which binds to alpha-synuclein. Biotechnol Lett 32:643–648
10. Morris KN, Jensen KB, Julin CM, Weil M, Gold L (1998) High affinity ligands from in vitro selection: complex targets. Proc Natl Acad Sci U S A 95:2902–2907
11. Pestourie C, Cerchia L, Gombert K, Aissouni Y, Boulay J, De Franciscis V, Libri D, Tavitian B, Duconge F (2006) Comparison of different strategies to select aptamers against a transmembrane protein target. Oligonucleotides 16:323–335
12. Ye M, Hu J, Peng M, Liu J, Liu H, Zhao X, Tan W (2012) Generating aptamers by Cell-SELEX for applications in molecular medicine. Int J Mol Sci 13:3341–3353
13. Noma T, Ikebukuro K, Sode K, Ohkubo T, Sakasegawa Y, Hachiya N, Kaneko K (2006) A screening method for DNA aptamers that bind to a specific, unidentified protein in tissue samples. Biotechnol Lett 28:1377–1381

14. Rajendran M, Ellington AD (2003) In vitro selection of molecular beacons. Nucleic Acids Res 31:5700–5713
15. Ikebukuro K, Kiyohara C, Sode K (2004) Electrochemical detection of protein using a double aptamer sandwich. Anal Lett 37:2901–2909
16. Ikebukuro K, Kiyohara C, Sode K (2005) Novel electrochemical sensor system for protein using the aptamers in sandwich manner. Biosens Bioelectron 20:2168–2172
17. Nonaka Y, Abe K, Ikebukuro K (2012) Electrochemical detection of vascular endothelial growth factor with aptamer sandwich. Electrochemistry 80:363–366
18. Abe K, Ikebukuro K (2011) Aptamer sensors combined with enzymes for highly sensitive detection. InTech: Rijeka, Croatia
19. Polsky R, Gill R, Kaganovsky L, Willner I (2006) Nucleic acid-functionalized Pt nanoparticles: Catalytic labels for the amplified electrochemical detection of biomolecules. Anal Chem 78:2268–2271
20. Numnuam A, Chumbimuni-Torres KY, Xiang Y, Bash R, Thavarungkul P, Kanatharana P, Pretsch E, Wang J, Bakker E (2008) Aptamer-based potentiometric measurements of proteins using ion-selective microelectrodes. Anal Chem 80:707–712
21. Centi S, Tombelli S, Minunni M, Mascini M (2007) Aptamer-based detection of plasma proteins by an electrochemical assay coupled to magnetic beads. Anal Chem 79:1466–1473
22. Zhou L, Ou LJ, Chu X, Shen GL, Yu RQ (2007) Aptamer-based rolling circle amplification: a platform for electrochemical detection of protein. Anal Chem 79:7492–7500
23. Pinto A, Bermudo Redondo MC, Ozalp VC, O'Sullivan CK (2009) Real-time apta-PCR for 20 000-fold improvement in detection limit. Mol Biosyst 5:548–553
24. Xiang Y, Xie M, Bash R, Chen JJ, Wang J (2007) Ultrasensitive label-free aptamer-based electronic detection. Angew Chem Int Ed Engl 46:9054–9056
25. Fukasawa M, Yoshida W, Yamazaki H, Sode K, Ikebukuro K (2009) An aptamer-based bound/free separation system for protein detection. Electroanalysis 21:1297–1302
26. Abe K, Hasegawa H, Ikebukuro K (2012) Electrochemical detection of vascular endothelial growth factor by an aptamer-based bound/free separation system. Electrochemistry 80:348–352
27. Abe K, Ogasawara D, Yoshida W, Sode K, Ikebukuro K (2011) Aptameric sensors based on structural change for diagnosis. Faraday Discuss 149:93–105 (Discussion 137–157)
28. Ogasawara D, Hachiya NS, Kaneko K, Sode K, Ikebukuro K (2009) Detection system based on the conformational change in an aptamer and its application to simple bound/free separation. Biosens Bioelectron 24:1372–1376
29. Xu D, Yu X, Liu Z, He W, Ma Z (2005) Label-free electrochemical detection for aptamer-based array electrodes. Anal Chem 77:5107–5113
30. Labib M, Zamay AS, Kolovskaya OS, Reshetneva IT, Zamay GS, Kibbee RJ, Sattar SA, Zamay TN, Berezovski MV (2012) Aptamer-based impedimetric sensor for bacterial typing. Anal Chem 84:8114–8117
31. Labib M, Zamay AS, Muharemagic D, Chechik AV, Bell JC, Berezovski MV (2012) Aptamer-based viability impedimetric sensor for viruses. Anal Chem 84:1813–1816
32. Rodriguez MC, Kawde AN, Wang J (2005) Aptamer biosensor for label-free impedance spectroscopy detection of proteins based on recognition-induced switching of the surface charge. Chem Commun (Camb), pp 4267–4269
33. Qi H, Shangguan L, Li C, Li X, Gao Q, Zhang C (2012) Sensitive and antifouling impedimetric aptasensor for the determination of thrombin in undiluted serum sample. Biosens Bioelectron 39:324–328
34. Deng C, Chen J, Nie Z, Wang M, Chu X, Chen X, Xiao X, Lei C, Yao S (2009) Impedimetric aptasensor with femtomolar sensitivity based on the enlargement of surface-charged gold nanoparticles. Anal Chem 81:739–745
35. Wang L, Xu M, Han L, Zhou M, Zhu C, Dong S (2012) Graphene enhanced electron transfer at aptamer modified electrode and its application in biosensing. Anal Chem 84:7301–7307
36. Stern E, Wagner R, Sigworth FJ, Breaker R, Fahmy TM, Reed MA (2007) Importance of the Debye screening length on nanowire field effect transistor sensors. Nano Lett 7:3405–3409

37. Maehashi K, Katsura T, Kerman K, Takamura Y, Matsumoto K, Tamiya E (2007) Label-free protein biosensor based on aptamer-modified carbon nanotube field-effect transistors. Anal Chem 79:782–787
38. Li D, Song S, Fan C (2009) Target-responsive structural switching for nucleic acid-based sensors. Acc Chem Res 43:631–641
39. Yamamoto R, Baba T, Kumar PK (2000) Molecular beacon aptamer fluoresces in the presence of Tat protein of HIV-1. Genes Cells 5:389–396
40. Hamaguchi N, Ellington A, Stanton M (2001) Aptamer beacons for the direct detection of proteins. Anal Biochem 294:126–131
41. Bang GS, Cho S, Kim BG (2005) A novel electrochemical detection method for aptamer biosensors. Biosens Bioelectron 21:863–870
42. Xiao Y, Lubin AA, Heeger AJ, Plaxco KW (2005) Label-free electronic detection of thrombin in blood serum by using an aptamer-based sensor. Angew Chem Int Ed Engl 44:5456–5459
43. Radi AE, Acero Sanchez JL, Baldrich E, O'Sullivan CK (2006) Reagentless, reusable, ultrasensitive electrochemical molecular beacon aptasensor. J Am Chem Soc 128:117–124
44. Baker BR, Lai RY, Wood MS, Doctor EH, Heeger AJ, Plaxco KW (2006) An electronic, aptamer-based small-molecule sensor for the rapid, label-free detection of cocaine in adulterated samples and biological fluids. J Am Chem Soc 128:3138–3139
45. Stojanovic MN, de Prada P, Landry DW (2001) Aptamer-based folding fluorescent sensor for cocaine. J Am Chem Soc 123:4928–4931
46. Lai RY, Plaxco KW, Heeger AJ (2007) Aptamer-based electrochemical detection of picomolar platelet-derived growth factor directly in blood serum. Anal Chem 79:229–233
47. Xiao Y, Uzawa T, White RJ, Demartini D, Plaxco KW (2009) On the signaling of electrochemical aptamer-based sensors: collision- and folding-based mechanisms. Electroanalysis 21:1267–1271
48. Xiao Y, Piorek BD, Plaxco KW, Heeger AJ (2005) A reagentless signal-on architecture for electronic, aptamer-based sensors via target-induced strand displacement. J Am Chem Soc 127:17990–17991
49. Zuo X, Song S, Zhang J, Pan D, Wang L, Fan C (2007) A target-responsive electrochemical aptamer switch (TREAS) for reagentless detection of nanomolar ATP. J Am Chem Soc 129:1042–1043
50. Lu Y, Li X, Zhang L, Yu P, Su L, Mao L (2008) Aptamer-based electrochemical sensors with aptamer-complementary DNA oligonucleotides as probe. Anal Chem 80:1883–1890
51. Das J, Cederquist KB, Zaragoza AA, Lee PE, Sargent EH, Kelley SO (2012) An ultrasensitive universal detector based on neutralizer displacement. Nat Chem 4:642–648
52. Cheng AK, Ge B, Yu HZ (2007) Aptamer-based biosensors for label-free voltammetric detection of lysozyme. Anal Chem 79:5158–5164
53. Lapierre MA, O'Keefe M, Taft BJ, Kelley SO (2003) Electrocatalytic detection of pathogenic DNA sequences and antibiotic resistance markers. Anal Chem 75:6327–6333
54. Ferri S, Kojima K, Sode K (2011) Review of glucose oxidases and glucose dehydrogenases: a bird's eye view of glucose sensing enzymes. J Diabetes Sci Technol 5:1068–1076
55. Yamaoka H, Sode K (2007) SPCE based glucose sensor employing novel thermostable glucose dehydrogenase, FADGDH: blood glucose measurement with 150 nL sample in one second. J Diabetes Sci Technol 1:28–35
56. Abe K, Sode K, Ikebukuro K (2010) Constructing an improved pyrroloquinoline quinone glucose dehydrogenase binding aptamer for enzyme labeling, Biotechnol Lett 32:1293–1298
57. Morita Y, Yoshida W, Savory N, Han SW, Tera M, Nagasawa K, Nakamura C, Sode K, Ikebukuro K (2011) Development of a novel biosensing system based on the structural change of a polymerized guanine-quadruplex DNA nanostructure. Biosens Bioelectron 26:4837–4841
58. Osawa Y, Takase M, Sode K, Ikebukuro K (2009) DNA Aptamers that Bind to PQQGDH as an Electrochemical Labeling Tool. Electroanalysis 21:1303–1308

59. Tsuya T, Ferri S, Fujikawa M, Yamaoka H, Sode K (2006) Cloning and functional expression of glucose dehydrogenase complex of Burkholderia cepacia in Escherichia coli. J Biotechnol 123:127–136
60. Kakehi N, Yamazaki T, Tsugawa W, Sode K (2007) A novel wireless glucose sensor employing direct electron transfer principle based enzyme fuel cell. Biosens Bioelectron 22:2250–2255
61. Xiang Y, Lu Y (2011) Using personal glucose meters and functional DNA sensors to quantify a variety of analytical targets. Nat Chem 3:697–703
62. Su J, Xu J, Chen Y, Xiang Y, Yuan R, Chai Y (2012) Personal glucose sensor for point-of-care early cancer diagnosis. Chem Commun (Camb) 48:6909–6911
63. Xu J, Jiang B, Xie J, Xiang Y, Yuan R, Chai Y (2012) Sensitive point-of-care monitoring of HIV related DNA sequences with a personal glucometer. Chem Commun (Camb) 48:10733–10735

Adv Biochem Eng Biotechnol (2014) 140: 203–219
DOI: 10.1007/10_2013_230

Published Online: 4 July 2013

Enzymatic Glucose Biosensors Based on Nanomaterials

Butaek Lim and Young-Pil Kim

Abstract Glucose biosensors have an important place in the diagnosis of diabetes as well as in various food and biotechnological processes. Recent advances in nanomaterials have directly improved enzymatic glucose biosensors owing to their distinguished structural and physiochemical properties. Here, we review the recent developments in electrochemical and fluorescent glucose biosensors based on nanomaterials. New technologies that combine nanomaterials with glucose-sensing enzymes will result in promising glucose biosensors with high specificity and sensitivity.

Keywords Diabete · Enzyme · Glucose biosensor · Nanomaterial · Nanoparticle

Abbreviations

GOx	Glucose oxidase
AuNP	Gold nanoparticle
QD	Quantum dot
CNT	Carbon nanotube
NAD	Nicotinamide adenine dinucleotide
GDH	Glucose dehydrogenase
PQQ	Pyrroloquinoline quinone
FET	Field effect transistor
SWNT	Single-wall nanotube
SCE	Short-channel effect
SWCNT	Single-wall carbon nanotube
FAD	Flavin adenine dinucleotide
CMF	Carbon microfiber
GR	Graphite rod
HRP	Horseradish peroxidase
OMC	Ordered mesoporous carbon
MCF	Mesocellular carbon foam
NP	Nanoparticle
SAM	Self-assembled monolayer

B. Lim · Y.-P. Kim (✉)
Department of Life Science, Hanyang University, Seoul 133-791, Republic of Korea
e-mail: ypilkim@hanyang.ac.kr

LSPR	Localized surface plasmon resonance
MNP	Magnetic nanoparticle
NMM	Nanostructured magnetic materials
PDDA-HCNT	Poly(diallyldimethylammonium chloride) functionalized helical carbon nanotube
PVA-Py-GOx	Poly(vinyl alcohol)-pyrene-GOx
FRET	Fluorescence resonance energy transfer

Contents

1 Introduction

Enzymes, as the most commonly used reagents, offer exquisite specificity when combined with different types of biosensors. To this end, enzymatic biosensors are attractive in spite of their relatively poor stability, which is associated with short lifetimes and limited ranges of applications. A great number of enzymatic biosensors have been proposed, but far fewer have been practically used; notable success has been achieved in the rapid diagnosis of blood glucose levels for patients with diabetes, which is one of the leading causes of death and disability in the world. Because the diagnosis and management of diabetes mellitus require a stringent control of blood glucose levels within the normal range of 80–120 mg/dL (4.4–6.6 mM), glucose biosensors account for about 85 % of the entire biosensor market [1], leading to the incessant development of innovative biosensors. Over the last few decades, glucose biosensors, especially those based on glucose oxidase (GOx), have played a pivotal role in simple glucose detection in blood as well as in vivo glucose monitoring, due to mass production and easy availability. However, enzyme-based glucose sensors remain formidable.

To expand the usability of enzymatic glucose biosensors, much research has focused on increasing their stability and sensitivity using nanomaterials. Recent

advances in nanomaterials offer some significant advantages owing to their enhanced structural and engineered complexity. For example, high surface area/volume ratios facilitate larger signals and greater catalytic activity by enzymes. Also, the enhanced electrical or optical properties of nanoparticles, including gold nanoparticles (AuNPs), quantum dots (QDs), and carbon nanotubes (CNTs), improved the accuracy and lifetime of the glucose biosensors. Therefore, enzymes and their coupling to nanomaterials will lead to new types of biosensors.

Here, we review recent advances in the field of enzymatic glucose biosensors based on nanomaterials. To avoid redundancy in a myriad of reviews of glucose biosensors [2–6], we outline nanomaterial-based enzymatic glucose biosensors, primarily focusing on distinguished detection methods by various nanomaterials. A short description regarding electrochemical and fluorescent glucose biosensors is presented with sensing principles and structural properties. Emphasis is given to the major strategies for enhancing their performance. We outline key challenges and opportunities for their further development and use.

2 Enzymatic Electrochemical Detection of Glucose Using Nanomaterials

The immobilizing technique of glucose oxidase directed the era of self-monitoring of blood glucose with reflectance meters in the 1970s [7]. However, since Clark and Lyons [8] and Updike and Hicks [9] first described the electrochemical enzymatic glucose sensors in the 1960s, electrochemical sensors have replaced reflectance meters due to their faster and more accurate properties. The most significant sensing material that is widely used in glucose biosensors is glucose oxidase (GOx), which catalyzes the oxidation of glucose to gluconolactone, followed by being hydrolyzed to gluconic acid in water. A good example is the traditional glucose sensor, which can detect the hydrogen peroxide produced in the oxidation process catalyzed by a glucose oxidase enzyme.

$$\text{Glucose} + O_2 + \text{GOx} \rightarrow \text{Gluconolactone} + H_2O_2$$

Along with flavoprotein GOx, nicotinamide adenine dinucleotide (NAD)-dependent glucose dehydrogenase (GDH) has been harnessed as an enzyme for glucose biosensors. In contrast with the oxidation systems of GOx, which involve membrane flavoproteins in the inner face of the cytoplasmic membrane, GDH is found in the periplasm of gram-negative bacteria, such as *Acinetobacter calcoaceticus*. Although these two enzymes have been primarily used for the construction of glucose biosensors, they have intrinsic problems: GOx is sensitive to oxygen fluctuations in blood samples and NAD–GDH has less stability due to the loss of the cofactor NAD. GDH also requires an additional redox mediator to lower the overvoltage for oxidation of the NADH product. To circumvent these problems, pyrroloquinoline quinone (PQQ)-dependent GDH has been used as an

alternative; it does not require an oxygen cofactor (that is, it is oxygen-insensitive) and has tightly bound PQQ in the enzyme [10–12]. PQQ can act as an electron acceptor instead of oxygen during the glucose oxidation.

$$\text{Glucose} + \text{PQQ}_{\text{Ox}}\text{ - GDH} \rightarrow \text{Gluconolactone} + \text{PQQ}_{\text{Red}}\text{ - GDH}$$

Compared to NAD-dependent GDH, PQQ-GDH contains a relatively tightly bound PQQ cofactor [13]. In addition, glucose kinetics for quinoprotein GDH are approximately 40 times greater than that for the flavoprotein GOx under identical conditions [10]. Although such PQQ enzymes are of limited use due to their limited stability by insoluble PQQ, the water-soluble PQQ-GDH is reported to be developed from *Acinetobacter calcoaceticus* [14]. The high catalytic activity and oxygen insensitivity make the PQQ-GDH biosensor suitable for in vivo blood glucose monitoring in the management of diabetes.

Recently, it has been revealed that the incorporation of nanomaterials into such enzymes offers a variety of advantages, including increased surface area, improved catalytic reaction, and more efficient electron transfer from enzyme to electrode. In particular, nanocomposites including carbon nanotubes and metal particles have been preferentially implemented to induce high performance of the electrochemical glucose sensing system. Other nanoparticles have been exploited to amplify the signal sensitivity by several orders of magnitude. In this chapter, we highlight recent advances in electrochemical glucose biosensors, including enzymes and nanomaterials.

2.1 Carbon Nanotubes

The CNT-based enzymatic glucose sensor was initially demonstrated as a field effect transistor (FET)-type sensor by Dekker et al. [15]. Through the controlled attachment of the GOx to the nanotube sidewall in Fig. 1, it was shown that the conductance change of the assembly was much more dependent on the pH than that of enzyme-free CNT. With increasing pH, GOx became more negative, thereby increasing the conductance of the semiconducting single-wall nanotube (SWNT). Accordingly, it was very effective to detect charge changes of about 50 protein molecules attached to a $\sim$600-nm long semiconducting SWNT. The low-potential (-0.2 V vs. SCE) reductive detection of the hydrogen peroxide product led to highly selective amperometric monitoring of the glucose, which showed the linearity up to 30 mM glucose and a detection limit of 0.08 mM. This system was very specific to glucose; glucose did not change the conductance of the bare SWNT but did increase the conductance after GOx was immobilized. It was presumed that this system would be suitable for real-time electronic glucose detection. However, because the immobilization of GOx can decrease the conductance (and many other factors in the real sample can also affect the conductance), a stringent control is a prerequisite for reliable measurement.

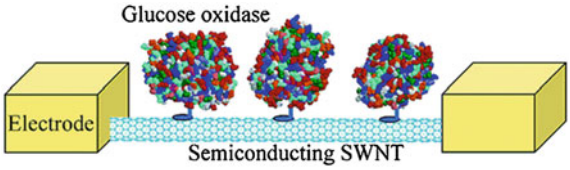

Fig. 1 Carbon nanotube (CNT)-based field effect transistor as the glucose biosensor. Two electrodes are connected to a semiconducting CNT with GOx enzymes immobilized on its surface. *SWNT*, Single-walled nanotube. Adapted from [15] with permission

Willner et al. demonstrated the incorporation of single-walled carbon nanotubes (SWCNTs) as electrical connectors between the GOx redox centers and the electrode [16]. The amino derivative of the flavin adenine dinucleotide (FAD) cofactor was coupled to the carboxy groups at the free edges of the standing SWCNTs that had been conjugated to a gold electrode via an EDC reaction. After passivation of the walls with Triton X-100 and polyethylene glycol, apo-GOx was reconstituted on the FAD unit. This assembly allowed the SWCNT to act as a nanoconnector that electrically contacted the active site of the enzyme and the electrode. The rate constants of electron transport were controlled by the length of the SWCNTs: 83, 42, 19, and 12 s^{-1} was estimated for the standing SWCNTs of 25, 50, 100, and 150 nm average length, respectively. The large surface coverage of the GOx–CNT units enabled the turnover rate of electrons sixfold faster than that between the GOx and its O_2 electron acceptor. This system suggested the hybrid system of CNTs and enzymes could be used for glucose detection, showing that CNTs served as the distance-dependent electron wire.

Davis and Coleman described an SWCNT glucose biosensor based on a diffusive ferrocene mediator [17]. This was achievable by adsorbing several metalloproteins and enzymes on both the sidewalls and termini of SWCNTs. As is characteristic with many similar enzyme systems, the tunnelling distance between the (redox) active site and any underlying support/electrode is still too far. Because direct electrochemical communication between the flavin active site of GOx immobilized in this way and the nanotube is not possible, the adsorption (π–π interaction) of cytochrome on oxidized SWNTs allowed for direct communication between the active site of GOx enzyme and nanotube through the ferrocene mediator to generate a quantifiable catalytic current in response to glucose substrate (Fig. 2).

Schmldtke et al. showed further utility of the CNT/enzyme assembly by incorporating SWNTs into redox polymer hydrogels containing the GOx enzymes [18]. The composite films were achieved by incubating the GOx in the SWNT solution and then the subsequent cross-linking within a poly[(vinylpyridine)Os(bipyridyl)$_2$$Cl^{2+/3+}$] polymer. This system resulted in a two- to tenfold increase in the redox peak currents during cyclic voltammetry, while the glucose oxidation current was also threefold higher in the current output than that of CNT-free electrode. This result clearly demonstrated that the incorporation of CNT into

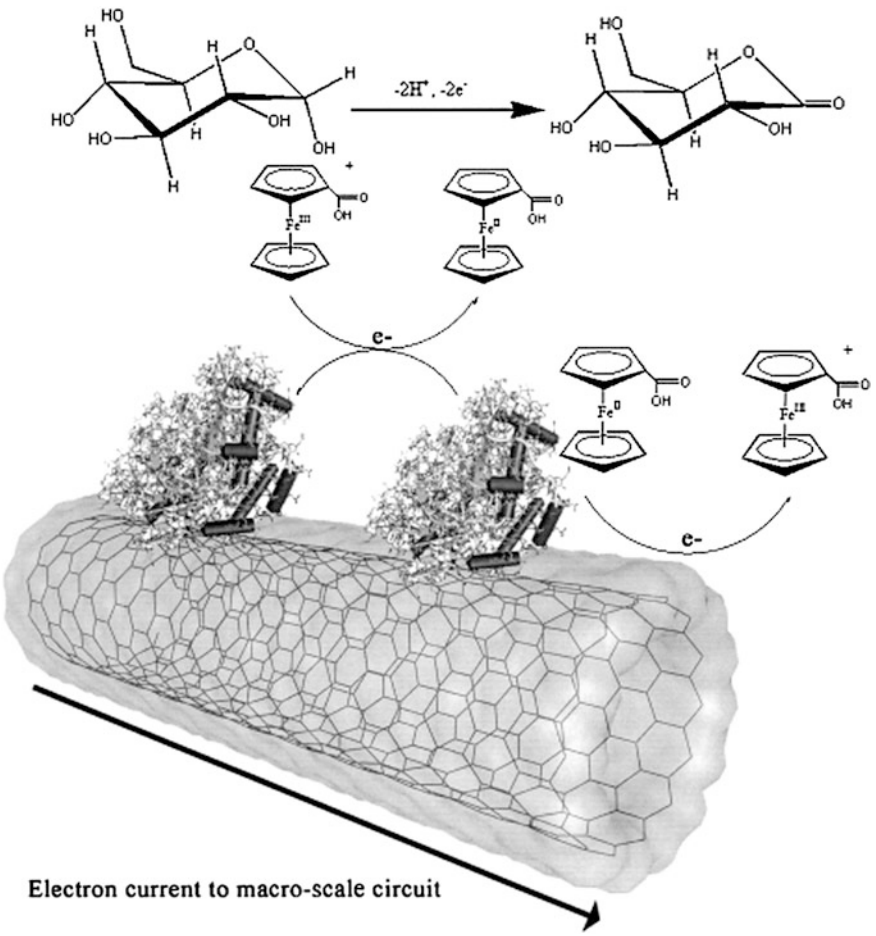

Fig. 2 Schematic representation of the single-walled nanotube glucose biosensor. Solution-phase D-glucopyranose is turned over by oxidase enzymes immobilized on the nanotubes. This redox process at the enzyme flavin moieties is communicated to the nanotube π system through the diffusive mediator ferrocene monocarboxylic acid. The redox action of the ferrocenes at the nanotube surface ultimately generates a quantifiable catalytic current characteristic of substrate detection and turnover. Adapted from [17] with permission

the films facilitated the electron transfer through the polymer film upon the addition of glucose.

In addition to electrochemical glucose sensors based on CNTs, a novel method to generate a high potential biocathode through a controlled electric connection between CNTs and the electrode was recently proposed by Schuhmann and Stoica [19]. The effective reduction of H_2O_2 was induced by co-immobilization of GOx at CNT/carbon microfiber (CMF)/graphite rod (GR) electrodes modified with 1-pyrenehexonic acid and horseradish peroxidase (HRP). This biocathode with suitable anodes would be useful as both a glucose sensor and a glucose-based biofuel cell.

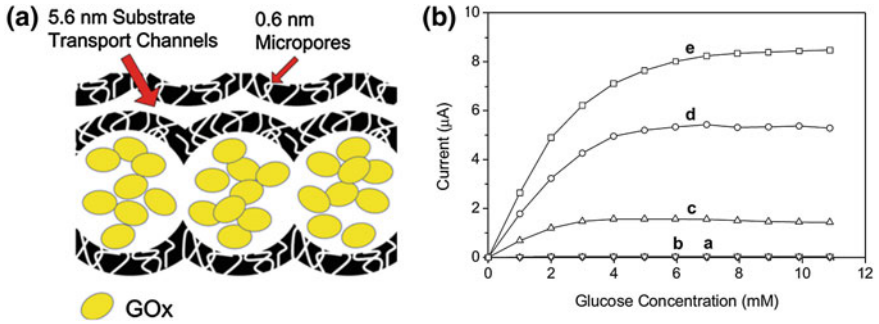

Fig. 3 **a** Schematic representation of MSU-F–C/glucose oxidase showing effective retention of enzymes within large mesopores and the role of small pores in the facile transport of a substrate. **b** The amperometric response on varied contents of MCF (*a* 0, *b* 0.5, *c* 1.0, *d* 2.0, and *e* 3.0 mg mL^{-1}) as a function of glucose concentration. Adapted from [22] with permission

2.2 Mesoporous Carbon

Ordered mesoporous carbon (OMC) could be a good candidate for glucose-sensing nanomaterials due to its unique structural properties, such as the uniform existence of mesopores (>2 and <50 nm), large pore volume, high specific surface area, and biocompatibility, which not only ensure highly homogeneous and reproducible immobilization of enzymes onto the biosensor electrode but also lead to large loading capacity for biocatalysts [20, 21]. Kim et al. reported highly sensitive glucose biosensors using enzymes immobilized in mesocellular carbon foam (MCF) [22]. To immobilize GOx with a molecular weight of ca. 160 kDa and with molecular dimensions of 5.2 nm × 6.0 nm × 7.7 nm, the OMC containing interconnected hollow cells with a diameter of ca. 30 nm was synthesized as foam. The loading density of GOx in MCF was about 4.7-fold higher than that in the activated carbon owing to the larger pore volume (Fig. 3a). As a result, the detection limit of glucose was about 0.07 mM and its dynamic range was extended up to ~2 mM (Fig. 3b) with a fast response time (less than 30 s after glucose addition). This was attributed to the effective transfer of substrate and products through MCF matrixes containing enzymes.

A mediator-free glucose sensor by the OMC–AuNP nanocomposite was demonstrated by Guo et al. [23]. They synthesized the AuNPs on OMC by a chemical reduction of gold seed ions via $NaBH_4$/sodium citrate. Thereafter, GOx was directly adsorbed on the nanocomposite-modified glassy carbon electrode. The surface coverage of the GOD/OMC–Au/GC electrode was calculated to be 2.99×10^{-9} mol cm^{-2}, which is much larger than that of the GOD/OMC/GC electrode (1.80×10^{-9} mol cm^{-2}). Also, the GOD/OMC–Au/GC electrode had better stability than the GOD/OMC/GC electrode, due to the good biocompatibility of the OMC–Au nanocomposites. Owing to this property, the nanocomposite-based glucose biosensor showed a linear range from 0.05 to 20.0 mM with good reproducibility and stability.

2.3 Gold Nanoparticle

A metallic nanoparticle (NP) with the appropriate dimensions and structures can serve as an excellent nanocollector and an electron relay to a macroelectrode when adjacent to the enzyme redox center. Willner et al. have been leading this field. They initially reported that improved electrical contacting of flavoenzymes was achieved by the surface-reconstitution of apo-GOx on a single gold nanoparticle (AuNP)-flavin adenine dinucleotide (FAD) unit, where a 1.4-nm AuNP was functionalized with FAD and then the FAD-AuNP was reconstituted with GOx [24]. The AuNP/FAD/GOx composite was assembled on an Au electrode functionalized with a 1,4-dimercaptoxylene monolayer, showing the denslely packed GOx monolayer (1×10^{-12} mol cm^{-2}). The electron transfer turnover rate of the reconstituted bioelectrocatalyst is $\sim$5,000 per second, compared with the rate at which molecular oxygen, the natural cosubstrate of the enzyme, accepts electrons ($\sim$700 per second). They emphasized the role of AuNP as an electrical nanoplug for the alignment of the enzyme on the conductive support.

Willner also demonstrated that this concept could be applied to the apo-GDH [25]. To construct an electrically contacted GDH electrode, the apo-GDH with PQQ-functionalized AuNPs (1.4 nm in diameter) was reconstituted on a Au electrode via 1,4-benzenedithiol bridges (Fig. 4). The electrical contacting of GDH by AuNPs was approximately 25-fold improved as compared to a system where polyaniline acts as the matrix for the electrical contacting of the reconstituted enzyme and the electrode support. When compared to that of the AuNP/FAD/GOx nanocomposite, the efficient electrical wiring of AuNP/PQQ/GDH led to the higher turnover rate (11,800 s^{-1}) between the enzyme and the electrode, suggesting that nonspecific oxidizable interfering compounds for biosensing of glucose would not significantly be considered because the oxidation of glucose by the PQQ-dependent GDH is known not to be affected by oxygen.

Intriguingly, it was reported by Kim et al. that the electrostatic binding of PQQ-incorporated GDH on an electrode was more efficient and easier in the fabrication of this enzymatic biosensor. It was revealed that the GDH glucose biosensor by electrostatic conjugation onto the self-assembled monolayers (SAMs) on the Au electrode gave rise to twofold higher detection sensitivity than that by covalent conjugation under the same condition, mainly due to the net charge of PQQ-GDH (pI $\sim$9.5). Thus, it is suggested that this enzyme should confer a strong electrostatic attraction to the carboxyl groups of SAM or AuNPs.

Willner et al. also described the biocatalytic growth of AuNPs by GOx and glucose [26]. By using a glucose sensor system, the catalytic growth of AuNPs was performed using $AuCl_4^-$ and H_2O_2 produced by the enzyme because numerous oxidases generated H_2O_2 upon the oxidation of the respective substrates by molecular O_2 (Fig. 5). Although the AuNPs exist in several morphologies (spheres, rhombs, triangles, and polygons) with a very narrow size distribution, 12 ± 1 nm, the absorbance values from the catalytically enlarged AuNPs increased as the concentration of glucose was elevated, enabling us to develop a new glucose biosensor based on the H_2O_2-mediated growth of the AuNPs.

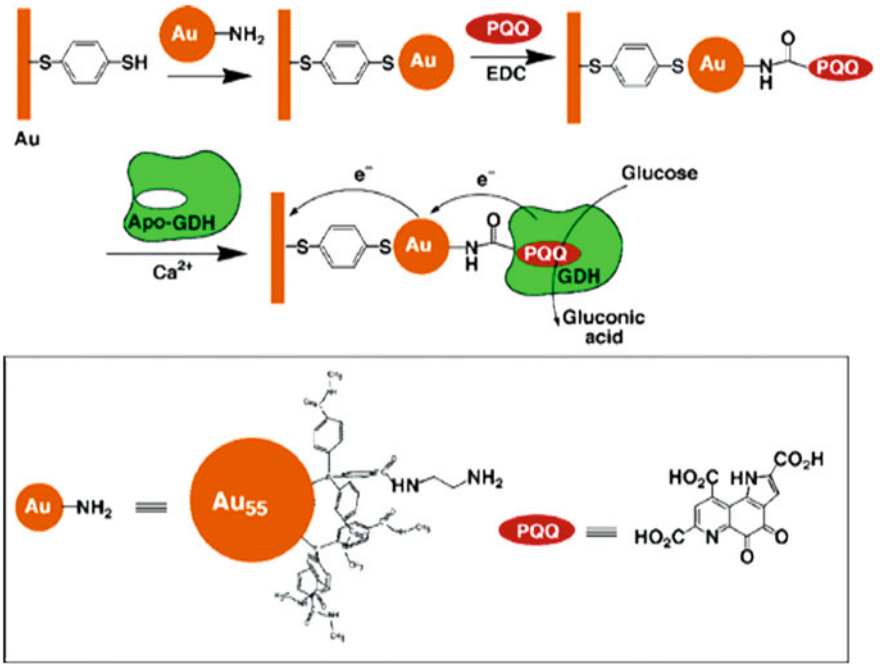

Fig. 4 Assembly of glucose dehydrogenase (GDH) reconstituted on the pyrroloquinoline quinone (PQQ)-functionalized gold (Au) nanoparticles associated with an Au electrode and the non-mediated electrical contacting of the enzyme. Adapted from [25] with permission

More recently, Stevens et al. developed the plasmonic nanosensors by means of GOx-mediated crystal growth [27]. This nanosensors are based on the localized surface plasmon resonance (LSPR), where GOx controls the rate of nucleation of silver nanocrystals on plasmonic transducers. That is, GOx generates hydrogen peroxide, which reduces silver ions to grow a silver coating around plasmonic nanosensors (gold nanostars): (i) At low concentrations of GOx the nucleation rate is slow, which favors the growth of a conformal silver coating that induces a large blueshift in the LSPR of the nanosensors; (ii) When GOx is present at high concentrations, the fast crystal growth conditions stimulate the nucleation of silver nanocrystals and less silver is deposited on the nanosensors, therefore generating a smaller variation of the LSPR. Therefore, this LSPR-generation step induces inverse sensitivity of GOx. By controlling the kinetics of crystal growth with an enzyme, this system opens up new opportunities and applications for biosensing.

2.4 Magnetic Nanoparticle

It is noteworthy that the combination of the OMC foams and nanostructured magnetic materials (NMMs) will facilitate a fast and reversible electrochemical

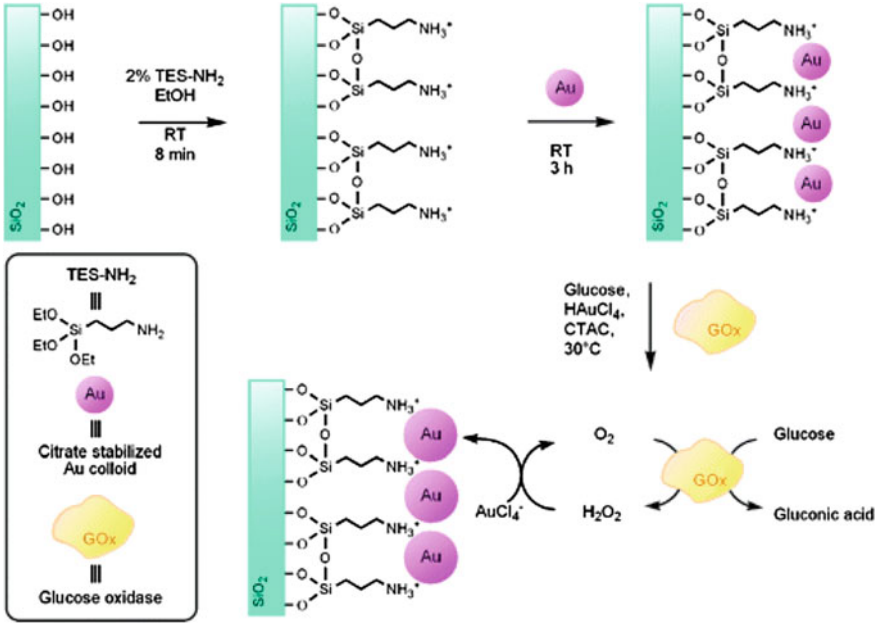

Fig. 5 Biocatalytic enlargement of gold (Au) nanoparticles by the glucose oxidase (GOx)-mediated oxidation of glucose on a glass support (*TES–NH_2*, 3-aminopropyltriethoxysilane). Adapted from [26] with permission

glucose biosensor. Kim et al. demonstrated that the OMC with embedded magnetic nanoparticles (MNPs) has the carbon structure and loading capacity, immobilization kinetics, and the stability for GOx similar to OMC forms, which was characterized by co-existence of three types of substructures: interconnected hollow spherical cells (diameter ca. 30 nm), channels (width ca. 6 nm) surrounding the cells, and micropores (width ca. 0.6 nm) present throughout the carbon framework [28]. Electron microscopy and analysis of the magnetic properties have revealed that ferromagnetic nanoparticles were generated and well distributed mainly on the exterior surface of magnetic OMC. A switchable glucose sensing system was made possible by GOx immobilized in the magnetic OMC and a diffusive ferrocene derivative (Fig. 6). By controlling the distance between the enzyme and the electrode using an external magnetic field, the mediated electron-transfer was able to be reversibly promoted or inhibited.

To further extend applications of the OMC-related materials, there seems to remain a need for the highly electroconductive materials so as to reach the most efficient electron-transfer reaction. For example, much faster reaction of enzyme-assembled electrodes would be attainable when using electrode-immobilized mediators, rather than using soluble free electron mediators. In this regard, co-immobilization of proper electron mediators with enzymes may enhance the performance of magnetic OMC-based glucose sensors.

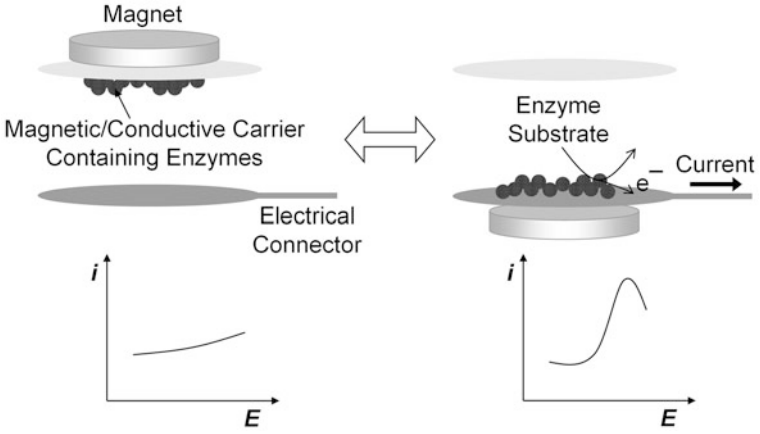

Fig. 6 Principle of the magnetically switchable electrochemical biosensing. Expected voltammetric results are also depicted schematically before (*left*) and after (*right*) applying a magnetic field to the working electrode

Cui et al. recently demonstrated a glucose biosensor based on poly(diallyldimethylammonium chloride) functionalized helical CNTs (PDDA-HCNTs) and magnetic electrodes [29]. An amperometric response to glucose by the developed GOx-functionalized PDDA-HCNTs was conducted on magnetic glass carbon electrode, which resulted in the excellent electrocatalytic activity and stability, with a linear range of glucose from 5 to 85 μM and a low detection limit of 0.72 μM at 3σ. Furthermore, the magnetic electrode has an advantage of eliminating the biofouling effect and of preventing the leaking loss of the enzyme. As an on–off bioelectrocatalytic glucose sensor, an MNP-assisted gate microelectrode was recently developed by Baker et al. [30]. As shown in Fig. 7, MNPs control reversibly the gate transport of an electroactive species (ferrocene) to the surface of the electrode in the center of single-coil microelectromagnetic traps; that is, GOx-modified MNPs were pulled on and off of the electrode surface by magnetite and the voltammetric response was recorded, which was proportional to the glucose concentration. It is anticipated that an MNP-modulated sensing system will be promising for developing on/off biosensors and drug delivery systems.

3 Enzymatic Fluorescent Detection of Glucose Using Nanomaterials

Although electrochemical sensors have taken up a large proportion of research and commercialized activity in glucose detection, fluorescence-based sensors can be used as an alternative. Fluorescence-based glucose sensors provide several advantages for in vivo continuous monitoring, due to the ability to optically see through the skin rather than having an electrode system implanted.

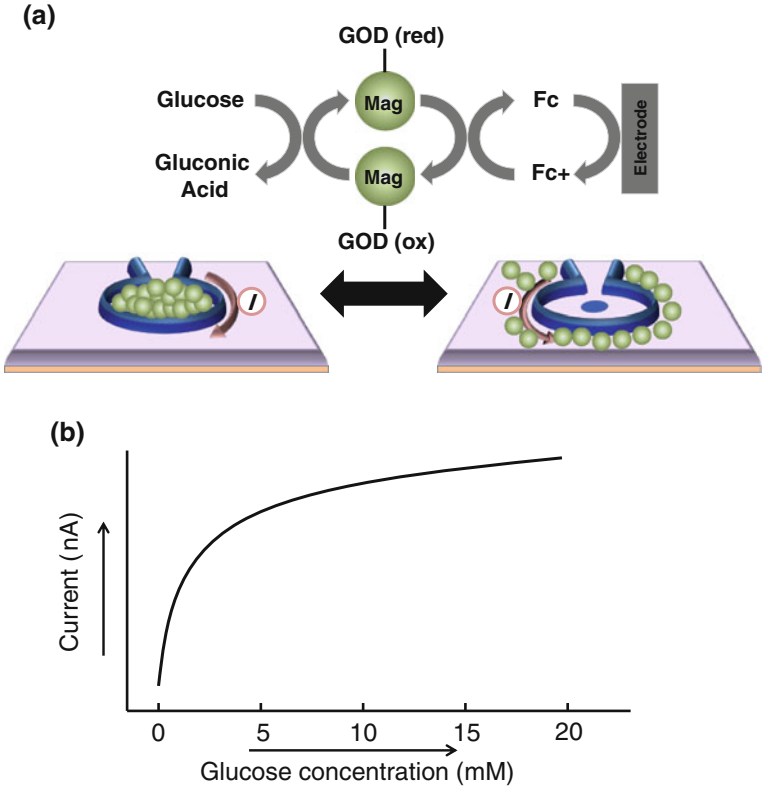

Fig. 7 **a** Schematic of mechanism of on/off ferrocene-mediated glucose detection. Glucose oxidase (GOx) is attached to magnetic particles that are pulled to the center of the coil. Various concentrations of glucose (0.5–20 mM), 0.5 mM ferrocene carboxylic acid, 50 mM phosphate, and 50 mM KCl buffer were used. When particles are at the coil periphery, the mediated reaction does not occur. **b** Glucose concentration is shown versus the limiting current measured

Initial work on the fluorescence-based detection of glucose was done by Trettnak and Wolfbeis [31], in which they examined changes in the intrinsic flavine fluorescence of glucose oxidase. Thereafter, it was reported that fluorophore-modified GOx was used for the detection of glucose by delayed energy transfer between the FAD and the fluorophore [32, 33]. However, a main hurdle in such research is that FAD fluorescence in response to glucose is too weak, making this system unsuitable for investigating a real monitoring system in many other interferences.

A convenient way of developing glucose sensors that involve measurements of fluorescence is to use a GOx-catalyzed reaction. During this process, oxygen consumption or hydrogen peroxide production can be monitored by fluorescent detection. For example, decacyclene (ex 385 nm, em 450–600 nm) and the ruthenium complex, tris(1,10-phenanthrolene)ruthenium chloride (ex 447 nm, em 604 nm), have been used as oxygen reactive materials in GOx-based glucose

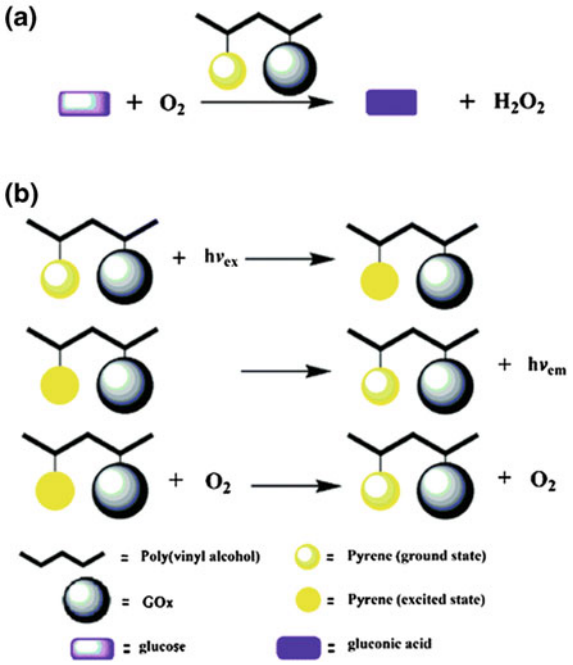

Fig. 8 Schematic representation of the mechanisms responsible for **a** glucose oxidation by the enzymatic reaction and **b** fluorescence emission and oxygen quenching of excited poly(vinyl alcohol)-pyrene-glucose oxidase (GOx). Adapted from [37] with permission

sensors, where their fluorescence is quenched by the oxygen [34, 35]. Rosenzweig et al. reported the fluorescence-based glucose sensors by using MNP/GOx and ruthenium phenanthroline fluorescent complex [36]. GOx was covalently attached using a cross-linking reagent (glutaraldehyde) to amino-modified magnetite (Fe_3O_4) NPs averaging 20 nm in diameter. The resulting GOx-coated magnetic particles had long-term stability (even for 3 months) and high enzymatic activity.

The Yagci et al. proposed the fluorescent glucose biosensor using the poly(vinyl alcohol)-pyrene-GOx (PVA-Py-GOx) having both fluorescent and oxidant sites in the structure [37]. Upon the consumption of glucose by GOx and dissolved O_2, the fluorescence intensity of pyrene groups of the probes was generated by the elimination of O_2. As a result, glucose concentration was analyzed quantitatively from 0.25 to 3.0 mM by the fluorescence measurement. The change in dissolved oxygen in the medium causes a quenching fluorescent intensity (Fig. 8).

As promising fluorescence-based glucose sensors, QDs have received great attention as a preferable material in enzyme-based biological analyses and applications, owing to their good optical characteristics, high catalytic effects, and high electron-transfer efficiency. Tang et al. demonstrated that a complex of CdTe QDs and GOx could be useful as a fluorescent nanosensor for the detection of glucose with high sensitivity [38]. When glucose was oxidized to gluconic acid and H_2O_2 in the presence of GOx, H_2O_2 was specifically reduced to O_2 on the surface of QDs via electron hole traps, resulting in fluorescence quenching (Fig. 9). The resultant O_2 was presumed to be further participated in the catalyzed

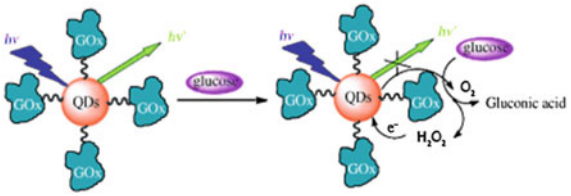

Fig. 9 Schematic illustration of the structure of the assembled CdTe quantum dots (QDs)–glucose oxidase (GOx) complex and its glucose-sensing principles. Adapted from [38] with permission

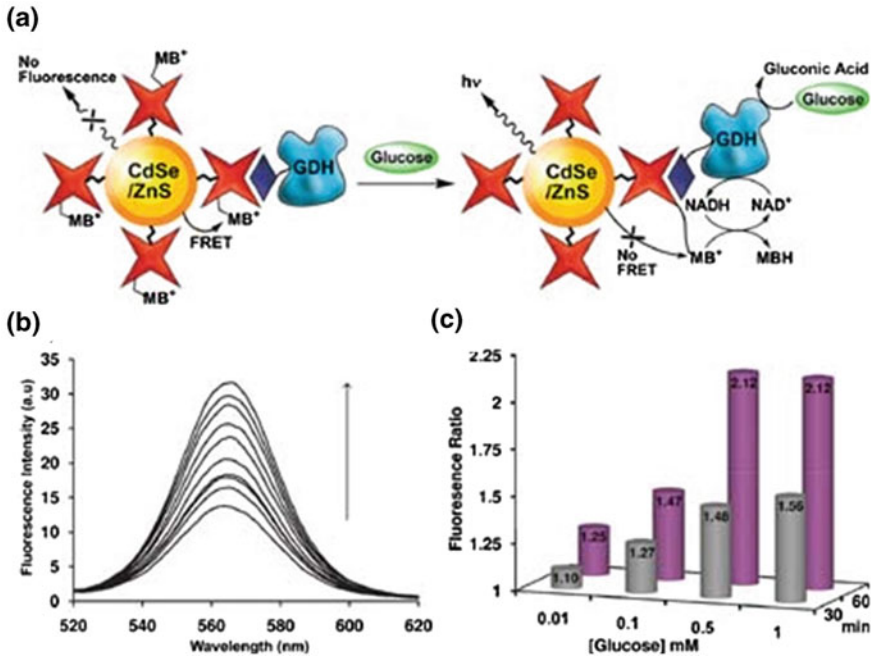

Fig. 10 **a** Sensing of glucose by the methylene blue (MB^+)-functionalized CdSe/ZnS quantum dots (QDs). **b** Time-dependent fluorescence changes upon the interaction of 0.5 mM glucose with the MBþ-functionalized QDs. Spectra were recorded at 6-min intervals. **c** Calibration curve corresponding to the optical analysis of different concentrations of glucose by the MB^+-functionalized QDs. Each sample was analyzed by reacting the functionalized QDs with different concentrations of glucose for two fixed time intervals of 30 and 60 min, respectively. *FRET*, Fluorescence resonance energy transfer; *GDH*, Glucose dehydrogenase; *NAD*, Nicotinamide adenine dinucleotide. Adapted from [40] with permission

reaction of GOx, producing a cyclic reaction of glucose oxidation. Therefore, the quenching efficiency of CdTe QDs increases as the glucose concentration increases. Compared to free GOx, GOx conjugated on the CdTe QDs showed the conformational changes in the process of assembly, leading to the considerably

enhanced enzyme activity. Not only that, the conjugated GOx remained active over a wide range of temperatures up to 80 °C, presumably due to the limited denaturation on the QD surface. This system, however, should be further validated to see whether one can eliminate many interfering species that affect the generation of O_2 and H_2O_2, which would not be easy, especially in real blood samples. By taking advantage of this principle, Li et al. constructed a layer-by-layer assembly consisting of CdTe QDs and GOx for the detection of glucose by using its fluorescence change [39]. Although this chip-based sensor is not reproducible, due to the partial recovery of fluorescence intensity under ambient conditions, this system has an advantage: it can be designed in an array format for rapid and high-throughput screening of blood glucose.

Similarly, Willner et al. developed an integrated hybrid system by combining NAD-dependent GDH with CdSe/ZnS QDs for the optical detection of glucose. QDs were functionalized with methylene blue (MB^+)-conjugated avidin via covalent linkage to a glutathione-protecting layer. Because MB^+ quenched the fluorescence of QD via a fluorescence resonance energy transfer (FRET) process, the production of NADH by glucose and NAD-GDH can reduce the MB^+, leading to the fluorescence activation of QDs (Fig. 10). When biotinylated GDH was associated with the complex of MB^+/avidin/QDs, the addition of glucose generated the fluorescent intensity, depending on its concentration; that is, higher glucose induced higher NADH and lower MB^+. However, this complicated nanoassembly is not validated in real blood samples and the free NAD^+ should be added to the reaction solution; therefore, this glucose-sensing system needs to be more optimized for high stability and reproducibility.

4 Summary, Conclusions, Outlook

Glucose sensing has an important place in the diagnosis and therapy of diabetes. In addition to medicinal applications, an advanced sensing system with online and in vivo monitoring properties is also desirable to control various food and biotechnological processes. Because enzymatic glucose reactions offer better selectivity in response to glucose rather than enzyme-free sensing, the combination of highly stable enzymes in association with glucose and nanomaterials is being harnessed at many stages of commercial and clinical implementation to achieve better performance of glucose-sensing systems. Although a variety of nanosensor technologies have been developed using both electrochemical and fluorescent methods, there is still a need to integrate such sensing systems with in vivo measurements. Implantation of electrochemical sensing chips and optical interrogation through the skin will be of great interest. In addition, a method to eliminate or reduce the need for patients to take blood samples is promising with the miniaturization of sensing systems for point-of-diagnosis in the future. Amplification strategies are another significant area in the development of enzymatic glucose biosensors, which can be possibly achieved by the incorporation of glucose-related enzymes or other detection molecules into nanomaterials.

Using the high-protein loading capacities of nanocarriers and co-immobilization with antibodies or avidin and multiple enzyme labels, the optical or electrochemical signals could be highly amplified, which will contribute to the detection of many metabolites with high sensitivity.

Acknowledgments This work was supported by the research fund of Hanyang University (HY-2012-G).

References

1. Heller A, Feldman B (2008) Electrochemical glucose sensors and their applications in diabetes management. Chem Rev 108(7):2482–2505
2. Yoo EH, Lee SY (2010) Glucose biosensors: an overview of use in clinical practice. Sens Basel 10(5):4558–4576
3. Chia CW, Saudek CD (2004) Glucose sensors: toward closed loop insulin delivery. Endocrin Metab Clin 33(1):175–195
4. Newman JD, Turner APF (2005) Home blood glucose biosensors: a commercial perspective. Biosens Bioelectron 20(12):2435–2453
5. Oliver NS, Toumazou C, Cass AEG, Johnston DG (2009) Glucose sensors: a review of current and emerging technology. Diabetic Med 26(3):197–210
6. Wang J (2008) Electrochemical glucose biosensors. Chem Rev 108(2):814–825
7. Sonksen PH, Judd SL, Lowy C (1978) Home monitoring of blood-glucose—method for improving diabetic control. Lancet 1(8067):729–732
8. Clark LC, Lyons C (1962) Electrode systems for continuous monitoring in cardiovascular surgery. Ann Ny Acad Sci 102(1):29–45
9. Updike SJ, Hicks GP (1967) The enzyme electrode. Nature 214(5092):986–988
10. Dcosta EJ, Higgins IJ, Turner APF (1986) Quinoprotein glucose-dehydrogenase and its application in an amperometric glucose sensor. Biosensors 2(2):71–87
11. Cletonjansen AM, Goosen N, Fayet O, Vandeputte P (1990) Cloning, mapping, and sequencing of the gene encoding escherichia-coli quinoprotein glucose-dehydrogenase. J Bacteriol 172(11):6308–6315
12. Yamada M, Elias MD, Matsushita K, Migita CT, Adachi O (2003) Escherichia coli PQQ-containing quinoprotein glucose dehydrogenase: its structure comparison with other quinoproteins. BBA Proteins Proteom 1647(1–2):185–192
13. Iswantini D, Kano K, Ikeda T (2000) Kinetics and thermodynamics of activation of quinoprotein glucose dehydrogenase apoenzyme in vivo and catalytic activity of the activated enzyme in *Escherichia coli* cells. Biochem J 350:917–923
14. Oubrie A, Rozeboom HJ, Kalk KH, Olsthoorn AJJ, Duine JA, Dijkstra BW (1999) Structure and mechanism of soluble quinoprotein glucose dehydrogenase. Embo J 18(19):5187–5194
15. Besteman K, Lee JO, Wiertz FGM, Heering HA, Dekker C (2003) Enzyme-coated carbon nanotubes as single-molecule biosensors. Nano Lett 3(6):727–730
16. Patolsky F, Weizmann Y, Willner I (2004) Long-range electrical contacting of redox enzymes by SWCNT connectors. Angew Chem Int Edit 43(16):2113–2117
17. Davis JJ, Coleman KS, Azamian BR, Bagshaw CB, Green MLH (2003) Chemical and biochemical sensing with modified single walled carbon nanotubes. Chem-Eur J 9(16): 3732–3739
18. Joshi PP, Merchant SA, Wang YD, Schmidtke DW (2005) Amperometric biosensors based on redox polymer-carbon nanotube-enzyme composites. Anal Chem 77(10):3183–3188
19. Jia W, Jin C, Xia W, Muhler M, Schuhmann W, Stoica L (2012) Glucose oxidase/horseradish peroxidase Co-immobilized at a CNT-modified graphite electrode: towards potentially implantable biocathodes. Chem-Eur J 18(10):2783–2786

20. Cao HM, Sun XM, Zhang Y, Hu CY, Jia NQ (2012) Electrochemical sensing based on hemin-ordered mesoporous carbon nanocomposites for hydrogen peroxide. Anal Methods UK 4(8):2412–2416
21. Ryoo R, Joo SH, Jun S (1999) Synthesis of highly ordered carbon molecular sieves via template-mediated structural transformation. J Phys Chem B 103(37):7743–7746
22. Lee D, Lee J, Kim J, Kim J, Na HB, Kim B, Shin CH, Kwak JH, Dohnalkova A, Grate JW, Hyeon T, Kim HS (2005) Simple fabrication of a highly sensitive and fast glucose biosensor using enzymes immobilized in mesocellular carbon foam. Adv Mater 17(23):2828–2833
23. Wang LX, Bai J, Bo XJ, Zhang XL, Guo LP (2011) A novel glucose sensor based on ordered mesoporous carbon-Au nanoparticles nanocomposites. Talanta 83(5):1386–1391
24. Xiao Y, Patolsky F, Katz E, Hainfeld JF, Willner I (2003) "Plugging into enzymes": nanowiring of redox enzymes by a gold nanoparticle. Science 299(5614):1877–1881
25. Zayats M, Katz E, Baron R, Willner I (2005) Reconstitution of apo-glucose dehydrogenase on pyrroloquinoline quinone-functionalized Au nanoparticles yields an electrically contacted biocatalyst. J Am Chem Soc 127(35):12400–12406
26. Zayats M, Baron R, Popov I, Willner I (2005) Biocatalytic growth of Au nanoparticles: from mechanistic aspects to biosensors design. Nano Lett 5(1):21–25
27. Rodriguez-Lorenzo L, de la Rica R, Alvarez-Puebla RA, Liz-Marzan LM, Stevens MM (2012) Plasmonic nanosensors with inverse sensitivity by means of enzyme-guided crystal growth. Nat Mater 11(7):604–607
28. Lee J, Lee D, Oh E, Kim J, Kim YP, Jin S, Kim HS, Hwang Y, Kwak JH, Park JG, Shin CH, Kim J, Hyeon T (2005) Preparation of a magnetically switchable bioelectrocatalytic system employing cross-linked enzyme aggregates in magnetic mesocellular carbon foam. Angew Chem Int Edit 44(45):7427–7432
29. Cui RJ, Han ZD, Pan J, Abdel-Halim ES, Zhu JJ (2011) Direct electrochemistry of glucose oxidase and biosensing for glucose based on helical carbon nanotubes modified magnetic electrodes. Electrochim Acta 58:179–183
30. Basore JR, Lavrik NV, Baker LA (2012) Magnetically gated microelectrodes. Chem Commun 48(7):1009–1011
31. Trettnak W, Wolfbeis OS (1989) Fully reversible fibre-optic glucose biosensor based on the intrinsic fluorescence of glucose-oxidase. Anal Chim Acta 221(2):195–203
32. de Marcos S, Galindo J, Sierra JF, Galban J, Castillo JR (1999) An optical glucose biosensor based on derived glucose oxidase immobilised onto a sol–gel matrix. Sensor Actuat B Chem 57(1–3):227–232
33. Sierra JF, Galban J, De Marcos S, Castillo JR (2000) Direct determination of glucose in serum by fluorimetry using a labeled enzyme. Anal Chim Acta 414(1–2):33–41
34. Xu H, Aylott JW, Kopelman R (2002) Fluorescent nano-PEBBLE sensors designed for intracellular glucose imaging. Analyst 127(11):1471–1477
35. Rosenzweig Z, Kopelman R (1996) Analytical properties and sensor size effects of a micrometer-sized optical fiber glucose biosensor. Anal Chem 68(8):1408–1413
36. Rossi LM, Quach AD, Rosenzweig Z (2004) Glucose oxidase-magnetite nanoparticle bioconjugate for glucose sensing. Anal Bioanal Chem 380(4):606–613
37. Odaci D, Gacal BN, Gacal B, Timur S, Yagci Y (2009) Fluorescence sensing of glucose using glucose oxidase modified by PVA-pyrene prepared via "click" chemistry. Biomacromolecules 10(10):2928–2934
38. Cao LH, Ye J, Tong LL, Tang B (2008) A new route to the considerable enhancement of glucose oxidase (GOx) activity: the simple assembly of a complex from CdTe quantum dots and GOx, and its glucose sensing. Chem-Eur J 14(31):9633–9640
39. Li XY, Zhou YL, Zheng ZZ, Yue XL, Dai ZF, Liu SQ, Tang ZY (2009) Glucose biosensor based on nanocomposite films of CdTe quantum dots and glucose oxidase. Langmuir 25(11):6580–6586
40. Bahshi L, Freeman R, Gill R, Willner I (2009) Optical detection of glucose by means of metal nanoparticles or semiconductor quantum dots. Small 5(6):676–680

Adv Biochem Eng Biotechnol (2014) 140: 221–251
DOI: 10.1007/10_2013_228

Published Online: 5 July 2013

Cascadic Multienzyme Reaction-Based Electrochemical Biosensors

Yong Duk Han, Yo Han Jang and Hyun C. Yoon

Abstract Since the first glucose biosensor was developed by Clark and Lyons, there have been great efforts to develop effective enzyme biosensors for wide applications. Those efforts are closely related to the enhancement of biosensor performance, including sensitivity improvement, elevation of selectivity, and extension of the range of analytes that may be determined. Introduction of a cascadic multienzyme reaction to the electrochemical biosensor is one of those efforts. By employing more than two enzymes to the biosensor, its sensitivity and accuracy can be enhanced. Also, the narrow application range that is a typical limitation of single enzyme-based biosensor can be overcome. This chapter will discuss the fundamental principles for the development of cascadic multienzyme reaction-based electrochemical biosensors and their applications in clinical and environmental fields.

Keywords Biosensors · Cascadic multienzyme reaction · Coupled enzyme assay · Electrochemical analysis · Enzyme electrode

Abbreviations

ACh	Acetylcholine
AChE	Acetylcholine esterase
ALT	Alanine transaminase
ALP	Alkaline phosphatase
AST	Aspartate transaminase
AuNP	Gold nanoparticle
BS^3	Bis(sulfosuccinimidyl) suberate
CE	Cholesterol esterase
Ch	Choline
ChOx	Choline oxidase
CK	Creatine kinase

Y. D. Han · Y. H. Jang · H. C. Yoon (✉)
Department of Applied Chemistry and Biotechnology and Department of Molecular Science and Technology, Ajou University, Suwon 443-749, Republic of Korea
e-mail: hcyoon@ajou.ac.kr

CNT	Carbon nanotube
CO	Cholesterol oxidase
Cyt-c	Cytochrome complex
DAP	Diaphorase
GA	Glutaraldehyde
GalDH	Galactose dehydrogenase
GOx	Glucose oxidase
G3PO	Glycerol-3-phosphate oxidase
HRP	Horseradish peroxidase
LDH	Lactate dehydrogenase
MP	Magentic microparticle
MWCNT	Multi-walled carbon nanotube
NAD	Nicotinamide adenine dinucleotide (oxidized)
NADH	Nicotinamide adenine dinucleotide (reduced)
NHS	N-hydroxysuccinimide ester
OAC	Oxaloacetate decarboxylase
OP	Organophosphorous
PANI	Polyaniline
p-AP	p-Aminophenol
PASA	Polyaniline sulfonic acid
PDMS	Polydimethylsiloxane
PLL	Poly-L-lysine
POx	Pyruvate oxidase
PPY	Polypyrrole
p-QI	p-Quinonimine
SAM	Self-assembled monolayer
SO	Sulfite oxidase

Contents

1 Introduction

Curiosity and the desire to understand the composition of certain objects have been strong driving forces for advances in analytical science. As the scientific knowledge about physics, chemistry, and biology has grown, analytical chemists and biochemists have developed various analytical methods to detect the amounts of biochemical components in complex systems such as the human body. Those analytical methods for chemical or biochemical assays have been performed in professional laboratories and facilities by experts using additional equipment. Rationally, we have sought more convenient and efficient biochemical assay methods that require minimal professional skills and equipment. These needs triggered the development of a brand-new analytical methodology: the biosensor [1].

A biosensor can be generally defined as an analytical device that is composed of a biological recognition part (the so-called bioreceptor) and a physico-chemical transducer to convert an observed biospecific response into a measurable signal whose intensity is proportional to the concentration of a target analytes. Briefly, biosensors can be classified as affinity biosensors and catalytic biosensors. In affinity biosensors, biomolecules having target-specific binding capabilities—such as antibodies, oligonucleotides, and cellular receptors—are used as bioreceptor elements. If the target analytes are composed of protein or oligonucleotide, one can select an affinity biosensor for an assay. In catalytic biosensors, enzymes possessing a biocatalytic activity with target analytes are employed as a bioreceptor element. Generally, this catalytic biosensor is used in detection of non-protein biochemical metabolites.

According to the utilized transducer type, biosensors also can be divided into several groups such as electrochemical, optical, piezoelectric, and calorimetric biosensors [1–5]. Among these various transducing strategies, electrochemical transducers are most widely used as biosensors due to their cost efficiency, operation convenience, good portability, and simplicity of construction. Also, the electrochemical transducer (especially an amperometric transducer) can be easily combined with catalytic bioreceptors (enzymes) generating bioelectro-catalytic signals when the target analytes recognized [2–4]. Figure 1 shows a scheme of a typical amperometric enzyme biosensor principle.

Since the first glucose biosensor using a catalytic biosensing concept was introduced by Clark and Lyons in 1962 [6], many researchers have struggled to develop efficient and sensitive enzyme-based electrochemical biosensors that can be applied to various fields, such as healthcare [1–3, 7–11], environmental monitoring [12–18], food analysis [16–18], and bioreactor monitoring [19]. By these efforts, there has been an explosive growth of research activities in the biosensor development area. Although there were huge advances in the academic fields, few commercially successful biosensor products exist, except for the blood-glucose biosensor in the industrial field [8].

Commercialized glucose biosensors employ an amperometric enzyme electrode as a biosensing platform. On the amperometric enzyme electrode, the enzyme–

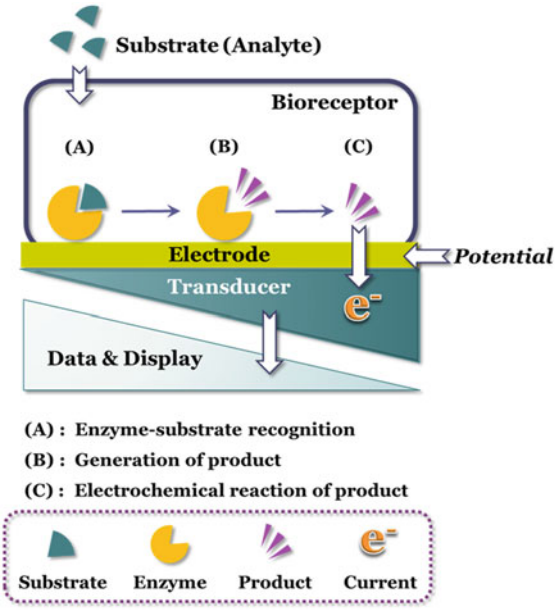

Fig. 1 Schematic illustration of a typical amperometric enzyme biosensor

substrate biocatalytic reaction results in an alteration of redox-active species concentrations. During an appropriate electric potential applied to the electrode, oxidation or reduction of these redox-active species generates measurable current whose magnitude has a stoichiometric relationship to the concentration of the analyte [7, 8]. The success of this glucose biosensor was affected by its comparably simple electrocatalytic reaction principle that requires only one redox enzyme to measure the concentration of blood glucose. Unfortunately, many analytes in nature require more complicated enzymatic assay methods involving more than two enzymes. Only a few enzymes that have the ability to directly generate or consume electroactive species. These limited numbers of analytes can be measured by a mono-enzymatic biosensor and thus hinder the expansion of biosensor applications [20].

To overcome this limitation, introduction of cascadic multienzyme-modified electrodes that couple the bioelectrocatalytic activities of different enzymes in a sequential manner should be considered [20, 21]. For instance, determination of triglycerides in serum sample cannot be achieved by using a monoenzymatic assay method because there is no enzyme that can directly oxidize the analytes and produce electroactive substances. However, triglycerides can be hydrolyzed into fatty acids and glycerol by the enzyme reaction of lipase. Sequentially, by using a glycerol kinase (GK) reaction, the generated glycerol is converted into glycerol-3-phosphate that can be oxidized by glycerol-3-phosphate oxidase (G3PO). Based on this three-enzyme involved cascadic reaction, triglycerides can be electrochemically determined [22].

This cascadic multienzyme-involved biosensing strategy provides not only an expansion of the biosensor application range but also an enhancement of the selectivity and sensitivity of the biosensor. To analyze the very low concentrations of target analytes, enhancement of enzymatic biosensor sensitivity is required. In this regard, Wollenberger et al. suggested a multienzyme system employing the recycling of substrates and electroactive species [20]. For example, a very sensitive measurement of glutamate has to be accomplished by employing an enzyme-modified carbon electrode that is comprised of glutamate dehydrogenase and alanine aminotransferase [23]. On the bienzyme-modified electrode, a sequential enzyme reaction allows the recycling and regeneration of the glutamate, a target analyte, and it provides amplified electrochemical signals that guarantee higher sensitivity. As discussed previously, the employment of cascadic multienzyme reactions to the electrochemical biosensor offers great advances to its sensitivity and extended usage to industrial fields. This chapter reviews the principles of the development of multienzyme-based electrochemical biosensors and their practical applications in various fields.

2 Basic Principles of the Development of Cascadic Multienzyme Reaction-Based Electrochemical Biosensors

Simply, the multienzyme-modified electrochemical biosensor might be considered as extra enzyme reactions added to the mono-enzymatic electrochemical biosensor. However, the practical realization of multienzyme reaction-involved biosensor demands more complicated conditions, such as appropriate strategy selections for immobilization and arrangement of different enzymes on the electrode, diffusion controls of substrate products in multienzyme-modified layers, adjustments of different enzyme activities, and electrochemical signaling efficiencies. On the basis of these considerations, this section will consider some essential knowledge for the development of cascadic multienzyme-modified electrochemical biosensor including (1) the kinds of analytes that require a cascadic multienzyme reaction-based assay method and their multienzyme reaction mechanisms, (2) electrochemical signaling principles, and (3) multienzyme immobilization strategies.

2.1 Cascadic Multienzyme Reaction for Enzymatic Analysis

From the 1960s, a full-scale analytical use of enzymes began, especially in the medical analysis field, and their accumulated experience has influenced other industrial fields, such as food analysis and environmental analysis [24].

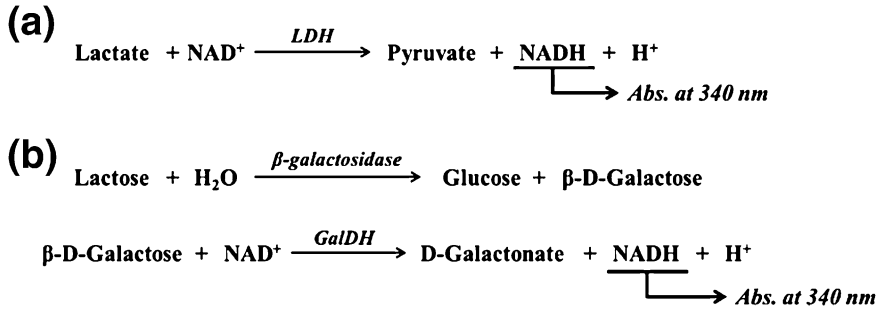

Scheme 1 Examples of conventional enzymatic analytical method. **a** Monoenzymatic assay for lactate determination. **b** Coupled enzymatic assay for lactose determination

In the most frequently used enzymatic analytical methods, stoichiometric measurements of targeted enzyme-substrate reactions are achieved by spectrophotometric observation of the optical density alterations of cofactors such as $NAD(P)^+$ or NAD(P)H, which are involved during enzyme-substrate reactions. For example, the determination of pyruvate involves the reaction of lactate dehydrogenase (LDH) and nicotinamide adenine dinucleotide (reduced; NADH) as shown in Scheme 1a.

By the LDH reaction, pyruvate is converted into lactate in the presence of NAD^+, and NAD^+ is reduced to NADH. By reading the appearance of NADH by an ultraviolet and visible absorption spectrophotometer, concentrations of pyruvate can be determined. When the target analytes have no adequate enzymes to directly catalyze them with cofactor-involving reactions, additional enzymes are employed to convert the target analytes into an accessible form that can be catalyzed by adequate cofactor-dependent enzymes. This enzymatic method, based on the coupling of conversion purpose-enzymes and indication-purpose enzymes, is called *coupled enzymatic assay* [24–27]. The measurement of lactose, for instance, can be accomplished by employing cascadic bienzyme reactions of *β*-galactosidase and galactose dehydrogenase (GalDH), as given in Scheme 1b. To our best knowledge, there is no redox enzyme (oxidase or dehydrogenase) that directly reacts with lactose and generates signals. However, a coupled enzyme reaction enables the lactose determination. By the reaction of *β*-galactosidase as a conversion-purposed enzyme, lactose is decomposed into glucose and galactose. In the presence of NAD^+, GalDH is employed as an indicating enzyme converts galactose into galacturonic acid. During the indication-purposed enzyme reaction, NAD^+ is reduced into NADH. Finally, the measured optical density of appeared NADH reflects the concentration of lactose in tested samples. A number of such coupled enzymatic assay methods for various analyte determinations are listed by Rudolph et al. [27] and some important analytes are listed in Table 1.

As shown in Table 1, many biochemicals require coupled enzymatic assay methods to be measured. The concept and principle of these coupling enzyme assay methods provide important clues to the development of cascadic-multienzymatic

Table 1 Examples of coupled enzyme assays

Target analyte	Coupling enzymes	Indication
Aspartate	AST, MDH	Disappearance of NADH
Alanine	ALT, LDH	Disappearance of NADH
Fructose	Hexokinase, G6PD	Formation of NADPH
Citrate	Citrate lyase, LDH or MDH	Disappearance of NADH
Creatine	CK, PK, LDH	Formation of NADH
Glycerol	GK, PK, LDH	Formation of NADH
TG	Lipase, GK, PK, LDH	Formation of NADH
ATP	Hexokinase, G6PD	Disappearance of NADPH
ADP	PK, G6PD	Disappearance of NADPH

electrochemical biosensors. First, most indicating enzymes used in coupled enzymatic assays are redox enzymes, and those are also essential components of electrochemical biosensors for bioelectrocatalytic signaling. The only difference between coupled enzymatic assays and electrochemical enzymatic biosensors is the type of redox enzymes that are frequently used in indication and signaling. In the case of traditional coupled enzymatic assays, $NAD(P)^+$ and NAD(P)H-dependent enzymes are predominantly used for optical indications. Contrary to this, enzymatic electrochemical biosensors employ the oxidase type of enzymes, using oxygen as an electron acceptor for signaling. Therefore, for the implantation of coupled enzyme reactions to an electrochemical biosensor, adjustment and modification of $NAD(P)^+$ and NAD(P)H-dependent enzyme couples into the type of enzyme couples to enable easy and efficient signaling should be considered [28]. A number of examples of enzyme couples that can be applied in a multienzymatic electrochemical biosensor are listed in Table 2.

As shown in Table 2, the cascadic enzyme reaction couples employed in a multienzymatic electrochemical biosensor can be briefly classified into two categories: non-redox enzyme/redox enzyme couple and redox enzyme/redox enzyme couple [29]. In the cascadic reaction of non-redox enzyme/redox enzyme couple, non-redox enzymes convert the analytes into a certain form that can be oxidized by the following redox enzyme reaction. As a non-redox enzyme, any possible enzymes such as kinase, transferase, invertase, and hydrolase can be employed for an analyte conversion reaction. For instance, maltose can be measured by using glucosidase-glucose oxidase (GOx) coupled reaction. Glucosidase hydrolyzes maltose into glucose that can be oxidized by GOx. Cascadic enzyme reactions of these non-redox and redox enzyme couples produce hydrogen peroxide (or reduced electron transferring mediators) as an electroactive product. By the electrochemical oxidation (or reduction) of these electroactive products, electrochemical signals can be generated on the electrode. This type of enzyme reaction is frequently used for determination of target analytes that have no directly related redox enzymes. Appropriate selection of these types of enzyme couples gives a strong chance to extend the biosensor application ranges. The schematic illustrations of non-redox enzyme and redox enzyme coupling reaction are depicted in Fig. 2a.

Table 2 Examples of enzyme couples used in multienzymatic electrochemical biosensors

Target analyte	Enzyme coupling type	Involved enzymes	Enzyme reaction mechanism
Ethanol	Redox/redux	AOx, HRP	$\text{Ethanol} + O_2 \rightarrow (\text{AOx}) \rightarrow \text{Acetaldehyde} + H_2O$ $2H_2O_2(\text{HRP}) \rightarrow H_2O$
Glucose	Redox/redox	GGx, HRP	$\text{Glucose} + O_2 \rightarrow (\text{GOx}) \rightarrow \text{Gluconic acid} + H_2O_2$ $2H_2O_2 \rightarrow (\text{HRP}) \rightarrow H_2O$
L-lactate	Redox/redox	LDH, DAP	$\text{L}-\text{Lactate} + NAD^+ \rightarrow (\text{LDH}) \rightarrow \text{Oxaloacetate} + \text{NADH} + H^+$ $\text{NADH} + H^+ \rightarrow (\text{DAP}) \rightarrow NAD^+$
L-malate	Redox/redox	MDH, DAP	$\text{L}-\text{Malate} + NAD^+ \rightarrow (\text{MDH}) \rightarrow \text{Oxaloacetate} + \text{NADH} + H^+$ $\text{NADH} + H^+(\text{DAP}) \rightarrow NAD^+$
β-D-glucan	Non-redox/redox/ redox	β-Glucanase, GGx, HRP	$\beta\text{-D-Glucan} + H_2O \rightarrow (\beta\text{-glucanase}) \rightarrow \beta\text{-D-Glucose} + H_2O$ $\beta\text{-D-Glucose} + O_2 \rightarrow (\text{GOx}) \rightarrow \text{Gluconic acid} + H_2O_2$ $2H_2O_2 \rightarrow (\text{HRP}) \rightarrow H_2O$
ACh	Non-redox/redox	AChE, ChOx	$\text{ACh} + H_2O \rightarrow (\text{AChE}) \rightarrow \text{Acetic acid} + \text{Ch}$ $\text{Ch} + O_2 \rightarrow (\text{ChOx}) \rightarrow \text{Betain} + H_2O_2$
Arginine	Non-redox/redox	Arginase 1, urease	$\text{L-Arginine} + H_2O \rightarrow (\text{Arginase I}) \rightarrow \text{L-Ornitine} + \text{Urea}$ $\text{Urea} + 2H_2O + H^+ \rightarrow (\text{Urease}) \rightarrow 2NH_4^+ + HCO_3^-$
ALT	Non-redox/redox	POx	$\text{ALA} + \alpha\text{-Ketoglutarate} \rightarrow (\text{ALT}) \rightarrow \text{Glutamate} + \text{Pyruvate}$ $\text{Pyruvate} + O_2 + H_2PO_4^- \rightarrow (\text{POx}) \rightarrow \text{Acetylphosphate} + H_2O_2$
AST	Non-redox/redox	OAC, POx	$\text{ASP} + \alpha\text{-Ketoglutarate} \rightarrow (\text{AST}) \rightarrow \text{Glutamate} + \text{Oxaloacetate}$ $\text{Oxaloacetate} \rightarrow (\text{OAC}) \rightarrow \text{Pyruvate} + CO_2$ $\text{Pyruvate} + O_2 + H_2PO_4^- \rightarrow (\text{POx}) \rightarrow \text{Acetylphosphate} + H_2O_2$
ATP	Non-redox/redox	GK, G3PO	$\text{Glycerol} + \text{ATP} \rightarrow (\text{GK}) \rightarrow \text{Glycerol-3-phosphate} + \text{ADP}$ $\text{Glycerol-3-phosphate} + O_2 \rightarrow (\text{G3PO}) \rightarrow \text{Dihydroxyacetone phosphate} + H_2O_2$

(continued)

Table 2 (continued)

Target analyte	Enzyme coupling type	Involved enzymes	Enzyme reaction mechanism
Total cholesterol	Non-redox/redox	CE, CO	Cholesterol ester → (CE) → Cholesterol + Fatty acid Cholesterol + O_2 → (CO) → Cholestenone + H_2O_2
Creatine	Non-redox/redox	CI, SOx	Creatine + H_2O → (CI) → Sarcosine + Urea Sarcosine + H_2O + O_2 → (SOx) → Formaldehyde + Glycine + H_2O_2
Creatinine	Non-redox/redox	CA, CI, SOx	Creatinine + H_2O → (CA) → Creatine Creatine + H_2O → (CI) → Sarcosine + Urea Sarcosine + H_2O + O_2 (SOx) → Formaldehyde + Glycine + H_2O_2
Glycerol	Non-redox/redox	GK, G3PO	Glycerol + AFP → (GK) → Glycerol-3-phosphate + ADP Glycerol-3-phosphate + O_2 → (G3PO) → Dihydroxyacetone phosphate + H_2O_2
D-lactosc	Non-redox/redox	β-Galactosldase, GalOx, GOx	D - Lactose + H_2O → (β-Galactosidase) → β-D-Glucose + D-Galactose β-D-Glucose + O_2 → (GOx) → Gluconic acid + H_2O_2 D-Galactose + O_2 → (GalOx) → Galactohexodialdose + H_2O_2
Sucrose	Non-redox/redox	Invertase, mutarotase, GOx	Sucrose + H_2O → (Invertase) → β-D-Glucose + Fructose α-D-Glucose → (Mutarotase) → β-D-Glucose β-D-Glucose + O_2 → (GOx) → Gluconic acid + H_2O_2
TG	Non-redox/redox	Lipase, GK, G3PO	TG + H_2O → (Lipase) → Fatty acid + Glycerol Glycerol + ATP → (GK) → Glycerol-3-phosphate + ADP Glycerol-3-phosphate + O_2 → (G3PO) → Dihydroxyacetone phosphate + H_2O_2

AChE Acetylcholine esterase; *AOx* Alcohol oxidase; *CA* Creatinine amidohydrolase; *CE* Cholesterol esterase; *ChOx* Choline oxidase; *CI* Creatine amidinohydrolase; *CO* Cholesterol oxidase; *DAP* Diaphorase; *G3PO* Glycerol-3-phosphate oxidase; *GalOx* Galactose oxidase; *GK* Glycerol kinase; *GOx* Glucose oxidase; *HRP* Horseradish peroxidase; *LDH* Lactate dehydrogenase; *MDH* Malate dehydrogenase; *OAC* Oxaloacetate decarboxylase; *POx* Pyruvate oxidase; *SOx* Sarcosine oxidase

The other cascadic enzyme reaction used in enzymatic biosensor is the redox enzyme/redox enzyme coupling reaction. In the cascadic reaction of the redox enzyme/redox enzyme couple, a primary redox enzyme reacts with a target analyte in the presence of electron acceptor (or donor) molecules, such as oxygen, and produces oxidized substrate and reduced (or oxidized) electroactive species, such as hydrogen peroxide. A secondary redox enzyme oxidizes the produced electroactive species and generates an electrochemical signal on the electrode [29]. This enzyme coupling of a redox enzyme is generally used for the enhancement of sensitivity and accuracy. For example, redox enzymes such as GOx can be combined with a peroxidase such as horseradish peroxidase (HRP). The oxidase-substrate reaction yields an oxidized substrate and hydrogen peroxide by oxygen involved in the electron transferring reaction. Sequentially, the oxidation of hydrogen peroxide by HRP occurs and it initiates generation of an electrochemical signal on the electrode. The electrochemical signaling of HRP-induced hydrogen peroxide oxidation can be accomplished under a relatively low potential range that can prevent signal interference by the overpotential of ascorbic acid, uric acid, and acetaminophen [30].

Similar to the oxidase–peroxidase couple, NAD^+-dependent dehydrogenase such as LDH can be coupled with diaphorase (DAP), which oxidizes NADH. As a result of the dehydrogenase-analytes reaction, oxidized substrates and NADH are generated. DAP re-oxidizes NADH into NAD^+ and generates electrochemical signals on the electrode. In this case, the employed DAP reaction efficiently recycles NAD^+/NADH and finally provides an amplified electrochemical signal [31]. In both cases, a secondary redox enzyme reaction can be combined with appropriate electron transferring mediators to provide an amplified signal, as will be discussed in the next section. The reaction schemes of the oxidase-HRP couple and dehydrogenase-DAP couple are illustrated in Fig. 2b, c respectively.

As a minor case, the determination of the enzyme itself in the sample can be considered. When the target analyte is a certain enzyme form, its own reaction and related substrate should be induced on the appropriate oxidase-modified electrode. In this case, careful preparations of conditions for the enzyme-substrate reaction, such as substrate solution and pre-reaction time, are required. For example, alanine transaminase (ALT) quantification can be achieved by using a pyruvate oxidase (POx)-modified electrode [32]. In the presence of α-ketoglutarate and alanine, ALT produces pyruvate as an oxidizable product in the solution phase. After the pre-reaction solution is applied to the POx-modified electrode, electrochemical signals can be registered by the POx-pyruvate reaction.

According to the target analytes, the non-redox enzyme/redox enzyme couple and redox enzyme/redox enzyme couple can be mixed and used for biosensing. For example, GK, G3PO, and HRP involving a cascadic multienzyme reaction are employed to quantify creatine kinase (CK) concentrations in serum. In this case, GK takes the conversion reaction and the G3PO-HRP couple performs the coupled redox enzyme reaction [33].

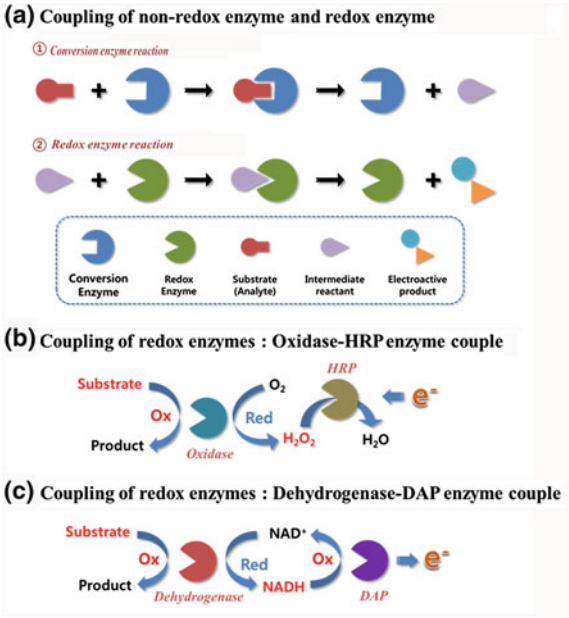

Fig. 2 Types of cascadic multienzyme reactions. **a** Cascadic reaction of non-redox enzyme and redox enzyme couple. **b** Cascadic reaction of oxidase-HRP enzyme couple. **c** Cascadic reaction of dehydrogenase-DAP enzyme couple. *DAP*, Diaphorase; *HRP*, Horseradish peroxidase

2.2 *Principles of the Electrochemical Signaling in a Cascadic Multienzymatic Electrochemical Biosensor*

The electrochemical signaling of an enzymatic electrochemical biosensor is mainly dependent on the reaction of redox enzymes with their corresponding substrate. In this section, principles of bioelectrocatalytic signaling using redox enzymes on the electrochemical biosensing surface will be discussed.

As described in the previous section, for the generation of electrochemical signals, most catalytic biosensors employ redox enzymes, such as oxidases, which produce hydrogen peroxide and dehydrogenases that produce NAD(P)H during the course of catalytic reaction with the enzyme substrate of interest. The enzymatic products from the redox enzyme reactions, such as hydrogen peroxide and NAD(P)H, can be directly oxidized on the biosensing electrode by applying a certain electrical potential, and this direct electrocatalytic oxidation provides a measurable electrical signal.

As shown in Scheme 2, products from redox enzyme reactions such as hydrogen peroxide and NADH can be measured amperometrically by electro-oxidation at the solid electrode (e.g., glassy carbon electrode), polarized at more than +0.65 and +0.8 V, respectively. This direct electrocatalytic oxidation provides a simple and convenient biosensor transducing strategy. However, in a complex sample such as human blood, at those potential levels where the direct electrocatalytic oxidation of hydrogen peroxide and NADH is accomplished, co-oxidation of various organic compounds, such as ascorbic acid and uric acid, can

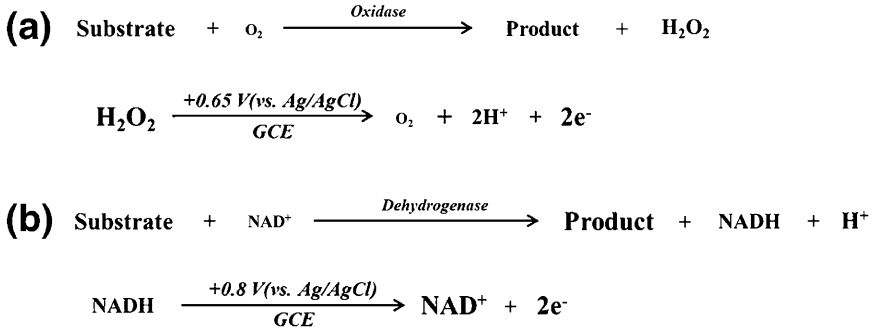

Scheme 2 Scheme for redox enzyme reactions and the direct electrocatalytic oxidations of electroactive products from enzyme reactions. **a** Oxidase enzyme reaction and direct electrocatalytic oxidation of hydrogen peroxide at electrodes. **b** Dehydrogenase enzyme reaction and direct electrocatalytic oxidation of NADH at electrodes

also occur and cause poor biosensor selectivity. It is a serious problem for practical applications of biosensor in clinical fields and bioreactor monitoring. Additionally, the high oxidative potential results in the fouling of the solid electrode surfaces. Although careful selection and use of biosensing electrode materials may solve this problem, it cannot be a fundamental solution.

To overcome the overpotential problems in direct electrocatalytic oxidation of hydrogen peroxide and NADH, the use of additional redox enzymes and electron transferring mediators has been studied [12, 28–31]. Generally, these additional redox enzymes and mediators are used to replace the natural electron acceptor. Electron transferring mediators are employed to participate in the electrocatalytic reaction of redox enzyme as an artificial electron acceptor instead of a natural electron acceptor such as oxygen or NAD^+(P). Those mediators were reduced by the redox enzyme reaction and oxidized on the electrode at relatively low oxidative potentials, which could prevent the co-oxidation of non-target interfering molecules. Also, during the bioelectrocatalytic reaction of the redox enzyme on the polarized electrode, mediators are regenerated in a reduced form by a cycling reaction of repetitive reduction and oxidation. The regeneration of the mediator results in the amplification of amperometric signals and a higher sensitivity of biosensors. Moreover, especially in the oxidase-based biosensor, the mediator recycling reaction minimizes the signal hindrance that may be caused by the oxygen depletion in the sample solution.

One thing that should be noted in the use of a mediator is the possible side reaction between the mediator and non-target molecules in the sample, which causes a signal interference during the biosensor operation. A detailed review for the required conditions that should be satisfied by an electron transferring mediator was reported by Turner [34]. A lot of work has been done in mediated biosensing systems, and the advantages from the use of mediators have been reported in comprehensive reviews [35, 36]. For the electron transferring mediators of amperometric enzyme biosensors, ferrocene derivatives, ferricyanides, organic

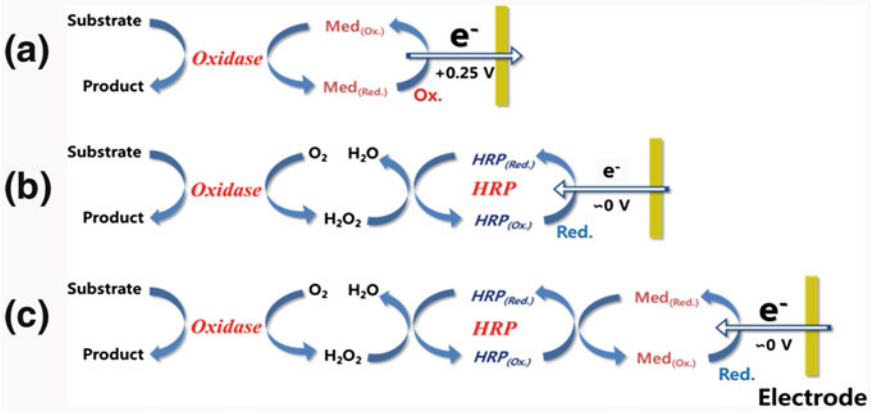

Fig. 3 Schematic illustrations for the electrocatalytic signaling of an oxidase-based biosensor. **a** Mediated mono-oxidase reaction. **b** Nonmediated oxidase-HRP cascadic enzyme reaction. **c** Mediated oxidase-HRP cascadic enzyme reaction. *HRP*, Horseradish peroxidase

dyes, quinone derivatives, and metal-conductive polymer complexes can be used. These mediators can be prepared by adsorption onto the enzyme electrode or by mixing with sample pre-treatment solution. In addition, mediators can be covalently immobilized on the electrode as mediator–polymer complex formats.

Similar to the use of electron transferring mediators, the use of additional redox enzymes lowering the electrocatalytic potential range is another promising route. This redox enzyme coupling was mentioned in the previous section. In this case, additional redox enzymes (e.g., HRP and DAP) catalyze products from the primary redox enzyme reaction (e.g., hydrogen peroxide or NADH) and accept the electrons to their own redox active site. Those activated additional redox enzymes can generate amperometric signals on the electrode by direct electrocatalytic oxidation with a certain electrocatalytic potential or again by mediator-involved electrocatalytic reaction. By using these combined redox enzyme couples, their electrocatalytic potential levels for the amperometric signal generation also can be reduced similarly to the case of a single redox enzyme-mediator system. Moreover, the high substrate specificity and fast catalytic rate of these additional redox enzymes provide enhanced signaling efficiency and accuracy.

These approaches employing mediators and extrinsic redox enzymes to minimize the side effects caused by high electrocatalytic working potential for direct oxidation of electroactive species can be classified into oxidase-based biosensing systems and dehydrogenase-based systems, as shown in Figs. 3 and 4, respectively.

In oxidase-based biosensing, the amperometric signaling methods could be divided into three cases: (1) Mediator-involved bioelectrocatalytic signaling using single oxidase-modified electrodes, (2) Direct electrocatalytic reduction of activated HRP using oxidase-HRP redox enzyme couple-modified electrodes, and (3) Mediator involved electrocatalytic signal generation using oxidase-HRP redox

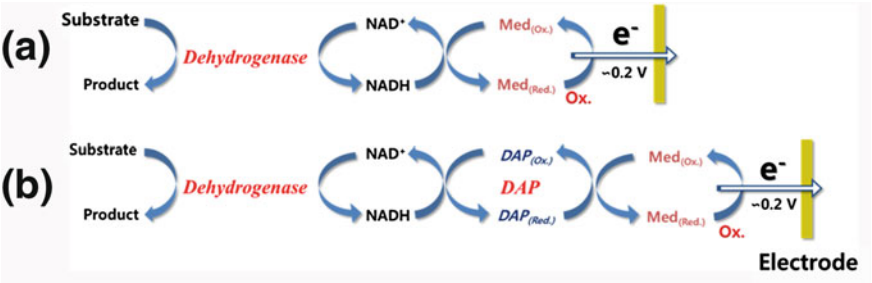

Fig. 4 Schematic illustrations of electrocatalytic signaling of a dehydrogenase-based biosensor. **a** Mediator-involved indirect measurement of NADH. **b** Mediated dehydrogenase-DAP cascadic enzyme reaction. *DAP*, Diaphorase; *NADH*, Nicotinamide adenine dinucleotide (reduced)

enzyme couple-modified electrodes. Also, distinctively in the dehydrogenase-based biosensing, the amperometric signaling methods follows in two cases: (1) Mediator-involved bioelectrocatalytic oxidation of NADH signaling using single dehydrogenase-modified electrodes and (2) Mediator-involved electrocatalytic signal generation using dehydrogenase-DAP redox enzyme couple-modified electrodes. All the cases that use mediators or extrinsic redox enzymes include regeneration and recycling of redox active species causing an amplification of signal. However, when redox enzyme couples and mediators are used together, the type of mediators should be carefully chosen to avoid possible distracted electron transfer, because some mediators participate in both coupled redox enzyme reactions and may generate false signals. For example, the most widely used mediator, ferrocenemethanol, can react with flavin adenine dinucleotide (oxidized)-dependent oxidase and HRP simultaneously. The distracted electron transfer reduces the signal accuracy and sensitivity of the biosensor. Similar problems appear in the mediated dehydrogenase-DAP system because some mediators can react with NADH and DAP simultaneously. To address these issues, rate constants of the redox enzymes and mediators should be carefully considered for the selection of mediators [28, 34].

On the basis of these bioelectrocatalytic reaction principles, recent advances in materials science and nanotechnology offer a great possibility to enhance the signaling performance of biosensors. A number of studies have reported on the application of newly developed nanomaterials having novel electrochemical properties that may improve of the performance of enzymatic biosensors [37–42]. For example, nanocarbon materials (e.g., carbon nanotubes [CNT], graphene) that show good electrical and mechanical properties—including high conductivity, stability under a high potential level, minimized surface fouling, high surface area, and biocompatibility—were used as electrode substrates or electrode additives for the fabrication of enzyme biosensors [39, 40]. Also, carbon-based nanomaterials remarkably decreased the oxidation potential level of NADH, which was ascribed to the edge-plane sites or defects present in the pyrolytic graphite and CNTs [43]. Another example of nanomaterial applications in biosensors is the use of metal

nanoparticles [37, 41, 42, 44]. Among the various metal nanoparticles, gold nanoparticles (AuNPs) are most widely used in enzymatic biosensors because of their convenient synthesis, biocompatibility, and novel electrical properties. The use of AuNPs in the enzyme electrode provides an enhanced electron transferring (hopping) between redox enzymes and electrode surfaces. These improvements in electrochemical activities are induced by AuNPs' own characteristics, such as the high surface-to-volume ratio and high surface energy. The effectively small size of AuNPs (a few nanometers) offers an opportunity to approach the active site of redox enzymes and facilitate the electron transfer. Also, AuNPs play a role as electro-conducting pathways between electroactive sites in redox enzymes and the electrode surface. Pingarron et al. reported a review on AuNP-based electrochemical biosensors [44]. Besides carbon-based nanomaterial and metal nanoparticles, nano metal-oxide materials (e.g., ZnO and TiO_2) and conducting polymers (e.g., polyaniline [PANI] and polypyrrole [PPY]) are also applied to the enzyme biosensor to improve the electrochemical signaling [45–48]. Although these nanomaterials provide an enhancement of electrochemical signaling performance, ill-prepared use of nanomaterials can cause some problems, including complicated sensor construction steps, an increase of background signals, and uneconomical fabrication costs. To develop a highly sensitive multi-enzymatic biosensor for practical use, appropriate selection and organization of enzyme couples and mediating scenarios are more important than the employment of new material.

2.3 Enzyme Immobilization Strategies for the Construction of Multienzyme-Modified Electrodes

To develop enzyme-based biosensors, enzymes have to be properly attached to the transducer surface. This process is known as immobilization. The optimal immobilization method retains the activity of biomolecules with long-term stability regarding their function [5]. Generally, there are a number of factors to be considered for the enzyme immobilization, including the characteristics of the supporting material, functional moiety on the enzyme surface, molecular weight of the enzyme, isoelectric point and polarity of enzyme, substrate diffusivity toward enzyme layer, and the transfer of electroactive product toward the electrode surface [5, 49–51]. To carry out the multienzyme immobilization, those factors for each enzyme should be individually satisfied. Certainly, if the characteristics of different enzymes to be immobilized are similar, optimization of those factors can be rather simple. Otherwise, careful selection of immobilization conditions for each enzyme, such as pH and the ionic strength of the treating solution, is required.

In addition, the efficient diffusion of an intermediate reactant that is generated from a primary enzyme reaction to the secondary enzyme location should be kept in mind for the multienzyme immobilization [5, 49–51]. Also, the amount of each

enzyme and the ratio for immobilization are critical factors for sensitive biosensor fabrication. These factors are related to the catalytic reaction of each enzyme, which is represented as the K_m value, exhibiting the lag period in the coupled reaction. Thus, it is highly necessary to evaluate the K_m values of each enzyme to fabricate the most effective multienzyme biosensor. The correlation between the K_m values of each enzyme and the total coupled enzyme assay was demonstrated by Tipton in 2002 [25]. Based on the evaluation according to the product generation, the total reaction rate of the cascadic coupled enzyme reaction is proportional to the reaction rate of the primary enzyme. In the enzyme biosensor, reaction of the final redox enzyme for signal generation is equivalently important as the primary enzyme reaction. Therefore, when the reaction rates of each enzyme are different, the ratio of immobilized enzymes would be changed to compensate for this imbalance. Thus, by understanding the enzyme reaction rate, we can calculate the optimal amount of enzymes to be immobilized, which provides an efficient multienzyme reaction and biosensing.

In addition to the ratio control, the compensation of enzyme reaction rates can be achieved by the arrangement of individual enzymes during the immobilization. When each enzyme is separately immobilized on the electrode, the delayed diffusion of the intermediate from primary enzyme location to the next enzyme layer occurs. This delayed diffusion provides time to produce a sufficient amount of intermediate that acts as a substrate for secondary enzymes. Regarding biosensor sensitivity, an intense immobilization of the redox enzyme that generates an electrochemical signal may enhance the electrochemical signal. Although this approach is not required for every multienzyme system, it is useful when the involved primary enzyme is remarkably slow in the cascadic multienzyme reaction. The mathematical modeling studies about the kinetic behavior of two enzyme reactions on the multienzyme-modified electrode were summarized by Baronas et al. [21].

The immobilization methods used for enzyme biosensors can be divided into physical and chemical approaches (Fig. 5) [5, 49–51]. Physical methods include adsorption, entrapment, and encapsulation. Chemical methods can be briefly categorized into cross-linking and covalent bonding. Adsorption is the simplest and involves minimal preparation. In this case, enzymes are randomly attached to surfaces of supporting material by low energy bonds such as electrostatic interaction, hydrogen interaction, van der Waals forces, and hydrophobic interactions [52]. However, the bonding is relatively weak. Therefore, this method is only suitable for exploratory work over a short timespan. In this method, arrangement of individual enzymes after immobilization cannot be achieved.

In entrapment and encapsulation methods, enzymes are held in three-dimensional polymeric lattices, polymeric membranes, and micellar polymers. Entrapment is normally achieved by forming a networked polymer gel, such as a starch gel, polyacrylamide gel, or PEG-based hydrogel, around the enzymes. Also, a sol–gel matrix can be applied to this method, such as tetraethyl orthosilicate [53, 54]. Conducting polymers including PPY and PANI are also useful [47, 48]. The polymeric network can be formed by traditional polymerization and electro-

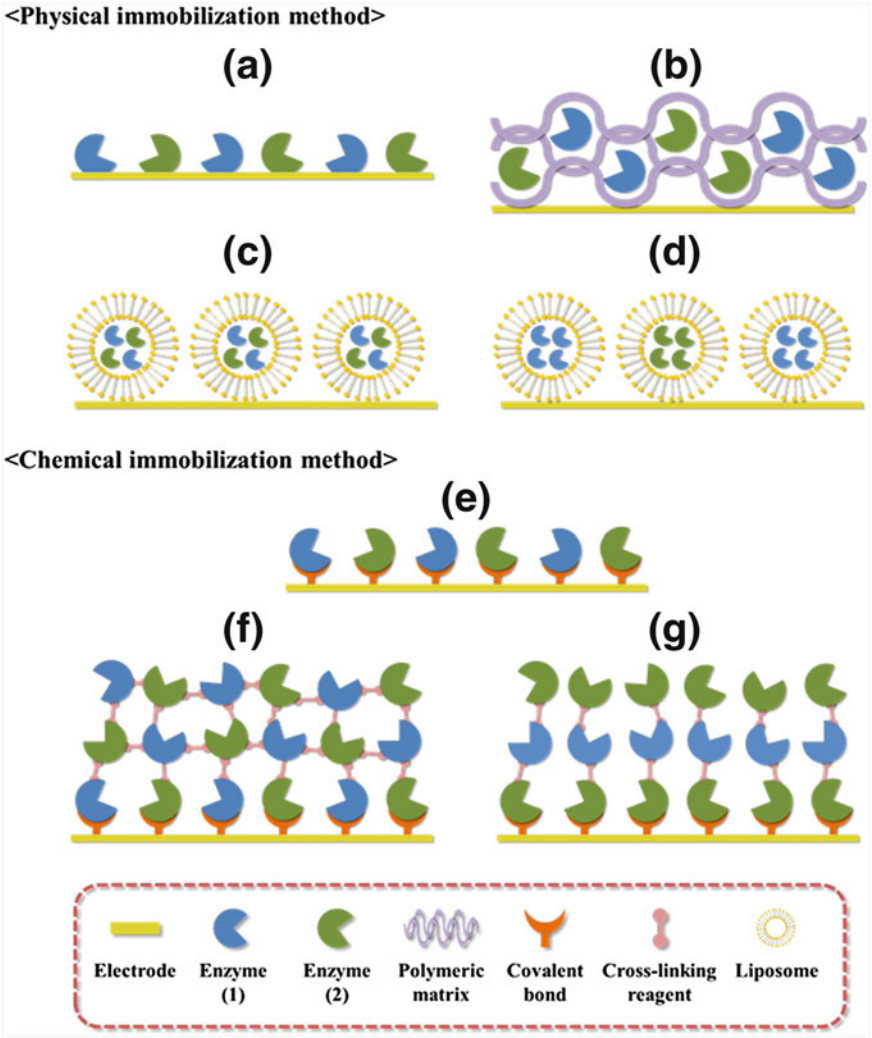

Fig. 5 Methods of enzyme immobilization. **a** Adsorption **b** Entrapment **c** Liposome-based encapsulation-random immobilization **d** Liposome-based encapsulation-isolated enzyme immobilization **e** Covalent bonding **f** Blended method using covalent bonding and cross-linking **g** Layer-by-layer (LBL) formation and LBL associated with covalent bonding

polymerization for entrapping enzymes [40]. Simple polymer membranes such as polyvinyl chloride, nylon, and Nafion also have been employed to hold enzymes [22]. In addition, electrostatic interaction-based multienzyme layer formation using linear polyelectrolytes such as polyethyleneimine, poly-L-lysine (PLL), and polyaniline sulfonic acid (PASA) are frequently used [55]. The entrapment method provides a definite enzyme immobilization with minimized leaching of enzymes as

a function of time. Moreover, by repeating the polymerization with different enzymes, separated enzyme layers can be achieved.

Encapsulation is similar to the entrapment method. In cases of encapsulation, enzymes are immobilized in a polymeric matrix having isolated pores, room, or film structure [56]. In the early type of biosensors, enzymes were held in place behind a permeable membrane such as a dialysis membrane, which allowed selective substrate and product penetration. Recently, enzyme micelle and enzyme liposome structures have been developed and used. However, during the polymerization step, enzyme activity can be reduced by uncertain denaturation. In addition, the polymeric networks such as polymeric matrix, micelle structures, and polyelectrolyte layers may act as barriers against the diffusion of substrates and intermediates; thus, reduction or loss of the cascadic multienzyme reaction rate can occur. To address this issue, polymerization degree and polymerization conditions should be carefully controlled [57].

Cross-linking and covalent bonding are the most stable immobilization methods for enzyme electrode fabrication [49–51]. In these methods, enzymes are bound to an activated electrode surface or other enzyme molecules by forming a covalent bond. Functional moieties of the enzyme surface, such as amine groups and carboxyl groups, are involved in covalent bonding. To attach the enzymes onto the electrode surface, electrode surfaces are preactivated by additional treatments such as silanisation of ITO glass, oxidation of carbon, and formation of self-assembled monolayers (SAM) on gold electrode surfaces. By this surface activation, various functional groups, such as amine groups, carboxyl groups, hydroxyl groups, thiol groups, N-hydroxysuccinimide ester (NHS) groups, and maleimide groups, can be exposed on the electrode. To these functional groups of electrode surfaces, functional moiety of the enzyme surface can be immobilized by direct covalent bonding or bifunctional cross-linking reagents (e.g., succinimidyl-4-[N-maleimidomethyl]cyclohexane-1-carboxylate, glutaraldehyde (GA), and bis[sulfosuccinimidyl] suberate [BS^3]). The reaction between electrode surface and enzyme was simply done by dipping the activated surface into an enzyme solution or applying a drop of this solution onto the surface.

To the enzyme immobilized electrode that is fabricated by covalent bonding, one can immobilize more enzymes repetitively by using a bifunctional cross-linking reagent. Using this strategy, one can construct an enzyme electrode in a layer-by-layer (LBL) format [32]. Cross-linking can be formed among enzymes in the same layer after LBL formation. This covalent bond-based enzyme immobilization necessarily causes a reduction of enzyme activities due to the covalent bonding. Therefore, the selection of relatively mild conditions of enzyme immobilization treatments such as low ionic strengths, low temperatures, near physiological pHs, and the selection of water-soluble chemical reagents are very important [57]. Recently, nanomaterials with unique properties such as high surface-to-volume ratio, mesoporous nanostructures, and good electrochemical activities (e.g., CNTs, mesoporous metal oxides, metal nanoparticles) have been applied to the enzyme immobilization for the construction of highly concentrated enzyme layers and sensitive multienzyme electrodes.

3 Practical Applications of Cascadic Multienzyme-Modified Biosensing Electrodes in Various Fields

The efforts of scientific and engineering research provide us with the knowledge to develop accurate and effective electrochemical multienzymatic biosensors. The theories and techniques include coupled enzyme reaction mechanisms, electrochemical signaling techniques, and enzyme immobilization strategies. On the basis of these findings, a number of studies about the development of biosensors employing cascadic multienzyme reactions have been reported. They are used in clinical diagnostics, food analysis, and environmental monitoring [1–3, 10–19]. This section discusses the practical applications of multienzyme-based electrochemical biosensors in various fields.

3.1 Applications in Clinical Diagnostics

Among many achievements in enzyme biosensor research and development, the most successful is the diagnostic use of blood glucose sensors. Although there exist many important target metabolites that need to be measured by biosensors, the list of commercialized enzyme biosensors is very short. Recent advances in multienzyme reactions involving biosensing techniques may offer an opportunity to overcome this situation. By using cascadic multienzyme-modified biosensing electrodes, more clinically significant analytes that require complicated analysis procedures for detection—including biochemical metabolites, cofactors, and metabolic enzymes—can be analyzed more efficiently. Moreover, a sensitive electrochemical immunoassay can be accomplished by using a multienzymatic reaction as a label of antibody molecules. D'Ozario reviewed the biosensing technologies for clinical chemistry [2].

Many researchers reported the development of multienzymatic electrochemical biosensors to quantify the concentration of biochemical metabolites such as acetylcholine [58, 59], arginine [60], cholesterol [52, 61], creatinine [62, 63], glucose [64–66], and triglycerides [22, 67]. Ahmadalinezhad et al. proposed a total cholesterol biosensor using a titanium electrode modified with three enzymes and nanoporous gold coating [61]. As enzymatic constituents, cholesterol esterase (CE), cholesterol oxidase (CO), and HRP were employed and were immobilized onto a nanoporous gold-coated Ti electrode by simple adsorption and chitosan-based entrapment. As shown in Fig. 6, the cascadic enzyme reaction for cholesterol detection is composed of non-redox enzyme/redox enzyme couple and redox/redox enzyme couple. The multienzyme-modified biosensing electrode (Ti/AuNP/CE-CO-HRP) exhibited a high sensitivity (29.33 $\mu A/mM \cdot cm^2$) and a wide linear range to 300 mg/dL. In addition, the apparent K_m constant of the proposed biosensor was very low (0.64 mM). The researchers explain that the effective enzyme immobilization strategy and the nanoporous structure of the electrode surface are the possible reasons for the observed biosensor performance.

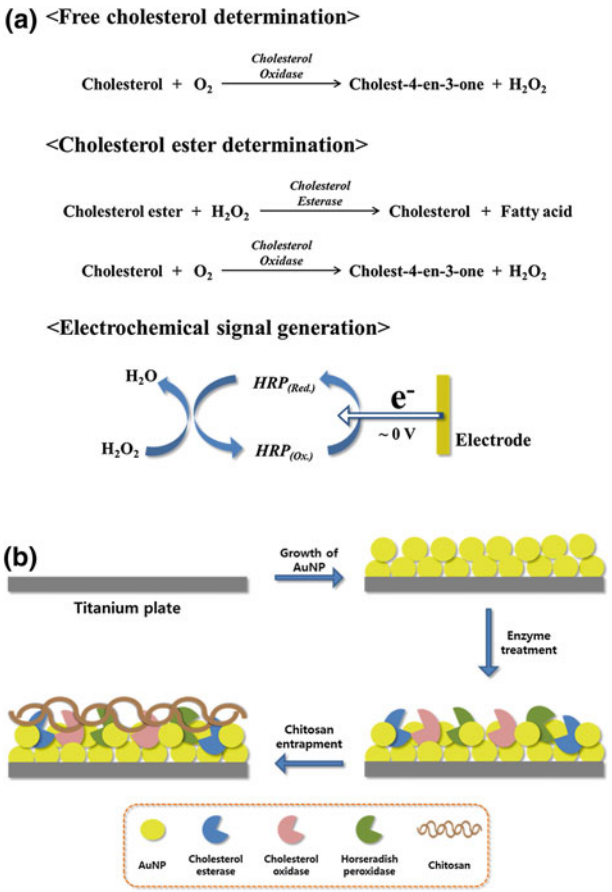

Fig. 6 Schematic illustration of cascadic tri-enzyme reaction mechanism and multienzyme electrode fabrication for the total cholesterol biosensor proposed by Ahmadalinezhad et al. [61]. **a** Cascadic multienzyme reaction mechanism and electrochemical signaling mechanism **b** Multienzyme electrode fabrication procedures. *AuNP*, Gold nanoparticle; *HRP*, Horseradish peroxidase

Yadav et al. reported a sensitive and stable serum creatinine biosensor employing carboxylated multiwalled carbon nanotube (c-MWCNT) and a PANI-modified electrode [63]. For the multienzyme-modified electrode fabrication, c-MWCNT/PANI nanocomposite film was electrodeposited over the surface of a platinum (Pt) electrode. To the carboxyl group on the activated electrode, enzymes (creatinine amidohydrolase, creatine amidinohydrolase, and sarcosine oxidase) for creatinine detection were covalently immobilized by using 1-ethyl-3-(3-dimethylaminopropyl)carbodiimide/NHS chemistry. The cascadic enzyme reaction and electrochemical signaling mechanism are shown in Scheme 3.

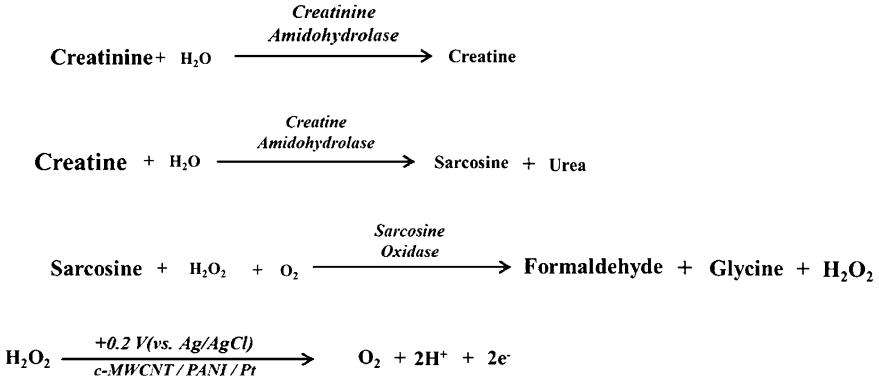

Scheme 3 Cascadic tri-enzyme reaction employed in electrochemical creatinine biosensor (Yadav et al. [63])

In this study, as an electrochemical signaling strategy, direct oxidation of hydrogen peroxide, which was generated from the cascadic enzyme reaction, was employed. The proposed biosensor exhibited a linear response range from 10 to 750 μM creatinine with a limit of detection of 0.1 μM. Also, Yadav et al. described that the proposed biosensor was successfully employed for the determination of creatinine in human serum samples. According to their report, the developed biosensor showed a 15 % loss in its initial response after 180 days storage at 4 °C.

Recently, the development of multienzymatic biosensors for the analysis of clinically meaningful metabolic enzymes including CK [33] and transaminase [32, 68] have been reported. Han et al. investigated a new method for the electrochemical detection of human serum transaminases (e.g., aspartate transaminase [AST] and ALT) by using a bienzyme-modified electrode [32]. For the electrochemical detection of AST and ALT, POx and oxaloacetate decarboxylase (OAC) were immobilized on the gold electrode surface using an amine-reactive SAM (DTSP) and a homobifunctional cross-linker (BS^3). AST and ALT were pre-reacted with a substrate such as L-aspartate, L-alanine, or α-ketoglutarate. Enzyme reactions of AST and ALT generated pyruvate as an end product. To determine the activities of AST and ALT, electroanalyses of pyruvate were conducted using POx/OAC-modified multienzyme electrode with ferrocenemethanol as an electron mediator. Generated biosensor signals from the multienzyme-mediated reaction were correlated to AST and ALT levels in human plasma. The calibration results for AST and ALT concentrations from 7.5 to 720 units/L in human plasma-based samples were found useful, covering the required clinical detection range for the liver disease diagnosis. For the enzyme immobilization, Han et al. employed an LBL technique associated with covalent bonding to enhance and control the biosensor sensitivity (Fig. 7).

Cascadic multienzyme reactions also can be applied to an affinity biosensor system such as immunoassays [69] and aptamer-based protein analyses [70, 71].

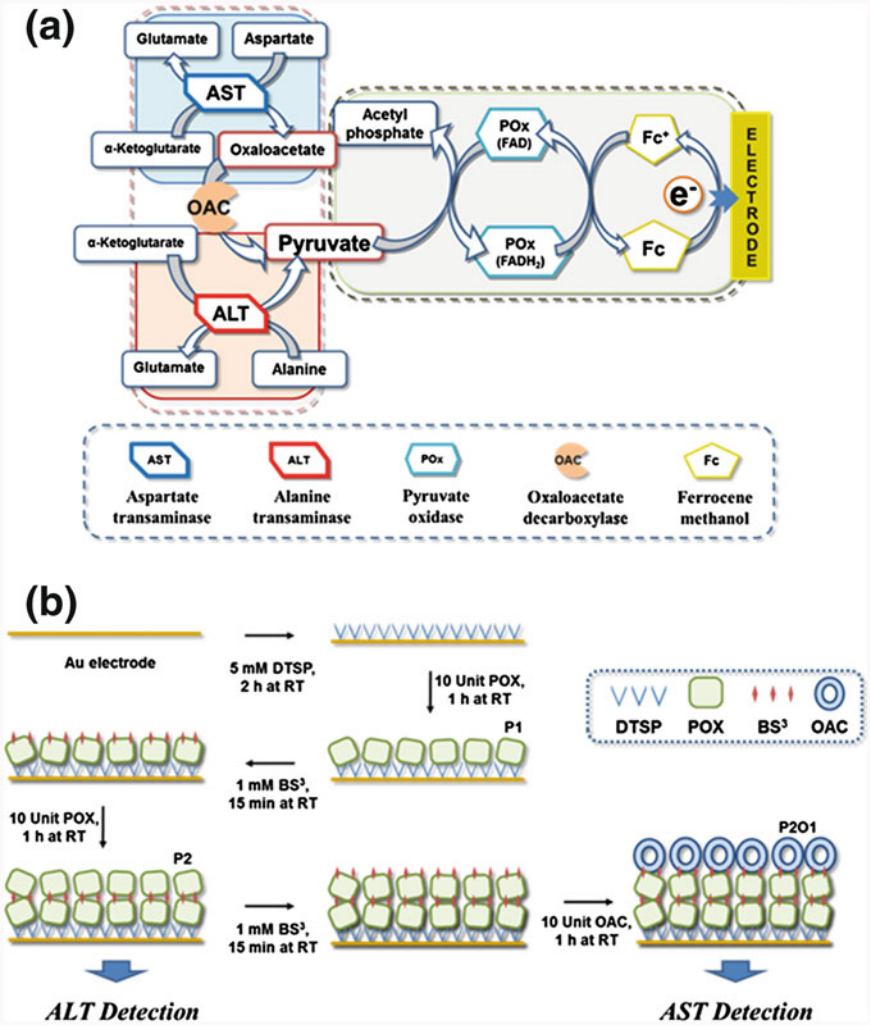

Fig. 7 Schematic illustration of a multienzyme reaction mechanism and electrode fabrication for an electrochemical transaminase biosensor proposed by Han et al. [32]. **a** Cascadic multienzyme reaction mechanism and electrochemical signaling mechanism **b** Multienzyme electrode fabrication procedures

Xiang et al. suggested an electrochemical sandwich-type aptasensor for the monitoring of proteins through a multienzyme reaction-based signal amplification strategy [70]. In this study, thrombin was employs as a model analyte, sandwiched between an electrode surface immobilized aptamer and an aptamer enzyme (alkaline phosphatase [ALP])-CNT bioconjugate. By coupling the ALP-DAP bienzymatic signal amplification with the biocatalytic signal enhancement from redox-recycling, the resulting analytical signal was significantly amplified. In the

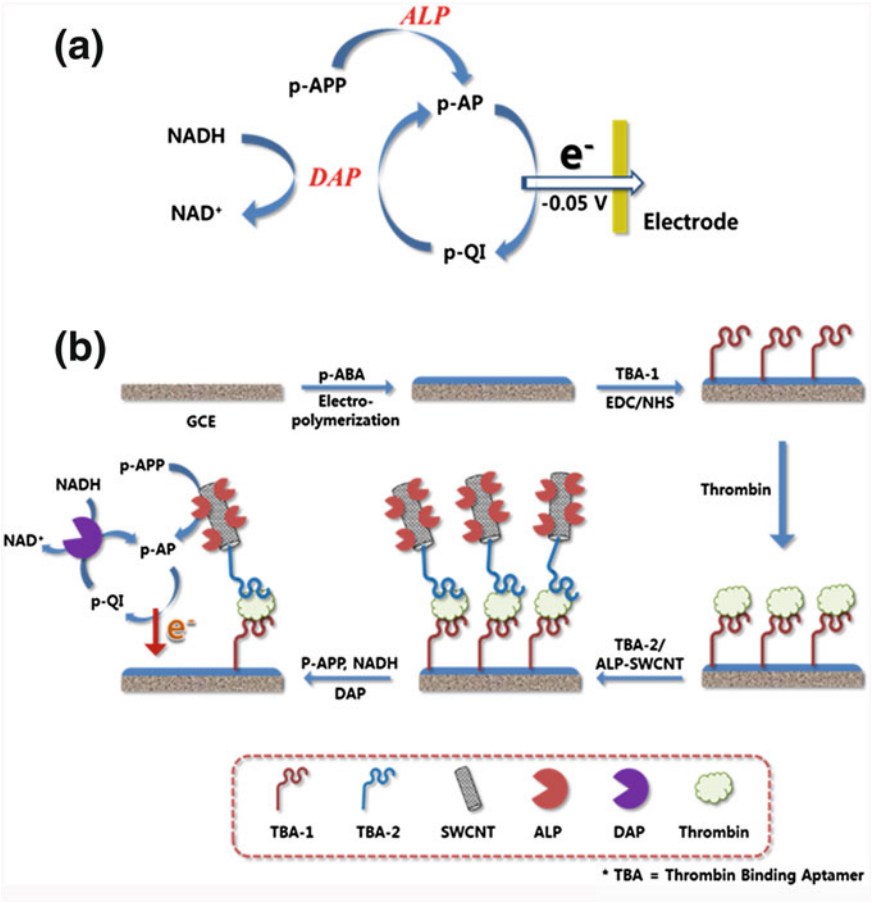

Fig. 8 Schematic illustration of an electrochemical aptasensor suggested by Xiang et al. [70]. **a** Cascadic bienzyme reaction-based electrochemical signaling **b** Fabrication and operation procedures of electrochemical aptasensors. *ALP*, Alkaline phosphatase; *DAP*, Diaphorase; *EDC*, 1-Ethyl-3-(3-dimethylaminopropyl) carbodiimide; *GCE*, Glassy carbon electrode; *NADH*, Nicotinamide adenine dinucleotide (reduced); *NHS*, N-hydroxysuccinimide ester; *p-AP*, p-Aminophenol; *p-QI*, p-Quinonimine; *p-APP*, p-Aminophenylphosphate; *SWCNT*, Single-walled carbon nanotube; *TBA*, Thrombin-binding aptamer

presence of DAP, p-aminophenylphosphate, and NADH, the electrochemically oxidized product p-quinonimine (p-QI) is reduced back to p-aminophenol (p-AP) by DAP, and NADH reduces the oxidized form of DAP to its native state. A redox-recycling between p-AP and p-QI is made accordingly, resulting in an increased electrocatalytic signal (Fig. 8). Xiang et al. demonstrated that the detection limit of the proposed aptasensor was as low as 8.3 fM, and it showed highly improved sensitivity for thrombin detection compared to a conventional single ALP-based aptamer assay.

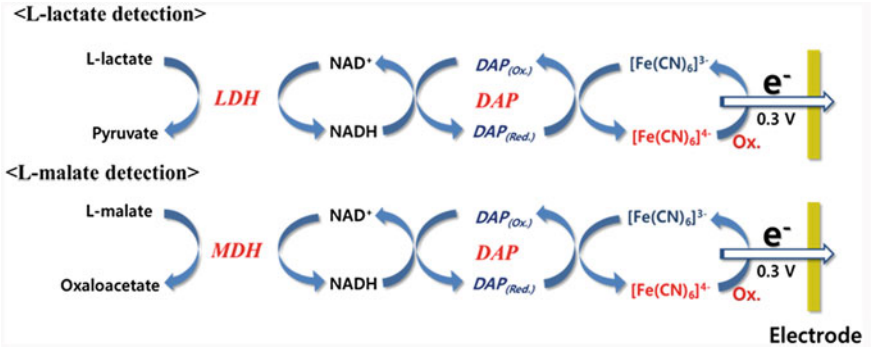

Fig. 9 Schematic illustration of a cascadic bienzyme reaction employed in an electrochemical L-lactate/L-malate biosensor suggested by Katrlík et al. [73]. *DAP*, Diaphorase; *LDH*, Lactase dehydrogenase; *MDH*, Malate dehydrogenase; *NAD*, Nicotinamide adenine dinucleotide (oxidized); *NADH*, Nicotinamide adenine dinucleotide (reduced)

3.2 Applications in Food Analysis and Environmental Monitoring

Accurate monitoring of contaminants in food and the environment, such as chemical compounds and toxins, is a significant issue to assess and prevent risks for human and environmental health. Moreover, in the food industry, the analysis of nutrients in a product is essential for quality control. On the basis of these requirements, a number of multienzyme-based biosensors for monitoring the food and environmental conditions have been developed [16–18].

Glucan [72], L-lactate [73], L-malate [73], polyphenol [74], and sulfites [55] are typical target analytes for the reported multienzyme-based biosensors for food analysis. Katrlík et al. presented bienzymatic electrochemical biosensors for the selective detection of L-lactate and L-malate in wine [73]. The developed electrode comprised a solid binding matrix (SBM) having a hydrophobic skeleton such as 2-hexadecanone, graphite, and NAD^+. As the enzymatic component, malate dehydrogenase or LDH and DAP were applied to the prepared electrode and covered by a dialysis membrane, which substantially reduced interferences from easily oxidizable compounds such as polyphenols in wine. As an electron transferring mediator, hexacyanoferrate (III) was used for DAP-involved bioelectrocatalytic signaling. During the biocatalytic reaction, the substrate (L-malate or L-lactate) is oxidized and NAD^+ is reduced to NADH. The reduced cofactor NADH is then reoxidized by DAP, which reacts with the electron mediator hexacyanoferrate (III). The reduced mediator is electrochemically oxidized on the electrode and generates a signal (Fig. 9). The response of the proposed bienzymatic biosensing electrode were found to be linear up to 1.1 mM for L-malate and 1.3 mM for L-lactate, respectively. The biosensing results obtained from wine samples were in good agreement with those obtained by liquid chromatography.

Spricigo et al. investigated an electrochemical biosensor for the detection of sulfite, which is a hazardous food additive [55]. An enzyme electrode was

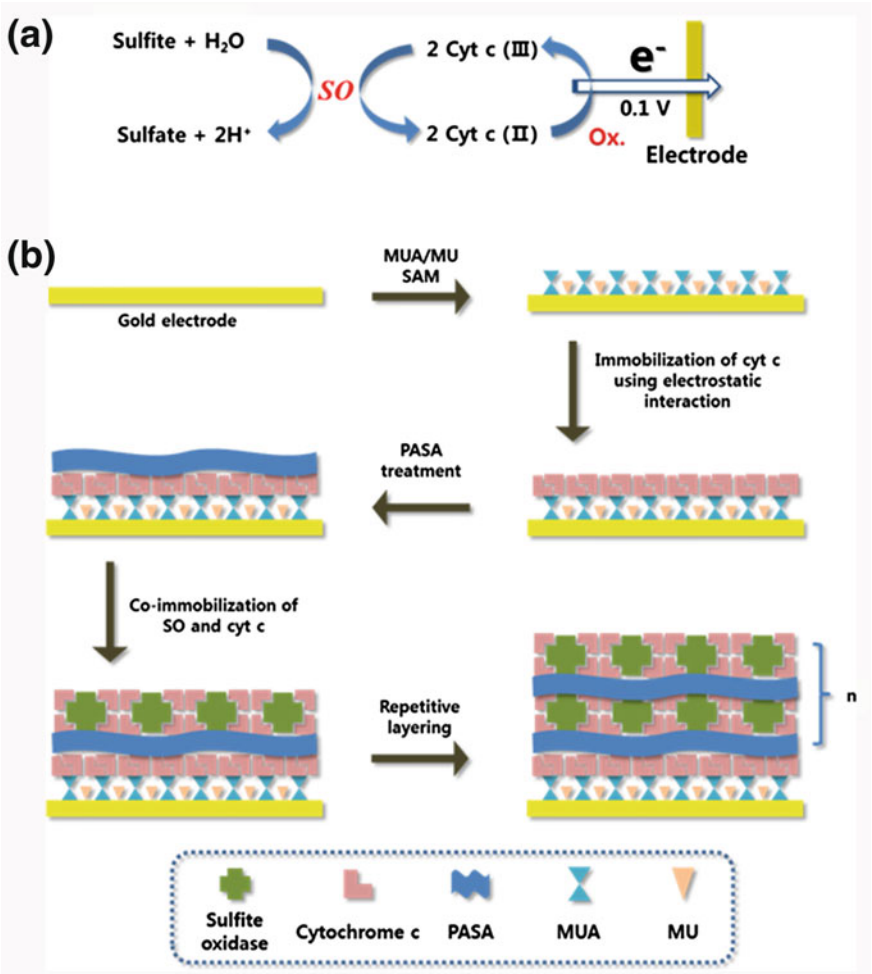

Fig. 10 Schematic illustration of a sulfite biosensor proposed by Spricigo et al. [55]. **a** Mechanism of SO/Cyt-c enzyme reaction and electrochemical signaling mechanism **b** Multienzyme electrode fabrication procedures. *Cyt-c*, Cytochrome compound; *MU*, 11-Mercapto-1-undecanol; *MUA*, 11-Mercapto-1-undecanol acid; *PASA*, Polyaniline sulfonic acid; *SAM*, Self-assembled monolayer; *SO*, Sulfite oxidase

fabricated by co-immobilizing sulfite oxidase (SO) and cytochrome complex (Cyt-c) with PASA on the gold wire electrode as an LBL assembly (Fig. 10). An electrostatic interaction between positively charged enzymes and negatively charged PASA was used as the driving force for immobilization. SO is a metalloprotein containing both the molybdenum cofactor (Moco) and a cytochrome b5-type heme. Sulfite is oxidized at the Moco cofactor of the SO enzyme. The resulting electrons from Moco are transferred to the heme b5 domain in the same SO and then transferred to the nearest Cyt-c molecule that is immobilized. Then,

the Cyt-c transfers received electrons further to the neighboring Cyt-c molecules and ultimately to the electrode, generating the sensor signal. A electro-oxidation current was measured in the presence of sulfite at the enzyme/cytochrome t-modified electrode under the working potential of +0.1 V versus Ag/AgCl, which is a relatively low potential level and advantageous in sensor operation. According to Spricigo et al., a 17-bilayer deposited electrode exhibited a linear range between 1 and 60 μM sulfite, with a sensitivity of 2.19 mA/M. The resulting enzyme electrode was found to be stable for extended uses (5 days of operational stability and 2 months of storage stability). By the sulfite testing using unspiked and spiked samples of red and white wine, Spricigo et al. verified that the suggested biosensor is applicable for real sample analysis.

In the environmental monitoring field, the development of a multienzyme reaction-based biosensor is focused on the detection of toxic chemicals such as pesticide [14, 15, 75] and formaldehyde [76]. Among them, the detection of organophosphorous (OP)-type pesticides has been one of the most popular subjects for multienzymatic biosensor development because it requires complicated enzyme inhibition assay procedures to be conducted. In a number of studies about OP compound determination, acetylcholine esterase (AChE)-related enzyme pathways have been widely employed because they are specifically inhibited by the OP compounds.

Recently, Han et al. developed an integrated microsystem for the OP detection using AChE and choline oxidase (ChOx) cascadic bienzyme bioelectrocatalysis [75]. The electrocatalytic signaling mechanism of the AChE–ChOx bienzyme reaction for OP determination is depicted in Fig. 11. Acetylcholine (ACh) is decomposed into choline (Ch) and acetic acid by the AChE reaction, and Ch is then used as a substrate for ChOx, generating an amplified electrochemical current based on its electrocatalytic reaction with mediators such as ferrocenemethanol. The changes in AChE activity by the irreversible inhibition of OP compounds can be tracked to determine the OP concentration. For field applications, a microsystem containing an enzyme biosensor and microfluidic sample treatment part was designed and fabricated. By using the microfluidic channel and chamber, all the required procedures of an OP test, including enzyme immobilization, sample injection, and washing procedures, are accomplished without any other external preparation.

In this report, enzymes were immobilized on the biosensing microchip in two different ways. As shown in Fig. 11, ChOx was immobilized on the electrode using PLL, GA, and an amine-rich interfacial surface such as cystamine SAM. In the other method, AChE was attached on the magentic microparticle (MP) surface via imine bond formation, and the enzyme-modified MPs were localized on the working electrode using a magnet installed under the microfluidic channel. By utilizing the developed OP biosensing chip, calibration results for OP from 0.05 to 0.8 ppm of diazinon were obtained. The concentrated enzyme arrangement and reduced distance between the enzymes participating in the cascade signaling reactions improved the biosensing performance. The suggested system is a good example of an integrated multienzyme biosensor for field use.

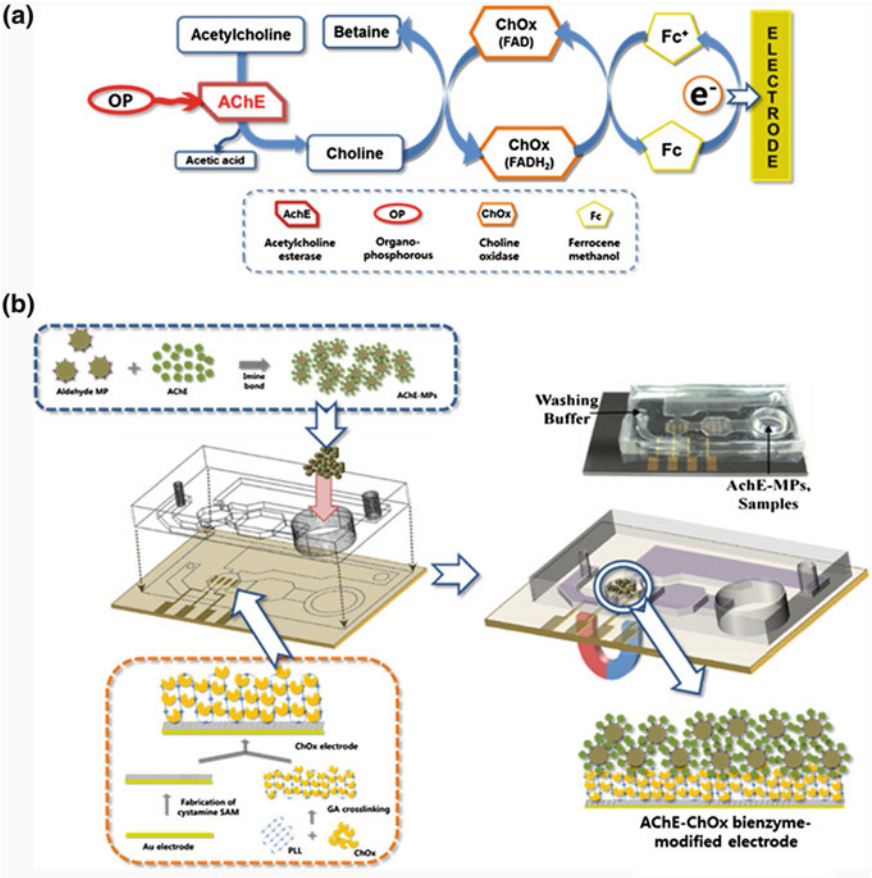

Fig. 11 Schematic illustration of a biosensor for OP-type pesticides proposed by Han et al. [75] **a** Mechanism of bienzyme reactions and electrochemical signaling for OP **b** Procedures of multienzyme electrode fabrication and integrated microchip construction. *OP*, Organophosphorous

4 Conclusion

This review described fundamental principles for multienzyme biosensor development and its applications in various fields. As mentioned in the text, an understanding of the enzyme reaction mechanisms is the most important factor in the development of effective biosensors. The selection of appropriate enzyme couples based on the mechanisms and molecular characteristics is the starting point of multienzyme reaction-based biosensor research.

The potential values and advantages of multienzyme reaction-based biosensors are clear. To expand the pipeline of enzyme biosensors, research on multienzyme reaction-based biosensors is highly important. For the commercialization of

multienzyme biosensors, a number of critical problems should be solved. First, signal interferences induced by non-target molecules should be determined. When employing more than two enzymes for the analysis, one should consider possible side reactions of the enzymes and chemical substances. Another issue is the stability of the biosensor. Because the sensor stability is directly related to the enzyme stability being used, one should find a way to maintain or enhance the enzyme stability. Also, the development of genetically engineered enzymes with improved stability can be another promising solution to the problem. A final concern is the cost of biosensor fabrication. By using new materials and microfabrication technologies, sensors containing small amounts of immobilized enzymes will be made to solve the issue. For the commercialization of biosensors, balanced approaches toward the biosensor performance and fabrication costs are required.

Acknowledgments This chapter includes research supported by the National Research Foundation (2011-0025819, 2012-0003042) and the Priority Research Center Program (2012-0006687).

References

1. Vo-Dinh T, Cullum B (2000) Biosensors and biochips: advances in biological and medical diagnostics. Fresenius J Anal Chem 366:540
2. D'Orazio P (2003) Biosensors in clinical chemistry. Clin Chim Acta 334:41
3. Newman JD, Setford SJ (2006) Enzymatic biosensors. Mol Biotechnol 32:249
4. Zhao Z, Jiang H (2010) Enzyme-based electrochemical biosensors. In: Serra PA (ed) Biosensors. InTECH, Rijeka
5. Ronkainen NJ, Halsallb HB, Heinemanb WR (2010) Electrochemical biosensors. Chem Soc Rev 39:1747
6. Clark L Jr, Lyons C (1962) Electrode systems for continuous monitoring in cardiovascular surgery. Ann NY Acad Sci 102:29
7. Bakker E (2004) Electrochemical sensors. Anal Chem 76:3285
8. Wang J (2008) Electrochemical glucose biosensors. Chem Rev 108:814
9. Kimmel DW, LeBlanc G, Meschievitz ME, Cliffel DE (2012) Electrochemical sensors and biosensors. Anal Chem 84:685
10. Wang Y, Xu H, Zhang J, Li G (2008) Electrochemical sensors for clinic analysis. Sensors 8:2043
11. Liang JF, Li YT, Yang VC (2000) Biomedical application of immobilized enzymes. J Pharm Sci 89(8):979
12. Prodromidis MI, Karayannis MI (2002) Enzyme based amperometric biosensors for food analysis. Electroanal 14(4):241
13. Raz SR, Haasnoot W (2011) Multiplex bioanalytical methods for food and environmental monitoring. TRAC—Trend Anal Chem 30(9):1526
14. Amine A, Mohammadi H, Bourais I, Palleschi G (2006) Enzyme inhibition-based biosensors for food safety and environmental monitoring. Biosens Bioelectron 21:1405
15. Shah J, Wilkins E (2003) Electrochemical biosensors for detection of biological warfare agents. Electroanal 15(3):157
16. Trojanowicz M (2002) Determination of pesticides using electrochemical enzymatic biosensors. Electroanal 14(19–20):1311

17. Mello LD, Kubota LT (2002) Review of the use of biosensors as analytical tools in the food and drink industries. Food Chem 77:237
18. Dorst BV, Mehta J, Bekaert K, Rouah-Martin E, Coen WD, Dubruel P, Blust R, Robbens J (2010) Recent advances in recognition elements of food and environmental biosensors: a review. Biosens Bioelectron 26:1178
19. Glindkamp A, Riechers D, Rehbock C, Hitzmann B, Scheper T, Reardon KF (2010) Sensors in disposable bioreactors status and trends. Adv Biochem Eng Biotech 115:145
20. Wollenberger U, Schubert F, Pfeiffer D, Scheller FW (1993) Enhancing biosensor performance using multienzyme systems. Trends Biotechnol 11:255
21. Baronas R, Ivanauskas F, Kulys J (2010) One-layer multi-enzyme models of biosensors. In: Baronas R, Ivanauskas F, Kulys J (eds) Mathematical modeling of biosensors, vol 9. Springer, Netherlands, p 113
22. Minakshi, Pundir CS (2008) Construction of an amperometric enzymic sensor for triglyceride determination. Sensor Actuat B Chem 133:251
23. Schubert F, Kirstein D, Scheller F, Appleqvist R, Gorton L, Johansson G (1986) Enzyme electrodes for L-glutamate using chemical redox mediators and enzymatic substrate amplification. Anal lett 19:1273
24. Godfrey T, Reichelt J (1983) Industrial enzymology—the application of enzymes in industry. Macmillan Publishers, England
25. Tipton KF (2002) Principles of enzyme assay and kinetic studies. In: Eisenthal R, Danson MJ (eds) Enzyme assays: a practical approach. Oxford University Press, New York
26. Holme DJ, Peck H (1983) Analytical biochemistry. Longman Group, New York
27. Rudolph FB, Baugher BW, Beissner RS (1979) Techniques in coupled enzyme assays. In: Purich DL (ed) Methods in enzymology. Academic Press Inc., New York
28. Turner APF, Karube I, Wilson GS (1987) Biosensors-fundamentals and applications. Oxford University Press, New York
29. Burton SG, Rose-Hill M (2008) Oxidizing enzymes in multi-step biotransformation processes. In: Garcia-Junceda E (ed) Multi-step enzyme catalysis: biotransformations and chemoenzymatic synthesis. Wiley-VCH Verlag, Weinheim
30. Gorton L, Jönsson-Pettersson G, Csöregi E, Johansson K, Domínguez E, Marko-Varga G (1992) Amperometric biosensors based on an apparent direct electron transfer between electrodes and immobilized peroxidases. Plenary lecture. Analyst 117:1235
31. Radoi A, Compagnone D (2009) Recent advances in NADH electrochemical sensing design. Bioelectrochemistry Bioener 76:126
32. Han YD, Song SY, Lee JH, Lee DS, Yoon HC (2011) Multienzyme-modified biosensing surface for the electrochemical analysis of aspartate transaminase and alanine transaminase in human plasma. Anal Bioanal Chem 400:797
33. Liu CX, Jiang LY, Wang H, Guo ZH, Cai XX (2007) A novel disposable amperometric biosensor based on trienzyme electrode for the determination of total creatine kinase. Sensor Actuat B Chem 122:295
34. Turner APF (1988) Redox mediators and their application in amperometric sensors. In: Guilbault GG, Mascini M (eds) Analytical uses of immobilized biological compounds for detection, medical and industrial uses. NATO ASI Series. Reidel Publ. Co., Dordrecht
35. Katakis I, Domínquez E (1997) Catalytic electrooxidation of NADH for dehydrogenase amperometric biosensors. Mikrochim Acta 126:11
36. Gorton L (1995) Carbon paste electrodes modified with enzymes, tissues, and cells. Electroanal 7:23
37. Li H, Liu S, Dai Z, Bao J, Yang X (2009) Applications of nanomaterials in electrochemical enzyme biosensors. Sensors 9:8547
38. Jianrong C, Yuqing M, Nongyue H, Xiaohua W, Sijiao L (2004) Nanotechnology and biosensors. Biotechnol Adv 22:505
39. Wang J (2005) Carbon-nanotube based electrochemical biosensors: a review. Electroanal 17(1):7

40. Shao Y, Wang J, Wu H, Liu J, Aksay IA, Lin Y (2009) Graphene based electrochemical sensors and biosensors: a review. Electroanal 22(10):1027
41. Willner I, Basnar B, Willner B (2007) Nanoparticle-enzyme hybrid systems for nanobiotechnology. FEBS J 274:302
42. De M, Ghosh PS, Rotello VM (2008) Applications of nanoparticles in biology. Adv Mater 20:4225
43. Wooten M, Gorski W (2010) Facilitation of NADH electro-oxidation at treated carbon nanotubes. Anal Chem 82:1299
44. Pingarron JM, Yanez-Sedeno P, Gonzalez-Cortes A (2008) Gold nanoparticle-based electrochemical biosensors. Electrochim Acta 53:5848
45. Ahmad M, Pan C, Luo Z, Zhu J (2010) A single ZnO nanofiber-based highly sensitive amperometric glucose biosensor. J Phys Chem C 114:9308
46. Cosnier S, Senillou A, Grätzel M, Comte P, Vlachopoulos N, Renault NJ, Martelet C (1999) A glucose biosensor based on enzyme entrapment within polypyrrole films electrodeposited on mesoporous titanium dioxide. J Electroanal Chem 469:176
47. Dhand C, Das M, Datta M, Malhotra BD (2011) Recent advances in polyaniline based biosensors. Biosens Bioelectron 26:2811
48. Gerard M, Chaubey A, Malhotra BD (2002) Application of conducting polymers to biosensors. Biosens Bioelectron 17:345
49. Sassolas A, Blum LJ, Leca-Bouvier BD (2012) Immobilization strategies to develop enzymatic biosensors. Biotechnol Adv 30:489
50. Schoffelen S, van Hest JCM (2012) Multi-enzyme systems: bringing enzymes together in vitro. Soft Matter 8:1736
51. Hanefeld U, Gardossi L, Magner E (2009) Understanding enzyme immobilisation. Chem Soc Rev 38:453
52. Li XR, Xu JJ, Chen HY (2011) Potassium-doped carbon nanotubes toward the direct electrochemistry of cholesterol oxidase and its application in highly sensitive cholesterol biosensor. Electrochim Acta 56:9378
53. Wang B, Dong S (2000) Sol–gel-derived amperometric biosensor for hydrogen peroxide based on methylene green incorporated in Nafion film. Talanta 51:565
54. Kandimalla VB, Tripathi VS, Ju H (2006) Immobilization of biomolecules in sol–gels: biological and analytical applications. Crit Rev Aanl Chem 36:73
55. Spricigo R, Dronov R, Lisdat F, Leimkühler S, Scheller FW, Wollenberger U (2009) Electrocatalytic sulfite biosensor with human sulfite oxidase co-immobilized with cytochrome c in a polyelectrolyte-containing multilayer. Anal Bioanal Chem 393:225
56. Park BW, Yoon DY, Kim DS (2010) Recent progress in bio-sensing techniques with encapsulated enzymes. Biosens Bioelectron 26:1
57. Moehlenbrock MJ, Minteer SD (2011) Introduction to the field of enzyme immobilization and stabilization. In: Minteer SD (ed) Methods in molecular biology, vol 679—Enzyme stabilization and immobilization. Springer, New York
58. Shi H, Zhao Z, Song Z, Huang J, Yang Y, Anzai J, Osa T, Chen Q (2005) Fabricating of acetylcholine biosensor by a layer-by-layer deposition technique for determining trichlorfon. Electroanal 17:1285
59. Hou S, Ou Z, Chen Q, Wu B (2012) Amperometric acetylcholine biosensor based on self-assembly of gold nanoparticles and acetylcholinesterase on the sol–gel/multi-walled carbon nanotubes/choline oxidase composite-modified platinum electrode. Biosens Bioelectron 33:44
60. Stasyuk N, Smutok O, Gayda G, Vus B, Koval'chuk Y, Gonchar M (2012) Bi-enzyme L-arginine-selective amperometric biosensor based on ammonium-sensing polyaniline-modified electrode. Biosens Bioeletron 37(1):46
61. Ahmadalinezhad A, Chen A (2011) High-performance electrochemical biosensor for the detection of total cholesterol. Biosens Bioeletron 26:4508

62. Yadav S, Devi R, Kumar A, Pundir CS (2011) Tri-enzyme functionalized ZnO-NPs/CHIT/c-MWCNT/PANI composite film for amperometric determination of creatinine. Biosens Bioeletron 28:64
63. Yadav S, Kumar A, Pundir CS (2011) Amperometric creatinine biosensor based on covalently coimmobilized enzymes onto carboxylated multiwalled carbon nanotubes/polyaniline composite film. Anal Biochem 419:277
64. Wang J (2001) Glucose biosensors: 40 years of advances and challenges. Electroanal 13(12):983
65. Moehlenbrock MJ, Meredith MT, Minteer SD (2012) Bioelectrocatalytic oxidation of glucose in CNT impregnated hydrogels: advantages of synthetic enzymatic metabolon formation. ACS Catal 2:17
66. Jeykumari DRS, Narayanan SS (2009) Functionalized carbon nanotube-bienzyme biocomposite for amperometric sensing. Carbon 47:957
67. Solanki PR, Dhand C, Kaushik A, Ansari AA, Sood KN, Malhotra BD (2009) Nanostructured cerium oxide film for triglyceride sensor. Sensor Actuat B Chem 141:551
68. Jamal M, Worsfold O, McCormac T, Dempsey E (2009) A stable and selective electrochemical biosensor for the liver enzyme alanine aminotransferase (ALT). Biosens Bioelectron 24:2926
69. Xiang Y, Zhang Y, Jiang B, Chai Y, Yuan R (2011) Multi-enzyme layer-by-layer assembly for dual amplified ultrasensitive electronic detection of cancer biomarkers. Sensor Actuat B Chem 155:317
70. Xiang Y, Zhang Y, Qian X, Chai Y, Wang J, Yuan R (2010) Ultrasensitive aptamer-based protein detection via a dual amplified biocatalytic strategy. Biosens Bioelectron 25:2539
71. Bai L, Yuan R, Chai Y, Yuan Y, Zhuo Y, Mao L (2011) Bi-enzyme functionlized hollow PtCo nanochains as labels for an electrochemical aptasensor. Biosens Bioelectron 26:4331
72. Bagal-Kestwal D, Kestwal RM, Hsieh BC, Chen RL, Cheng TJ, Chiang BH (2010) Electrochemical $\beta(1 \rightarrow 3)$-d-glucan biosensors fabricated by immobilization of enzymes with gold nanoparticles on platinum electrode. Biosens Bioelectron 26:118
73. Katrlík J, Pizzariello A, Mastihuba V, Švorc J, Stred'anský M, Miertuš S (1999) Biosensors for L-malate and L-lactate based on solid binding matrix. Anal Chim Acta 379:193
74. Diaconu M, Litescu SC, Radu GL (2011) Bienzymatic sensor based on the use of redox enzymes and chitosan–MWCNT nanocomposite. Evaluation of total phenolic content in plant extracts. Microchim Acta 172:177
75. Han YD, Jeong CY, Lee JH, Lee DS, Yoon HC (2012) Microchip-based organophosphorus detection using bienzyme bioelectrocatalysis. Jpn J Appl Phys 51:06FK01
76. Nikitina O, Shleev S, Gayda G, Demkiv O, Gonchar M, Gorton L, Csöregi E, Nistor M (2007) Bi-enzyme biosensor based on NAD^+- and glutathione-dependent recombinant formaldehyde dehydrogenase and diaphorase for formaldehyde assay. Sensor Actuat B Chem 125:1

Adv Biochem Eng Biotechnol (2014) 140: 253–298
DOI: 10.1007/10_2013_236

Published Online: 16 November 2013

Protein Multilayer Architectures on Electrodes for Analyte Detection

Sven C. Feifel, Andreas Kapp and Fred Lisdat

Abstract This chapter provides an overview of different assembly methodologies used for the construction of multilayer architectures with biomolecules for application in sensors. Besides the use of bioaffinity interactions and covalent strategies, special attention will be paid to the electrostatic layer-by-layer technique. Different building blocks can be used for the formation of multilayers with a clear preference for polymers and nanoparticles. Among the biomolecules, enzymes and redox proteins are in the focus. Because of the high importance of multilayers formed on electrodes, the chapter will concentrate on sensor systems with electrochemical transduction. Particularly advantageous are schemes that can avoid diffusible shuttling molecules between the biomolecule and the electrode and that represent artificial signal chains by exploiting direct protein–protein communication in the immobilized state.

Keywords Biosensors · Electrochemical · Enzyme · Layer-by-Layer · Multilayer · Nanomaterials · Self-assembly

Abbreviations

AOx	Ascorbate oxidase
AChE	Acetylcholine esterase
AuNP	Gold nanoparticle
BSA	Bovine serum albumin
BOD	Bilirubin oxidase
Bpy	Bipyridyl
CDH	Cellobiose dehydrogenase
CHIT	Chitosan
ChE	Choline esterase
ChOx	Choline oxidase
COx	Cholesterol oxidase

S. C. Feifel · A. Kapp · F. Lisdat (✉)
Biosystems Technology, Technical University of Applied Sciences Wildau, Wildau, Germany
e-mail: flisdat@th-wildau.de

CE	Cholesterol esterase
CEA	Carcinoembryonic antigen
Con A	Concanavalin A
CNT	Carbon nanotube
cyt *c*	Cytochrome c
cyt *b*	Cytochrome b
DET	Direct electron transfer
DIDS	4,4′-diisothiocyanate-2,2′-stilbene-sulfonic acid
DIP	2,6-dichloro-indophenol
DNA	Desoxyribonucleic acid
dsDNA	Double-stranded deoxyribonucleic acid
DSP	3,3′-dithiodipropionic acid bis(N-hydroxysuccinimide ester)
EACC	6-Ethoxytrimethylammoniochitosan chloride
ECL	Electrochemiluminescence
EIS	Electrochemical impedance spectroscopy
FAD	Flavin adenine dinucleotide
FIA	Flow injection analysis
FITC	Fluoresceinisothiocyanate
GCE	Glassy carbon electrode
GDH	Glucose dehydrogenase
GOx	Glucose oxidase
GN	Graphene sheet
Hb	Hemoglobin
HBs-Ab	Hepatitis B antibody
HRP	Horseradish peroxidase
HX	Hypoxanthine
IgG	Immunoglobulin G
LOx	Lactate oxidase
LBL	Layer-by-layer
Mb	Myoglobin
MU	11-mercapto-1-undecanol
MUA	Mercaptoundecanoic acid
MWCNT	Multiwall carbon nanotube
MPS	3-mercapto-1-propanesulfonic acid
NADH	Nicotinamide adenine dinucleotide
NHS	N-hydroxysuccinimide
NP	Nanoparticle
PAA	Poly(acrylic acid)
PAMAM	Polyamidoamine
PAH	Poly(allylamine hydrochloride)
PANI	Polyaniline
PASA	Poly(aniline-sulfonic acid)
PAPSA	Poly(anilinepropane-sulfonic acid)
PDDA	Poly(dimethyl-diallylammonium chloride)

PEI	Poly(ethyleneimine)
PLL	Poly(L-lysin)
PMA	Poly(methacrylic acid)
PSS	Poly(styrene-sulfonate)
PSAA	Poly(sulfanilic acid)
PVP	Poly(vinyl-pyridine
PVS	Poly(vinylsulfonate)
QCM	Quartz crystal microbalance
QD	Quantum dot
SOx	Sulfite oxidase
SiNP	Silica nanoparticle
SPR	Surface plasmon resonace
SWV	Square wave voltammetry
SWCNT	Single-wall carbon nanotube
ssDNA	Single-stranded deoxyribonucleic acid
TB	Toluidine blue
THI	Thionine
XOD	Xanthine oxidase

Contents

1 Introduction

First conceptualized in the 1960s, the development of biosensors has continuously progressed since then. A biosensor can be defined as a device incorporating a biological sensing element connected to a transducer to convert an observed biomolecular interaction into a measurable signal, the magnitude of which is

proportional to the concentration of a specific molecule [1]. Among the various kinds of biosensors, electrochemical biosensors are the most common devices [2].

The immobilization process of the biocomponent, which specifically recognizes the analyte, is a key step in the construction of biosensors [3]. However, there is often limited activity of the biomolecules at the solid–liquid interface, which is related to the need for the biomaterial to be well arranged on the surface (or within) an assembly [4]. Furthermore, the amount of biomolecules immobilized is connected to the sensitivity of the whole sensing device. This gives rise to the development of immobilization procedures that moved away from simple mixing of the biocomponent with a matrix to methods that allow a layered and controlled deposition of the recognition element, resulting in multilayered architectures on the transducer surface. This chapter gives an overview of the methods available for arranging biomolecules in a layer-by-layer (LBL) design [5]. Furthermore, applications in sensor construction are illustrated, with a focus on electrochemical transduction.

2 Multilayer Architectures: Assembly Methods

Immobilization is an essential part of biosensor construction. The main aim is that the biomolecules are properly attached to the surface or the supporting matrix and thereby maintain their activity. Furthermore, it is desirable to use simple but also reproducible procedures for the fixation.

The local chemical environment can have profound effects on the activity and stability of the biological recognition element. Therefore, several factors have to be considered before selecting an appropriate immobilization method, such as the following:

- The nature of the biological component
- The accessibility of the biomolecule within the assembly after immobilization
- The essential functionalities of the bioelement, which should not be blocked or affected during the assembly process
- The physico-chemical properties of the analyte, which need to reach the recognition element
- The type and the surface of the transducer
- The desired lifetime of the device
- The response time of the sensor needed for application
- The operating conditions under which the biosensor has to function.

Considering all of these factors, it is often not easy to develop a procedure for maximum biomolecule activity under certain conditions. The issue of sensitivity is particularly important for an efficient biosensor. The sensitivity depends on several factors: the recognition properties of the selected biomolecule, the density distribution and/or orientation of the biological material near the sensor surface, and the sensitivity of the transduction system. Thus, the last decade can be characterized by

the development of more complex immobilization schemes. One direction is connected to the preparation of multilayer architectures on transducers. The concept is based on the combination of individual layers of the biocomponent or even several biomolecules. Thus, the techniques used are often called LBL methods. Several advantages can be seen for such an approach:

(i) Surface density can be controlled by the number of layers and also by the composition of each layer.
(ii) A high surface density may result in higher response at a given concentration.
(iii) Control of the permeation of substrates (or cofactors) will influence the dynamic range of the sensor and also the response time.
(iv) The deposition in a layered fashion can be beneficial in the exclusion of interfering substances.
(v) Additional layers can also be deposited on top of the assembly to improve stability and specificity.

Different strategies for arranging biomolecules in multiple layers have been developed. They can be classified according to the basic interaction principle used: biospecific interactions (e.g. antibody–antigen), covalent binding/cross-linking of the layer constituents, or adsorption of differently charged molecules or particles. These strategies are discussed in the following sections. In addition, examples of biosensorial applications are illustrated. Because of the importance of electrostatic LBL constructions, sensor systems based on this approach are treated in more detail in Chap. 3.

2.1 Biospecific Interactions

One strategy for preparing protein multilayer films makes use of biospecific interactions between two biomolecules. These interactions are noncovalent by nature but can be rather strong. Examples include avidin–biotin, lectin–sugar, and antibody–antigen interactions. When weaker interactions are used, such as DNA hybridization, reversible binding becomes feasible. To exploit these highly specific and stable binding reactions for multilayer construction, first the biomolecule that is supposed to be used as a recognition element needs to be coupled to such a biospecific molecule. Alternatively, the sensing component may already be a carrier of ligands for biospecific interactions (e.g. glycosylated enzymes/proteins, which can be bound by lectins).

2.1.1 Biotin–Avidin Interaction

Biotin, also known as vitamin H, is a small molecule (molecular weight [Mw] = 244.3 Da) that is present in tiny amounts in all living cells. The valeric acid side chain of the biotin molecule can be derivatized to incorporate various reactive

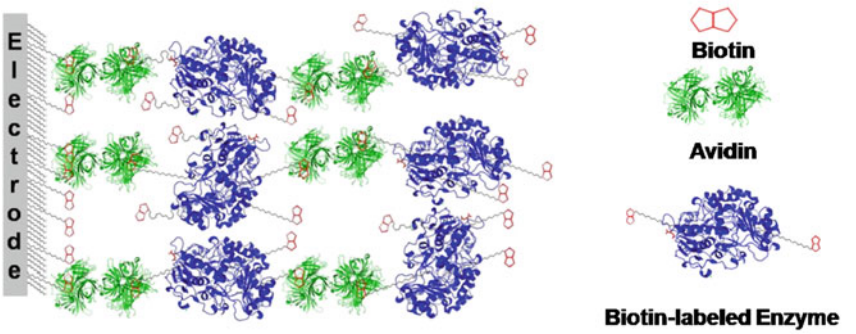

Fig. 1 Multilayer architecture on an electrode surface using avidin and a biotin-labeled enzyme. Figure adapted from Ref. [8]

groups that are used to attach biotin to other molecules. Once biotin is attached to a molecule, it can be immobilized through interaction with avidin.

Avidin (MW 66 kDa) is a glycoprotein found in the egg white and tissues of birds, reptiles, and amphibia. It has nearly a globular shape and contains four identical biotin-binding sites arranged in two pairs on opposite faces of the molecule, with a high affinity for biotin (binding constant, $K_a \sim 10^{15}\ M^{-1}$) [6, 7]. In addition to avidin, streptavidin (from *streptomyces avidnii*) and neutravidin (deglycosylated avidin) have been used for similar purposes.

Alternating and repeated deposition of avidin and biotin-labeled enzymes or proteins produces a multilayer structure composed of monomolecular layers, as schematically shown in Fig. 1. Several enzymes have been integrated in the multilayer architecture with avidin, such as glucose oxidase (GOx), lactate oxidase (LOx), and alcohol oxidase (AOx) [8–15]. The enzymes are catalytically active in the multilayer films. Signal generation can be performed via hydrogen peroxide conversion at the subjacent electrode (first-generation biosensor).

In other examples, a mediator has been introduced into multilayer systems for signal transfer (second-generation biosensor). Thus, in a hydrogenase-based system, methyl-viologen is used as a diffusional mediator [16]. The mediator can also be integrated into the multilayer system by stably coupling it to the matrix. Thus, for example, the charge transfer in multilayer films with covalently linked ferrocene has been studied [17].

In addition to constructing enzyme multilayers with one kind of protein, it is possible to combine different enzymes immobilized in different layers. This route allows for the buildup of multienzyme sensing schemes, such as the use of sequential reactions. In this case, the analyte is first converted by one enzyme to a product that is subsequently converted into a second product by another enzyme. The overall reaction is finally detected by analyzing the formation of a coproduct or using a redox mediator, for example.

This principle can be demonstrated in an acetylcholine biosensor that has been constructed by optimizing the loading of choline esterase (ChE) and choline oxidase (ChOx) on a Pt-black electrode [18]. In this case, the idea of sequential enzyme reactions is confined to the sensor surface: The part of choline, which is in its esterified form, is first cleaved within the ChE layer before it can react in the underlying ChOx-layers to form H_2O_2, which subsequently reacts at the Pt electrode (first-generation biosensor). A sensor modified with 10-layer ChOx exhibits its maximum response to acetylcholine when two additional layers of ChE are added to the surface of the ChOx layer. The (ChOx)/(ChE)-based biosensor displays a concentration-dependent amperometric response to acetylcholine. The response time is fast for all sensors (10 s or faster). This is attributed to the rather thin ChOx/ChE membranes, which do not significantly alter the transport of acetylcholine and products of the enzymatic reactions in the membrane.

Bienzyme sensors have also been constructed with a different background. For example, GOx/ascorbate oxidase (AsOx) and LOx/AOx multilayers are used to effectively eliminate ascorbic acid interference. Such a biosensor can determine the normal blood level of glucose (5 mM) and lactate (1 mM) in the presence of physiological level of ascorbic acid (0.1 mM) [19, 20]. The response time of both sensors is 10 s or faster, irrespective of the number of the AOx layer, confirming the smooth transport of substrates across the AOx layers.

2.1.2 Lectin–Sugar Interaction

Another way to construct enzyme multilayers has been achieved by the use of lectin–sugar interactions. Concanavalin A (Con A) appears to be a promising building block for preparing enzyme multilayer films. Con A is a lectin protein (MW 104,000 Da) that contains four identical binding sites to sugars, such as D-mannose or D-glucose. The binding between Con A and sugar is not covalent and reversible [21]. Lvov et al. [22, 23] were the first to use Con A to develop multilayer films in combination with glycogen, a polysaccharide composed of D-glucose units through biological affinity, without extending the application of such multilayer films to the construction of biosensors. One of the benefits of using Con A for the formation of multilayers is that certain kinds of enzymes, such as GOx and horseradish peroxidase (HRP), can be used without labeling because such enzymes intrinsically contain polysaccharide chains on their molecular surface. This is advantageous because the glycosylation of the proteins is not connected to the catalytic function. Thus, the assembly process is used to construct multilayer-based biosensors with Con A and glycoenzymes via sugar chains (Fig. 2).

For example, the sensitivity of a flow-through glucose monitoring cartridge, integrated into a flow injection analysis system, is improved significantly by increasing the amount of immobilized GOx via bioaffinity layering [24]. A cartridge bearing six layers of GOx on a Sepharose support can be used effectively and repeatedly for analysis of medium glucose concentration during a fed-batch

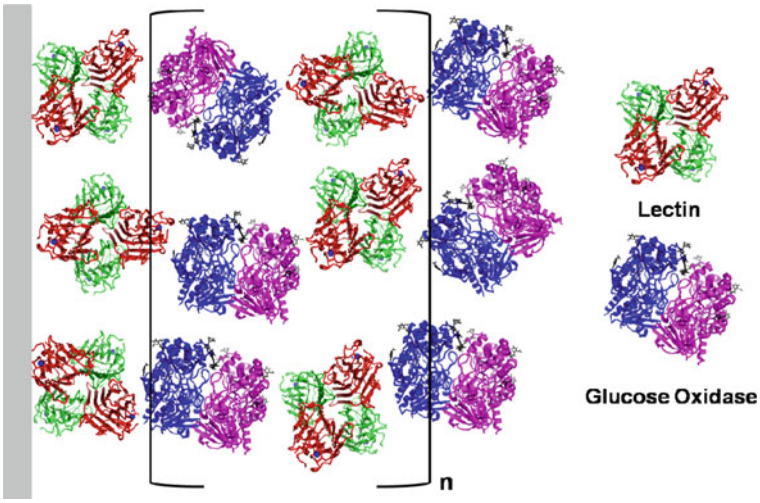

Fig. 2 Multilayer system of ConA (lectin)–glucose oxidase on an electrode. Figure adapted from Ref. [24]

cultivation of yeast *Saccharomyces cerevisiae*. Signal detection is based on the liberation of H_2O_2 during glucose oxidation. However, the formation of more than five bioaffinity layers on the Sepharose matrix is ineffective in further enhancing the sensitivity.

In addition, bienzyme multilayer films using lectin and glycoenzymes, such as GOx and HRP, have been used for biosensor applications [25]. During glucose oxidation in the GOx layers, hydrogen peroxide is produced, which is subsequently converted in the HRP layers. The enzymes are catalytically active and stable in the multilayer films and the response of the sensing electrode depends linearly on the number of enzyme layers. The $(HRP)_5(GOx)_5$ film-modified electrode is used to determine 10^{-6}–10^{-3} M H_2O_2 and 10^{-5}–10^{-2} M glucose, with nearly the same maximum current ($\sim$ 8.0 mA). Based on the same enzymes, other systems have been developed to make use of mediated electron transfer by means of an Osmium polymer [26, 27]. Also, mannose-labeled LOx (which contains intrinsically no sugar chain) has been successfully integrated in the construction of multilayer films [28].

Another approach uses pH-dependent electrocatalysis on electrodes modified with multiple layers composed of Con A and redox proteins (myoglobin) or enzymes (HRP) [29–32]. A dextran/Con A/myoglobin multilayer-coated electrode has been constructed, and the catalytic reduction of O_2 and H_2O_2 at the electrode is studied [29]. The electrode reactions are regulated as a function of the number of protein layers (up to eight) in the assembled films.

These findings support the possible use of Con A/enzyme layered systems for the development of biosensor interfaces. However, multilayer films constructed

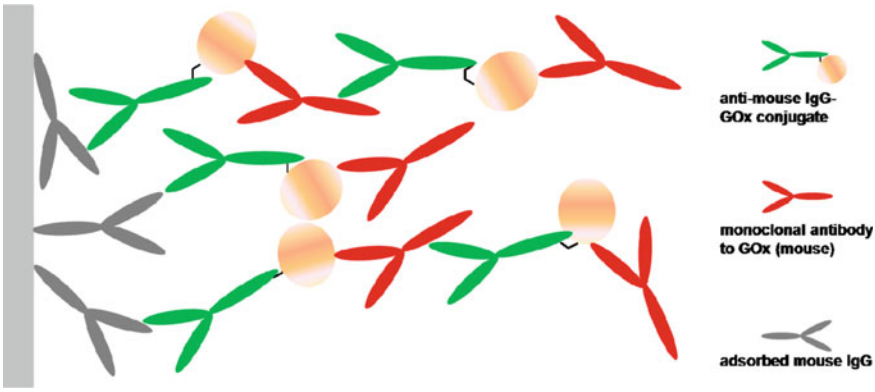

Fig. 3 Scheme of the construction of multilayers of glucose oxidase on a glassy carbon electrode surface. Figure adapted from Ref. [33]

with Con A may be sensitive to sugars because these structures rely on the reversible binding between Con A and sugar residues.

2.1.3 Antibody–Antigen Interaction

To make further use of biospecific interactions, antibody–antigen reactions have been employed to organize multilayers for electrochemical biosensors. The antibody (also known as immunoglobulin [Ig]) recognizes a unique part of a target, called an antigen. Each antibody contains a paratope that is specific for one particular epitope on an antigen, allowing these two molecules to bind together with specificity and precision to form very stable noncovalent bonds. For this approach, the (bio)molecule has to be fixed to one of the partners of the antibody–antigen couple or it possesses an antigenic structure by itself.

For example, an immunological method has been developed, allowing the layered assembly of IgG-labeled GOx and anti-GOx IgG onto an electrode surface. A glassy carbon electrode is coated with gelatin, and mouse IgG antibodies are adsorbed onto the gelatin [33–38]. A conjugate consisting of GOx linked to the antimouse IgG antibody is bound to the antibody associated with the gelatin to yield an enzyme-modified electrode on which further GOx-layers are assembled by the use of monoclonal antibodies against GOx produced in mouse (Fig. 3). The immunological procedure has been extended up to 10 enzyme monolayers. The immobilized enzyme is fully active and its kinetic properties are the same as those of the native enzyme in solution. For signal generation, a mediator-type scheme is applied. For this purpose, ferrocene is used to transfer the electrons from GOx through the network towards the electrode (second-generation biosensor).

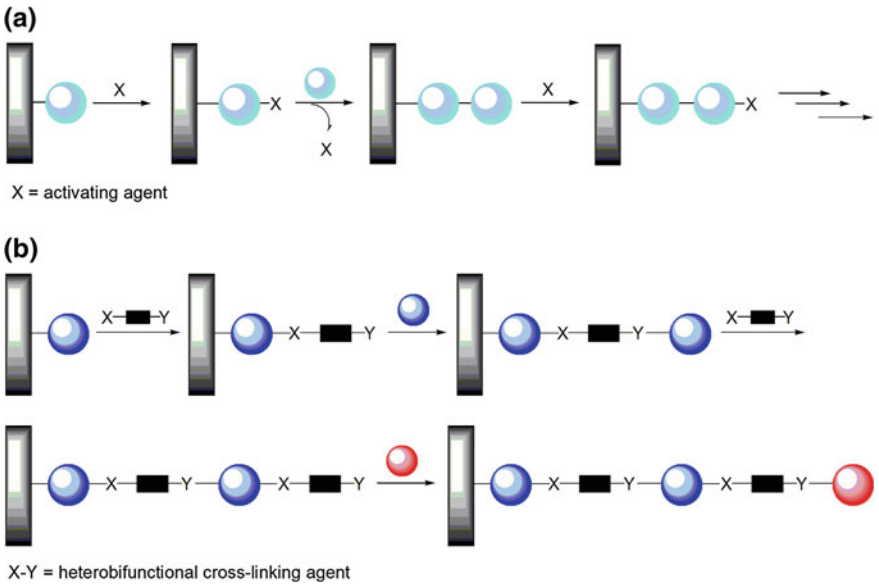

Scheme 1 Covalent biomolecule immobilization. **a** Step-by-step covalent coupling route via activating agents. **b** Cross-linking by the use of a bifunctional reagents. The *blue* and *red spheres* represent the respective biomolecules used

2.2 Covalent Binding/Cross-Linking

An alternative approach for the immobilization of biomolecules to a sensor surface is through covalent binding. In this approach, biomolecules are immobilized on solid surfaces through the formation of defined chemical linkages [39, 40]. Immobilization by other methods is sometimes associated with instability or leakage of proteins; these problems are common when biomolecules are trapped on sensor surfaces by means of polymer matrices or adsorption, but they can be overcome by using covalent immobilization procedures.

Covalent binding of biomolecules to the surface can result in loss of biomolecule activity because of unwanted reactions. Therefore, care has to be taken in the choice of linkers and coupling strategies to achieve minimal loss of specific recognition or catalytic activity [41–46]. Covalent coupling has been employed to improve uniformity, density, and distribution of the bound proteins in a multilayer fashion onto a surface. It has the advantage that the biomolecule is generally stable when immobilized and therefore unlikely to detach from the surface during use [46–51].

Covalent coupling between the enzyme or protein and the solid support is best achieved through functional groups on the biomolecule surface that are not required for its biological activity. Biomolecules such as enzymes and proteins have several functional groups present for covalent immobilization onto surfaces;

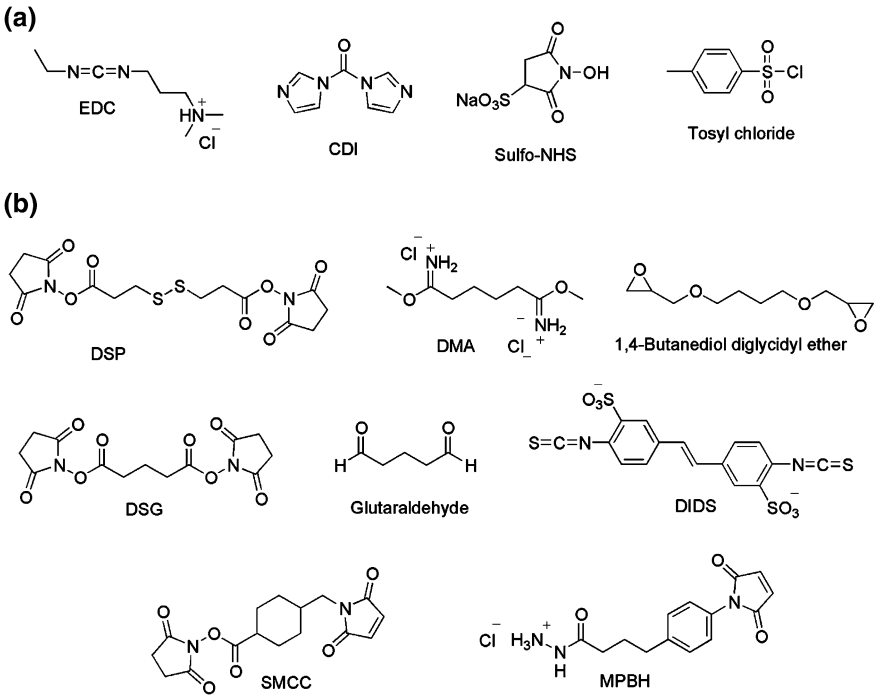

Fig. 4 **a** Activating agents. **b** Homo- and heterobifunctional cross-linking agents. *EDC* 1-ethyl-3-(3-dimethylaminopropyl)carbodiimide, *CDI* N,N′-carbonyldiimidazol; *Sulfo-NHS* N-hydroxysulfo-succinimide, *DSP* dithiobis succinimidylpropionate, *DSG* disuccinimidyl glutarate, *DMA* dimethyl adipimidate dihydrochloride, *SMCC* succinimidyl-4-(N-maleimido-methyl)cyclohexane-1-carboxylate; *MPBH* (4-N-maleimidophenyl)butyric acid hydrazide hydrochloride, *DIDS* 4,4′-diisothiocyanate-2,2′-stilbene-disulfonic acid

these include carboxylic acid groups, amino groups, hydroxyl groups, sulfhydryl groups, phenolic groups, and imidazole groups.

There are two main approaches used for covalent coupling on sensor surfaces (Scheme 1). In the first approach, activation reagents are used to mediate the conjugation of two molecules by forming a bond between a group of one biomolecule with a group of the other one. Thus, one atom is covalently attached to an atom of a second molecule with no intervening linker or spacer. The chemistry of reactive groups and how they can be activated covers a broad spectrum of different reagents; however, because of the fragility of biomolecules, only a limited number of them can be applied for bioconjugation reactions. The agents described in this section can initiate the formation of four types of bonds: an amide linkage made by the condensation of a primary amine with a carboxylic acid, a phosphoramidate linkage made by the reaction of an organic phosphate group with a primary amine, an ester linkage and a Schiff base or amine linkage made by the reaction of a primary amine with an aldehyde group. A Schiff base (the first reaction product of an amine with an aldehyde) can be reduced to a secondary amine linkage. All of

the reactions are quite efficient. Depending on the reagent chosen and the desired application, they may be performed in aqueous or nonaqueous environments.

For the activation of the functional groups as illustrated in Scheme 1a, different activation agents can be used. Some examples are shown in Fig. 4. *Carbodiimides* are used to mediate the formation of an amide linkages between carboxlates and amines or phosphoramidate linkages between phosphates and amines. The water-soluble carbodiimides are the most common choice for biochemical conjugations because most macromolecules of biological origin are stable only in aqueous buffer solutions. *EDC (1-ethyl-3-(3-dimethylaminopropyl)* carbodiimide is the most popular carbodiimide used for conjugating biomolecules. Another example is *CMC 1-cyclohexyl-3-(2-morpholinoethyl)carbodiimide*.

Carbonyldiimidazoles, such as *CDI* (*N,N′-carbonyldiimidazole*), are highly active carbonylating agents that contain two imidazole leaving groups. They can be used to activate carboxylic acids or hydroxyl groups for conjugation with other nucleophiles, thereby creating either a zero-length amide bond or one-carbon-length N-alkyl carbamate linkage between the coupled molecules. The active carboxylate can further react with amines to form amide bonds or with hydroxyl groups to form ester linkages. If a carbonyldiimidazole is used to activate a hydroxyl functional group, the reaction proceeds differently because the active intermediate formed by the reaction of a carbonyldiimidazole with a hydroxyl group is an imidazoyl carbamate, which can be attacked by an amine releasing the imidazole but not the carbonyl. Thus, a hydroxyl-containing molecule may be coupled to an amine-containing molecule with the result of a one-carbon spacer, forming a stable urethane (N-alkyl carbamate) linkage.

N-hydroxysuccinimides, such as *NHS (N-hydroxysulfo-succinimide),* can also be used to activate carboxylic groups to form active esters to react with an attacking amine from the other molecule to form an amide linkage. N-hydroxysuccinimide esters are more stable in aqueous solutions but still couple rapidly with amines on target molecules.

Tosylates, such as *4-toluenesulfonyl chloride,* are used to activate hydroxyl groups. The modification of the hydroxyl group (which is a relatively poor leaving group) by the tosylate transforms it into a good leaving group, and thus it reacts with other nucleophiles such as amines.

Another type of activation agent is *$NaIO_4$*. $NaIO_4$ allows the oxidative conversion of sugar structures (e.g. on protein surfaces) to aldehydes, which in turn can be used to react with another nucleophile, such as an amine, to form a linkage between the two molecules.

In a second approach, bifunctional reagents are used (so-called cross-linkers). Cross-linking is achieved with the use of reagents containing (at least two) reactive end groups. The bifunctional reagents are characterized as either homobifunctional or heterobifunctional. Most of the compounds containing the same functionality at both ends are symmetrical in design, with a carbon chain spacer connecting the two reactive ends. The length of the spacer may be designed to achieve the optimal distance between two molecules to be conjugated. Therefore, these reagents glue one protein to another by covalently reacting with the same group on both

molecules. Thus, for example, amino groups on the surface of a protein are modified with a cross-linker (e.g. glutaraldehyde) in such a way that the amine group is coupled to one end of the cross-linker, exposing the other (reactive) end for further protein coupling (see Scheme 1b).

In addition, heterobifunctional cross-linkers may be used, which contain two different reactive groups that can couple to different functional targets on proteins and other macromolecules. This results in the ability to direct the cross-linking reaction to selected parts of target molecules, thus gathering better control over the conjugation process.

There are mainly four functional groups that have been found to be successful cross-linking targets: primary amines, carboxyls, sulfhydryls, and hydroxyls. The cross-linkers discussed in the following sections are the types most often referred to in literature or are commercially available.

Homobifunctional Cross-linkers

Bis-NHS-esters are highly reactive towards amine nucleophiles. *Bis-imidoesters* carry one of the most specific acylating groups available for the modification of primary amines, with minimal cross-reactivity toward other nucleophilic groups in proteins. *Bis-maleimides* can react with sulfhydryls to form stable thioether linkages. *Bis-aldehydes* are likely used to react with primary or secondary amines. *Bis-epoxides* can be used to cross-link molecules containing nucleophiles, including amines, sulfhydryls, and hydroxyls (the reaction proceeds with epoxide ring opening).

Heterobifunctional Cross-linkers

In several heterobifunctional linkers, the previously mentioned functionalities are combined, such as an NHS ester on one side and a maleimide group on the other side of the linker. In Fig. 4, some homo- and hetero-crosslinkers are shown. To illustrate the covalent multilayer concept, several examples for sensor construction are described here. A multilayered arrangement of GOx has been achieved by previous modification of functional groups on the protein surface. Thereby, the carbohydrate groups on the peripheral surface of GOx are first oxidized to aldehydes by periodate [53–55]. Thereafter, a cross-linker with a large number of amine groups, such as on poly(L-lysin) (PLL) and polyamidoamine (PAMAM) dendrimer, is used to react with periodate-oxidized GOx (aldehyde groups formed on the surface) to form a Schiff base. The sensor signal can be monitored by detection of H_2O_2, which is produced during the oxidation of glucose. The sensitivity of the constructed multilayer is tunable by the number of layers (five), with the possibility to extend this immobilization method for the construction of multilayer films with other enzymes.

The approach of bifunctional reagents has been used to construct a multilayer enzyme electrode through covalent attachment of quinoprotein glucose dehydrogenase (PQQ-GDH) onto a gold electrode surface [52]. The gold electrode surface is modified with 3,3′-dithiodipropionic acid bis-N-hydroxy succinimide ester

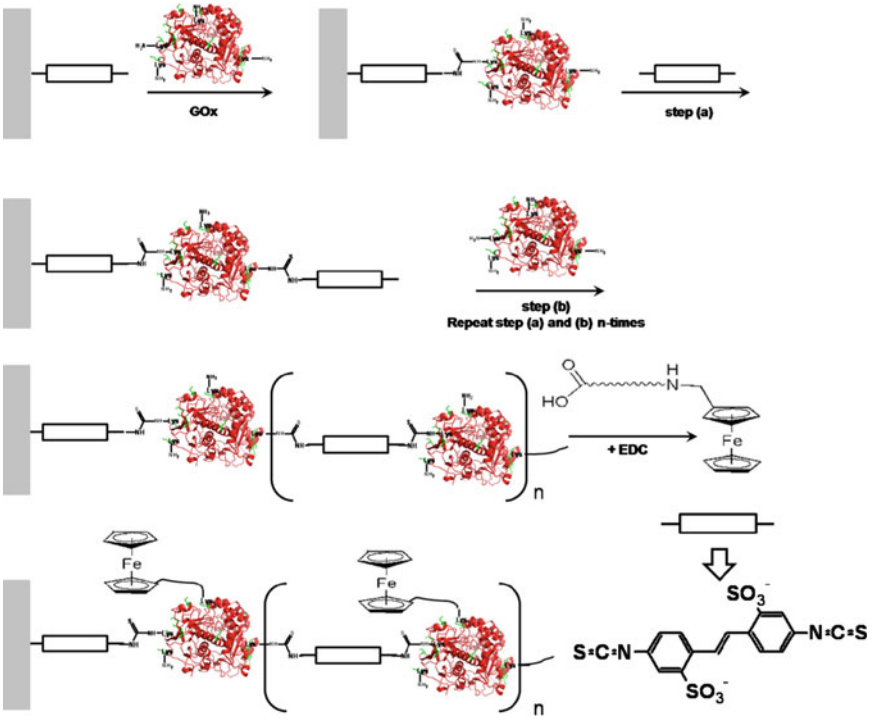

Fig. 5 Stepwise assembly of a covalently-linked multilayer system of glucose oxidase (GOx) on a gold electrode (Au). The linkage is formed by the reaction of the amino groups on GOx with the isothiocyanate groups of the bifunctional reagent. Electrical contact between the enzyme molecules and the electrode is established via the multiple ferrocene moieties. Figure adapted from Ref. [56]

(DSP), which has a disulfide linkage that rapidly chemisorbs onto the gold surface and possessing an activated succinimide ester (NHS) group for efficient coupling of the protein. When the activated electrode is dipped into an GDH solution, the enzyme spontaneously binds to the modified gold. The resulting monolayer-GDH electrode is then activated by the bifunctional reagent 4,4′-diisothiocyanate-2,2′-stilbene-disulfonic acid (DIDS); further layers of GDH have been stepwise coupled to the primary layer. This system can be applied as recycling sensor for *p*-aminophenol, which is oxidized at the electrode and re-reduced by the enzyme GDH. The steady-state current of the multilayer electrode to *p*-aminophenol concentrations is linear in the range of 10 nM to 10 mM, with a detection limit of 5 nM. After 2 months of storage, the multilayered biosensor maintains 75 % of its original activity.

This concept has also been used to construct enzyme multilayer biosensors for sensing of glucose, choline, and acetylcholine. By the use of bivalent cross-linking reagents, the enzymes are fixed in the layered films through covalent bonds [56].

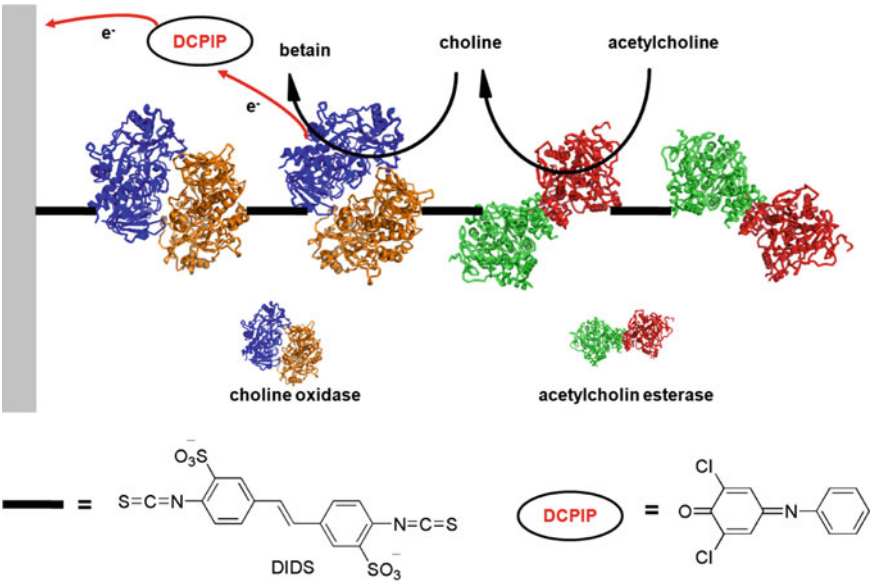

Fig. 6 Layered assembly of two enzymes for amperometric sensing of acetylcholine. *AChE* acetylcholine esterase, *ChO* choline oxidase, *DCPIP* dichlorophenol indophenol. Figure adapted from Ref. [63]

As an electron mediator, ferrocene carboxylic acid is used for the electrical communication of the enzyme with the electrode (Fig. 5). The linear range of the glucose biosensor is up to 15 mM. The layered GOx network electrodes reveal unaltered activity for 6 months when stored dry at 4–8 °C.

As described previously, enzyme multilayers can be constructed by combining different enzymes immobilized in different layers; thereby, the buildup of multienzyme sensing schemes, such as sequential reactions, becomes feasible. Here, the analyte is first converted by one enzyme to a product that in turn is subsequently converted to a second product by another enzyme. Such an amperometric acetylcholine biosensor is established using a multilayered network consisting of choline oxidase (ChO) and acetylcholine esterase (AChE) bienzyme layers [63]. In this system, choline generated by AChE hydrolysis of acetylcholine is converted by the ChO layers in the presence of soluble dichlorophenol indophenol (DCPIP). DCPIP acts as diffusional electron mediator and is amperometrically detected at the electrode (Fig. 6).

Both covalent attachment and cross-linking of entrapped enzymes or proteins in multilayer systems can often alleviate the problem of biomolecule leakage. Cross-linking of biological components by means of a bifunctional or multifunctional reagent affords an enhanced stability of the deposited proteins that are supposed to be fixed onto the support. Glutaraldehyde, which couples with the amino groups of enzymes, is by far the most common cross-linking agent used in biosensor applications. A selected example includes the cross-linking of proteins such as

BSA with GOx using glutaraldehyde to produce a thin layer on the sensor surface [57].

The approach of cross-linking can also be combined with different strategies for the multilayer formation. One example is shown for glucose and lactate biosensors combining electrostatic LBL deposition (see Sect. 2.3) and chemical cross-linking [60]. Cross-linking is accomplished here by exposing the thin film to glutaraldehyde vapor, thus inducing linkage formation between lysine and arginine residues present on the enzyme periphery with amine groups on a redox polymer, poly[vinylpyridine Os(bisbipyridine)2Cl]-co-allyamine. Reproducible analyte response curves from 2 to 20 mM (glucose-GOx) and 2–10 mM (lactate-LOx) can be obtained. The electron transfer between the redox polymer and enzyme is improved and the cross-linked films are able to retain nearly 100 % of their activity for 3 weeks. The authors explain that cross-linking of the multilayer structure likely decreases the distance between enzyme active sites and redox sites while providing direct routes of charge transfer. For more insights in the combination of different immobilization strategies, the reader is referred to other references [57–64]. Immobilization problems associated with leakage of proteins can be overcome using covalent immobilization routes, resulting in very stable systems. However, as for many immobilization strategies, there are also some disadvantages associated with this method, such as the following:

- It is often difficult to control the cross-linking reaction.
- Loss of activity of the proteins or enzymes in the multilayer system may occur after covalent coupling reactions.
- Rather large diffusion barriers can be formed because of tight binding of biomolecules, resulting in slow response.

The suitability of the covalent coupling is also very much dependent on the biomolecule used, the cross-linking agent, and the spacing capability, as well as on the kind of signal generation, such as the diffusion of generated species or a hopping of electrons between the redox-active sites within the immobilization matrix.

2.3 Electrostatic Interactions

Adsorption of biomolecules from solution onto solid surfaces can proceed via either physical or chemical interactions. Physical adsorption involves van der Waals forces, ionic binding, or hydrophobic forces [65]. For multilayer formation, electrostatic interactions are mainly used, although other interactions may contribute to the binding. This method is also called polyelectrolyte adsorption technique or electrostatic LBL assembly. The method is based on the constrcution of a multilayer thin film from oppositely charged species deposited in succession on a solid support (Fig. 7).

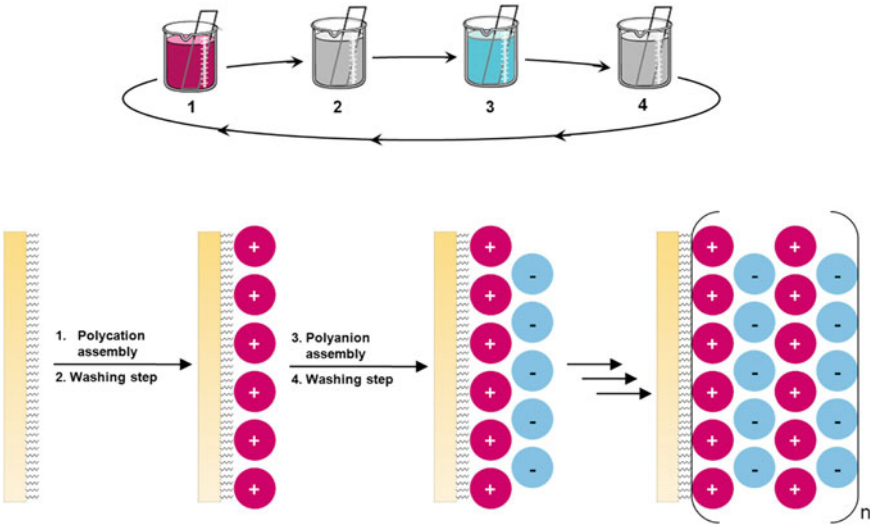

Fig. 7 Layer-by-layer method: initially a base electrode is modified with a charged layer. This negatively charged substrate is then immersed in a polycation and a polyanion aqueous solution, respectively (e.g. protein, nanoparticles, polyelectrolytes, DNA). Figure adapted from Ref. [5]

The method is very advantageous because it is more versatile than other film fabrication techniques. In addition, a large range of different materials, including polyelectrolytes [66, 67], nanoparticles [68, 69], dendrimers [70, 71], carbon materials [72], and many others [73] can be employed in the fabrication of multilayer films. Moreover, parameters such as roughness, thickness, and porosity of films can be controlled by changing experimental conditions, such as pH, temperature, concentration of the building blocks, and ionic strength of the media [74].

The main driving force in alternate LBL assembly is the electrostatic interaction between oppositely charged species [75]. Therefore, the layer formation can be described as the kinetic trapping of charged species from solution on a surface. Multilayer film assembly is possible because of charge reversal on the film surface after each adsorption step. Surface charge therefore depends on the last adsorbed layer, permitting a degree of control over surface and interface properties. A high charge density in the adsorbing species will result not only in strong attraction between molecules in neighboring layers but also in strong repulsion between like-charged molecules in the same layer. That is, electrostatics both drives layer assembly and limits it. Several layers of material applied in succession create a solid, multilayer coating. Subtle changes in organization and composition of the used building blocks as well as several experimental factors influence layer structure (e.g. thickness, stability) and functionality (e.g. permeability). Because the layer formation is induced by electrostatic interactions, the ionic strength of the working solution will modifiy the appearent charge density because of partial shielding of the charges in the building blocks used. The ionic strength influences the amount of deposited material and also the structure of the multilayer film.

Table 1 Advantages of layer-by-layer deposition over other methods for multilayer construction

Main advantages	Further specifications	
Wide range of materials used	Polyelectrolytes	- Biological polymers - Artificial polymers
	Nanoparticles	- Nonbiological origin (e.g. AuNPs, SiNPs, QDs) - Biological origin (e.g. viruses, bacteria)
	Nonpolyelectrolytes	Co-entrapment with charged polymers
Various surfaces for deposition	Nonbiological surfaces	e.g. metals, glass, plastic
	Colloids	e.g. SiNP, AuNP, vesicles
	Biological particles	e.g. cells, bacteria, viruses
Tuning parameters for optimization of layer formation and structure	Ionic strength	
	Concentration	
	pH	
	Temperature	
	Solvent composition	
	Adsorption time	
Post deposition processing by	pH	
	Ionic strength	
	Temperature	
	Deposition of protecting layer	
"Infinite" number of layers		
Low-cost production		
Environmental friendly process		
Automation possible		

Therefore, ionic strength appears as a valuable tool to govern and adjust the LBL formation process.

A further tuning parameter is the pH of the working solution, which can also affect the charge density of the deposited polyelectrolyte, particularly if it contains functional groups which can be protonated or deprotonated. The concentration of the building blocks is another criterium affecting the layer assembly and its functionality. If the concentration of the building blocks is too high, repulsion may be enforced or displacement of the already assembled molecules may occur. Otherwise, if the concentrations of the building blocks are too low, an imperfect film may be formed. For every system, there will be an optimum range for the building block concentration. Another factor is the temperature used during layer formation, as it can slow down or speed up the adsorption process but also subsequent interpenetration of deposited layers. In a similar way, the adsorption time affects the building block deposition, particularly at low adsorption rates. The choice of the solution composition also needs to be considered because some additives may influence the stability and functionality of the biomolecules to be

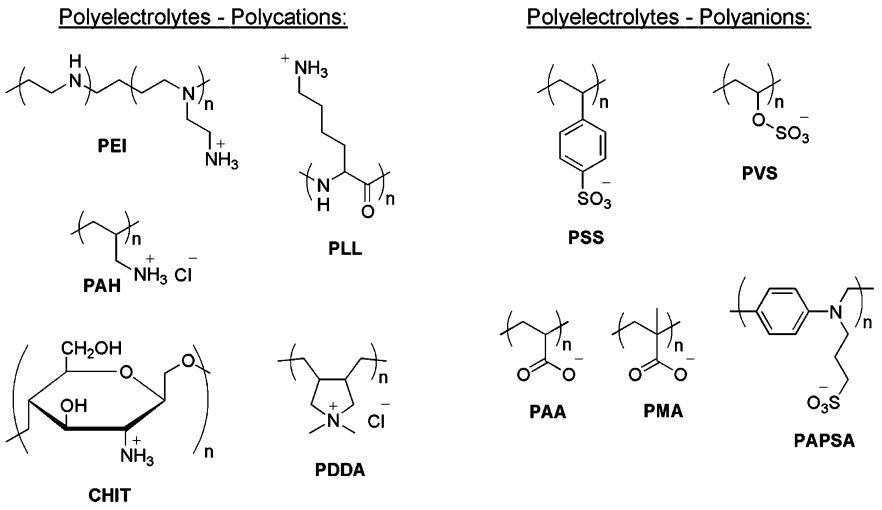

Fig. 8 Structures of commonly used polyelectrolytes for multilayer assembly. *CHIT* chitosan, *PAA* poly(acrylic acid), *PAH* poly(allylamine hydrochloride), *PAPSA* poly(anilinepropane-sulfonic acid), *PDDA* poly(dimethyl-diallylammonium chloride); *PEI* poly(ethyleneimine), *PLL* poly(L-lysin), *PMA* poly(methacrylic acid), *PSS* poly(styrene-sulfonate), *PVS* poly(vinylsulfonate)

deposited. To fix biomolecules, one can exploit their inherent charge at a given pH or one can codeposite weekly or uncharged species together with a polyelectrolyte. The advantages of the LBL deposition method over other approaches of multilayer construction are summarized in Table 1.

3 Multilayer-Based Sensing Architectures Using Electrostatic Interactions of the Building Blocks

3.1 Polyelectrolyte-Based Biosensors

Electrostatic multilayer assembly of proteins and oppositely charged polyelectrolytes was developed in the 1990s [5]. Polycations that have predominantly been used to construct multilayer architcutres include PLL, poly(ethyleneimine) (PEI), poly(dimethyl-diallylammonium chloride) (PDDA), poly(allylamine hydrochloride) (PAH), and chitosan (CHIT). The most commonly used polyanions are: poly(styrene-sulfonate) (PSS), poly(vinylsulfonate) (PVS), poly(anilinepropane-sulfonic acid) (PAPSA), poly(acrylic acid) (PAA), and poly(methacrylic acid) (PMA). The chemical structures of the polymers are shown in Fig. 8.

The polyelectrolyte-based multilayer assemblies provide an excellent control of layer thickness and have been extended to immobilize proteins, enzymes, DNA, and nanoparticles for the construction of biosensors. Biomolecules in a buffer

Table 2 Polyelectrolyte-based protein multilayer assemblies on electrodes for substrate detection

Enzymes in multilayer films	Analyte	References
Peroxidase	H_2O_2	[85–89, 97]
Cytochrome *c* oxidase	Cyt *c*	[109]
Fructose dehydrogenase	Fructose	[90]
Polyphenol oxidase	Dopamine, catechol	[91–93]
Glucose oxidase	Glucose	[76–82]
Lactate oxidase	Lactic acid	[60, 83, 84]
Uricase	Uric acid	[96, 110]
Alcohol dehydrogenase	Ethanol	[111]
Sorbitol dehydrogenase	Sorbite	[111]
Glucose dehydrogenase	Glucose	[112]
Glutamate oxidase	Glutamate	[113]
Hemoglobin	O_2	[98–100]
Myoglobin	O_2	[101–104]
Cytochrome *c*	Superoxide	[105–107]
Catalase	H_2O_2	[108]
Cytochrome P450	O_2	[101]
Cholesterol oxidase	Cholesterol	[94, 95]

solution of pH smaller or larger than their isoelectric point can take positive or negative charges, which make them suitable for incorporation in polyelectrolyte layers. Initially, an electrode has to be modified with a charged layer. This negatively (or positively) charged surface is then immersed in a polycation (or polyanion) solution to form the first positively (or negatively)-charged layer. Negatively-charged biomolecules are immobilized subsequently during the next incubation step. These deposition processes are carried out repeatedly to obtain the desired number of layers. When the protein has only a weak charge on the surface, it can also be mixed with a polyelectrolyte, resulting in a codeposition of both materials. However, for this kind of procedure, a rather high concentration of the proteins has to be applied.

The LBL approach is generic and provides a strategy to rationally design the properties of immobilized architectures. With this approach, almost all types of enzymes have been immobilized to form multilayered biosensors. Some representative examples are collected in Table 2.

3.1.1 Polyelectrolyte-Based Monoprotein Systems

Currently an ideal model, GOx was first incorporated in multilayer assemblies and applied for biosensing in 1996. In this example, the multilayered GOx sensor was prepared via GOx and PLL coadsorption on a negatively charged monolayer made of mercaptopropionic acid [114]. The glucose concentration can be directly correlated to the byproduct H_2O_2, which is than detected at the underlying electrode.

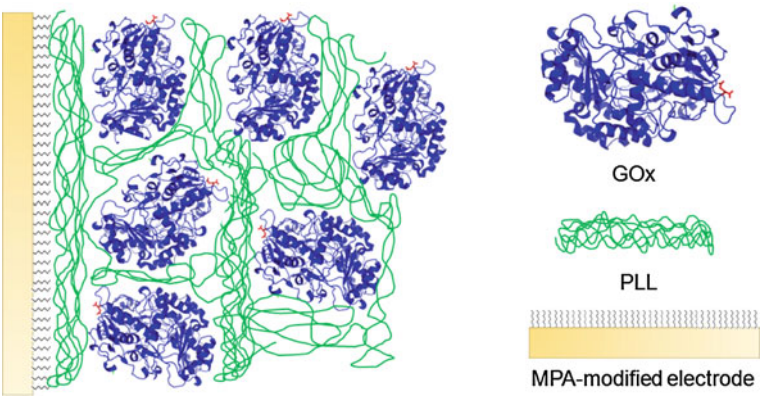

Fig. 9 Schematic illustration of glucose oxidase (GOx) incorporated into a matrix consisting of poly-L-lysine (PLL) by co-immobilization of the enzyme with polymer. Figure adapted from Ref. [114]

The sensor is build up to seven layers, with an signal increase with each layer. Therefore, the sensitivity of the constructed system can be tuned by the number of deposited enzyme layers. The presented GOx multilayer system is an example of a first-generation biosensor (Fig. 9).

In a similar approach, a multilayer-based biosensor using ChOD and 6-O-ethoxytrimethylammoniochitosan chlorid (EACC) deposited on a Prussian blue (PB)-modified platinum electrode, is constructed [118]. The chitosan building block provides multilayer-forming ability, sufficient permeability towards water and small molecules, good adhesion, and biocompatibility. The signal is generated by the conversion of the ChOD-generated H_2O_2 at the PB-modified Pt electrode. With this multilayered biosensor PB[EACC/ChOD]$_{10}$, the analyte (choline) can be detected in a linear range between 5×10^{-7} and 1×10^{-4} M. The sensing system retains around 85 % of its initial response to choline after 2 month of storage. A similar amperometric glucose biosensor based on the alternating deposition of a quaternized chitosan derivative and GOx on a Nafion-modified electrode has been developed [119]. For this system, the sensitivity is enhanced by the increase of the number of layers up to 10 bilayers. The glucose concentration has been correlated to the arising byproduct H_2O_2, which is then detected at the modified electrode. This sensor is quite selective because the presence of uric acid and ascorbic acid does not interfere with the electrochemical response due to the charge repulsive properties of Nation.

A further evolutionary step is shown by a reagentless glucose biosensor, which is prepared by successive alternate deposition of ferrocene-attached polypyridine or ferrocene-modified polyallylamin polymer and anionic GOx, on an Au electrode surface initially thiolated with negatively charged sulfonic acid groups [78, 115]. In these systems, ferrocene is used as a mediating agent attached to the polymers. In an similar way, this kind of GOx multilayer sensor is prepared by the use of a

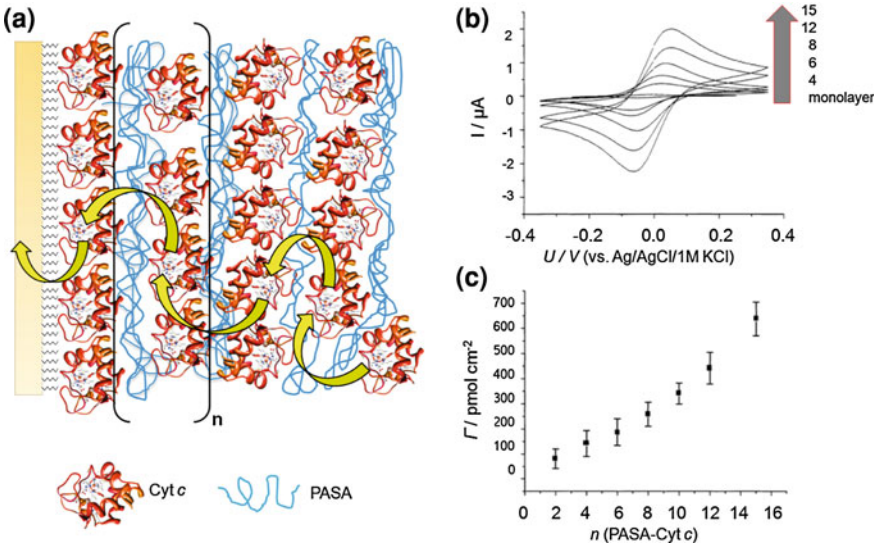

Fig. 10 **a** Schematic depiction of a cytochrome *c* (cyt *c*)/poly(aniline-sulfonic acid) (PASA) multilayer electrode. Arrows indicate the suggested pathway for electron transfer through the cyt *c* assembly with rotational flexibility of the protein. **b** Cyclic voltammetry in order of increasing magnitude: monolayer, 4, 6, 8, 12, 15 layers of cyt *c*. **c** Electrochemically determined concentration of cyt *c* in 2–15 multilayers. Figure adapted from Ref. [105]

charged Os-based redox polymer for the electrochemical communication of GOx. The analytical performance of the sensor can be controlled by the number of GOx/redox polmer bilayers [116]. The progress here is that the reaction process is followed more directly as the relase of electrons during the oxidation reaction is monitored without the liberation or consumption of byproducts. Electrons are transferred through the assembly by hopping from redox center to redox center (second-generation biosensor).

In an almost equal approach, a multilayer-based sensor for hydrogen peroxide is constructed by the use of a positively charged osmium-derivatized polymer and a negatively charged HRP [117]. The resulting architectures are shown to be stable and exhibit some advantages, such as fast response times and good chemical/mechanical stability.

The multilayer construction with the LBL method also seems to be a promising approach for the fabrication of mediator-free biosensors. In this context, the construction of layered architectures with positively charged myoglobin (Mb) and negatively charged PSS on a pyrolytic graphite (PG) electrode surface is shown [102]. Cyclic voltammetry of $[PSS/Mb]_n$ films exhibit a pair of well-defined, quasi-reversible peaks, characteristic for the Mb heme Fe^{2+}/Fe^{3+} redox couple. Electroactivity of the multilayer system is extended up to seven $[PSS/Mb]_7$ bilayers. Unfourtunately, not all of the Mb in the multilayer system can be addressed because only an slight signal increase is monitored with the number of

layers. In this system, the electron transfer of myoglobin may be explained by direct electron transfer from one Mb to the other towards the underlying electrode. Additionally, oxygen and trichloroacetic acid catalysis have been observed.

Based on the idea of direct electron transfer, a multilayer assembly combining cytochrome *c* (cyt *c*) as a small redox protein and sulfonated polyaniline (PASA) as a counter polyelectrolyte has been developed (Fig. 10). Thereby, a fully electroactive assembly based on interprotein electron transfer is prepared without the need of redox mediators [105, 106]. These multilayer architectures containing up to 15 protein layers show a quasi-reversible electron transfer. The propotional increase of electroactivity with the number of deposited cyt *c* layers also results in an enhanced sensitivity of such an electrode for the analysis of superoxide radicals because cyt *c* is able to oxidize this radical [107].

The increased number of recognition sites on the electrode generates a higher current. However, as in the case of several other multilayer systems, above a certain thickness, diffusion through the multilayer becomes rate limiting. This phenomenon is shown for superoxide sensors with more than six cyt *c* layers deposited by the polyelectrolyte adsorption technique [107]. This appears here with a rather small number of layers because the analyte is not a stable molecule and decomposes by spontanous disproportionation into O_2 and H_2O_2.

On the basis of cyt *c* multilayers constructed with sulfonated polyaniline (PASA), some further work has been performed. An additional envelop-S-layer can be assembled on top of the multilayer architecture to construct a permselective system [120]. The recrystallization of a bacterial protein surface layer (S-layer-envelop) of SbpA (recrystallized protein, from *Bacillus sphaericus* CCM 2177) on the PASA-cyt *c* multilayer film is feasible in the case when a different polyelectrolyte, PSS, is used as bridging layer before immobilization of SbpA. Notably, the recrystallization process of the S-layer does not significantly diminish the amount of electroactive cyt *c* within the multilayer arrangement. Therefore, the described approach of self-assembled protein multilayers with S-layer recrystallization can offer new advantages for the construction of permselective functional systems.

Additional investigations of cyt *c* multilayer architectures, constructed with chemically modified sulfonated polyanilines as polyelectrolyte [121], have been performed. The comparison of the different sulfonated polyanilines points out that the redox activity of the polyelectrolyte can significantly contribute to the overall activity of the assembly, if not carefully chosen. This may cause side reactions if the system is applied in sensorics. It is also shown that the polyanilline is not acting as a conducting matrix between the cyt *c* but as a kind of glue holding the proteins in small distances from each other.

Instead of using synthetic polymers, biopolymers can be also applied as building blocks for the construction of multilayer systems. In a rather unique example, DNA and cytochrome *c* are used to build up electroactive multilayers [122]. DNA, which habours a negatively charged phosphate backbone, ensures electrostatic interactions to facilitate the immobilization of cyt *c* in multiple layers. A significant increase in the amount of cyt *c* with the number of layers is shown for up to six bilayers by spectrophotometric, quartz crystal microbalance (QCM) and

electrochemical studies. Multilayers containing up to six DNA–cyt *c* bilayers exhibit a quasi-reversible electron transfer. The most striking difference compared to polymer-based systems, however, is the significantly higher amount of electroactive cyt *c* bound within this type of architecture (six bilayers = 190 ± 12 pmol/cm^2). This finding is accompanied by much higher surface roughness, indicating that a three-dimensional structure is formed on the electrode surface. Furthermore, the long-term stability of the DNA/cyt *c* multilayer assembly has been studied for at least 40 days, and only a slight decrease in electroactive protein amount (<5 %) is found during this period of dry storage.

Another example for the use of polyelectrolytes to build up multilayers are dendrimers, which are new types of polymers with a globular structure mimicking the three-dimensional structure of biomacromolecules, with a highly branched dendritic structure and unique properties, such as a high density of active groups, good structural homogeneity, internal porosity, and good biocompatibility. Thin multilayer films of heme proteins, including hemoglobin (Hb), myoglobin (Mb), and catalase (Cat), are assembled layer by layer with polyamidoamine (PAMAM) dendrimers on different solid surfaces [123]. At pH 7.0, protonated PAMAM possesses positive surface charges, whereas the proteins have net negative surface charges at pH above their isoelectric points, allowing defined electrostatic interactions for film preparation. The assembly process is monitored by QCM and visible ultraviolet (UV–Vis) spectroscopy. The growth of the protein multilayer films proceeds regular and linear, whereas the electroactivity of the films can only be extended up to a few bilayers. Cyclic voltammetries of $[\text{PAMAM/protein}]_n$ films display a pair of defined and nearly reversible peaks characteristic for the protein heme Fe^{2+}/Fe^{3+} redox couple. Several substrates with biological or environmental significance, such as oxygen, hydrogen peroxide, trichloroacetic acid, and nitrite, are catalytically reduced at $[\text{PAMAM/protein}]_n$ film electrodes, showing that the multilayers are based on direct electrochemistry of the proteins because no shuttle molecules are needed.

3.1.2 Polyelectrolyte-Based Multiprotein Systems

More sophisticated approaches have been reported, which integrate more than one biomolecule in the multilayer assembly to achieve a cooperative mechanism (so-called biprotein assemblies). For example, a multilayer biosensor for direct determination of cholesterol was constructed using cholesterol oxidase (COx) and PSS on a monolayer of microperoxidase that was covalently immobilized on a Au-alkanethiolate electrode (Fig. 11) [124]. The biosensor diplays a linear current response for cholesterol in the concentration range of 0.2–3.0 mM with a rather fast response time (<20 s). The catalytic current increases with the number of layers up to three bilayers of $[\text{COx/PSS}]_3$. Thus, the reactions involved in the observation of a cathodic current response for cholesterol is the generation of hydrogen peroxide by the enzymatic reaction between COx and cholesterol followed by electrocatalytic reduction of H_2O_2 at the microperoxidase (MP). The

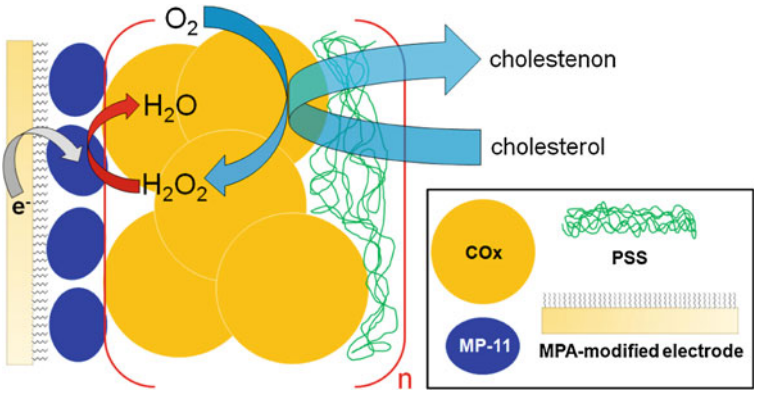

Fig. 11 Schematic depiction of a cholesterol oxidase (COx) multilayer illustrating the enzymatic and electrochemical reaction. *PSS* poly(styrenesulfonate). Figure adapted from Ref. [124]

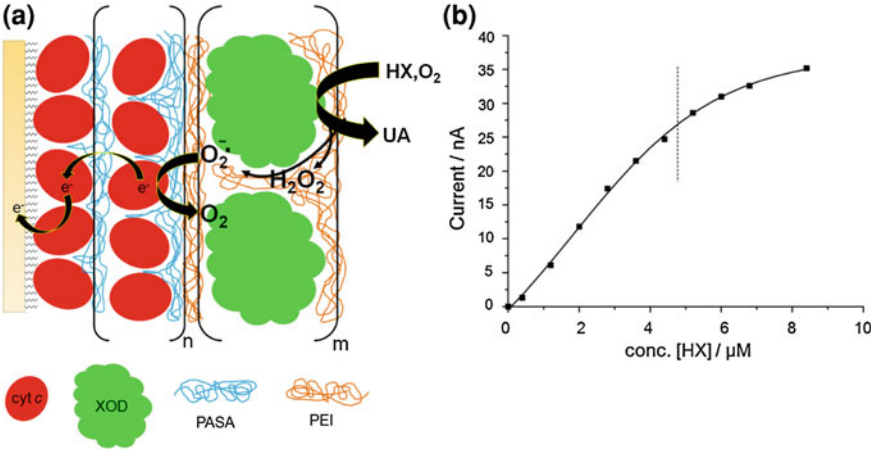

Fig. 12 **a** Scheme of a cyt *c*/XOD biprotein sensor for HX and electron transfer. *HX* hypoxanthine, *UA* uric acid, *black arrows* electron transfer/reaction pathway. **b** Increase of the amperometric sensor current with increasing HX concentration. Figure adapted from Ref. [125]

COx/MP biosensor is a multilayer system only with respect to COx; the microperoxidase only serves as transducing monolayer.

However, various kinds of real biprotein multilayer assemblies have been developed, including a xanthine oxidase-based multilayer system [125]. Here, xanthine oxidase (XOD) has been combined with cyt *c* and two different polyelectrolytes (PASA and PEI). On the basis of this arrangement, a signal chain starting from hypoxanthine (HX) is established. A schematic view of the protein assembly is given in Fig. 12. Here, XOD is immobilized on top of a cyt *c*/PASA assembly. In contrast to cyt *c*, XOD is a slightly acidic enzyme (pI = 5.1). Therefore, a cationic polyelectrolyte and a higher pH is necessary to assemble

XOD on the cyt *c* multilayer. As cationic polyelectrolyte, PEI is used. Voltammetric measurements indicate that cyt *c* is still electrochemically active in the polyelectrolyte multilayer after PEI and XOD immobilization. When the electrode is exposed to a buffer solution containing hypoxanthine, a well-defined oxidation current can be detected, thereby verifying that a signal chain from hypoxanthine via the two proteins towards the electrode is formed. The conversion of hypoxanthine can only occur at the XOD. During this oxidation process, oxygen is reduced and hydrogen peroxide and superoxide are liberated simultaneously. Because the cyt *c* multilayer electrode gives no response to hydrogen peroxide at the chosen potential, superoxide radicals serve as shuttle molecules, transferring the signal from XOD to cyt *c*. Therefore, the multilayer system relies on the internal generation of a shuttle molecule, ensuring the communication of both proteins.

Another example is also based on the immobilization of the biocatalyst on top of the cytochrome *c* multilayer. This is exemplified by the assembly of laccase on top of cyt *c* multilayers [126]. The assembly reflects the structure of the previously mentioned cyt *c*/XOD system; however, the operation is based on direct electron exchange between the two proteins. Electrons are delivierd by cyt *c* for the catalytic reaction at the copper enzyme laccase. The oxygen reduction current linearly follows the oxygen concentration in solution up to oxygen saturation. Because the laccase is assembled on top of the cyt *c* multilayer, the catalytic current cannot be enhanced by simply increasing the number of layers. After two or three layers of laccase, this system reaches saturation because additional enzyme layers are not in contact with the cyt *c* molecules in the multilayer architecture anymore.

A similar approach can be shown by the layered assembly of quinoprotein glucose dehydrogenase (PQQ-GDH) on cytochrome *c*, where DNA is used as second building block [127]. The LBL deposition technique is applied to build up cyt *c*/DNA bilayers and a terminal layer of PQQ-GDH on top. It is found that the catalytic current flows when substrate (glucose) is present, indicating that this system also relies on interprotein electron transfer.

In a more advanced system, it would be favorable to incoporate the biocatalyst into the whole layered architecture. This new principle of signal chain has been first demonstrated with multilayers comprising cyt *c* and bilirubin oxidase (BOD) [128]. The structure of this system is schematically given in Fig. 13. Proteins are assembled here in complexes on electrodes in such a way that direct protein–protein electron transfer is achieved. This design does not need a redox mediator in analogy to natural protein communication, such as in the respiratory chain. The concept relies on the direct electron exchange between proteins, which has been investigated in solution or in monolayer systems but is confined here to the immobilized state of both partners.

For demonstration of the principle, cyt *c* and the enzyme BOD are coimmobilized by means of the polyelectrolyte sulfonated polyanilin on gold electrodes. Although these two proteins are not natural reaction partners, they can exchange electrons directly in solution [129]. Immobilized in multilayers, the protein architecture facilitates electron transfer from the electrode via multiple protein

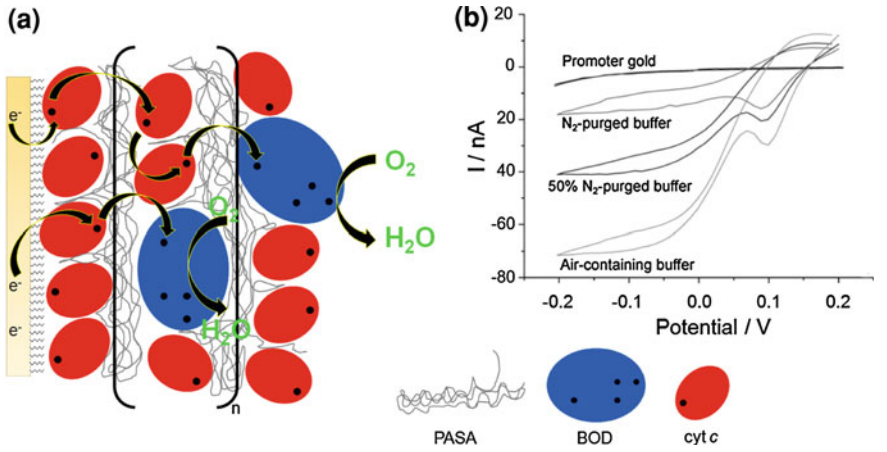

Fig. 13 **a** Schematic illustration of the redox chain in cyt *c*/BOD multilayer electrodes. *Red circles* cyt *c* protein, *blue shapes* BOD enzyme, *arrows* indicate electron transfer pathways between cyt *c* and BOD within the polyelectrolyte network and the four-electron oxygen reduction process. **b** Dependency of the reduction current of a three-layer assembly on oxygen concentration. Figure adapted from Ref. [128]

layers to molecular oxygen in solution, resulting in a significant catalytic reduction current. The electrode architecture is fabricated starting from a cyt *c* electrode (Au/MUA/MU/cyt *c*) by alternating incubations in the protein mixture of cyt *c* and BOD and the polyelectrolyte PASA. When the cyt *c*/BOD multilayer electrode is exposed to an air-saturated solution and a cathodic potential sweep is performed, a substantial reduction current can be observed at neutral pH. The catalytic current results from reduction of cyt *c*, most of which is oxidized by the electron transfer to neighboring BOD molecules. By varying the number of [cyt *c*/BOD] layers on the electrode, not only the electroactive amount of cyt *c* is increasing with every deposition step but also the catalytic oxygen current.

Increasing the number of catalytic sites (BOD amount) obviously enhances the electrocatalytic conversion. This result implies that the deposited BOD molecules are in electrical contact with the electrode. Because a large part of the enzyme is immobilized rather far from the electrode surface, it is concluded that cyt *c* is providing the electrons for the enzyme reaction. For the sensorial application, this also means that the sensitivity can be tuned by the number of deposited [BOD/cyt *c*] layers. Notably, a current limit is not observed up to 12 bilayers because of the direct communication between the enzyme and the redox protein in every layer and a rather fast diffusion of oxygen.

In a further study on the basis of this principle, different forms of cyt *c* have been investigated with respect to their behavior as electron donors to the enzyme BOD incorporated in multilayer assemblies [130]. It is shown that cyt *c* from different species as well as single-point mutations in the human form of cyt *c* can influence the reaction rate with BOD in solution. In addition, it is observed that the amount of

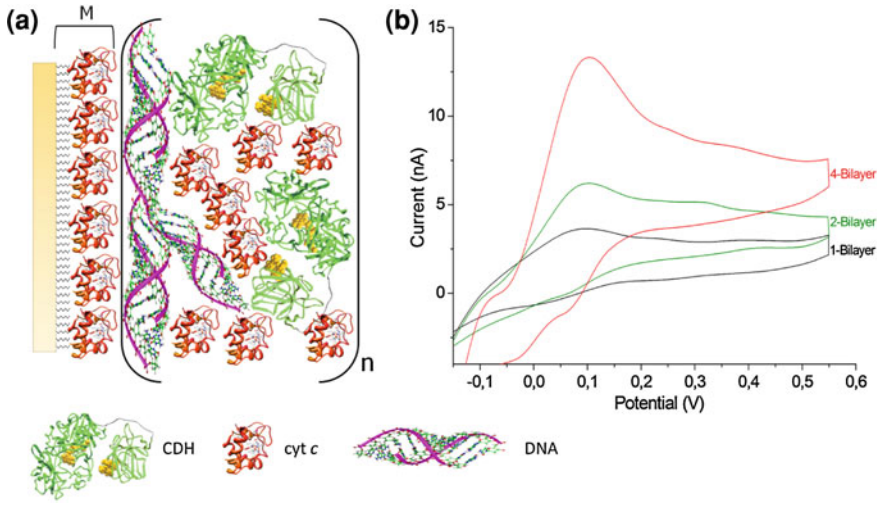

Fig. 14 **a** Schematic representation of DNA/cytochrome *c* (cyt *c*)·cellobiose dehydrogenase (CDH) architectures prepared on cyt *c* monolayer electrodes (M). The cyt *c* monolayer is assembled on a mixed thiol layer (11-mercapto-1-undecanol [MU]/mercaptoundecanoic acid [MUA]). **b** Cyclic voltammograms of Au-MUA/MU-cyt *c*-[DNA/dCDH·cyt *c*]$_n$ multilayer electrodes. Multilayers ($n = 1, 2, 4$) in the presence of lactose (5 mM). Figure adapted from Ref. [133]

protein deposited by the LBL approach can be influenced by exchange of one amino acid and thus can limit the current density. The kinetic analysis of the multilayer system with different cyt *c* forms shows that a decreased cyt *c* self-exchange rate can also be a limiting factor. This corroborates a dominating role of the redox protein for the electron transfer through the system. Thereby, it is illustrated that protein engineering can be a helpful instrument to study protein–protein reactions, as well as the electron transfer mechanisms of complex multilayer systems.

Another biprotein multilayer is shown by a sulfite oxidase SOx/cyt *c* arrangement, with both proteins assembled together on the electrode. SOx–cyt *c* multilayers are successfully formed as fully electroactive assemblies with the help of the polyelectrolyte PASA [131, 132]. The multilayer architecture diplays catalytic activity for the oxidation of sulfite. Increasing numbers of biprotein layers result in a linear increase of both: electroactive cyt *c* amount and catalytic sulfite oxidation. Thus, again a protein assembly is constructed on modified electrodes, establishing a signal chain from the enzyme substrate via the enzyme and cyt *c* towards the electrode and allowing sensitive sulfite detection, even in real samples.

Instead of a synthetic polymer, DNA can be used as natural polyelectrolyte (see [122]). This has also been used for the construction of biprotein assemblies, in which cellobiose dehydrogenase (CDH) and cytochrome *c* are used as protein building blocks [133]. CDH and cyt *c* are co-immobilized on a cyt *c* modified monolayer electrode by alternating incubation steps in DNA and [CDH/cyt *c*]

solutions. The biosensor is used to monitor the substrate (lactose) concentration in solution (Fig. 14). The electrons that are generated during the oxidation process at CDH are transfered via interprotein electon transfer by the cyt *c* molecules towards the electrode. Therefore, no additional shuttle molecule is needed. The catalytic response increases with the number of deposited [DNA/CDH·cyt *c*] bilayers. A further analysis of the system reveals a dynamic range from 0.01 to 20 mM lactose.

3.1.3 Polyelectrolyte-Based Immunosensors

In the past few years, there have been several reports on the development of immunosensors for clinical and environmental purposes as a result of the possibility of generating a large number of antibodies for the analysis of numerous chemical species, with the advantage of analyzing samples with less pretreatment and because of a rather fast and direct signal generation. The construction of the biological recognition layer is fundamental for tailoring the sensing properties of such biosensors. Increasing the binding layer capacity and maintaining its immunological activity are two key issues for an increased sensitivity. To develop such immunosensors, the arrangement of one partner of the immune reaction by means of multilayer architectures has also drawn some attention [134–137]. However, compared to enzyme-based systems, here the permeability for the analyte (antigen) can be a major drawback, particularly when the antigen is a molecule of higher molecular weight.

One of the first approaches is shown with a multilayer immunosensor prepared by embedding anti-immunoglobulin G (anti-IgG) monoclonal antibodies into polyelectrolyte multilayer films [135]. Alternating polyelectrolyte films constructed by the sequential adsorption of anti-IgG and PSS have been used as sensors for IgG. The assembly process of the multilayer films can be monitored using QCM and surface plasmon resonance (SPR). Multilayer film growth is achieved up to at least five anti-IgG layers. The sensitivity, determined using IgG mass uptake data from quartz crystal microgravimetry, is found to be linearly dependent on the number of anti-IgG layers (and hence the amount of IgG incorporated) in the polyelectrolyte film when the anti-IgG layers are separated by one PSS layer. In contrast, for films where anti-IgG layers are separated by five polyelectrolyte ($PSS(PAH/PSS)_2$) layers, only the outer anti-IgG layer is found to be immunologically active. This is attributed to the formation of a densely packed polyelectrolyte film through which antigen permeation is restricted. The assembly strategy is promising because the sensitivity can be controlled by the number of protein layers, whereas the selectivity can be modified by selecting the desired antibody.

Another layered immunosensor is fabricated by alternating adsorption of anti-horseradish peroxidase (anti-HRP) antibodies and dextran sulfate [138, 139]. A sensor employing mutiple layers of antibodies exhibits an enhanced sensitivity to

the HRP antigen compared with those using two-dimensional monolayers, mainly because of the higher number of receptors and their accessibility to the antigens.

For many immunosensor systems, polyelectrolyte layers haven been extensively used as the first modication step because antigens or antibodies can be easily immobilized on top of the polyelectrolytes by simple adsorption, as well as by covalent linkage with the reactive groups on the polymer. The adsorption method is very attractive for single-use immunosensor devices and the covalent one is favorable for multiple-use sensors. The high amount of recognition molecules immobilized in such a way allows for more sensitive detection of antigens or antibodies, respectively.

3.1.4 Polyelectrolyte-Based DNA Biosensors

Specificity with respect to biomolecular recognition has also been explored extensively using DNA fragments on modifed electrode surfaces [140–143]. DNA is known as a polymeric molecule with a specific base sequence that determines the genomic characteristics of living organisms. The identification of specific changes in the base sequences is very important for detecting diseases or identifying organisms [144, 145].

Another aspect is that oxidative DNA damage may lead to aging, cancer, and mutaganesis. Therefore, the application of DNA sensors has been extended to the detection of chemical toxicity [146–149]. Such methods are based on two facts: (1) guanine is the most easily oxidized of the four DNA bases and (2) single-stranded DNA is more easily oxidized at the guanine or adenine sites than double-stranded DNA (dsDNA) because of the easier access to the bases. When multilayer films of dsDNA are exposed to a solution harboring toxic chemicals, the dsDNA in the film is damaged and the double helix is unwound. Easier access to the nucleobases is enabled, leading to faster reaction rates and larger electrochemical signals. In conventional electrochemical approaches, DNA is preconcentrated on electrodes by adsorption prior to analysis, and a larger voltammetric signal can be obtained when oxidative damage has occured. DNA voltammetry with higher sensitivity can be achieved by using electrocatalytic oxidation with transition metal complexes.

Based on this principle, films of $[Ru(bpy)_2(PVP)_{10}Cl]Cl$ (in which PVP is poly[vinyl-pyridine]) and dsDNA are assembled as multilayers by alternate electrostatic interactions [148]. The redox polymer $[Ru(bpy)_2(PVP)_{10}Cl]Cl$ in the multilayer architecture is used to catalyze the voltammetric oxidation of guanine bases of dsDNA. This multilayer-based system provides a reagentless sensor for toxicity screening of new chemicals based on the detection of DNA damage. In another example, DNA films containing $[Os(bpy)_2(PVP)_{10}Cl]Cl$ and $[Ru(bpy)_2(PVP)_{10}Cl]Cl$ are assembled as multilayers on pyrolytic graphite electrodes to obtain sensors selectively detecting oxidized DNA [149]. The assemblies display independent reversible electrochemistry for Os^{3+}/Os^{2+} and Ru^{3+}/Ru^{2+} centers. The combination of ruthenium and osmium metallopolymers in the multilayer

structures allows for the detection of 8-oxogunanine and other oxidized nucleobases simultaneously. The catalytic osmium square wave voltammetry (SWV) peak is mainly selective for 8-oxoguanine because Os^{3+} selectively oxidizes 8-oxogunaine but not guanine [150].

3.2 Nanomaterial-Based Biosensors

Materials at the nanoscale level have received significant attention in the last decade because of their interesting properties associated with quantum confinement and surface energy effects. The main advantages of using nanomaterials for multilayer construction are based on their morphology, size, and surface properties. Because these parameters can be controlled to a large extent, it offers the possibility to regulate the composition and structure of the resulting layered architecture. The use of nanoparticles for the construction of multilayered systems allows the following:

- The introduction of new functionalities
- An enhanced interaction with biomolecules
- An easy adjustment of the surface charges by suitable modification protocolls of the nanostructure.

Colloidal noble metal nanoparticles (NPs) have been the subject of many studies owing to their particular electronic and electrocatalytic properties [151–153]. Many electrochemical approaches use various types of NPs, including gold [154–156], platinum [157], silver [158, 159], palladium [160], and others [161–163]. The introduction of NPs in multilayer construction has developed into an important approach in biosensor research. Gold nanoparticles (AuNPs) are one of the most studied nanomaterials in literature [164–166]. This is assocciated with their intensive absorption in the visible range, electrocatalytic properties, high mass (density), and ease of modification by thiol compounds. Besides their electronic properties, they exhibit excellent biocombatibility [167], and colloidal solutions of AuNPs can be synthesized relatively simply.

Carbon nanotubes (CNTs) have attractive conducting and electochemical properties with several applications as electrode materials [168–171]. The tubular structure of CNTs is formed from sp^2-carbon atoms arranged in a hexagonal pattern, with a diameter in the order of nanometers and length of micrometers [172]. Furthermore, the adsoprtion of biological molecules, such as proteins [173–176], antibodies [177], and DNA [178], has been reported in an active form.

A further representative example of nanomaterials are colloidal quantum dots (QDs), which are fluorescent semiconductor particles. They have been intensively studied for several years because of their unique photophysical properties. QDs have been recently discussed as new building blocks for the construction of electrochemical biosensors [179–184]. Upon illumination, electron hole pairs are generated inside QDs [185]. Because of these charge carriers, electron transfer

from or to the QDs becomes feasible. The nanoparticles thus can be oxidized or reduced. They can serve as a light-controlled redox-active element and can be integrated into electrochemical signal chains [182, 186–188]. The key advantage hereby is that the redox reaction on the QDs surface can be switched on and off by light. QDs have also been used as signal transducting elements of enzymatic reactions [189, 190]. In another application, they are used as electrochemoluminescence labels during biorecognition reactions; here, electrochemical reactions are used to excite QDs with subsequent emission of light, appearing as an analytical signal [191].

3.2.1 Multilayered Enzyme Sensors Based on Nanomaterials

Because the surface charge of different nanomaterials can be adjusted, they can be used as new building blocks for the formation of multilayer assemblies [192–194]. For example, myoglobin multilayers have been constructed by the use of MnO_2 nanoparticles [195]. The alternate adsorption of manganese oxide nanoparticles with myoglobin (Mb) onto silver, quartz, or rough pyrolytic graphite results in stable, porous, and thin films. QCM and UV–Vis absorbance reveal regular film growth after each adsorption step for MnO_2 and Mb. These multilayered films feature reversible interconversion of the protein's heme Fe^{3+}/Fe^{2+} redox couple up to 10 electroactive layers of protein. Nevertheless, a linear increase in electroactive protein is not observed because only a fraction of the assembled protein layers are electrochemically active. Shifts in redox potential caused by CO complexation of the heme Fe^{2+} and electrochemically driven catalytic reduction of oxygen suggest that the Mb/MnO_2 films on pyrolytic graphite are porous for easy access of gas molecules.

Another example are stable films of clay particles and hemoglobin (Hb), which are assembled LBL on various solid substrates by alternate adsorption of negatively charged clay platelets from their aqueous dispersions and positively charged Hb [196]. This is based on earlier developments incorporating heme proteins in thicker clay layers [197, 198]. The multilayer film growth can be monitored by QCM and UV–Vis spectroscopy. Cyclic voltammetries of $[clay/Hb]_n$ multilayers on pyrolytic graphite electrodes show a pair of well-defined, nearly reversible peaks. Although the amount of Hb adsorbed in each bilayer has been found to be almost the same (QCM), the fraction of electroactive Hb decreases with the number of $[clay/Hb]_n$ bilayers. Electroactivity of Hb extends to six clay/Hb bilayers. The Soret absorption band of Hb in $[clay/Hb]_6$ films shows that Hb-heme environment remains in its structure similar to its native state. Additionally, the electrodes can catalyze the electrochemical reduction of trichloroacetic acid, oxygen, and hydrogen peroxide.

Another approach for multilayer construction can be seen by core–shell nanocluster films of proteins, polyelectrolytes, and silica nanoparticles (SiNPs) [199]. Thereby, SiNPs are used as "core" materials and the $(enzyme/polyion)_n$ multilayers are deposited on this core particles to form a bioactive shell. These

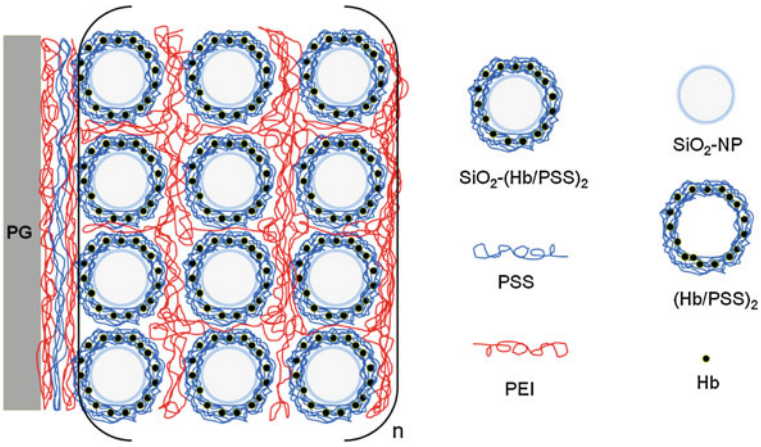

Fig. 15 Schematic diagram of the idealized structure of [SiNP-(protein/PSS)$_m$/PEI]$_n$ multilayer on a PG/PEI/PSS/PEI surface. PEI is used as polycation and PSS is used as polyanion. *Hb* hemoglobin, *NP* nanoparticle, *PEI* poly(ethylenimine), *PG* pyrolytic graphite, *PSS* poly(styrenesulfonate). Figure adapted from Ref. [199]

core–shell nanoclusters are then assembled by the use of oppositely charged polyions on electrodes (Fig. 15).

For the construction, hemoglobin and myoglobin can be used as redox proteins. {[SiO_2 − (protein/PSS)$_m$]/PEI}$_n$ films at pyrolytic graphite (PG) electrodes exhibit well-defined, reversible cyclic voltammetric reduction–oxidation peaks characteristic of the heme Fe^{3+}/Fe^{2+} redox couple. For this system, it is also found that only a relative fraction of the incorporated redox protein is electroactive (Γ^*/Γ). Therefore, not all of the Hb is able to contribute to the electrochemical signal. However, the electroactivity of the [SiNP − (protein/PSS)$_m$/PEI]$_n$ system can be tailored by adjusting both the shell thickness (m) and the film thickness (n).

Multilayer formation has also been studied with negatively charged gold nanoparticles (AuNPs) and positively charged myoglobin (Mb) to ensure electrostatic interactions [200]. The AuNP/Mb multilayers are used to catalyze the electroreduction of oxygen and hydrogen peroxide, showing that the electrochemical and electrocatalytic properties are strongly effected by the size of the AuNPs. Unfortunately, not all of the assembled Mb is able to contribute to the electrochemical reaction because it is also found that only a relative fraction of the immobilized Mb is electroactive (Γ^*/Γ).

Based on the same construction principle, a layered architecture with cyt *c* and colloidal AuNPs has been decribed [156]. Prepared on a MU/MUA-modified gold electrode, the AuNP/cyt *c* multilayers give a well-defined, quasi-reversible response of cyt *c*. A highlight here, compared to the systems described above, is that this system exhibits a linear increase of the cyt *c* amount and electrochemical response with the number of adsorption steps. For a six-bilayer assembly, an

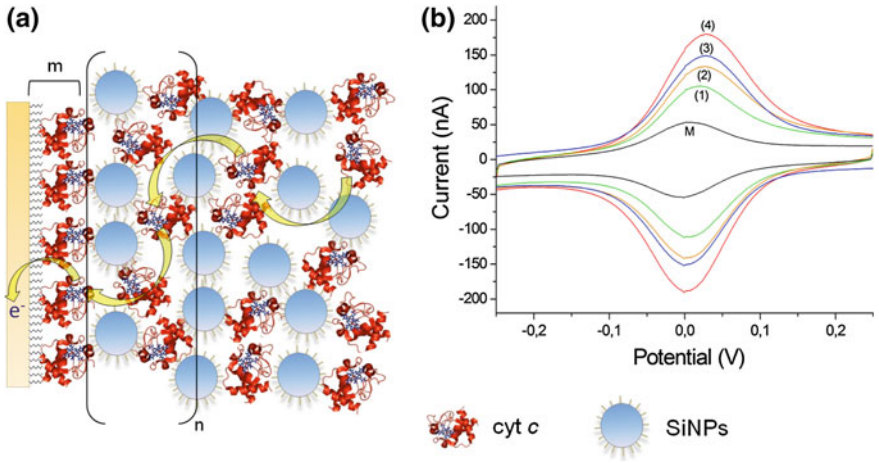

Fig. 16 **a** Schematic representation of the SiNPs/cyt *c* multilayer architecture. The SiNPs/cyt *c* assembly was prepared on a cyt *c* monolayer electrode (M). *Yellow arrows* indicate the electron transfer between the cyt *c* molecules towards the electrode. **b** Cyclic voltammetry of 1, 2, 3, 4-bilayer assemblies of cyt *c*/SiNPs. Figure adapted from Ref. [203]

electroactive surface concentration of 90 ± 25 pmol/cm^2 is found. The combination of cyt *c* with small-diamater AuNPs (5 nm) for multilayer construction demonstrates its potential for application in biosensor development.

Semiconducting nanoparticles have also been applied for layered protein immobilization. Different properties of the nanoparticles are the focus here, including biocompatibility and a light-induced charge carrier generation [185]. For example, two QD multilayer architectures are constructed by the use of the positively charged polyelectrolyte polyallylamine (PAH) or the redox-protein cyt *c* and mercaptopropionic acid-modified CdSe/ZnS-QDs [201]. The assembly with PAH and QDs reveals a proportional increase of the accumulated mass and the light-induced current with the number of deposited layers. Obviously, here an electron exchange between the immobilized and illuminated QDs is feasible.

In summary, a QD-based multilayer electrode system can be constructed and its properties can be tuned in a controlled way. This has also been shown with DNA-coupled QDs for multilayer construction by means of hybridization [202]. Because photocurrent measurements can be used for sensorial purposes, such as in the detection of redox active substances, the higher amount of electrode contacted QDs can be beneficially used for enhanced analytical signals [191]. It needs to be mentioned that assemblies constructed with cyt *c* and QDs do not show an increase of the redox signal from cyt *c*, but for the photocurrent mesurements an enhancement is found, which depends on the number of deposited layers [201].

In contrast to the previously described systems, nonconducting nanoparticles can also be used for the construction of fully electroactive protein multilayers. Here, carboxy-modified SiNPs and cytochrome *c* are used to construct a layered entity [203]. For this system, it can be demonstrated that smaller SiNPs (5 nm) in the size

range of cyt *c* are more favorable for construction than larger silica particles because more cyt *c* is assembled in the layered system. For the cyt *c*/SiNPs multilayers, a well-defined, quasi-reversible response of cyt *c* has been detected with a rather small peak separation, which is indicative for a fast electron transfer within the system (Fig. 16). A spotlight here is that the SiNPs-based cyt *c* multilayer system exhibits a linear increase of the electroactive cyt *c* amount with the number of deposited bilayers. Compared to AuNPs-based assemblies [156], the system clearly demonstrates that protein–protein electron exchange is the dominating mechanism for electron transport through the layered entity because SiNPs are nonconductive. Therefore, the construction strategy of this multilayer system provides a controllable route to immobilize proteins or enzymes in mutiple layers featuring direct and interprotein electron transfer without the need for mediating shuttle molecules.

SiNPs have also been used to construct enzyme-based multilayers. For example, aminated SiNPs and GOx are assembled in multiple layers [204]. Here, cross-linking by means of glutaraldehyde is applied for improved stability. By a different approach, mesoporous silica spheres have been used to immobilize different enzymes (catalase, peroxidase, lysozyme) in the hollow spheres, followed by encapsulation with PDDA and PSS in mutiple layers [205].

Because of the high conductivity, the use of carbon nanotubes (CNTs) represents a very different multilayer construction principle for electrochemical biosensors. The CNTs can be used to effectively convert reaction products within the assembly and transport electrons toward the electrode. Furthermore, it is possible to connect enzymes in such a way with CNTs that DET becomes feasible. To ensure the electrostatic force of attraction for multilayer assembly, the surface of CNTs is functionalized with carboxy groups or wrapped with a polyelectrolyte, such as CHIT, PDDA, poly(aminobenzensulfonic acid) [206–213], or even DNA.

GOx can be immobilized on the negatively charged carbon nanotube surface (functionalized with carboxy-groups) by alternatingly assembling a cationic PDDA layer and a GOx layer [206, 207]. The sandwich-like structure of (PDDA/GOx/PDDA/CNT) provides a microenvironment to contain the bioactivity of GOx and prevent enzyme molecule leakage. During the reaction, glucose is oxidized in the presence of oxgen into D-glucono-lactone and hydrogen peroxide. Therefore, the catalytic reaction can be monitored by the detection of the liberated hydrogen peroxide. The high electrochemical activity for H_2O_2 indicates that the polyelectrolyte-protein multilayer does not affect the electrocatalytic properties of CNTs, enabling sensitive determination of glucose.

In a similar way, a bienzyme nerve agent biosensor can be prepared using the LBL assembly of PDDA, HRP and ChO on CNTs [208, 209]. A bioactive multilayer/nano-composite film of [CNT/PDDA/HRP/PDDA/ChO/PDDA] is fabricated on a glassy carbon electrode (Fig. 17). Owing to the electrocatalytic effect of CNTs, the measurement of a Faradayic response is realized at low potential. The signal results from the enzyme reactions, in which choline is oxidized in the presence of oxygen into betain aldehyde and hydrogen peroxide,

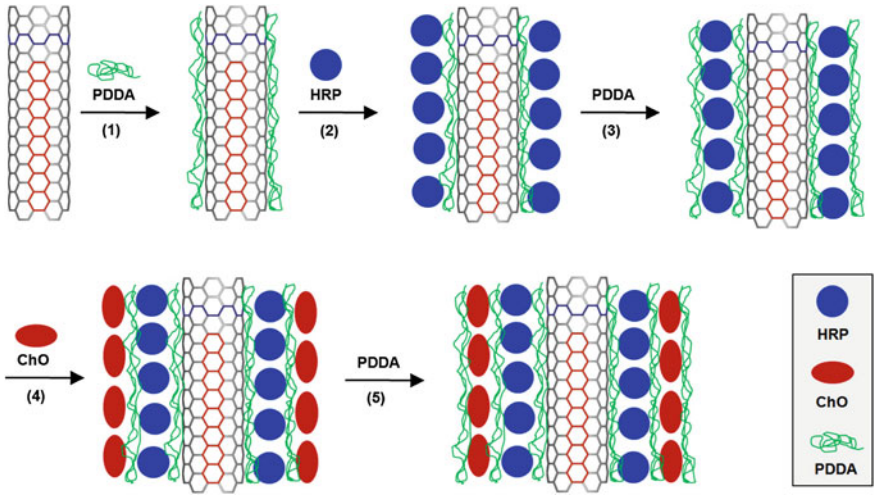

Fig. 17 Layer-by-layer coating of carbon nanotubes with enzymes. Schematic illustration of the procedure for the attachment of choline oxidase (ChO) and horseradish peroxidase (HRP) on carbon nanotube surface. *PDDA* poly(dimethyldiallylammonium chloride). Figure adapted from Ref. [208]

which is converted by HRP. For this system, it has been demonstrated that the CNT-modified GC electrodes offer a significant catalytic effect for the reduction of hydrogen peroxide and faciliate the direct electron transfer reaction of the enzyme (HRP) on the electrode surface.

In an even more sophisticated approach, SiNPs are used to construct a fully catalytically active biprotein system for analyte (lactose) detection [214]. Here, cellobiose dehydrogenase (CDH) and cyt *c* are used as biomolecules for analyte conversion and signal transfer. SiNPs in this system are used as second building block with a negative surface charge to enhance electrostatic interaction with the biomolecules. The supramolecular system is assembled on a cyt *c* monolayer electrode by alternating incubation steps in solutions of SiNP and a CDH/cyt *c* mixture. The co-immobilization of CDH and cyt *c* is faciliated by different isoelectric points of the two proteins. A schematic representation of the complex artificial onion-like architecture is given in Fig. 18. The system shows a distinct increase in the catalytic current and the amount of addressable cyt *c* with the growing number of deposited biomolecular layers and thereby provides evidence for efficient interprotein electron transfer. In a reverse conclusion, this means that by increasing the number of catalytic sites (amount of enzyme) within the system the specific bioelectrocatalytic conversion of lactose can be enhanced. This circumstance, however, also implies that CDH molecules deposited in different layers are in electrical contact with the electrode. Because a large portion of the enzyme molecules are immobilized rather far away from the electrode surface, it can be concluded that the catalytic oxidation reaction at CDH provides the electrons for the catalytic current, which are in turn transferred by cyt *c*–cyt *c* interprotein electron transfer steps towards the electrode.

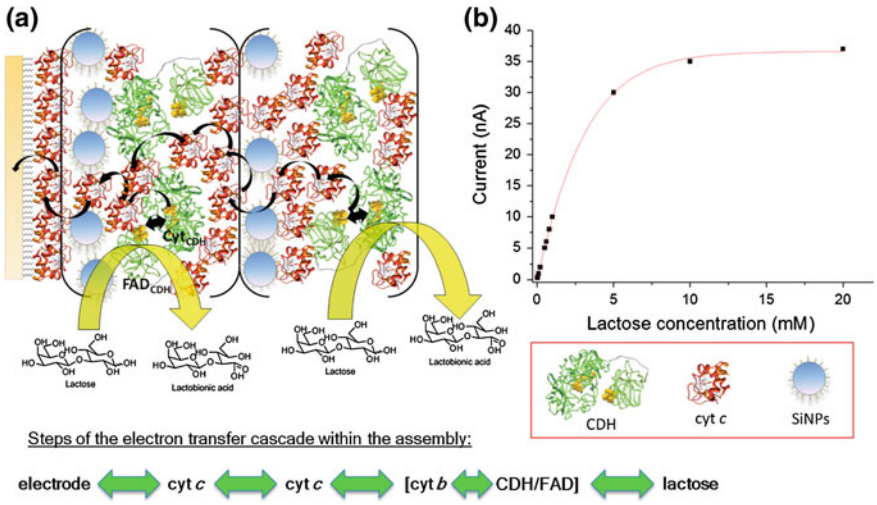

Fig. 18 Schematic representation of a supramolecular [SiNP/CDH·cyt *c*] architecture prepared on a cytochrome *c* (cyt *c*) monolayer electrode (M). The cyt *c* monolayer is assembled on a mixed thiol layer (MU/MUA). The different electron transfer steps for this architecture can be summarized in a simple way as follows: First lactose is oxidized at the flavin adenine dinucleotide (FAD)-domain of cellobiose dehydrogenase (CDH) and then the electrons are transferred to the cyt *b*-domain of CDH and from there on to the next neighboring cyt *c* and then they are transferred towards the electrode by cyt *c*–cyt *c* self-exchange. Figure adapted from Ref. [214]

For applications of such supramolecular nanoarchitectures, this means that the sensitivity towards the enzyme substrate (here, lactose) can be tuned to a large extent by the number of deposited protein layers without being limited by mediator diffusion or leakage.

In addition, the study of this system provides some information on the influence of protein glycosylation, as it can be shown that glycosylation of CDH can hinder the defined deposition of material during layer formation and decrease electron transfer between the immobilized protein molecules [214]. Approaches using direct protein–protein communication are expected to have a considerable impact on the development of further multilayer-based architectures and also represent a significant advance in modeling biological electron-transfer processes.

3.2.2 Nanomaterial-Based Immunosensors

Nanomaterials can also be a helpful tool to construct multilayer immunobiosensors. However, here the focus is not on the preparation of antibody multilayers but mainly to use multilayers of nanoparticles to increase electrochemical signals and/or the amount of bound antibodies [215, 216]. A large number of systems based on nanoparticles [134, 217–220] have been developed in this direction. However,

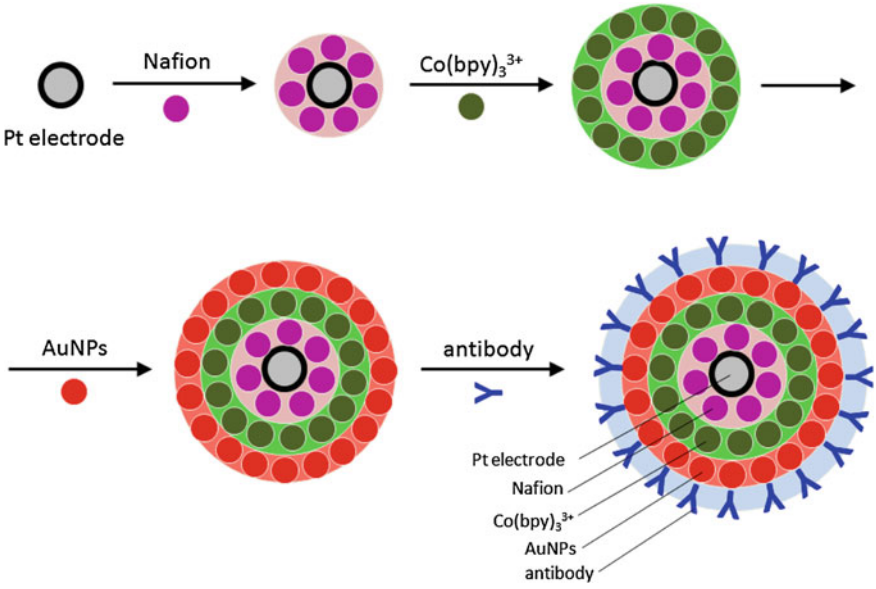

Fig. 19 Schematic illustration of the carcinoembryonic antigen immunosensor. Schematic illustration of the assembly of antibody/{nanogold/Co(bpy)$_3^{3+}$}$_n$/Nafion multilayers on the platinum electrode surface to core–shell particles. Figure adapted from Ref. [136]

because of the limited importance for the construction of protein multilayers, only a selected example will be illustrated in this section (Fig. 19).

This system combines electrochemically active Co(bpy)$_3^{3+}$ and AuNPs for the construction of [AuNP/Co(bpy)$_3^{3+}$]$_n$ multilayers [136]. Thereafter, a hepatitis B antibody (HBs-Ab) is immobilized on the gold nanoparticle surface. The multilayer immunosensor is used for hepatitis B surface antigen (HBsAg) determination via an amperometric and a potentiometric method. The electrochemical response of Co(bpy)$_3^{3+}$ is tuned by the number of bilayers. Because of the interaction of the immobilized antibodies with the antigens, an insulating antigen–antibody complex is formed, diminishing electron transfer reactions; accordingly, the amperometric response decreases. The linear range of the system for HBs-Ag is 0.05–4.5 μg/mL, with different detection limits for the voltammetric system (0.005 μg/mL) and the potentiometric system (0.015 μg/mL).

3.2.3 Nanomaterial-Based DNA Sensors

Carbon nanotubes have been proposed as support materials for numerous applications, including the development of DNA sensors [221, 222]. One of the challenges is the immobilization of DNA or other biological molecules on the sidewall of CNTs. Therefore, several methods have been developed, such as

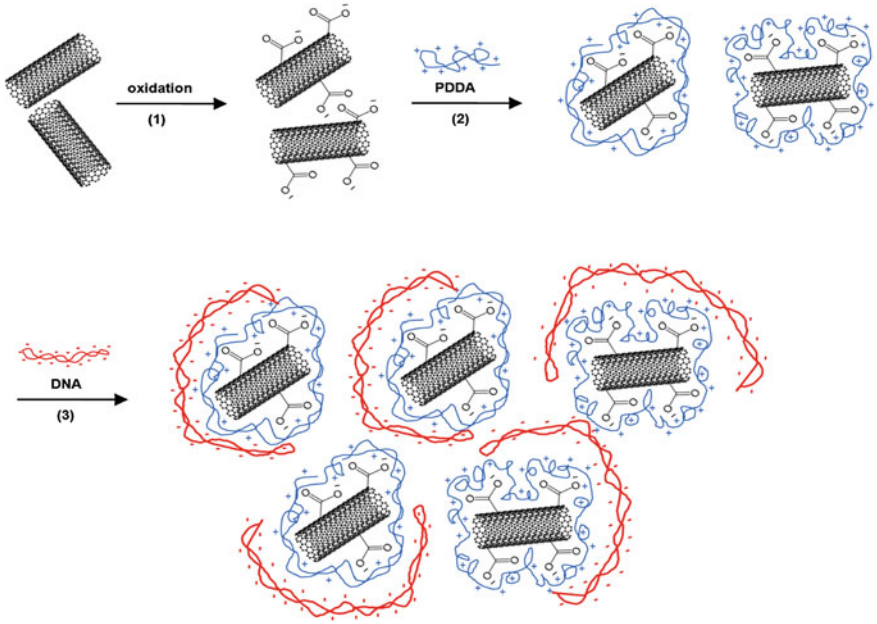

Fig. 20 Schematic illustration of the DNA/poly(dimethyl-diallylammonium) (PDDA)/single-wall carbon nanotube (SWCNT) multilayer. Figure adapted from Ref. [143]

for modification with Π-system containing compounds, partial surface oxidation, electropolymerization of thin films, or wrapping of CNTs in polymers. This can be exemplified with a system immobilizing DNA on single-wall carbon nanotubes (SWCNTs) in mutiple layers (Fig. 20) [143].

PDDA, a positively charged polyelectrolyte, and DNA as a negatively charged counterpart macromolecule are alternatingly deposited on oxidized SWCNTs. The electrode modified by the DNA/PDDA/SWCNTs particles shows a dramatic change of the electrochemical signal in solutions of tris(2,2′-bipyridyl)-ruthenium(II) ((Ru-(bpy)$_3^{2+}$) as a reporting redox probe. The DNA/PDDA/SWCNTs multilayer electrode is used to monitor DNA damage through the presence of nitric oxide. Here, the signal increases after oxidative damage of DNA.

Other examples are reported on the fabrication of multilayer films for the improvement of the electrochemical detection of DNA hybridization, such as through the modification of gold or ITO electrode surfaces with PSS and PAH multilayers and subsequent DNA adsorption [223].

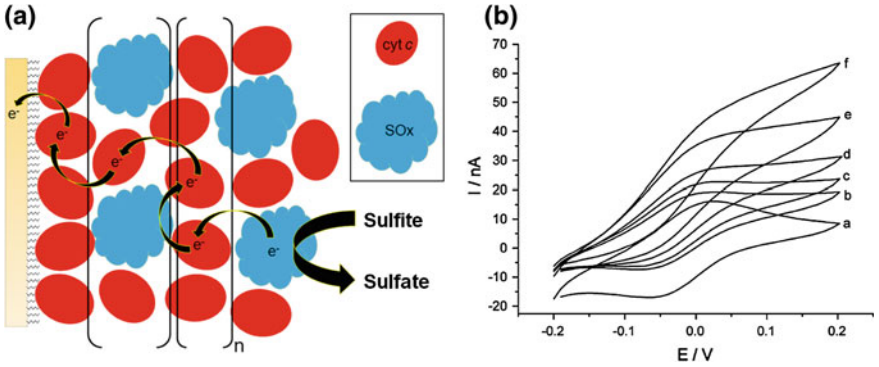

Fig. 21 **a** Schematic image of a multilayer electrode comprising cyt *c* and SOx constructed by electrostatic layer-by-layer self-assembly: *red circles* cyt *c*, *blue objects* SOx. *Black arrows* indicate electron transfer steps and sulfite oxidation. **b** Cyclic voltammograms of an eight-bilayer cyt *c*/SOx electrode with increasing sulfite concentration (0, 60, 125, 250, 0.5, 1 mM; scan rate 100 $mV \cdot s^{-1}$). Figure adapted from Ref. [224]

3.3 Protein–Protein Interaction-Based Biosensors

In this section, a rather unique approach to construct multilayer architectures is presented. Previously, we have seen that, in most cases, a supporting polyelectrolyte or different kinds of nanomaterials are used for the construction of multilayer films, but it can also be shown that the electrostatic interactions between proteins can be strong enough to result in multilayer formation on surfaces without any supporting material. This fact relys on a very different charge situation on the surface of the two proteins used for the construction at a given pH.

The principle can be exemplified with a system in which the redox protein cytochrome *c* is combined with the enzyme sulfite oxidase (SOx) in a self-assembling process, thereby forming a fully catalytically and electrochemically active multilayer electrode for sulfite detection [224]. One of the fundamentals for the successful multilayer development in this case is that the isoelectric points of the two proteins are rather separated and the density of charged amino acids is high enough to ensure that the electrostatic interactions between them are sufficient to form stable layers. This approach may have an advantge because both proteins are natural reaction partners with opposite charge on the protein interaction surface. Electron transfer (mediator-free) through the multilayer film is achieved by co-immobilization of the enzyme and the redox protein from a mixture rather than pure solutions. The cyt *c* and SOx are assembled by alternating incubations of a cyt *c* monolayer electrode into a SOx/cyt *c* mixture and a pure cyt *c* solution. The mixture of SOx/cyt *c* is necessary because a pure SOx interlayer would prevent the electron transport through the system, as it is based on cyt *c*–cyt *c* electron exchange. The mass accumulation during the assembly process can be confirmed by QCM measurements.

Atomic force microscopy measurements analyzing the multilayer thickness clearly show that with every deposition cycle approximately a monolayer of

proteins is immobilized on the surface. A schematic layer profile is given in Fig. 21. Voltammetric analysis shows a distinct catalytic oxidation current in the presence of sulfite in solution. It is a result of SO_3^{2-} oxidation by SOx, subsequent enzyme oxidation by cyt *c*, followed by electron transfer toward the electrode. In addition, the current is found to correlate with the number of immobilized [cyt *c*/SOx]$_n$ layers. This indicates that the two proteins are able to maintain efficient electronic communication being co-immobilized in multiple layers on the electrode. Notably, the fast reaction of cyt *c* with SOx in solution ($k = 4.47 \pm 0.13\ \mu M^{-1}\ s^{-1}$, pH 8.5) [225] can also occur in the immobilized state. The experiments indicate that the electron transfer cascade from the enzyme to the electrode is fast enough to follow the catalytic reaction and, thus, is not the rate-limiting step. Thus, a catalytically active multilayered protein architecture is established, which relys only on the electrostatic protein–protein interaction without any supporting material.

4 Summary

Electrochemical biosensors represent a wide area of research, which continues to develop at a rapid pace. As a rather simple, reliable, and cost-effective method for biomolecule immobilization, the LBL assembly technique has been paid much attention over the past decade. Therefore, the method is considered to be a very interesting approach for the fabrication of nanostructured architectures with rather high molecular order. Many studies have focused on maintaining the molecular integrity of biomolecules when they are immobilized on solid supports using polymers as well as several nanosized materials. However, the main focus is clearly the increase in biomolecular interaction sites on the electrode surface because this is attributed to the sensitivity of the system when applied for sensorial analysis.

Various LBL assembly strategies have been developed to incorporate enzymes, proteins, immunoglobulins, and DNA in the organized multilayer films for the design of biosensors. Mainly, biospecific interactions, covalent reactions, or electrostatic interactions have been applied. The LBL assembly allows control on the properties of the nanoarchitectures, such as charge, thickness, polarity, permeability, and roughness of the multilayer films. Special attention has been paid to an improved signal transfer based on the use of redox polymers or the construction of systems with protein–protein electron transfer. The rather large interest in multilayered sensor electrodes can be attributed in part to the possibility of developing miniaturized devices capable of a more sensitive and selective analysis and of detecting small quantities of analyte molecules.

References

1. Eggins BR (1996) Biosensors: an introduction. Wiley, New York
2. Dzyadevych SV, Arkhypova VN, Soldatkin AP, Elskaya AV, Martelet C, Jaffrezic-Renault N (2008) Amperometric enzyme biosensors: past, present and future. IRBM 29:171
3. Cassidy JF, Doherty AP, Vos JG (1998) Principles of chemical and biological sensors. Wiley, Toronto
4. Ramanavicius A, Ramanaviciene A, Malinauskas A (2006) Electrochim Acta 51:6025
5. Decher G (1997) Science 277:1232
6. Wilchek M, Bayer E (1988) Anal Biochem 171:1
7. Pugliese L, Coda A, Malcovati M, Bolognesi M (1993) J Mol Biol 231:698
8. Hoshi T, Anzai J, Osa T (1995) Anal Chem 67:770
9. Du X, Anzai J, Osa T, Motohashi R (1996) Electroanalysis 8:813
10. Anzai J, Kobayashi Y, Suzuki Y, Takeshita H, Chen Q, Osa T, Hoshi T, Du X (1998) Sens Actuators B 52:3
11. Anzai J, Takeshita H, Hoshi T, Osa T (1995) Chem Pharm Bull 43:520
12. Decher G, Lehr B, Lowack K, Lvov Y, Schmitt J (1994) Biosens Bioelectron 9:677
13. He P, Takahashi T, Hoshi T, Anzai J, Suzuki Y, Osa T (1994) Mater Sci Eng C2:103
14. Ebato H, Herron JN, Muller W, Okahata Y, Ringsdorf H, Suci PA (1992) Angew Chem Int Ed 31:1087
15. Anzai J, Kobayashi Y, Nakamura N, Nishimura M, Hoshi T (1999) Langmuir 15:221
16. De Lacey AL, Detcheverry M, Moiroux J, Bourdillon C (2000) Biotechnol Bioeng 68(1):1
17. Steiger B, Padeste C, Grubelnik A, Tiefenauer L (2003) Electrochim Acta 48(6):761
18. Chen Q, Kobayashi Y, Takeshita H, Hoshi T, Anzai J (1998) Electroanalysis 10:94
19. Anzai J, Takeshita H, Kobayashi Y, Osa T, Hoshi T (1998) Anal Chem 70:811
20. Anzai J, Takeshita H, Hoshi T, Osa T (1995) Denki Kagaku 63:1141
21. Becker JW Jr, Reeke GN, Cunningham BA, Edelman GM (1976) Nature 259:406
22. Lvov Y, Ariga K, Ichinose I, Kunitake T (1995) Chem Commun 31:2313
23. Lvov Y, Ariga K, Ichinose I, Kunitake T (1996) Thin Solid Films 284:797
24. Farooqi M, Saleemuddin M, Ulber R, Sosnitza P, Scheper T (1997) J Biotechnol 55:171
25. Anzai J, Kobayashi Y (2000) Langmuir 16:2851
26. Pallarole D, von Bildering C, Pietrasanta LI, Queralto N, Knoll W, Battaglini F, Azzaroni O (2012) Phys Chem Chem Phys 14(31):11027
27. Pallarole D, Queralto N, Knoll W, Ceolin M, Azzaroni O, Battaglini F (2010) Langmuir 26(16):13684
28. Kobayashi Y, Anzai J (2001) J Electroanal Chem 507:250
29. Yao H, Guo X, Hu N (2009) Electrochim Acta 54:7330
30. Yao H, Hu N (2009) J Phys Chem B 113:16021
31. Yao H, Hu N (2010) J Phys Chem B 114:3380
32. Yao H, Hu N (2010) J Phys Chem B 114:9926
33. Bourdillon C, Demaille C, Moiroux J, Saveant JM (1994) J Am Chem Soc 116:10328
34. Bourdillon C, Demaille C, Moiroux J, Saveant JM (1995) J Am Chem Soc 117:11499
35. Bourdillon C, Demaille C, Moiroux J, Saveant JM (1996) Acc Chem Res 29:529
36. Anne A, Demaille C, Moiroux J (1999) J Am Chem Soc 121:10379
37. Bourdillon C, Demaille C, Moiroux J, Saveant JM (1999) J Am Chem Soc 121:2401
38. Demaille C, Moiroux J (1999) J Phys Chem B 103:9903
39. Lin JN, Herron J, Andrade JD, Brizgys M (1988) IEEE Trans Biomed Eng 35:466
40. Peterman JH, Tarcha PJ, Butler JE (1988) J Immunol Methods 111:27
41. Muramatsu H, Dicks JM, Tamiya E, Karube I (1987) Anal Chem 59:2760
42. Muramatsu H, Kajiwara K, Tamiya E, Karube I (1986) Anal Chim Acta 188:257
43. Thompson M, Arthur CL, Dhaliwal GK (1986) Anal Chem 58:1206
44. Thompson M, Dhaliwal GK, Arthur CL, Calabrese GS (1987) IEEE Trans Ultrason Ferroelec Freq Contr UFFC 34:127

45. Prusak-Sochaczewski E, Loung JHT (1990) Anal Lett 23:401
46. Leggett GJ, Roberts CJ, Williams PM, Davies MC, Jackson DE, Tendler SJB (1993) Langmuir 9:2356
47. Hegner M, Wagner P, Semenza G (1993) FEBS Lett 336:452
48. Cullen DC, Lowe CR (1990) Sens Actuators B 1:576
49. Cullen DC, Lowe CR (1994) J Colloid Interface Sci 166:102
50. Leavitt AJ, Wenzler LA, Williams JM, Beebe TP (1994) J Phys Chem 98:8742
51. Caruso F, Rodda E, Furlong DN (1995) J Colloid Interface Sci 178:104
52. Jin W, Bier F, Wollenberger U, Scheller F (1995) Biosens Bioelectron 10:823
53. Zhang SX, Yang WW, Niu YM, Sun CQ (2004) Anal Chim Acta 523:209
54. Zhang SX, Yang WW, Niu YM, Sun CQ (2004) Sens Actuators B 101:38741
55. Yoon HC, Hong MY, Kim HS (2000) Anal Chem 72:4420
56. Willner I, Riklin A, Shoham B, Rivenson D, Katz E (1993) Adv Mater 5:912
57. Luong GHT, Nguyen AL, Guilbault GG (1993) Adv Biotechnol Bioeng 50:86
58. Means GE, Peeney RE (1971) Chemical modification of proteins. Holden-Day, San Francisco
59. Ji TH (1979) Biochim Biophys Acta 559:39
60. Sirkar K, Revzin A, Pishko MV (2000) Anal Chem 72:2930
61. Willner I, Liom-Degan M, Marx-Tibbon S, Katz E (1995) J Am Chem Soc 117:6581
62. Shoham B, Migron Y, Riklin A, Willner I, Tartakovsky B (1995) Biosens Bioelectron 10:341
63. Riklin A, Willner I (1995) Anal Chem 67:4118
64. Chen Z, Kaplan DL, Gao H, Kumar J, Marx KA, Tripathy SK (1996) Mater Sci Eng C4:155
65. Gerard M, Chaubey A, Malhotra BD (2002) Biosens Bioelectron 17:345
66. Clark SL, Montague MF, Hammond PT (1997) Macromolecules 30:7237
67. Lutkenhaus JL, Hammond PT (2007) Soft Matter 3(7):804
68. Siqueira JR, Caseli L, Crespilho FN, Zucolotto V, Oliveira ON (2010) Biosens Bioelectron 25(6):1254
69. Mahmoudi M, Lynch I, Ejtehadi M, Monpoli M, Bobelli F, Laurent S (2011) Chem Rev 111:5610
70. Zhang HY, Fu Y, Wang D, Wang LY, Wang ZQ, Zhang X (2003) Langmuir 19:8497
71. Astruc D, Boisselier E, Ornelas C (2010) Chem Rev 110:1857
72. Olek M, Ostrander J, Jurga S, Mohwald H, Kotov N, Kempa K, Giersig M (2004) Nano Lett 4:1889
73. Zhang MN, Yan YM, Gong KP, Mao LQ, Guo ZX, Chen Y (2004) Langmuir 20:8781
74. Schonhoff M, Ball V, Bausc AR, Dejugnat C, Delorme N, Glinel K, Klitzing RV, Steitz R (2007) Colloids Surf A: Physicochem Eng Aspects 303:14
75. Iler RK (1966) J Colloid Interface Sci 21:569
76. Sun Y, Zhang X, Sun C (1996) J Shen Macromol Chem Phys 197:147
77. Zhang S, Yang W, Niu Y, Sun C (2004) Sens Actuators B 101:387
78. Hodak J, Etchenique R, Calvo EJ, Singhal K, Bartlett PN (1997) Langmuir 13:2708
79. Calvo EJ, Etchenique R, Pietrasanta L, Wolosiuk A, Danilowicz C (2001) Anal Chem 73:1161
80. Calvo EJ, Danilowicz C, Wolosiuk A (2002) J Am Chem Soc 124:2452
81. Calvo EJ, Wolosiuk A (2004) ChemPhysChem 5:235
82. Hou S, Wang J, Martin CR (2005) Nano Lett 5:231
83. Hoshi T, Noguchi T, Anzai J (2004) New Technol Med 5:345
84. Xu JJ, Zhao W, Luo XL, Chen HY (2005) Chem Commun 41:792
85. Calvo EJ, Battaglini F, Danilowicz C, Wolosiuk A, Otero M (2000) Faraday Discuss 116:47
86. Sun C, Li W, Sun Y, Xi Z, Shen J (1999) Electrochim Acta 44:3401
87. Anzai J, Kobayashi Y (2000) Langmuir 16:2851
88. Rosca V, Catalin Popescu I (2002) Electrochem Commun 4:904
89. Yu X, Sotzing GA, Papadimitrakopoulos F, Rusling JF (2003) Anal Chem 75:4565

90. Narvaez A, Suarez G, Popescu IC, Katakis I, Dominguez E (2000) Biosens Bioelectron 15:43
91. Forzani ES, Solis VM, Calvo EJ (2000) Anal Chem 72:5300
92. Coche-Guerente L, Labbe P, Mengeaud V (2001) Anal Chem 73:3206
93. Coche-Guerente L, Desbrieres J, Fatisson J, Labbe P, Rodriguez MC, Rivas G (2005) Electrochim Acta 50:2865
94. Ram MK, Bertoncello P, Ding H, Paddeu S, Nicolini C (2001) Biosens Bioelectron 16:849
95. Yang M, Yang Y, Yang H, Shen G, Yu R (2005) Biomaterials 27:246
96. Hoshi T, Saiki H, Anzai J (2003) Talanta 61:363
97. Patel DS, Aithal RK, Krishna G, Lvov YM, Tien M, Kuila D (2005) Colloids Surf B 43:13
98. Wang LW, Hu NF (2001) Bioelectrochemistry 53:205
99. Zhou YL, Li Z, Hu NF, Zeng YH, Rusling JF (2002) Langmuir 18:8573
100. Shi GY, Sun ZY, Liu MC, Zhang L, Liu Y, Qu YH, Jin LT (2007) Anal Chem 79:3581
101. Lvov YM, Lu ZQ, Schenkman JB, Zu XL, Rusling JF (1998) J Am Chem Soc 120:4073
102. Ma HY, Hu NF, Rusling JF (2000) Langmuir 16:4969
103. Panchagnula V, Kumar CV, Rusling JF (2002) J Am Chem Soc 124:12515
104. Li Z, Hu NF (2002) J Colloid Interface Sci 254:257
105. Beissenhirtz MK, Scheller FW, Stocklein WFM, Kurth DG, Möhwald H, Lisdat F (2004) Angew. Chem Int Ed 43:4357
106. Beissenhirtz MK, Kafka J, Schäfer D, Wolny M, Lisdat F (2005) Electroanalysis 17:1931
107. Beissenhirtz MK, Scheller FW, Lisdat F (2004) Anal Chem 76:4665
108. Yu AM, Caruso F (2003) Anal Chem 75:3031
109. Lindholm-Sethson B, Gonzalez JC, Puu G (1998) Langmuir 14:6705
110. Moraes ML, Rodrigues UP, Oliveira ON, Ferreira M (2007) J Solid State Electrochem 11:1489
111. Hassler BL, Kohli N, Zeikus JG, Lee I, Worden RM (2007) Langmuir 23:7127
112. Loew N, Scheller FW, Wollenberger U (2004) Electroanalysis 16:1149
113. Harper AC, Anderson MR (2006) Electroanalysis 18:2397
114. Mizutani F, Sato Y, Yabuki S, Hirata Y (1996) Chem Lett 4:251
115. Hou SF, Fang HQ, Chen HY (1997) Anal Lett 30:1631
116. Hou SF, Yang KS, Fang HQ, Chen HY (1998) Talanta 47:561
117. Li W, Wang Z, Sun C, Xian M, Zhao M (2000) Anal Chim Acta 418:225
118. Shi H, Yang Y, Huang J, Zhao Z, Xu X, Anzai J (2006) Talanta 70:852
119. Miscoria SA, Desbrieres J, Barrera GD, Labbé P, Rivas GA (2006) Anal Chim Acta 578:137
120. Dronov RV, Kurth DG, Möhwald H, Scheller FW, Friedmann J, Pum D, Sleytr UB, Lisdat F (2008) Langmuir 24(16):8779
121. Sarauli D, Tanne J, Xu C, Schulz B, Trnkova L, Lisdat F (2010) Phys Chem Chem Phys 12(42):14271
122. Sarauli D, Tanne J, Schafer D, Schubart IW, Lisdat F (2009) Electrochem Commun 11:2288
123. Shen L, Hu NF (2005) Biomacromolecules 6:1475
124. Gobi KV, Mizutani F (2001) Sens Actuators B 80:272
125. Dronov R, Kurth DG, Möhwald H, Scheller FW, Lisdat F (2007) Electrochim Acta 53:1107
126. Balkenhohl T, Adelt S, Dronov R, Lisdat F (2008) Electrochem Commun 10:914
127. Wettstein Ch, Möhwald H, Lisdat F (2012) Bioelectrochemistry 88:9
128. Dronov RV, Kurth DG, Möhwald H, Scheller FW, Lisdat F (2008) Angew Chem Int Ed 47(16):3000
129. Dronov RV, Kurth DG, Scheller FW, Lisdat F (2007) Electroanalysis 19:1642
130. Wegerich F, Turano P, Allegrozzi M, Möhwald H, Lisdat F (2011) Langmuir 27(7):4202
131. Spricigo R, Dronov R, Rajagopalan KV, Lisdat F, Leimkühler S, Scheller FW, Wollenberger U (2008) Soft Matter 4(5):972
132. Spricigo R, Dronov R, Lisdat F, Leimkühler S, Scheller FW, Wollenberger U (2009) Anal Bioanal Chem 393(1):225–233
133. Feifel SC, Kapp A, Ludwig R, Gorton L, Lisdat F (2013) RSC Advances 3:3428

134. Wang MJ, Wang LY, Yuan H, Ji XH, Sun CY, Ma L, Bai YB, Li TJ, Li JH (2004) Electroanalysis 16:757
135. Caruso F, Niikura K, Furlong DN, Okahata Y (1997) Langmuir 13:3427
136. Tang DP, Yuan R, Chai YQ, Fu YZ, Dai JY, Liu Y, Zhong X (2005) Biosens Bioelectron 21:539
137. Calvo EJ, Danilowicz C, Lagier CM, Manrique J, Otero M (2004) Biosens Bioelectron 19:1219
138. Brynda E, Houska M, Skvor J, Ramsden JJ (1998) Biosens Bioelectron 13:165
139. Brynda E, Homola J, Houska M, Pfeifer P, Skvor J (1999) Sens Actuators B 54:132
140. Diederich A, Losche M (1997) Adv Biophys 34:205
141. Wong ELS, Gooding JJ (2006) Anal Chem 78:2138
142. Zhang Y, Hu NF (2007) Electrochem Commun 9:35
143. He PG, Bayachou M (2005) Langmuir 21:6086
144. Teles FRR, Fonseca LP (2008) Talanta 77:606
145. Batchelor-McAuley C, Wildgoose GG, Compton RG (2009) Biosens Bioelectron 24:3183
146. Munge B, Estavillo C, Schenkman JB, Rusling JF (2003) ChemBioChem 4:82
147. Rusling JF (2004) Biosens Bioelectron 20:1022
148. Wang B, Rusling JF (2003) Anal Chem 75:4229
149. Mugweru A, Wang B, Rusling J (2004) Anal Chem 76:5557
150. Ropp PA, Thor HH (1999) Chem Biol 6:599
151. Park S, Xie Y, Weaver MJ (2002) Langmuir 18:5792
152. El-Deab MS, Ohsaka T (2002) Electrochem Commun 4:288
153. Bharathi S, Nogami M (2001) Analyst 126:1919
154. Lin JH, Zhang LJ, Zhang SS (2007) Anal Biochem 370:180
155. Daniel MC, Austric D (2004) Chem Rev 104:293
156. Bonk S, Lisdat F (2009) Biosens Bioelectron 25(4):739
157. Hrapovic S, Liu YL, Male KB, Luong JHT (2004) Anal Chem 76:1083
158. Liu CY, Hu JM (2009) Biosens Bioelectron 24:2149
159. Lin JH, He CY, Zhao Y, Zhang SS (2009) Sens. Actuators B: Chem. 137:768
160. Lim SH, Wei J, Lin JY, Li QT, KuaYou J (2005) Biosens Bioelectron 20:2341
161. Fiorito PA, Goncales VR, Ponzio EA, de Torresi SIC (2005) Chem Commun 3:366
162. Zong SZ, Cao Y, Zhou YM, Ju HX (2006) Langmuir 22:8915
163. Slowing II, Trewyn BG, Giri S, Lin VSY (2007) Adv Funct Mater 17:1225
164. Baptista P, Pereira E, Eaton P, Doria G, Miranda A, Gomes I, Quaresma P, Franco R (2008) Anal Bioanal Chem 391:943
165. Nietzold C, Lisdat F (2012) Analyst 137(12):2821
166. Moriggi L, Cannizzo C, Dumas E, Mayer CR, Ulianov A, Helm L (2009) J Am Chem Soc 131:10828
167. Pingarrón JM, Yãnez-Sedẽno P, González-Cortés A (2008) Electrochim Acta 53:5848
168. Gooding JJ (2005) Electrochim Acta 50:3049
169. Coleman JN, Khan U, Gunko YK (2006) Adv Mater 18:689
170. Durkop T, Getty SA, Cobas E, Fuhrer MS (2004) Nano Lett 4:35
171. Keren K, Berman RS, Buchstab E, Sivan U, Braun E (2003) Science 302:1380
172. Tasis D, Tagmatarchis N, Bianco A, Prato M (2006) Chem Rev 106:01105
173. Gooding JJ, Wibowo R, Liu JQ, Yang WR, Losic D, Orbons S, Mearns FJ, Shapter JG, Hibbert DB (2003) J Am Chem Soc 125:9006
174. Schubert K, Göbel G, Lisdat F (2009) Electrochim Acta 54(11):3033
175. Tanne C, Göbel G, Lisdat F (2010) Biosens Bioelectron 26:530
176. Zhao W, Xu JJ, Chen HY (2005) Front Biosci 10:1060
177. Erlanger BF, Chen BX, Zhu M, Brus L (2001) Nano Lett 1:465
178. Staii C, Johnson AT (2005) Nano Lett 5:1774
179. Stoll C, Kudera S, Parak WJ, Lisdat F (2006) Small 2:741
180. Katz E, Zayats M, Willner I, Lisdat F (2006) Chem Commun 42:1395

181. Stoll C, Gehring C, Schubert K, Zanella M, Parak WJ, Lisdat F (2008) Biosens Bioelectron 24:260
182. Schubert K, Khalid W, Yue Z, Parak WJ, Lisdat F (2010) Langmuir 26:1395
183. Liu Q, Lu XB, Li J, Yao X, Li JH (2007) Biosens Bioelectron 22:3203
184. Wang Z, Xu Q, Wang HQ, Yang Q, Yu JH, Zhao YD (2009) Sens Actuators B-Chem 138:278
185. Bawendi MG, Steigerwald ML, Brus LE (1990) Annu Rev Phys Chem 41:477
186. Kucur E, Riegler J, Urban GA, Nann T (2003) J Chem Phys 119:2333
187. Ehlert O, Tiwari A, Nann T (2006) J Appl Phys 100:98
188. Kucur E, Bucking W, Arenz S, Giernoth R, Nann T (2006) ChemPhysChem 7:77
189. Niemeyer CM (2003) Angew Chem Int Ed 42:5796
190. Willner I, Basnar B, Willner B (2007) FEBS J 274:302
191. Lisdat F, Schäfer D, Kapp A (2013) Anal Bioanal Chem 405:3739
192. Pereira AR, Iost RM, Martins MVA, Yokomizo CCH, da Silva WC, Nantes IL, Crespilho FN (2011) Phys Chem Chem Phys 13:12155
193. Cosnier S, Mousty C, Gondran C, Lepellec A (2006) Mater Sci Eng, A 26:442
194. Tam PD, Hieu NV, Chien ND, Le A-T, Tuan MA (2009) J Immunol Methods 350:118
195. Lvov Y, Munge B, Giraldo O, Ichinose I, Suib S, Rusling JF (2000) Langmuir 16:8850
196. Zhou Y, Li Z, Hu N, Zeng Y, Rusling JF (2002) Langmuir 18:8573
197. Kröning S, Scheller FW, Wollenberger U, Lisdat F (2004) Electroanalysis 16(4):253
198. Lei Ch, Lisdat F, Wollenberger U, Scheller FW (1999) Electroanalysis 11(4):274
199. Liu HY, Rusling JF, Hu NF (2004) Langmuir 20:10700
200. Zhang Y, Lu H, Hu N (2005) J Phys Chem B. 109:10464
201. Göbel G, Schubert K, Schubart IW, Khalid W, Parak WJ, Lisdat F (2011) Electrochim Acta 56(18):6397
202. Willner I, Patolsky F, Wassermann J (2001) Angew Chem Int Ed 40(10):1861
203. Feifel SC, Lisdat F (2011) Journal of Nanobiotechnology 9:59
204. Sun YY, Yan F, Yan WS, Sun CQ (2006) Biomaterials 27(21):4042
205. Wang YJ, Caruso F (2005) Chem Mater 17(5):953
206. Liu G, Lin Y (2006) Electrochem Commun 8:251
207. Liu G, Lin Y (2006) J Nanosci Nanotechnol 6:948
208. Liu G, Lin Y (2006) Anal Chem 78:835
209. Wang J, Liu G, Lin Y (2006) Analyst 131:477
210. Qu FL, Yang MH, Jiang JH, Shen GL, Yu RQ (2005) Anal Biochem 344:108
211. Zhao HT, Ju HX (2006) Anal Biochem 350:138
212. Zhang MN, Gong KP, Zhang HW, Mao LQ (2005) Biosens Bioelectron 20:270
213. Liu JY, Tian SJ, Knoll W (2005) Langmuir 21:5596
214. Feifel SC, Ludwig R, Gorton L, Lisdat F (2012) Langmuir 28:9189
215. Yu X, Munge B, Patel V, Jensen G, Bhirde A, Gong JD, Kim SN, Gillespie J, Gutkind JS, Papadimitrakopoulos F, Rusling JF (2006) J Am Chem Soc 128(34):11199
216. Das J, Aziz A, Yang H (2006) J Am Chem Soc 128(50):16022
217. Cui XQ, Pei RJ, Wang ZX, Yang F, Ma Y, Dong SJ, Yang XR (2003) Biosens Bioelectron 18:59
218. Olkhov RV, Parker R, Shaw AM (2012) Biosens Bioelectron 1(36):1
219. Luppa PB, Sokoll LJ, Chan DW (2001) Clin Chim Acta 314:1
220. Ou CF, Yuan R, Chai YQ, Tang MY, Chai R, He XL (2007) Anal Chim Acta 603:205
221. Xu K, Huang JR, Ye ZZ, Ying YB, Li YB (2009) Sensors 9(7):5543
222. Iost RM, Madurro JM, Brito-Madurro AG, Nantes IL, Caseli L, Crespilho FN (2011) Int J Electrochem Sci 6(7):2965
223. Lee TMH, Li LL, Hsing IM (2003) Langmuir 19:4338
224. Dronov RV, Kurth DG, Möhwald H, Spricigo R, Leimkühler S, Wollenberger U, Rajagopalan KV, Scheller FW, Lisdat F (2008) J Am Chem Soc 130(4):1122
225. Speck SH, Koppenol WH, Dethmers JK (1981) J Biol Chem 256(14):7394

Adv Biochem Eng Biotechnol (2014) 140: 299–326
DOI: 10.1007/10_2013_224

Published Online: 10 August 2013

Biosensors Based on Enzyme Inhibition

Fabiana Arduini and Aziz Amine

Abstract The present chapter describes the use of biosensors based on enzyme inhibition as analytical tools. The parameters that affect biosensor sensitivity, such as the amount of immobilized enzyme, incubation time, and immobilization type, were critically evaluated, highlighting how the knowledge of enzymatic kinetics can help researchers optimize the biosensor in an easy and fast manner. The applications of these biosensors demonstrating their wide application have been reported. The objective of this survey is to give a critical description of biosensors based on enzyme inhibition, of their assembly, and their application in the environmental, food, and pharmaceutical fields.

Keywords Biosensor · Enzyme · Inhibition

Contents

F. Arduini (✉)
Dipartimento di Scienze e Tecnologie Chimiche, Università di Roma Tor Vergata, Via della Ricerca Scientifica, 00133 Rome, Italy
e-mail: fabiana.arduini@uniroma2.it

F. Arduini
Consorzio Interuniversitario Biostrutture e Biosistemi "INBB", Viale Medaglie d'Oro, 305 Rome, Italy

A. Amine
Faculté des Sciences et Techniques, B.P.146, Mohammadia, Morocco

1 Introduction

According to the IUPAC (International Union of Pure and Applied Chemistry) definition, a biosensor may be defined as a device incorporating a biocomponent (antibody, enzyme, microorganism, tissue, nucleic acid) in intimate contact with a suitable physicochemical transducer. The transducer converts the biochemical signal into a quantifiable electronic signal, which is proportional to the concentration of a specific analyte or group of analytes. As reported in a technical report in the *Biosensor and Bioelectronics Journal*,

> Biosensors may be classified according to the biological specificity-conferring mechanism or, alternatively, to the mode of physico-chemical signal transduction. The biological recognition element may be based on a chemical reaction catalyzed by, or on an equilibrium reaction with macromolecules that have been isolated, engineered or present in their original biological environment. In the latter cases, equilibrium is generally reached and there is no further, if any, net consumption of analyte(s) by the immobilized biocomplexing agent incorporated into the sensor. Biosensors may be further classified according to the analytes or reactions that they monitor: direct monitoring of analyte concentration or of reactions producing or consuming such analytes; alternatively, an indirect monitoring of inhibitor or activator of the biological recognition element (biochemical receptor) may be achieved [1].

In the case of an enzymatic biosensor, in which the enzyme is the biocomponent, we can summarize that the measurement of analytes can be performed by means of two different approaches: if the enzyme metabolizes the analyte, the analyte can be determined measuring the enzymatic product, or if the analyte inhibits the enzyme, the decrease of the enzymatic product formation can be measured and correlated to the analyte concentration. In the latter case, this type of biosensor is called a "biosensor based on enzyme inhibition." Nowadays, several reviews of biosensors based on enzyme inhibition have been published. Taking into consideration the papers published from 2000, there are just three reviews in the literature. The first one in chronological order was reported in the *Biosensor and Bioelectronics* Journal by Luque de Castro and Herrera, in which an overview of biosensors and biosensing systems was given. In this case the authors highlighted that the inhibition effect is not selective, and for this reason the title is "Enzyme Inhibition-Based Biosensors and Biosensing Systems: Questionable Analytical Devices" [2]. Another review was reported by our research group, also published in the *Biosensors and Bioelectronics* Journal with the title, "Enzyme

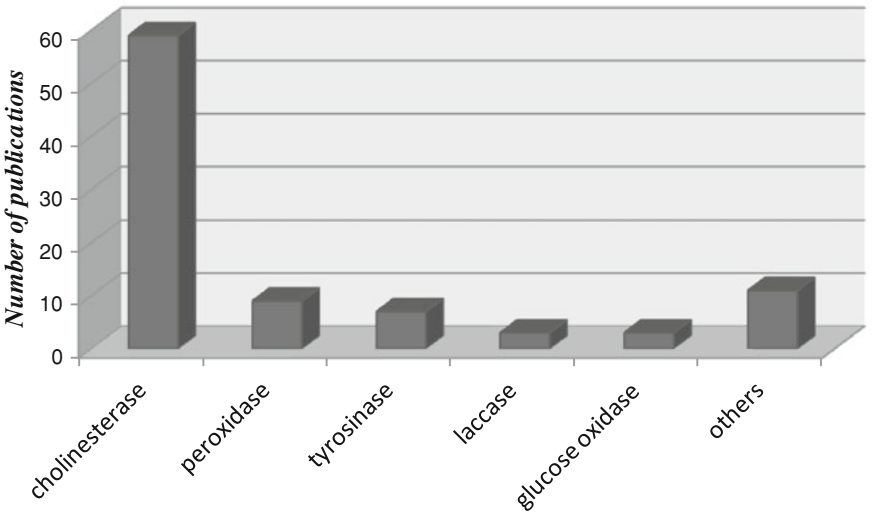

Fig. 1 Distribution of enzymes used to construct biosensors based on enzyme inhibition (period 2006–2012)

Inhibition-Based Biosensors for Food Safety and Environmental Monitoring" [3]. The review highlighted research carried out during 2000–2005 on biosensors that are based on enzyme inhibition for determination of pollutants and toxic compounds in a wide range of samples. Here the different enzymes implicated in the inhibition, different transducers forming the sensing devices, and the different contaminants analyzed were considered. The last one was reported in the *Analytical Letters* Journal also by our research group with the title of, "Reversible Enzyme Inhibition Based Biosensors: Applications and Analytical Improvement Through Diagnostic Inhibition," in which research carried out from 2000 up to 2009 on biosensors based on *reversible* enzyme inhibition for determination of drugs, pollutants, and toxic compounds was reported [4].

We highlight that, to our knowledge, these reviews are the only ones totally dedicated to biosensors based on enzyme inhibition; in fact, in other reviews such as, "Determination of Pesticides Using Electrochemical Enzymatic Biosensors" [5] or "Design and Development of Biosensors for the Detection of Heavy Metal Toxicity" [6], only a section dedicated to the biosensor based on enzyme inhibition is present. However, taking into consideration the three reviews mentioned above, it seems that the world of biosensors based on enzyme inhibition is confined to a restricted field of applications in analytical chemistry. However, this is not true if we consider that the cholinesterase biosensor is a biosensor based on cholinesterase inhibition; in fact, including the period between 2000 and 2012, there are eight reviews concerning the cholinesterase biosensor [7–14]. In Fig. 1 we show the distribution of enzymes used for the design of biosensors in the period 2006–2012 demonstrating that the cholinesterase biosensor is the most used enzyme for developing enzyme-based biosensors. We have found the same trend also in the

period 2000–2005 [3]. In this chapter, after highlighting research activity in this field reported in the literature, we describe how to design a biosensor based on enzyme inhibition and which parameters need to be investigated accurately in order to reach a low detection limit, together with their analytical application.

2 Biosensors Based on Irreversible and Reversible Inhibition

The detection of analyte is based on the determination of the difference in enzyme activity in the presence and absence of inhibitor according to the equation:

$$\mathrm{I}\% = (\mathrm{A}_0 - \mathrm{A}_\mathrm{i}/\mathrm{A}_0) \times 100$$

where A_0 is the activity in the absence of inhibitor and A_i in the presence of inhibitor. This procedure is always used in the case of reversible inhibition and, sometimes, in the case of irreversible inhibition in which a different protocol is usually adopted in order to obtain an increase in sensitivity, as described in detail in the successive protocol of the measurement section. The different protocol is due to a different kind of inhibition: reversible inhibition is characterized by noncovalent interaction between inhibitor and enzyme, with the consequent restoration of the initial activity after the inhibition measurement. On the contrary, in the case of irreversible inhibition characterized by covalent bonding between the enzyme and the inhibitor, the restoration of the initial activity requires a reactivation of the enzyme using specific compounds. Thus, in order to choose the best measurement protocol, it is important to know the type of inhibition. The research study should start with the calculation of the Michaelis–Menten constant ($\mathrm{K_{Mapp}}$) using the Michaelis–Menten equation

$$V = \frac{V_{\max}[S]}{K_M + [S]}$$

where V is the reaction rate, $V_{\max}$ is the maximum reaction rate, $[S]$ is the substrate concentration and $K_{M\mathrm{app}}$ is the Michaelis–Menten apparent constant, apparent because the enzyme is immobilized. The enzymatic activity is measured as a function of the substrate concentration and a typical response is reported in Fig. 2. The substrate concentration that produces exactly half of the maximum reaction rate (Fig. 2) is numerically equal to the $K_{M\mathrm{app}}$ and gives information about the affinity of the enzyme towards the substrate: a low value of $K_{M\mathrm{app}}$ indicates a high affinity for the substrate. A good biosensor should have the $K_{M\mathrm{app}}$ value near the K_M value of the enzyme free in solution.

To understand if the enzyme is inhibited by the analyte in an irreversible or reversible way, the procedure should be the one described in Fig. 3; if the enzyme restores the initial enzymatic activity after the measurement, then the inhibition is of reversible type (Fig. 3a); if the enzyme does not restore its initial enzymatic activity instead, the inhibition is of irreversible type (Fig. 3b).

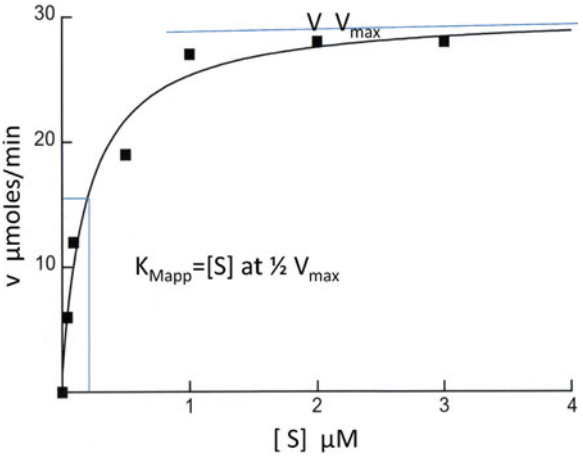

Fig. 2 Typical Michaelis–Menten plot

In the case of irreversible inhibition, the reaction scheme is reported in Fig. 4a. In the case of reversible inhibition, there are different mechanisms involved in interactions between enzyme and inhibitor. Most of the developed biosensors are based either on a *competitive* or *noncompetitive* mechanism. In the first case (Fig. 4b), the inhibitor may bound to the active site center and compete with the substrate for the active site. This equilibrium is regulated by the inhibition constant that describes the affinity of the inhibitor for the enzyme. In competitive inhibition, a high concentration of substrate competes with the inhibitor and prevents the detection of a low concentration of inhibitor. For this reason, in order to reach a low detection limit, the substrate concentration should be chosen as a compromise between a good analytical signal and an inhibition effect still detectable for the needed level. In the case of noncompetitive inhibition (Fig. 4c), the inhibitor binds to both the enzyme and the enzyme–substrate complex, most likely at a site other than the active site, such that the inhibitor does not compete directly with the substrate. In this case, the degree of inhibition is not dependent on the substrate concentration, and this format permits reaching a low detection limit of the analyte/inhibitor more easily, because there is no limitation on using an amount of substrate giving the optimal analytical signal.

The other two mechanisms of inhibition are *uncompetitive inhibition* and *mixed inhibition*. For the case of uncompetitive inhibition (Fig. 4d), the inhibitor binds only the enzyme–substrate complex, so that the degree of inhibition is independent of the substrate when the substrate concentration is higher than the Michaelis–Menten constant value. For the latter case of a mixed inhibition (Fig. 4e), the inhibitor binds the enzyme and enzyme–substrate complex with different affinities as regulated by K_i in the case of the inhibitor–enzyme complex, and αK_i for the inhibitor enzyme–substrate complex. The inhibition is designated *mixed, predominantly competitive* when $\alpha > 1$, or *mixed predominantly uncompetitive* when $\alpha < 1$, and *noncompetitive* when $\alpha = 1$. Thus, noncompetitive inhibition is one of the cases of mixed inhibition. For the evaluation of the inhibition type and the determination of K_i, an exact

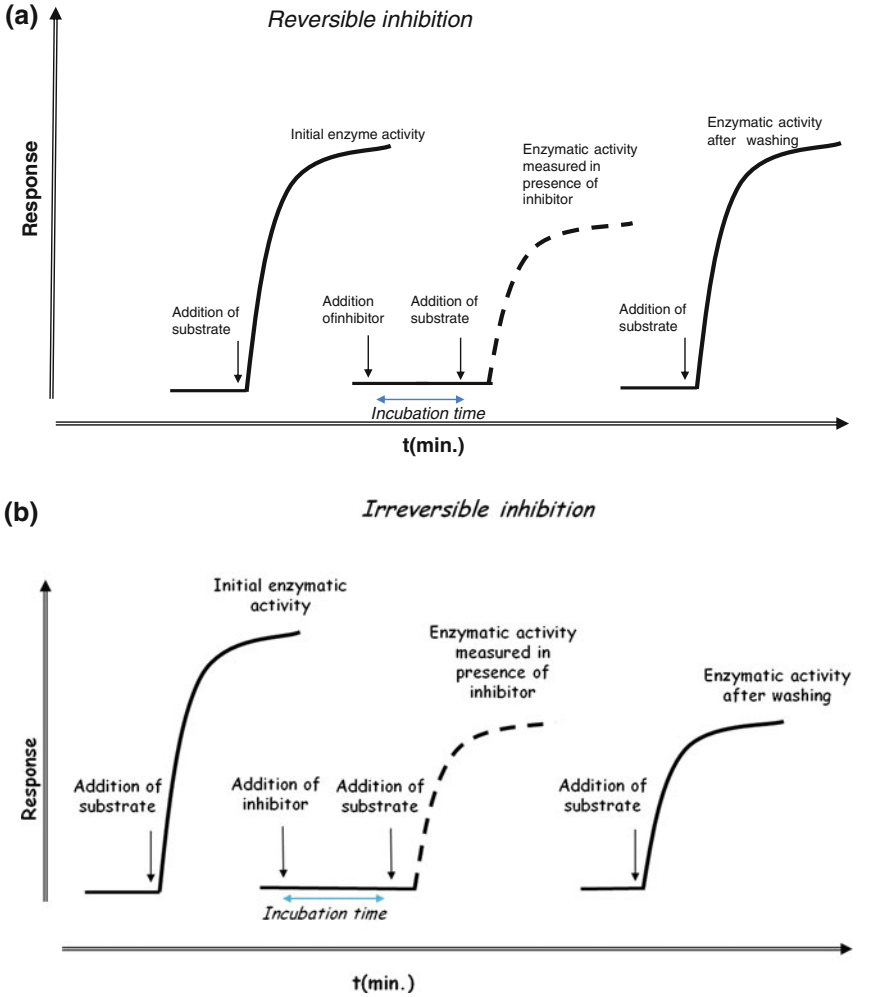

Fig. 3 **a** A typical response before and after inhibition in the case of a biosensor based on reversible inhibition, or **b** irreversible inhibition

evaluation of the mechanism [15–17] can be made by use of the Lineawever–Burk plot, Dixon plot, and Cornish–Bodwen plot. Often in pharmacological and toxicological fields, the I_{50} is commonly reported; it designates the inhibitor concentration required for 50 % of inhibition. I_{50} is often regarded as simply equal to K_i, albeit this is only true for purely noncompetitive inhibition.

Table 1 shows the relations between I_{50} and K_i and calculates the values of I_{50}/K_i ratios when [S] increases from 0.1 to 10 km. Under competitive inhibition, the ratio I_{50}/K_i increases by increasing [S], particularly when $[S] > K_m$. In the opposite case, under uncompetitive inhibition, the ratio I_{50}/K_i decreases by increasing [S],

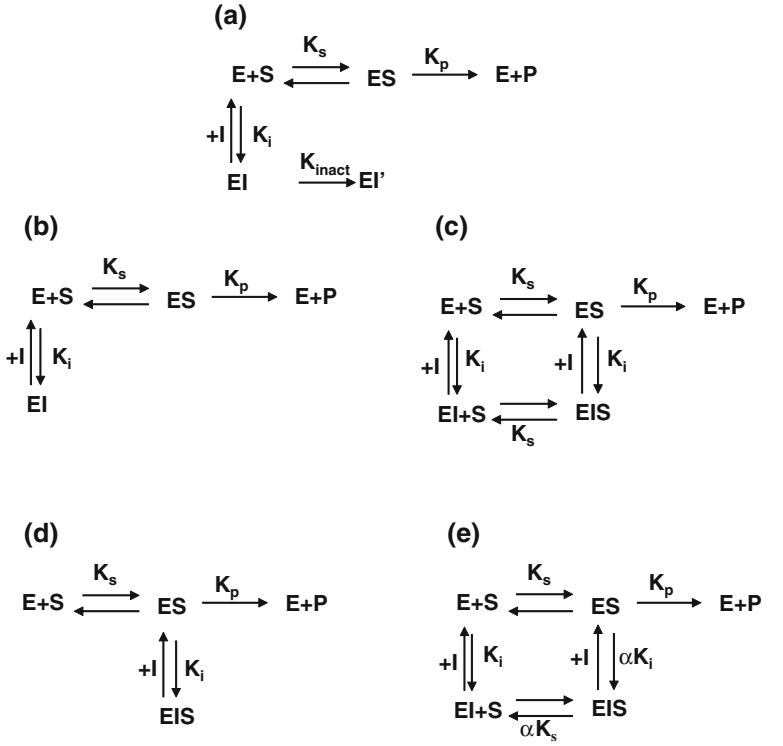

Fig. 4 **a** Scheme of enzyme inhibition in the case of irreversible inhibition, and **b** reversible inhibition competitive, **c** noncompetitive, **d** uncompetitive, and **e** mixed type inhibition

Table 1 Relations between I_{50} and K_i for pure inhibition and for different ratios of $[S]/K_m$

	Competitive inhibition	Noncompetitive inhibition	Uncompetitive inhibition	Mixed inhibition
I_{50}	$(K_m + [S])$ K_i/K_m	K_i	$(K_m + [S])$ $K_i/[S]$	$(K_m + [S])\alpha K_i/$ $(\alpha Km + [S])$
I_{50}/K_i	$1 + ([S]/K_m)$	1	$1 + (K_m/[S])$	$\alpha\ (1 + ([S]/K_m))/$ $(\alpha + ([S]/K_m))$
I_{50}/K_i when $[S]/K_m = 0.1$ and $\alpha = 2$	1.1	1	11	1.05
I_{50}/K_i when $[S]/K_m = 1$ and $\alpha = 2$	2	1	2	1.33
I_{50}/K_i when $[S]/K_m = 10$ and $\alpha = 2$	11	1	1.1	1.83

particularly when $[S] < K_m$. Slight variation of the ratio I_{50}/K_i was obtained in all ranges of substrate concentration studied under mixed inhibition. The I_{50} and I_{50}/K_i equations are obtained and rearranged from general equations of pure inhibition reported in the literature [18].

3 Parameters Affecting the Analytical Performance of Reversible and Irreversible Inhibition Biosensors

The goal of this section is to give useful suggestions for easily developing a biosensor based on enzyme inhibition to the researcher starting to work in this field. The parameters that can affect the sensitivity of an enzyme inhibition-based biosensor can be summarized as follows.

- *Measurement protocol:* The measurement can be carried out applying several protocols.
- *Immobilization:* How the enzyme is immobilized on the sensor.
- *Enzyme loading:* Amount of enzyme immobilized.
- *Incubation time:* Time of contact between enzyme and only inhibitor.
- *Substrate concentration*: Concentration of substrate used to monitor enzymatic activity.

In this section we described how these parameters affect the analytical performances of the biosensor and how to choose the best conditions in order to obtain a sensitive measurement.

3.1 Measurement Protocol

In the case of *reversible* inhibition, the most used approach is based on the measurement of initial enzymatic activity by adding the substrate to the working solution in which the biosensor is immersed (first protocol). Subsequently, the biosensor reaction reaches the steady state and the initial enzyme activity is evaluated (A_0). Next, the inhibitor is added to the same working solution. The addition of inhibitor leads to a decrease of enzyme activity, and, in fact, the signal immediately decreases; after a certain time, the steady state is again reached and corresponds to the enzyme residual activity (A_i; Fig. 5a). Knowing the initial activity (A_0) and residual activity (A_i), it is then possible to calculate the degree of inhibition correlated to inhibitor concentration.

The second protocol is characterized by two different measurements (Fig. 3a). The first one is carried out in the absence of inhibitor (A_0), after which the working solution is replaced with a new working solution to which the inhibitor is then added. Subsequently, the substrate is added and the steady-state signal is recorded

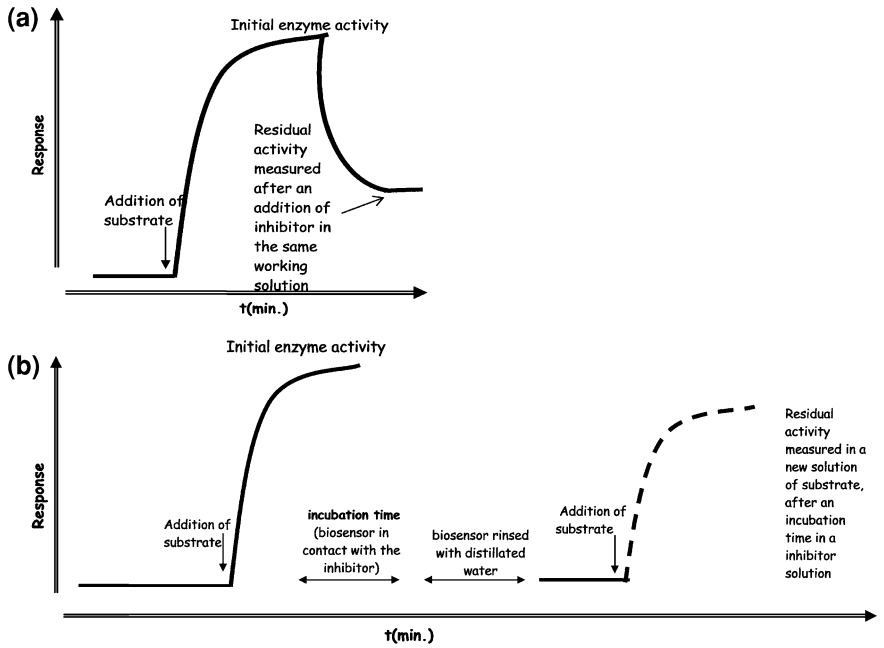

Fig. 5 Different protocols of inhibitor measurement using a biosensor based on enzyme inhibition

and corresponds to the residual activity (A_i). In this case the incubation step is absent. In the case of irreversible inhibitor, the first and second protocols are usually not recommended because they are characterized by a high detection limit. The protocols usually used for the detection of an irreversible inhibitor are the third and fourth protocols. In the third protocol (Fig. 3a), the biosensor is immersed in a buffer solution; the substrate is then added and the signal registered. The biosensor is then immersed in the inhibitor solution for a certain period (incubation time) and afterward, in the same inhibitor solution, the substrate is added and the residual activity measured, registering the signal. The fourth one (also called the "medium exchange method;" Fig. 5b) is performed as follows: the biosensor is immersed in a buffer solution, the substrate is then added, and the signal registered. Afterwards, the biosensor is immersed in the inhibitor solution for a certain period (incubation time). Next, the biosensor is rinsed several times with distillate water. The biosensor is then immersed in a new buffer solution and the substrate added, and the residual activity measured.

In the case of reversible inhibition the first protocol is usually suggested because it is faster and can be carried out in the same step. In the case of irreversible inhibition the fourth protocol is suggested because it allows reaching lower detection limits than the ones obtained using the first and second protocols, and, with respect to the third protocol, it allows avoiding (1) electrochemical and (2) enzymatic interferences. The electrochemical interferences, which can be

present in the real sample tested, are eliminated because the residual enzymatic activity is measured in a new substrate buffered solution in the absence of a real sample. Enzymatic interferences such as reversible inhibitors [19] as well as detergents [20, 21] are avoided because, after the incubation step, the biosensor is washed with distilled water and in this way, only the inhibitor covalently linked to the enzyme is measured. The need for adopting a "medium exchange method" has been demonstrated in the literature as effective for pesticide measurements using a cholinesterase biosensor enzyme, for example [22]. In detail, using the medium exchange method in the presence of 200 ppb of sodium dodecyl sulfate (SDS, limit value for wastewater), no inhibition was observed, whereas following the third protocol, an inhibition of 88 % was observed. With this procedure, the enzyme acts as a high-affinity capture agent for the pesticide, and, because of the irreversibility of the inhibition, the successive enzymatic reaction can be carried out in a fresh buffer solution, thereby circumventing the effect of reversible inhibitors of cholinesterase present in real samples.

However, there is an exception: in the case of irreversible inhibitor nerve agent detection using a cholinesterase biosensor, rapid measurement is an important issue, thus the first protocol can be used to reach this requirement taking into consideration that, even if this protocol is characterized by lower sensitivity, the nerve agents are very strong inhibitors [23]. Recently the same approach was reported by Alonso et al. in whose paper the slope of the biosensor response measurement in the presence of inhibitor is reported, coupled with an artificial neural network and arrays of biosensors with acetylcholinesterase from *Drosophila melanogaster* wildtype and genetically for a rapid determination of a pesticide mixture [24].

3.2 Immobilization

Immobilization is a key step to obtaining a robust and sensitive biosensor. There are several methods for immobilizing the enzyme, such as physical adsorption, cross-linking method, and self-assembled monolayer (SAM) formation. Physical immobilization such as adsorption is one of the simplest procedures to immobilize the biocomponent onto the transducer [25]. Acetylcholinesterase (AChE) was immobilized by adsorption on screen-printed electrodes modified with multiwall carbon nanotubes (MWCNTs): some μL of AChE solution were dropped on the MWCNT modified electrode surface and allowed to dry at room temperature under a current of air. The electrode was then rinsed twice with buffer to remove the loosely adsorbed enzyme molecules [26]. In order to avoid enzyme leakage during the measurement, a Nafion membrane can also be added [27]. An interesting approach was also the one based on the layer-by-layer electrostatic self-assembly of AChE on MWCNTs modified glassy carbon electrodes [28]. The CNTs were initially NaOH treated in order to assume a negative charge and then dipped into a solution of cationic poly(diallyldimethylammonium chloride) (PDDA), which

leads to the adsorption of a positively charged polycation layer (CNT–PDDA). Afterward, the negatively charged AChE was adsorbed on CNT–PDDA to obtain CNT–PDDA–AChE. Finally, in order to avoid the leakage of AChE from the electrode surface, another PDDA layer was absorbed, resulting in a sandwich structure of PDDA/AChE/PDDA. This system allows a low detection limit for paraoxon (4×10^{-13} M).

One of the most common methods of enzyme immobilization is chemical immobilization by means of cross-linking with glutaraldeyde. This method confers high working stability to the biosensor even if it usually causes a decrease of the enzymatic affinity towards its substrate. This behavior is due to the distortion of the enzyme structure with a consequent $K_{M\text{app}}$ higher than K_M obtained for ChE in solution [22, 29]. A valuable approach to immobilize the enzyme is the use of layered double hydroxides, a layered structure built on a stacking of positive layers ($[M^{II}_{1-x}\ M^{III}_{x}(OH)^2]^{x+}$). Their intercalation properties were used for an easy and biocompatible immobilization of enzyme molecules; however, in order to strengthen the resulting inorganic biocoating, glutaraldehyde can be added inducing a partial covalent binding between adjacent enzyme molecules. This approach was used, for example, to assemble a xanthine oxidase biosensor and to investigate the inhibitory effect by allopurinol [30].

The SAM can be an alternative method to immobilize the enzyme close to the electrode surface with a high degree of control over the molecular architecture of the recognition interface. An example can be the biosensor based on AChE enzyme immobilization via glutaraldehyde on a preformed cysteamine (SAM) on gold-screen printed electrodes (Au–SPEs). This method allows the detection of 2 ppb of paraoxon pesticide [31]. Another approach can be step-by-step self-assembly, such as in the case of horseradish peroxidase incorporated into a laponite/chitosan modified glassy carbon electrode for sulfite detection [32]. The enzyme can also be immobilized by means of a polymerization reaction such as the case of peroxidase immobilized on a screen-printed electrode in which acrylamide was used as monomer and the polymerization reaction was initiated by adding $K_2S_2O_8$ [33].

Recently an alternative way to realize a biosensor is enzyme immobilization on magnetic beads. The measurement was performed by the retention of the enzyme-functionalized magnetic beads onto a magnetized electrode. An example reported in the literature is the case of tyrosinase immobilized onto glutaraldehyde-activated streptavidine magnetic particles with a carbon paste electrode for the evaluation of the inhibitory potency of the most frequently used active substances in a cosmetic product [34].

How does the immobilization type affect the kinetic inhibition? In the case of irreversible inhibition, the different types of immobilization used can change the $K_{M\text{app}}$ or the sensitivity towards the inhibitor. In the case of a reversible inhibitor, the immobilization can change the sensitivity such as in the case of an irreversible inhibitor; moreover, the immobilization can also change the type of inhibition as in the case of the inhibition of the polyphenol oxidase [35] immobilized in conducting polymer matrices. The immobilized enzyme modifies the inhibition type

when compared with the free enzyme in the case of cinnamic and sorbic acid, and also changes the inhibition constant (affinity of the inhibitor for the enzyme) as a function of the characteristics of the polymeric films. A clear example about the sensitivity change in the enzyme immobilization function was reported in the research work carried out by Vidal et al. [36], in which the different analytical performances using different immobilization types are reported in Table 1 of the paper for dichlorvos detection using tyrosinase as the enzyme. This means that although the type of inhibition in solution is well known, it is better to restudy the type of inhibition when using a biosensor, in order to know the type of inhibition exactly and easily optimize the parameters for obtaining a sensitive biosensor.

3.3 Effect of Incubation Time

The *incubation time* is the reaction time between the enzyme and the inhibitor. For irreversible inhibition, it is possible to achieve lower detection limits using longer incubation times; in fact, the degree of enzyme inhibition increases with the incubation time [37] until reaching a plateau [38]. The incubation time is usually chosen as a compromise between a sensitive measurement and a measurement carried out in a reasonable time. In the case of reversible inhibition, the degree of inhibition is theoretically independent of the incubation time, which means that the analysis time can be very short because no incubation time is required. The term "theoretically" is required because in the case of an enzyme free in solution, this behavior is always confirmed, whereas in the case of an enzyme immobilized on a sensor, such behavior is not always observed. An example could be the dependence on incubation time reported by Cosnier et al. [39] in the case of As(V) detection through the reversible inhibition of acid phosphatase and polyphenol oxidase entrapped in anionic clays. In this case the use of incubation time was useful to increase the sensitivity only due to specific electrostatic interactions between the positively charged layers of the clay and the As(V) anion that allows a preconcentration fo As(V) in the clay.

3.4 Effect of Enzyme Loading

Enzyme loading is another critical factor to be evaluated. In the case of reversible inhibition using enzyme free in solution, the enzyme concentration does not affect the degree of inhibition if the enzyme concentration is lower than the concentration of the inhibitor. Instead, for irreversible inhibition, the degree of inhibition depends on the enzyme concentration. Specifically, the enzyme concentration should be chosen taking into consideration that (1) the amount of enzyme immobilized should give a measurable signal and (2) the lowest amount of enzyme is necessary to achieve the lowest detection limit. In this view, it is very useful to

have a highly sensitive enzymatic product detection and an enzyme immobilization that does not decrease enzymatic activity. In this approach, the use of nanomaterial can be an added value. In fact, using sensors modified with nanomaterials such as carbon nanotubes, carbon black, and gold nanoparticles [40–43] it is possible to reach a lower detection limit for the enzymatic product, because of the promoted electron transfer reaction catalyzed by the nanomaterials. The high sensitivity for the enzymatic product allows the use of a lower amount of enzyme and consequently in the case of irreversible inhibition, better sensitivity of the biosensor. In the case of reversible inhibition, the amount of enzyme should not affect the degree of inhibition; however, for an immobilized enzyme, this behavior is not so strictly respected, such as in the case of a tyrosinase biosensor reported by Shan et al. [44]. In this case the authors studied a set of five membranes with different amounts of enzyme loading, observing an increase of sensitivity up to 30 μg of tyrosinase loading, and then a gradual decrease due to the film thickness effect [44].

3.5 *Effect of Substrate Concentration*

In the case of irreversible inhibition, a high substrate concentration can be selected in order to obtain a higher output signal; usually the minimum substrate concentration to have the maximum reaction rate is chosen [22]. In the case of reversible inhibition, the choice of substrate amount is not so predictable. For reversible competitive inhibition, the best analytical performance can be obtained using (1) substrate at a concentration lower than that of inhibitor or (2) using a substrate with low affinity for the enzyme. In the first case, as demonstrated by Benilova et al., the degree of inhibition decreases at a high concentration of substrate for butyrylcholinesterase inhibited by α-chaconine [45], whereas in the second case, analytical performance can be improved by choosing the best substrate as demonstrated by Shan et al. [44]. In their study, the inhibition of tyrosinase by benzoic acid was investigated as a function of five different phenolic compounds as substrate (catechol, p-cresol, m-cresol, phenol, and p-chlorophenol). It was found that the highest degree of inhibition was obtained using catechol as the substrate, which showed the highest value of K_M among the five phenolic compounds tested, corresponding to a lower affinity of the enzyme for this substrate.

3.6 *Biosensor Stability*

As reported by Gibson [46], "One of the main problems of many biosensors is their intrinsic stability…. However, the majority of enzymes used in biosensors are labile and require stabilization to produce viable devices." This means that in order to develop a successful biosensor, it is important to reach low detection

limits but it is also true that the biosensor should be characterized by a satisfactory working and shelf stability where (1) the working stability may be defined as the retention of activity of an enzyme when the biosensor is in use and (2) shelf stability is defined as the enhancement or improvement of activity retention of an enzyme when stored under specified conditions after manufacture [46]. The problem of low shelf stability at room temperature in dry conditions is probably the reason for the gap between academic research and the biosensor presence in the market. This is a relevant problem; in fact, the reduction of the gap between the real market and on-going research is one of the policy priorities of the Horizon 2020 strategy. In this context, for example, we have performed a study to develop a biosensor for organophosphate detection characterized by high working and storage stability [47]. In this study we have investigated several immobilization types also with stabilizers using both AChE and BChE. Briefly, for the construction of AChE or BChE biosensors we have used three approaches: in the first approach, the enzyme was adsorbed onto the working electrode surface, storage at 4 °C overnight, and after that some μL of several stabilizers were added to the working electrode surface. The biosensors were tested when the working electrodes of biosensors were completely dry.

An another approach a similar protocol to the aforementioned was adopted but followed by a final step of Nafion® coverage by simple addition of some μL of Nafion on the working electrode surface and waiting to be dry. The last approach was made using the cross-linking method by means of glutaraldehyde, Nafion, and bovine serum albumin (BSA). In the case of AChE the best result in terms of shelf stability was obtained in the case of AChE immobilized by gelatin, retaining its activity up to 5 months when maintained at RT in dry conditions; however, we observed the possibility of using this biosensor no more than five times because after that, there is a probable solubilization of the membrane. In the case of BChE, the best shelf life stability was obtained using the biosensor constructed immobilizing the BChE by means of glutaraldeyde, Nafion, and BSA. This type of BChE biosensor demonstrated a shelf stability of at least 6 months and a working stability of 10 h, confirming that this biosensor is characterized by high working and storage stability; for this reason this biosensor was chosen to be assembled to a prototype for nerve agent detection for future commercialization [48]. However, in the case of inhibitor measurement the working stability can also be affected by the change of pH, temperature, and matrix composition [49]. In the case of a decrease of enzymatic activity due to the change of these parameters, the degree of inhibition is overestimated, and thus is very important during enzyme inhibition to evaluate the matrix effect in order to avoid false-positive results. In addition, in the case of irreversible inhibition, the enzyme can't recover its original activity and thus only few experiments are carried out with the enzyme. The addition of activator can allow 60–90 % of the initial activity [50–52], but after a few generations the enzyme is totally inhibited. That is why it is recommended to adopt a procedure for the single use of an enzymatic biosensor using, for example, a disposable biosensor [22, 29, 31].

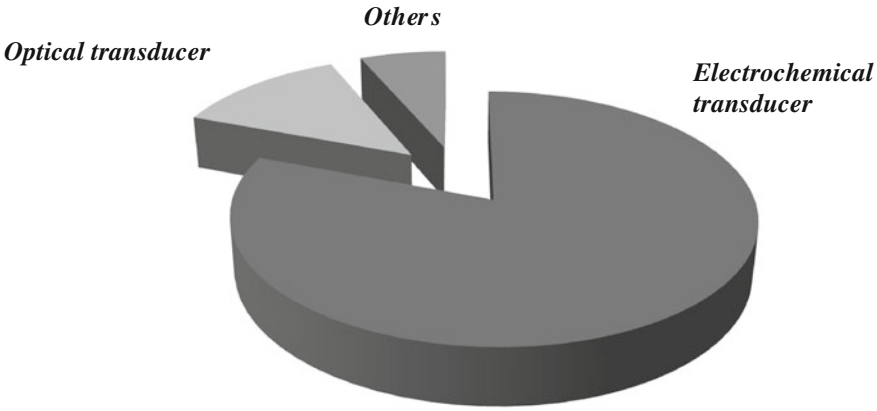

Fig. 6 Distribution of transducers used to construct biosensors based on enzyme inhibition (period 2006–2012)

3.7 Transducer

The choice of transducer is also important in order to have a sensitive, robust, and cost-effective system. As reported in Fig. 6, the most used type of transducer is the electrochemical one (81 % of the biosensors based on enzyme inhibition reported in the literature are electrochemical biosensors) for several reasons, because it is robust, cost-effective, fast, miniaturizable, and used also in the case of colored solutions. In addition, the possibility of using screen-printed electrodes renders this kind of sensor suitable for an easy, fast, and cost-effective measurement for each type of inhibitor both reversible and irreversible, avoiding reactivation in the latter case.

3.8 Electrochemical Transduction

In our first review we discussed the transducer for a cholinesterase biosensor and we divided the electrochemical biosensors into bienzymatic and monoenzymatic ones; on the contrary, in the 2006–2012 period we found only two systems based on the bienzymatic approach, confirming that the monoenzymatic system is the preferable one [53, 54]. As reported in the literature [13], it is possible to obtain a monoenzymatic biosensor employing both a potentiometric or conductimetric transducer, using the natural substrate acetylcholine with acetylcholinesterase. However, in the case of a cholinesterase amperometric monoenzymatic biosensor, the nonnatural acetylcholinesterase substrate acetylthiocholine should be used,

because it generates an electroactive product. Moreover, in order to reduce the applied potential and the electrochemical interferences, thiocholine detection can be measured using redox mediators such as cobalt phthalocyanine (CoPc) [55], Prussian Blue [56], tetracyanoquinodimethane (TCNQ) [57], cobalthexacyanoferrate [58], potassium ferricyanide [59], or nanomaterial [26, 43, 60] such as carbon nanotubes, carbon black, or also nanomaterial (carbon nanotubes) coupled with redox mediator (CoPc), as we have recently demonstrated [61].

Conductimetric biosensors such as in the case of peroxidase biosensors for cyanide detection [62] or square wave voltammetric biosensors such as in the case of peroxidase biosensors for glyphosate [63] are also present in the literature. However, amperometric detection is the most common, due to its high sensitivity coupled with the possibility to miniaturize the system in an easy way, as we have demonstrated in the case of the prototype for nerve agent detection based on a butyrylcholinesterase amperometric biosensor [48].

3.9 Optical Transduction

Optical transducers were also utilized in the case of a biosensor based on enzyme inhibition. A colorimetric method was developed by Pohanka et al. for nerve agent and organophosphate pesticide detection. The principle of the assay is based on the enzymatic hydrolysis of acetylcholine into acetic acid and choline by acetylcholinesterase. Acidification of the reaction medium due to accumulation of acetic acid was visible using a pH indicator strip. The achieved limit of detection was 5×10^{-8} M for paraoxon-ethyl and 5×10^{-9} M for sarin and VX [64].

A biosensor composed of nanostructured multilayers of the enzyme AChE and photoluminescent CdTe QDs was reported in the literature for organophosphate detection [65]. The decrease of enzymatic activity in the presence of organophosphate leads to the decrease of thiocholine production and then the photoluminescent quenching rate of QDs. By measuring the quenching rate before and after an incubation step with the pesticide, one can calculate the concentration of organophosphate with a very low detection limit, 2.89 ppt.

An interesting approach was reported by Li et al. although the format is a bioassay and not a biosensor because the enzyme is used in solution. The system is based on acetylcholinesterase inhibition by an organophosphate compound, and citrate-coated Au nanoparticles were used with a colorimetric probe. The catalytic hydrolysis of acetylthiocholine into thiocholine by acetylcholinesterase induces the aggregation of Au nanoparticles and the color change from claret-red to purple or even grey; in the presence of pesticides the aggregation and the relative color change is absent, whereas in the absence of pesticides there is an AuNP aggregation. The linear range value found was from 0.02 to 1.42 ppm [65].

3.10 Surface Plasmon Resonance (SPR) Biosensor

Recently, cholinesterase biosensors using a SPR were reported in the literature. The acetylcholinesterase was immobilized on a SPR biosensor chip surface and in the presence of pesticides, a changing of intensity of SPR angles was observed [66, 67]. The SPR biosensor was also developed in the case of AFB_1 detection obtaining higher sensitivity when compared with the one obtained using an amperometric biosensor [68].

3.11 Piezoelectric Transduction

The insecticide inhibitors can also be measured by means of piezoelectric biosensors [69, 70]. The detection of organophosphate and carbamate was carried out measuring the precipitation of an enzymatic reaction product over a quartz crystal microbalance (QCM) [71].

3.11.1 Analytes

Pesticides

The detection of pesticide residues in food, water, and soil is one of the major issues of analytical chemistry. Pesticides are, in fact, among the most important environmental pollutants because of their increasing use in agriculture. Among the several pesticides used, organophosphorus and carbammic insecticides are often used due to their high toxicity coupled with low persistency in the environment. This type of insecticide has the power to inhibit the cholinesterase enzyme in an irreversible way, thus they can be detected by means of a cholinesterase biosensor. The amperometric monoenzymatic biosensor based on acetyl or butyrilcholinesterase was principally applied in water samples (drinking water, river water, and wastewater) with good recovery values [22, 31, 61]. An adopted procedure and the typical response for pesticide (paraoxon) detection using a butyrilcholinesterase biosensor based on screen-printed electrode modified with Prussian Blue are shown in Fig. 7a, b, respectively, using the portable instrumentation shown in Fig. 7c. The electrochemical bienzymatic AChE–ChOx was used to detect coumaphos in honey samples [52].

The cholinesterase biosensor was also applied to detect organophosphorus and carbammic insecticides in fruit, vegetables, and dairy products as reported in the literature before 2006 [72]. An interesting application published in 2008 reported the detection of insectides in tomato without any previous manipulation of the sample; in fact, the amperometric biosensor was immersed directly in the tomato pulp during the incubation time, obtaining a recovery of 83.4 % for 50 μM

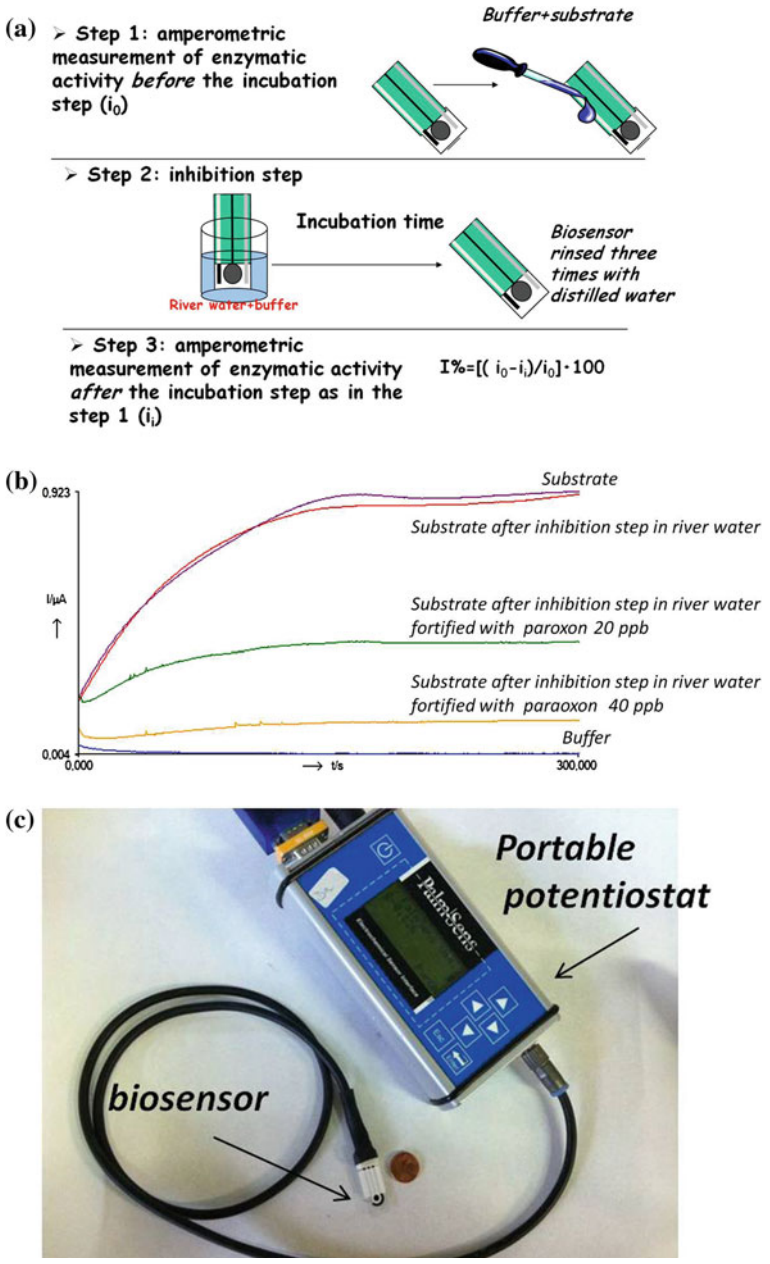

Fig. 7 **a** Procedure used to detect pesticides using the "medium exchange method;" **b** amperograms obtained using the following conditions: applied potential + 0.2 V versus Ag/AgCl, phosphate buffer 0.05 M + KCl 0.1 M, pH 7.4 using BChE biosensor based on Prussian Blue modified screen-printed electrode; and **c** the portable instrumentation used (unpublished data)

carbaryl and showing very low interference from the matrix components [73]. The results reported showed the real possibility to detect organophosphorous and carbamic insecticides using an AChE biosensor in real samples. In the case of organothiophosphate, it is important to stress that these insecticides usually were electrochemically oxidized before the analysis because the oxidized form is able to inhibit the enzyme more strongly [74]. This means that organothiophosphate insecticides themselves are weak inhibitors of ChE: in fact, only their oxo-form is highly toxic. However, in the literature sometimes low detection limits using organothiophosphate are shown, and this could be ascribed to (1) a possible mistake using parathion spontaneously oxidated to paraoxon, (2) the use of organothiophosphate coupled with chemical or electrochemical oxidation in order to have organophosphate–oxo, or (3) the use of a very sensitive biosensor.

Another approach to detect pesticides is the use of tyrosinase, laccase, or peroxidase enzyme. The herbicide glyphosate [N-(phosphonometyl)glycine] was detected using a biosensor with atemoya peroxidase [63]. Carbamate methomyl was measured using a biosensor based on laccase obtained from a genetically modified fungus (*Aspergillus oryzae*) immobilized in a new supported ionic liquid phase formed by platinum nanoparticles/1-butyl-3-methylimidazolium tetrafluoroborate ionic liquid/montmorillonite [75]. A tyrosinase biosensor was used to detect the herbicides atrazine and diuron with a conductimetric biosensor [76]; the insecticide dichlorvos was detected by means of a chronocoulometric biosensor [77]. In the case of tyrosinase, the inhibition is of reversible type with the advantage of using the same biosensor for several measurements, but without the possibility of (1) the use of the medium exchange method in order to avoid electrochemical interferences, and (2) to increase the sensitivity increasing the incubation time.

Heavy Metals

For heavy metal detection, several enzymes can be used such as alkaline phosphatase, glucose oxidase, and acetylcholinesterase. However, in the period 2006–2012, an interesting system for Hg^{2+} was presented by Cosnier et al. [39] using an amperometric bienzymatic system based on the competitive activities of glucose oxidase and laccase [78]. The As^{3+} was detected using acetylcholinesterase immobilized on screen-printed electrodes. As reported by the authors, the As^{3+} is a powerful inhibitor, more so than other metal ions such as mercury, nickel, and copper. The biosensor was challenged in spiked tapwater samples with good recovery values [79]. The same authors instead used acid phosphatase immobilized on screen-printed electrodes for As^{5+} detection at the μM level [80]. The amperometric biosensor based on glucose oxidase for the detection of metallic cations, cadmium, copper, lead, and zinc was developed by Ghica and Brett [81] or coupled with a flow-injection system by Guascito et al. for heavy metal ion (Hg^{2+}, Ag^{+}, Cu^{2+}, Cd^{2+}, Co^{2+}, Ni^{2+}) measurements [82].

Toxins

Okadaic acid is a toxin that accumulates in bivalves; this toxin can be detected by means of a biosensor based on protein phosphatase-2A (PP2A) due to the ability of okadaic acid to inhibit this enzyme [83]. The same enzyme was also used to realize a biosensor for microcystin detection, applied to detect this cyanobacterial toxin with a 50 % inhibition coefficient (IC50) of 83 ppb and a limit of detection (LOD; 35 % inhibition) of 37 ppb. Real samples of cyanobacterial blooms from the Tarn River (France) have been analyzed using the developed amperometric biosensor and the toxin contents have been compared to those obtained by a conventional colorimetric protein phosphatase inhibition assay and high-performance liquid chromatography (HPLC). The authors found higher values of R.S.D. (35 %) in the case of the biosensor due to the less steep slope of the curve (which induces a higher uncertainty on the concentration values) coupled with reproducibility problems associated with the electrode construction and with fouling phenomena [84].

Recently we have demonstrated the possibility of detecting the toxin AFB_1 by means of acetylcholinesterase [85]. Prior to developing a biosensor, a bioassay using a choline oxidase biosensor was applied to detect AFB_1 in olive oil obtaining recovery values higher than 75 % [86]. In the case of a biosensor in which the enzyme was immobilized, a higher detection limit was found. For example, Hansmann et al. developed an AChE biosensor depositing 3 μL of a 1:1 mixture of polyvinylalcohol and enzyme on cobalt–phthalocyanine-modified screen-printed electrode and polymerized the mixture under neon light at 4 °C for 3 h. This sensor allows the detection of a minimum concentration of 3 μM of AFB_1 corresponding to 1 ppm [87]. We have developed an amperometric biosensor for detecting AFB_1 at ppb levels using AChE immobilized on Prussian Blue-modified screen-printed electrodes by means of physical immobilization. The AChE immobilized in a gelatin layer allows obtaining a LOD of 100 ppb. Pohanka et al. have developed a biosensor immobilizing the enzyme with a gelatin layer, obtaining IC_{50} = 100 ppb [88]. Recently Puiu et al. have immobilized AChE via its primary amine groups (lysine residues) through 1-ethyl-3-(3-dimethylaminopropyl carbodiimide) hydrochloride and N-hydroxysuccinimide on the (SAM) functionalized surface of the surface plasmon resonance chip. The LOD was 0.94 ppb for AFB_1 which is lower than the ones previously reported [68].

Drugs and Clinical Application

In the case of drugs, the application of a biosensor is rather limited to academic research because, at this time, for quality measurement the US Food and Drug Administration requires highly selective methods. However, this does not mean that in the future the US Food and Drug Administration could not also accept the biosensor as a screening method in the pharmaceutical industry.

In order to detect amaryl and acorbose, which are therapeutic drugs that prevent high blood glucose levels, α-glucosidase enzyme was immobilized on bismuth-

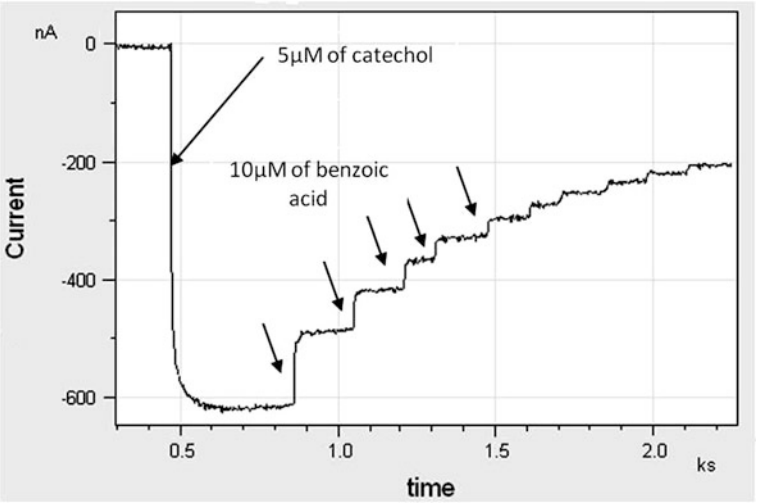

Fig. 8 A typical amperogram in the case of benzoic acid measurement using a tyrosinase biosensor. Enzyme tyrosinase cross-linked with glutaraldehyde and deposited on a carbon paste electrode. Applied potential is −0.15 V versus Ag/AgCl, phosphate buffer pH 7.0. After stabilization of the catechol signal, successive additions of benzoic acid were added (unpublished data)

modified glassy carbon electrodes, obtaining a linear range of 0.002–0.24 mg/mL and 0.0008–0.0066 mg/mL for amaryl and acorbose, respectively [89]. Allopurinol is used to treat hyperuricemia and it was measured by means of an amperometric xanthine oxidase biosensor [30]. Glutathione is detected by means of an amperometric biosensor based on pyranose oxidase inhibition [90]. Several thiols such as glutathione, N-acetylcysteine, and cysteine were detected using amperometric biosensors based on peroxidase inhibition [91, 92].

Others

The chemical warfare nerve agent can be detected by means of a cholinesterase biosensor. Our group developed a butyrylcholinesterase biosensor immobilizing the enzyme on screen-printed electrodes modified with Prussian Blue. The system was challenged towards two different concentrations of Sarin gas (0.1 mg/m^3 and 0.5 mg/m^3) at different incubation times (from 30 s up to 10 min) demonstrating that it is possible to detect the Sarin at a concentration of 0.1 mg/m^3 with only 30 s of incubation time [29]. A butyrylcholinesterase biosensor was also integrated into a miniaturized prototype composed of the cell in which the biosensor is inserted, a little fan for sampling the air, and an electronic circuit. The circuit was able to

Table 2 Practical considerations of biosensors based on reversible and irreversible inhibition

	Reversible inhibition	Irreversible inhibition
Enzyme loading	Medium	Very low
Time of incubation of enzyme with inhibitor	No incubation is required	10–60 min
Method of enzyme immobilization	Immobilization does not change the inhibition type	Covalent attachment or adsorption methods involving low amount of enzyme/gr or/cm^2
Concentration required of substrate	Low concentration if the inhibition is competitive	Minimum concentration to have the maximum enzymatic reaction rate ($\approx$2 km)
Total time of analysis	Short	Long
Batch analysis	Yes	Yes
Flow injection analysis	Yes	No
Regeneration	Yes with water or buffer	No unless specific reagent (reactivator) is used for few regenerations
Frequency of analysis per hour	High	Low
Limit of detection	Very low if K_i is very low	Very low
Matrix effect	Exposed to interfering species of the matrix	Less sensitive to matrix effect using the "medium exchange method" (see Fig. 5b)

apply the potential, to register the current, to turn the fan on and off, and eventually give an alarm [47].The acetylcholinesterase electrochemical biosensor was also developed to measure Tabun, Sarin, Soman, Cyclosarin, and VX in solution [93].

Cyanide is a substance commonly used worldwide in industrial applications often resulting in contamination of groundwater. Biosensors prepared through immobilization of bovine liver catalase in a photoreticulated poly(vinyl alcohol) membrane on the surface of a conductimetric transducer was reported in the literature. The biosensor allows cyanide detection with LOD of 6 μM [94].

Fluoride is a reversible inhibitor of tyrosinase, thus it can be detected by means of an amperometric tyrosinase biosensor as reported by Asav et al. reaching a linear range from 1.0 to 20 μM [95].

Sulfide is able to inhibit peroxidase and thus, a biosensor using horseradish peroxidase has been developed characterized by a detection limit of 5 μM [32], whereas using a biosensor based on *Coprinus cinereus* peroxidase, a detection limit of 0.3 μM was found [96].

Benzoic acid is extensively used as a preservative in food, beverages, mouthwashes, cosmetics, and pharmaceuticals. Amperometric tyrosinase-based biosensors for benzoic acid determination with the use of a flow-batch monosegmented sequential injection system were reported in the literature with the detection limit of 0.03 μM [97]. Highly sensitive biosensors based on the immobilization of tyrosinase by calcium carbonate nanomaterials were applied from the determination of

benzoic acid in real beverage samples [46]. A typical amperogram of benzoic acid measurement using a tyrosinase biosensor is shown in Fig. 8. The tyrosinase biosensor for evaluation of the inhibitory potency of the most frequently used active substances in marketed cosmetic products against hyperpigmentation such as kojic acid, azelaic acid, and benzoic acid was also reported in the literature [34].

4 Conclusion

Biosensors based on enzyme inhibition can be applied to monitoring several analytes with the advantage of being a cost-effective, easy to use, and miniaturized analytical tool. The knowledge of the enzymatic kinetic (knowing if the inhibition is an irreversible or reversible inhibition type) can help the researcher reach the optimized procedure in a faster and easier way, as schematized in Table 2 in respect to the optimization obtained by changing one variable at time. Wide application in the environmental, food, and pharmaceutical fields demonstrates the suitability of this tool also with real samples.

We also highlight that in the case of organophosphate detection, low detection limits using organothiophosphate could be ascribed to a possible mistake using parathion spontaneously oxidated to paraoxon, thus the presence of the oxo-form in the standard solution used should be checked.

In this overall scenario, it is important to highlight the low selectivity to the biosensor based on enzyme inhibition. This characteristic can be an advantage as in the case of the cholinesterase inhibition that can be considered a "family doctor," whereas in the presence of inhibition, a specialist doctor such as an HPLC instrument can be used with a decrease in terms of time analysis and cost. However, sometimes the selectivity of the biosensor can be improved by optimizing the procedure knowing the enzymatic kinetic [13] or also optimizing the sample treatment; thus it can be very useful during biosensor-based inhibition development to evaluate interferences or demonstrate selectivity using a sample fortified with several analytes, because very often in the papers based on enzyme inhibition reported in the literature the authors focused their attention on a single analyte detection instead of which the biosensor is able to detect a class of compounds instead of a single compound. In this direction, we propose using the biosensor based on enzyme inhibition as a first alarm system in order to give, even if not specific, a fast and cost-effective response.

Development of an array of enzyme electrodes for multianalyte detection and the use of the chemiometric method for interpretation of experimental data in the analysis of these mixtures of inhibitors may allow in the near future the conversion of biosensing systems to marketable devices suitable for large-scale applications.

References

1. Thévenot DR, Toth K, Durst RA, Wilson GS (2001) Electrochemical biosensors: recommended definitions and classification. Biosens Bioelectron 16(1–2):121–131
2. Luque De Castro MD, Herrera MC (2003) Enzyme inhibition-based biosensor and biosensing systems: questionable analytical devices. Biosens Bioelectron 18:279–294
3. Amine A, Mohammadi H, Bourais I, Palleschi G (2006) Enzyme inhibition-based biosensor for food safety and environmental monitoring. Biosens Bioelectron 21(8):1405–1423
4. Arduini F, Amine A, Moscone D, Palleschi G (2009) Reversible enzyme inhibition based biosensors: applications and analytical improvement through diagnostic inhibition. Anal Lett 42:1258–1293
5. Trojanowicz M, Trojanowicz M (2002) Determination of pesticides using electrochemical enzymatic. Biosens Electroanal 14(19-20):1311–1328
6. Turdean GL (2011) Design and development of biosensors for the detection of heavy metal toxicity. Int J Electrochem, Article ID 343125, p 15. doi:10.4061/2011/343125
7. Andreescu S, Marty JL (2006) Twenty years research in cholinesterase biosensors: from basic research to practical applications. Biomol Eng 23:1–15
8. Pohanka M, Jun D, Kalasz H, Kuca K (2009) Cholinesterase biosensor construction-A review. Protein Pept Lett 15:795–798
9. Pohanka M, Musilek K, Kuca K (2009) Progress of biosensors based on cholinesterases inhibition. Curr Med Chem 16:1790–1798
10. Pohanka M (2009) Cholinesterase based amperometric biosensors for assay of anticholinergic compounds. Interdisc Toxicol 2:52–54
11. Manco G, Nucci R, Febbraio F (2009) Use of esterase for the detection of chemical neurotoxic agents. Protein Pept Lett 16:1225–1243
12. Periasamy AP, Umasankar Y, Chen SM (2009) Nanomaterials acetylcholinesterase enzyme matrices for organophosphorus pesticides electrochemical sensors: a review. Sensors 9:4034–4055
13. Arduini F, Amine A, Moscone D, Palleschi G (2010) Biosensors based on cholinesterase inhibition for pesticides, nerve agents and aflatoxin B1 detection (review). Microchim Acta 170:193–214
14. Sun X, Zhai C, Wang X (2012) Recent advances in amperometric acetylcholinesterase biosensor. Sens Transducers J 137:199
15. Lineawever H, Burk D (1934) The determination of enzyme dissociation constants. J Am Chem Soc 6:658–666
16. Dixon M (1953) The determination of the enzyme inhibitor constants. Biochem J 55:170–171
17. Cornish-Bowden A (1974) A simple graphical method for determining the inhibition constants of mixed, uncompetitive and non-competitive inhibitors. Biochem. J 137:143–144
18. Segel IH (1975) Enzyme kinetics. Wiley-Interscience, New York
19. Evtugyn GA, Ivanov AN, Gogol EV, Marty JL, Budnikov HC (1999) Amperometric flow-through biosensor for the determination of cholinesterase inhibitors. Anal Chim Acta 385:13–21
20. Jaganathan L, Boopathy R (2000) Distinct effect of benzalkonium chloride on the esterase and aryl acylamidase activities of butyrylcholinesterase. Bioorg Chem 28:242–251
21. Kucherenko IS, Soldatkin OO, Arkhypova VM, Dzyadevych SV, Soldatkin AP (2012) A novel biosensor method for surfactant determination based on acetylcholinesterase inhibition. Meas Sci Technol 23:065801
22. Arduini F, Ricci F, Tuta CS, Moscone D, Amine A, Palleschi G (2006) Detection of carbammic and organophosphorus pesticides in water samples using cholinesterase biosensor based on Prussian Blue modified screen printed electrode. Anal Chim Acta 580:155–162
23. Pohanka M, Jun D, Kuca K (2008) Amperometric biosensors for real time assays of organophosphate. Sensors 8:5303–5312

24. Alonso GA, Istamboulie G, Noguer T, Marty JL, Munoz R (2012) Rapid determination of pesticide mixtures using disposable biosensors based on genetically modified enzymes and artificial neural networks. Sens Actuators B 164:22–28
25. Bonnet C, Andreescu S, Marty JL (2003) Adsorption: an easy and efficient immobilisation of acetylcholinesterase on screen-printed electrodes. Anal Chim Acta 481:209–211
26. Joshi KA, Tang J, Haddon R, Wang J, Chen W, Mulchandani A (2005) A disposable biosensor for organophosphorus nerve agents based on carbon nanotubes modified thick film strip electrode. Electroanal 17:54–58
27. Scognamiglio V, Pezzotti I, Pezzotti G, Cano J, Manfredonia I, Buonasera K, Arduini F, Moscone D, Palleschi G, Giardi MT (2012) Towards an integrated biosensor array for simultaneous and rapid multi-analysis of endocrine disrupting chemicals. Anal Chim Acta 751:161–170
28. Liu G, Lin Y (2006) Biosensor based on self-assembling acetylcholinesterase on carbon nanotubes for flow injection/amperometric detection of organophosphate pesticides and nerve agents. Anal Chem 78:835–843
29. Arduini F, Ricci F, Amine A, Moscone D, Palleschi G (2007) Fast, sensitive and cost-effective detection of nerve agents in the gas phase using a portable instrument and an electrochemical biosensor. Anal Bioanal Chem 388:1049–1057
30. Shan D, Wanga Y, Zhua M, Xuea H, Cosnierb S, Wanga C (2009) Development of a high analytical performance-xanthine biosensor based olayered double hydroxides modified-electrode and investigation of the inhibitory effect by allopurinol. Biosens Bioelectron 24:1171–1176
31. Arduini F, Guidone S, Amine A, Palleschi G, Moscone D (2013) Acetylcholinesterase biosensor based on self-assembled monolayer-modified gold-screen printed electrodes for organophosphorus insecticide detection. Sens Actuators B 179:201−208
32. Shan D, Li QB, Ding SN, Xu JQ, Cosnier S, Xue HG (2010) Reagentless biosensor for hydrogen peroxide based on self-assembled films of horseradish peroxidase/laponite/chitosan and the primary investigation on the inhibitory effect by sulfide. Biosens Bioelectron 26:536–541
33. Savizi ISP, Kariminia HR, Ghadiri M, Roosta-Azad R (2010) Amperometric sulfide detection using Coprinus cinereus peroxidase immobilized on screen printed electrode in an enzyme inhibition based biosensor. Biosens Bioelectron 35:297–301
34. Harceaga Sima V, Patris S, Aydogmus Z, Sarakbi A, Sandulescu R, Kauffmann JM (2011) Tyrosinase immobilized magnetic nanobeads for the amperometric assay of enzyme inhibitors: application to the skin whitening agents. Talanta 83:980–987
35. Narh I, Kiralp S, Toppare L (2006) Preventing inhibition of tyrosinase with modified electrodes. Anal Chim Acta 572:25–31
36. Vidal JC, Esteban S, Gil J, Castillo JR (2006) A comparative study of immobilization methods of a tyrosinase enzyme on electrodes and their application to the detection of dichlorvos organophosphorus insecticide. Talanta 68:791–799
37. Zhang S, Zhao H, John R (2001) Development of a quantitative relationship between inhibition percentage and both incubation time and inhibitor concentration for inhibition biosensors-theoretical and practical consideration. Biosens Bioelectron 16:1119–1126
38. Kok FN, Hasirci V (2004) Determination of binary pesticides mixture by an acetylcholinesterase-choline oxidase biosensor. Biosens Bioelectron 19:661–665
39. Cosnier S, Mousty C, Cui X, Yang X, Dong S (2006) Specific determination of As(V) by an acid phosphatase−polyphenol oxidase biosensor. Anal Chem 78:4985–4989
40. Du D, Huang X, Cai J, Zhang A (2007) Amperometric detection of triazophos pesticide using acetylcholinesterase biosensor based on multiwall carbon nanotube–chitosan matrix. Sens Actuators B 127:531–535
41. Du D, Chena S, Cai J, Zhang A (2007) Immobilization of acetylcholinesterase on gold nanoparticles embedded in sol–gel film for amperometric detection of organophosphorous insecticide. Biosens Bioelectron 23:130–134

42. Liu G, Riechers SL, Maria Consuelo Mellen MC, Lin Y (2005) Sensitive electrochemical detection of enzymatically generated thiocholine at carbon nanotube modified glassy carbon electrode. Electrochem Comm 7:1163–1169
43. Arduini F, Majorani C, Amine A, Moscone D, Palleschi G (2011) Hg^{2+} detection by measuring thiol groups with a highly sensitive screen-printed electrode modified with a nanostructured carbon black film. Electrochim Acta 56:4209–4215
44. Shan D, Li Q, Huaiguo H, Cosnier S (2008) A highly reversible and sensitive tyrosinase inhibition based amperometric biosensor for benzoic acid monitoring. Sens Actuators B 134:1016–1021
45. Benilova IV, Arkhypova VN, Dzyadevych SV, Jaffrezic-Renault N, Martelet C, Soldtkin AP (2006) Kinetics of human and horse sera cholinesterass inhibition with solanaceous glycoalkaloids: Study by potentiometric biosensor. Pestic Biochem Physiol 86:203–210
46. Gibson TD (1999) Biosensors: the stability problem. Analusis 27:633–638
47. Arduini F, Palleschi G (2012) Disposable electrochemical biosensor based on cholinesterase inhibition with improved shelf-life and working stability for nerve agent detection. In: NATO science for peace and security series a: chemistry and biology portable chemical sensors weapons against bioterrorism, p 261−278
48. Arduini F, Neagu D, Dall'Oglio S, Moscone D, Palleschi G (2012) Towards a portable prototype based on electrochemical cholinesterase biosensor to be assembled to soldier overall for nerve agent detection. Electroanal 24:581–590
49. Suprun E, Evtugyn G, Budnikov H, Ricci F, Moscone D, Palleschi G (2005) Acetylcholinesterase sensor based on Screen-Printed carbon electrode modified with Prussian Blue. Anal Bioanal Chem 377:624–631
50. Okazaki S, Nakagawa H, Fukuda K, Asakura S, Kiuchi H, Shigemori T, Takahashi S (2000) Re-activation of an amperometric organophosphate pesticide biosensor by 2-pyridinealdoxime methochloride. Sens Actuators B 66:131–134
51. Gulla KC, Gouda MD, Thakur MS, Karanth NG (2002) Reactivation of immobilized acetylcholinesterase in an amperometric biosensor for organophosphorus pesticide. Biochim Biophys Acta 1597:133–139
52. Du D, Wang J, Smith JN, Timchalk C, Lin Y (2009) Biomonotoring of organophosphorus agent exposure by reactivation of cholinesterase enzyme based on carbon nanotubes-enhanced flow-injection amperometric detection. Anal Chem 81:9314–9320
53. Del Carlo M, Pepe A, Sergi M, Mascini M, Tarentini A, Compagnone D (2010) Detection of coumaphos in honey using a screening method based on an electrochemical acetylcholinesterase bioassay. Talanta 81:76–81
54. Campanella L, Lelo D, Martini E, Martini (2007) Organophosphorus and carbamate pesticide analysis using an inhibition tyrosinase organic phase enzyme sensor; comparison by butyrylcholinesterase + choline oxidase opee and application to natural waters. Anal Chim Acta 587:22–32
55. Hart JP, Hartley IC (1994) Voltammetric and amperometric studies of thiocholine at a screen-printed carbon electrode chemically modified with cobalt phthalocyanine: studies towards a pesticide sensor. Analyst 119:259–263
56. Ricci F, Arduini F, Amine A, Moscone D, Palleschi P (2004) Characterisation of Prussian Blue modified screen printed electrodes for thiol detection. J Electroanal Chem 563:229–237
57. Hernandez S, Palchetti I, Mascini M (2000) Determination of anticholinesterase activity for pesticides monitoring using a thiocholine sensor. Int J Environ Anal Chem 78:263–278
58. Arduini F, Cassisi A, Amine A, Ricci F, Moscone D, Palleschi G (2009) Electrocatalytic oxidation of thiocholine at chemically modified cobalthexacyanoferrate screen-printed electrodes. J Electroanal Chem 626:66–74
59. Neufeld T, Eshkenazi I, Cohen E, Rishpon J (2000) A micro flow injection electrochemical biosensor for organophosphorus pesticides. Biosens Bioelectron 15:323–329
60. Wang J, Timchalk Lin Y (2008) Carbon nanotube-based electrochemical sensor for assay of salivary cholinesterase enzyme activity: an exposure biomarker of organophosphate pesticides and nerve agents. Environ Sci Technol 42:2688–2693

61. Ivanov AN, Younusova RR, Evtugyn GA, Arduini F, Moscone D, Palleschi G (2011) Acetylcholinesterase biosensor based on single-walled carbon nanotubes–Co phtalocyanine for organophosphorus pesticides detection. Talanta 56:4209–4215
62. Bouyahia N, Hamlaoui ML, Hnaien M, Lagarde F, Nicole Jaffrezic-Renault N (2011) Impedance spectroscopy and conductometric biosensing for probing catalase reaction with cyanide as ligand and inhibitor. Bioelectrochemistry 80:155–161
63. Oliveira GC, Moccelini SK, Castilho M, Terezo AJ, Possavatz J, Magalhães MRL, Dores EFGC (2012) Biosensor based on atemoya peroxidase immobilised on modified nanoclay for glyphosate biomonitoring. Talanta 98:130–136
64. Pohanka M, Karasova JZ, Kuca K, Pikulac J, Holas O, Korabecny J, Cabal J (2010) Colorimetric dipstick for assay of organophosphate pesticides and nerve agents represented by paraoxon, sarin and VX. Talanta 81:621–624
65. Zheng Z, Zhou Y, Li X, Liu S, Tang Z (2011) Highly-sensitive organophosphorous pesticide biosensors based on nanostructured films of acetylcholinesterase and CdTe quantum dots. Biosens Bioelectron 26:3081–3085
66. Huang X, Tu H, Zhu D, Zhang A (2009) A gold nanoparticles labelling strategy for the sensitive kinetic assay of the carbamate-acetylcholinesterase interaction by surface plasmon resonance. Talanta 78:1036–1042
67. Lin TJ, Huang KT, Liu CY (2006) Determination of organophoshorous pesticides by a novel biosensor based on localised surface plasmon resonance. Biosens Bioelectron 22:513–518
68. Puiu M, Istrate O, Rotariu L, Bala C (2012) Kinetic approach of aflatoxin B1–acetylcholinesterase interaction: a tool for developing surface plasmon resonance biosensors. Anaytical biochem 421:587–594
69. Zeng H, Jiang Y, Xie G, Yu J (2007) Novel piezoelectric DDVP sensor based on self-assembly method. Anal Lett 40:67–76
70. Halamek J, Teller C, Zeravik J, Fournier D, Makower A, Scheller FW (2006) Characterization of binding of cholinesterases to surface immobilized ligands. Anal Lett 39:1491–1502
71. Kim H, Park IS, Kim DK (2007) High-sensitivity detection for model organophosphorus and carbamate pesticides with quartz crystal microbalance-precipation sensor. Biosens Bioelectron 22:1593–1599
72. Schulze H, Scherbaum E, Anastassiades M, Vorlovà S, Schmid RD, Bachmann TT (2002) Development, validation, and application for an acetylcholinesterase-biosensor test for the direct detection of insecticide residues in infant food. Biosens Bioelectron 17:1095–1105
73. Caetano J, Machado SAS (2008) Determination of carbaryl in tomato ''in natura'' using an amperometric biosensor based on the inhibition of acetylcholinesterase activity. Sens Actuators B 129:40–46
74. Lee HS, Kim YA, Cho YA, Lee YT (2002) Oxidation of organophosphorus pesticides for the sensitive detection by a cholinesterase-based biosensor. Chemosph 46:571–576
75. Zappa E, Brondani D, Vieiraa IC, Scheeren CW, Dupont J, Barbosa AMJ, Ferreira VS (2011) Biomonitoring of methomyl pesticide by laccase inhibition on sensor containing platinum nanoparticles in ionic liquid phase supported in montmorillonite. Sens Actuators B 155:331–339
76. Anh TM, Dzyadevych SV, Prieur N, Duc CN, Pham TD, Jaffrezic Renault N, Chovelon Jean-Marc (2006) Detection of toxic compounds in real water samples using a conductometric tyrosinase biosensor. Mater Sci Eng, C 26:453–456
77. Vidal JC, Esteban S, Gil J, Castillo JR (2006) A comparative study of immobilization methods of a tyrosinase enzyme on electrodes and their application to the detection of dichlorvos organophosphorus insecticide. Talanta 68(3):791–799
78. Cosnier S, Mousty C, Guelorget A, Sanchez-Paniagua Lopez M, Shan D (2011) A fast and direct amperometric determination of Hg^{2+} by a bienzyme electrode based on the competitive activities of glucose oxidase and laccase. Electroanal 23(8):1776–1779
79. Sanllorente-Méndez S, Sanllorente-Méndez S, Sanllorente-Méndez S, Domínguez-Renedo O, Domínguez-Renedo O, Arcos-Martínez MJ, Arcos-Martínez MJ (2010) Immobilization of

acetylcholinesterase on screen-printed electrodes. application to the determination of arsenic(III). Sensors 10(3):2119–2128
80. Sanllorente-Mendez S, Dominguez-Renedo O, Arcos-Martinez MJ (2012) Development of acid phosphatase based amperometric biosensors for the inhibitive determination of As(V). Talanta 93:301–306
81. Ghica ME, Brett CMA (2008) Glucose oxidase inhibition in poly(neutral red) mediated enzyme biosensors for heavy metal determination. Microchim Acta 163(3–4):185–193
82. Guascito MR, Malitesta C, Mazzotta E, Turco A (2009) Screen-printed glucose oxidase-based biosensor for inhibitive detection of heavy metal ions in a flow injection system. Sens Lett 7(2):153–159
83. Campas M, Marty JL (2007) Enzyme sensor for the electrochemical detection of the marine toxin okadaic acid. Anal Chim Acta 605:87–93
84. Campas M, Szydłowska D, Trojanowicz M, Marty JL (2007) Enzyme inhibition-based biosensor for the electrochemical detection of microcystins in natural blooms of cyanobacteria. Talanta 72:179–186
85. Arduini F, Errico I, Amine A, Micheli L, Palleschi G, Moscone D (2007) Enzymatic spectrophotometric method for aflatoxin B detection based on acetylcholinesterase inhibition. Anal Chem 79:3409–3415
86. Ben Rejeb I, Arduini F, Arvinte A, Amine A, Gargouri M, Micheli L, Bala C, Moscone D, Palleschi G (2009) Development of a bio-electrochemical assay for AFB_1 detection in olive oil. Biosens Bioelectron 24:1962–1968
87. Hansmann T, Sanson B, Stojan J, Weik M, Marty JL, Fournier D (2009) Kinetic insight into the mechanism of cholinesterasterase inhibition by aflatoxin B1 to develop biosensors. Biosens Bioelectron 24(7):2119–2124
88. Pohanka M, Kuca K, Jun D (2008) Aflatoxin assay using an amperometric sensor strip and acetylcholinesterase as recognition element. Sens Lett. 6:450–453
89. Yazgan I, Aydin T, Odaci D, Timur S (2008) Use of pyranose oxidase enzyme in inhibitor biosensing. Anal Lett 41(11):2088–2096
90. Timur S, Anik U (2007) Glucosidase based bismuth film electrode for inhibitor detection. Anal Chim Acta 598:143–146
91. Lijun L, Fengna X, Yiming Z, Zhichun C, Xianfu L (2009) Selective analysis of reduced thiols with a novel bionanomultilayer biosensor based on the inhibition principle. Sens Actuator B Chem B135(2):642–649
92. Yu DY, Blankert B, Kauffmann JM (2007) Development of amperometric horseradish peroxidase based biosensors for clozapine and for the screening of thiol compounds. Biosens Bioelectron 22(11):2707–2711
93. Pohanka M, Dobes P, Dritinova L, Kuca K (2009) Nerve Agents assay using cholinesterase based biosensor. Electroanal 21:1177–1182
94. Bouyahia N, Larbi Hamlaoui M, Hnaien M, Lagarde F, Jaffrezic-Renault N (2011) Impedance spectroscopy and conductometric biosensing for probing catalase reaction with cyanide as ligand and inhibitor. Bioelectrochemistry 80(2):155–161
95. Asav E, Yorganci E, Akyilmaz E (2009) An inhibition type amperometric biosensor based on tyrosinase enzyme for fluoride determination. Talanta 78:553–556
96. Shahidi Pour Savizi I, Kariminia HR, Ghadiri M, Roosta-Azad R (2012) Amperometric sulfide detection using Coprinus cinereus peroxidase immobilized on screen printed electrode in an enzyme inhibition based biosensor. Biosens Bioelectron 35:297–301
97. Kochana J, Kozak J, Skrobisz A, Woźniakiewicz M (2012) Tyrosinase biosensor for benzoic acid inhibition-based determination with the use of a flow-batch monosegmented sequential injection system. Talanta 96:147–152

Adv Biochem Eng Biotechnol (2014) 140: 327–331
DOI: 10.1007/978-3-642-54143-8

Index